New Approaches to Combating Drug Resistance via Saturated Chemical Architectures

Jasmine Rebecca Hind

A thesis submitted for the degree of
Doctor of Philosophy

Cardiff University

September 2025

Abstract

Tamoxifen, an aryl containing tetrasubstituted olefin, is an essential drug used to treat breast cancer. Despite its clinical success, intraindividual differences in plasma concentration of non-therapeutic metabolites can cause variation in tamoxifen's efficacy and could contribute to acquired tamoxifen resistance. One approach to address this issue includes the introduction of a benzene bioisostere that has an improved metabolic stability. An example of a C(sp^3)-rich benzene bioisostere that may offer improved metabolic stability is cubane, a highly strained cage structure first synthesised by Eaton and Cole. Consequently, in this thesis, we aimed to synthesise cubane derivatives of tamoxifen as a method to improve its metabolic profile. Several synthetic strategies were explored to construct a tetrasubstituted olefin bearing a cubane scaffold, ultimately leading to the successful preparation of a cubane-containing derivative of tamoxifen.

In addition, bioisosteric replacement of benzene for cubane in pharmaceuticals has primarily been used to mimic terminal or *para*-substituted benzene rings, arising from the lack of general synthetic methods for the functionalisation of cubane. Given the prevalence of phenols in pharmaceuticals, it is noteworthy that synthetic routes to cubanols are virtually unknown. We postulated that the Bayer-Villiger rearrangement of cubane ketones, with a subsequent ester hydrolysis, could readily provide access to functionalised cubanols for applications in medicinal chemistry. Initially, we determined how steric and electronic factors influence the migratory aptitude of functionalised cubanes. We also demonstrate the synthetic utility of the hydrolysis of cubyl acetates to yield cubanols; this strategy was successfully applied to two analogues of the biologically active compound resveratrol.

Acknowledgements

I would like to thank my supervisor Matthew for all the support and guidance during my PhD. I am grateful for you providing an environment that allowed me to try new things and for helping me develop greater confidence in my own abilities. I have thoroughly enjoyed being a member of your research group. I would also like to thank my second supervisor Ian, for your feedback and support.

To Pawan, I am grateful for all your help, laughter and advice along the way. To Brandon, Tim, Annika and Marong, thank you for your friendship and well needed coffee breaks.

I would like to thank my mum, dad, sister and grandparents for their constant support, encouragement and late-night calls. To my partner Louise, thank you for being my constant over the last decade, your endless support during the stressful moments and the countless hours spent on GWR trains coming to Cardiff.

Lastly, thank you to the EPSRC for the funding my PhD.

Table of Contents

Table of Figures

Table of Tables

Table of Schemes

Abbreviations

BCP	Bicyclo[1.1.1]pentane
BCH	Bicyclo[2.1.1]hexane
BCHep	Bicyclo[2.1.1]heptane
BCO	Bicyclo[2.2.2]octane
BV	Baeyer-Villiger
CHI	Chromatographic hydrophobicity index
CUB	Pentacyclo[4.2.0.0^{2,5}.0^{3,8}.0^{4,7}]octane = Cubane
COSY	Correlation spectroscopy
d	Doublet
DCC	*N*,*N*'-Dicyclohexylcarbodiimide
DCM	Dichloromethane
DES	Diethylstilboestrol
DIPEA	*N*,*N*-Diisopropylethylamine
DMAP	4-(Dimethylamino)pyridine
DME	Dimethoxyethane
DMF	Dimethylformamide
ER	Oestrogen receptor
E_1	Unimolecular elimination
E_2	Biomolecular elimination
m	Multiplet
HPLC	High performance liquid chromatography
HRMS	High resolution mass spectrometry
HSQC	Heteronuclear single quantum coherence spectroscopy
HWE	Horner-Wadsworth-Emmons
LED	Light-emitting diode
LRMS	Low resolution mass spectrometry
m-CPBA	*meta*-Chloroperoxybenzoic acid

rt	Room temperature
s	Singlet
SERM	Selective oestrogen receptor modulator
t	Triplet
TFA	Trifluoroacetic acid
THF	Tetrahydrofuran
TLC	Thin-layer chromatography

Chapter 1 Introduction

1.1 Tamoxifen

1.1.1 Overview

Tamoxifen is a blockbuster drug that has been used to treat breast cancer for the last five decades worldwide, although its origins date back to the 1960s where it was originally evaluated by ICI pharmaceuticals (currently known as AstraZeneca) as a potential antifertility agent (Figure 1).[1-3] Unfortunately, after extensive studies it was discovered that tamoxifen failed to elicit anti-oestrogenic effects in the ovaries in women, causing ICI pharmaceuticals to reconsider the future of tamoxifen.[4] In fact, ICI pharmaceuticals were prepared for this eventuality and already had approval to carry out therapeutic studies of tamoxifen for the treatment of breast cancer.[2] Notably at the time, the standard endocrine treatment for advanced breast cancer involved high doses of diethylstilboestrol (DES), a compound structurally similar to tamoxifen (Figure 2).[5]

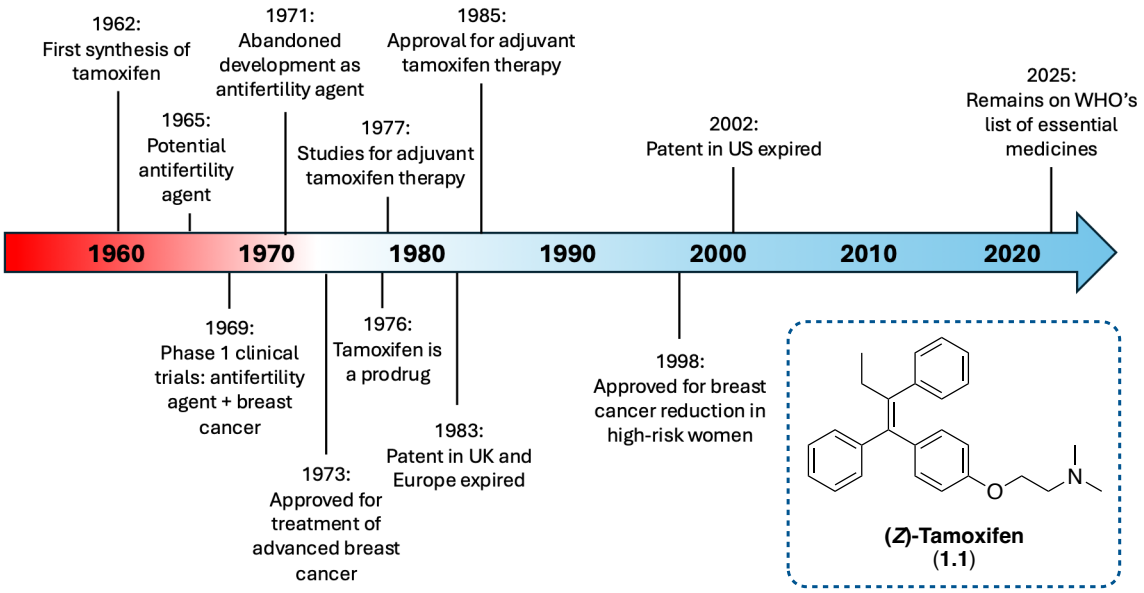

Figure 1: Timeline of tamoxifen development.

The clinical trial evaluating tamoxifen's effectiveness to treat breast cancer revealed it produced an equivalent response to DES, albeit with fewer side effects.[6] In addition,

tamoxifen was found to have a response for post-menopausal women, a group of patients that in the past had previously been insensitive to DES hormone therapy.[6] Based on these encouraging results tamoxifen was approved in the UK for the treatment of advanced breast cancer, despite incomplete understanding of its mode of action.[1] Interestingly, around the same time period other pharmaceutical companies abandoned their own development of breast cancer drugs over concerns of serious side effects with long-term use (e.g. cataract formation).[1] The breast cancer drugs in development were triparanol, ethamoxytriphetol and clomiphene; all compounds structurally similar to tamoxifen (Figure 2).[1]

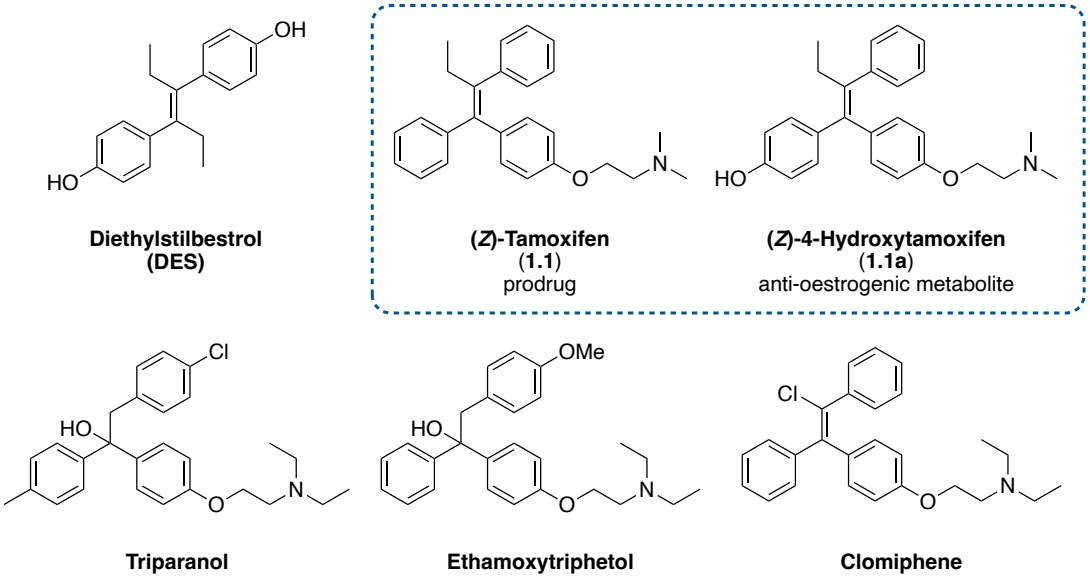

Figure 2: Pharmaceuticals for breast cancer treatment.

A few years later it was discovered that tamoxifen was in fact a prodrug that was converted into the anti-oestrogenic metabolite (*Z*)-4-hydroxytamoxifen (**1.1a**), which has a high affinity for the oestrogen receptor (ER) (Figure 2).[1, 7] The mode of action for **1.1a** is to competitively inhibit the binding of the hormone oestrogen to the ERs in breast cancer cells, thus preventing oestrogen-stimulated breast tumour growth.[8-10] Tamoxifen was later classified as a selective oestrogen-receptor modulator (SERM) that has anti-oestrogenic properties in breast tissue, but can act as an oestrogen-like compound elsewhere in the body.[9, 10] With a better understanding of the mode of action, ICI pharmaceuticals and others began to investigate how effective tamoxifen would be as

an adjuvant therapy.[11, 12] The Early Breast Cancer Trialist's' Collaborative Group collated information obtained from 37,000 women over 55 randomised clinical trials, to evaluate the optimal timeframe for tamoxifen adjuvant therapy treatment for women diagnosed with early-stage oestrogen positive or negative breast cancer.[13] In clinical trials of 1, 2 or 5 years of adjuvant tamoxifen there was a reduction in tumour recurrence of 21 %, 29 % and 47 % respectively and a decrease of mortality of 13 %, 26 % and 47 % respectively after a 10-year follow-up.[13] Based on these results, the collaborative group concluded that better clinical outcomes were observed with longer dose regimes, leading to 5 years of tamoxifen adjuvant therapy becoming the standard treatment for individuals with early-stage breast cancer. Tamoxifen's clinical application continued to expand; it was later shown it could be used for chemoprevention, reducing the incidence of invasive breast cancer by 50 % in high-risk patients.[14]

Currently breast cancer is the second most commonly diagnosed cancer and has the fourth highest mortality rate worldwide.[15] The most common form of breast cancer is oestrogen-receptor-positive (ER positive), accounting for around 80 % of all cases.[16] In the UK, tamoxifen is offered as a first-line treatment to men, pre- and perimenopausal women with ER positive advanced breast cancer, as a form of endocrine therapy.[17] In early and localised ER positive breast cancer, tamoxifen is also used as an adjuvant endocrine therapy, usually taken for 5 years after initial cancer treatment to supress secondary tumour formation.[17] In addition, it is licenced for chemoprevention in premenopausal women who have been identified as being at moderate to high-risk of developing breast cancer based on family history.[17] The multiple clinical applications of tamoxifen is partly why it is one of the most successful breast cancer drugs. Tamoxifen's development as an orally administered drug also makes it accessible and with all patents expired, generic versions make tamoxifen treatment highly affordable.[18] This is reflected by the World Health Organisation including tamoxifen on its list as an essential medicine for the treatment of breast cancer.[18]

1.1.2 Mechanism of action of tamoxifen

Shortly after Harper and Walpole first synthesised tamoxifen in the 1960s the antiestrogenic properties of the *Z*- and *E*-geometric isomers were first examined in immature rats (Table 1).[3] When (*Z*)-tamoxifen was administered the weight of the uterus decreased, which was indicative of antiestrogenic activity, whereas for (*E*)-tamoxifen the weight of the uterus increased, which suggested it behaved as a conventional oestrogen.[3] Based on the positive antiestrogenic properties of (*Z*)-tamoxifen the first clinical trial was funded.[6] In the clinical trial individuals with advanced breast cancer were given 10 mg of (*Z*)-tamoxifen daily, after 3 months of treatment a reduction in tumour mass in 22 % of patients was observed.[6] This provided strong evidence that in breast tissues (*Z*)-tamoxifen behaves as an antioestrogen for the ER. However, in different species and tissues (*Z*)-tamoxifen can behave as a partial or full oestrogen agonist, for example, a clinical trial evaluating tamoxifen as an antifertility agent found it actually induced ovulation in women by acting as a full oestrogen.[4, 19]

Table 1: Geometric isomers of tamoxifen.[20]

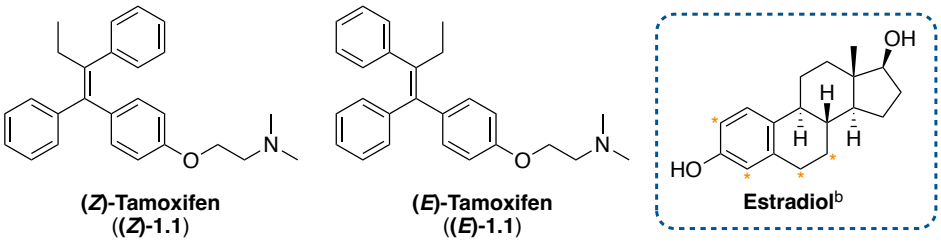

(*Z*)-Tamoxifen ((***Z*)-1.1**)

(*E*)-Tamoxifen ((***E*)-1.1**)

Estradiol[b]

	(*Z*)-Tamoxifen	**(*E*)-Tamoxifen**
Effect on MCF-7 oestrogen receptor	Weak antioestrogen	Weak oestrogen
Binding affinity [a] / %	2.5	0.3

[a] percentage of binding to MCF-7 estrogen receptor compared to estradiol (a type of oestrogen).[b] [2,4,6,7-^{3}H]estradiol with asterisk indicating the position of tritium labelling.

The binding affinity of (*Z*)-tamoxifen (and (*E*)-tamoxifen) *in vitro* (MCF-7 breast cancer cell line) is low compared to estradiol, a type of oestrogen hormone that has a high affinity for the ER (Table 1). One study measured the concentration of (*Z*)- and (*E*)-tamoxifen required to produce a 50 % decrease in specific binding of tritiated estradiol,

which indicated that (*Z*)-tamoxifen and (*E*)-tamoxifen had an affinity of 2.5 % and 0.3 % respectively for the ER compared to estradiol.[20] In addition, (*Z*)-tamoxifen also has a high binding affinity to serum albumin, with one study reporting up to 98 % of (*Z*)-tamoxifen was protein bound.[21] In this instance the protein binding was determined by ultracentrifugation of a patient's serum (40 mg of tamoxifen twice daily for 78 days) and measuring the percentage of serum albumin that co-sedimented with tamoxifen.[21]

It was only after (*Z*)-tamoxifen was initially approved for treatment of advanced breast cancer in the UK, that metabolic studies revealed (*Z*)-tamoxifen was a acting as a prodrug.[7] The first study to investigate (*Z*)-tamoxifen metabolism in humans included multiple women receiving a single dose of ^{14}C-labelled (*Z*)-tamoxifen (20 mg tamoxifen containing 1.5 MBq [^{14}C]tamoxifen).[22] Following a single dose, after 4 hours 33 % of the radiolabelled material from a serum sample was attributed to the parent compound and after an additional 6 hours only 8 % of the parent compound remained (Table 2).[22] Two weeks after receiving the labelled dose over 65 % (faeces = 51 %, urine = 14 %) of the dose was accounted by excretion, with still detectable radioactivity remaining in the blood samples (although components were not measured).[22] [^{14}C]4-Hydroxytamoxifen was identified as one of the metabolites of [^{14}C](*Z*)-tamoxifen, and only a few years later Jordan *et al* confirmed (*Z*)-4-hydroxytamoxifen had a higher binding affinity and potency for the ER than (*Z*)-tamoxifen.[23] Jordan and co-workers also identified several other important metabolites of the prodrug (*Z*)-tamoxifen.[23] Notably, the detectable levels of [^{14}C](*Z*)-tamoxifen observed in both the serum and faecal samples after one week demonstrated that (*Z*)-tamoxifen has a long half-life, which could be attributed to (*Z*)-tamoxifen having a high affinity to plasma proteins, thus reducing the rate the prodrug is metabolised *in vivo* (Table 2).[21]

Table 2: Average percentage of [^{14}C](*Z*)-tamoxifen in serum and faecal samples over two weeks.

		[^{14}C](*Z*)-Tamoxifen / %	[^{14}C]Metabolites / %
Serum sample / hours	4	33	39
	10	8	57
	25	11	49
	75	4	53
	172	4	65
Faecal sample / days	6	16	67
	8	12	66
	13	4	67

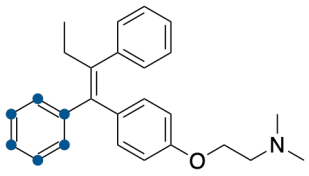

[^{14}C](*Z*)-Tamoxifen
1 dose of 1.5 MBq

The metabolism of (*Z*)-tamoxifen (**1.1**) begins with phase I metabolism in the liver by cytochrome P450 enzymes, generating the two primary metabolites 4-hydroxytamoxifen (**1.1a**) and *N*-desmethyltamoxifen (**1.1b**), with the major metabolic pathway highlighted with bold arrows in Table 3.[24, 25] Secondary metabolism of the two primary metabolites **1.1a** and **1.1b** produces endoxifen (**1.1c**). The metabolites **1.1a** and **1.1c**, which both have a phenolic group in common, notably have much lower plasma concentrations compared to (*Z*)-tamoxifen and metabolite **1.1b** (Table 3). The metabolites **1.1a** and **1.1c** are widely considered the most important metabolites for the antiestrogenic activity, due to their binding affinities to the ER being 60-fold greater than (*Z*)-tamoxifen and metabolite **1.1b** (Table 3). [26, 27] In addition, the IC_{50} (MCF-7 breast cancer cell line with ER overexpression) of metabolites **1.1a** and **1.1c** are in the low nM range (0.51 nM and 1.45 nM respectively) compared to (*Z*)-tamoxifen and metabolite **1.1b** (81.8 nM and 96.2 nM respectively), making metabolites **1.1a** and **1.1c** far more potent and effective at supressing breast cancer cell growth (Table 3).[26, 27]

Table 3: Important metabolites of (*Z*)-tamoxifen.[24, 28]

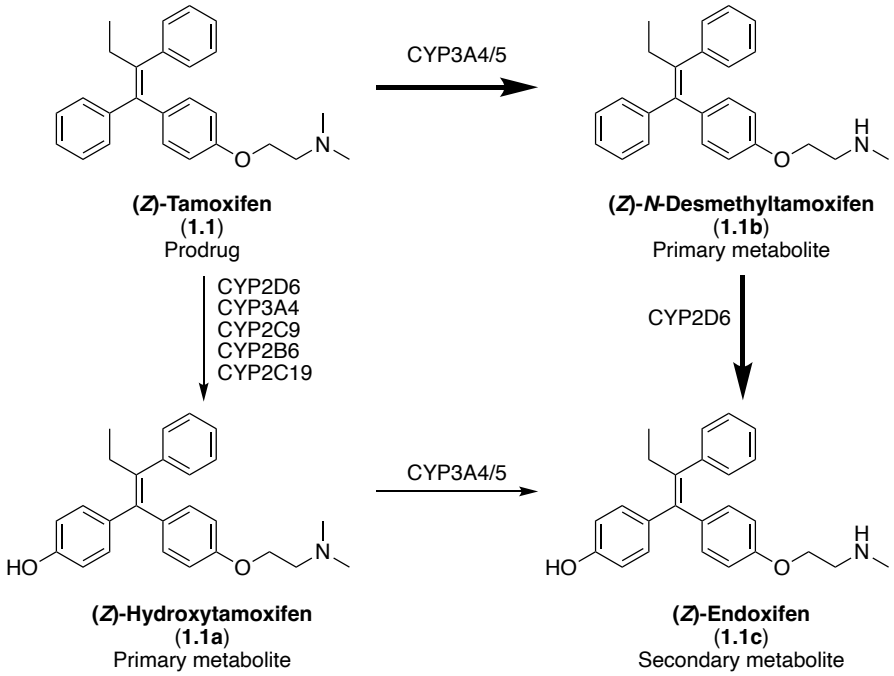

	1.1	**1.1a**	**1.1b**	**1.1c**
Effect on oestrogen receptor	Weak antioestrogen	Strong antioestrogen	Weak antioestrogen	Strong antioestrogen
Relative binding affinity [a] / %[26]	2.8	181	2.4	181
IC_{50} (MCF-7 / nM)[27]	81.8	0.51	96.2	1.45
Plasma concentration [b] (nM)[29]	377	9	655	63
Approximate half-life (days)	7[23, 30, 31]	n.d	14[23]	2[31]

[a] Compared to estradiol. [b] Mean concentration for subjects taking (Z)-tamoxifen (20 mg/day by oral administration) after 4 months; n.d – not determined.

In the literature it remains unclear as to whether metabolite **1.1a** or **1.1c** contributes more significantly to the antioestrogen activity of the drug. The primary difference between metabolites **1.1a** and **1.1c** is the enzymes that are used to generate them (Table 3).[28] Notably, metabolite **1.1c** is formed predominately by CYP2D6 enzymes whereas for **1.1a** several enzymes contribute to its formation. Some clinical studies have shown an association between genetic variations in the enzyme CYP2D6 and poor clinical outcomes, which implies metabolite **1.1c** has a more important role in reducing breast cancer growth, whilst other authors have reported no association between the two.[32-34] Therefore the question remains whether metabolite **1.1c** is the most important

and if it is, should we consider **1.1c** as a novel SERM over (*Z*)-tamoxifen. Early findings from a phase I clinical study evaluating **1.1c** against (*Z*)-tamoxifen for patients with estrogen positive metastatic breast cancer concluded it had an acceptable half-life (49-55 hours) and toxicity, whilst maintaining antitumour activity.[35-37] This supports the suggestion that there could be clinical advantages of using **1.1c** over (*Z*)-tamoxifen in the future if it is proven that genetic variations in the enzyme CYP2D6 impact the anti-tumour activity of (*Z*)-tamoxifen.

The biological target of (*Z*)-tamoxifen and the antioestrogen metabolites (which are all SERMs) is the estrogen receptor (ER), a hormone-regulated transcription factor that controls cell division and differentiation (Figure 3).[38] The two tamoxifen metabolites 4-hydroxytamoxifen (**1.1a**) and endoxifen (**1.1c**) have a high affinity for the ER due to the appropriately positioned phenolic group, which forms important hydrogen bonds with key amino acid residues in the ER binding pocket (Glu353 and Arg394) (Table 3 and Figure 3a).[39, 40] These interactions anchor a SERM into the binding pocket. The alkylaminoethoxy side chain of the SERM forms an ionic interaction to the anionic β-carboxylate of the ASP351 amino acid residue (Figure 3a).[39, 40] The binding extends outside the ligand binding domain, inducing a conformational change of the ER which promotes inhibition of oestrogen-stimulated breast cancer growth.[10, 39, 40]

A) Key binding interactions of **1.1a** (SERM) in the ER binding pocket

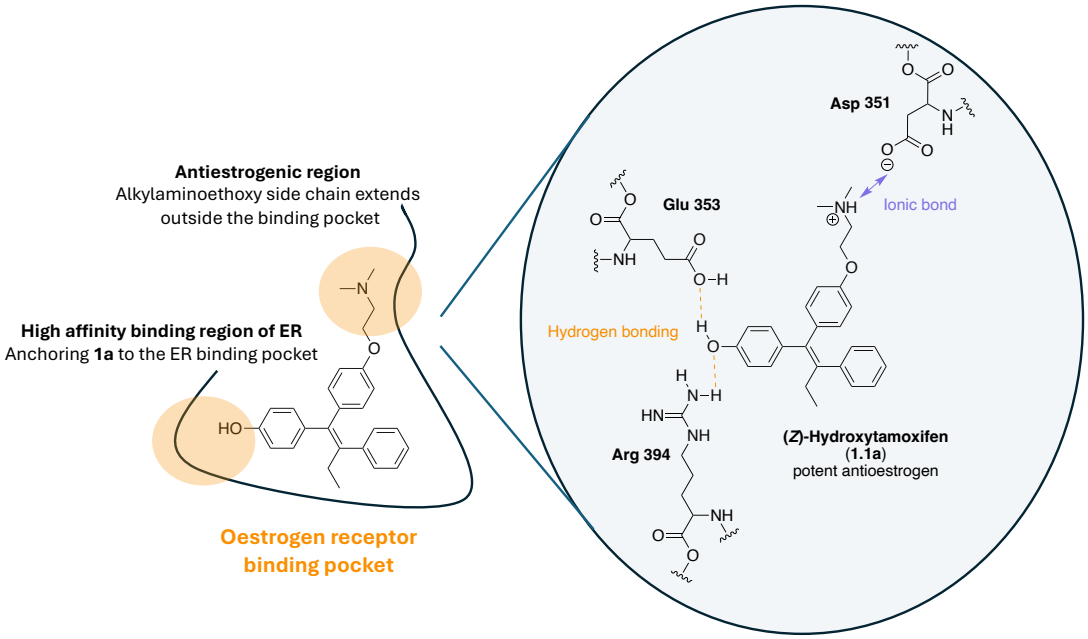

B) SERM versus oestrogen mode of action at the ER

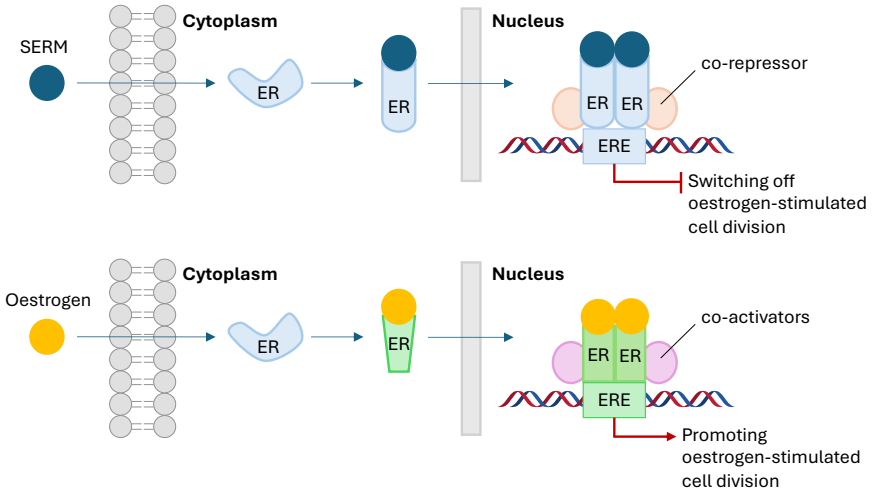

Figure 3: Mechanism of action of SERMs at oestrogen positive breast cancer cells.[9, 39-41]

SERM = selective oestrogen receptor modulator, ER = oestrogen receptor, ERE = oestrogen response elements.

When a SERM binds to an ER it induces a distinct conformational change in the receptor, which promotes the heat shock proteins to dissociate and allows two SERM-bound ER's to dimerise (Figure 3b).[9, 41] The role of the heat shock proteins is to regulate ER-mediated cell proliferation, without ER activation the heat shock proteins would not dissociate and ER-simulated cell division will not occur.[9] In addition, different ER ligands induce different conformational changes in the receptor, influencing which co-

regulator proteins can subsequently interact with the ER receptor dimer to regulate gene transcription.[9, 41] For SERM's, the two co-regulator proteins that bind to the ER dimer are called co-repressors, which switch off oestrogen-responsive gene transcription when the ER dimer binds to the oestrogen response elements (EREs) of the DNA.[9, 41] The downstream effects include a reduction in ER-stimulated breast cancer cell division and differentiation.[39]

1.1.3 Acquired Tamoxifen resistance

The efficacy of tamoxifen can widely vary between individuals who have oestrogen-receptor-positive breast cancer, with approximately 35 % not responding to this hormone therapy.[29] Tumours that do not respond well to tamoxifen will typically become resistant to this treatment.[29] Therefore, developing methods to minimise acquired resistance to tamoxifen is highly important for continued clinical success. One mechanism for acquired tamoxifen resistance includes variations in how tamoxifen is metabolised by different individuals.[42-44]

The metabolism of (*Z*)-tamoxifen was previously discussed, although only the principal metabolites were mentioned. In fact, the metabolism of (*Z*)-tamoxifen is significantly more complex and variations in metabolite formation are believed to contribute to an individual's clinical response to therapy. Despite tamoxifen being administered as the (*Z*)-geometric isomer, *in vivo* it has been shown that phenolic metabolites can isomerise into their respective (*E*)-geometric isomers by CYP450 enzymes, particularly by CYP1B1 (Scheme 1).[45-48] Based on how CYP-mediated oxidations usually proceed, the isomerisation may begin with the abstraction of a hydrogen atom from the phenolic group by a reactive iron-oxo species (Scheme 1).[46] Subsequently, the generated radical species **1.2a** could undergo an electron abstraction to form the cationic species **1.2b**, in which the resonance structure of both **1.2c** and **1.2d** would facilitate *Z*/*E* isomerisation.[46] DFT calculations by Eriksson *et al* revealed that the *Z*/*E* isomerisation is energetically more favourable via the cationic species rather than the radical species for 4-hydroxytamoxifen (**1.1a**), although this may be different for other (*Z*)-tamoxifen phenolic metabolites.[49] In addition, **1.1a** has been reported to isomerise to a *Z*/*E*

mixture in acidic solvent, therefore, *in vivo* pH dependant isomerisation may also occur for the (*Z*)-tamoxifen phenolic metabolites.[50]

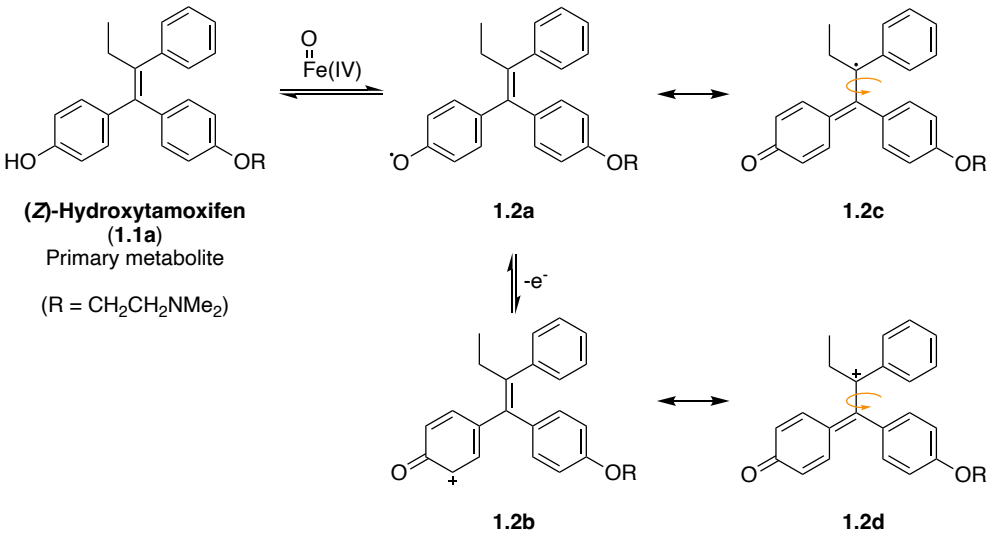

Scheme 1: Proposed isomerisation mechanism of (*Z*)-4-hydroxytamoxifen (**1.1a**) via radical and cationic intermediates.[46, 49]

A major clinical trial revealed that increased concentrations of (*E*)-4-hydroxytamoxifen (**1.1a'**), primarily a weak antioestrogen which can exhibit some estrogenic activity, compared to (*Z*)-4-hydroxytamoxifen (potent antioestrogen, **1.1a**) were found in tumour samples for patients not responding to tamoxifen treatment (n = 14).[42, 47] Whereas, higher concentrations of (*Z*)-4-hydroxytamoxifen (**1.1a**) were observed in patients responding to tamoxifen treatment.[42, 47] Thus, it has been implied that tamoxifen resistance could be reduced by finding a way to minimise isomerisation.[43, 44] Evidence that supports this includes a two to six-fold overexpression of the enzyme CYP1B1, which predominately catalyses the isomerisation of (*Z*)-4-hydroxytamoxifen to (*E*)-4-hydroxytamoxifen in tamoxifen resistance breast cancer cell lines (Scheme 2).[51, 52]

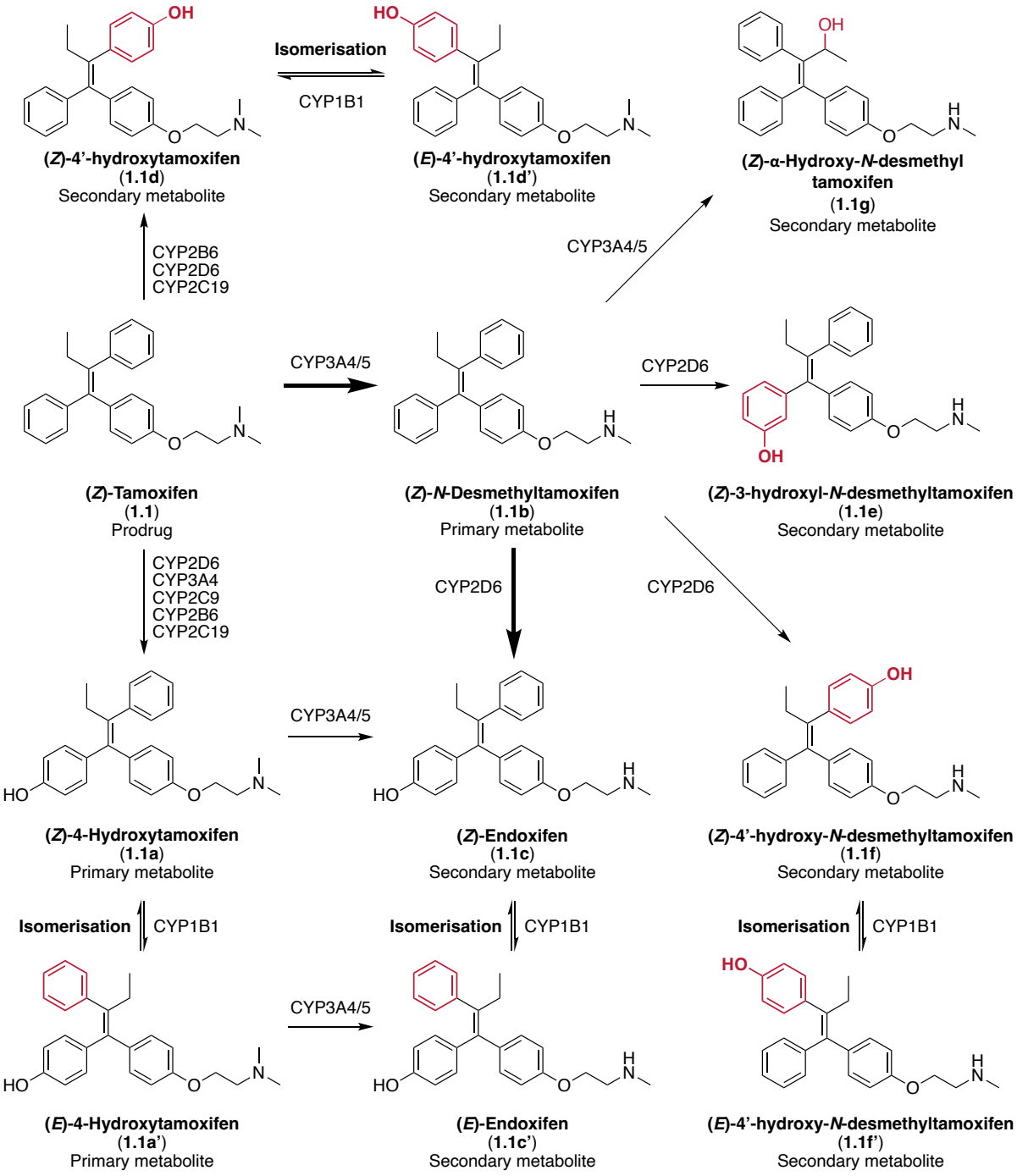

Scheme 2: Primary metabolites of (*Z*)-tamoxifen (**1.1a** – **1.1c**) and the major non-therapeutic metabolites from either undesired hydroxylation (oxidation) or isomerisation are displayed in red.

Tamoxifen metabolites that have been identified to isomerise *in vivo* are those with a phenolic group.[47] This includes the potent antioestrogens (*Z*)-4-hydroxytamoxifen (**1.1a**) and (*Z*)-endoxifen (**1.1c**) and the non-therapeutic metabolites **1.1d** and **1.1f** (Scheme

2).[53] These 4'-isomers of hydroxytamoxifen (**1.1d**) and endoxifen (**1.1f**) have no inhibitory effect on the ER, as the phenolic groups are no longer appropriately positioned to form hydrogen bonds in the ER binding pocket (Table 4 and Figure 3).[53] Unfortunately the steady state concentration of the 4'-isomers (**1.1d**: 9 nM; **1.1f**: 21 nM) are comparable to 4-hydroxytamoxifen (**1.1a**: 6 nM) and endoxifen (**1.1c**: 29 nM), ultimately reducing the efficacy of tamoxifen (Table 4).[53] A potential approach to overcome having high plasma concentrations of the non-therapeutic hydroxyl metabolites, that can also isomerise to their respective *E*-geometric isomers, would be to stop hydroxylation altogether at the 4'-position altogether.

Table 4: Inhibitory effect and plasma concentration of (*Z*)- tamoxifen and its major (*Z*)- and (*E*)-metabolites.

Compound	**IC_{50} (MCF7, nmol/L)**	**Mean steady state concentration (nM)**[a,b]
(*Z*)-Tamoxifen (**1.1**)	n.r	428 ± 157
(*Z*)-4-Hydroxytamoxifen (**1.1a**)	7	5.81 ± 2.17 (0.56 ± 1.06)
(*Z*)-*N*-Desmethyltamoxifen (**1.1b**)	n.r	762 ± 297
(*Z*)-Endoxifen (**1.1c**)	3	29.1 ± 14.4 (1.17 ± 3.56)
(*Z*)-4'-Hydroxytamoxifen (**1.1d**)	n.r	9.12 ± 3.53 (0.63 ± 0.73)
(*Z/E*)-3-Hydroxy-*N*-desmethyltamoxifen (**1.1e**)	n.r	3.16 ± 1.66
(*Z*)-4'-Hydroxy-*N*-desmethyltamoxifen (**1.1f**)	n.r	21.3 ± 8.00 (0.99 ± 1.52)
(*Z*)-α-Hydroxy-*N*-desmethyltamoxifen (**1.1g**)	n.r	3.35 ± 1.74

n.r = 50% inhibition was not reached. [a] After 6 months of adjuvant treatment of tamoxifen 20mg/day. [b] Mean steady state concentration for the respective E-geometric isomer in brackets.

In terms of preventing isomerisation of the potent antioestrogen metabolites of (*Z*)-tamoxifen *in vivo,* one strategy that could be utilised is the introduction of a scaffold that has a fixed geometry that prevents conformational rotation.[54, 55] An example of this approach is the substitution of the central *Z*-double bond in (*Z*)-tamoxifen for a 7-member heterocyclic scaffold (**1.3**) by Meegan *et al* (Scheme 3a).[54] Computational docking studies indicated that **1.3** had a similar orientation to (*Z*)-4-hydroxyltamoxifen (**1.1a**) in the binding pocket of the ER, providing evidence that the increase in structural rigidity was not preventing compound **1.3** entering the ER binding pocket.[54] This was

supported by *in vitro* studies, with **1.3** exhibiting a similar antiestrogenic potency to (*Z*)-tamoxifen (**1.1**) in human MCF-7 breast cancer cell line, which are known to overexpress the ER (IC_{50}: **1.1** = 11.3 μM and **1.3** = 16.2 μM).[54] Interestingly raloxifene, a next generation SERM of (*Z*)-tamoxifen has a central ring system which also prevents isomerisation (Scheme 3a).[55, 56]

A) Fixed ring systems.[54]

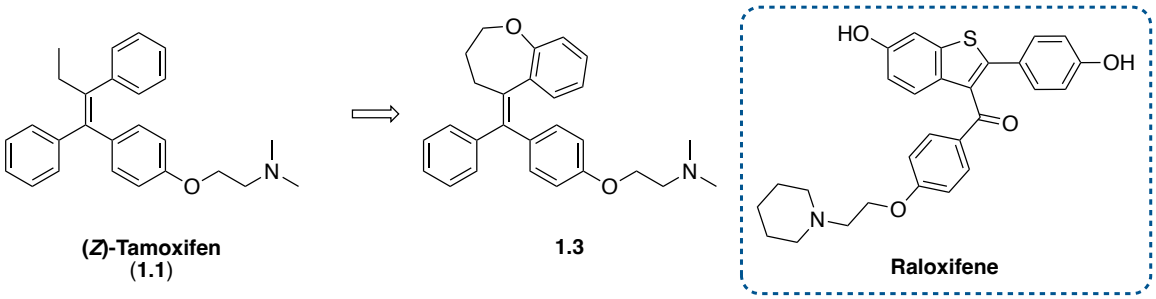

(*Z*)-Tamoxifen (1.1) **1.3** **Raloxifene**

B) Addition of EWG's adjacent to alkene to impede isomerisation

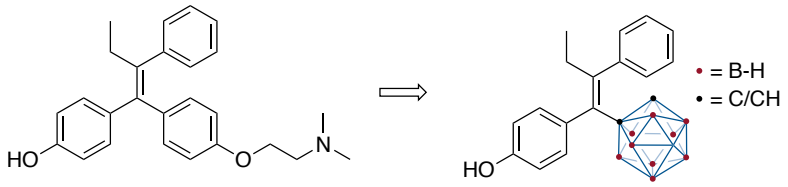

(*Z*)-4-Hydroxytamoxifen (1.1a) Primary metabolite **1.4**

Scheme 3: Literature approaches to prevent or reduce alkene isomerisation *in vivo*.[57]

An alternative approach investigated by Valliant and co-workers to disfavour isomerisation of (*Z*)-tamoxifen phenolic metabolites, was to replace the 4-substituted phenyl ring in (*Z*)-4-hydroxytamoxifen (**1.1a**) for a bulky carborane ring system (Scheme 3b).[57] It was reported that the (*E*)-carborane analogue **1.4** did not isomerise using microwave irradiation at 120 °C for 20 minutes, with only 15 % isomerisation when increasing the temperature to 160 °C.[57] In the discussion they did not include isomerisation percentages for (*Z*)-4-hydroxytamoxifen (**1.1a**) under the same conditions, although they did state the carborane analogues had a superior stability in solution. The reasoning behind the slower *E*/*Z* isomerisation of the carborane analogue **1.4** compared to **1.1a** was explained by considering the mechanism of isomerisation.

As previously discussed, for the phenolic metabolites CYP-mediated isomerisation can occur via a radical or cation mechanism, with computational studies suggesting *Z*/*E* isomerisation is energetically more favourable to proceed via the cationic mechanism for **1.1a**.[49] Considering just a cationic mechanism to begin with, the *Z*/*E* isomerisation of carborane analogue **1.4** should be unfavourable as the cation formation at the carbon adjacent to an electron withdrawing carborane scaffold would provide destabilisation. This is reflected in the experimental results, in which slow *E*/*Z* isomerisation of the carborane analogue **1.4** in solution was observed compared to (*Z*)-4-hydroxytamoxifen (**1.1a**).[57, 58] Notably, the *Z*/*E* isomerisation of carborane analogue **1.4** via a radical mechanism is unlikely to have the same effect as the radical at the carbon adjacent to a carborane scaffold should not be unfavourable. To conclude the study, the authors tested the potency of carborane **1.4** against (*Z*)-tamoxifen. Evaluation of the antiestrogenic activity of (*Z*)- and (*E*)-**1.4** using human MCF-7 breast cancer cell line showed that cell growth was inhibited by 60 % over 10 days, comparable to 50 % inhibition observed for (*Z*)-tamoxifen over the same time period.[57]

Despite the data from the carborane study providing strong evidence that bioisosteric substitution of one of the aromatic groups in (*Z*)-tamoxifen can occur without loss in biological activity, only a handful of other studies have explored this approach.[57, 59, 60] Furthermore, given the low metabolic stability of (*Z*)-tamoxifen and the resulting high plasma concentrations of non-therapeutic hydroxylated metabolites *in vivo*, replacing a benzene ring for a scaffold that is more resistant to CYP-mediated oxidation could offer another approach to improve the clinical outcomes of tamoxifen treatments (Scheme 4).[61]

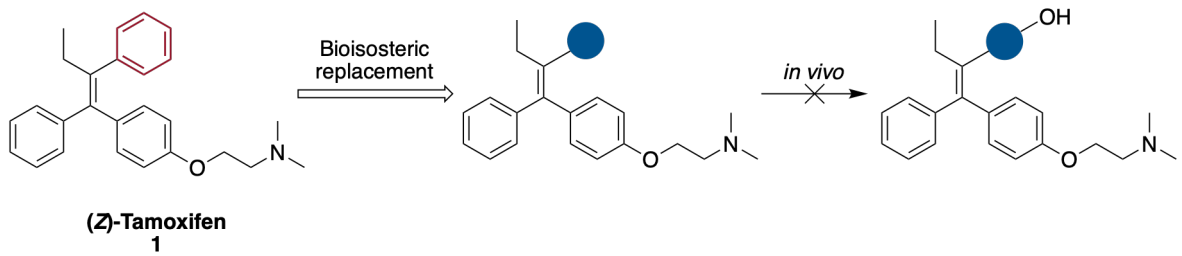

Scheme 4: An example of bioisosteric replacement to increase the metabolic stability of (*Z*)-tamoxifen.

An objective of this thesis is to investigate this strategy of bioisosteric replacement of the aryl ring(s) in (*Z*)-tamoxifen in order to produce (*Z*)-tamoxifen derivatives with a better *in-vivo* profile. In particular, we are interested in aryl bioisosteres that are more metabolically stable than benzene to oxidation, with the aim of limiting the formation of non-therapeutic metabolites via *Z*/*E* isomerisation.

1.2 Benzene bioisosteres

Benzene rings remain the most prevalent ring system in FDA approved small drug molecules, followed by pyridine, which appears almost 10 times less frequently.[62, 63] However, drugs that are rich in aromatic rings can often suffer from poor pharmacokinetic properties, such as metabolic instability and poor aqueous solubility.[61] A recent approach to improve the overall pharmacokinetic properties of drugs that contain a benzene ring, includes replacing this motif for an strained sp^3 hybridised ring system (Figure 4).[61] Bioisosteric replacement of flat sp^2 hybridised aromatic rings for saturated ring systems also increases the three-dimensional shape of a compound, creating more complex molecules that are more natural product-like that have access to an expanded area of chemical space for novel target interactions.[64, 65] In terms of drug discovery this is extremely valuable as it offers a route to discover additional libraries of bioactive compounds, thus providing greater opportunities for a drug to be optimised towards a biological target.[64, 65]

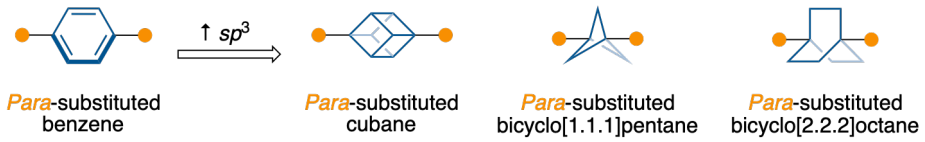

Figure 4: Examples of bioisosteric replacement of a flat *para*-substituted benzene for saturated three-dimensional ring systems.[64-67]

In the past decade these strained saturated ring systems have proven to be valuable in drug discovery, therefore in recent years research has focussed on developing methodologies to synthesise structurally more complex strained saturated ring systems.[61, 66-69]

1.2.1 Isosteres

The concept of isosterism was first considered by Moir, however, it was formally defined by Langmuir years later.[70, 71] Langmuir stated that compounds such as CO and N_2 that have the same number of atoms and valence electrons, also have similar physical properties, which led him to define these compounds as isosteric. The definition of isosterism was expanded by Grimm with his hydride displacement law, stating that isosteres are groups of atoms that have the same number of valence electrons but not necessarily the same number of atoms. For instance, elements of a lower periodic group (up to four groups) were isosteres to elements of a higher period group by the addition of hydrogen atoms (up to four groups) (Table 5).[72]

Table 5: Grimm's hydride displacement law - expanded definition of an isostere

C	N	O	F
	CH	NH	OH
		CH_2	NH_2
			CH_3

Grimm's definition of isosteres was later extended by Erlenmeyer as "elements, molecules or ions in which the peripheral layers of electrons may be considered identical". [72]

1.2.2 Bioisosteres

Friedman introduced the term bioisostere to relate the concept of isosteres to biological systems, in which he defined the term as "isosteres that exhibit a similar biological activity to the parent compound".[73] Therefore, according to this definition a compound can be isosteric but not necessarily bioisosteric, thus a bioisostere for one biological target may not be for an alternative target. The modern definition of a bioisostere has since expanded to "groups or molecules which have chemical and physical similarities producing broadly similar biological effects". [74]

With a definition of a bioisostere being this broad, introducing a bioisostere has the potential to alter the overall size, shape, electronic distribution, lipophilicity, polarity, pK_a and target binding for the better or worse.[61, 70, 74] Therefore, how beneficial a bioisosteric replacement is will depend on which properties are most important, how well the bioisostere can mimic these characteristics and how the molecule interacts with its biological target. In terms of the wider context, making modifications to the properties of a compound through bioisosteric replacement can be used as an additional tactic to improve the potency and selectivity; whilst reducing the metabolism and toxicity of lead compounds. To simplify the term bioisostere, Burger divided the groups or molecules that are used for bioisosteric replacement into the category of either classical or non-classical bioisosteres.[75]

1.2.2.1 Classical bioisosteres

A classical bioisostere can be divided into the five categories: monovalent, divalent, trivalent, tetravalent and ring equivalent.[75] For a bioisosteric substitution to be classified into of these categories, the substitution must follow the traditional isosteric replacement principles of (1) Grimm's Hydride Displacement Law or (2) Erlenmeyer's definition of an isostere.[72]

A common example of a monovalent bioisosteric replacement is the substitution of hydrogen for fluorine.[70, 75] While the van der Waal radius of fluorine is larger than hydrogen (F: 1.47 Å verses H:1.20 Å), fluorine substitution of hydrogen can often occur without imparting unfavourable steric interactions. However, there is a large difference in the electronegativity between fluorine and hydrogen (3.98 verses 2.20), which is reflected by a stronger C-F bond (105.4 kcal/mol verses 98.8 kcal/mol) and larger dipole moment (1.41μ verses -0.4 μ).[76] Therefore, bioisosteric replacement with fluorine can often be used to modulate properties such as metabolism, lipophilicity and conformation.[70, 76] The chemotherapy agent 5-fluorouracil is an excellent example of a monovalent bioisosteric replacement of hydrogen for fluorine (Scheme 5).[72, 77] The C-F bond in the active metabolite of 5-fluorouracil prevents the enzyme thymidylate synthases performing its normal function of methylating the active metabolite. A

consequence of this is the 5-fluorouracil active metabolite and the enzyme (thymidylate synthases) remain strongly bound, which effectively inhibits the enzyme. The downstream impact of this is a reduction in DNA synthesis, leading to cell death.

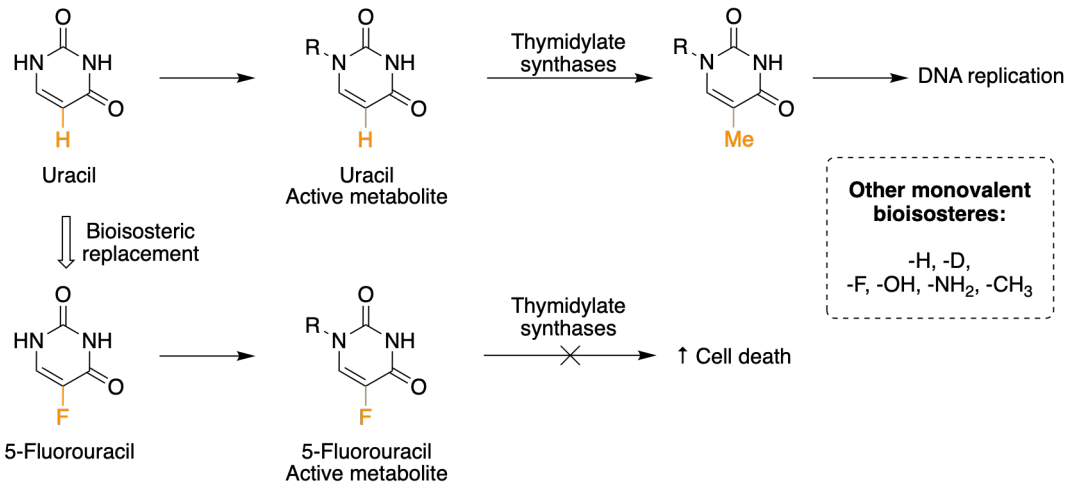

Scheme 5: Chemotherapy agent 5-fluorouracil - a monovalent classical bioisostere.

A divalent bioisostere includes substitution of an atom in a double bond (C=**C**, C=**N**, C=**O** and C=**S**) or the substitution of an atom or group involved in two single bonds (-**CH₂**-, -**NH**-, -**O**- and -**S**-).[75] An application of the latter is the antihypertensive drug Rilmenidine, in which bioisosteric replacement of C-**O**-C for C-**CH₂**-C reduced non-specific binding (receptor: α_2ARs), whilst maintaining a similar potency (receptor: I_1Rs) (Figure 5a).[78] Similar to a divalent bioisosteric replacement, a trivalent substitution can include a double bond (-**CH**= and -**N**=,) or three single bonds (**CH**R_3 and **N**R_3).[75] For instance, the bioisosteric replacement of a **CH** group in cholesterol for a **N** creates a compound that acts as a potent inhibitor to cholesterol biosynthesis (Figure 5b).[79] Finally, a tetravalent bioisostere can be defined as the substitution of an atom with four single bonds (**C**R_4, **N**$^+R_4$ and **Si**R_4).[75] A good example of a tetravalent bioisosteric substitution includes the replacement of a *tert*-butyl group for a trimethylsilyl group in Doramapimod, a phase II drug candidate for the treatment of Crohn's disease (Figure 5c). Barnes *et al* reported the silyl analogue had a comparable potency, with a slightly improved metabolic stability in human liver microsomes.[80]

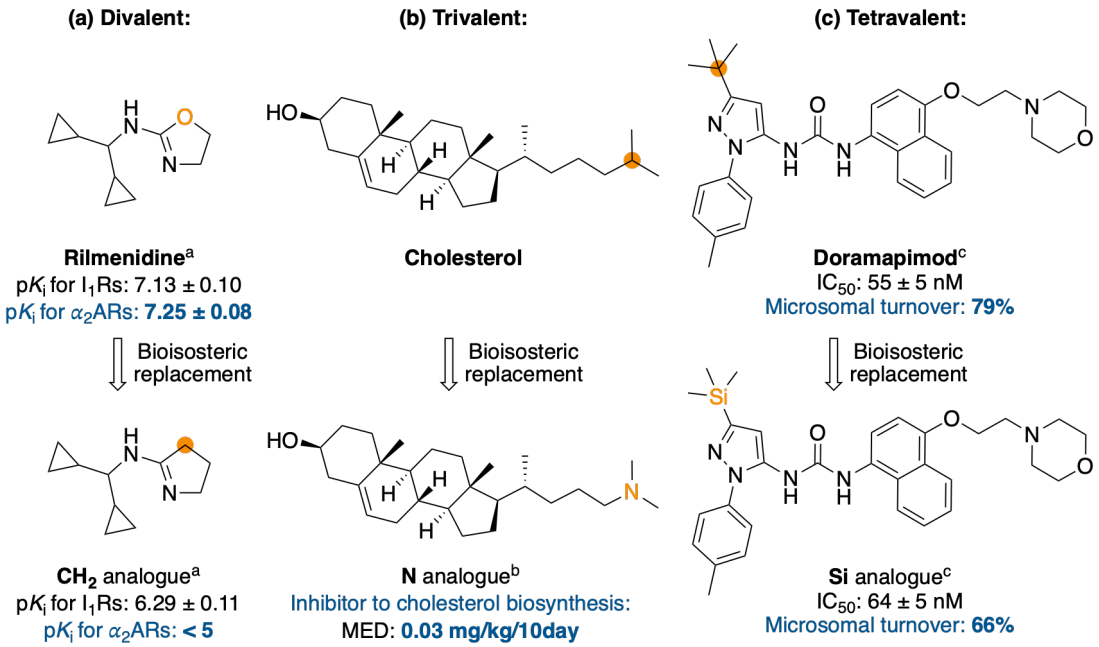

Figure 5: Examples of classical bioisosteres.

[a] pKi = -log(binding affinity to receptor), α_2ARs = receptor associated with side effects, I_1Rs = receptor associated with activity. [b] MED = minimal effective dose for a 10% reduction in serum cholesterol levels. [c] Human liver microsomes.

The final sub-class of classical bioisosteres are ring equivalents. The most common examples include the interchange between a phenyl and pyridine ring or a furan and thiophene.[75] Although, there are instances where classical bioisosteric substitutions fit into the sub-class of ring equivalents and another. The antihypertensive drug Rilmenidine discussed earlier is an example of this, in which the substitution of the oxazoline ring for a pyrroline ring can also be classified as a ring equivalent or a divalent classical bioisostere (Figure 5a).[78]

1.2.2.2 Benzene non-classical bioisosteres

A non-classical bioisostere includes any substitution that does not obey the principles of (1) Grimm's Hydride Displacement Law or (2) Erlenmeyer's definition of an isostere, whilst producing a similar biological effect.[72] Therefore, non-classical bioisosteres can be structurally distinct but must mimic or ideally improve the physicochemical properties of the parent compound.[75]

As previously mentioned, a benzene ring is the most frequently used ring scaffold in small drug molecules. [62, 63] The abundance of this functional group has been attributed to the ease at which benzene rings can be introduced synthetically, with a variety of functional groups and varying substitution pattern.[61] Unfortunately, benzene rings in drug candidates can lead to poor ADME profiles (e.g. metabolic instability) or pharmacokinetic properties (e.g. poor aqueous solubility).[61] This notion was supported by detailed analysis of 280 compounds in the GSK pipeline, which found on average the number of aromatic rings in the drug candidates decreased from pre-clinical studies to clinical trials.[81] One strategy to tackle this problem includes increasing the number of sp^3 hybridised carbon atoms and stereogenic centres in drug candidates, which will tune the physicochemical properties and allow more chemical space to be explored at a biological target.[65] Accordingly, there has been a growing interest around using sp^3 hybridised saturated scaffolds as a non-classical bioisosteres to benzene rings.[67, 69]

Scaffolds that are commonly evaluated in structure-activity relationship (SAR) studies currently, include the caged structures bicyclo[1.1.1]pentane (BCP), bicyclo[2.1.1]hexane (BCH), bicyclo[2.1.1]heptane (BCHep), bicyclo[2.2.2]octane (BCO) and pentacyclo[4.2.0.$0^{2,5}$.$0^{3,8}$.$0^{4,7}$]octane/cubane (CUB).[67-69] Each of these benzene bioisosteres have a rigid cage structure, which when functionalised leads to well-defined bond angles between substituents (Figure 6).[67, 69] The defined spatial arrangement between functional groups provides the basis to mimic the *para*-, *ortho*- and *meta*-substituted benzene ring patterns found in pharmaceutical drugs. Their success as a benzene bioisosteres is dependent on the role the benzene ring, whether that be to control the conformation (e.g. used as a rigid spacer) or as a pharmacophore (e.g. π-π stacking interaction with biological target).[61] In the circumstances the benzene ring acts as a 'spacer' unit, the dimensions of the bioisostere will influence how efficiently the pharmacophore regions can interact with the biological target. However, if the benzene ring is a pharmacophore, bioisosteric substitution could detrimentally affect the target binding interactions of the drug.

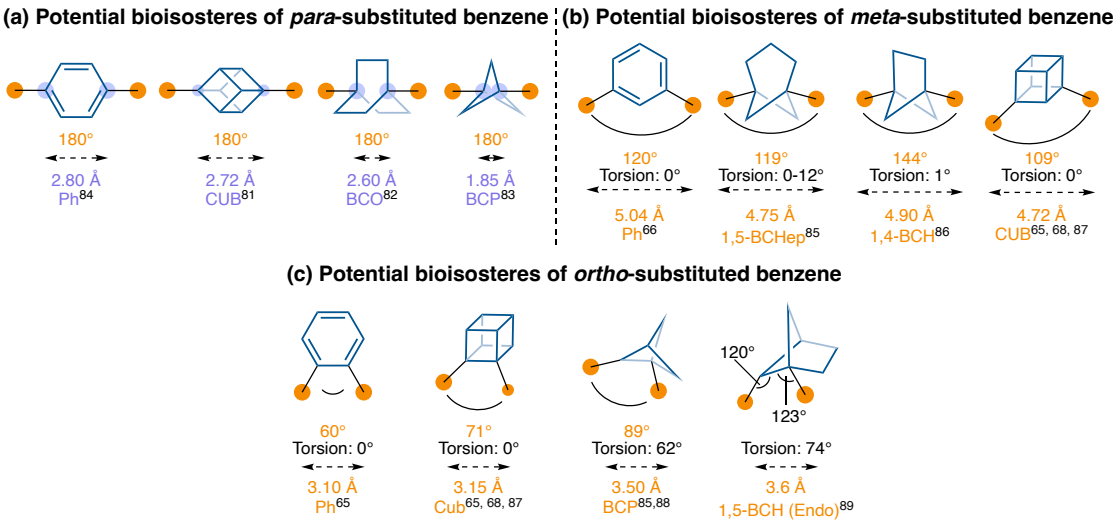

Figure 6: Reported dimensions of potential benzene bioisosteres[67] (a) *para*-substituted[82-85] (b) *meta*-substituted[66, 67, 69, 86-88] (c) *ortho*-substituted[66, 67, 69, 86, 88-90]

In general, bioisosteric replacement of benzene for any of the C(sp^3)-rich three-dimensional rigid cage scaffolds in Figure 6 could be utilised to improve the following properties:[67, 68] (1) aqueous solubility: replacement of the aromatic ring will remove strong π-π stacking interactions, which could reduce the lipophilicity of the overall structure. In addition, the three-dimensionality of these scaffolds will reduce the molecular planarity of the entire compound, which has been shown to increase aqueous solubility.[91] (2) metabolic stability: sp^3 hybridised rich scaffolds are usually more stable in CYP450 environments than benzene rings due to unusually strong C-H bonds, thus increasing metabolic stability.[61] (3) potency: these non-classical bioisosteres have access to greater chemical space due to their three-dimensional structure compared to benzene, which is planar, creating opportunities for novel target interactions.[65] As a result of these strained saturated scaffolds offering improved physicochemical properties over benzene; in the last decade SAR studies evaluating bioisosteric replacement have been on the rise.

1.2.2.2.1 Bicyclo[1.1.1]pentane (BCP):

The application of bicyclo[1.1.1]pentane (BCP) as a benzene bioisostere has been evaluated extensively, with numerous examples that have exhibited improved physicochemical properties (e.g. aqueous solubility, lipophilicity, metabolism and

potency) compared with their equivalent aromatic species.[67-69, 92] One successful example was reported by a team from Pfizer who found potency was retained when replacing the *para*-substituted fluorophenyl group in the γ-secretase inhibitor **1.5** with a 1,3-BCP scaffold (**1.5a**) (**1.5** IC_{50} = 0.225 nM compared to **1.5a** IC_{50} = 0.178 nM) (Table 6).[85] The work by the Pfizer team demonstrated that bioisosteric replacement can be valuable tool in SAR studies, as no reduction in potency of **1.5a** demonstrated that the fluorophenyl moiety in **1.5** was not involved in any critical enzyme inhibition interactions. Introduction of the BCP skeleton also increased the thermodynamic solubility by an order of magnitude at both pH 6.5 and 7.4, therefore improving the oral absorption of the drug (Table 6). This increase in aqueous solubility was attributed to the three-dimensional structure of BCP disrupting the planarity of the overall structure, thus obstructing intermolecular π-stacking interactions of the remaining aromatic ring. The outcomes of the solubility measurements are also consistent with the ELog*D* values, with the BCP analogue **1.5a** having a lower lipophilicity (**1.5** = 4.7 compared to **1.5a** = 3.8). Evaluation of the metabolic stability of both compounds revealed that the BCP analogue exhibited a greater resistance to metabolic turnover in human hepatocytes (apparent intrinsic clearance: **1.5** = 15 μL/min/10^6 cells compared to **1.5a** = < 3.8 μL/min/10^6 cells).

Table 6: BCP replacement of the *para*-substituted benzene in the γ-secretase inhibitors **1.5**.[85]

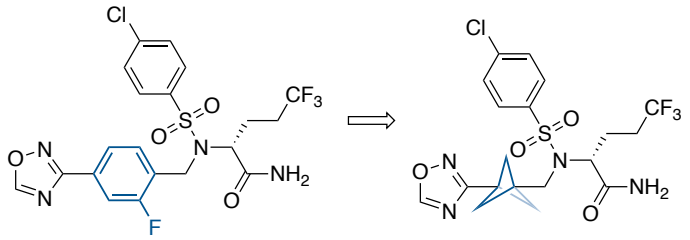

Avagacestat (1.5) γ-secretase inhibitor

1.5a

	1.5	**1.5a**
IC_{50} ($A\beta_{42}$, nM)	0.225	0.178
Thermodynamic solubility pH 6.5 (μM)	1.7	19.7
Thermodynamic solubility pH 7.4 (μM)	0.9	29.4
Elog*D*	4.7	3.8
Human hepatocytes CL_{int} (μL/min/10^6 cells)	15.0	< 3.8

Alongside BCP acting as a bioisostere for *para*-substituted benzene rings, 1,2-disubstituted bicyclo[1.1.1]pentanes can mimic *ortho*-substituted benzene rings.[68, 69, 93] Replacing the *ortho*-substituted benzene ring in the drug Telmisartan (**1.6**, angiotensin II receptor antagonist) with a 1,2-BCP scaffold gave the individual enantiomers **(+)-1.6a** and **(-)-1.6a** (separated by chiral HPLC), that had a potency and lipophilicity comparable to Telmisartan (Table 7).[94] Solubility of **(+)-1.6a** and **(-)-1.6a** at pH 2 was also comparable to Telmisartan, however, at pH 7 the solubility of both enantiomers was an order of magnitude greater compared to Telmisartan (**1.6** = 20 mg/mL, **(+)-1.6a** = 131 mg/mL and **(-)-1.6a** = 144 mg/mL).[94] The pH-independent solubility of the two BCP enantiomers could improve the compounds absorption throughout the gastrointestinal tract, addressing the solubility limitations that currently restricts Telmisartan's bioavailability.[95] The geometry of the three-dimensional BCP skeleton also had an impact on metabolic stability, with enantiomer **(+)-1.6a** being twice as resistant to metabolism compared to **(-)-1.6a**.[94] The authors do not comment on the difference in metabolic stability between the enantiomers, although enantioselective drug metabolism is commonly reported in the literature due to the intrinsic chirality of enzyme active sites.[96]

Table 7: BCP replacement of the *ortho*-substituted benzene in Telmisartan.[94]

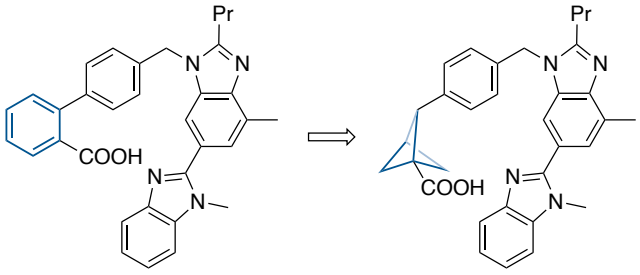

Telmisartan (1.6) **(±)-1.6a**

	1.6	**(+)-1.6a**	**(-)-1.6a**
IC_{50} (AT_1 antagonist, nM)	1.0	4.3	5.9
IC_{50} (AT_1 agonist, nM)	n.e	n.e	n.e
Solubility pH 2 (mg/mL)	152	146	160
Solubility pH 7 (mg/mL)	20	131	147
Log*D*	1.58	1.54	1.54
Human hepatocytes CL_{int} (µL/min/10^6 cells)	n.r	7.3	15.1

n.e = no significant effect; n.r = not reported

1.2.2.2.2 Bicyclo[2.1.1]hexane (BCH):

Bicyclo[2.1.1]hexanes have been validated as a suitable bioisostere for *ortho*- and *meta*-substituted benzene rings.[90, 97] The 1,5-bicyclo[2.1.1]hexane (1,5-BCH) scaffold that mimics the *ortho*-substituted benzene ring are chiral structures, therefore the diastereo- and enantioselectivity needs to be considered when constructing the 1,5-BCH scaffold.[90, 98-100] Recently, the Tortosa group synthesised several enantioenriched 1,5-BCH analogues of bioactive molecules, including the oncology drug Axitinib (**1.7**) that is approved for the treatment of advanced renal cell carcinoma.[98] The mechanism of action relies on inhibiting the phosphorylation of a tyrosine kinase receptor (VERGFR2), in which Axitinib (**1.7**) exhibited an IC_{50} value in the low nanomolar range (**1.7** IC_{50} = 5 nM) in this study (Table 8).[98]

Table 8: BCH replacement of the *ortho*-substituted benzene in Axitinib.[98]

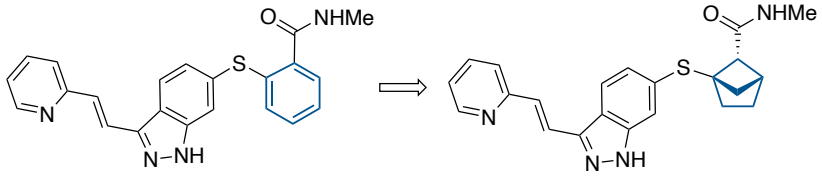

Axitinib
(1.7)
Treatment of renal cell carcinoma

(-)-1.7a

	1.7	**(+)-1.7a**	**(-)-1.7a**
IC_{50} (VEGFR2, nM)	5	15	9
EC_{50} (MB-231, μM)	1253	98	71
EC_{50} (HCT-116, μM)	505	64	45
EC_{50} (Mel-202, μM)	100	18	19

Both 1,5-BCH enantiomers were able to inhibit phosphorylation, with a slightly elevated IC_{50} value compared to Axitinib, but notably still in the low nanomolar range (IC_{50} = 15 and 9 nM for (+)-**1.7a** and (-)-**1.7a** respectively).[98] Enantiomer (-)-**1.7a** was 1.5x more active than (+)-**1.7a**, demonstrating the importance of enantioselective synthesis to maximise the biological activity of a drug.[98] In addition, both 1,5-BCH enantiomers and Axitinib were evaluated against three different human cancer cell lines (MB-231= breast cancer, HCT-116 = colon cancer and Mel-202 = eye cancer). Remarkably, for each cell line (+)-**1.7a** and (-)-**1.7a** cytotoxicity was much greater than Axitinib, with a 17-fold

increase in activity for (-)-**1.7a** compared with Axitinib for the MB-231 cell line (EC_{50} = 71 and 1253 μM for (-)-**1.7a** and Axitinib respectively).[98] Altogether, these results demonstrate the 1,5-BCH scaffold has a promising application as a bioisostere for *ortho*-substituted benzene rings.

1.2.2.2.3 Bicyclo[2.1.1]heptane (BCHep):

The exit vectors of the bridgehead substituents on the 1,3-disubstituted BCHep scaffold closely resemble those of a *meta*-substituted benzene ring (Figure 6b). This encouraged the Anderson group to prepare a 1,3-BCHep analogue of the skin cancer drug Sonidegib (**1.8**), to access 1,3-BCHep viability as a novel bioisostere (Table 9).[86] Introduction of the 1,3-BCHep scaffold increased the membrane permeability (AB/BA: **1.8** = 0.6/0.7 and **1.8a** = 3.7/2.7), in which the intestinal absorption of **1.8a** (AB = 3.7) was greater than the efflux value (BA = 2.7) (Table 9).

Table 9: BCH replacement of the aryl ring in Sonidegib.[86]

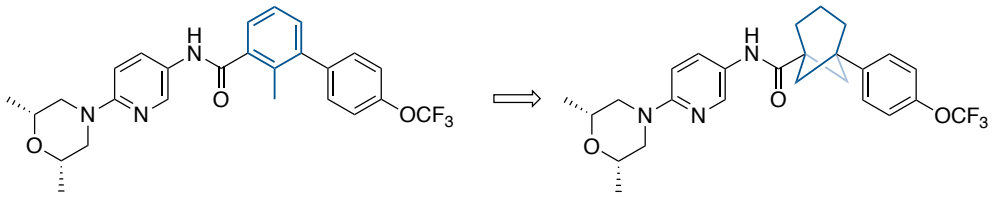

Sonidegib (1.8) Treatment of skin cancer

1.8a

	1.8	**1.8a**
Membrane permeability: Caco-2, AB/BA P_{app} (10^{-6} cm s-1)	0.6/0.7	3.7/2.7
Membrane permeability: Efflux ratio	1.1	0.7
Human hepatocytes CL_{int} (μL/min/mg)	20	18
IC_{50} (CYP3A4, μM)	>50	>50
IC_{50} (CYP2C19, μM)	>50	13.9
Kinetic solubility pH 7.4 (μM)	<1.6	<1.6
clog*P*	6.8	6.2

Meanwhile aqueous solubility, lipophilicity and metabolic stability of **1.8a** were all comparable to Sonidegib. Notably, there was no significant difference in the inhibition of CYP3A4 (IC_{50} = >50 μM for **1.8a** and Sonidegib), which is the enzyme responsible for the majority of drug metabolism.[101] Happily, the inhibition of enzyme CYP2C19 by **1.8a**

was 3-fold higher than Sonidegib in the low micro-molar range (IC_{50} = 13.9 and >50 μM for **1.8a** and Sonidegib respectively), demonstrating a difference in selectivity between the two enzymes. Overall, the SAR data related to the 1,3-BCHep analogue of Sonidegib are promising and validates its role as a non-classical isostere for *meta*-substituted benzene rings. However, as the study does not compare the antitumor activities of **1.8a** verses Sonidegib, its application in medicinal chemistry as a bioisostere is yet to be determined.

1.2.2.2.4 Bicyclo[2.2.2]octane (BCO):

One of the most widely used bicyclic bioisosteres for *para*-substituted arenes includes 1,4-bicyclo[2.2.2]octane (1,4-BCO), with the substituents located on the bridgehead positions. An extensive structure-activity relationship study on a class of MDM2 inhibitors, which regulate tumour suppression in almost all cancers, examined if replacing the *para*-substituted aryl ring in their lead compound **1.9** with 1,4-BCO (**1.9a**) would improve the oral pharmacokinetic properties (Table 10).[102] The results of the *in vitro* studies were promising, with **1.9a** exhibiting an improved binding affinity for MDM2 (IC_{50} = 4.4 and 3.7 nM for **1.9** and **1.9a** respectively) and a comparable potency for inhibiting cell growth in the SJSA-1 cell line (IC_{50} = 100 and 89 nM for **1.9** and **1.9a** respectively), in comparison to the aromatic led compound **1.9**. When examining the oral pharmacokinetic properties of **1.9** and **1.9a** in rats, the plasma concentration of **1.9a** was multiple orders of magnitude higher based on the C_{max} (1553 verses 8234 ng/mL) and AUC values (6799 and 73603 h·ng/mL) (Table 10). Despite the improved oral pharmacokinetic properties, the *in vivo* studies revealed that the 1,4-BCO analogue was unable to reduce tumour volume. It was hypothesised the poor antitumoral activity in mice was due to poor penetration of **1.9a** into the tumour tissue, which was resolved by ethylating the nitrogen in the pyrrolidine core (**1.9b**). The pharmacodynamic experiments of **1.9b** revealed that an oral dose (100 mg/kg) taken daily for 14 days resulted in full tumour regression for at least 30 days. As a result of great oral pharmacokinetic and pharmacodynamic properties, compound **1.9b** also known as Alrizomadlin, has now advanced to stage I and II clinical trials for the treatment of various human cancers.[103]

Table 10: BCO replacement of the *para*-substituted benzene.[102]

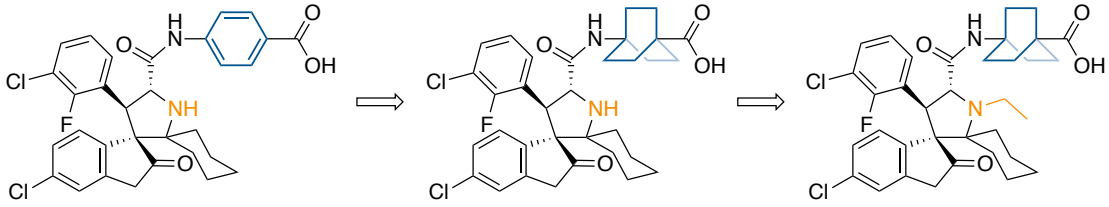

1.9 | **1.9a** | **Alrizomadlin (1.9b)** Stage I and II clinical trails for various human cancers

	1.9	1.9a	1.9b
IC_{50} (MDM2, nM)	4.4	3.7	3.8
K_i (MDM2, nM)	<1	<1	<1
IC_{50} (SJSA-1, nM)	100	89	60
po C_{max} (ng/mL)	1553	8234	5453
po AUC (h·ng/mL)	6,799	73,603	39,083
iv AUC (h·ng/mL)	8,633	82,241	38,265
Bioavailability / *F* (%)[a]	31.5	35	40.3
Antitumour efficacy (% regression)	86	0	100

[a] *po dose (mg/kg) for each compound = 25; iv dose (mg/kg) for each compound = 10. Po: oral administration; iv does: intravenous administration; C_{Max}: maximum plasma concentration; AUC: area under the plasma drug concentration-time curve.*

1.2.2.2.4 Pentacyclo[4.2.0.0 ^{2,5}.0^{3,8} .0^{4,7}]octane (Cubane):

Cubane is a rigid, highly strained cage structure that was first synthesised by Eaton and Cole.[104] Since the initial synthesis, Eaton proposed that cubane could have an application in medicinal chemistry as a benzene bioisostere, based on the diameter of the cubane scaffold (2.72 Å) closely resembling the distance between the *para*-substituted carbons in a benzene ring (2.80 Å).[82, 105] Each carbon in the cubane scaffold is a bridgehead carbon, therefore the substituent exit vectors are relatively fixed. Fortunately, the exit vectors for 1,2 and 1,3-disubstituted cubanes are similar to *ortho* and *meta*-substituted benzenes respectively, with 1,4-disubstituted cubane exit vectors matching *para*-substituted benzene (Figure 6). Since Eaton's initial hypothesis the synthesis of pharmaceutical drugs incorporating the cubane framework are mostly

mimicking terminal or *para*-substituted benzene rings, with limited reports of alternative substitution patterns.[67, 90]

The mono-substituted cubane **1.10a** was synthesised to evaluate its application as a non-classical bioisostere to the terminal aryl ring in the chemotherapy drug Vorinostat (**1.10**), which is a deacetylase inhibitor approved for treatment of cutaneous T-cell lymphoma (Table 11).[106] Both compounds inhibited the growth of two tumour cell lines, with similar IC_{50} values between the range of 0.03-0.05 ug/mL. Furthermore, when conducting *in vivo* studies on mice, 63 % tumour regression was reported for **1.10** and **1.10a**. Overall, the authors demonstrated that cubane could mimic the geometry of the benzene ring whilst retaining biological activity, as the potency of the cubane analogue **1.10a** was comparable to Vorinostat for two cancer cell lines.[106]

Table 11: Cubane replacement of the terminal benzene ring in the chemotherapy drug Vorinostat.[106]

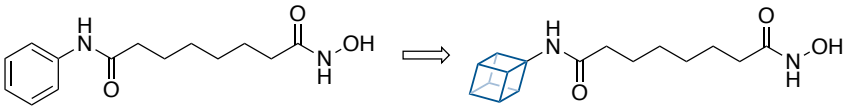

Vorinostat
(1.10)
Treatment for T-cell lymphoma

1.10a

	1.10	**1.10a**
IC_{50} (MM96L, μg/mL)	0.03	0.05
IC_{50} (MCF7, μg/mL)	0.03	0.05
LogP_{HPLC}	0.99	1.52
Antitumour efficacy (% regression)	63	63

The lipophilicity of the cubane analogue **1.10a** was slightly higher (logP_{HPLC} = 0.99 and 1.52 for **1.10** and **1.10a** respectively) but was still considered to be in a good range for oral administration.[107] Notably, in this study the Log*P* of six other cubane analogues of biologically active drugs were also evaluated.[106] In the instances where cubane was replacing a terminal benzene ring the lipophilicity increased. Whereas, for the instances cubane was acting as a *para*-linker the lipophilicity generally remained the same or decreased.[106] This connection between the extent of cubane substitution and lipophilicity has also been reported in other SAR studies examining cubane as a

benzene bioisostere.[108] The insecticide drug Diflubenzuron (**1.11**) is an example of the latter, in which replacement of the *para*-substituted benzene ring for cubane marginally decreased the lipophilicity (LogP_{HPLC} = 3.33 and 3.13 for **1.11** and **1.11a** respectively) (Table 12).[106] Potency of **1.11** and **1.11a** was evaluated by measuring the mortality rate of larvae in *Tribolium castaneum* beetles. At concentrations as low at 18 μmol, the cubane derivative **1.11a** was nearly twice as effective as the parent benzene compound **1.11**.

Table 12: Cubane replacement of the *para*-substituted benzene ring in the insecticide drug Diflubenzuron.[106]

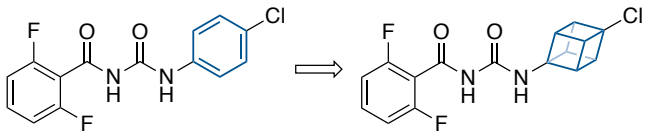

Diflubenzuron (**1.11**) Insecticide

1.11a

	1.11	**1.11a**
Larvae mortality at 18 μmol (%)	50	90
LogP_{HPLC}	3.33	3.13

The enhanced larvae mortality for **1.11a** was attributed to the cubane scaffold being less susceptible to metabolic oxidation compared to the benzene ring by CYP450 enzymes, which led to a higher bioavailability.[106, 108, 109] This hypothesis is likely based on differing pathways that exist for CYP450-mediated oxidation of a saturated system (cubane) compared to an aromatic ring (benzene).[61] For instance, CYP450-mediated oxidation of mono-substituted benzene (**1.12**) usually occurs readily and typically proceeds via the formation of an epoxide (**1.12a**), followed by rearrangement to a phenol (**1.12b**, Scheme 6a).[61] In contrast, a radical rebound mechanism has been proposed for CYP450-mediated oxidation of saturated systems (**1.13**), in which a hydrogen is first abstracted from a C-H bond generating a carbon-centred radical (**1.13a**), that then reacts with the Fe-OH intermediate to afford a hydrolysed metabolite (**1.13b**, Scheme 6b).[61] However, for cubane scaffolds the abstraction of a hydrogen atom for the radical rebound mechanism is likely not facile, as the C-H bonds in cubane are strong with a bond dissociation energy of 104 kcal/mol.[109] The strength of the C-H

bonds in cubane arises from the carbon atoms having 32 % s-character (based on $^{1}J_{CH}$ coupling constant = 155 Hz), resulting in the C-H bonds in cubane being closer to sp^2 hybridised than sp^3 hybridised.[110] To put into perceptive the strength of the tertiary centred C-H bonds in cubane, the bond dissociation energy for the tertiary centred C-H bond in isobutane has a much lower value of 93 kcal/mol.[109] In addition, cubane does not occur in nature, therefore specific biological processes have not evolved to metabolise this scaffold. The theory is that these two factors could each contribute to cubane generally being perceived as more metabolically stable to CYP450 than benzene.

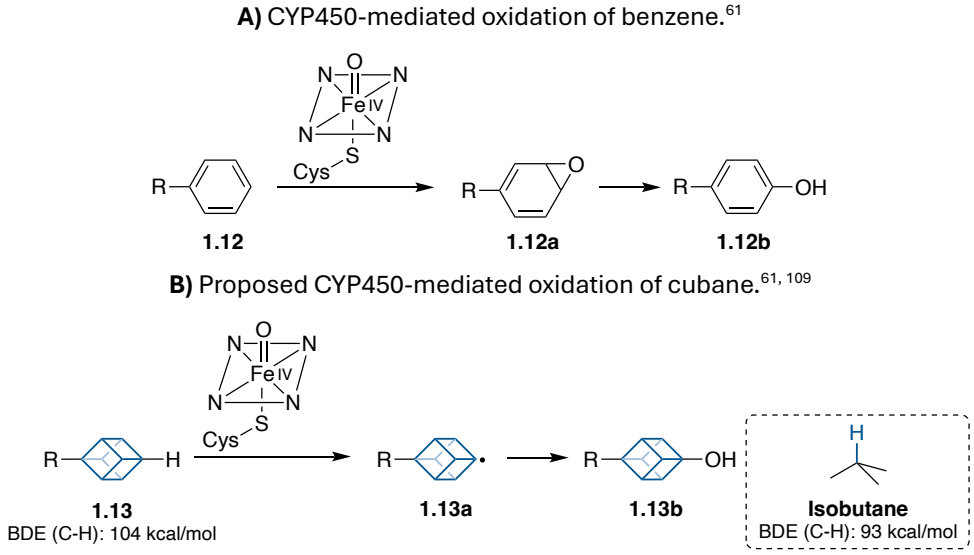

Scheme 6: CYP450-mediated oxidation.

Evidence that supports cubane as a poor substrate for CYP-mediated oxidation is provided by Coon *et al*.[111] In this study methylcubane was subjected to several CYP-mediated oxidations affording a mixture of hydroxylated products, with preferential hydroxylation of the methyl group over the cubane core being reported in each experiment (Table 13). In addition, Todd and co-workers recently reported a late-stage biofunctionalisation of **1.15** to **1.15a** and **1.15b** via an enzyme mediated oxidation (dog liver microsomes), demonstrating that cubane is still susceptible to CYP-mediated oxidation (Scheme 7).[112] Unfortunately, the yields for these two late-stage biofunctionalisations were not reported, making it difficult to comment on how reactive the cubane core is to these metabolic enzymes and which position on the cubane core

was more susceptible to oxidation under the reactions in scheme 7. Overall, these two studies on CYP-mediated oxidation of cubane compounds revealed that oxidation can occur, although the relative rate of oxidation compared to a benzene ring is still unknown.

Table 13: Products from enzymatic oxidation of methylcubanes.[111]

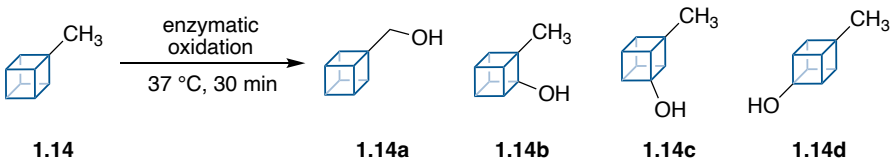

1.14 **1.14a** **1.14b** **1.14c** **1.14d**

	Yield[a] / %			
	1.14a	**1.14b**	**1.14c**	**1.14d**
Rat CYP2B1	62	12	19	7
Rat CYP2B4	88	4	1	7
Rat CYP2E1	55	13	16	10

[a] *The percentage yields represent product distribution not isolated yields. Overall yield was not reported.*

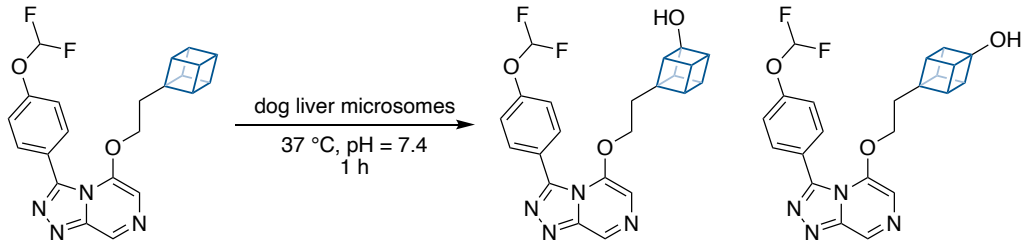

1.15 **1.15a** **1.15b**

Scheme 7: Late-stage biofunctionalisation of cubane **1.15** to afford cubanols **1.15a** and **1.15b**.[112]

Recently a synthetic strategy towards 1,3-disubstituted cubanes was reported, which was inspired by the earlier work of the Pettit group.[88, 113] To demonstrate the medicinal application of 1,3-disubstituted cubane as potential new bioisostere for *meta*-substituted benzenes, a cubane analogue (**1.16a**) of the cystic fibrosis drug Lumacaftor **1.16** was prepared (Table 14). Compound **1.16a** remained active, although an order of magnitude less active than Lumacaftor (RC_{50} = 0.15 and 2.1 μM for **1.16** and **1.16a** respectively). The reduction in potency of the **1.16a** could be attributed to the structural

replacement being proximal to carboxylic acid binding moiety. In this interaction the carboxylic acid forms a salt bridge to the CFTR protein, thus replacement of the aromatic carboxylic acid with a tertiary aliphatic carboxylic acid is expected to increase the p*K*a value, which would weaken this interaction.[114] Despite the two compounds having a comparable lipophilicity and surface area, **1.16a** was significantly more soluble at pH 2 (1 and 155 mg/mL for **1.16** and **1.16a** respectively) with a similar solubility at pH 7. In addition, the compound **1.16a** was found to have an improved metabolic stability based on an *in vitro* study measuring the intrinsic clearance rate of the two compounds (CL_{int} = 11.96 and 6.98 μL/min/10^6 cells for **1.16** and **1.16a** respectively).

Table 14: Cubane replacement of the *meta*-substituted benzene ring in the cystic fibrosis drug Lumacaftor.[88]

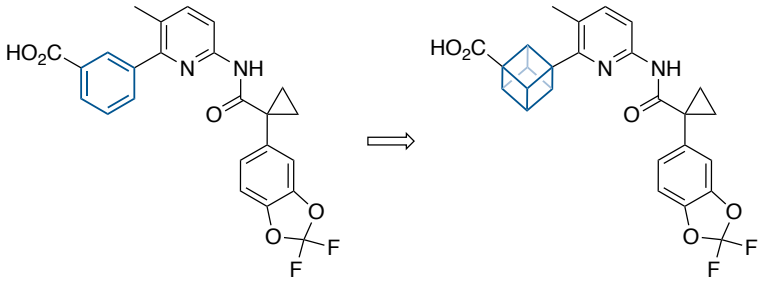

Lumacaftor (**1.16**) Treatment of cystic fibrosis

1.16a

	1.16	**1.16a**
RC_{50} (CFTR, μmol)	0.15	2.1
log*D*	1.99	2.03
EPSA	113	101
Solubility pH 7 (mg/mL)	139	171
Solubility pH 2 (mg/mL)	1	155
Human CL_{int} (μL/min/10^6 cells)	11.96	6.98

RC_{50} = half-maximal rescue concentration; EPSA = experimental polar surface area

To the best of our knowledge, no SAR studies have been performed on biologically active molecules that incorporate the 1,2-disubstituted cubane scaffold. Therefore, the application of cubane as a bioisostere for *ortho*-substituted benzene rings are still unknown. Despite well-established synthetic routes to synthesise various substitutions

patterns on the cubane framework, in general the number of SAR studies evaluating cubanes' suitability as a non-classical benzene bioisostere are still limited, especially compared to bicyclo[1.1.1]pentane and bicyclo[2.2.2]octane. It is likely this could be attributed to the cost of cubane scaffolds, which are generally far more expensive than bicyclo[1.1.1]pentanes and bicyclo[2.2.2]octanes. Although, the application of cubanes in medicinal chemistry is growing, with the number of patents that include cubane analogues of biologically active compounds on the rise.[67]

1.3 Benzene bioisosteric replacement in (*Z*)-tamoxifen

Individuals with estrogen-receptor-positive breast cancer that do not respond to (*Z*)-tamoxifen (**1.1**) therapy typically develop tumours that become resistant to this treatment, widely referred as acquired resistance.[29] It has been proposed that variations in the polymorphism of metabolic CYP450 enzymes in different individuals may play a role in acquired resistance, particularly in individuals with low or absent CYP2D6 activity and over overexpression of CYP1B1.[43, 44, 47, 115]

The role of CYP2D6 is to catalyse the hydroxylation of (*Z*)-tamoxifen (**1.1**) to 4-hydroxytamoxifen (**1.1a**) and *N*-desmethyltamoxifen (**1.1b**) to endoxifen (**1.1c**), which is critical as both **1.1a** and **1.1c** are the most potent antiestrogenic metabolites of (*Z*)-tamoxifen (Scheme 8).[24, 25] However, the first problem with CYP2D6-mediated oxidation of aromatic rings is its lack of selectivity, resulting in the formation of the undesired hydroxylated metabolites **1.1d-f,** which reduces the overall effectiveness of tamoxifen treatment (Scheme 8).[53] The second issue is the activated hydroxylated metabolites **1.1a**, **1.1c**, **1.1d** and **1f** can undergo CYP1B1-mediated isomerisation to their respective *E*-geometric isomers, which are either weak antioestrogen or inactive. [43, 44, 53] This is problematic as it has been reported that patients with acquired tamoxifen resistance have increased ratios of (*E*)-4-hydroxytamoxifen (**1.1a'**) compared to (*Z*)-4-hydroxytamoxifen (**1.1a**). [42, 47, 51, 52]

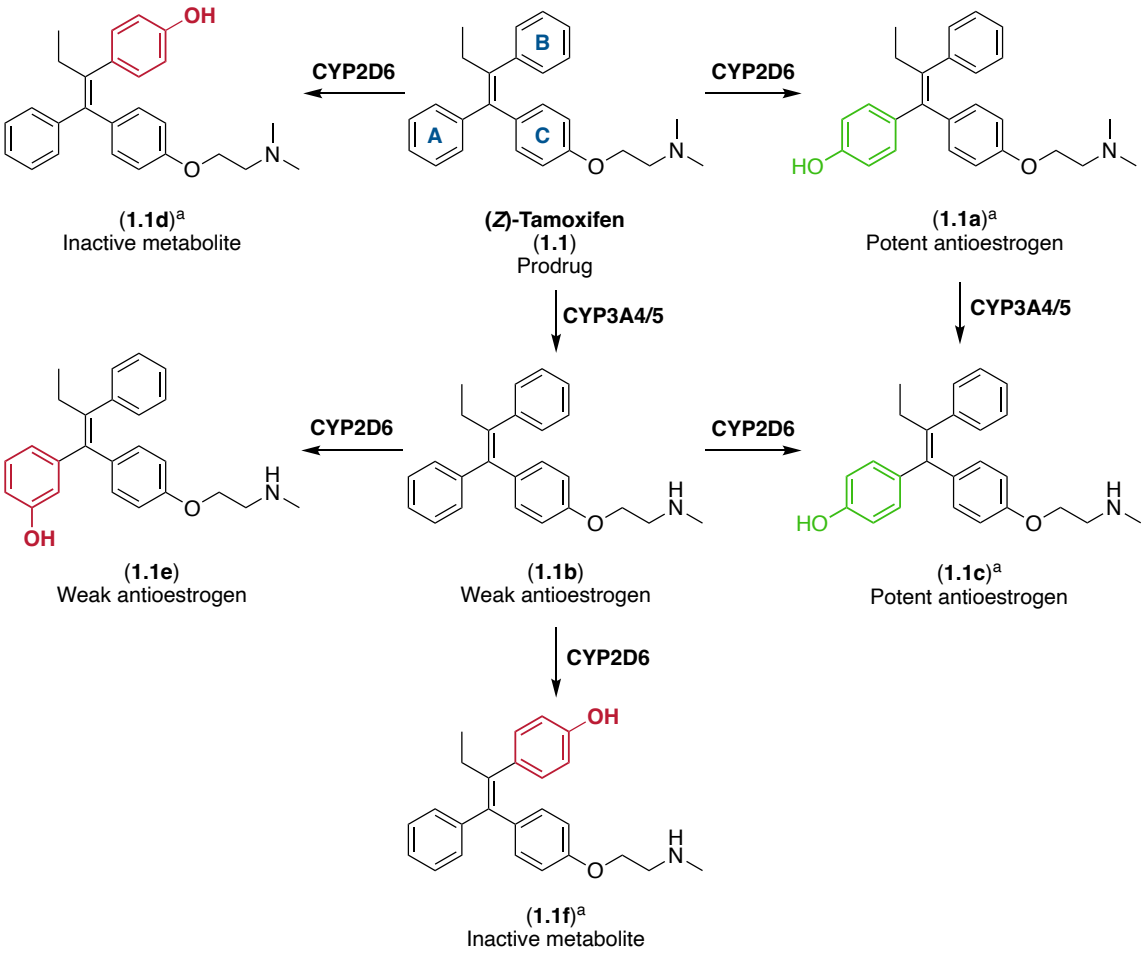

Scheme 8: CYP2D6-mediated hydroxylation towards therapeutic metabolites and non-therapeutic metabolites.[49, 53]

[a] *Susceptible to CYP1B1-mediated isomerisation to respective E-geometric isomer.*

We propose formation of non-therapeutic metabolites by CYP2D6-mediated hydroxylation and subsequently CYP1B1-mediated isomerisation of the hydroxylated metabolites could be reduced by replacing a benzene ring in (*Z*)-tamoxifen for a sp^3-rich bioisostere, which are scaffolds that can improve the metabolic stability of compounds. To explore if this approach can reduce acquired tamoxifen resistance, we plan to initially consider cubane as a suitable sp^3-rich bioisostere to benzene (Scheme 9).

Scheme 9: (*Z*)-Tamoxifen bioisosteric replacement with cubane.

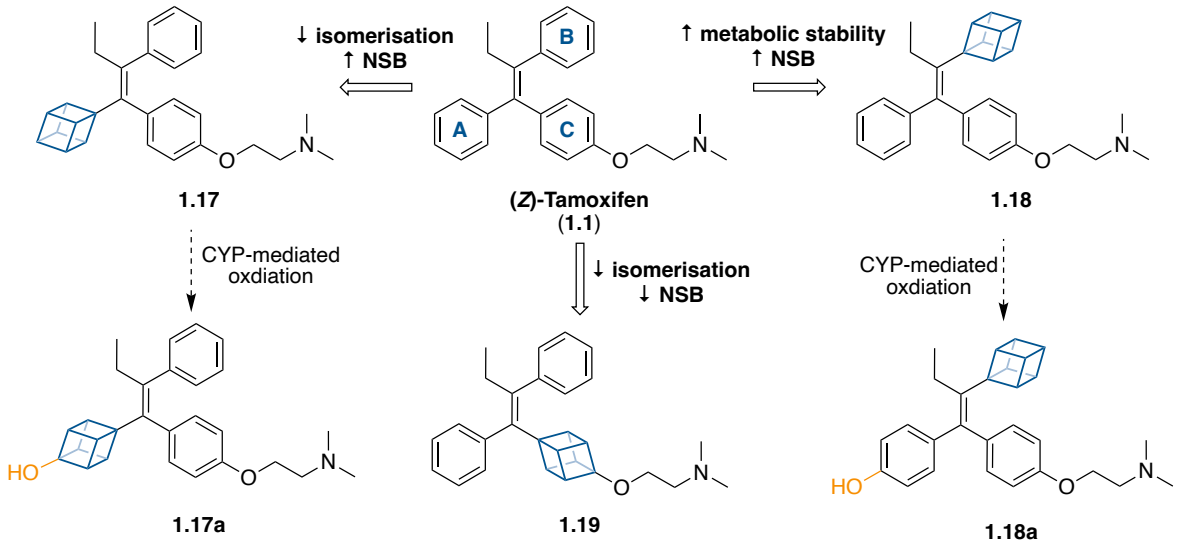

(*Z*)-Tamoxifen (**1.1**) is a prodrug that has three aromatic rings that could each be replaced with a cubane scaffold (Scheme 9). *In vivo* (*Z*)-Tamoxifen is metabolised into the two potent antioestrogens **1.1a** and **1.1c** (Scheme 8), both with a phenol group on benzene ring A that has proven to play an important role for binding in the ER (Figure 3a).[39, 40] Therefore, we can envision for a bioisosteric replacement at this position to be successful CYP450-mediated oxidation of the cubane core must occur. If **1.17a** can be formed and is stable *in vivo*, a cubane scaffold at this position may be beneficial to reduce isomerisation, as the cubane core would provide little stabilisation to the proposed cationic intermediate. Alternatively, if CYP-mediated oxidation on the cubane core is poor then bioisosteric replacement of aromatic ring B would be favoured as the number of non-therapeutic metabolites would decrease. Finally, aromatic ring C is not metabolically modified in any of the major non-therapeutic metabolites of (*Z*)-tamoxifen, therefore we suspect the metabolic stability will largely be unaffected when introducing a cubane scaffold in this position. However, based on studies by Valliant *et al* who observed restricted isomerisation of a carborane analogue of (*Z*)-Tamoxifen,[58] which was on aromatic C, cubane may also reduce isomerisation by having differing steric and electronic properties to the parent compound.

In addition to modulating the metabolic stability of (*Z*)-tamoxifen, bioisosteric replacement of a benzene ring with cubane may improve other pharmacokinetic

properties, such as lipophilicity and non-specific binding.[106, 116] The latter is of particularly relevant given (*Z*)-tamoxifen has a high binding affinity to serum albumin (98 %).[21] Overall, each mono-substituted cubane analogues of (*Z*)-tamoxifen has the potential to either reduce the formation of non-therapeutic metabolites by CYP2D6-mediated hydroxylation or decrease CYP1B1-mediated isomerisation, which has been identified as one mechanism contributing to tamoxifen acquired resistance.

1.4 Aim of the project

This work aims to develop a protocol to synthesise cubane analogues of the breast cancer drug (*Z*)-tamoxifen. If successful, we will begin to assess whether cubanes bioisosteric replacement for arenes in (*Z*)-Tamoxifen can improve the metabolic profile of the drug, towards the broader application of reducing acquired tamoxifen resistance. The project also aims to address a major limitation more generally associated with using cubane as a benzene bioisostere, which is the lack of general synthetic methods reported for functionalisation of cubane. This work will examine various multistep synthetic routes for synthesising cubane analogues of (*Z*)-tamoxifen, with the aim of expanding current protocols for cubane functionalisation.

To reach this goal, we will develop a protocol to synthesise unsymmetrical cubane containing tetrasubstituted alkenes, starting with the commercially available 4-methoxycarbonylcubanecarboxylic acid (Chapter 2). In this chapter we will also begin to assess how bioisosteric replacement of an arene in tamoxifen for cubane affects the drug's pharmacokinetic properties. In order to replace the *para*-substituted phenyl ring bearing a (dimethylamino)ethoxy side chain in tamoxifen for cubane, we anticipate that ethoxy side chain could be introduced via a cubanol intermediate. The synthesis towards cubanol begins with exploring the Baeyer-Villiger oxidation of cubyl ketones and investigating how steric and electronic factors influence the migratory aptitude (Chapter 3). Next, we will develop a general method to convert the cubyl ester products from the Baeyer-Villiger oxidation studies, where cubane migrated, to synthesise cubanols (Chapter 4). To test the utility of the approach we plan to synthesise a cubane analogue of the phenol containing natural product resveratrol (Chapter 4).

Chapter 2 Synthesis of cubyl-tamoxifen

2.1 Introduction

2.1.1 Routes towards (*Z*)-tamoxifen

(*Z*)-Tamoxifen (**1.1**) is marketed for the treatment of oestrogen-receptor-positive breast cancer and the prevention of breast cancer in high-risk individuals.[17] Stereoselective synthesis of tamoxifen is critical as the two geometric isomers have opposing effects on breast tissue, with (*Z*)-tamoxifen's active metabolites acting as potent antioestrogens whilst the metabolites of (*E*)-tamoxifen are weak oestrogens.[3, 42, 47] In the literature there are a variety of synthetic routes towards the preparation of (Z)-tamoxifen, although the vast majority are non-stereoselective and rely on purification to separate (*Z*)-tamoxifen from the unwanted (*E*)-tamoxifen.[117, 118]

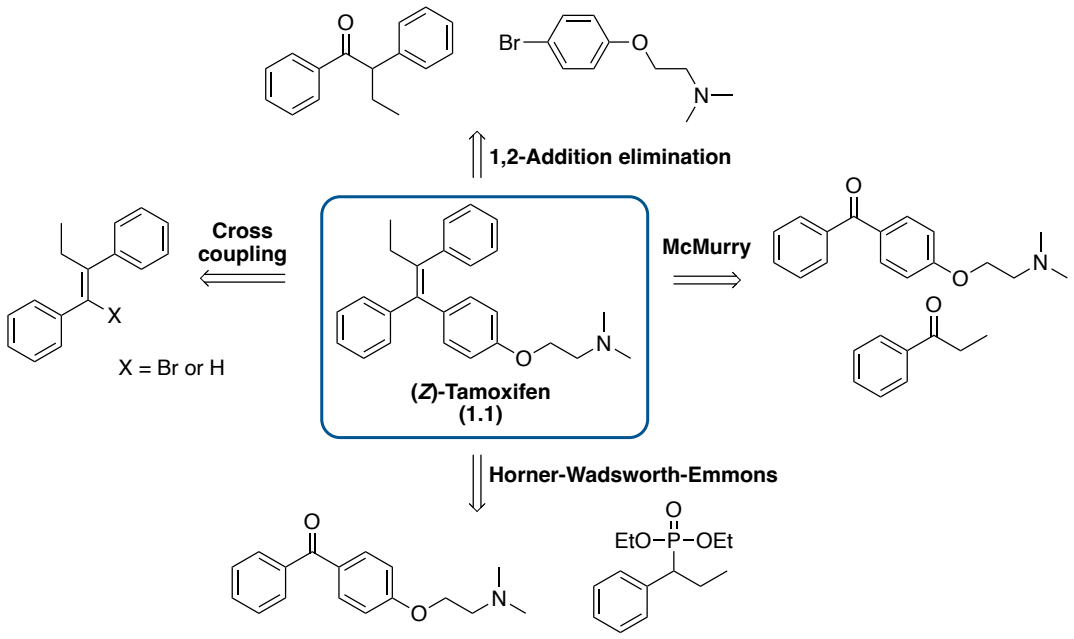

Figure 7: Common literature routes towards (*Z*)-tamoxifen.

One established synthetic strategy for the preparation of tamoxifen includes the McMurry reaction, in which two un-symmetrical ketones are reductively coupled (Figure 7).[119] Additionally, the 1,2-addition of an aryl Grignard or aryl organolithium to a ketone yields a tertiary alcohol, which can subsequently undergo acidic dehydration to afford

the olefin core of tamoxifen.[120-122] Other synthetic procedures involve transition metal catalysed cross-couplings, such as a Suzuki-Miyaura or the Heck coupling.[123, 124] An alternative, though less widely reported methodology, includes the Horner-Wadsworth-Emmons reaction between a phosphonate and a ketone.[125]

2.1.2 Routes towards alkenylcubanes

To the best of our knowledge there are no examples of all-carbon tetra-substituted olefins that incorporate cubane as a substituent, with only limited literature examples of tri- and di-substituted olefins that incorporate cubane as a substituent (Scheme 10-11). Notably, each of the cubane olefins were prepared by either a Wittig or Horner-Wadsworth-Emmons reaction using a cubyl aldehyde as the precursor (Scheme 10), with only one patent reporting a Wittig reaction with a cubyl ketone (Scheme 11).[108, 126-130]

The first example of an alkenylcubane was the synthesis of the vinylcubane **2.3a** by Carroll *et al* via a Wittig reaction (Scheme 10a).[126] The vinylcubane was prepared by treating methyltriphenylphosphonium bromide (**2.2a**) with *n*-BuLi in THF which afforded a ylide, followed by the addition of the cubyl aldehyde **2.1a** providing **2.3a** in 88 % yield. Similarly, the Williams group performed a Wittig reaction using cubyl aldehyde **2.1b** with two different phosphonium ylides (**2.2b** and **2.2c**).[108, 127] Treatment of cubyl aldehyde **2.1b** (1 eq) with the phosphonium ylide **2.2b** (2 eq) in toluene at reflux for an undisclosed time gave the olefin (*E*)-**2.3b** in 60 % yield (Scheme 10b).[108] In contrast, the Wittig reaction between **2.1b** (1 eq) and the phosphonium ylide **2.2c** (1.5 eq) at a lower temperature of 60 °C for 6 hours gave the cyclooctatetraene **2.4** in 52 %.[127] These two reactions by the Williams group suggest that leaving the reaction at elevated temperatures likely promotes cubane rearrangement. However, the substituents of the olefins could also have an influence on the stability of the cubane scaffold. Overall, these two factors could be contributing to why there are limited examples of alkenylcubane species reported in the literature. Switching the solvent from toluene to DCM and performing the reaction at a lower temperature of 40 °C allowed Willams and co-workers to isolate the olefin (*E*)-**2.3c** in 68 % yield.[127] The stereochemistry of **2.3b** and **2.3c** was established using ^{1}H NMR coupling constants of the vinyl protons (**2.3b**:

$^3J_{HH}$ = 15.5 Hz; **2.3c**: $^3J_{HH}$ = 16.0 Hz) that are indicative of the *E*-geometric isomer and consistent with stereoselectivity of Wittig reactions using stabilised ylides.[108, 127, 131]

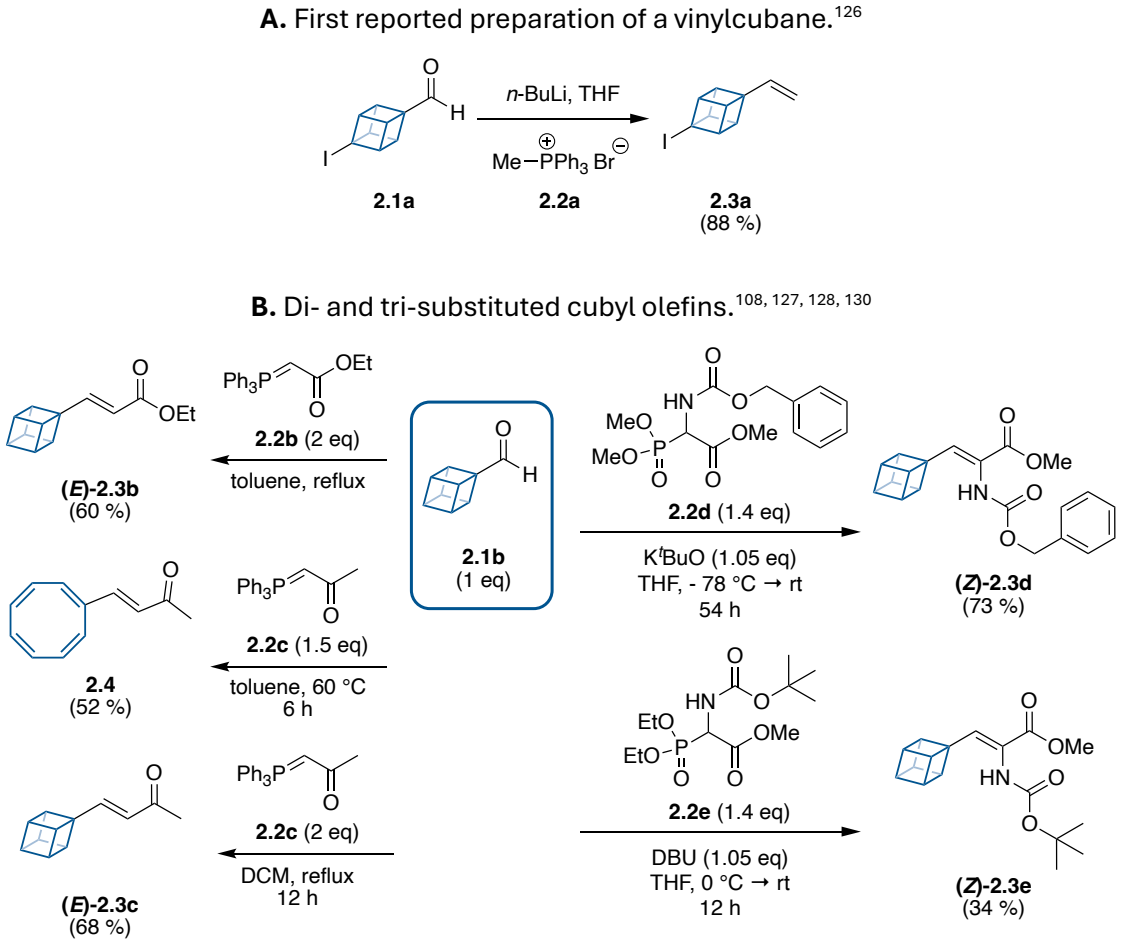

Scheme 10: Literature examples of Wittig and Horner-Wadsworth-Emmons reactions with cubyl aldehydes.

Churches' and co-workers were the first to prepare a tri-substituted olefin that incorporated cubane as a substituent (Scheme 10b).[128] The olefination proceeded via a Horner-Wadsworth-Emmons reaction beginning with deprotonation of the CBz-protected phosphonate **2.2d** (1.4 eq) in DCM as - 78 °C using ^{t}BuOK (1.05 eq). Subsequent addition of the cubyl aldehyde **2.1b** (1 eq) and warming the reaction mixture to room temperature afforded (*Z*)-**2.3d** in a yield of 73 %. ^{1}H and ^{13}C NMR analysis of the crude and purified product indicated that only one geometric isomer was formed, with **2.3d** confirmed to be the *Z*-geometry from X-ray crystallography studies. Building on the work by Churches' and co-workers, Wlochal *et al* adapted Churches

Horner-Wadsworth-Emmons conditions to prepare the tri-substituted olefin (*Z*)-**2.3e** as an intermediate towards a cubane analogue of the amino acid alanine (Scheme 10b).[130] In this work, the Boc-protected phosphonate **2.2e** (1.1 eq) was used over the CBz-protected phosphonate **2.2d**, DBU (1.05 eq) was chosen as the base and formation of ylide was performed at 0 °C rather than - 78 °C.[128, 130] The olefination was stereoselective with Wlochal *et al* reporting the (*Z*)-**2.3e** was formed exclusively, albeit in a reduced yield of 34 %.[130] In this work the alkene geometry of (*Z*)-**2.3e** was assigned based on similar ^{1}H NMR shifts to (*Z*)-**2.3d**, which was reported earlier by Churches *et al*.[128, 130]

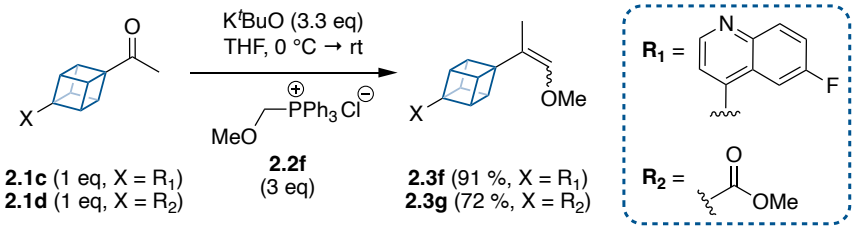

Scheme 11: The single example of a Wittig-Horner reaction using cubyl ketones.[129]

Notably all the olefination reactions described have been with structurally simple cubyl aldehydes, which are well-documented in the literature to be more reactive in the Wittig and Horner-Wadsworth-Emmons reaction than ketones.[132] A patent submitted by Qilu pharmaceuticals recently reported using cubyl ketones in a Wittig reaction, in yields exceeding 70 % using similar conditions as described by Churches *et al* for cubyl aldehydes (Scheme 11).[129] The treatment of cubyl ketone **2.1c** and **2.1d** at room temperature with ylide derived from **2.2f**, formed from the phosphonium chloride being treated with ^{t}BuOK in THF at 0 °C, gave **2.3f** and **2.3g** in 91 % and 72 % yield respectively after silica gel column chromatography. Unfortunately, as these two Wittig reactions were described in a patent no details regarding the stereoselectivity were revealed. However, based on the existing literature that shows the construction of all-carbon tetra-substituted alkenes via a Wittig or Horner-Wadsworth-Emmons usually proceeds in poor selectivity, it is likely **2.3f-g** are a mixture of geometric isomers.[133, 134] Therefore, exploring a range of different strategies is critical to find a robust synthetic method to access cubyl analogues of (*Z*)-tamoxifen and therefore other cubane containing tetra-substituted olefins in the future.

2.2 Results and discussion

2.2.1 Route 1: McMurry approach

2.2.1.1 Literature

We began our synthetic journey towards analogues of (*Z*)-cubyl-tamoxifen with exploring the suitability of the McMurry reaction, with a retrosynthetic analysis of (*Z*)-tamoxifen disclosed in Scheme 12. The alkene moiety in the target compounds would be constructed via a McMurry coupling between either ketone **2.6** and **2.5** or ketone **2.6** and **2.5a**, dependant on whether disconnection A or B are selected (Scheme 12). Ketones **2.6** and **2.5** are commercially available, with carbonyl **2.5a** expected to be accessible from the alkylation of the phenol moiety in **2.5** using 2-chloro-*N*,*N*-dimethylethylamine hydrochloride in the presence of a base.

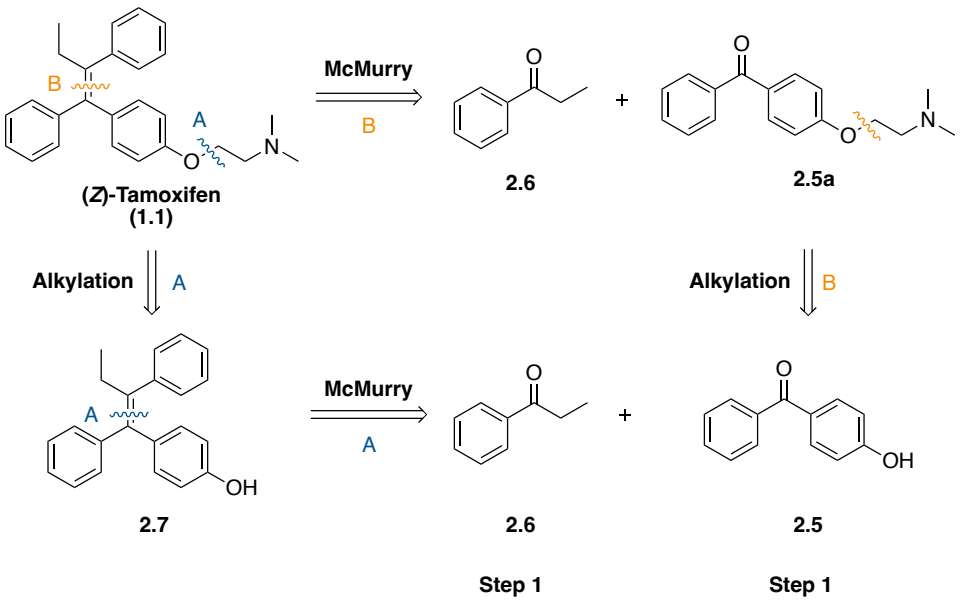

Scheme 12: Two disconnections of (*Z*)-tamoxifen (**1.1**).

In the McMurry reaction two carbonyl compounds, two ketones in the case of tamoxifen, are reductively coupled together to afford the corresponding olefin using a low-valent titanium species (Scheme 13).[135, 136] Common methods to prepare low-valent titanium (Ti^0) include refluxing titanium trichloride or titanium tetrachloride with a strong reducing agent such as $LiAlH_4$ or zinc, in either THF or DME.[137] The exact mechanism of

the reductive coupling of carbonyls with freshly prepared low-valent titanium (Ti^0) remains unclear, with multiple mechanistic routes considered since the discovery of the McMurry reaction.[138] In the classical mechanism the reductive coupling can be divided into two steps: (1) reduction of the carbonyl by a single electron transfer from the low-valent titanium species, to afford a ketyl radical that dimerises with another ketyl radical to give a metallopinacolate intermediate; (2) deoxygenation to afford the alkene (Scheme 13).[138] In the first step of the mechanism two keto-radical species dimerise, therefore the McMurry reaction is very effective for the preparation of symmetrical alkenes through homocoupling of a ketyl radical species. The synthesis of (*Z*)-tamoxifen via a McMurry coupling is far more challenging, as in the reaction two different asymmetric ketones are being reductively coupled. Therefore, conditions that minimise homocoupling whilst controlling the stereoselectivity of the olefin product are essential.

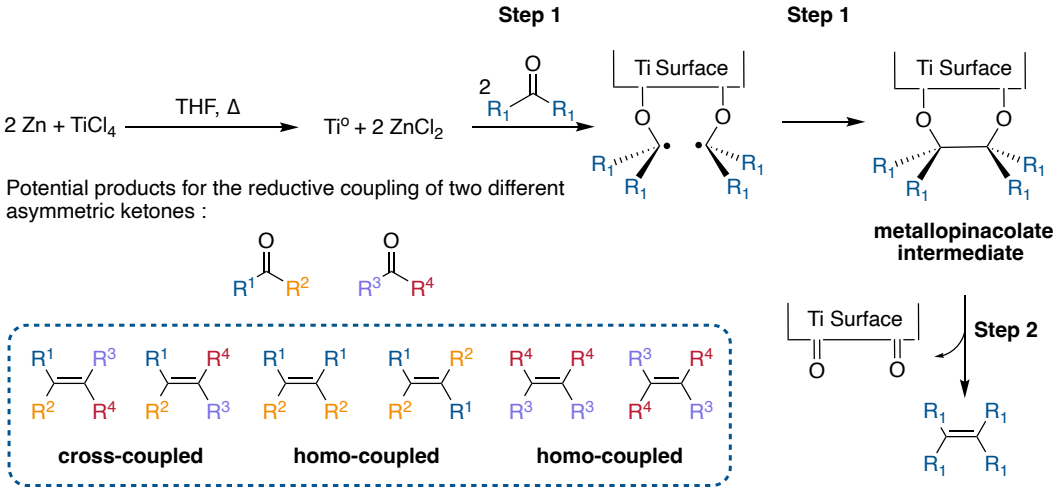

Scheme 13: Classical mechanism of the McMurry reaction.[138]

The first stereoselective synthesis of (*Z*)-tamoxifen utilising the McMurry reaction was described by Coe and Scriven.[119] Two pathways were explored to determine which carbonyl compounds in the McMurry reaction maximised the yield and stereoselectivity for the *Z*-geometric isomer (Scheme 14). In route A the low-valent titanium species was prepared by reducing titanium tetrachloride (3.1 eq) with excess zinc powder (6.2 eq) in refluxing DME for 2 hours. The heterogenous mixture was cooled to 0 °C and a 1:1

mixture of 4-hydroxybenzophenone (**2.5**, 1 eq) and propiophenone (**2.6**, 1 eq) was added and refluxed for 4 hours. After an aqueous work-up the coupled product 4-hydroxytamoxifen (**2.7**) was obtained in 98 % yield with a 7:1 *Z*/*E* isomer ratio, calculated by ^{1}H NMR analysis of the crude mixture. No further purification was attempted, instead the authors opted to directly alkylate the crude 4-hydroxytamoxifen **2.7** (7:1 *Z*/*E*) with 2-chloro-*N*,*N*-dimethylethylamine hydrochloride (3 eq) in refluxing toluene to obtain a mixture of (*Z*/*E*)-tamoxifen (**1.1**). Unfortunately, the ratio of geometric isomers after the work-up and the purification with silica gel column chromatography were not revealed. Although, the authors did report that recrystallisation of the purified *Z*/*E* mixture of tamoxifen with chloroform:hexane improved the ratio (*Z*/*E*)-tamoxifen to 9:1 (from 7:1 in the previous McMurry step) in a 24 % yield. Overall, using the conditions described in route A (*Z*)-tamoxifen (**1.1**) was synthesised in two steps with a high stereoselectivity (9:1 *Z*/*E*) in a moderate yield of 24 %.

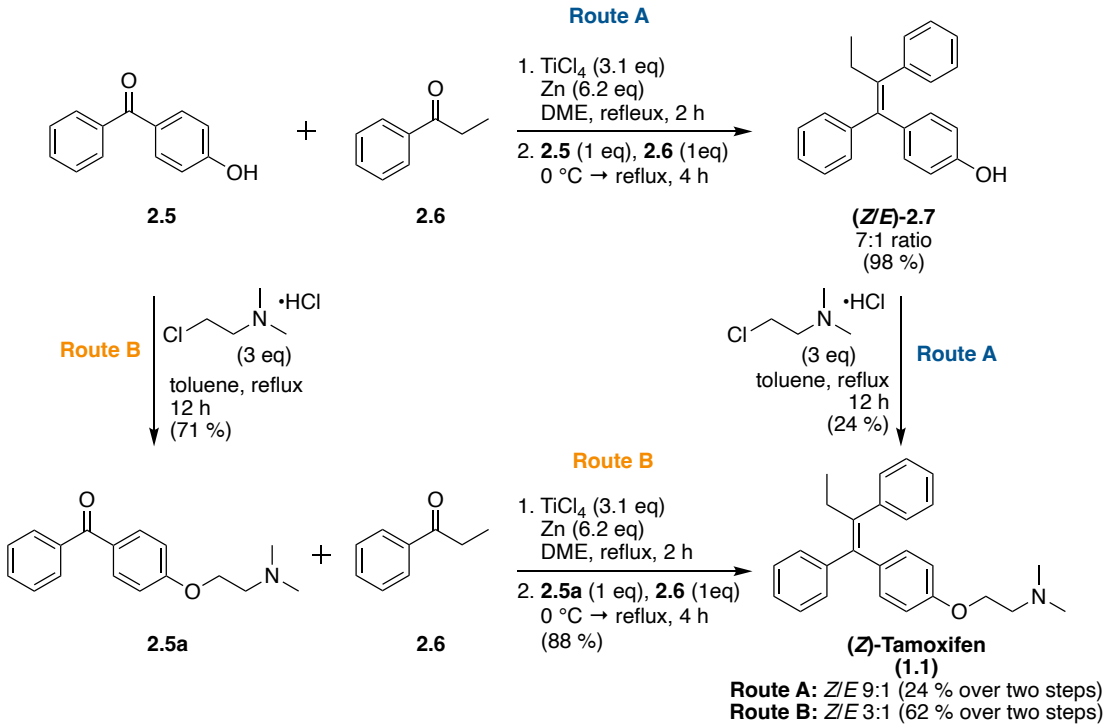

Scheme 14: Two McMurry literature examples towards the synthesis of (*Z*)-tamoxifen.[119]

Route B reverses the reaction order. Instead of starting with the McMurry reaction, Coe and Scriven began by treating 4-hydroxybenzophenone (**2.5**) with 2-chloro-*N*,*N*-

dimethylethylamine hydrochloride (3 eq) under the same alkylation conditions discussed in Route A. After purification by vacuum distillation the alkylated benzophenone **2.5a** was isolated in a good yield of 71 %. In the second step carbonyl **2.5a** was reductively coupled to propiophenone (**2.6**) using a low-valent titanium reagent, which was prepared in the same manner as previously described in route A. The authors found when using carbonyl **2.5a** in the McMurry reaction the stereoselectivity was reduced, with 3:1 ratio of (*Z*/*E*)-tamoxifen isolated after the work-up in a yield of 88 %. Despite the overall yield of route B being greater (yield = **route A**: 24 %; **route B**: 62 %), the poor stereoselectivity for (*Z*)-tamoxifen over (*E*)-tamoxifen made route A more favourable ((*Z*/*E*)-tamoxifen = **route A**: 9:1; **route B**: 3:1).

2.2.1.2 Our work

2.2.1.2.1 Synthesis of (*Z*/*E*)-tamoxifen

We opted to trial both route A and B before performing a McMurry reaction with a cubane carbonyl compound, to enable us to evaluate which route provides greater stereoselectivity and yield. This approach would also provide the opportunity to determine the optimal method to purify any mixture of olefin products, without loss of valuable cubane precursors. Once validated we would prepare a cubane analogue of one of the aromatic carbonyls to evaluate the viability of the McMurry approach to acquire a cubane analogue of (*Z*)-tamoxifen, and more generally tetra-substituted olefins that incorporate cubane as a substituent.

Our study began by examining route A (Scheme 15). When reviewing more recent literature for the McMurry coupling of ketone **2.5** and ketone **2.6**, we found the number of equivalents of titanium tetrachloride and zinc powder were generally in the range of 5 and 10 equivalents respectively.[139, 140] Therefore, we chose to approximately double the equivalents of titanium tetrachloride (3.1 eq $\rightarrow$ 6 eq) and zinc powder (6.2 eq $\rightarrow$ 13 eq) used in the protocol previously described by Coe and Scriven for our McMurry studies.[119] The equivalents of zinc are twice that of titanium tetrachloride to maximise the metal's reduction towards a low valent titanium species, which promotes the carbonyl coupling step. Unlike Coe and Scriven who used a 1:1 ratio of propiophenone

(**2.6**) and 4-hydroxybenzophenone (**2.5**), we opted to use a 3:1 ratio of propiophenone to 4-hydroxybenzophenone. By having the diaryl carbonyl as the limiting reagent, which are generally more readily reduced than monoaryl carbonyls in the McMurry reaction, theoretically should promote the desired cross-coupling between **2.5** and **2.6**.[135] The homo-coupled side product of carbonyl **2.6**, as a result of using this carbonyl in a three-fold excess, should then be readily separated from the target product 4-hydroxytamoxifen (**2.7**) during purification by silica gel column chromatography owing to their differing polarities.

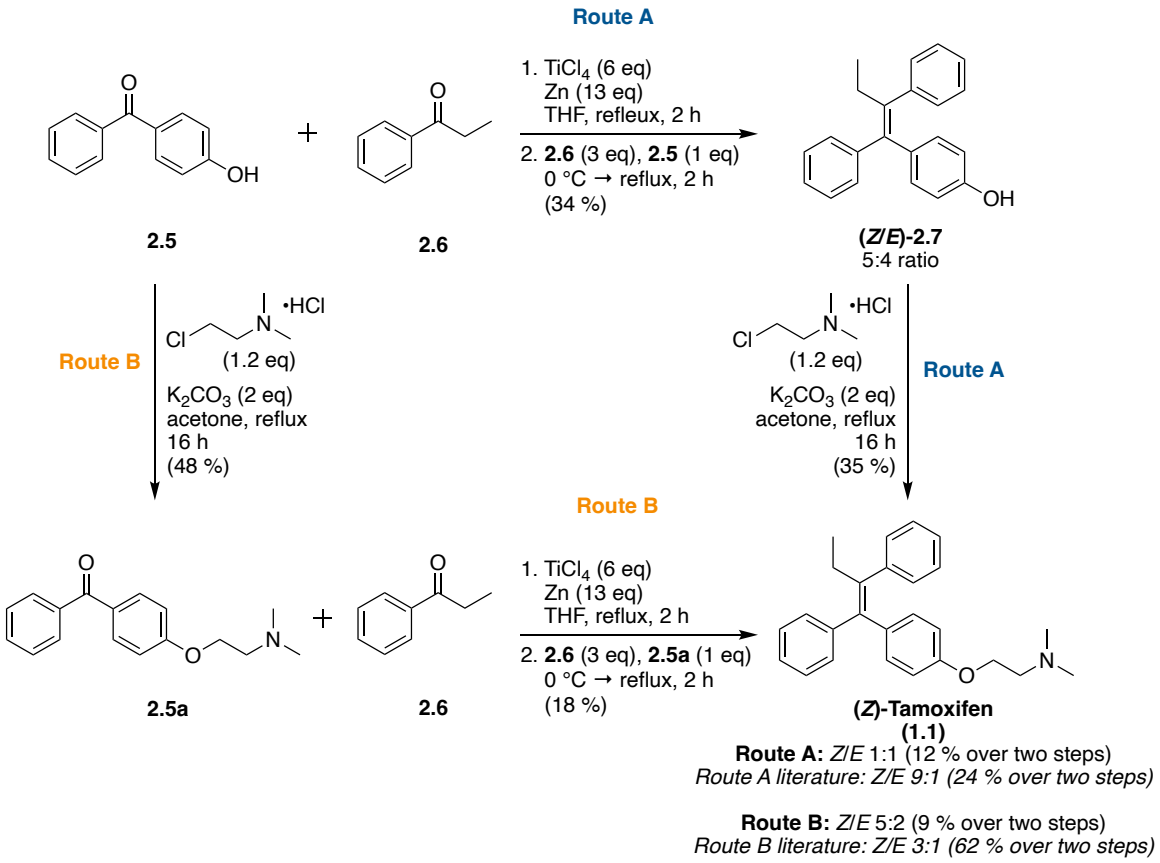

Scheme 15: Two routes investigated to synthesise (*Z*/*E*)-tamoxifen (**1.1**) via a McMurry coupling.

In our hands there was limited stereoselectivity for the McMurry reaction in route A using our adapted reaction conditions, with the crude mixture containing (*Z*/*E*)-4-hydroxytamoxifen (**2.7**) in a 5:4 ratio respectively by ^{1}H NMR analysis (Scheme 15). Despite the crude mixture containing multiple products and unreacted carbonyls the ratio of (*Z*/*E*)-4-hydroxytamoxifen could be determined, as the aromatic protons of the

4-substituted phenol ring in the *Z*-isomer are between 6.4 - 6.8 ppm whereas those for the *E*-isomer are more downfield between 6.8 - 7.2 ppm.[119] The same is observed in the ^{1}H NMR of (*Z/E*)-tamoxifen (**1.1**, Figure 8). Purification of the crude product by silica gel column chromatography afforded (*Z/E*)-4-hydroxytamoxifen (**2.7**) in a moderate yield of 34 % and unchanged 5:4 ratio of the *Z/E*-isomers. (*Z/E*)-4-Hydroxytamoxifen (**2.7**) was then converted into (*Z/E*)-tamoxifen by the alkylation of the phenol group in **2.7** using 2-chloro-*N*,*N*-dimethylethylamine hydrochloride (3 eq), potassium carbonate (2 eq) in refluxing acetone overnight. During the reaction we suspect there was partial isomerisation of the alkene, due to the crude mixture containing a 1:1 ratio of (*Z/E*)-tamoxifen indicative of a loss of stereoselectivity. Overall, we found route A was unselective with an overall yield of 11 %, due to poor yields of both the McMurry (34 %) and alkylation (35 %) reactions.

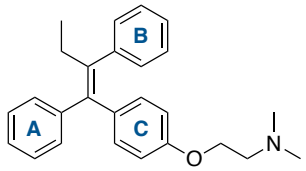

(*Z*)-Tamoxifen (1.1)
^{1}H NMR (300 MHz, $CDCl_3$) δ **6.60 - 6.52** (m, 2H)
(Ar*H ortho* to $O(CH_2)_2NMe_2$ - ring C)

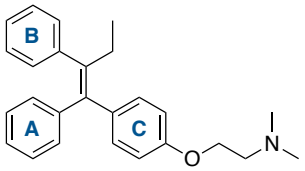

(*E*)-Tamoxifen (1.1)
^{1}H NMR (300 MHz, $CDCl_3$) δ **6.93 - 6.85** (m, 2H)
(Ar*H ortho* to $O(CH_2)_2NMe_2$ - ring C)

Figure 8: Shielding effect in ^{1}H NMR of (*Z*)-tamoxifen and (*E*)-tamoxifen.

We then examined route B, in which the McMurry and alkylation reaction were in the reverse order compared to route A (Scheme 15). Using the same alkylation conditions as described in route A, 4-hydroxbenzophenone (**2.5**) was converted into carbonyl **2.5a** in yield of 48 % after purification by silica gel column chromatography. Typically using this protocol purification by aqueous work up is sufficient to obtain pure material, although due to the sensitivity of the McMurry reaction and the poor yield of the McMurry reaction in route A we opted to purify the crude product as a precaution. In the McMurry reaction between carbonyl **2.5a** (1 eq) and **2.6** (3 eq), under identical conditions to those previously discussed in route A, we observed an improved stereoselectivity. The crude mixture contained (*Z/E*)-tamoxifen in a 5:2 ratio, which remained unchanged during the purification process by silica gel column

chromatography. Notably, the purification of the McMurry reaction in route B was more challenging than route A which is reflected in the lower isolated yield of 18 % versus 34 % respectively. As a whole the stereoselectivity and yields for both route A and B were lower than those reported by Coe and Scriven (Scheme 14 and 15). The most striking difference between the two studies was, we observed the greatest stereoselectivity for route B (**route A**: Z/E 1:1; **route B**: Z/E 5:2) whereas Coe and Scriven had a higher stereoselectivity for route A (**route A**: Z/E 9:1; **route B**: Z/E 3:1).

2.2.1.2.2 Preparation of cubane carbonyl for McMurry reaction

Having explored both routes with aromatic carbonyls we next turned our attention to performing the McMurry reaction with a cubyl ketone. To begin with we opted to use route A, while we realised this route was unselective for the aromatic substrates it offered a higher overall yield and thus would still allow us to test both isomers in any future biological studies. In total there are three phenyl rings between the ketones propiophenone (**2.6**) and 4-hydroxybenzophenone (**2.5**), therefore there are three locations to introduce a cubane scaffold via an isosteric replacement. Based on synthetic accessibility, we opted to prepare cubanylpropan-1-one (**2.13**) as a cubane analogue of propiophenone (**2.6**) starting from the commercially available 4-methoxycarbonylcubanecarboxylic acid (**2.8**) (Scheme 16). In our retrosynthetic plan, we envisioned performing the decarboxylation at the start of the synthetic sequence to afford the mono-substituted methyl-cubanecarboxylate (**2.10**) would be the best strategy.

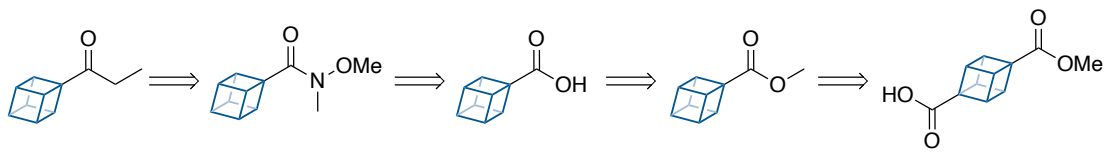

2.13 **2.12** **2.11** **2.10** **2.8**

Scheme 16: Synthetic plan of cubanylpropan-1-one (**2.13**).

Traditionally, the transformation of 4-methoxycarbonylcubanecarboxylic acid (**2.8**) to methyl-cubanecarboxylate **2.10** has been achieved via a Barton decarboxylation (Scheme 17a).[141] A more recent approach has utilised cubane redox-active esters, with Baran *et al* reporting a Ni-catalysed decarboxylation (Scheme 17b) and MacMillan *et al* publishing an Ir-catalysed photoredox-mediated decarboxylation (Scheme 17c) all with comparable yields.[88, 142] At the onset of our synthesis of cubanylpropan-1-one (**2.13**), MacMillan *et al* had not yet published their photoredox decarboxylation conditions for cubyl systems.[88] There were literature reports of visible-light induced radical decarboxylative fragmentation of *N*-(acyloxy)phthalimides, discovered by Okada *et al*[143], and the Macmillan's group research using iridium photocatalysts in the presence of blue LED light to generate radical species for cross-coupling reactions.[144, 145] Based on this literature, we proposed that blue light irradiation of the cubyl *N*-(acyloxy)phthalimide **2.9** in the presence of an iridium photocatalyst would generate a cubyl radical, which when trapped by a suitable proton source would afford methyl-cubanecarboxylate **2.10**.

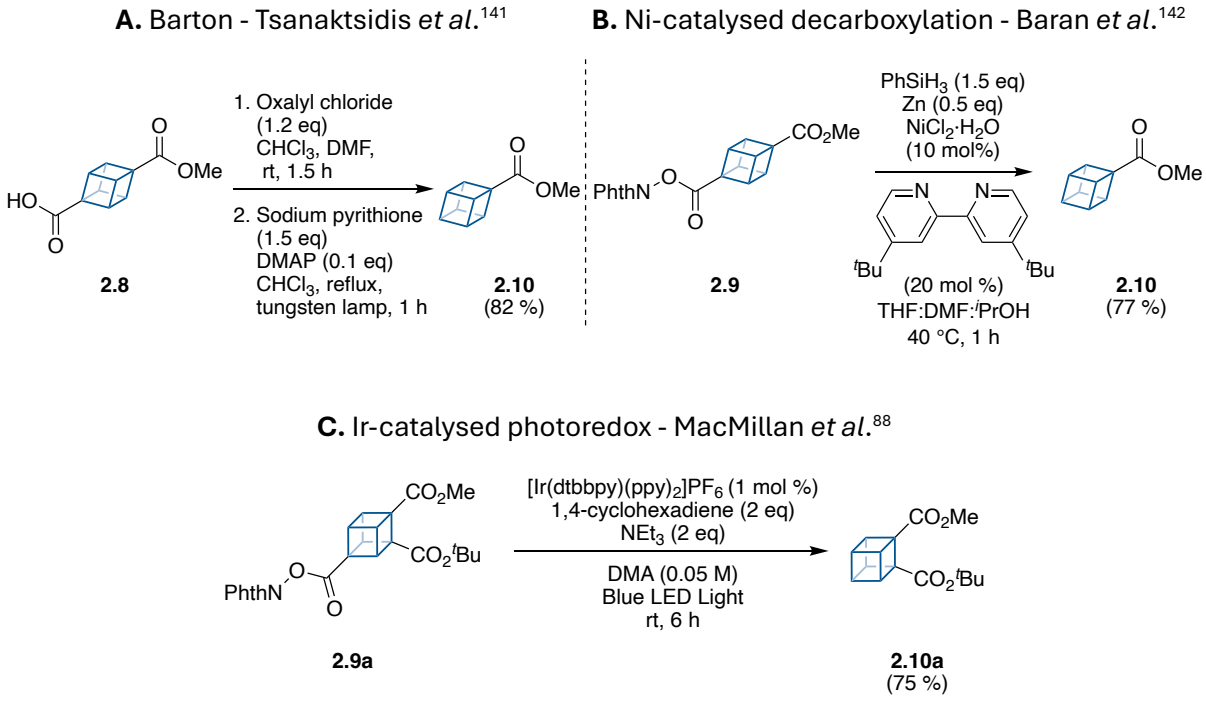

Scheme 17: Literature protocols for cubyl decarboxylation.

To test this hypothesis, we began by synthesising the cubyl *N*-(acyloxy)phthalimide **2.9** from the commercially available cubane **2.8** (Scheme 18). Our preferred route was to first convert the carboxylic acid moiety in **2.8** to an acid chloride using oxalyl chloride (1.2 eq. 2 M in DCM) and a catalytic quantity of DMF (10 mol %) in DCM at room temperature. Subsequent addition of *N*-hydroxyphthalimide (1.2 eq) and triethylamine (2.5 eq) to the freshly prepared acid chloride (1 eq) gave cubyl phthalimide **2.9** in a 94 % yield with no purification required. Alternatively, the phthalimide **2.9** could be synthesised via a peptide coupling by treating **2.8** (1 eq) directly with DCC (1.1 eq), DMAP (10 mol %) and *N*-hydroxyphthalimide (1.1 eq) in DCM at room temperature for 2 hours, albeit in a reduced yield of 53 % (Scheme 18). A further disadvantage of the peptide coupling route was the phthalimide **2.9** required purification by silica gel column chromatography, this was unfavourable as it was unstable on silica gel.

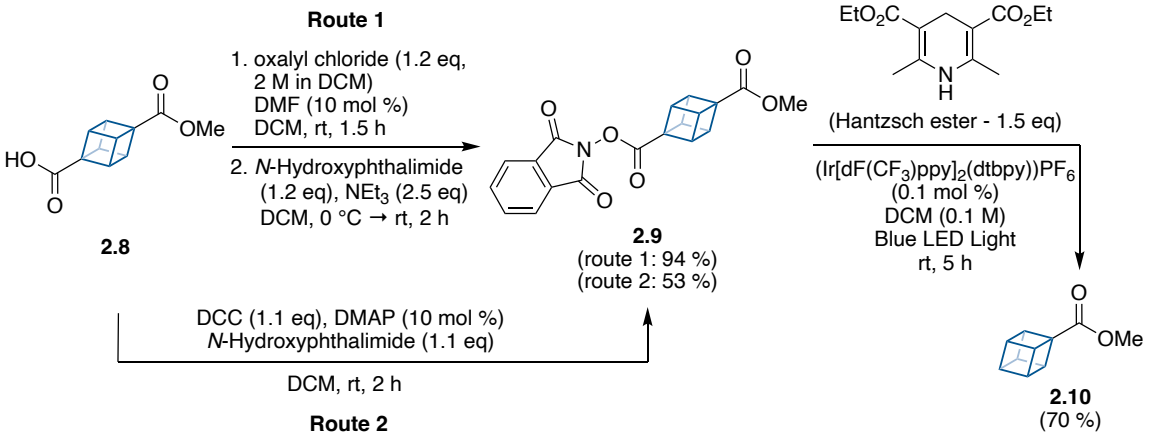

Scheme 18: Our photoredox decarboxylation protocol of cubyl phthalimide **2.9**.

With the cubyl *N*-(acyloxy)phthalimide **2.9** in hand, we next examined the photoredox decarboxylation on this substrate (Scheme 18). To start with we opted to use the photocatalyst (Ir[dF(CF_3)ppy]$_2$(dtbpy))PF_6 and the Hantzsch ester as the proton donor source, based on a Macmillan report that used this catalyst to promote the decarboxylation of secondary carboxylic acids and a review article on the application of Hantzsch esters in photoredox chemistry.[144, 146] In our initial attempt, a solution of **2.9** (1 eq), (Ir[dF(CF_3)ppy]$_2$(dtbpy))PF_6 (0.1 mol %) photocatalyst and Hantzsch ester (1.5 eq) in degassed DCM was irradiated with blue light at room temperature. After 5 hours, the

cubyl phthalimide **2.9** was fully consumed (determined by TLC analysis) and methyl-cubanecarboxylate (**2.10**) was isolated by silica gel column chromatography in a 70 % yield. No further optimisation of the reaction was performed.

After the decarboxylation of cubyl phthalimide **2.9**, we then turned our attention to converting methyl-cubanecarboxylate (**2.10**) into cubanylpropan-1-one (**2.13**, Scheme 19). The direct synthesis of a ketone from a carboxylic acid derivative, for example from a methyl ester, is often not efficient due to the newly formed ketone being highly susceptible to attack from any remaining organometallic reagent in the reaction. To avoid the formation of the tertiary alcohol we decided to proceed via a Weinreb amide. Preparation of the Weinreb amide **2.12** began with the hydrolysis of methyl-cubanecarboxylate (**2.10**, 1 eq) using lithium hydroxide (2.5 eq) in THF:MeOH:H_2O (3:3:1, 0.34 M) at room temperature. After an aqueous work-up the carboxylic acid **2.11** was isolated in an excellent yield of 95 %.

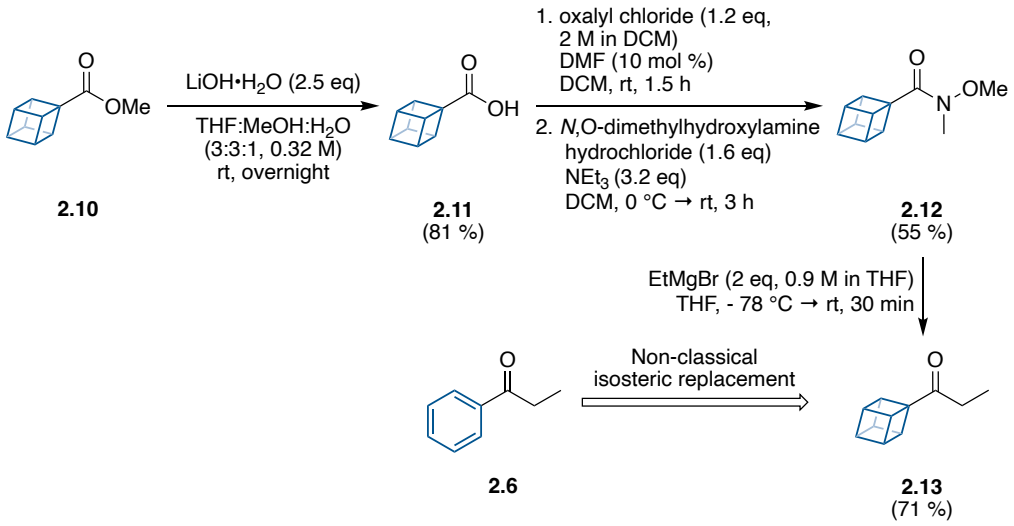

Scheme 19: Continued synthesis of cubanylpropan-1-one (**2.13**).

Following a protocol similar to that described previously, the carboxylic acid **2.11** was then converted to the acid chloride with oxalyl chloride (1.2 eq), which when treated directly with *N,O*-dimethylhydroxylamine and triethylamine afforded the Weinreb amide **2.12** in 55 % yield after purification by silica gel column chromatography (Scheme 19).[147] Subsequent addition of the Grignard ethylmagnesium bromide (2 eq, 0.9 M in THF) to

2.12 (1 eq) at - 78 °C followed by stirring at room temperature for 30 minutes, gave the target compound cubanylpropan-1-one (**2.13**) in 71 % isolated yield. In summary, **2.13** was prepared in 5 steps from commercial material **2.8** in an overall yield of 21 %.

2.2.1.2.3 McMurry reaction with cubanylpropan-1-one (2.13)

Next, we examined the McMurry reaction between cubanylpropan-1-one (**2.13**) and 4-hydroxybenzophenone (**2.5**) (Scheme 20). In our previous studies when we synthesised (*Z/E*)-tamoxifen via a McMurry coupling we used a 3:1 ratio of propiophenone (**2.6**) to the more readily reduced 4-hydroxybenzophenone (**2.5**) (Scheme 15). However, as cubanylpropan-1-one (**2.13**) was a valuable starting material, in this instance we chose to adjust the ratio of ketones cubanylpropan-1-one (**2.13**) and 4-hydroxybenzophenone (**2.5**) to a ratio of 1:1. Similar to the previous McMurry reactions described, we began by preparing the low-valent titanium species by reducing titanium tetrachloride (6 eq) with excess zinc powder (13 eq) in refluxing THF for 2 hours (Scheme 20). The heterogenous mixture was cooled to 0 °C and a 1:1 mixture of cubanylpropan-1-one (**2.13**, 1 eq) and 4-hydroxybenzophenone (**2.5**, 1 eq) were added and refluxed for a further two hours. ^{1}H NMR analysis of the crude product revealed that cubanylpropan-1-one (**2.13**) was fully consumed, although the reaction conditions failed to deliver the desired olefin product (*Z*)-**2.14a**. Upon further investigation, the ^{1}H NMR revealed multiplets between 3-4 ppm. Purification of the crude mixture by silica gel column chromatography allowed us to isolate this compound of interest.

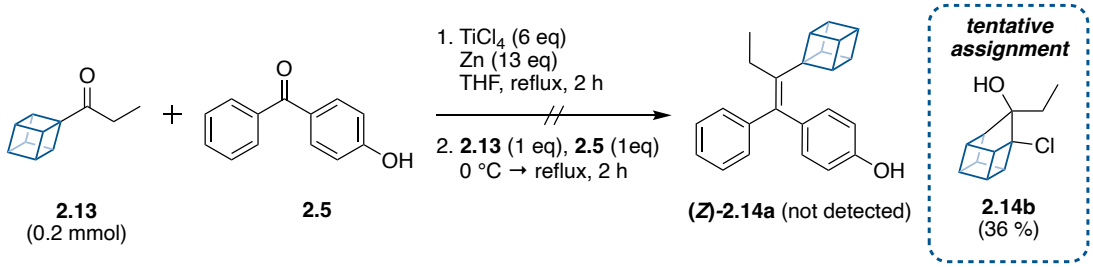

Scheme 20: Attempted McMurry reaction between cubanylpropan-1-one (**2.13**) and 4-hydroxybenzophenone (**2.5**).

The ^{1}H NMR spectrum for the compound of interest showed the cubyl framework was no longer intact (Figure 9). In addition, the proton environments were shifted up-field between 3-4 ppm compared to cubanylpropan-1-one (**2.13**) [4.30 – 4.22 (m, 3H), 4.05 – 3.93 (m, 4H)], indicative of a cubane ring-opened homocubane system.[148] We propose that in the McMurry reaction the carbonyl group in cubanylpropan-1-one (**2.13**) likely coordinated to the Lewis acid $ZnCl_2$, which was present in stochiometric quantities as a by-product of the reaction between $TiCl_4$ and Zn, promoting a Wagner-Meerwein type rearrangement which we tentatively propose gives **2.14b** (Scheme 20). This is highly plausible, as cubylmethanols in the presence of acid or Lewis acids are well documented to undergo the Wagner-Meerwein type rearrangements to afford homocubane systems (Scheme 21).[149]

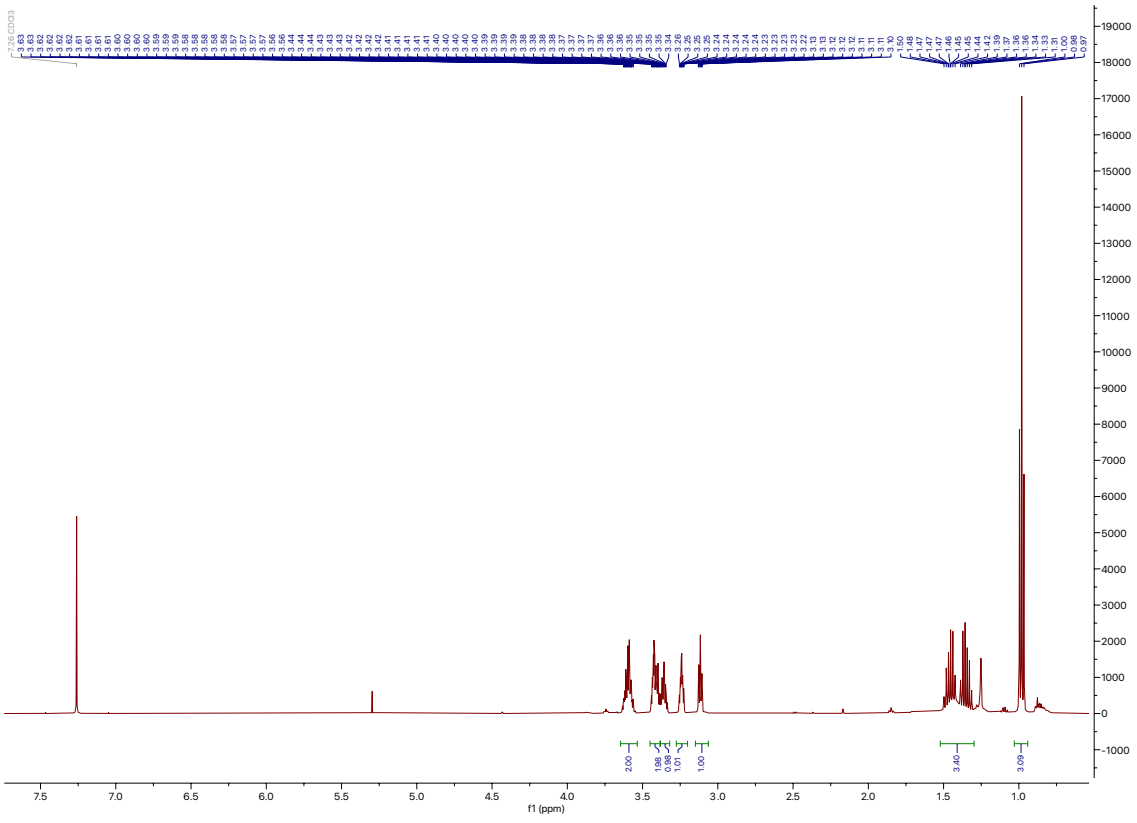

Figure 9: ^{1}H NMR (500 MHz, $CDCl_3$) spectrum of isolated product from McMurry reaction, tentatively assigned as **2.14b**.

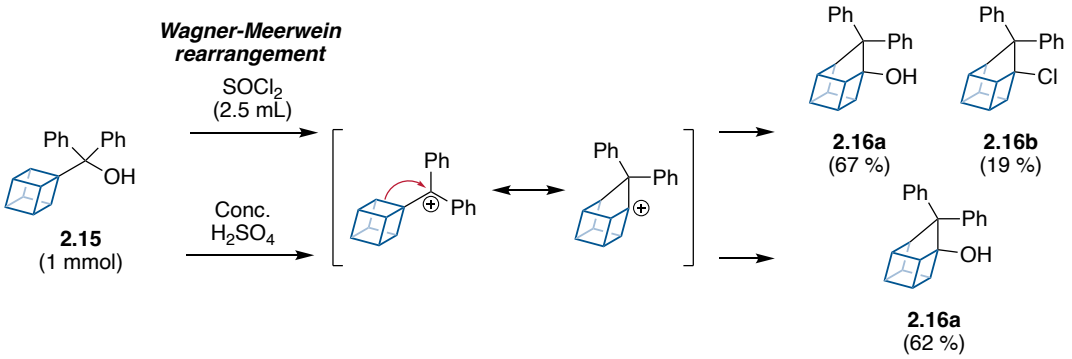

Scheme 21: Literature examples of Wagner-Meerwein rearrangement of cubylmethanols.[149]

The 2D-NMR data collected for **2.14b** supports our proposed assignment. Two quaternary centres were observed in the HSQC analysis at 93.2 ppm and 79.6 ppm, which is consistent with the presence of a tertiary alcohol and tertiary chloride (highlighted in Figure 10 in orange and red respectively). The observation of a doublet of multiplets at 1.50 – 1.30 in the proton NMR is consistent with diastereotopic protons of the C***H₂*** moiety in **2.14b**, further supported by HSQC analysis that showed the two protons in the C***H₂*** moiety coupling to the same carbon. Additionally, in the HSQC we observed 7 carbons between 35 - 40 ppm each individually coupling to a hydrogen between 3.0 - 3.7 ppm, once again consistent with our tentative assignment of **2.14b**.

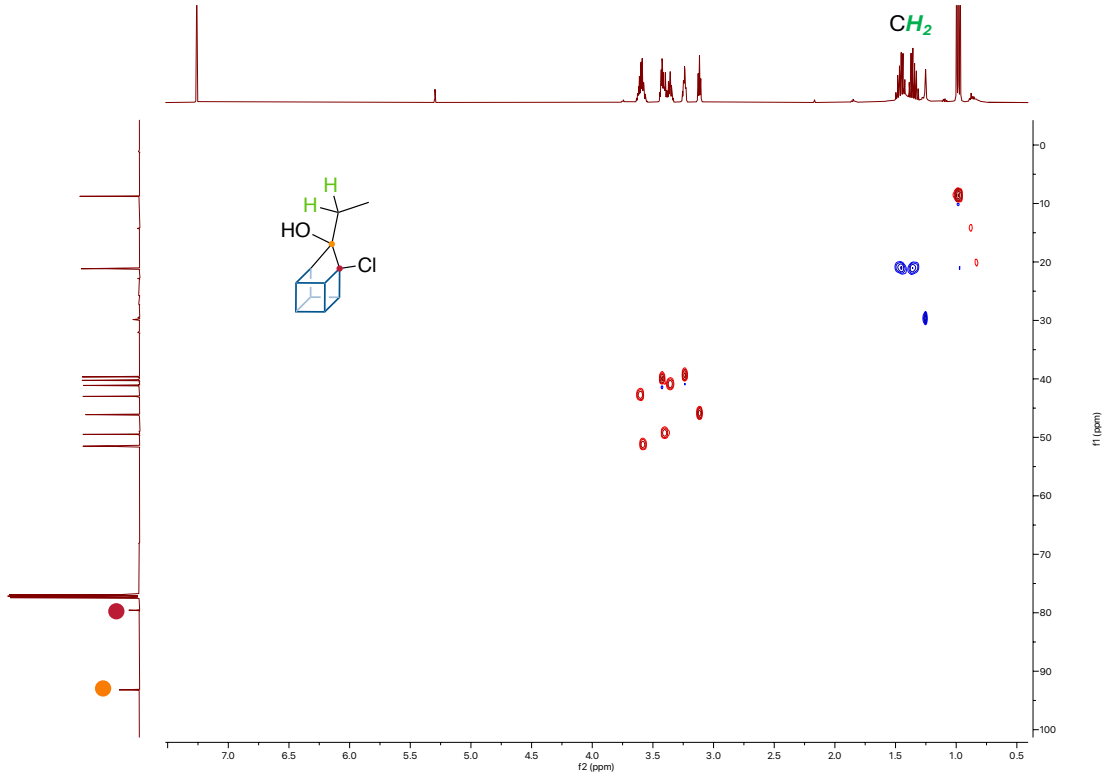

Figure 10: HSQC NMR (500 MHz, $CDCl_3$) spectrum of proposed **2.14b**.

On the basis of these results, we believed it was not worth further pursuing the McMurry route and began to investigative alternative approaches towards a cubane analogue of tamoxifen.

2.2.2 Route 2: Organometallic approach

2.2.2.1 Literature

ICI pharmaceuticals' original patent for (*Z/E*)-tamoxifen in the early 1960s disclosed their process to prepare a mixture of geometric isomers of tamoxifen.[120, 150] The patent described how the dehydration of the tertiary alcohol **2.18**, catalysed by hydrochloric acid and the application of heat, afforded (*Z/E*)-tamoxifen (Scheme 22). In addition, the patent stated that alcohol **2.18** was prepared by the addition of phenylmagnesium bromide to a solution of carbonyl **2.17** in diethyl ether under refluxing conditions. Since

the original patent submission several publications have followed this general approach to synthesise tamoxifen and its derivatives.[121, 122, 151-154]

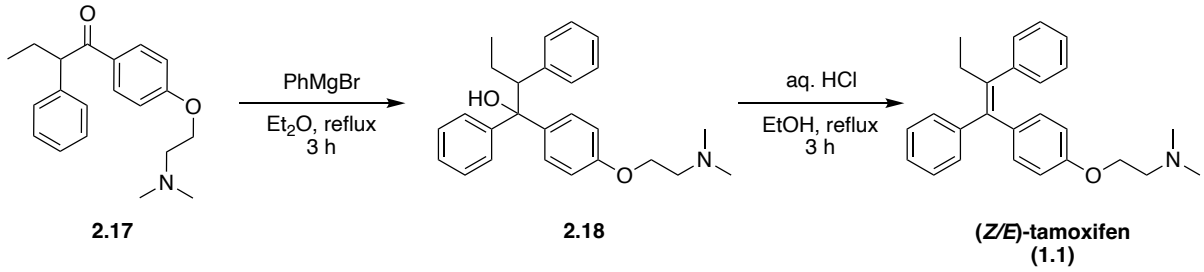

2.17 **2.18** **(*Z*/*E*)-tamoxifen (1.1)**

Scheme 22: ICI pharmaceuticals patent to prepare (*Z*/*E*)-tamoxifen.[120]

Under the acidic dehydration conditions outlined in Scheme 22 (compound **2.18** → **1.1**) the dominant elimination pathway is likely to be E_1, which would generate a carbocation intermediate. There are three aromatic rings in tertiary alcohol **2.18**, therefore we can envision three opportunities to perform a bioisosteric replacement of a phenyl ring for cubane (Scheme 23, compound **2.19** - **2.21**). The generation of the carbocation alpha to the cubane framework in compound **2.19a** and **2.21a** we suspect will provide a pathway for the strained cubane framework to rearrange via a Wagner-Meerwein rearrangement (Scheme 23, pathway A).[155, 156] Although, we hypothesised that in compound **2.20a** rearrangement of the cubane framework would be minimised as the carbocation is one carbon unit further from the cubane framework. To minimise or prevent cubane rearrangement for compound **2.19** and **2.21** during the dehydration step we envisioned that conditions that favour an E_2 pathway over E_1 may be more favourable for olefin bond formation.

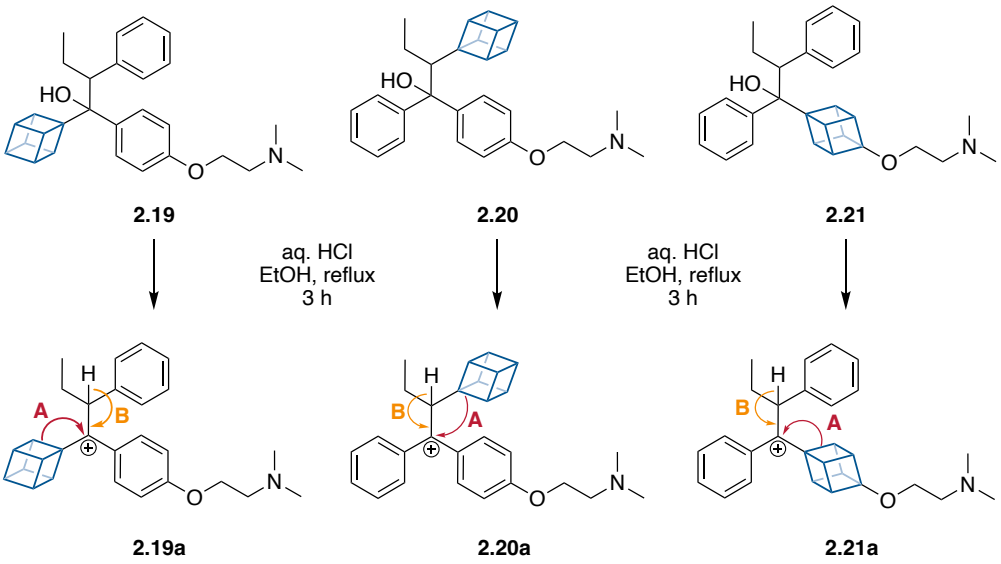

Scheme 23: Consequences of E_1 dehydration in compound **2.19** – **2.21**.

If route A is faster than route B cubane ring-opening will be favoured over alkene bond formation.

Alcohols are poor leaving groups for an E_2 elimination therefore if we were to pursue this route it would be necessary to first activate the alcohol group. Functionalisation of a sterically hindered tertiary alcohol is challenging and so perhaps unsurprisingly there are limited reports that describe the synthesis of tamoxifen via an E_2 elimination pathway. An alternative approach to construct the olefin bond which solves the blocked trajectory of the base in the E_2 pathway, includes promoting a *syn*-elimination. The Gosselin group recently reported the stereoselective synthesis of more than 20 tetra-substituted olefins using a *syn*-elimination approach, including the stereoselective synthesis of (*Z*)-tamoxifen (**1.1**, *Z*/*E* ratio of 97:3).[157] Similar to the original patent by ICI pharmaceuticals, the Gosselin group began their synthetic sequence with the addition of the Grignard 4-iodophenylmagnesium iodide to the carbonyl 1,2-diphenylbutan-1-one (**2.22**, 1 eq), affording tertiary alcohol (1SR, 2SR)-(±)-**2.23** in a 95 % yield with a 98:2 dr (Scheme 24). The stereochemical assignment for this transformation was confirmed by X-ray crystal studies and the ratio of each diastereomer was measured by HPLC. Subsequently, bis(2,6-dimethylphenyl)phosphoryl chloride (1.5 eq) was added to a solution of (1SR, 2SR)-(±)-**2.23** containing KHMDS (3 eq) in 1,4-dioxane. After 16 hours at 45 °C and two silica gel column chromatography purifications, olefin **2.24** was isolated in 85 % yield with 97:3 *Z*/*E* isomer ratio. In the final step, the work described

that the ethoxy(dimethylamino) side chain was introduced by a copper-catalysed C-O cross-coupling, using copper iodide (20 mol %) and *N*,*N*-dimethyl-2-hydroxyethylamine (4 eq). In this copper-catalysed Ullman-type reaction no scrambling of the *Z*/*E* isomer ratio was observed, affording (*Z*)-tamoxifen in an excellent yield of 96 % (97:3 *Z*/*E*).

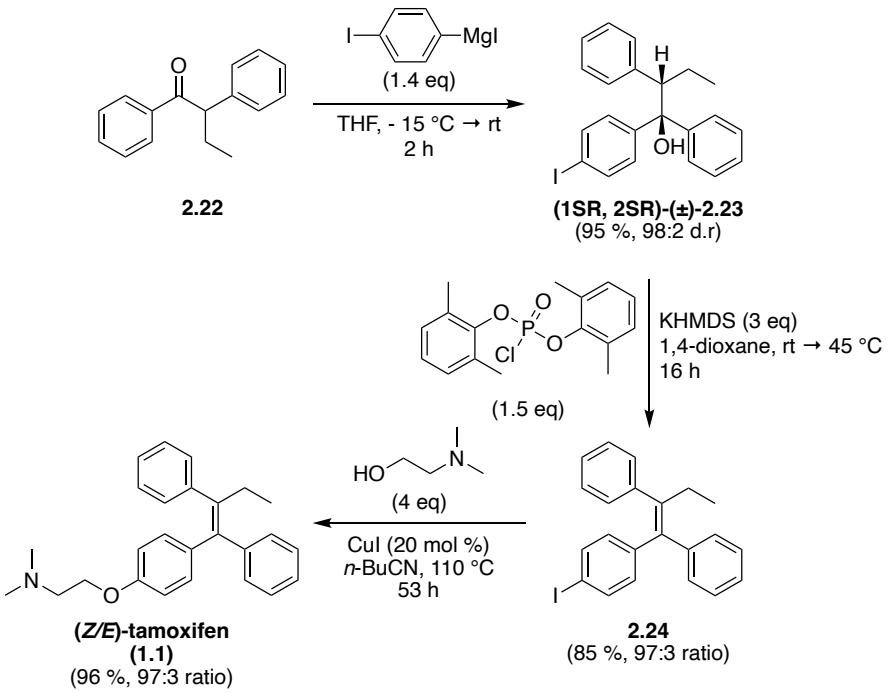

Scheme 24: *Syn*-elimination of tertiary alcohol **2.23** towards the stereoselective synthesis of (*Z*)-tamoxifen - Gosselin group.[157]

Considering these encouraging results by the Gosselin group, we were keen to explore if the *syn*-elimination approach with our cubyl alcohol substrates **2.19** - **2.21** (Scheme 23) would generate the desired tetra-substituted olefin without or limited cubane rearrangement.

2.2.2.2 Our work

2.2.2.2.1 Retrosynthetic analysis of cubylmethanol 2.21

From the outset, we were aware that extensive method development would be required to acquire cubylmethanol **2.21**, as introducing the (dimethylamino)ethoxy side chain directly onto the cubane framework would not be trivial based on literature precedent.

One method to install this motif could include transition metal-mediated C-O cross-coupling with a suitable cubane precursor (Scheme 25).

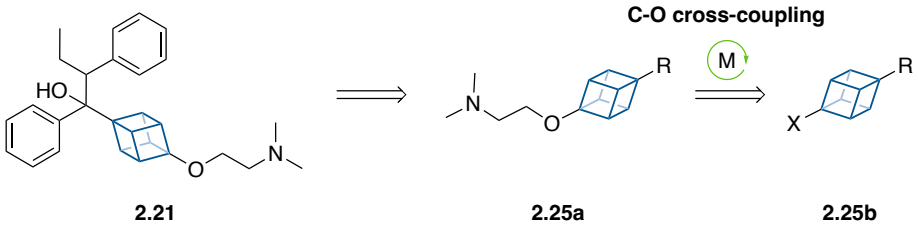

Scheme 25: Retrosynthesis of cubylmethanol **2.21** via a cubane C-O cross-coupling.

In general cubane cross-coupling remains a challenge, with only a handful of reported methodologies that do not promote metal-catalysed strain-releasing valence bond isomerisation. For instance, transition metals like palladium, ruthenium and silver are known to promote cubane decomposition, generating products such as cuneane and cyclooctatetraene species (Scheme 26).[158-160] One decomposition pathway proposed is oxidative addition of the transition metal into the cubane framework (**2.26a**), the second is from slow reductive elimination of the metal-cubane complex (**2.26b**).[158, 160] In the literature copper-mediated cross-couplings are reported to undergo slow oxidation addition and fast reductive elimination, the MacMillan group realised this and recently reported the first copper-mediated C-N and C-C cross coupling with cubane.[88, 161] For the C-N cross-coupling the MacMillan group reported the copper-mediated decarboxylative amination of 4-methoxycarbonylcubanecarboxylic acid (**2.8**), in yields exceeding 50 %.[88] In the examples of copper-mediated C-C cross-couplings the cubane photo-redox-active ester **2.9** was instead employed, with at least 5 examples for both arylation and alkylation in yields between 40-50 % included in the substrate scope.[88] Unfortunately, the only other cubane cross-couplings reported in the literature are the Baran group's Fe-mediated and the Senge group's Ni-mediated arylation of cubanes.[162, 163] Each of the cubane cross-coupling methodologies discussed are mechanistically similar, proposed to proceed via a cubyl radical.[88, 162, 163]

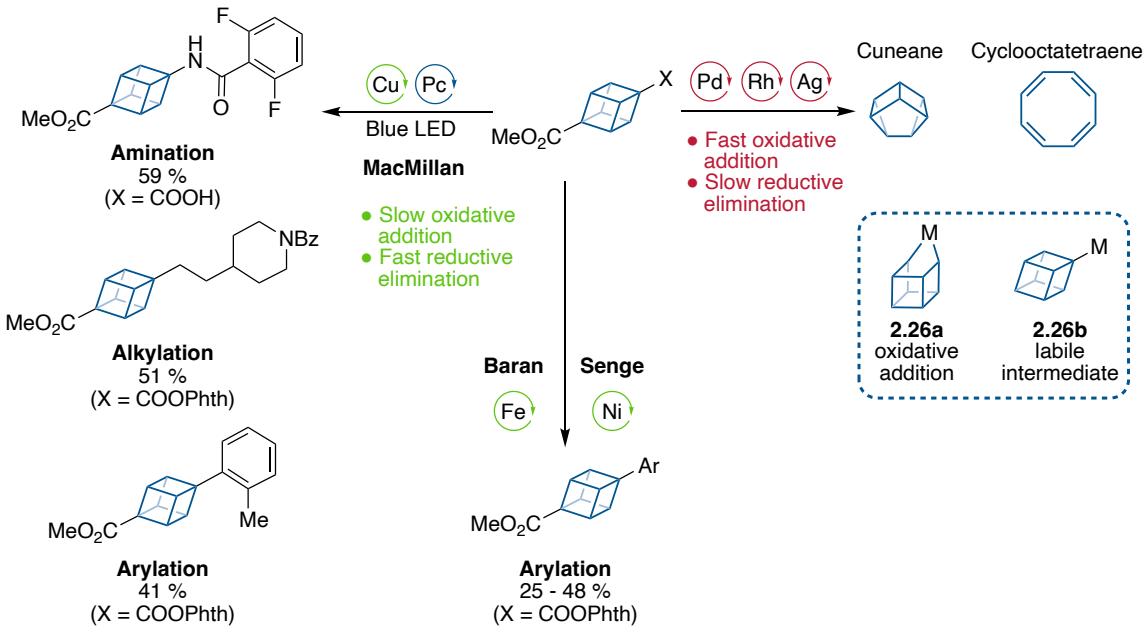

Scheme 26: Cubane metal-mediated cross-coupling literature methods.

Pc = Ir photocatalyst.

Currently there are no examples of cubane C-O cross-coupling, although methods for synthesising cubyl ethers do exist. Linclau and Brown reported a method to access alkoxy cubanes under electrochemical flow conditions via a Hofer-Moest reaction (Scheme 27a), while a limited number of cubyl ethers have been synthesised from the photolysis of cubyl iodides in methanol (Scheme 27b).[164-166] In each of these methodologies the alcohol employed to generate the alkoxylated cubanes also served as the reaction solvent. We were interested in developing a general method for the synthesis of cubanols in order to evaluate their utility as a useful synthetic building block for accessing structurally more complex alkoxylated cubanes. We envisioned the alkylation of cubanol **2.25c** with 2-chloro-*N*,*N*'-dimethylethylamine would provide **2.25a**, an intermediate that should then allow us synthesise cubyl-tamoxifen **1.19** (Scheme 27c). We expect to encounter challenges whilst exploring this approach, as the chemistry to alkylate a cubanol does not exist and cubanols themselves have been reported to be unstable and prone to rearrangement in the literature.[105, 167-169] Therefore, the development of a method to access a range of cubanol precursors and their transformation into cubanols are first needed, these topics are addressed in Chapter 3 and 4 respectively.

A. Flow electrochemistry – Linclau and Brown.[164]

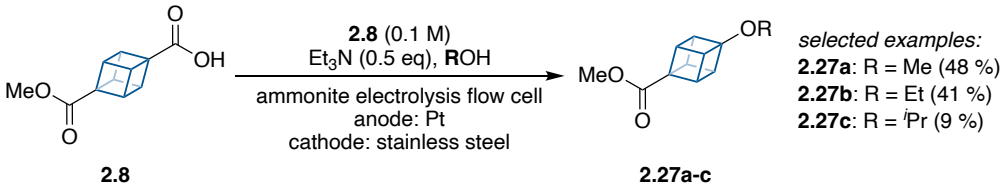

B. Photolysis of cubyl iodides – Irngartinger *et al*.[166]

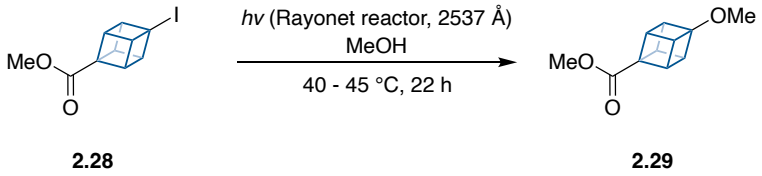

C. Synthesis plan of cubyl-tamoxifen via cubanol.

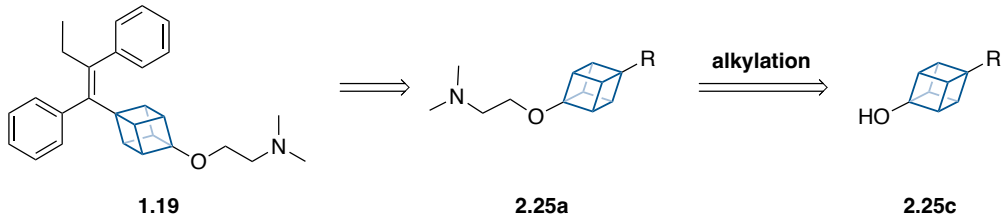

Scheme 27: Methods towards alkoxylated cubanes.

2.2.2.2.2 Synthesis of cubylmethanol 2.19

In our retrosynthetic analysis for cubylmethanol **2.19** the formation of the tertiary alcohol moiety would occur by the organometallic addition of aryl bromide **2.34** into carbonyl **2.31** (Scheme 28), resembling the method reported in the original tamoxifen patent and work by the Gosselin group. In the forward direction, it was envisioned that carbonyl **2.30** could be constructed by the addition of benzylmagnesium bromide to Weinreb amide **2.12**. A subsequent alkylation of the ketone **2.30** with iodoethane would then afford carbonyl **2.31**.

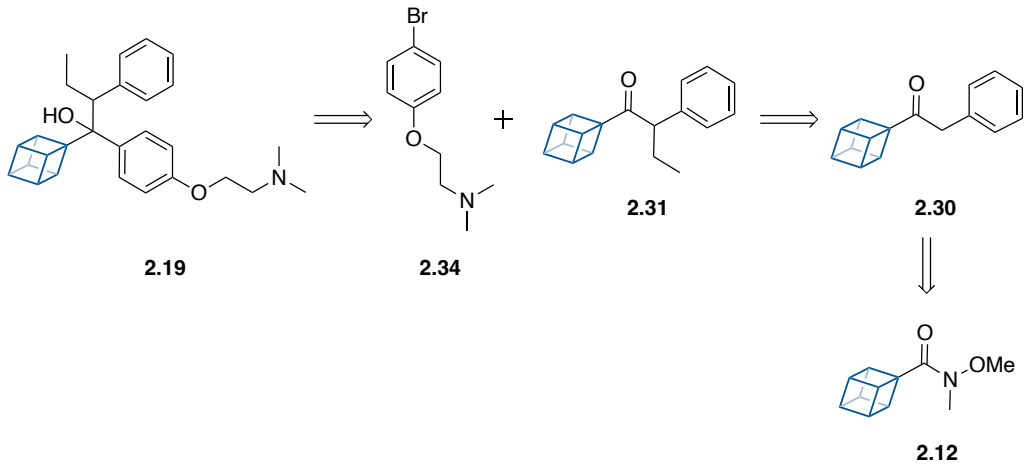

Scheme 28: Retrosynthetic analysis of cubylmethanol **2.19**.

Our forward synthesis commenced by preparing cubyl Weinreb amide **2.12** from commercially available 4-methoxycarbonylcubanecarboxylic acid **2.8** (5-steps, 21 % overall yield), which was previously described in **Section 2.2.1.2** (Scheme 18-19). In our first attempt to generate the Grignard benzylmagnesium bromide we began by activating the magnesium turnings (3.8 eq) with iodine (0.1 eq) in a solution of THF, followed by the slow addition of benzyl bromide (3.3 eq) at room temperature (Scheme 29, left arrow). Titration of the reaction mixture revealed we failed to generate the Grignard benzylmagnesium bromide under these conditions. A review on benzyl Grignard reactions stated that conducting the Grignard formation step in diethyl ether instead of THF and at 0 °C rather than room temperature, shifts the percentage of Grignard formation from 30 % to 80 %.[170] To further promote Grignard formation the magnesium turnings (3.8 eq) were activated by stirring and heating them for 5 minutes at 40 °C in the presence of a pellet of iodine (0.1 eq) (Scheme 29, right arrow). Subsequently, we found the slow addition of benzyl bromide (3.3 eq) over 20 minutes to a suspension of the activated magnesium turnings in diethyl ether pre-cooled to 0 °C, produced a 1.6 M solution of benzyl magnesium bromide (determined by titration). To our delight, when Weinreb amide **2.12** was treated with 1.1 equivalents of the freshly prepared benzylmagnesium bromide, carbonyl **2.30** was isolated in a yield of 74 % following purification by silica gel column chromatography.

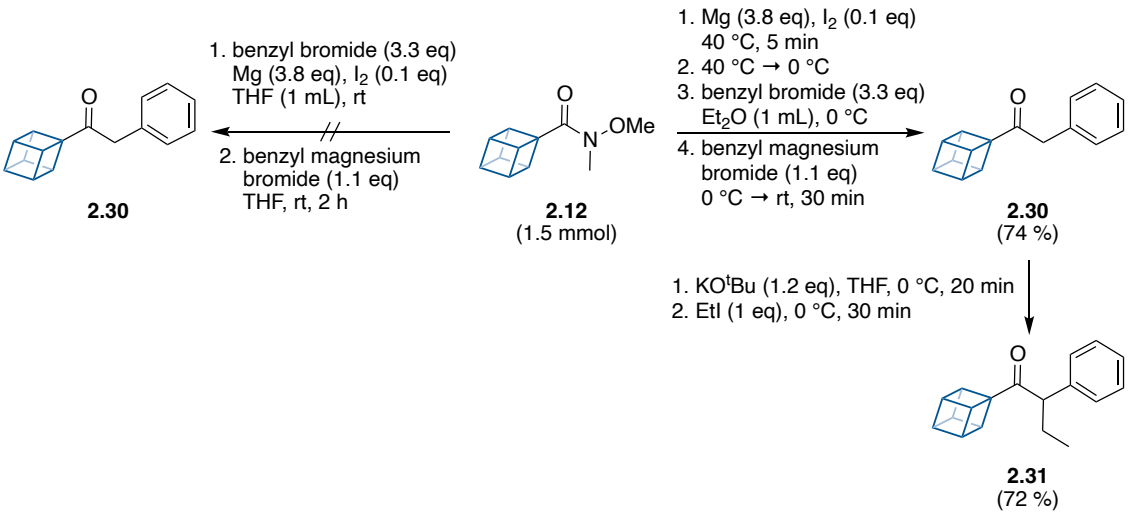

Scheme 29: Preparation of carbonyl **2.31** via an alkylation reaction.

The potassium enolate of ketone **2.30** was formed using the base potassium *tert*-butoxide (1.2 eq) in THF at 0 °C, generating a dark red solution instantly (Scheme 29). After 20 minutes at 0 °C, iodoethane (1 eq) was added and within 30 minutes ketone **2.30** was fully consumed (determined by TLC analysis). From TLC analysis we observed the formation of more polar by-products within this 30-minute timeframe, therefore close monitoring via TLC is recommended. Based on the integration pattern in the ^{1}H NMR of the crude mixture we confirmed that the mono-alkylated product **2.31** was the major species present, subsequent purification by silica gel column chromatography gave carbonyl **2.31** in 72 % yield. To the best of our knowledge, this is the first example of an alkylation of a cubyl ketone.

Referring to the work by the Gosselin group, in their study the tertiary alcohol (1SR, 2SR)-(±)-**2.23** was prepared by the addition of 4-iodophenylmagenisum iodide to carbonyl **2.22** (95 % yield, 98:2 dr, Scheme 30a).[157] In a latter step, the ethoxy(dimethylamino) side chain was introduced by a late-stage copper-catalysed C-O cross-coupling between iodo-arene **2.24** (1 eq) and *N*,*N*-dimethyl-2-hydroxyethylamine (4 eq) in *n*-butyronitrile (Ullmann type reaction). *n*-Butyronitrile typically favours *O*-arylation using amino alcohols and its high boiling point (117 °C) allows the reaction to be performed at elevated temperatures.[157, 171] The Gosselin group performed the C-O

cross-coupling at 110 °C for 53 hours, which gave (*Z*)-tamoxifen in 96 % with *Z*/*E* ratio of 97:3 (Scheme 30a).[157]

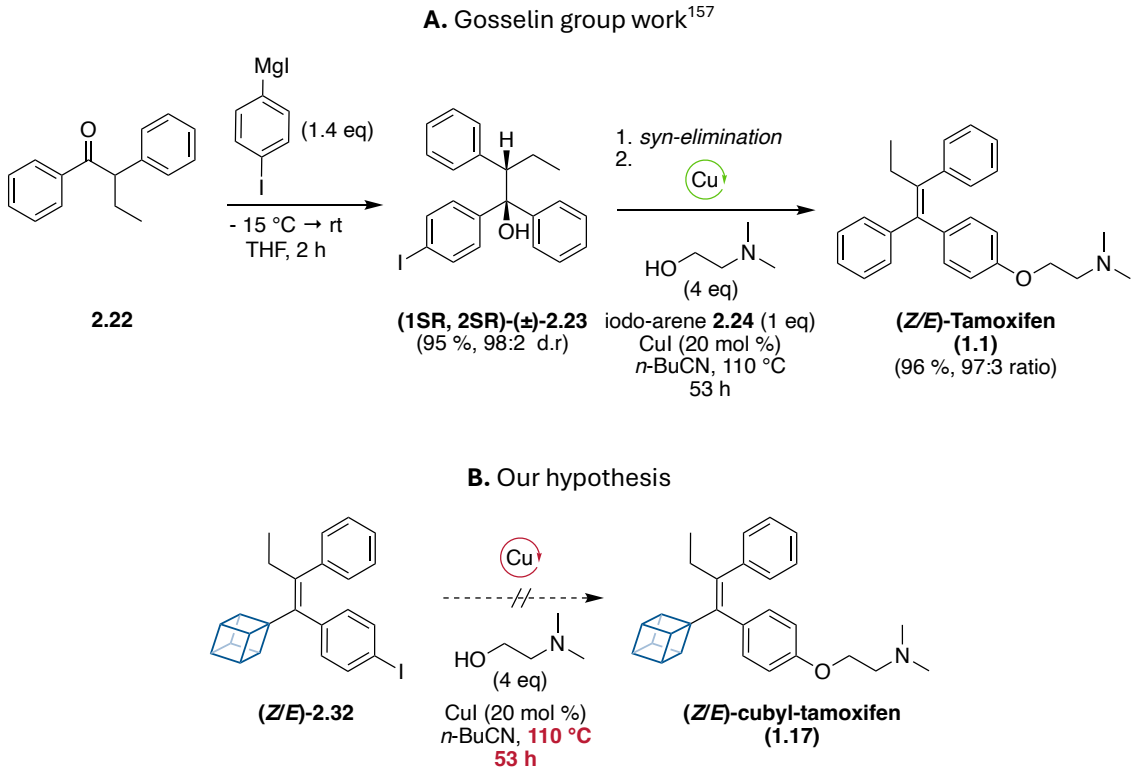

Scheme 30: Deviation from Gosselin group approach required to synthesise cubyl-tamoxifen (**1.17**).

In our studies the late-stage copper-catalysed C-O cross-coupling would be unfavourable, due to evidence in the literature demonstrating the tendency of cubanes to rearrange in the presence of transition metals.[158-160] The MacMillan group have shown that the cubane scaffold was stable in a copper-mediated C-N and C-C cross-coupling with no observation of cubane decomposition, however in these reactions the cubane scaffold was only in solution with the transition metal catalyst for 1 hour at room temperature.[88] Whereas, the Ullmann type reaction in our study would require much harsher conditions, with the cubane olefin (*Z*/*E*)-**2.32** being heated in the presence of CuI at 110 °C for 53 hours (Scheme 30b).[157] Based on this information we opted to deviate from the Gosselin approach and install the ethoxy(dimethylamino) side chain on the aryl ring of 4-bromophenol (**2.33**) before the organometallic reaction, therefore eliminating the cross-coupling reaction altogether (Scheme 31).

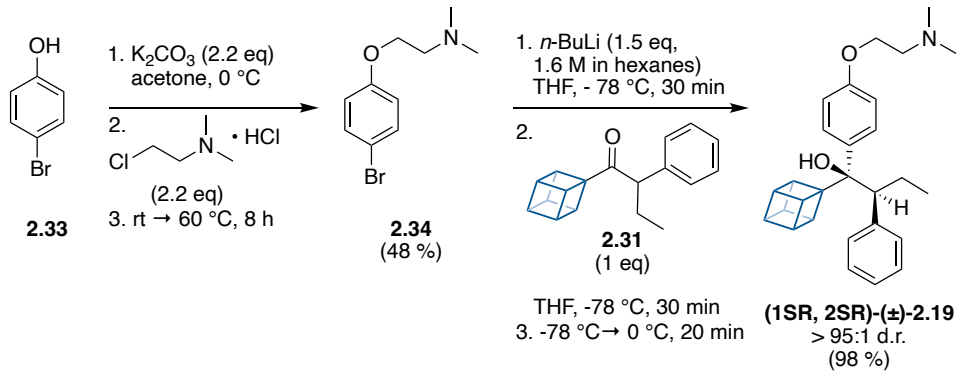

Scheme 31: Synthesis of cubylmethanol **2.19** via 1,2-addition of an aryl organolithium.

Alkylation of 4-bromophenol (**2.33**, 1 eq) with 2-chloro-*N*,*N*'-dimethylethylamine hydrochloride (1.2 eq), in the presence of the base K_2CO_3 (2.2 eq) in refluxing acetone gave pure arylbromide **2.34** after an acid/base work-up in a yield of 48 % (Scheme 31). Formation of the Grignard derived from arylbromide **2.34** was challenging, even when the magnesium turnings were pre-activated with iodine or 1,2-dibromoethane. Therefore, we preferred to use halogen-lithium exchange of **2.34** with *n*-butyl lithium (1 eq, 1.6 M in hexanes) at - 78 °C in THF, this method easily and reliably generated the required aryllithium species. 1,2-Addition of the freshly prepared aryllithium reagent (~ 1.5 eq) into carbonyl **2.31** (1 eq) at - 78 °C, followed by warming the reaction to 0 °C resulted in full consumption of carbonyl **2.31** within 20 minutes. ^{1}H NMR analysis of the crude mixture revealed the 1,2-nucleophilic addition into carbonyl **2.31** led to the formation of cubylmethanol (1SR, 2SR)-(±)-**2.19** as the major diastereoisomer (> 95:1 d.r.). Purification of the crude mixture by silica gel column chromatography gave (1SR, 2SR)-(±)-**2.19** in an excellent yield of 98 % with the same diastereomeric ratio > 95:1 d.r. An X-ray of crystalline (1SR, 2SR)-(±)-**2.19**, grown by the slow evaporation of DCM over one week, confirmed the stereochemical assignment of (1SR, 2SR)-(±)-**2.19** as shown in Scheme 32b.

A. Major diastereoisomer isolated by the Gosselin group.

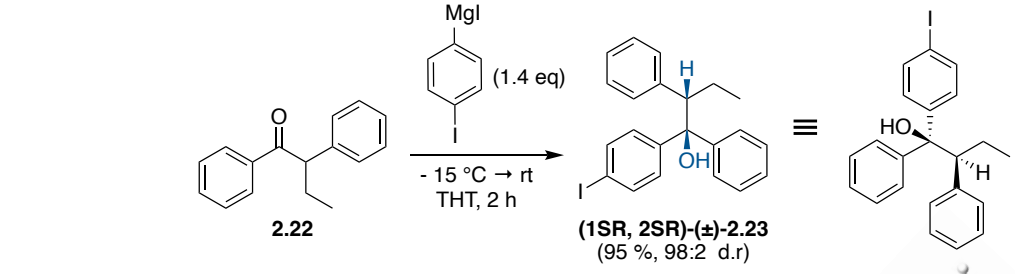

2.22

(1SR, 2SR)-(±)-2.23
(95 %, 98:2 d.r)

B. Major diastereoisomer in our work.

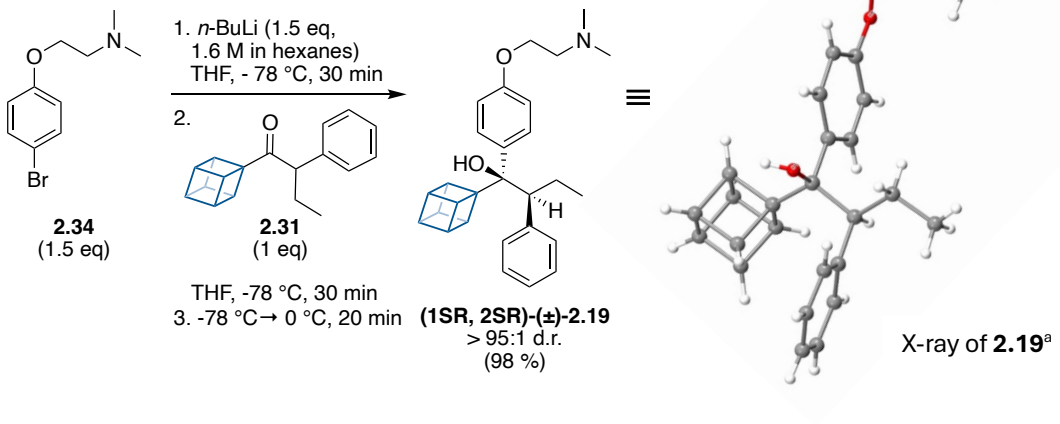

2.34
(1.5 eq)

2.31
(1 eq)

(1SR, 2SR)-(±)-2.19
> 95:1 d.r.
(98 %)

X-ray of **2.19**[a]

Scheme 32: Same major diastereoisomer of 1,2-addition of aryllithium into cubyl ketone **2.31** (*our work*) and aryl ketone **2.22** (*Gosselin group*).

[a] *X-ray crystal structure collected by Dr Benson Kariuki (Cardiff University).*

The 1,2-nucleophilic addition reaction was repeated using 1,2-diphenylbutan-1-one (**2.22**), the aromatic analogue of cubane carbonyl **2.31**, to examine if bioisosteric replacement affects the diastereoselectivity of this transformation (Scheme 33a). Using the same conditions, aryl bromide **2.34** (1 eq) was treated with *n*-BuLi (1 eq) at - 78 °C in THF to prepare the respective aryllithium reagent. The 1,2-addition of the aryllithium (1.5 eq) to 1,2-diphenylbutan-1-one (**2.22**, 1 eq) gave the tertiary alcohol (1SR, 2SR)-(±)-**2.35a** in a moderate yield of 58 % with a >95:1 dr. Based on the chemical shift of the aryl protons *ortho* to (dimethylamino)ethoxy side chain being δ 6.94 – 6.87 (m, 2H), we were able to assign the structure of the major diastereoisomer as shown in Scheme 33a, which is consistent with the spectroscopic data reported by McCague *et al* and Sohár *et al* when performing the same reaction (Scheme 33b).[121, 172] Overall, this experiment demonstrated the 1,2-addition of aryllithium reagent, derived from arylbromide **2.34**, to

the aromatic and cubane carbonyl proceeded with the same diastereoselectivity. Preparation of the alterative diastereoisomer (1SR, 2RS)-(±)-**2.35b** can be achieved by treating 1-(4-(2-(dimethylamino)ethoxy)phenyl-2-phenylbutan-1-one with phenylmagnesium bromide (Scheme 33b).[121]

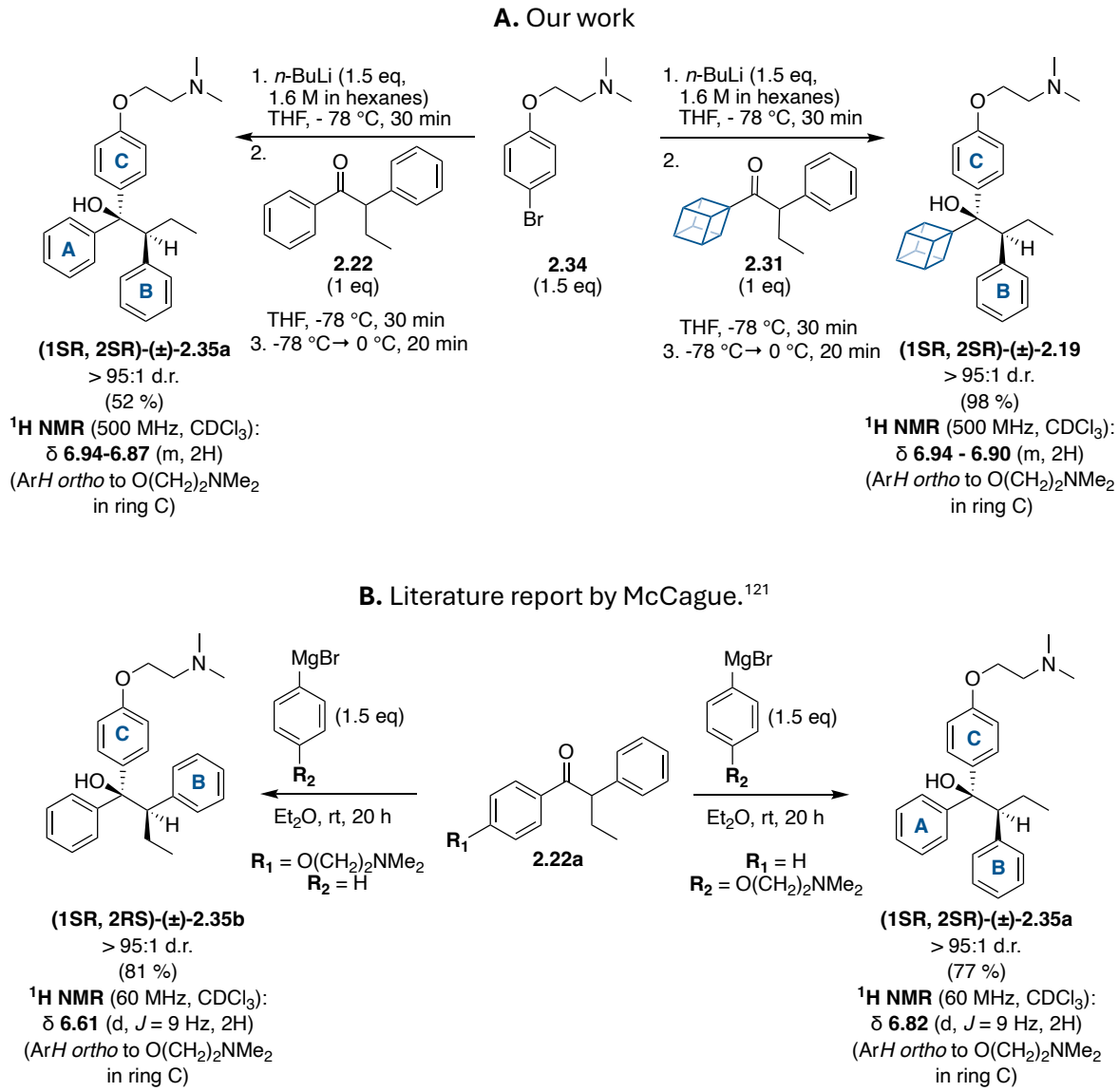

Scheme 33: Diastereoselectivity for the 1,2-nucleophilc addition into carbonyl **2.22** and **2.31**.

2.2.2.2.3 *Syn*-elimination of cubylmethanol 2.19

The next objective was to examine the *syn*-elimination of cubylmethanol (1SR, 2SR)-(±)-**2.19**, although to save this valuable precursor we began by testing the elimination

conditions reported by the Gosselin group using the tertiary alcohol (1SR, 2SR)-(±)-**2.35a** as the model substrate (Scheme 34). Treatment of (1SR, 2SR)-(±)-**2.35a** (1 eq) with diphenylphosphoryl chloride (1.5 eq) and NaHMDS (3 eq) in 1,4-dioxane for 16 hours at 45 °C, gave a *Z*/*E* mixture of tamoxifen (**1.1**). Due to overlapping signals in the ^{1}H NMR of the crude mixture we were unable to determine the ratio of geometric isomers. After purification by silica gel column chromatography (silica pre-treated with triethylamine) we were able to confirm (*Z*)-tamoxifen was predominately formed in 3:1 *Z*/*E* ratio (Scheme 34a).

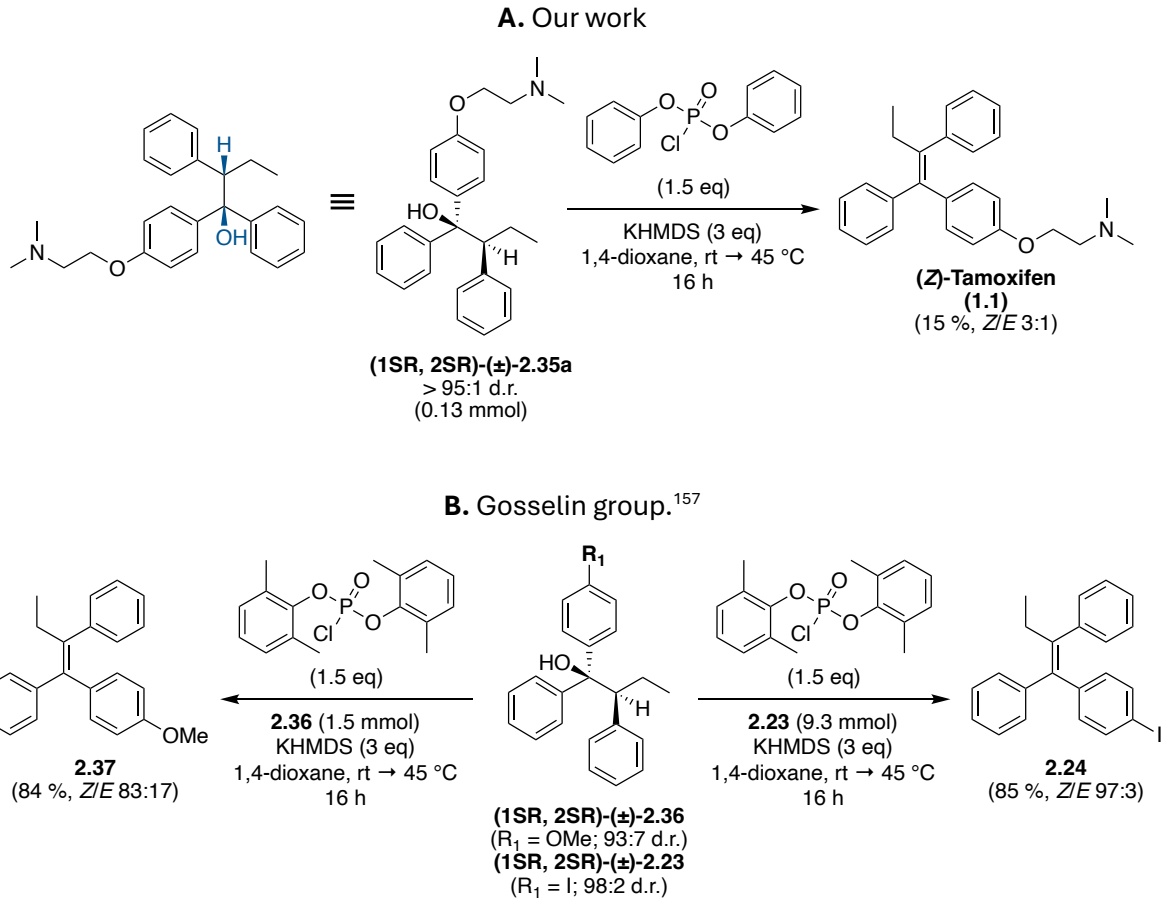

Scheme 34: *Syn*-elimination of tertiary alcohols via a phosphate intermediate.

We were pleased with the stereoselectivity of (*Z*/*E*)-tamoxifen we obtained (3:1 respectively), as the Gosselin group also found when electron rich arenes were employed the elimination was less selective. For instance, the elimination of (1SR, 2SR)-(±)-**2.36** resulted in a 83:17 mixture of the *Z*/*E*-isomers (Scheme 34b).[157] Despite

our model substrate (1SR, 2SR)-(±)-**2.35a** having a comparable *Z*/*E*-stereoselectivity the yield was only 15 %, compared to the Gosselin group reporting a 84 % yield for the methoxy analogue (1SR, 2SR)-(±)-**2.37** under similar reaction conditions. The poor yield for our transformation may explain why the Gosselin group opted to perform the elimination on the 4-iodo-substituted arene (**2.23**) which proceeded with a much improved stereoselectivity (*Z*/*E* 97:3, Scheme 34b) and yield (85 %), followed by the installation of the (dimethylamino)ethoxy side chain through a copper-mediated cross-coupling at the final step.[157] However, as explained previously we did not want to install the (dimethylamino)ethoxy side chain via a cross-coupling reaction due to the instability of the cubane motif in the presence of transition metals, particularly at elevated temperatures for prolonged reaction times (110 °C for 53 hours).[158-160]

Despite the low yield for the elimination reaction on our model aromatic substrate (1SR, 2SR)-(±)-**2.35a**, we opted to trial the elimination reaction on cubylmethanol (1SR, 2SR)-(±)-**2.19** under identical reaction conditions (Scheme 35). When monitoring the reaction by TLC no non-polar spots which would correlate to (*Z*/*E*)-cubyl-tamoxifen **1.17** were observed. Analysis of the ^{1}H NMR of the crude mixture appeared to include unreacted alcohol (1SR, 2SR)-(±)-**2.19**, although based on the noisy baseline particularly between 1-4 ppm we could not be certain (Figure 11).

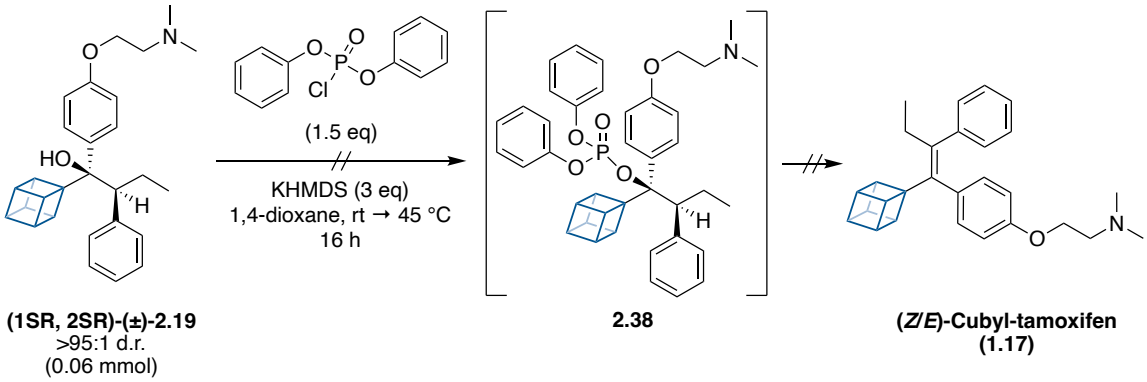

(1SR, 2SR)-(±)-2.19
>95:1 d.r.
(0.06 mmol)

2.38

(*Z*/*E*)-Cubyl-tamoxifen (1.17)

Scheme 35: Attempted elimination of cubylmethanol **2.19** via phosphate intermediate **2.38**.

Overall, the ^{1}H NMR of the crude product demonstrated that (1SR, 2SR)-(±)-**2.19** was more fragile than our aromatic model substrate (1SR, 2SR)-(±)-**2.35a** to the elimination

conditions, which aligns with our initial prediction that cubylmethanols may undergo ring-opening under these conditions. One potential pathway for decomposition is by strain-releasing valence bond isomerisation, due to the proximity of the phosphate leaving group to the strained cubane framework.

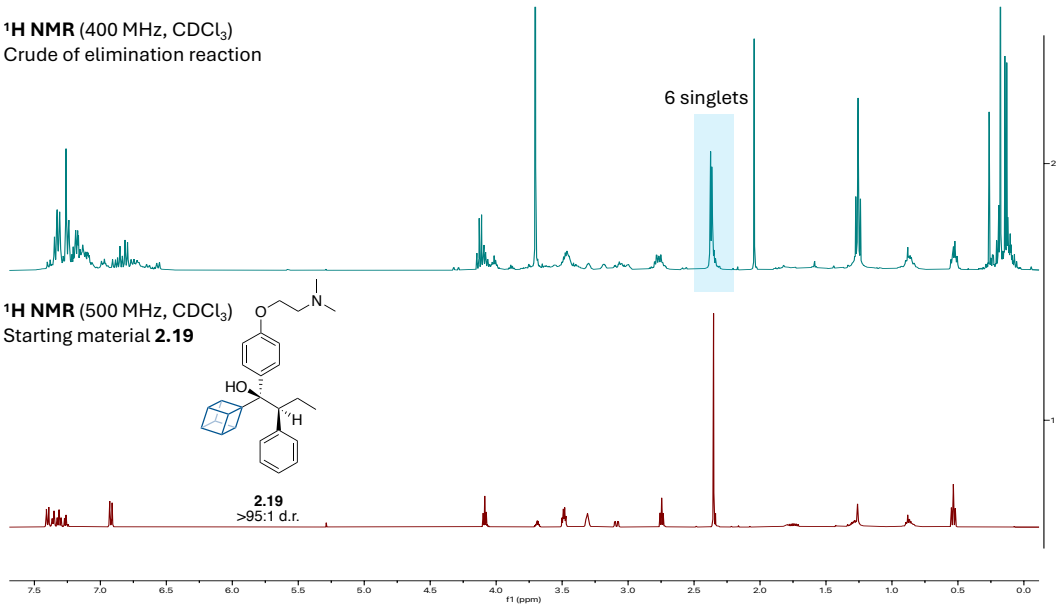

Figure 11: ^{1}H NMR overlay of cubylmethanol **2.19** and the *syn*-elimination crude mixture.

Despite no indication of olefin formation in the ^{1}H NMR of the crude, electrospray ionisation mass spectrometry included signals that matched the phosphate intermediate **2.38** ($[M+H]^+$ m/z = 648.29) and the final product **1.17** ($[M+H]^+$ m/z = 398.25), in addition to the starting material **2.19** ($[M+H]^+$ m/z = 416.26) (Figure 12). Based on the mass spectroscopy data indicating the presence of product **1.17** and phosphate intermediate **2.38** the crude product was purified by silica gel column chromatography, which gave an inseparable mixture of compounds. Examination of the isolated mixture by ^{1}H NMR (300 MHz, $CDCl_3$) revealed two singlets in a 1:1 at 2.44 ppm and 2.42 ppm (Figure 13 – highlighted in blue). In the starting material (**2.19**, d.r >95:1) the two-methyl groups in the (dimethylamino)ethoxy side chain appear as a singlet at 2.35 ppm in the ^{1}H NMR (500 MHz, $CDCl_3$) (Figure 11), whilst under the *syn*-elimination reaction conditions we would not expect interconversion of the two diastereoisomers of **2.19**. Therefore, we propose the isolated mixture contains the starting material **2.19** and phosphate intermediate **2.38** (Figure 13).

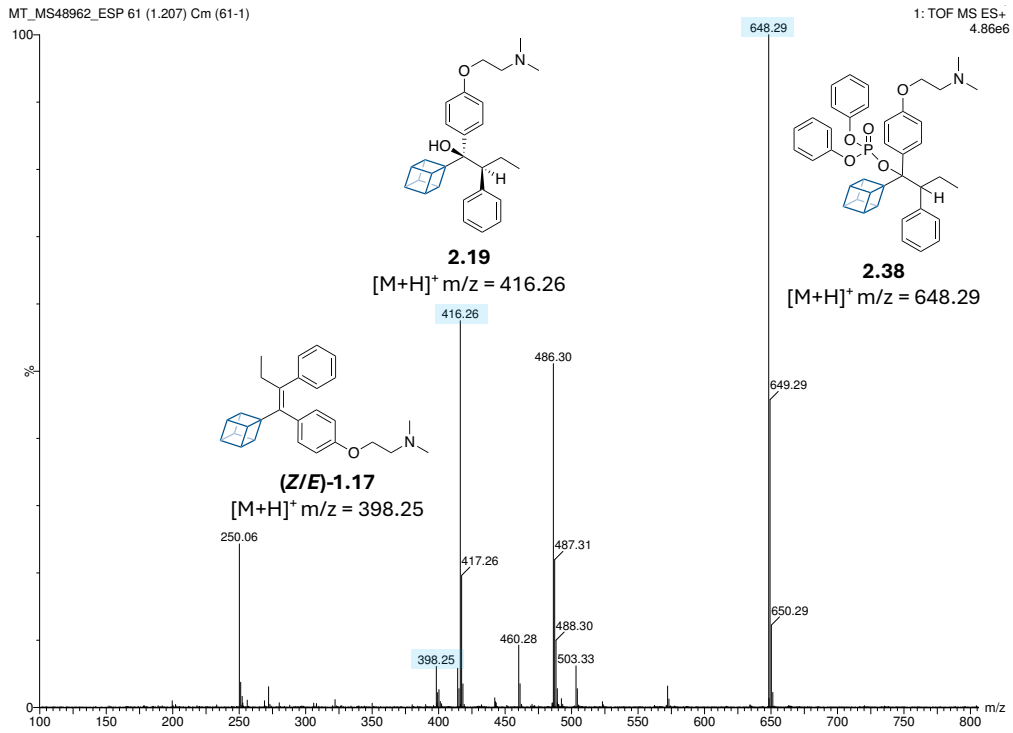

Figure 12: LRMS (ESI$^+$) spectrum of the crude mixture for the *syn*-elimination of cubylmethanol **2.19**.

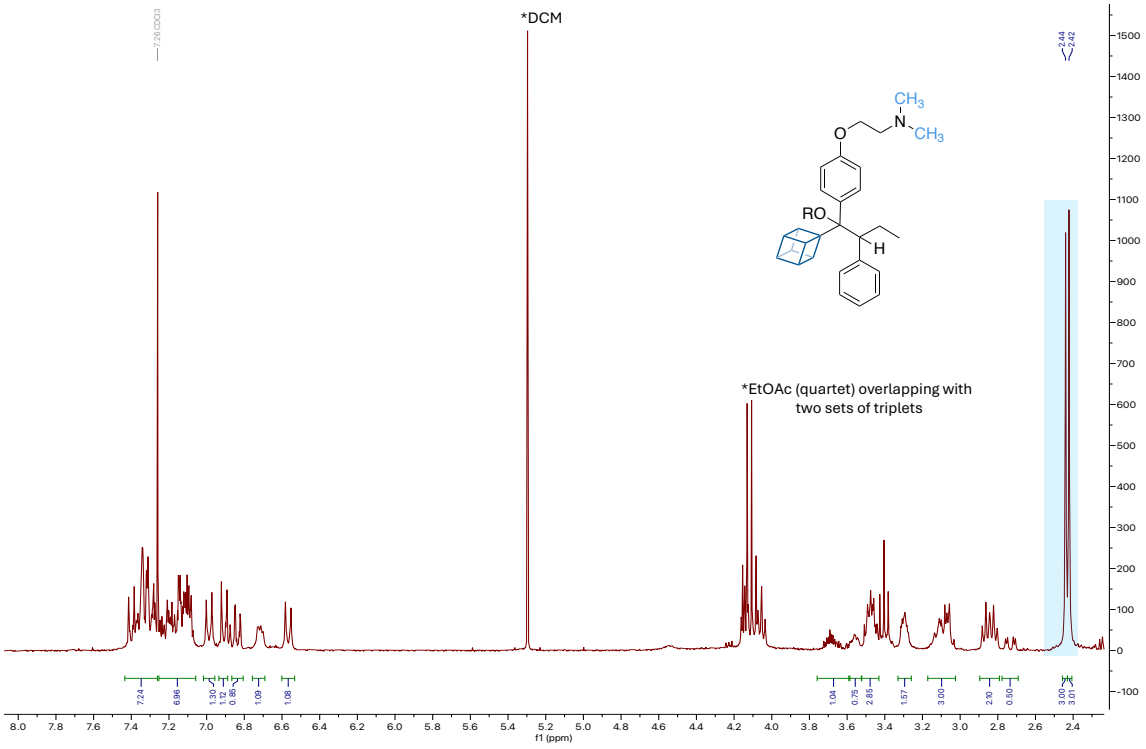

Figure 13: ^{1}H NMR (300 MHz, $CDCl_3$) of isolated mixture post purification from the *syn*-elimination of cubylmethanol **2.19**.

Ultimately, the *syn*-elimination of cubylmethanol **2.19** via a phosphate intermediate was unsuccessful as we were unable to isolate any of the final product cubyl-tamoxifen **1.17** using this synthetic approach.

2.2.2.2.4 Additional elimination studies

In the previous section the treatment of our aromatic model substrate (1SR, 2SR)-(±)-**2.35a** with NaHMDS (3 eq) and diphenyl phosphoryl chloride (1.5 eq) in 1,4-dioxane at 45 °C gave the desired product (*Z*/*E*)-tamoxifen (**1.1**) in 15 % yield (Table 15, entry 1).

Table 15: Elimination optimisation for aromatic model substrate **2.35a**.

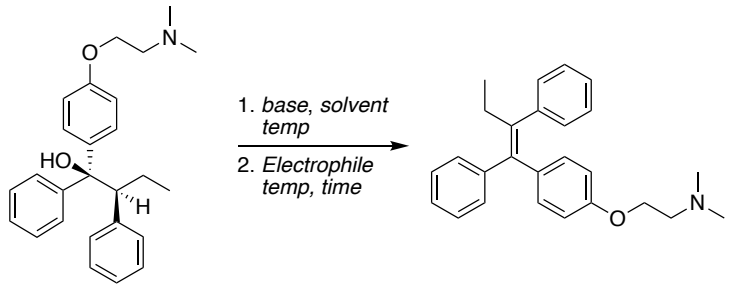

(1SR, 2SR)-(±)-2.35a
> 95:1 d.r.

(*Z*)-Tamoxifen (1.1)

Entry	Base (eq)	Electrophile (eq)	Solvent	Temp / °C	Time / h	Yield of 1 / %[b]	(*Z*/*E*) ratio[c]
1	NaHMDS[d] (3)	diphenyl phosphoryl chloride (1.5)	1,4-dioxane	rt → 45	16	15	3:1
2	NaHMDS[d] (3)	tosyl chloride (1.5)	1,4-dioxane	rt → 45	16	0	-
3	NaH[e] (1.2)	tosyl chloride (1.2)	THF	rt → 45	5	0	-
4	Pyridine (1.2)	tosyl chloride (1.2)	DCM	rt → rt	5	0	-
5[a]	*n*-BuLi[f] (1.1)	TFAA[g] (2)	THF	-78 to rt	1	60	5:1
6	*n*-BuLi[f] (1.1)	Ac_2O[h] (2)	THF	-78 to rt	1	35	2:1
7	*n*-BuLi[f] (1.1)	benzyl chloride (2)	THF	-78 to rt	4	4	1:1

[a] Optimised reaction conditions. [b] Isolated yield. [c] Determined by ^{1}H NMR. [d] Sodium bis(trimethylsilyl) amide (2 M in THF). [e] Sodium hydride (60 % dispersion in mineral oil). [f] n-Butyl lithium (1.6 M in hexanes). [g] Trifluoroacetic anhydride. [h] Acetic anhydride.

Our optimisation studies began by examining if replacing diphenyl phosphoryl chloride for tosyl chloride, a less sterically hindered electrophile, could enhance the yield of (*Z*/*E*)-tamoxifen. The treatment of (1SR, 2SR)-(±)-**2.35a** (1 eq) with NaHMDS (3 eq) and tosyl chloride (1.5 eq) in 1,4-dioxane unfortunately resulted in no formation of (*Z*/*E*)-tamoxifen, despite heating the reaction at 45 °C for 16 hours (Table 15, entry 2). Furthermore, no product formation was observed by ^{1}H NMR analysis when employing the base sodium hydride (1.2 eq) or pyridine (1.2 eq) in the presence of alcohol (1SR, 2SR)-(±)-**2.35a** (1 eq) and tosyl chloride (1.5 eq) (entry 3-4 respectively).

Leh and co-workers developed a continuous flow protocol to synthesise (*Z*/*E*)-tamoxifen (**1.1**) using commercially available precursors, with equipment designed to withstand organometallic chemistry (Scheme 36).[173] In the protocol a stream of a freshly prepared aryl lithium, formed by treating aryl bromide **2.34** with *n*-BuLi (1.1 eq), was mixed with a stream of ketone **2.22** to give the lithium alkoxide **2.39**. A subsequent input stream of trifluoroacetic anhydride, followed by triethylamine at an elevated temperature of 100 °C and under 7 bar of pressure gave (*Z*/*E*)-tamoxifen.

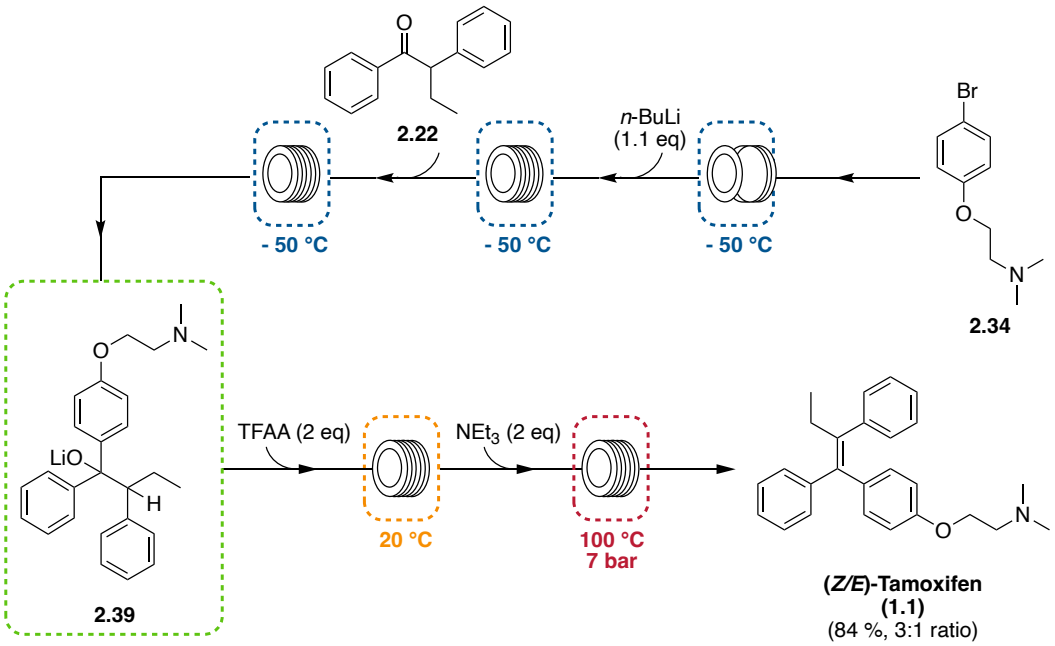

Scheme 36: Leh *et al* continuous-flow method to synthesise (*Z*/*E*)-tamoxifen, by the treatment of lithium alkoxide **2.39** with trifluoroacetic anhydride.[173]

Inspired by this work we treated a solution of (1SR, 2SR)-(±)- **2.35a** in THF at - 78 °C with *n*-BuLi (1.1 eq, 1.6 M in hexanes), followed by the addition of trifluoroacetic anhydride (2 eq) at room temperature (Table 15, entry 5). Notably, we opted to use milder reaction conditions compared to Leh and co-workers (room temperature at atmospheric pressure verses 100 °C under 7 bar) and without the addition of triethylamine. Pleasingly, under the adapted conditions described (*Z*/*E*)-tamoxifen was isolated in a 5:1 ratio and yield of 60 % (entry 5). Interestingly, the *Z*/*E* ratio of tamoxifen in our study (5:1) was greater than Leh and co-workers (3:1), despite our protocol deviations. Replacing trifluoroacetic anhydride for acetic anhydride decreased the yield to 35 % and reduced the stereoselectivity for the formation of the desired *Z*-geometric isomer to 2:1 (*Z*/*E*)-tamoxifen (entry 6). Switching trifluoroacetic anhydride for benzyl chloride resulted in no stereoselectivity, giving a 1:1 ratio of (*Z*/*E*)-tamoxifen in a very poor yield of 4 %. Based on the optimisation experiments for the aromatic model substrate (1SR, 2SR)-(±)-**2.35a**, we opted to subject cubylmethanol (1SR, 2SR)-(±)-**2.19** to the optimised reaction conditions in Table 15, entry 5 (Scheme 37).

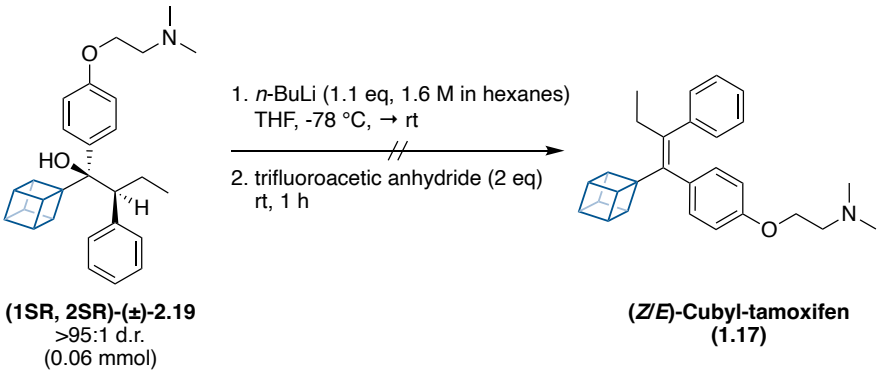

(1SR, 2SR)-(±)-2.19
>95:1 d.r.
(0.06 mmol)

(*Z*/*E*)-Cubyl-tamoxifen
(1.17)

Scheme 37: Elimination of cubylmethanol **2.19** via trifluoroacetate intermediate.

Similar to our earlier studies on the elimination of cubylmethanol (1SR, 2SR)-(±)-**2.19**, in the LRMS (ESI$^+$) of the crude mixture we observed signals that matched cubylmethanol **2.19** ([M+H]$^+$ m/z = 416.26), the trifluoroacetate intermediate **2.40** ([M+H]$^+$ m/z = 512.24) and the desired product (*Z*/*E*)-cubyl-tamoxifen **1.17** ([M+H]$^+$ m/z = 398.25) (Figure 14). Unfortunately, only the starting material **2.19** and signals likely a result of **2.19** decomposition were observed in ^{1}H NMR of the crude product. After silica gel column

chromatography 37 % of (1SR, 2SR)-(±)-**2.19** was recovered and desired product **1.17** was not isolated. Repeating the reaction with the addition of triethylamine, similar to Leh and co-workers, did not change the reaction outcome.

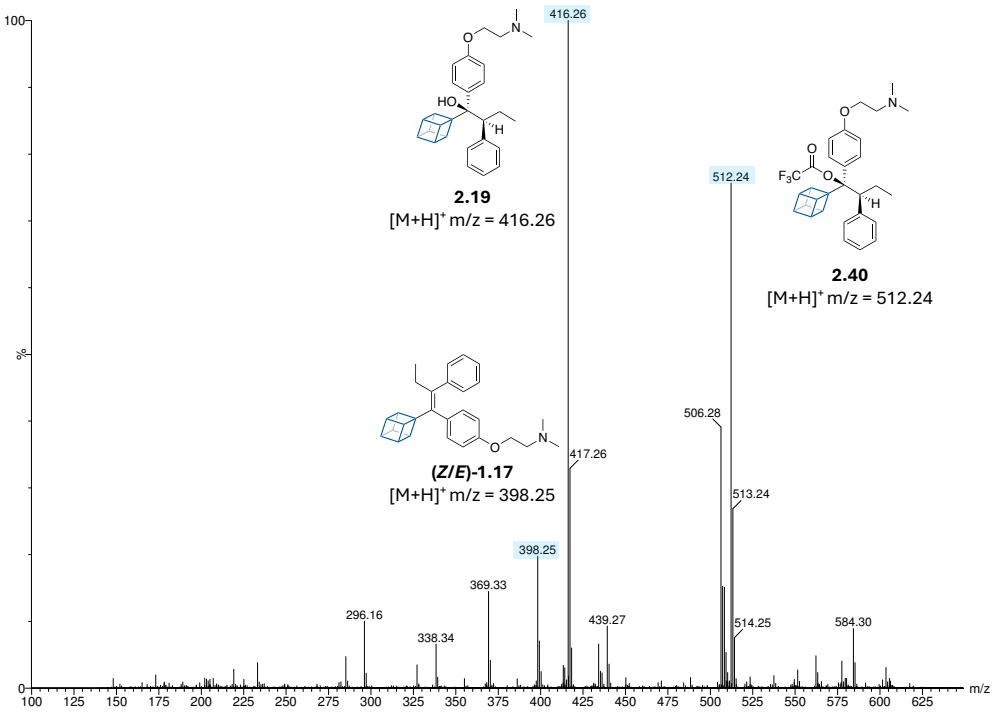

Figure 14: LRMS (ESI$^+$) spectrum of the crude mixture for the elimination of cubylmethanol **2.19** via a trifluoroacetate intermediate.

Based on these results, we redirected our efforts to the synthesis of cubylethanol **2.20**. The additional carbon unit between the alcohol moiety and the cubane scaffold in **2.20** could reduce or prevent cubane decomposition pathways during the elimination reaction.

2.2.2.2.5 Synthesis towards cubylethanol 2.20

In the design for the retrosynthetic analysis of cubyl-tamoxifen **1.18**, we first opted to disconnect the olefin bond to reveal the cubylethanol **2.20** (Scheme 38). The alcohol moiety in **2.20** could be accessed from the cubyl ester **2.44** in 4 steps, by a series of aryl organometallic additions, first to a Weinreb amide followed by an aryl organometallic addition to ketone **2.45**. In the forward direction we envisioned that the α-alkylation of

2.43 may afford cubyl ester **2.44**, which to the best of our knowledge has not been reported in the literature. To prepare ester **2.43**, a C-homologated analogue of ester **2.10**, we planned to use a Kowalski homologation procedure previously described by Burton *et al*.[174]

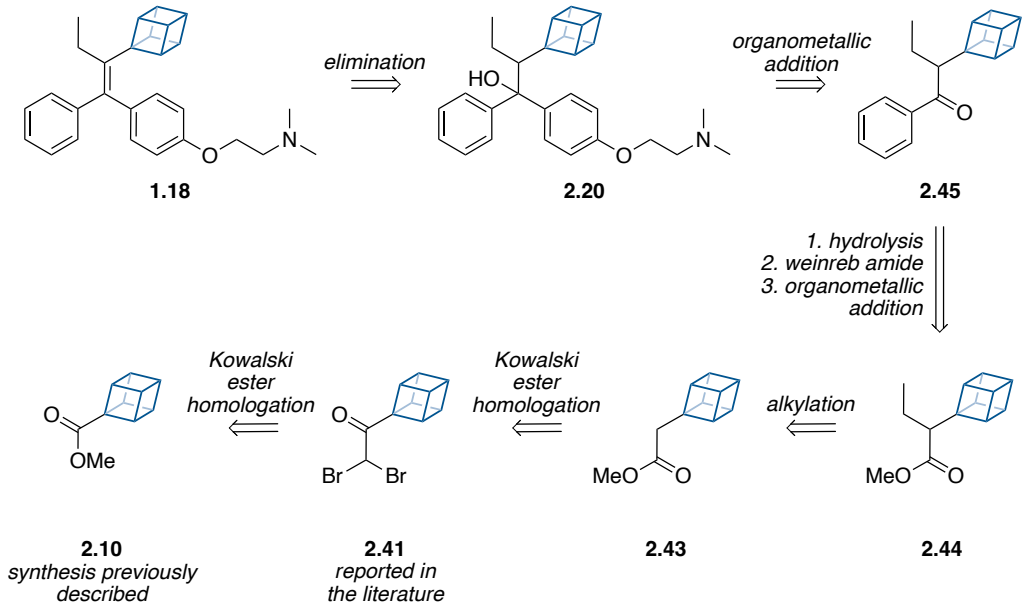

Scheme 38: Retrosynthetic analysis of cubyl-tamoxifen **1.18** via cubylethanol **2.20**.

Our synthesis commenced with methyl cubane-1-carboxylate (**2.10**), that was prepared from commercially available 4-methoxycarbonylcubanecarboxylic acid (**2.8**) in two steps and 66 % overall yield (previously described in **Section 2.2.1.2.2**, Scheme 18). With **2.10** in hand, we set out to prepare cubane acetate **2.43** via a Kowalski homologation reaction following the protocol reported by Burton and co-workers, who described the efficient conversion of **2.10** to **2.42** over two steps in an overall yield of 53 % (Scheme 39a).[174] Burton *et al* reported that when the second step of the Kowalski homologation reaction was quenched with acidic methanol the carboxylic acid **2.42** was isolated, which contradicts other literature sources that states quenching with acidic methanol yields the methyl ester in this reaction.[175, 176]

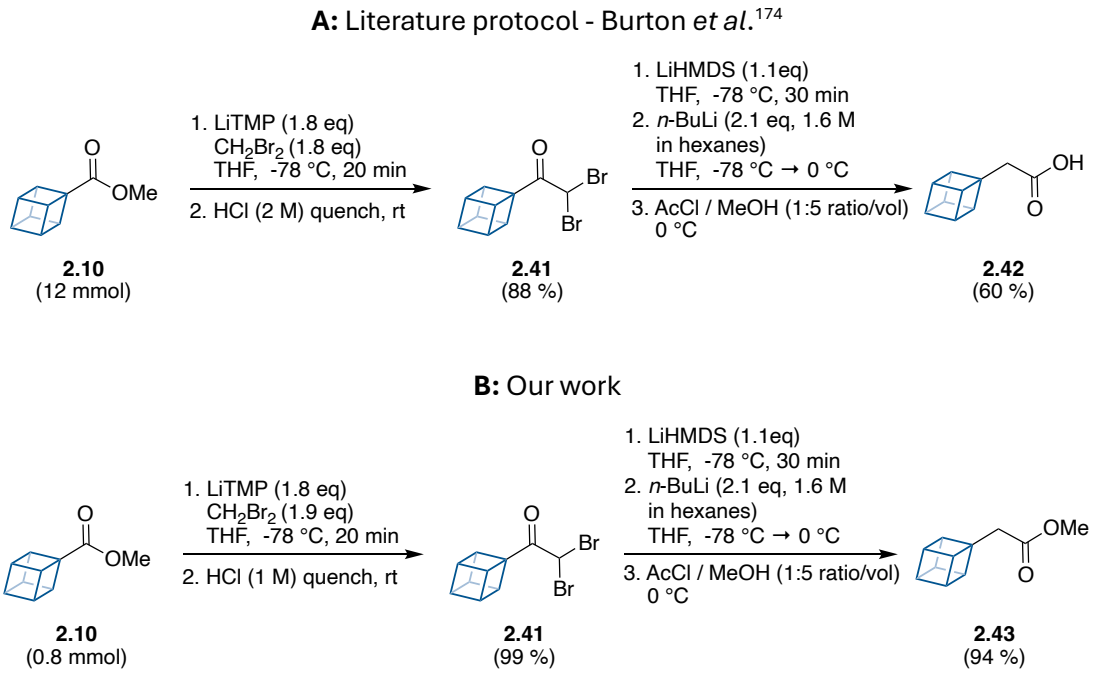

Scheme 39: Kowalski homologation reaction of cubyl ester **2.10.**

In the literature the Kowalski homologation reaction is usually a one-pot reaction in which the dibromide **2.41** is not isolated.[176] However, we opted to follow the protocol by Burton *et al* and perform the two steps independently. In the first step of the Kowalski homologation a solution of **2.10** (1 eq) and dibromomethane (1.8 eq) in THF cooled to -78 °C was added to a solution of lithium tetramethylpiperidide (1.8 eq) in THF at the same temperature, freshly prepared from the treatment of tetramethylpiperidide (2 eq) with *n*-BuLi (1.8 eq) (Scheme 39b). The intermediate was quenched with 1 M HCl to afford the dibromoketone **2.41** in a 99 % yield after extraction of the aqueous layer using hexane. We found **2.41** to be stable at room temperature for at least 5 hours. In the second step, **2.41** (1 eq) was cooled to -78 °C in THF and treated with LiHMDS (1.1 eq) followed by *n*-BuLi (2.1 eq). Quenching the reaction with acidic methanol at 0 °C (prepared from the addition of acetyl chloride to ice cold methanol) gave cubane acetate **2.43** after an aqueous extraction with diethyl ether (Figure 15). This is in contrast to Burton *et al* who isolated the carboxylic acid **2.42** under the same reaction conditions and quenching protocol.[174] Purification of the crude mixture by silica gel column chromatography afforded **2.43** in 94 % yield, which was found to be volatile below 150 mbar at room temperature and therefore should be handled with care.

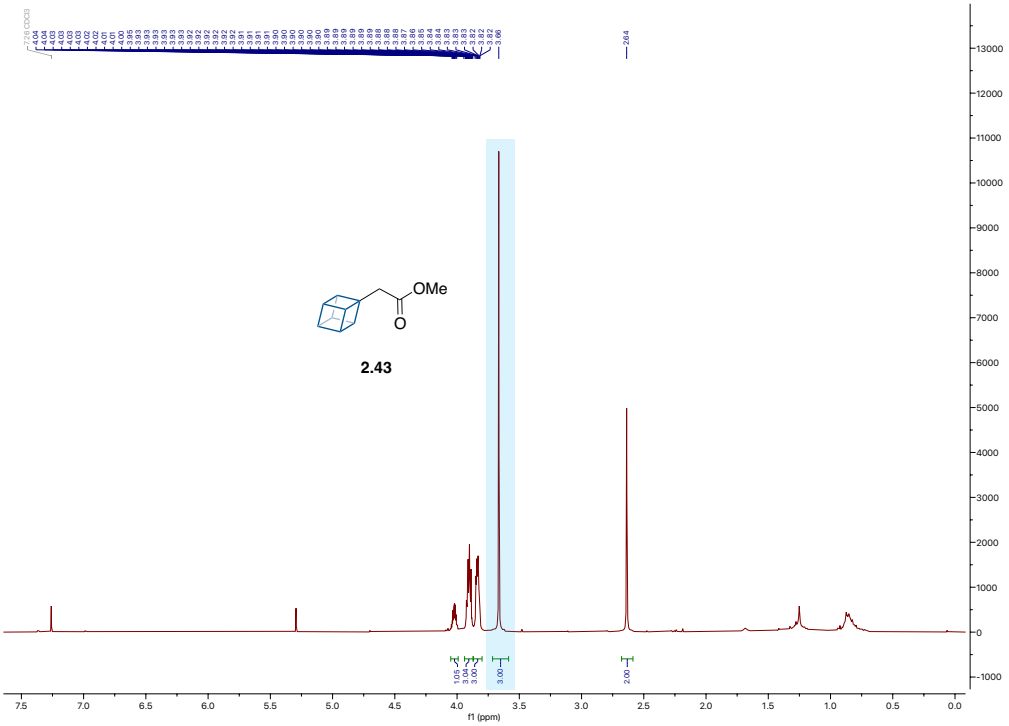

Figure 15: ^{1}H NMR (400 MHz, $CDCl_3$) of ester **2.43** formed in the Kowalski homologation reaction.

*Methyl ester C**H**$_3$ signal highlighted in blue.*

Next, we focused our attention on the α-alkylation of ester **2.43**. In the literature Klunder and Zwanenburg reported that cubane acetate **2.46** was converted into the rearranged products **2.48a** and **2.48b** within 30 minutes, upon treatment with lithium diisopropylamide in THF at - 30 °C (Scheme 40a).[177] It was found refluxing this mixture in benzene converted **2.48a** and **2.48b** into a tricyclooctatriene **2.50a** and tricyclooctatetraene **2.50b** respectively. Similar results were obtained when cubane methylcyanide **2.47** was subjected to the same conditions.[177] On the other hand, Chi reported the treatment of 1,4-bis(nitromethyl)cubane **2.52** with sodium methoxide, followed by the addition of either CH_3OD or bromine at room temperature gave **2.53** and **2.54** respectively (Scheme 40b).[178] In both these examples it is assumed the reaction proceeded via the nitro-stabilised cubylcarbinyl anion intermediate (**2.52a**), without any ring opening product formation. Therefore, we were intrigued if the cubylcarbinyl anion of cubane acetate **2.43** would be more stable if generated at a lower temperature of - 78 °C, which upon treatment with iodoethane would give the desired α-alkylated product **2.44** (Scheme 40c).

A: Base induced cubane ring opening via cubylcarbinyl anion - Klunder and Zwaneburg.[177]

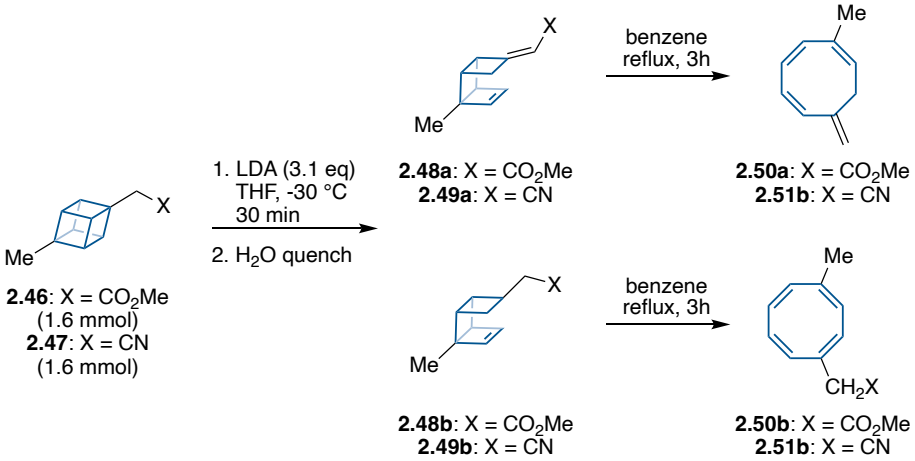

B: Hydrogen/deuterium exhange and bromination via cubylcarbinyl anion - Chi.[178]

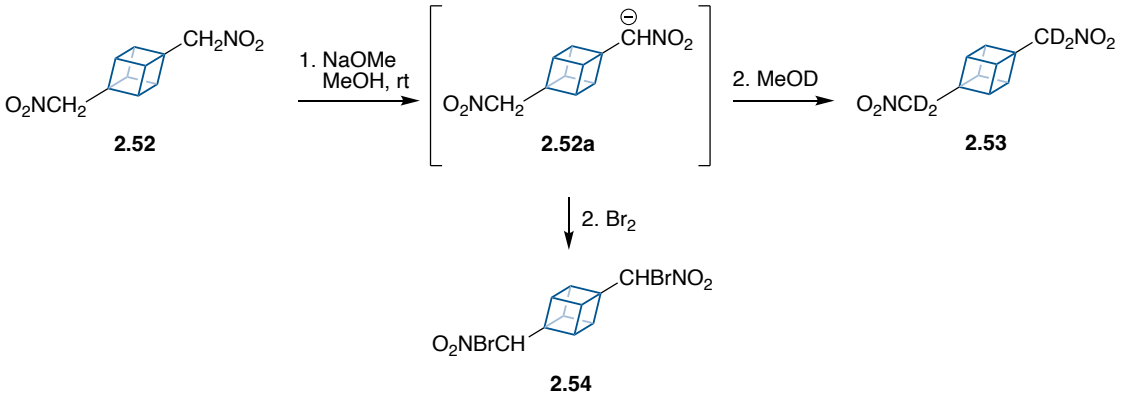

C: Our test conditions for the α-alkylation of **42**.

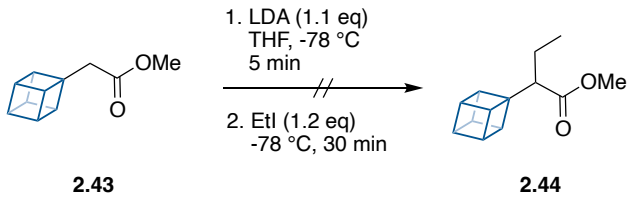

Scheme 40: Cubylcarbinyl anion formation.

A trial reaction was performed in which freshly prepared lithium diisopropylamide (1.1 eq) was added to a solution of cubane acetate **2.43** (1 eq) in THF cooled to - 78 °C, which turned the solution from colourless to yellow (Scheme 40c). After 5 minutes, iodoethane was added to the reaction, followed by stirring at - 78 °C for 30 minutes before quenching the reaction with a saturated solution of ammonium chloride. By TLC analysis, cubane acetate **2.43** (R_f **2.43** = 0.4 using 5 % EtOAc/hexane) was fully consumed with two new spots visible using a $KMnO_4$ stain (R_f = 0.45 and R_f = 0.3 using 5

% EtOAc/hexane). Based on the ^{1}H NMR of the crude, we could confirm the rearranged products in Scheme 40a were not present due to the absence of olefinic protons between 5 - 7 ppm (Figure 16, highlighted in green). In addition, we believe the compound isolated had the cubane scaffold intact, based on multiplet and integration pattern present in ^{1}H NMR being consistent with monosubstituted cubanes (Figure 16, highlighted in blue).[179] However, we were uncertain which substituent was attached to the cubane framework, as the OC***H***$_3$ signal in methyl ester group only had an integration value of 1 (Figure 16, highlighted in red). In addition, if the α-alkylation was successful a chiral centre would have formed and the protons in the C***H***$_2$ group would be diastereotopic and have a distinctive resonance pattern, which was not observed in the crude ^{1}H NMR spectrum. The ESI$^+$ LRMS of the crude was also inconclusive.

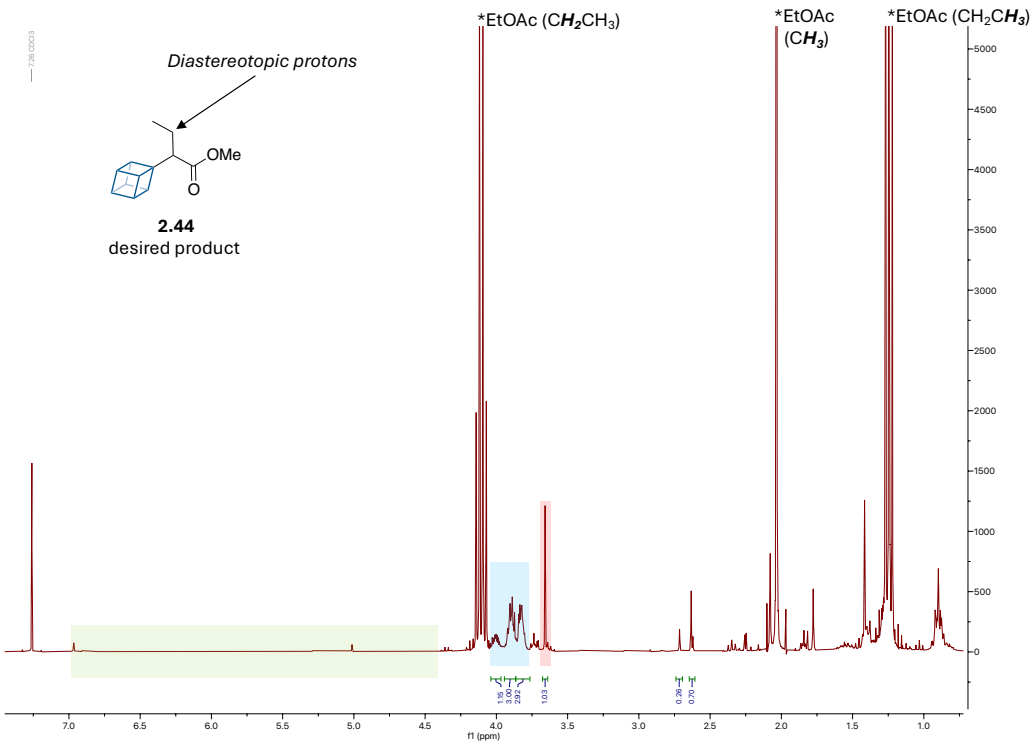

Figure 16: Crude ^{1}H NMR (300 MHz, $CDCl_3$) of the α-alkylation of cubane acetate **2.43** with iodoethane.

Considering this information, we decided to purify the crude mixture by silica gel column chromatography to isolate the individual species, however despite our best efforts the two isolated compounds still could not be identified. Overall, we can conclude that the trial α-alkylation of ester **2.43** was unsuccessful at the lower

temperature of - 78 °C and the products isolated are not consistent with those reported by Klunder and Zwanenburg for a similar transformation (Scheme 40a). On this basis, we decided to consider an alternative approach to give cubane analogues of (*Z*/*E*)-tamoxifen. At the start of this section the methodologies for cubane cross-couplings were introduced, with cubane arylations the most widely reported. We envisioned that we could use one of those cross-coupling protocols to couple cubane to a tetra-substituted bromoalkene species. The major advantage of this approach includes a late-stage functionalisation of the cubane scaffold, compared to this organometallic approach in which we slowly built-up functionality around the cubane scaffold.

2.2.3 Route 3: Cross-coupling approach

2.2.3.1 Literature

To the best of our knowledge there is no general methodology for the metal-mediated alkenylation of cubanes. Although, the metal-mediated arylation of cubane redox-active esters have been reported, including the Ni-mediated by the Senge group[163], Fe-mediated by the Baran group[162] and Cu-mediated by the MacMillan group[88] (Scheme 41). These cross-coupling reactions for cubane rely on activating the carboxylic acid as their redox-active ester derivatives, either as the *N*-hydroxyphthalimide (**2.9**) or the *N*-hydroxy-tetrachlorophthalimide (**2.9a**).

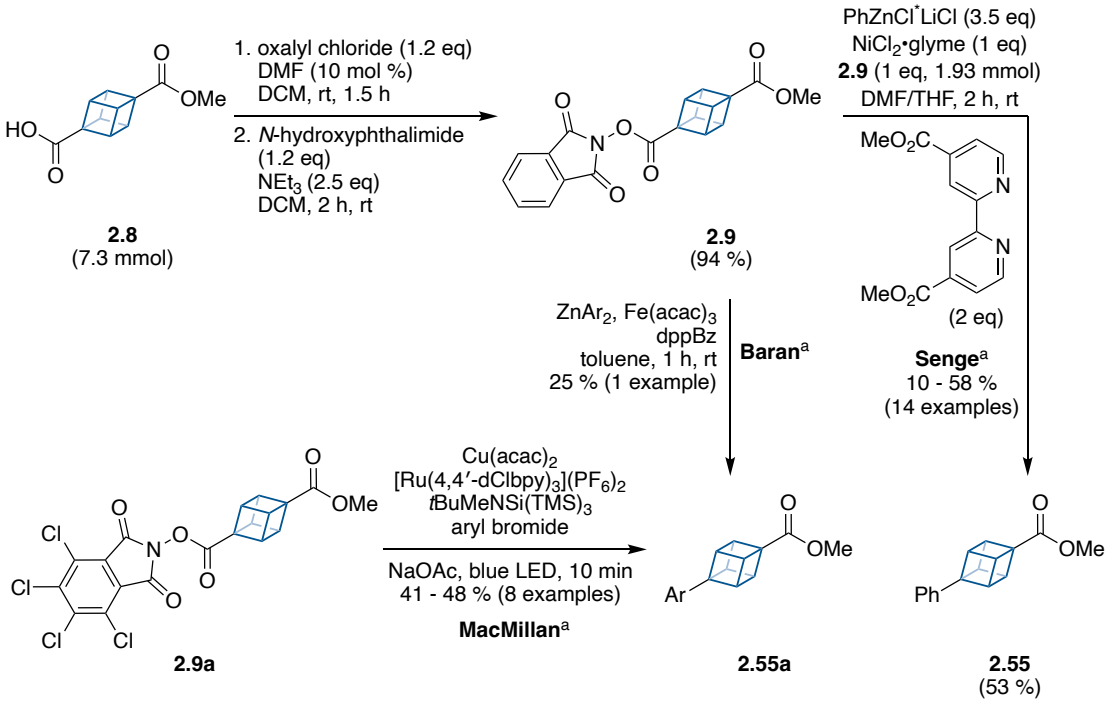

Scheme 41: Metal-mediated arylation of cubane.

[a] *Literature methods for metal-mediated C-C cross-coupling arylations for cubane.*[88, 162, 163]

We opted to explore the Ni-mediated cubane cross-coupling conditions reported by Senge *et al*, as the substrate scope in this methodology included three examples of cubane cross-coupling to a porphyrin system.[163] In these examples, the organozinc of the iodo-porphyrin was synthesised and cross-coupled to the cubane redox-active ester **2.9** (Scheme 42a).[163] Based on this report, we considered if the tetra-substituted bromoalkene **2.58** could also cross-couple to the cubane redox-active ester **2.9** under similar reaction conditions (Scheme 42b).

A: Cross-coupling between cubane and porphyrins – Senge group. [163]

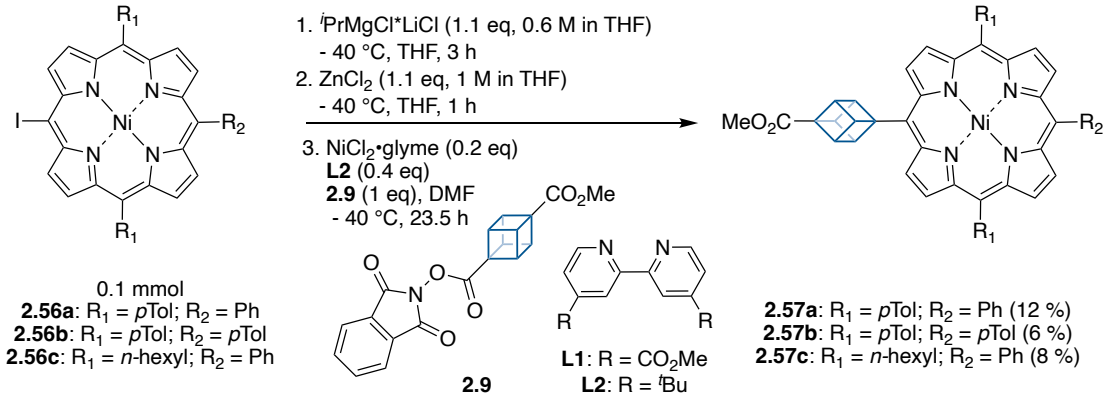

B: Proposed forward synthesis: Cross-coupling between cubane **2.59** and olefin **2.58**.

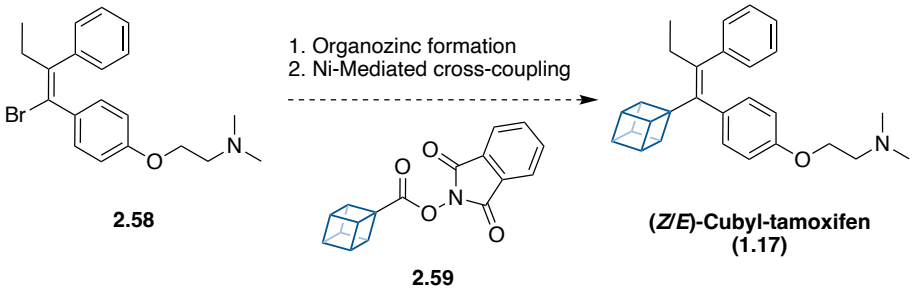

C: Selected test substrates for the Ni-mediated cross-coupling.

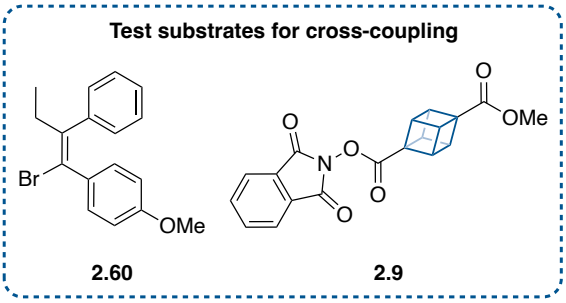

Scheme 42: Ni-mediated cubane cross-coupling.

In the literature Potter and McCague reported the synthesis of alkenylbromide **2.58**.[180] However, to test this approach we opted to prepare the alkenylbromide **2.60** to simplify the reaction and purification by removing the tertiary amine group (Scheme 42c). In addition, we planned to use cubane redox-active ester **2.9** over **2.59**, as the former was employed in the Senge report and can be prepared in one step from commercially available material **2.8** versus 4 steps for **2.59**.

2.2.3.2 Our work

2.2.3.2.1 Synthesis of precursors for Ni cross-coupling

As previously described cubane redox-active ester **2.9** can be prepared by converting the carboxylic acid moiety in 4-methoxycarbonylcubanecarboxylic acid (**2.8**) to the acid chloride, using oxalyl chloride (1.2 eq) and catalytic quantities of DMF (10 mol %). The subsequent addition of *N*-hydroxyphthalimide (1.2 eq) and triethylamine (2.5 eq) provided the cubane redox-active ester **2.9** in 94 % yield (Scheme 41). Following literature protocols alkenylbromide **2.60** was prepared in two steps from commercially available propiophenone (**2.6**, Scheme 43a). In the first step triphenylphosphine (4 eq) and tetrabromomethane (2 eq) were refluxed in toluene for 15 minutes to generate an ylide, subsequent addition of propiophenone (**2.6**, 1 eq) promoted a Wittig reaction to afford the dibromoalkene **2.61**. Purification of the crude mixture was achieved by silica gel column chromatography, affording **2.61** in 61 % isolated yield. In the second step we envisioned a Suzuki-Miyaura cross-coupling between the dibromoalkene **2.61** and boronic acid **2.62** would give alkenylbromide **2.60**, although we suspected controlling the regioselectivity may be challenging (Scheme 43a).

A: Our synthesis of dibromoalkene **2.61** and planned Suzuki-Miyaura C-C cross-coupling.

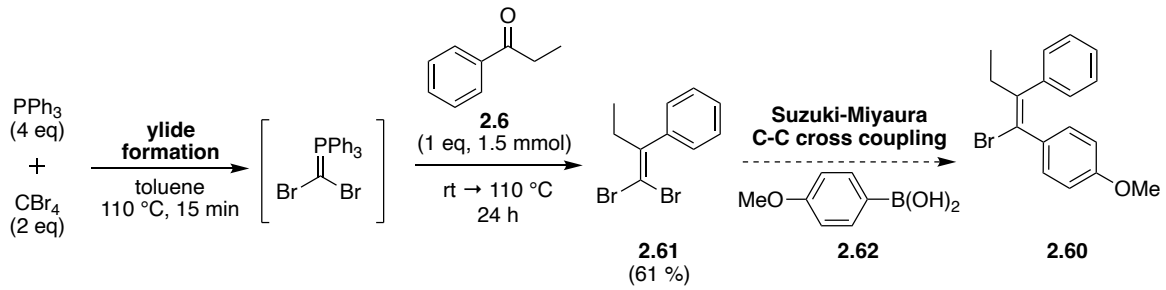

B: Regioselective C-C Suzuki-Miyaura cross-coupling – Florent group.[181]

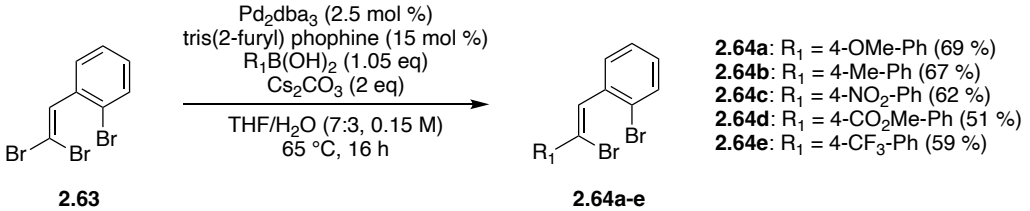

Scheme 43: Synthesis towards alkenylbromide **2.60**.

In the literature the preparation of alkenylbromide **2.60** by a Suzuki-Miyaura cross-coupling is not reported, although Florent *et al* have described a regioselective Suzuki-Miyaura C-C cross-coupling between unsymmetrical dibromoalkene **2.63** and various electron rich and electron poor boronic acids in good yields (Scheme 43b).[181] With this in mind, we first applied Florent's protocol for the treatment of dibromoalkene **2.61** (1 eq) and 4-methoxyphenyl boronic acid (**2.62**, 1.05 eq) with catalyst Pd_2dba_3 (2.5 mol %) and ligand tri(2-furyl) phosphine (15 mol %), in the presence of cesium carbonate (2 eq) in THF:H_2O (7:3, 0.15 M) at 65 °C (Table 16, entry 1). Unlike Florent *et al* who reported yields often exceeding 60 % with these cross-coupling conditions, in our hands **2.60** was obtained in a poor yield of 28 % with a *Z*/*E* ratio of 2:1. The regioselectivity in our reaction also favoured the formation of the *Z*-geometric isomer, this would result in (*E*)-cubyl-tamoxifen (**1.17**) being obtained as the major isomer in the next step (Ni-mediated cubane cross-coupling) providing no alkene isomerisation occurred. To try and improve the yield and the regioselectivity we screened a range of conditions (Table 16).

Table 16: Reaction screening of Suzuki-Miyaura cross-coupling.

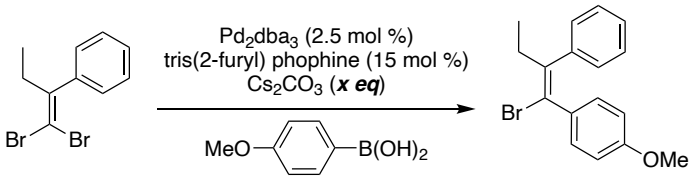

2.61 | **2.62** (***x eq***) ***solvent***, 65 °C, ***time*** | (***E***)-**2.60** desired regioisomer

Entry	2.61 (mmol)	2.62 (eq)	Base (eq)	Solvent (ratio and concentration	Time / h	Ratio of *Z*/*E*-2.60[a]	(*Z*/*E*)-2.60 yield[a] / %
1	0.35	1.05	2	THF: H_2O (7:3 0.15 M)	16	2:1	28
2	0.35	1.05	2	Et_2O:THF:H_2O (2:1:1 0.1 M)	16	2:1	32
3	0.35	1.05	2	Et_2O:THF:H_2O (2:1:1 0.01 M)	5	3:2	26
4	0.35	1.05	2	THF:H_2O (3:1 0.1 M)	5	3:2	27
5	0.35	1.3	2	THF:H_2O (3:1 0.1 M)	16	2:1	28
6	0.35	1.3[b]	2	THF:H_2O (3:1 0.1 M)	16[c]	2:1	23
7	0.35	1.05	1.1	THF:H_2O (3:1 0.1 M)	5	3:2	27
8[d]	3.3	1.05	1.1	THF:H_2O (3:1 0.1 M)	6	3:2	36

[a] after silica-gel chromatography. [b] dropwise addition over 40 minutes. [c] reaction at 45°C. [d] Optimised conditions.

In the literature Nishihara *et al* adapted Florent's Suzuki-Miyaura C-C cross-coupling protocol to include diethyl ether as a third solvent and with a lower concentration of 0.1 M (from 0.15 M).[182] Switching the solvent system to Et_2O:THF:H_2O (2:1:1 0.1 M) we observed a slight increase in yield (32 %) and no change in regioselectivity (*Z*/*E* 2:1), which was determined by ^{1}H NMR analysis after silica-gel column chromatography (Table 16, entry 2). Decreasing the reaction time from 16 hours to 5 hours resulted in a minor decrease in yield (26 %) but with an improved regioselectivity (*Z*/*E* ratio of 3:2, entry 3). Similar results were obtained when removing the solvent diethyl ether and only using THF:H_2O at the same concentration (3:1 0.1 M), with **2.60** obtained in 27 % yield with a *Z*/*E* ratio of 3:2 (entry 4). Increasing the number of equivalents of 4-methoxyphenyl boronic acid (1.05 eq → 1.3 eq) and increasing the reaction length to 16 hours decreased the regioselectivity with the *Z*/*E* ratio dropping back to 2:1 (28 % yield, entry 5). Dropwise addition of the boronic acid in THF over 40 minutes did not improve the regioselectivity (*Z*/*E* ratio of 2:1) and resulted in the lowest yield observed of 23 % (entry 6). Reverting to 1.05 equivalents of boronic acid, we next decreased the number of equivalents of base (2 eq → 1.1 eq), which did not improve the yield but saw a small increase in regioselectivity to favour the *E*-isomer (28 %, *Z*/*E* ratio of 3:2, entry 7). Despite the conditions in entry 7 resulting in a lower yield than those in entry 2, when scaling the reaction from 0.35 mmol of dibromoalkene **2.61** to 3.3 mmol we opted to use the conditions described in entry 7 as it favoured the formation of the desired *E*-geometric isomer. Pleasingly, we obtained **2.60** in an improved yield of 36 % in an unchanged *Z*/*E* ratio of 3:2. With an established route to prepare (*Z*/*E*)-**2.60** (ratio of 3:2) in an overall yield of 22 % over two-steps from affordable commercially available material, we opted to not pursue further reaction screening to enhance the regioselectivity or yield.

2.2.3.2.2 Cubane Ni cross-coupling

With alkenylbromide (*Z*/*E*)-**2.60** (ratio of 3:2) in hand, we turned our attention to the synthesis of **2.65** by a Ni-catalysed cross-coupling between bromide (*Z*/*E*)-**2.60** and cubane redox-active ester **2.9** (Scheme 44). In the protocol reported by Senge *et al*, for the coupling of cubane to several electron poor porphyrin systems an electron-rich ligand (L2) proved to beneficial to overcome decomposition (see above Scheme 42a).[163] On the other hand, for electron-rich arenes an electron poor ligand (L1) was found to promote product formation.[163] In our work, the alkenylbromide (*Z*/*E*)-**2.60** is electron-rich, thus we opted to employ the electron poor ligand (L1) in the cross-coupling reaction.

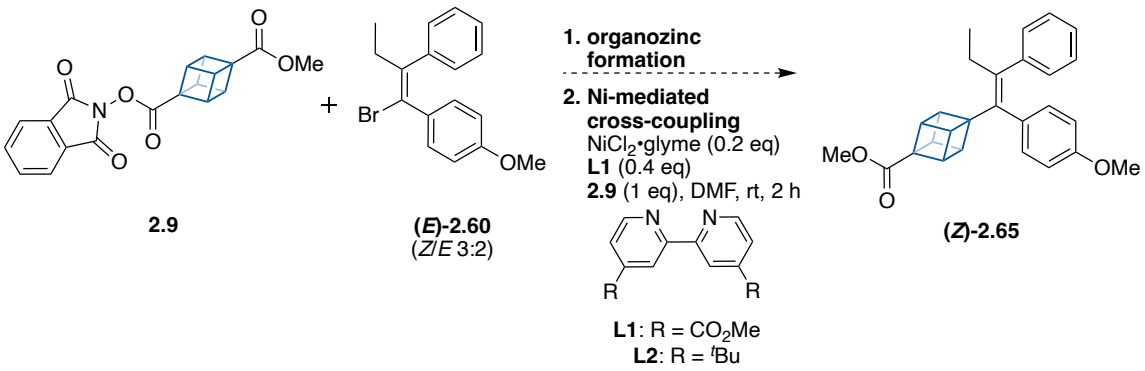

Scheme 44: Synthetic plan for the cubane Ni-catalysed cross-coupling.

Also, in the study by Senge and co-workers, the I/Mg exchange of iodo-porphyrins using ^{i}PrMgCl*LiCl was carried out at - 40 °C.[163] However, literature reports have shown that Br/Mg exchange of similar substrates using ^{i}PrMgCl*LiCl does not proceed at these lower temperatures.[183] Therefore, we opted to prepare the Grignard of alkenylbromide (*Z*/*E*)-**2.60** by the addition of ^{i}PrMgCl*LiCl (1.1 eq, 2 M in THF) to a solution of alkenylbromide (*Z*/*E*)-**2.60** (ratio of 3:2) in THF at 0 °C, which was subsequently warmed to room temperature. To confirm Grignard formation, a sample of the mixture was taken and quenched with water. In the LRMS (ESI^{+}) of the sample we observed signals that matched **2.66** ([M+H]$^{+}$ m/z = 238.14) and the starting material **2.60** ([M+H]$^{+}$ m/z = 316.05) (Scheme 45).

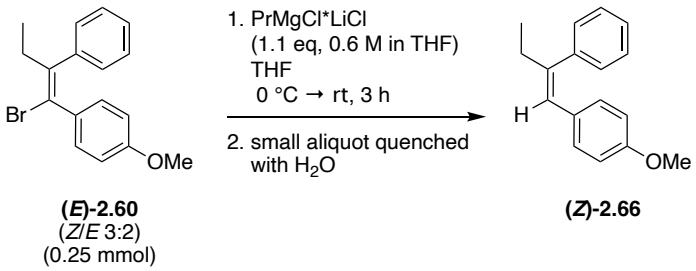

(*E*)-2.60
(*Z*/*E* 3:2)
(0.25 mmol)

(*Z*)-2.66

Scheme 45: Grignard derived from alkenylbromide (*Z*/*E*)-**2.60** analysed by LRMS (ESI^+).

Based on this data, we proceeded with the next steps of the reaction, which first included the addition of $ZnCl_2$ (1.1 eq) in THF to the Grignard solution to generate an organozinc species. Next the organozinc species was added to a solution containing cubane redox-active ester **2.9** (0.3 eq), $NiCl_2$ (0.3 eq) and ligand L1 (0.6 eq) in DMF at room temperature in one fast addition (Scheme 46). The reaction mixture changed from a dark green to brown colour, which was indicative of a failed cross-coupling based on previous experience of cubane arylations using these conditions. Nevertheless, the reaction was monitored over the next two hours by TLC, but as suspected no product formation was observed. ^{1}H NMR of the crude mixture indicated the major signals belonged to both starting materials alkenylbromide **2.60** and cubane redox-active ester **2.9**. In fact, no singlet corresponding to the alkene proton in **2.66** was observed, suggesting that Grignard formation was likely limited. The crude material was purified by silica gel column chromatography, with 36 % of cubane redox-active ester **2.9** recovered. The poor Grignard formation prompted us to explore alternative protocols to prepare the Grignard of alkenylbromide (*Z*/*E*)-**2.60**. One methodology explored was the preparation of the Grignard derived from alkenylbromide (*Z*/*E*)-**2.60** (ratio of 3:2, 1 eq) using magnesium turnings (1.25 eq, preactivated by stirring and addition of iodine) in the presence on LiCl (1.25 eq) at room temperature. However, despite our best efforts we could not initiate Br/Mg exchange (Scheme 46).

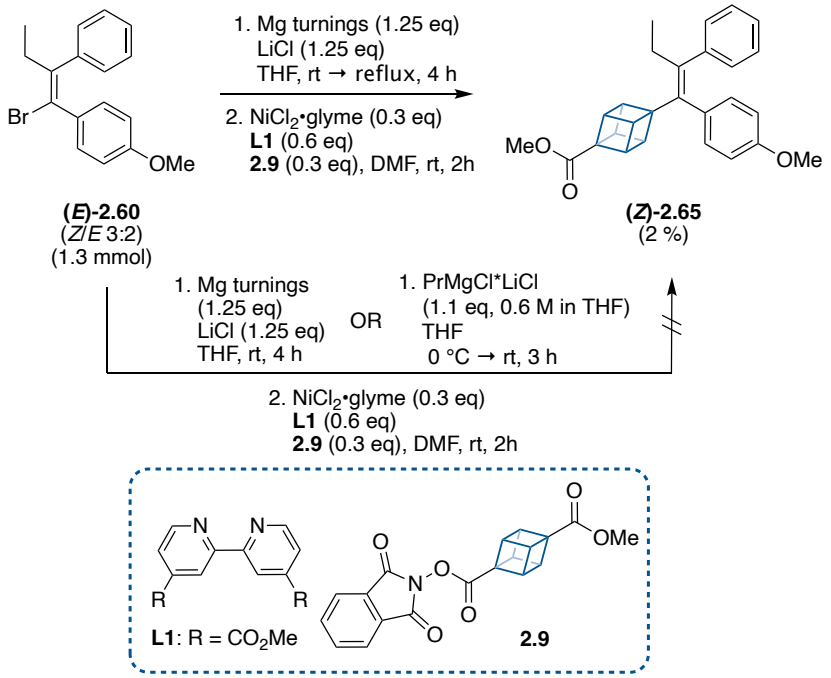

Scheme 46: Stereoselective synthesis of (*Z*)-**2.65** via a Ni-mediated cubane cross-coupling.

As a result of the bromoalkene (*Z*/*E*)-**2.60** being so unreactive towards Grignard formation, we refluxed (*Z*/*E*)-**2.60** (ratio of 3:2, 1 eq) in the presence of magnesium turnings (1.25 eq, preactivated by stirring and addition of iodine) and LiCl (1.25 eq) in THF (Scheme 46). After 4 hours the red solution turned dark brown/black and a visual loss of magnesium turnings was observed, both indicative of Grignard formation. The solution was cooled to room temperature and subsequently added to a solution containing cubane redox-active ester **2.9** (0.3 eq), $NiCl_2$ (0.3 eq) and ligand L1 (0.6 eq) in DMF at room temperature. This time the green mixture turned purple, which from our experience with cubane-arylations using this method normally indicated a successful cubane cross-coupling, although TLC analysis of the reaction mixture revealed many side products (8 spots off the baseline in 10 % EtOAc/hexane). ^{1}H NMR analysis of the crude mixture revealed the protons in the cubane scaffold had the same chemical shift, with no indication of product formation (Figure 17 – highlighted in blue). Encouragingly there was a broad singlet at 6.36 ppm that we assigned to the alkene proton in **2.66**, providing additional evidence that Grignard formation was successful (Figure 17 – highlighted in red). Based on this information, we opted to purify the crude mixture to investigate if one of the minor spots visible during TLC analysis of the crude belonged to

the desired product **2.65**. Pleasingly, after a lengthy purification by silica gel column chromatography we isolated the single geometric isomer (*Z*)-**2.65** in 2 % yield. An overlay of the ^{1}H NMR of purified (*Z*)-**2.65** against the crude mixture and the two starting material cubane redox-active ester **2.9** and bromoalkene (*Z*/*E*)-**2.60** (ratio of 3:2), show how similar the chemical environments are between starting materials and the product. Thus, monitoring the cross-coupling by ^{1}H NMR was extremely challenging. For instance, in the ^{1}H NMR of the product (*Z*)-**2.65** all 6 protons in the cubane scaffold appear as one multiplet at the same chemical shift as the cubane protons in the cubane redox-active ester **2.9** (Figure 17).

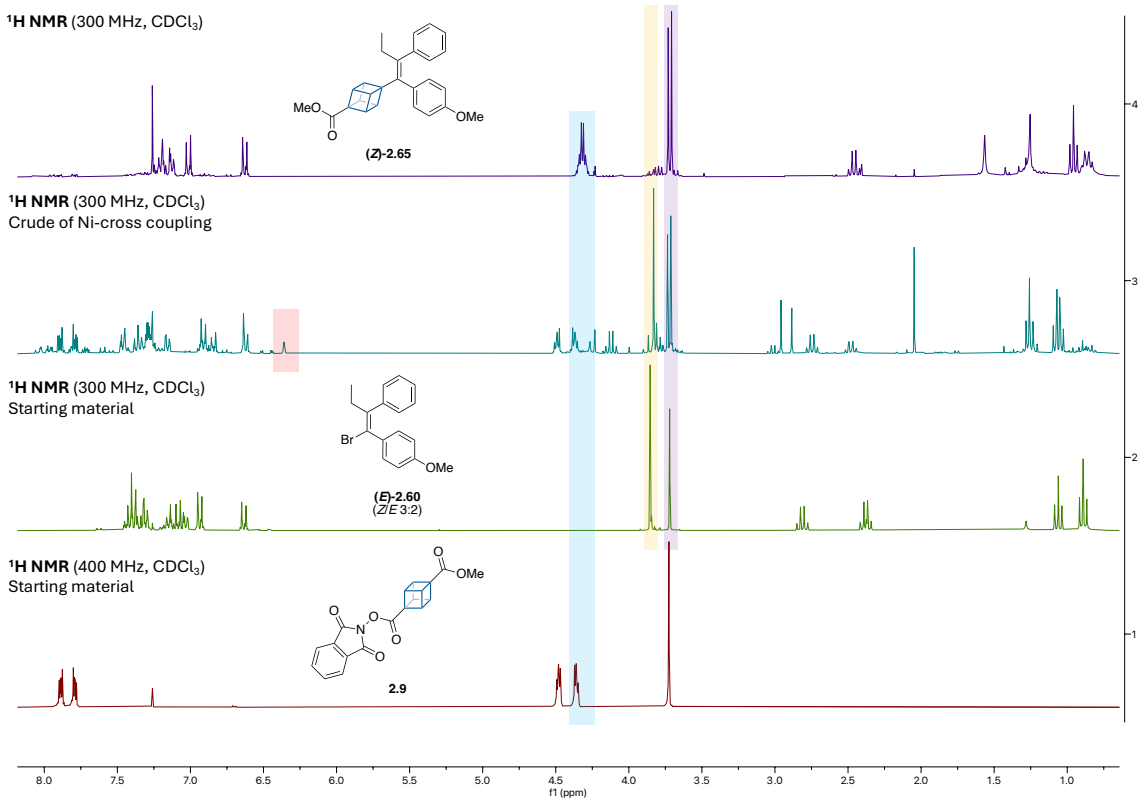

Figure 17: ^{1}H NMR overlay of isolated (*Z*)-**2.65** via a Ni-mediated cubane cross-coupling, against crude reaction mixture and starting materials.

*Highlighted in red = alkene proton in **2.66** (formed by Grignard being quenched with H_2O); blue = similar chemical shift for cubane protons in (Z)-**2.65** compared to **2.9**; yellow = methoxy group (OC**H**$_3$) in (Z)-**2.60**; purple = methoxy group (OC**H**$_3$) in (E)-**2.60**.*

The chemical shift of the protons in methoxy group (OC***H***$_3$) in (*Z*)-**2.65** was observed at 3.71 ppm, which corresponded to the same chemical shift as the *E*-geometric isomer of

bromoalkene **2.60** (Figure 17 – highlighted in purple). Based on this data, we inferred that the stereochemistry of the product **2.65** was likely the desired *Z*-geometric isomer. In a subsequent section we will show how the chemical shifts of cubane protons in tetra-substituted alkenes bearing a cubane substituent can vary significantly depending on the geometric isomer, providing additional evidence for our proposed alkene assignment of **2.65**. However, to prove **(*Z*)-2.65** was the geometric isomer isolated from the Ni-mediated cross-coupling**,** in the future a NOESY NMR or an X-ray crystal is required.

Overall, the Ni-mediated cross-coupling between **2.9** and (*Z*/*E*)-**2.60** (ratio of 3:2) demonstrated that tetra-substituted alkenes bearing a cubane substituent can be synthesised. The 2 % yield of the cross-coupling was poor, although the Senge group also reported low yields for the preparation of the cubane-porphyrin substrates using the same methodology (6 % - 12 %).[163] Given the low yield we explored one further route.

2.2.4 Route 4: Horner-Wadsworth-Emmons approach

2.2.4.1 Literature and retrosynthetic analysis

The final methodology explored towards a cubane analogue of tamoxifen, in which one of the aromatic rings have been replaced with a cubane framework, was the Horner-Wadsworth-Emmons (HWE) olefination. At the start of this chapter several examples of a HWE and Wittig reaction were described (**Section 2.1.2**, Scheme 10-11). Notably, in all but two examples the more reactive cubyl aldehyde (**2.1b**) was used over a cubyl ketone (**2.1c-d**) and not one of examples included the preparation of a tetra-substituted olefin.[108, 126-130]

In the previous section (**Section 2.2.3** – Cross-couplings), we demonstrated that a Ni-mediated cross-coupling between a bromoalkene and cubane redox-active ester was successful, albeit in a poor yield of 2 % (Scheme 46). Rather than optimising the reaction conditions, we initially thought that the installation of the cubane framework to an alkene bond may be formed more readily via a HWE or Wittig reaction. As hindered

ketones have been found to react under milder conditions in HWE olefinations, compared to an analogous reaction using Wittig reagents, we were initially interested in utilising HWE conditions to prepare a mono-substituted analogue cubane-tamoxifen.[184, 185] The preferred strategy included a HWE olefination between cubyl ketone **2.69** and phosphonate **2.70** or cubyl ketone **2.13** and phosphonate **2.71**, which would afford two mono-substituted analogues of cubane-tamoxifen (**1.17** and **1.18**, Scheme 47). Unfortunately, as the HWE olefination usually proceeds with high (*E*)-selectivity, a HWE between those substrates would likely result in the un-desired (*E*)-geometric isomer of cubyl-tamoxifen being the major product. On the other hand, a HWE between cubyl ketone **2.13** and the commercially available diethyl benzylphosphonate (**2.67**) would provide the tri-substituted olefin (*E*)-**2.68**; a Heck cross-coupling of (*E*)-**2.68** with 2-(4-bromophenoxy)-*N*,*N*-dimethylethan-1-amine (**2.34**) would then afford the first cubane analogue of tamoxifen (**1.18**) with the desired *Z*-stereochemistry.

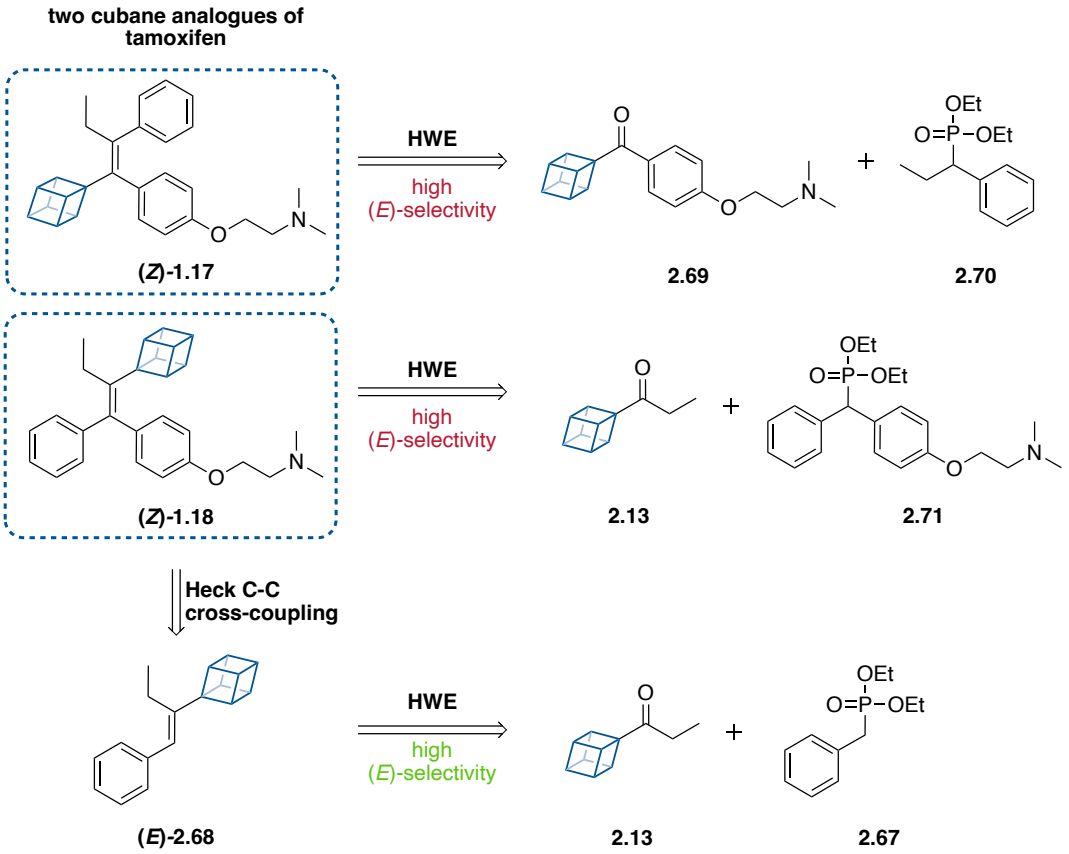

Scheme 47: Retrosynthetic analysis for the HWE olefination of cubyl-tamoxifen **1.17** and **1.18**.

2.2.4.2 Our work

2.2.4.2.1 HWE reaction followed by Heck cross-coupling

The details regarding the synthesis of cubyl ketone **2.13** were previously described in **Section 2.2.1.2** over 5 steps in a total yield of 21 % (Scheme 18-19). In the HWE reaction, diethyl benzylphosphonate (**2.67**, 2.1 eq) was added to a solution of potassium *tert*-butoxide (2 eq) in THF at 0 °C, followed by the addition of cubyl ketone **2.13** (1 eq) at the same temperature (Scheme 48). The reaction was monitored by TLC analysis and after 15 minutes at 0 °C we observed **2.13** was fully consumed. The reaction was quenched and ^{1}H NMR analysis of the crude revealed the formation of **2.68** was successful. As predicted the reaction proceeded with greater selectivity for the *E*-isomer, with a *Z*/*E* ratio of 1:4 in the crude mixture. Purification by silica gel column chromatography gave (*E*)-**2.68** in a good yield of 52 % with an improved *Z*/*E* ratio of 1:10. A NOESY experiment was used to confirm the major geometric isomer had the *E*-configuration, in which we observed correlation between the singlet at δ 6.13 (s, 1H, C=C**H**) and multiplet at δ 4.15 – 4.10 (m, 3H, three C-H bonds in cubane) (Figure 18).

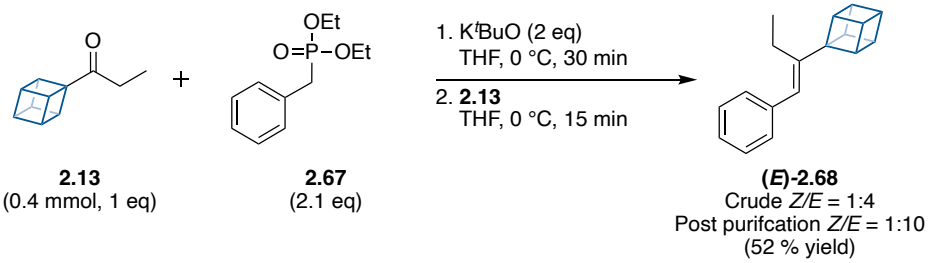

Scheme 48: HWE olefination between cubyl ketone **2.13** and diethyl benzylphosphonate **2.67**.

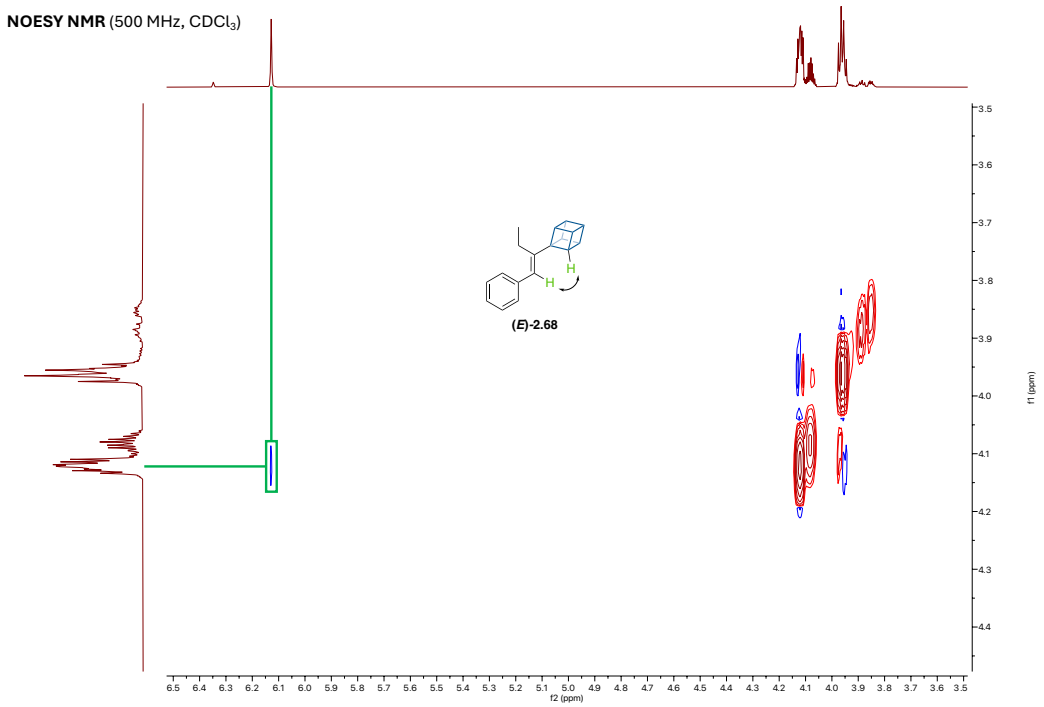

Figure 18: ^{1}H NOESY NMR spectrum of the 1:10 mixture of (*Z*/*E*)-**2.68** post silica gel column chromatography revealed the major geometric isomer has the *E*-configuration.

With a stereoenriched sample of (*E*)-**2.68** (*Z*/*E* ratio of 1:10) in hand, we next investigated the Heck cross-coupling between (*E*)-**2.68** and 2-(4-bromophenoxy)-*N*,*N*-dimethylethan-1-amine (**2.34**), with the latter being prepared by the *O*-alkylation of 4-bromophenol with 2-chloro-*N*,*N*'-dimethylethylamine hydrochloride (previously described in **Section 2.2.2.2**, Scheme 31). In the literature, Chang *et al* reported a $Pd(OAc)_2$ catalysed Heck cross-coupling between the aromatic analogue of (*E*)-**2.68** and aryl bromide **2.34** gave (*Z*)-tamoxifen in a yield of 65 % (Scheme 49a).[123] Initially, we were concerned about using this method for our cubyl olefin (*E*)-**2.68** as Cassar and co-workers reported that cubane undergoes strain-releasing valence isomerisation to cuneane in the presence of Pd(II) species.[160] This conclusion was based on their observation that the treatment of cubane **2.73a** or **2.73b** in concentrations between 10^{-2} – 10^{-1} M (in chloroform) with 10^{-2} – 10^{-1} M bis(benzonitrile)palladium (II) chloride in chloroform, resulted in rapid isomerisation of cubane at room temperature to several cuneane products (Scheme 49b).[160] Since this original report other groups have documented how Pd(II)-catalysed cross couplings promote cubane decomposition pathways.[158, 186] One example includes Eaton's attempt to prepare alkynylcubanes by

palladium-catalysed reaction of iodocubane **2.73c** with a terminal acetylene under Heck-type reaction conditions, resulting in the formation of a cyclooctatetraene product (Scheme 49b).[186]

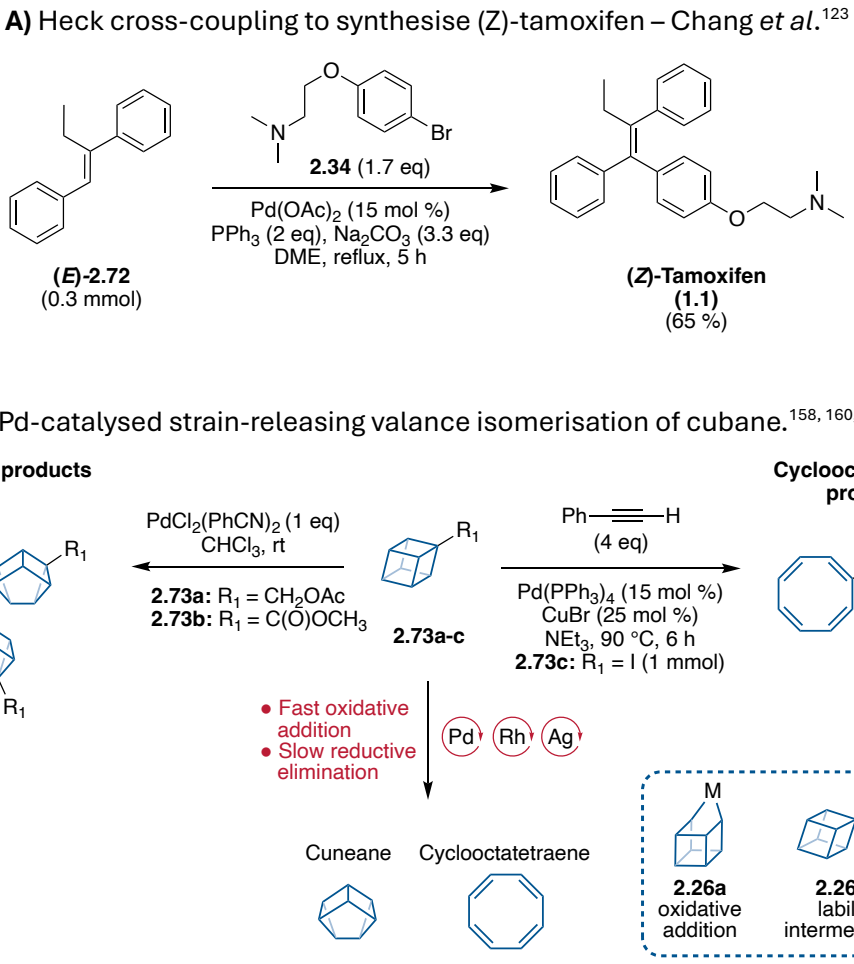

Scheme 49: Pd-catalysed cross-coupling for aromatic verses cubane species.

Due to these earlier reports in the field of cubane chemistry there is a general misconception that cubane is just inherently unstable towards palladium catalysis. However, recently the Senge group demonstrated that the cubane framework remained intact during the Pd-catalysed Sonogashira coupling of alkynyl cubanes with arylhalides at room temperature (Scheme 50a).[163] The stability of alkynyl cubanes under these Pd(II) catalysed conditions prompted us to consider if the Pd-catalysed Heck between our stereoenriched sample of (*E*)-**2.68** (*Z*/*E* ratio of 1:10) and aryl bromide **2.34** could be a viable route towards (*Z*)-cubyl-tamoxifen **1.18** (Scheme 50b).

a) Pd-catalysed Sonogashira coupling of alkynyl cubanes – Senge group.[163]

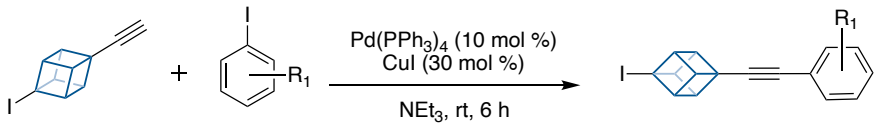

2.74 (0.3 mmol) **2.75** (3 eq) **2.76** 5 examples (> 75 % yield)

b) Heck cross-coupling between olefin **2.68** and aryl bromide **2.34** – Our work.

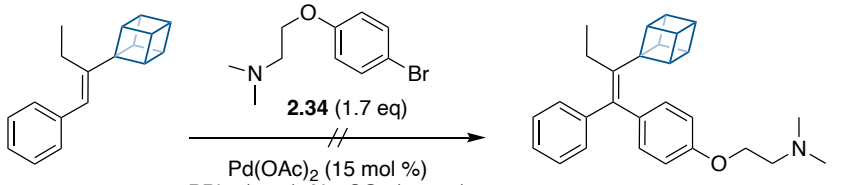

(*E*)-2.68 (*Z*/*E* = 1:10) (0.1 mmol)

(*Z*)-1.18 (not detected)

after 5 h: **(*Z*/*E*)-2.68** intact
after 20 h: **(*Z*/*E*)-2.68** decomposed

Scheme 50: Cubane stability in the presence of Pd-catalysts.

The procedure previously described by Chang *et al* for the Heck cross-coupling was followed in the first instance. Under this protocol, (*E*)-**2.68** (1 eq, *Z*/*E* = 1:10) and aryl bromide **2.34** (2 eq) were refluxed in DME in the presence of $Pd(OAc)_2$ (15 mol %), triphenylphosphine (2 eq) and sodium carbonate (3.3 eq) for 5 hours (Scheme 50b). After 5 hours an aliquot of the reaction mixture was removed, quenched with H_2O and analysed by ^1H NMR. Analysis of the data revealed that the relative ratio of the integration values of the Ar*CH* protons in aryl bromide **2.34** and the cubane *CH* protons in (*E*)-**2.68** was 2:1, which was consistent with the numbers of equivalents of each reagent used at the start of the reaction (Scheme 50b and Figure 19). While no Heck cross-coupling occurred in the first five hours of the reaction, this shows that no decomposition of the cubane framework occurred under these reaction conditions which itself is informative. Only when leaving the reaction overnight at reflux did we observe complete decomposition of the cubane framework.

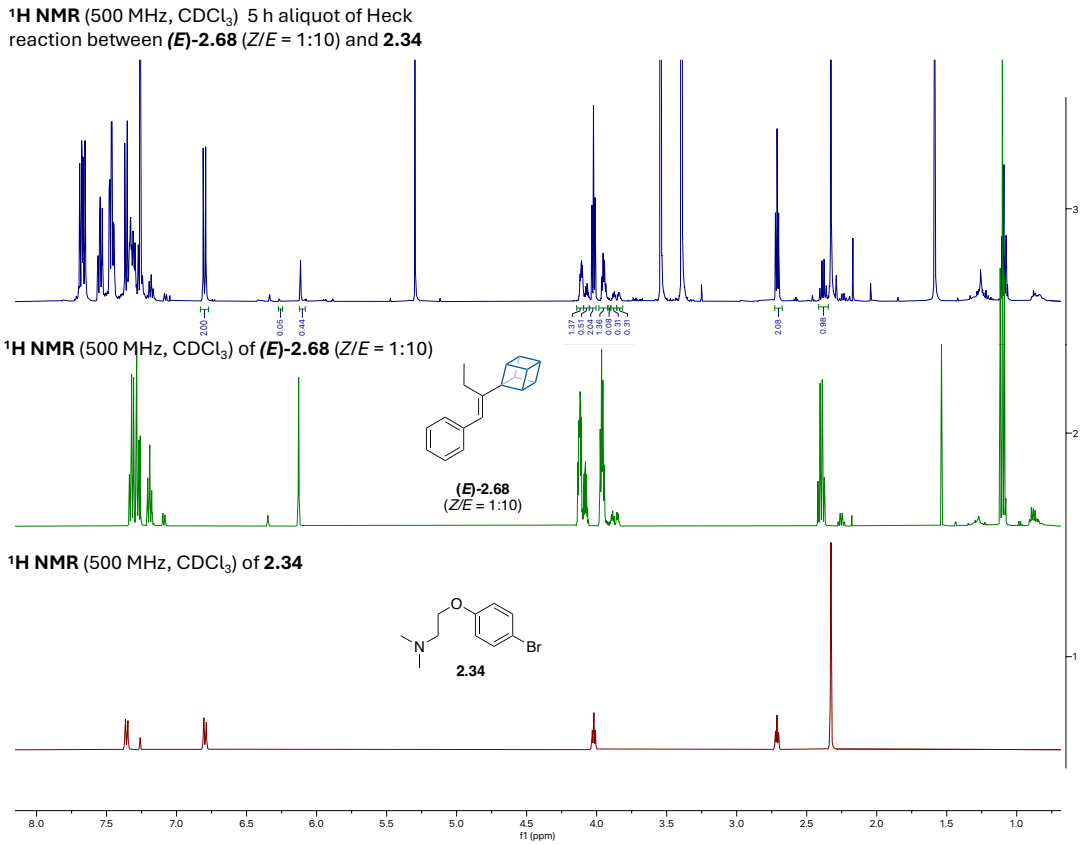

Figure 19: [1]H NMR overlay of the Heck reaction between olefin (*E*)-**2.68** (*Z*/*E* ratio of 1:10) and aryl bromide **2.34** after 5 hours.

While Chang *et al* reported a 65 % yield for the Heck reaction between the aromatic olefin (*E*)-**2.72** and aryl bromide **2.34** (Scheme 49a)[123], when we subjected (*E*)-**2.68** (1 eq, *Z*/*E* = 1:10) under identical reactions conditions the target compound (*Z*)-cubyl-tamoxifen **1.18** was not formed (Scheme 50b). In addition, when we subjected the aromatic olefin (*Z*)-**2.72** (*Z*/*E* = 46:1) to the conditions described by Chang *et al* no formation of (*Z*/*E*)-tamoxifen (**1.1**) was observed (Scheme 51a). Since the rate of Heck reactions can be strongly influenced by the degree of substitution of the olefin, we opted to also test these Heck conditions with the commercially available *trans*-stilbene (Scheme 51b).[187] Under identical conditions, the C-C coupling between *trans*-stilbene (**2.77**) and aryl bromide **2.34** was unsuccessful, with the target compound **2.78** not detected by TLC or [1]H NMR analysis. Given these findings, this promoted us to explore alternative Heck reaction conditions.

A) Heck cross-coupling with tri-substituted olefins – our work.

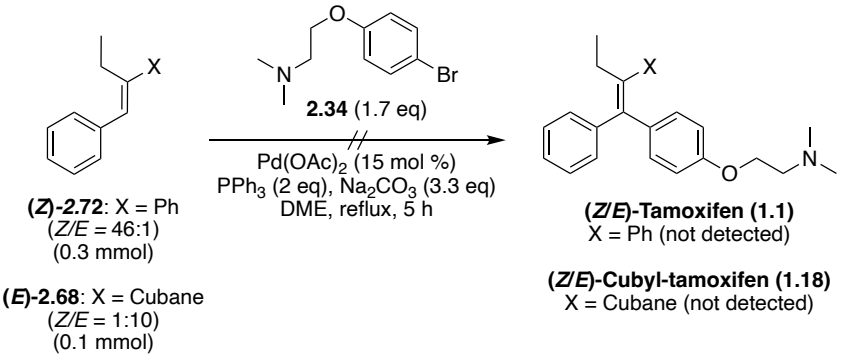

B) Heck cross-coupling with di-substituted olefin – our work.

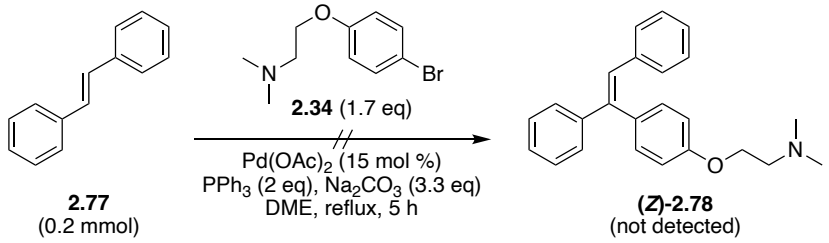

Scheme 51: Heck cross-coupling outcomes using the conditions described by Chang *et al*.[123]

The aryl halide chosen for this investigation was 4-iodoanisole (**2.79**), as the methoxy group mimicked the (dimethylamino)ethoxy side chain in aryl bromide **2.34** but would simplify the purification by removing the tertiary amine moiety. Secondly, 4-iodoanisole was selected over 4-bromoanisole, as the former is known to undergo oxidative addition to Pd(0) more readily, owing to the weaker C-I bond and better leaving group characteristics.[187] Subjecting *trans*-stilbene (**2.77**, 1 eq) and 4-iodoanisole (**2.79**, 1.2 eq) with catalytic quantities of $Pd(OAc)_2$ (3 mol %) and potassium carbonate (1.5 eq) in degassed DMF at 80 °C for 5 hours, in the presence of *N*-tetraethylammonium bromide (2 eq) and KBr (1.2 eq) gave the desired product (*Z*/*E*)-**2.80** (ratio of 1:6) in a 30 % yield post purification by silica gel column chromatography (Scheme 52). When subjecting the more sterically crowded tri-substituted olefin (*Z*)-**2.72** (*Z*/*E* = 46:1) to the same Heck conditions, no product formation was observed by TLC or ^{1}H NMR analysis (Scheme 52).

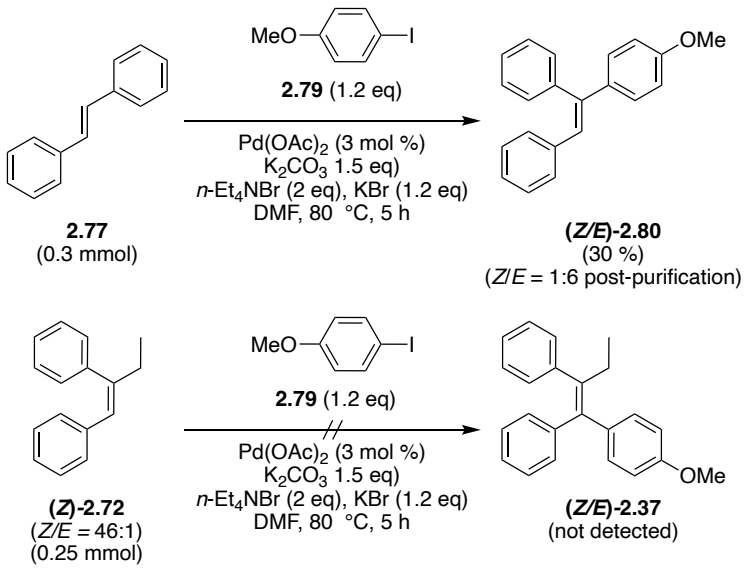

Scheme 52: Heck reaction of di- and tri-substituted olefins.

Given we were unable to develop conditions for the Heck cross-coupling with tri-substituted alkenes and knowing the HWE olefination using cubyl ketones occurs readily, we opted to focus our attention on the HWE olefination between cubyl ketone **2.69** and phosphonate **2.70**. We predicted a mixture of geometric isomers would form in this HWE reaction, therefore, optimisation of the reaction conditions to control the *Z*/*E* stereoselectivity or the development of a purification method to separate the two geometric isomers would be required.

2.2.4.2.2 Direct HWE olefination

The HWE olefination between cubyl ketone **2.69** and phosphonate **2.70** was selected over cubyl ketone **2.13** and phosphonate **2.71** as from a retrosynthetic perspective, phosphonate **2.71** would likely be more challenging to prepare (Scheme 53).

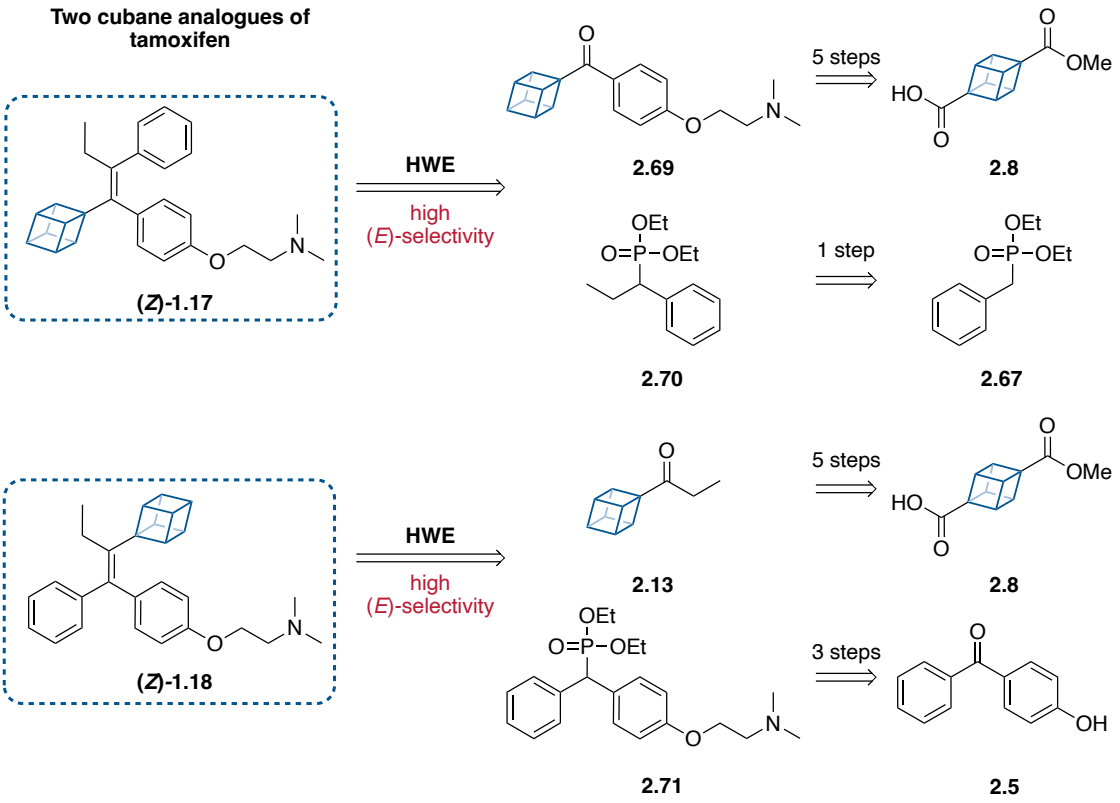

Scheme 53: Retrosynthetic analysis of two remaining HWE olefination.

Before we could examine the HWE reaction we first needed to prepare the two starting materials, cubyl ketone **2.69** and phosphonate **2.70**. The synthesis of the former began by converting 4-methoxycarbonylcubanecarboxylic acid (**2.8**) to the cubyl Weinreb amide **2.12** over 4 steps in an overall yield of 29 %, with all steps previously described in detail (**Section 2.2.1.2,** Scheme 18-19). Lithium-bromine exhange of aryl bromide **2.34** (1.5 eq) using *n*-butyl lithium (1.5 eq, 1.6 M in hexanes) in THF at - 78 °C generated the organolithium reagent. After 15 minutes, cubyl Weinreb amide **2.12** (1 eq) in THF was added and during the next two hours at this temperature the Weinreb amide was fully consumed (Scheme 54). Purification by silica gel column chromatography (pre-treated with 2 % NEt_3) gave ketone **2.69** in 77 % yield. With one of the starting materials in hand, we switched to the preparation of the phosphonate **2.70** via the alkylation of diethyl benzylphosphonate (**2.67**). The addition of *n*-BuLi (1.2 eq, 1.6 M in hexanes) to a solution of **2.67** (1 eq) in THF at - 78 °C followed by iodoethane (1.2 eq) gave **2.70** in 84 % yield (Scheme 54). No purification of the crude product was required for the product.

With both the cubyl ketone **2.69** and functionalised phosphonate **2.70** prepared, we then looked at the HWE between these two substrates.

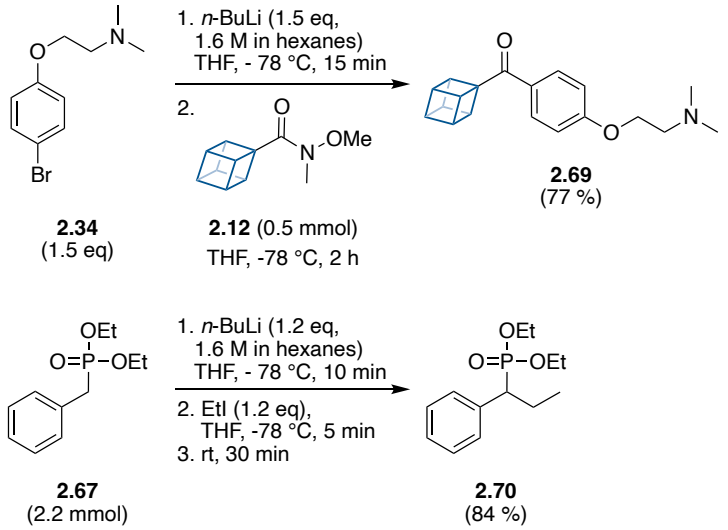

Scheme 54: Preparation of starting materials for cubyl HWE reactions.

In the previous HWE reaction we described in **Section 2.2.4.2.1**, diethyl benzylphosphonate (**2.67**, 2.1 eq) and ketone **2.13** in the presence of potassium *tert*-butoxide (2 eq) in THF gave olefin (*E*)-**2.68** (*Z*/*E* ratio of 1:4) within 15 minutes at 0 °C (Scheme 55, 52 % yield, *Z*/*E* 1:10 post purification).

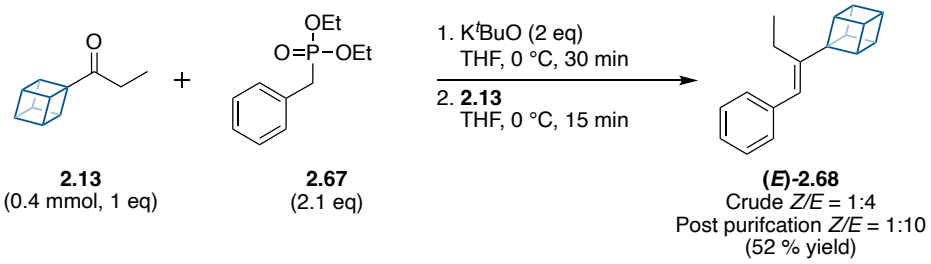

Scheme 55: Previous HWE between cubyl ketone **2.13** and phosphonate **2.67**.

We found the treatment of the functionalised phosphonate **2.70** (3 eq) with the base potassium *tert*-butoxide (3 eq) at 0 °C, followed by the addition of the bulkier ketone **2.69** (1 eq) under similar conditions did not provide the final product (*Z*)-cubyl-tamoxifen **1.17** (Table 17, entry 1). Allowing the HWE reaction to stir at room

temperature for 16 hours did not promote the HWE reaction, with 98 % of ketone **2.69** recovered from silica gel column chromatography (entry 2). Increasing the temperature to 50 °C for 16 hours resulted in 96 % of ketone **2.69** being recovered (entry 3), and replacing potassium *tert*-butoxide (3 eq) for the stronger base sodium hydride (3 eq, 60 % dispersion in mineral oil) was also ineffective with 93 % recovery of ketone **2.69** post silica gel column chromatography (entry 4).

Table 17: HWE reaction screening.

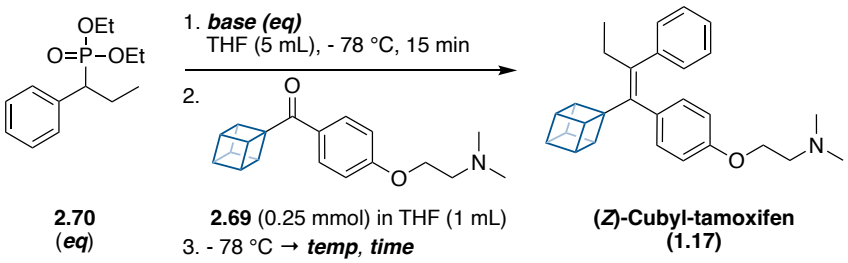

Entry	2.70 (eq)	Base (eq)	Temp / °C	Time / h	Recovered 2.69 / %	Ratio of (*Z*)-1.17: (*E*)-1.17 in crude[a]	(*Z*/*E*)-1.17 yield / %[b]
1	3	K^{t}BuO (3)	0[c]	0.25	97	-	-
2	3	K^{t}BuO (3)	25[c]	16	98	-	-
3	3	K^{t}BuO (3)	50[c]	16	96	-	-
4	3	NaH (3)	50[c]	16	93	-	-
5	3.1	*n*-BuLi (3)	50	21	34	1:3 (1:3)	40
6[d]	3.1	*n*-BuLi (3)	50	21	46	1:2 (1:2)	40
7	2.1	*n*-BuLi (2)	50	21	31	1:3 (1:3)	29
8	2.1	*n*-BuLi (2)	25	2	51	2:3 (2:3)	12
9	2.1	*n*-BuLi (2)	- 78	48	92	-	-

*[a] ratio of (Z)-**1.17** : (E)-**1.17** in brackets after purification by silica gel column chromatography. [b] isolated yield. [c] K^{t}BuO was added at 0 °C instead of -78 °C. [d] concentration reduced by 25 %.*

Pandey and co-workers described the synthesis of (*Z*)-tamoxifen (**1.1**) via a HWE reaction between ketone **2.5a** and phosphonate **2.81**, in the presence of *n*-BuLi (1.2 eq, 15 % in hexanes) (Scheme 56). [125] When maintaining the temperature of the reaction at -78 °C for 48 hours a 7:3 mixture of *Z*- and *E*-tamoxifen was reported in the crude mixture.[125] By silica gel column chromatography the authors reported that the two isomers were separated, with *Z*- and *E*-tamoxifen (**1.1**) being isolated in 28 % and 12 % yield respectively. [125] To the best of our knowledge this is the only report of tamoxifen being synthesised via a HWE reaction using a ketone. With this paper in mind, we continued the HWE optimisation by using *n*-BuLi. Treatment of the functionalised phosphonate **2.70** (3 eq) in THF at -78 °C with *n*-BuLi (3 eq, 1.6 M in hexanes), followed by the addition of cubyl ketone **2.69** (1 eq) and heating to 50 °C for 21 hours resulted in olefin formation (Table 17, entry 5). The ^{1}H NMR of the crude product revealed a 1:3 ratio of (*Z*/*E*)-cubyl-tamoxifen **1.17**, determined by the ^{1}H NMR integration values combined with a ^{1}H NOESY experiment (*vide infra*). Purification of the crude product by silica gel column chromatography (pretreated with NEt_3) gave (*Z*/*E*)-**1.17** in a good yield of 40 % with an unchanged *Z*/*E* ratio (1:3). In addition, 34 % of unreacted ketone **2.69** was recovered during the purification, suggesting there was scope to further optimise the conditions to enhance the yield.

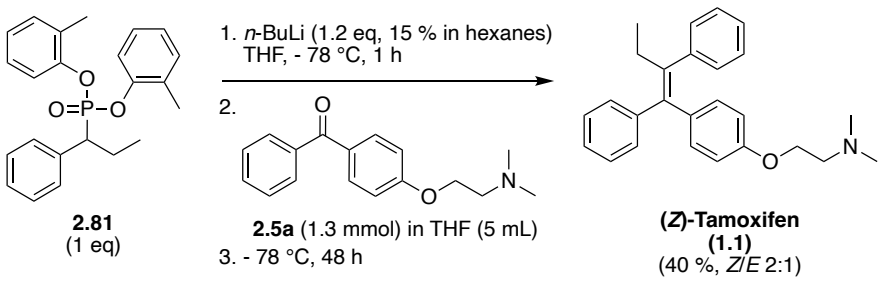

Scheme 56: Pandey and co-workers synthesis of tamoxifen via a HWE olefination.[125]

Increasing the concentration of the HWE reaction by 25 % gave (*Z*/*E*)-**1.17** in the same yield (40 %), although there was a slight difference in the *Z*/*E* ratio (1:2) and percentage of recovered ketone **2.69** (46 %) (Table 17, entry 6). Decreasing the equivalents of phosphonate **2.70** (3.1 eq → 2.1 eq) and *n*-BuLi (3 eq → 2 eq, 1.6 M in hexanes) reduced the yield of (*Z*/*E*)-**1.17** to 29 %, with poorer selectivity for (*Z*)-**1.17** (*Z*/*E* 1:3) and recovery

of unreacted ketone **2.69** (entry 7). Lowering the temperature from 50 °C to room temperature (25 °C) resulted in a 12 % isolated yield of (*Z*/*E*)-**1.17** with a 2:3 ratio after only 2 hours, with 51 % of ketone **2.69** recovered (entry 8). This data suggested that performing the HWE reaction at lower temperatures favoured selectivity for (*Z*)-**1.17**, which was earlier observed by Pandey and co-workers (Scheme 56). However, when we reduced the temperature to - 78 °C for 48 hours no HWE reaction occurred, and 92 % of ketone **2.69** was recovered post silica gel column chromatography (Table 17, entry 8).

In all our HWE reaction screening experiments between cubyl ketone **2.69** and functionalised phosphonate **2.70** poor stereoselectivity was observed (Table 17). Instead of screening conditions further we opted to develop a purification method to separate the geometric isomers, thus allowing us to test both isomers against tamoxifen in future biological studies. An extensive screening of solvent systems was tested by TLC analysis to determine if the two isomers of (*Z*/*E*)-**1.17** could be separated by normal-phase silica gel column chromatography, but none provided adequate separation. We proposed the geometric isomers could be separated by reverse-phase (C18) semi-preparative HPLC. In preparation for this, method development with an analytical HPLC was first required. The purified mixture from entry 5 of the HWE optimisation (Table 17), which contained a 1:3 ratio of (*Z*/*E*)-**1.17** (determined by ^{1}H NMR analysis) was selected as the test sample. No separation was observed when using a gradient with an eluent system of MeCN/H_2O containing 0.1 % TFA. Although, when switching to an isocratic system of 75 % MeCN / 25 % H_2O containing 0.1 % TFA, there was good resolution between the signals for (*E*)-**1.17** (retention time = 5.2 min) and (*Z*)-**1.17** (retention time = 6.0 min) (Figure 20).

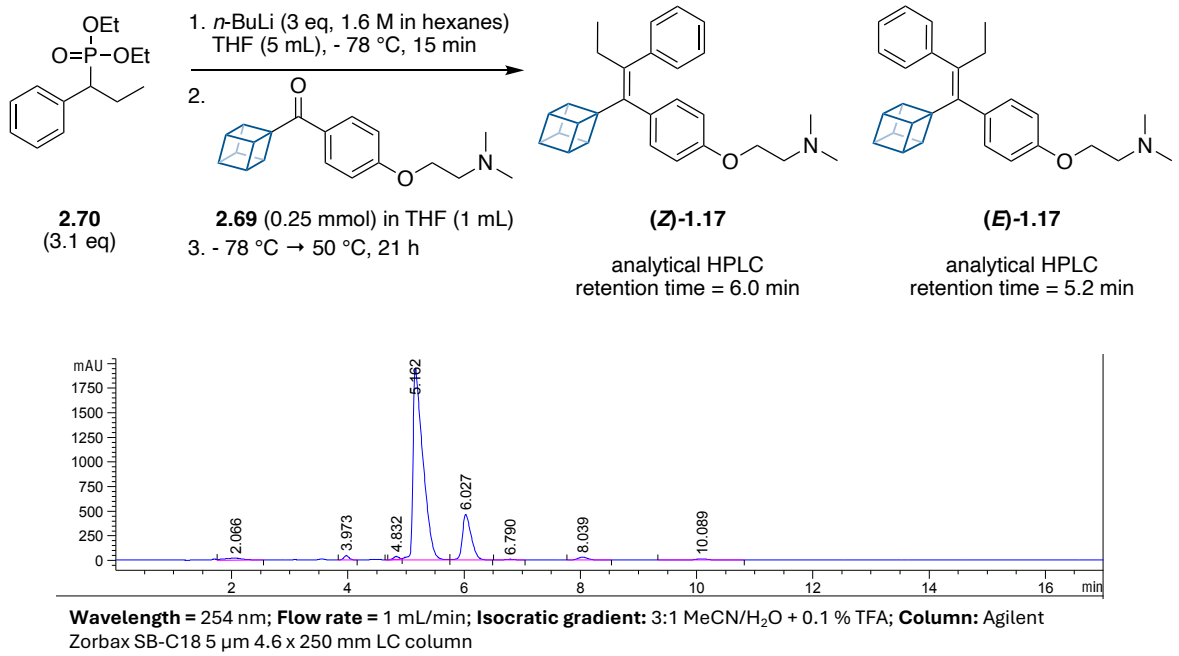

Figure 20: Analytical HPLC trace of HWE 1:3 mixture of (*Z*/*E*)-**1.17** post silica gel column chromatography.

The conditions established on the analytical HPLC were then evaluated on a semi-preparative HPLC with the same sample of 1:3 mixture of (*Z*/*E*)-**1.17** (38 mg) isolated post silica gel column chromatography (HWE described in Table 17, entry 5). The first step in the sample preparation included dissolving the 38 mg of (*Z*/*E*)-**1.17** in 1 mL of HPLC grade MeCN. For the initial semi-preparative run, 100 µL of this solution was transferred to a HPLC vial containing 50 µL of H_2O with 0.1 % TFA. Pleasingly, we found the separation of the two geometric isomer was sufficient using this sample preparation and the isocratic system of 75 % MeCN / 25 % H_2O containing 0.1 % TFA (Figure 21). There was a small overlap in retention time, but this did not prevent the isolation of pure fractions of both (*E*)-**1.17** and (*Z*)-**1.17**. When increasing the loading of sample from 100 µL to 150 µL of the MeCN solution (containing the 1:3 mixture of (*Z*/*E*)-**1.17**) no separation of the geometric isomers was achieved.

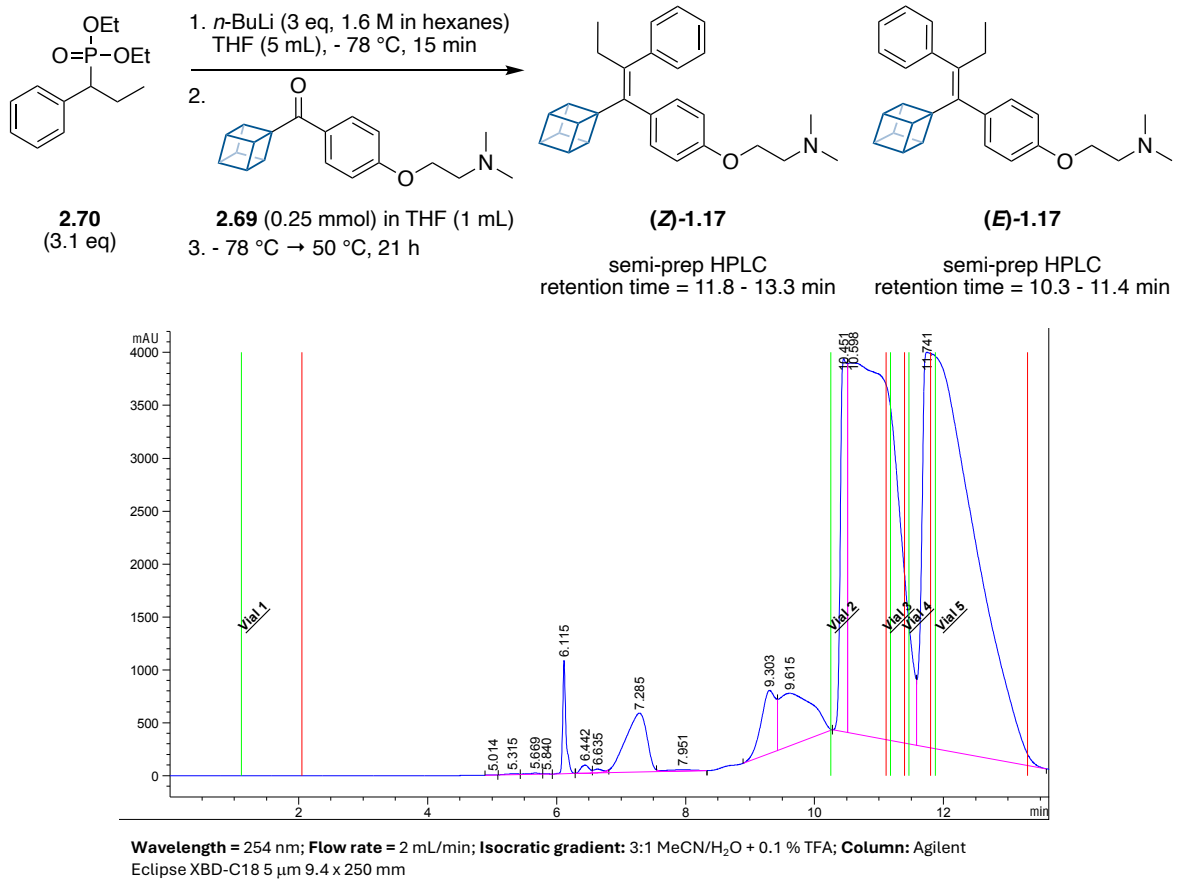

Figure 21: Semi-preparative HPLC trace of HWE 1:3 mixture of (*Z*/*E*)-**1.17** post silica gel column chromatography.

Post semi-preparative HPLC the fractions for (*E*)-**1.17** and (*Z*)-**1.17** were combined separately and concentration *in vacuo* to remove the bulk of MeCN and H_2O. The products were susceptible to decomposition in this solution, therefore evaporation of the solvent was performed immediately after reverse-phase purification. Furthermore, to limit product decomposition the water bath was maintained at 35 °C and additional HPLC grade MeCN was used to azeotropically remove the bulk of the water. An aqueous work-up for each geometric-isomer was also required, with the aqueous layer basified with 1 M NaOH before the addition of the organic solvent diethyl ether to generate the free amine of each product. Subsequent washes of the organic layer with 1 M NaOH removed traces of TFA. We found going directly from semi-preparative HPLC to an aqueous work-up resulted in substantial loss of both compounds (*E*)-**1.17** and (*Z*)-**1.17**. Therefore, prior concentration of the fractions for (*E*)-**1.17** and (*Z*)-**1.17** was found to be critical for maximising the recovery of final products. Post aqueous work-up, a TLC of

isolated (*E*)-**1.17** and (*Z*)-**1.17** was performed, which revealed weak UV peaks that were more polar likely a result of slight product decomposition. Therefore, each sample was passed through a short silica-gel plug to remove these impurities before analysis, providing (*E*)-**1.17** and (*Z*)-**1.17** in an overall yield of 17 % and 3 % respectively (40 % combined yield before semi-preparative purification). Overall, this complicated purification process to separate the *Z*- and *E*-geometric isomers of our target compound *Z*- and *E*-cubyl-tamoxifen (**1.17**) resulted in only 50 % being recovered (Scheme 57). In addition, the batch semi-preparative runs were both resource heavy and time consuming, making scalability challenging. Therefore, in the future the focus should be on the development of a stereoselective HWE olefination for these cubyl systems.

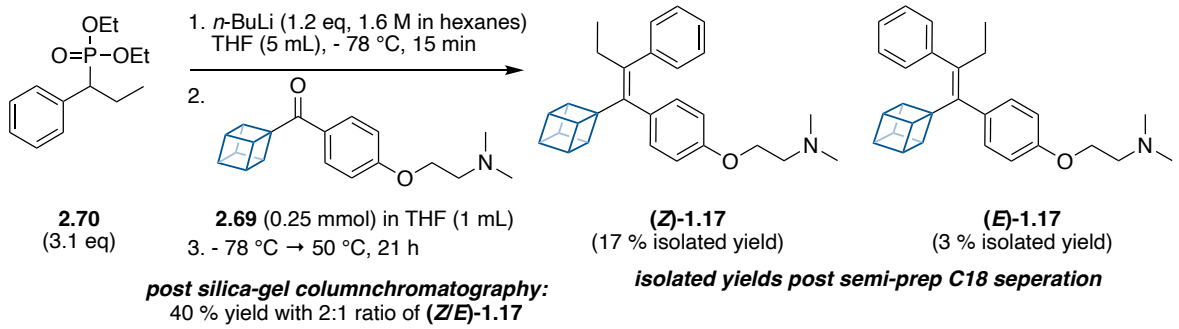

Scheme 57: Overview of HWE to synthesise (*Z*/*E*)-cubyl-tamoxifen **1.17** and separation of the two geometric isomers.

The final step was to confirm the stereochemistry of each isomer by ^{1}H NOESY experiments. Correlation between the peak at δ 3.45 – 3.39 (m, 3H, β-hydrogens of cubane) and 7.23 – 7.19 (m, 2H, *ortho*-hydrogens of unsubstituted phenyl ring) confirmed the *E*-stereochemistry (Figure 22a, red relationship), which was the major isomer in all the HWE reaction tested (Table 17). In this ^{1}H NOESY spectrum we could also observe correlation between signal at δ 3.45 – 3.39 (m, 3H, β-hydrogens of cubane) and 7.10 – 7.04 (m, 2H, Ar*H meta* to $O(CH_2)_2NMe_2$) (Figure 22a, orange relationship).

a) ^{1}H NOESY NMR (400 MHz, $CDCl_3$) spectrum of **(*E*)-1.17.**

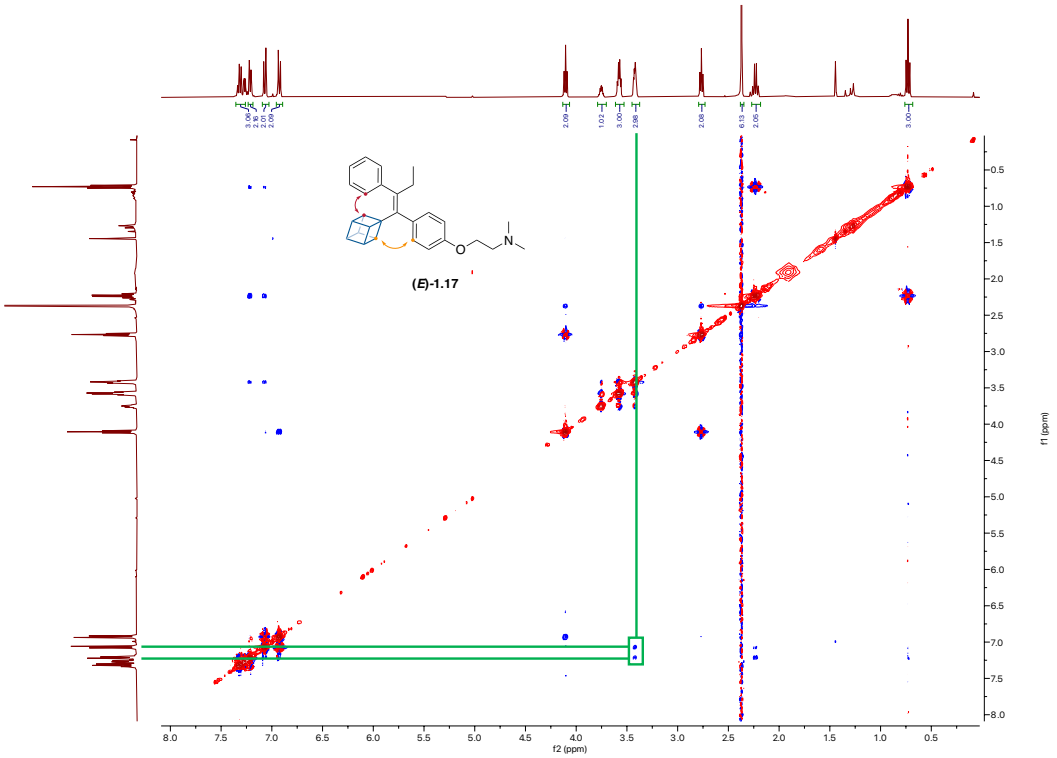

b) ^{1}H NMR (400 MHz, $CDCl_3$) spectrum of **(*Z*)-30.**

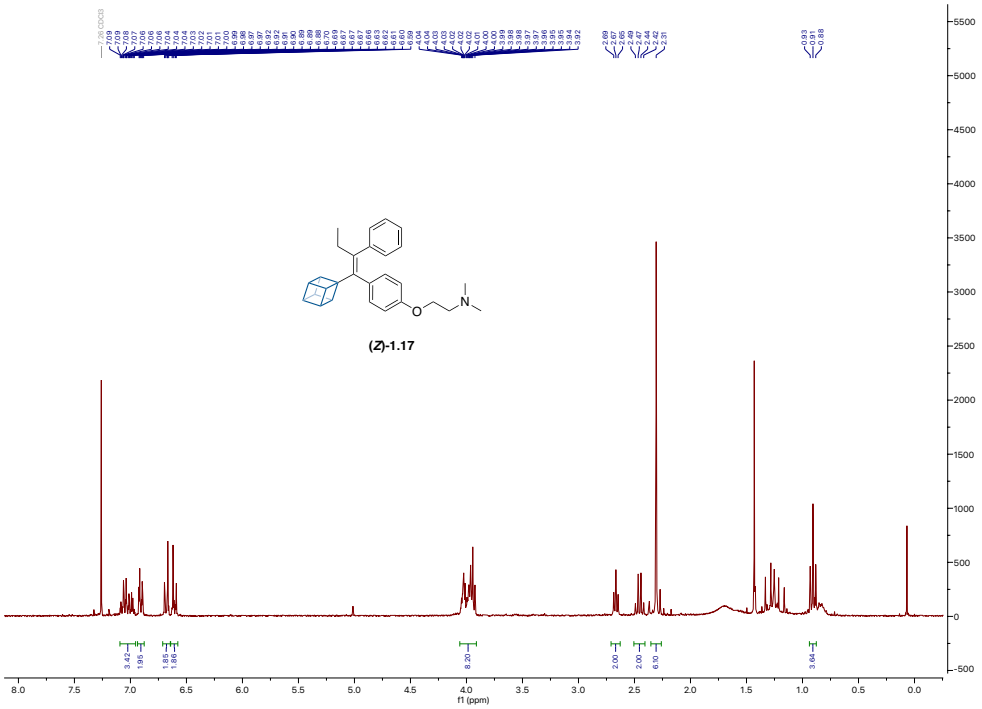

Figure 22: Selected NMR data of (*E*)-**1.17** and (*Z*)-**1.17**.

Overall, the HWE olefination has shown to be the most effective approach to synthesise all-carbon tetra-substituted olefins including cubane as a substituent. Through optimisation of both the HWE conditions and steps required for purification and isomer separation, we have synthesised and isolated the first ever mono-substituted analogues of cubyl-tamoxifen (***E*-1.17** and ***Z*-1.17**). We propose adaption of this strategy could be used to access other mono-substituted analogues of cubane tamoxifen in the future or more generally to access more complex olefin cubane derivatives.

2.3 Log*P*

In Chapter 1 we presented numerous examples of bioisosteric replacement of benzene for cubane in biologically active compounds, providing a comparison between physicochemical properties. One common property examined in these studies were differences in lipophilicity, determined experimentally by estimating the Log*P* for both the aromatic parent compound and the cubane analogue using reverse phase C-18 HPLC. A general trend observed in the literature indicated that substituting a terminal benzene ring with cubane typically results in an increase in Log*P*, therefore an increase in lipophilicity.[106, 108] Conversely, when cubane functions as a *para*-linker, the lipophilicity generally remained unchanged or reduced.[106, 108] Thus we were keen to experimentally determine the Log*P* of (*E*)-cubyl-tamoxifen (**1.17**) and (*Z*)-cubyl-tamoxifen (**1.17**) against the parent compound (*Z*)-tamoxifen (**1.1**).

Reverse phase C-18 HPLC provides a fast and practical method to estimate the Log*P* of compounds, when using a fast acetonitrile gradient. Following a well-documented protocol by Valko *et al,* the Log*P* of a compound can be obtained from its respective retention time (t_r) by using Equation 1 and 2.[188]

$$CHI = a \cdot t_r + b \quad (1)$$

$$CHI\ \text{Log}P = (0.054 \cdot CHI) - 1.467 \quad (2)$$

To determine the values for *a* and *b* in Equation 1, it is first necessary to calibrate the HPLC-system using a Valko test mixture which contained 10 compounds with a known chromatographic hydrophobicity index (*CHI*) value (*see experimental section 5.2.5.2*). By plotting the retention time of each compound against its literature *CHI* value, the trendline can be used to obtain the values of *a* and *b*. In terms of what the *CHI* value represents, it approximates the percentage of acetonitrile required for the compound to elute off the C-18 column. It includes an assumption that the compound is bound to the stationary phase (C-18 column) before the CHI value, and only at the CHI value is the compound equally distributed between the stationary phase and mobile phase.

Using the *CHI* value the *CHI* Log*P* can be determined using Equation 2. This equation is derived from fitted data of 98 known drug molecules, in which the *CHI* values were plotted against the measured Log*P* values determined by octanol-water partitioning (shake-flask method). Valko *et al* validated this protocol by showing good correlation between the *CHI* Log*P* values and the Log*P* values determined by the shake-flask method ($r^2 = 0.88$). For that reason, using reverse phase C-18 HPLC with a gradient method has become a common technique to estimate the Log*P* of compounds and thus the lipophilicity.

As the drug (*Z*)-tamoxifen is administered orally, we decided to measure Log$D_{7.4}$ to reflect the ionisation state of the drug under physiological conditions. Measuring the retention time of the 10 compounds in the Valko test C-18 mix at pH 7.4 (*see experimental section 5.2.5.2, HPLC conditions B)* and plotting this data against the literature *CHI* value of each compound, gave a calibration plot (Figure 23). The calibration runs were repeated three further times to ensure good reproducibility, therefore the retention times in Figure 23 are an average of these multiple runs.

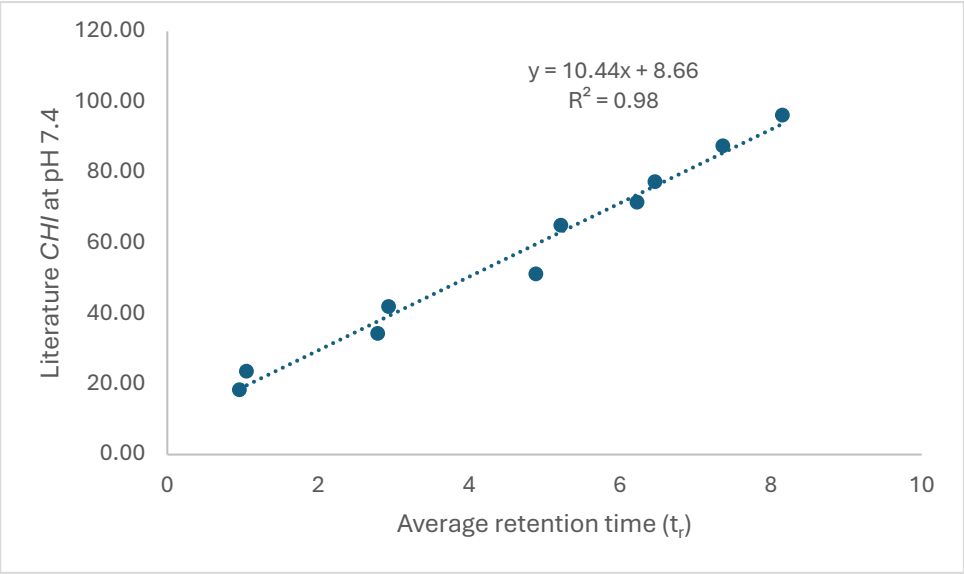

Figure 23: Calibration plot of Valko test C-18 mix (10 compounds) at pH 7.4.

Using the same HPLC method for the calibration measurements (*see experimental section,* gradient B) a sample of (*Z*)-tamoxifen (**1.1**), (*E*)-cubyl-tamoxifen (**1.17**) and a 3:1 ratio mixture of (*Z*/*E*)-cubane-tamoxifen (**1.17**) were measured twice with a chromatogram for each displayed in Figure 24.

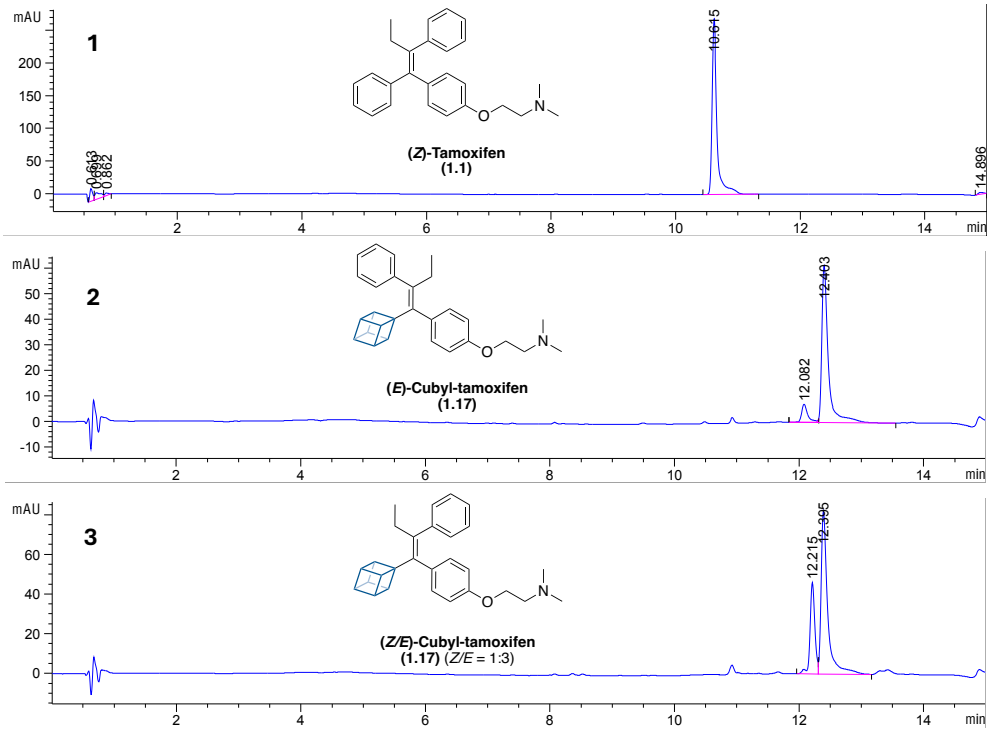

Figure 24: HPLC (C-18) chromatograms of (*Z*)-tamoxifen (**1.1**), (*E*)-cubyl-tamoxifen **1.17** and a 3:1 ratio mixture of (*Z*/*E*)-cubane-tamoxifen **1.17** at pH 7.4.

Comparison between chromatogram 1 to chromatogram 2 and 3 firstly showed that the difference in retention time of (*Z*)-tamoxifen to cubyl-tamoxifen (**1.17**) was between 1.5-2 minutes. Secondly, the sample of (*E*)-cubyl-tamoxifen **1.17** purified by semi-preparative HPLC (chromatogram 2), which by ^{1}H NMR analysis did not contain the *Z*-isomer of **1.17**, did in fact contain 6 % (*Z*)-cubyl-tamoxifen **1.17** (measured by the area under both peaks). This conclusion was based on the similar retention times measured for our sample of 3:1 ratio mixture of (*Z*/*E*)-cubane-tamoxifen (**1.17**) in chromatogram 3. Using the average retention time of **1.1**, (*E*)-**1.17** and (*Z*)-**1.17** in combination with the trendline from the calibration plot (Figure 23), a *CHI* value for each compound was calculated using equation 3. The *CHI* was then converted into Log$D_{7.4}$ using equation 2, with the results displayed in Figure 25.

$$CHI = 10.44 \cdot t_r + 8.66 \quad (3)$$

$$CHI\ \text{Log}D_{7.4} = (0.054 \cdot CHI) - 1.467 \quad (2)$$

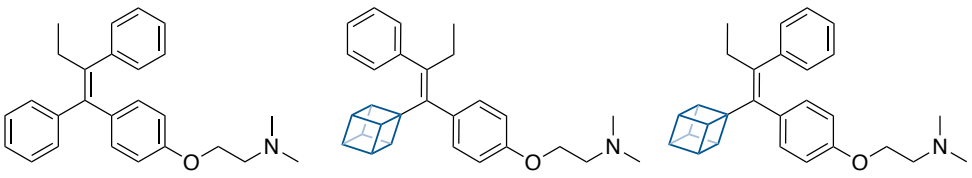

(*Z*)-Tamoxifen (1.1)

CHI = 119
log $D_{7.4}$ = 5.0

(*E*)-Cubyl-tamoxifen (1.17)

CHI = 138
log $D_{7.4}$ = 6.0

(*Z*)-Cubyl-tamoxifen (1.17)

CHI = 136
log $D_{7.4}$ = 5.9

Figure 25: HPLC-determined Log $D_{7.4}$ values.

Our data has shown that (*Z*)-tamoxifen (**1.1**, Log$D_{7.4}$ = 5.0) was less lipophilic than both (*E*)-cubyl-tamoxifen (**1.17**, Log$D_{7.4}$ = 6.0) and (*Z*)-cubyl-tamoxifen (**1.17**, Log$D_{7.4}$ = 5.9), with both isomers of cubyl-tamoxifen (**1.17**) having a comparable lipophilicity. Overall, this result supports the existing evidence in the literature that substituting a terminal benzene ring with cubane typically results in an increase in lipophilicity.

Chapter 3 Baeyer-Villiger oxidation of cubyl ketones

3.1 Introduction

3.1.1 Context

The pharmaceutical drug (*Z*)-tamoxifen is a tetrasubstituted olefin that contains three phenyl rings, with one featuring an ether substituent (Scheme 58). To substitute the functionalised phenyl ring in tamoxifen for the sp^3-hybidised bioisostere cubane (**1.19**), we envisioned that the ether bond would be constructed from the cubyl alcohol (**3.3**). Given the prevalence of phenols in medicinal chemistry, transformations that would provide access to cubyl alcohol analogues would ultimately advance the synthetic utility of cubane in drug discovery programmes.[189] From a retrosynthetic analysis, we identified that the cubane C-O bond could be installed by using the Baeyer-Villiger (BV) oxidation to transform a cubyl ketone (**3.5**) into the cubyl ester (**3.4**). We predict the conversion of the cubyl ester (**3.4**) to the cubyl alcohol (**3.3**) will be challenging. This predication is based on the work by Eaton who explored the synthesis of cubyl alcohols, which highlighted their instability and the tendency for the cubane framework to ring open.[105]

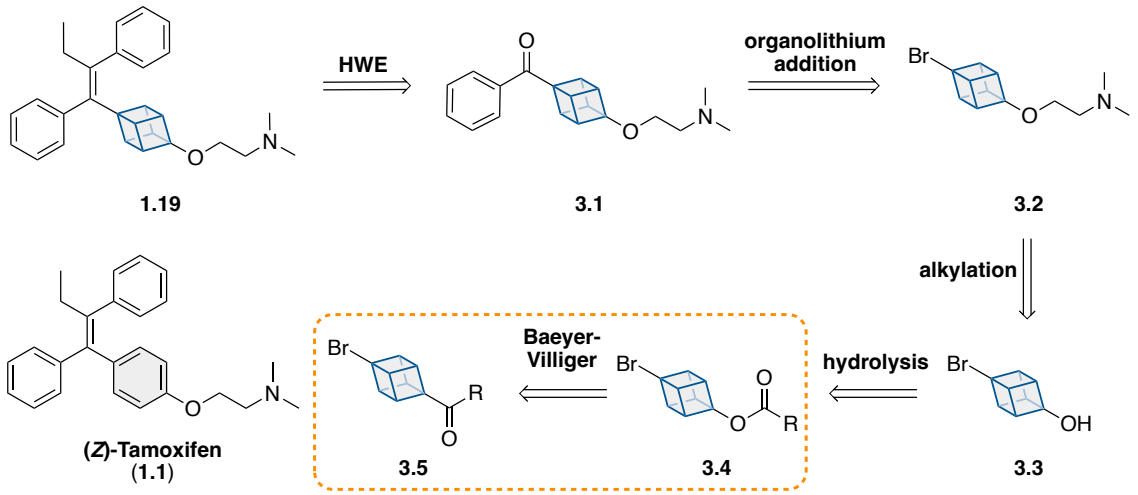

Scheme 58: Retrosynthetic analysis of cubane-tamoxifen.

The Baeyer-Villiger oxidation of cubyl ketones to cubyl esters is relatively unexplored. The Baeyer-Villiger oxidation of cubyl methyl ketones(**3.6a-e**) have been reported to give exclusively the respective cubyl acetates (**3.7a-e**) resulting from the migration of the cubyl group. (Scheme 59a).[109, 169, 190] In contrast, the Baeyer-Villiger oxidation of the cubyl phenyl ketone **3.6f**, in which the phenyl group exclusively migrated, is the only other example of cubyl ketones being used in this reaction (Scheme 59b).[191]

A. BV oxidation of cubyl methyl ketones.[109, 169, 190]

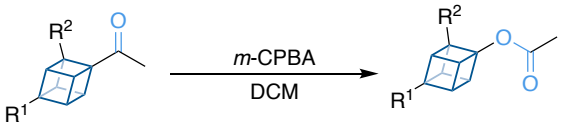

3.6a R^1 = $Si(Me)_3$, R^2 = H
3.6b R^1 = $Sn(Me)_3$, R^2 = H
3.6c R^1 = F, R^2 = H
3.6d R^1 = Me, R^2 = H
3.6e R^1 = H, R^2 = Me

3.7a 98 % yield
3.7b 71 % yield
3.7c 65 % yield
3.7d 91 % yield
3.7e 80 % yield

B. BV oxidation of cubyl phenyl ketone.[191]

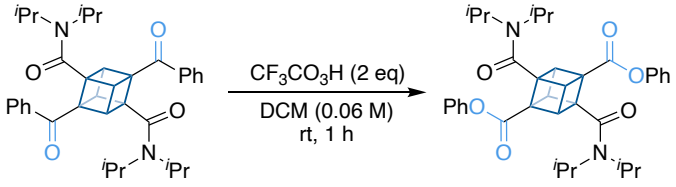

3.6f
(0.35 mmol)

3.7f

Scheme 59: Literature examples for the Baeyer-Villiger oxidation cubyl ketones.

The alternative protocols to the Baeyer-Villiger oxidation to synthesise cubyl esters in good yields all require either the addition of a directing group, large excess of oxidant or pre-functionalised reagents. For instance, Eaton and Cunkle reported an approach to treat the iodocubane (**3.8**) with peracetic acid or *m*-CPBA to generate a hypervalent iodine intermediate, which then decomposed to the cubyl acetate (**3.9a**) or cubyl benzoate (**3.9b**) respectively (Scheme 60a).[192] Unfortunately, to generate **3.9a** in a good yield, a large excess of peracetic acid was found to be required. When treating iodocubane (**3.8**) with the peracid *m*-CPBA, Eaton and Cunkle reported a shorter reaction time and fewer equivalents of oxidant were required, but the yields for the reaction were not consistent (Scheme 60a). Moriarty and co-workers reported an

extension of this methodology by treating an iodocubane (**3.10**) with hypervalent iodine reagent $C_6H_5I(OH)(OCOCF_3)$, to encourage a displacement reaction between the cubyl iodine atom and the ligand of the hypervalent reagent (Scheme 60b).[193] A large excess of the hypervalent iodine reagent was not required for this improved protocol, although the reagent did need to be preprepared and prolonged reaction times between 1-3 days were reported.

A. Oxidative deiodination – Eaton and Cunkle.[192]

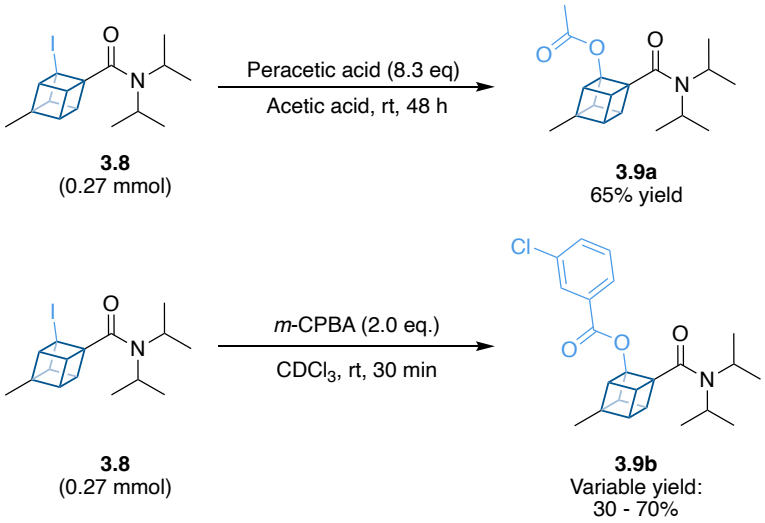

B. Hypervalent iodine reagents – Moriarty *et al*.[193]

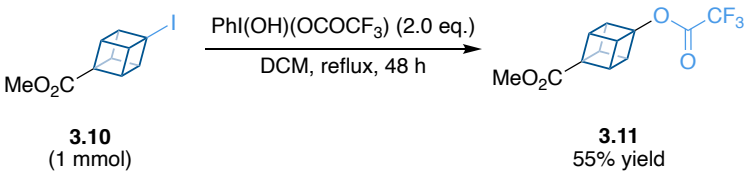

C. Direct C-H acetoxylation – Nagasawa *et al*.[194]

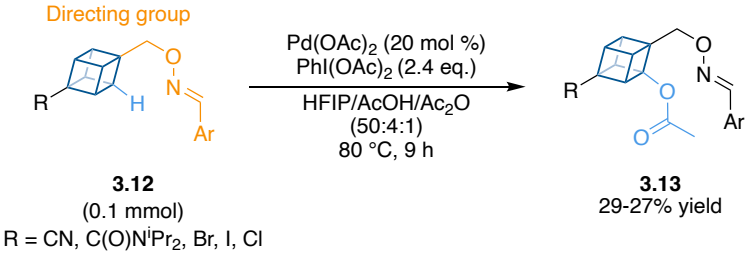

Scheme 60: Alternative routes to the Baeyer-Villiger oxidation to synthesise cubyl esters.

More recently, Nagasawa and co-workers reported a strategy to use palladium catalysed C-H functionalisation of cubane to introduce an acetate group (Scheme 60c).[194] A major drawback of this approach was the requirement of directing group (**3.12**), which took three steps to install from a carboxylic acid and two steps to reinstate the carboxylic acid. In addition, for the halide substrates a mixture of mono- and diacetoxylated products were formed. Given the drawbacks of the alternative approaches to generate cubyl acetates outlined in Scheme 60, and the relative simplicity around synthesising cubyl ketones, we sought to explore using the Baeyer-Villiger oxidation approach as a more efficient route to access cubyl esters.

3.1.2 The Baeyer-Villiger oxidation

In 1899, Adolf Baeyer and Victor Villiger discovered that the alicyclic ketones menthone (**3.14a**) and carvomenthone (**3.14b**) were converted into their respective lactones using potassium peroxymonosulfate (Scheme 61).[195] This process of converting a ketone to an ester or a lactone using a peroxyacid was later named after them as the Baeyer-Villiger oxidation. More recently, the definition of the reaction has expanded to include the oxidation an aldehyde to its respective carboxylic acid or formate.[196-198]

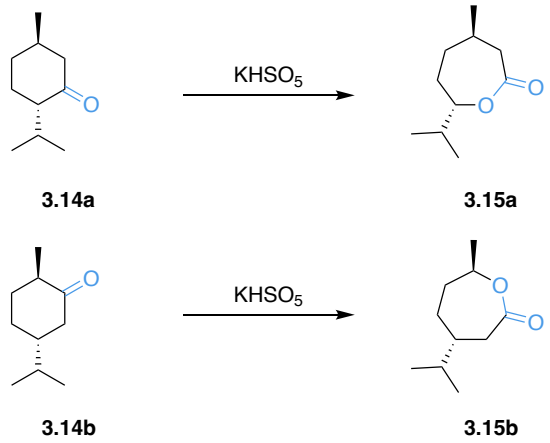

3.14a **3.15a**

3.14b **3.15b**

Scheme 61: Baeyer-Villiger oxidation of menthone (**3.14a**) and carvomenthone (**3.14b**) using potassium peroxymonosulfate.[195]

Since the discovery of the Baeyer-Villiger oxidation, the reaction has been used extensively in organic chemistry towards the synthesis of natural products[199-201], steroids[202-204], antibiotics[205], antifungal agents[206] and cancer drugs[207, 208]. The broad range

of applications that the Baeyer-Villiger reaction has been employed in, demonstrates what a versatile synthetic tool it has become since its discovery. The widespread utilisation of this reaction can be attributed to its high degree of regioselectivity, stereoselectivity and its broad functional group tolerance.[196] For instance, alcohols[209, 210], ethers[211-213], esters[214, 215] and amides[215, 216] are all well-tolerated in the Baeyer-Villiger reaction.

The Baeyer-Villiger oxidation has also found industrial application. For example, for over 30 years a manufacturing plant was producing more than 25,000 tonnes per year of ε-caprolactone (**3.17**), via the Baeyer-Villiger oxidation of cyclohexanone (Scheme 62).[217] The efficient production of ε-caprolactone attracted increasing attention from the biomedical and food packaging industry, as the lactone could be used to manufacture biocompatible and biodegradable polyesters like poly(ε-caprolactone, **3.18**) via a ring-opening polymerisation reaction.[218-220]

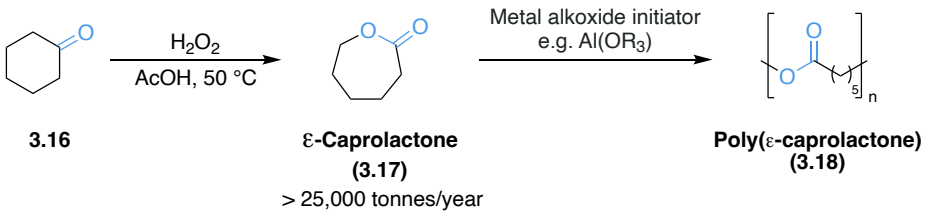

Scheme 62: 25,000 tonnes of ε-caprolactone was produced yearly by the Baeyer-Villiger oxidation of cyclohexanone.[217-220]

Recently, Snead and co-workers began to develop a more cost-efficient route to access cyclopropanol (**3.19**), which includes incorporating the Baeyer-Villiger oxidation (Scheme 63a).[221] As a synthetic intermediate, cyclopropanols are a valuable building block in organic synthesis due to their inherent reactivity.[222, 223] For instance, cyclopropanols have been widely used to facilitate the total synthesis of natural products, through ring opening or expansion reactions (Scheme 63b).[224, 225] Recently, the inclusion of a cyclopropanol motif in a clinical drug candidate (MRTX1719) that has antitumour activity has highlighted their emerging recognition as a suitable and valuable structure for future drug development (Scheme 63c).[226] The supply of

cyclopropanol has traditionally relied on a multistep synthesis starting from bromocyclopropane (**3.26**), a volatile and expensive precursor (Scheme 63d).[227] Snead and co-workers have reported a protocol that addresses the cost limitation of scaling the synthesis of cyclopropanol, by starting from the cheaper commercially available cyclopropyl methyl ketone (**3.21**) (Scheme 63d).[221]

A. Retrosynthetic analysis of cyclopropanol – Snead *et al*.[221]

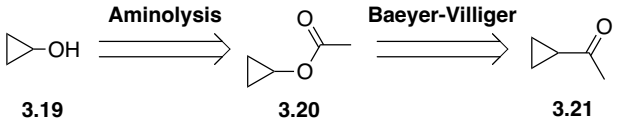

B. Total synthesis of β-araneosene via a cyclopropanol derivative.[224, 225]

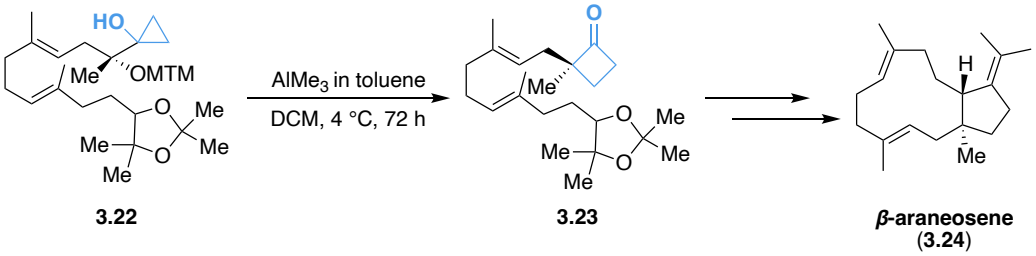

C. Clinical drug candidate for cancer treatment.[226]

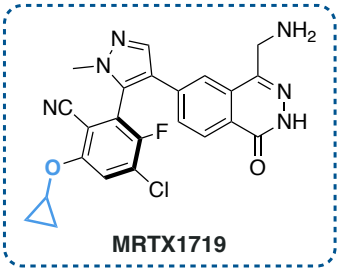

D. Synthesis of cyclopropanol.[a]

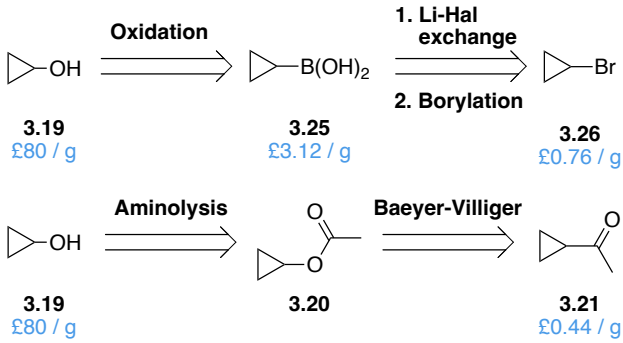

Scheme 63: Synthesis of cyclopropanol via a Baeyer-Villiger oxidation.[221]

[a] *Prices obtained from Fluorochem on 27/12/2024.*

The cyclopropyl methyl ketone (**3.21**) is oxidised via the Baeyer-Villiger reaction with trifluoroperacetic acid, which is prepared *in-situ* by mixing urea hydrogen peroxide with trifluoroacetic anhydride (Scheme 64).[221] In order to safely perform the Baeyer-Villiger oxidation on a hundreds of kilogram scale, the authors optimised a continuous flow protocol. Within 40 minutes of operation 380 g of cyclopropyl methyl ketone (**3.21**) was

oxidised under these conditions, generating a mixture of the methyl and trifluoromethyl esters (**3.20** and **3.27**) in a combined yield of 79 %. A small batch of the combined esters (15 g) was treated with ammonium hydroxide to generate cyclopropanol (**3.19**), which was directly telescoped into the S_NAr reaction to afford aryl ether **3.28** (Scheme 64). Overall, Snead and co-workers demonstrated that Baeyer-Villiger oxidation can be incorporated into a continuous flow protocol on a scale of hundreds of grams, with future work focussed on moving towards tonne scale. In addition, the authors showed the cyclopropanol prepared can be used as a valuable building block, by their synthesis of the aryl ether **3.28** which is a precursor to the clinical drug candidate MRTX1719 (Scheme 63c).

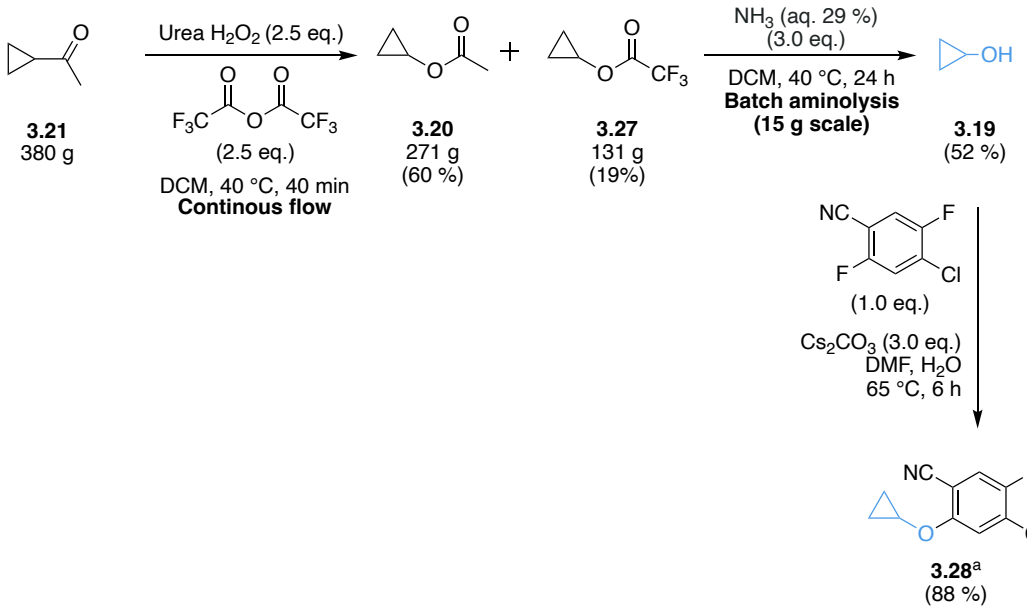

Scheme 64: Snead and co-workers work on developing a continuous flow methodology towards cyclopropanol via a Baeyer-Villiger oxidation.

[a] *Precursor used in the synthesis of the clinical drug candidate MRTX1719 (Scheme 63c).*

3.1.3 Mechanism

There were several mechanisms that were consistent with the experimental results for the Baeyer-Villiger oxidation of ketones: (a) Criegee mechanism[228] (**3.30a**); (b) Baeyer-Villiger mechanism[195] (**3.30b**); (c) Wittig and Pieper mechanism[229] (**3.30c**) (Scheme 65). To clarify which intermediate was formed during the Bayer-Villiger oxidation Doering and

Dorfman isotopically labelled benzophenone with oxygen-18 (**3.29**), treated the labelled ketone with perbenzoic acid and subsequently reduced the [^{18}O]phenyl benzoate (**3.31a** and **3.31c**) with $LiAlH_4$.[230] If the oxidation proceeded via the Criegee mechanism then the oxidation would afford [^{18}O]benzyl alcohol (**3.32a**) exclusively. The Baeyer-Villiger mechanism would result in a mixture of [^{18}O]benzyl alcohol (**3.32a**) and [^{18}O]phenol (**3.32c**); while the Wittig and Pieper mechanism would exclusively yield [^{18}O]phenol (**3.32c**). Using mass spectrometry it was reported that [^{18}O]benzyl alcohol (**3.32a**) was exclusively formed during this study, which supported the Criegee mechanism and demonstrated that the other two mechanisms were inconsistent with the experimental data.[230]

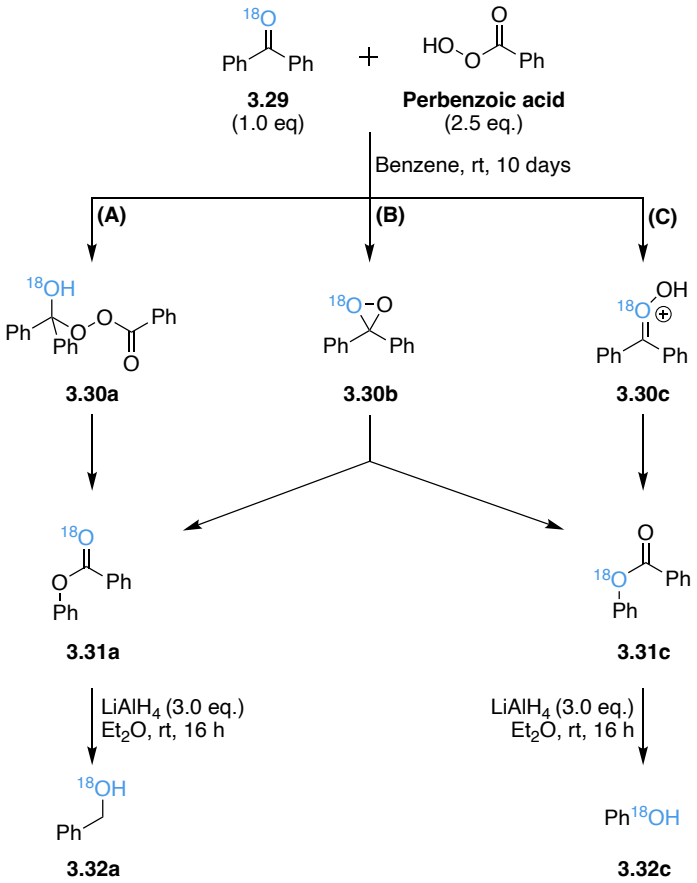

Scheme 65: The ^{18}O-labeling experiment designed by Doering and Dorfman to clarify the mechanism of the Bayer-Villiger oxidation.

(A) Concerted version of the Criegee mechanism[228] (B) Baeyer and Villiger mechanism[195] (C) Wittig and Pieper mechanism.[229]

Currently, the two-step concerted mechanism outlined by Criegee is still the accepted mechanism (Scheme 66).[228] In the initial step the ketone (**3.33**) is protonated by the peroxyacid (**3.34**). The anionic peroxyacid (**3.36**) then attacks the electrophilic carbonyl (**3.35**) to form a tetrahedral intermediate, widely referred to as the Criegee intermediate (**3.37**). In the transition state, the migratory substituent (**R^m**) migrates as the O-O single bond breaks (**3.38**), releasing the carboxylate in a concerted process. Whether the rate determining step in the Baeyer-Villiger oxidation is the addition of the peroxyacid to the carbonyl or the migration step of the Criegee intermediate, is still a topic of controversy. However, the consensus is the limiting step is largely dependent on the electronic and steric properties of the ketone substituents and the reaction conditions being used.[231] For instance, cyclohexanone reacts 200 times slower with peracetic acid than trifluoroperacetic acid.[232] Since peracetic acid is a stronger nucleophile than trifluoroperacetic acid, the carbonyl addition should be faster. However, as the observed reaction rates between trifluoroperacetic acid and cyclohexanone are significantly fast, this would suggest that for this substrate the decomposition of the Criegee intermediate is the rate-determining step.

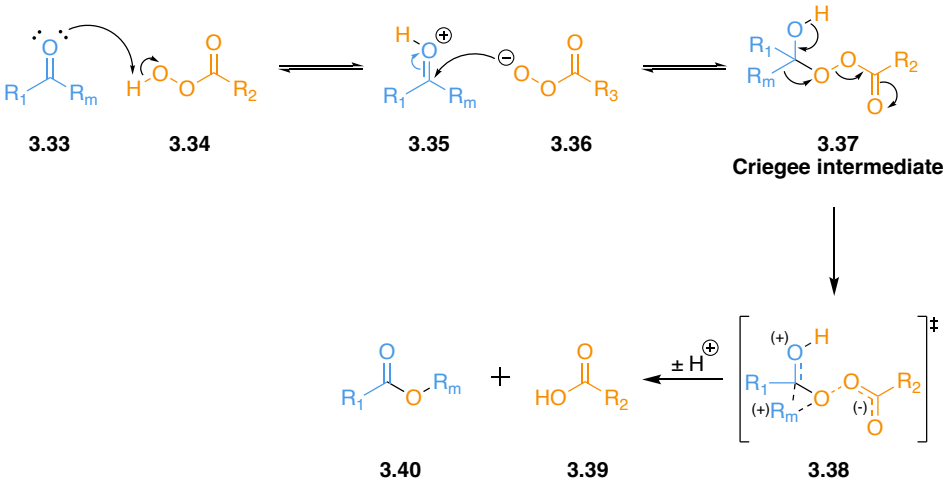

Scheme 66: The Baeyer-Villiger oxidation mechanism.

The migratory step in the Baeyer-Villiger oxidation occurs with retention of stereochemistry at the migrating carbon. This was first demonstrated by Turner when optically pure *cis*-1-acetyl-2-methylcyclohexane (**3.41**) was treated with perbenzoic

acid and the stereochemistry at the migrating centre was retained (Scheme 67a).[233] The authors determined the optical purity of the acetate (**3.42**) by measuring the melting point depression of the respective acid phthalate (**3.43**) when adding an authentic reference to it. As there was no depression in the melting point value for the acid phthalate, Turner concluded that there was no loss of stereochemistry during the Baeyer-Villiger oxidation. Mislow and Brenner provided additional evidence that the Baeyer-Villiger oxidation proceeded with retention of stereochemistry, when reporting the oxidation of (*S*)-(+)-3-phenyl-2-butanone (**3.44**) with perbenzoic acid afforded (*S*)-(-)-1-phenylethyl acetate (**3.45**) (Scheme 67b).[234] In this instance the stereochemistry of the acetate was confirmed by measuring the optical rotation of the alcohol **3.46** ($[\alpha]_D^{27}$ = - 34.1 (*c* 1.95, $CHCl_3$), 57% ee), obtained by the saponification of the acetate **3.45**, against an authentic reference of (*S*)-(-)-phenylethanol (**3.46**) (lit.[235] $[\alpha]_D^{25}$ = - 54.0 (*c* 1.0, $CHCl_3$), 97% ee). The optical rotation values were in agreement which provided strong evidence the Baeyer-Villiger oxidation proceeded with retention of stereochemistry. These two studies also demonstrated that the oxidation usually occurs with a high degree of regioselectivity, where in general the more substituted substituent will migrate (tertiary alkyl > secondary alkyl > benzyl > phenyl > H > primary alkyl > methyl). Although, there are exceptions.

A. BV oxidation of *cis*-1-acetyl-2-methylcyclohexane - Turner.[233]

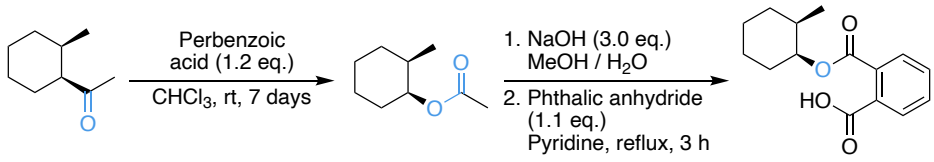

3.41 (14.3 mmol) | **3.42** | **3.43** (63 % over 3 steps)

B. BV oxidation of (*S*)-(+)-3-phenyl-2-butanone - Mislow and Brenner.[234]

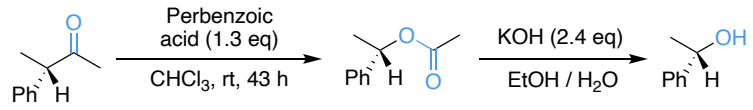

(*S*)-(+)-**3.44** 58 % ee (54 mmol) | (*S*)-(-)-**3.45** 56 % ee | (*S*)-(-)-**3.46** 57 % ee $[\alpha]_D^{27}$= -34.1° (80 % over 2 steps)

Scheme 67: Two early examples that provided evidence that the Baeyer-Villiger oxidation proceeds with retention of stereochemistry.

The observed stereospecificity and regioselectivity in the Baeyer-Villiger oxidation can be accounted for by the concepts of the primary and secondary stereoelectronic effects in the Criegee intermediate (Scheme 68a).[236-238] The primary stereoelectronic effect dictates that the migrating substituent (R_m) must be antiperiplanar to the oxygen-oxygen single bond of the peroxide. Within the Criegee intermediate, this effect ensures the σ orbital of the C-C bond (associated with R_m) has the maximum overlap with the σ* orbital of the O-O bond (Scheme 68b). This antiperiplanar alignment of the σ and σ* orbitals are critical, as it facilitates the migration of the migratory group and the cleavage of the O-O bond to occur in a concerted process with retention of stereochemistry. For the secondary stereoelectronic effect, the migrating substituent (R_m) should have an antiperiplanar alignment to one of the nonbonding electron pairs of the hydroxyl group (Scheme 68a). This alignment allows donation of electron density from the lone pair of the hydroxyl group to assist in the breaking of the R_m-C bond. When both the primary and secondary stereoelectronic effects are in place, there is an uninterrupted flow of electrons allowing the C=O bond formation, migration of R_m and O-O bond breaking to take place in a concerted process.

A. Criegee intermediate - Newman projection. **B.** Orbital interactions - Criegee intermediate.

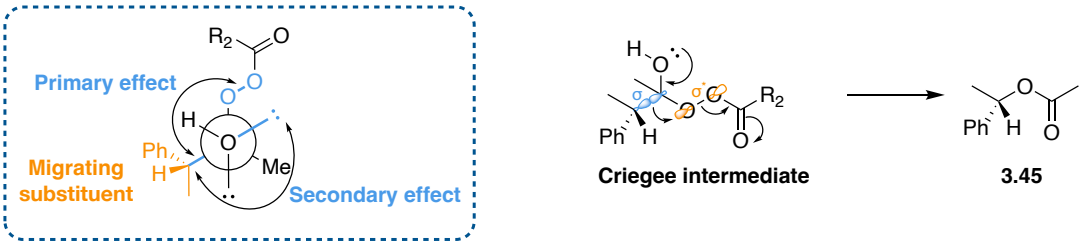

Scheme 68: Primary and secondary stereoelectronic requirements for the Criegee intermediate in the Baeyer-Villiger oxidation.

3.1.4 Primary and secondary stereoelectronic effects

Chandrasekhar and Roy were the first to provide evidence of the primary stereoelectronic effect in the Baeyer-Villiger oxidation.[236] In the study 2-oxocyclohexane acetic acid (**3.46**) was treated with peracetic acid to generate the 2-oxocyclohexane peracetic acid (**3.47**), to promote an intramolecular Baeyer-Villiger reaction (Scheme

69). The authors postulated that the breakdown of the conformationally restricted bicyclic Criegee intermediate (**3.48**) could take place by migration of either bond 'a' (under stereoelectronic control) or bond 'b' (based on migratory aptitude of the substituent). If the rearrangement of the Criegee intermediate did not require the antiperiplanar alignment of the migrating group to the O-O bond, then the tertiary centre would be anticipated to migrate in preference of the secondary centre. However, the authors reported that **3.50** was formed exclusively, from the migration of bond 'a' which had the required antiperiplanar alignment. The formation of **3.50** supports the notion that the primary stereoelectronic effect is more important than the relative migratory aptitude of substituents (tertiary alkyl > secondary alkyl > benzyl > phenyl > primary alkyl > methyl). The only drawback of the study was the product of the Baeyer-Villiger oxidation **3.49** was never isolated, as under the acidic reaction conditions the lactone was susceptible to ring-opening to form the di-acid **3.50** in a 62 % yield. The low mass balance of the product unfortunately weakens the argument that only **3.50** was formed exclusively.

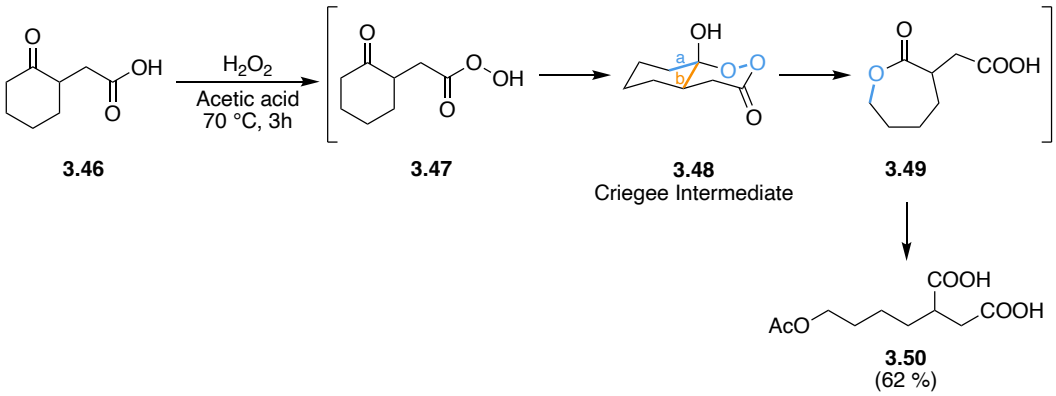

Scheme 69: Chandrasekhar and Roy's model to demonstrate the primary stereoelectronic effect in the Baeyer-Villiger oxidation.[236]

Crudden and co-workers built upon the work by Chandrasekhar and Roy to provide more compelling evidence to support the notion that the primary stereoelectronic effect has the most influence on the Baeyer-Villiger regioselectivity.[236, 238] Crudden and co-workers focussed on two systems, the oxidation of *trans*- and *cis*-4-*tert*-butyl-2-fluorocyclohexanone (**3.51** and **3.54**) with *m*-CPBA (Scheme 70).[238] In the *trans* isomer

(**3.51**) the sterically larger *tert*-butyl adopts an equatorial position forcing the smaller fluorine substituent to adopt the axial position. The major product isolated from the oxidation of **3.51** resulted from the non-fluorinated substituent migrating (**3.53b**). This was expected, as it has been widely reported that α-halo substituents of ketones supress migratory aptitude during the Baeyer-Villiger oxidation.[239, 240] For the *cis* isomer **3.54**, the sterically bulky *tert*-butyl still adopts the equatorial position, forcing the smaller fluorine to also adopt the equatorial position. When **3.54** was oxidised the regioselectivity was reversed and the α-fluoro substituent migrated preferentially (**3.56a**).

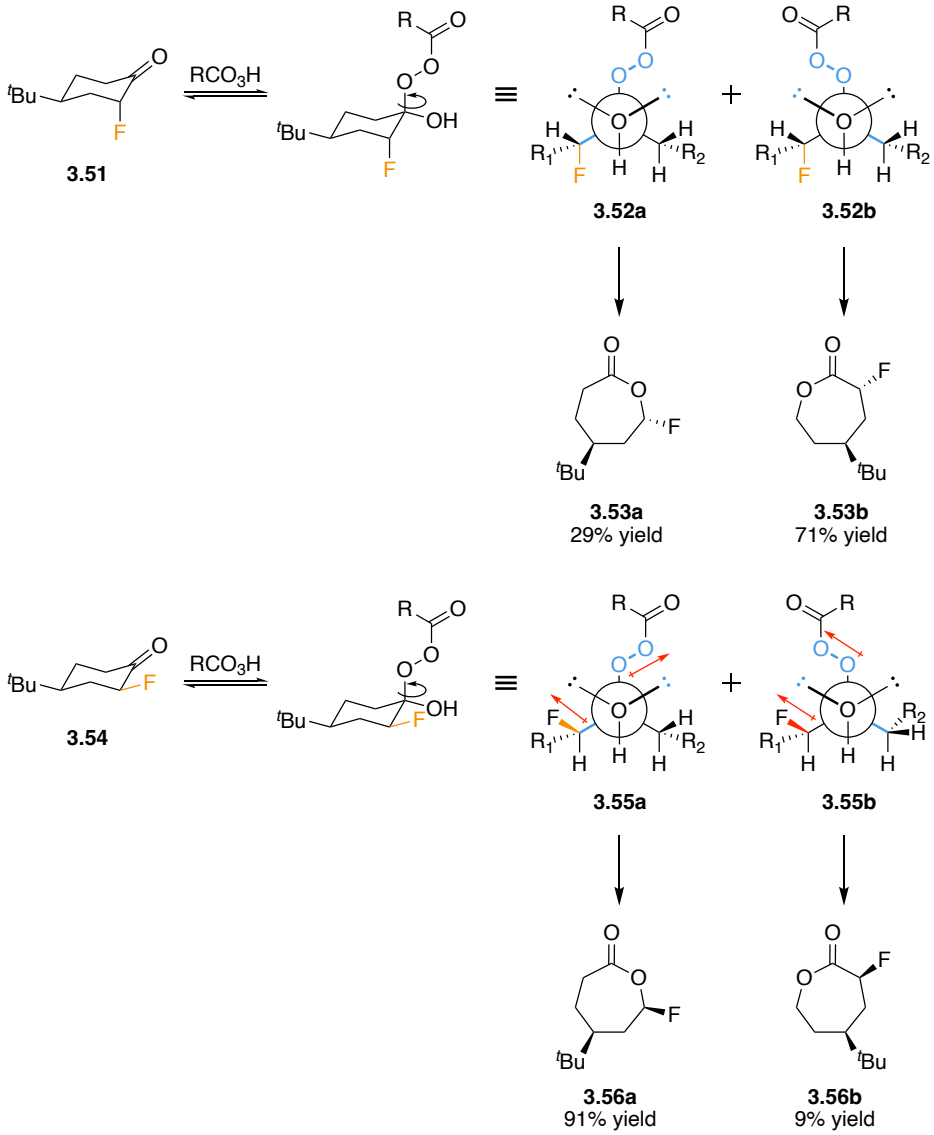

Scheme 70: Crudden and co-workers' model to demonstrate the primary stereoelectronic effect in the Baeyer-Villiger oxidation.[238]

The difference in the regioselectivity for the *cis* and *trans* ketone was understood when looking at the two reactive conformations of the Criegee intermediate (**3.55a** and **3.55b**) that obey the primary and secondary stereoelectronic rules (Scheme 70). In conformer **3.55b** the dipoles of the C-F bond and the O-O bond are pointing in the same direction, this unfavourable dipole/dipole interaction promotes the reaction to proceed via the conformer **3.55a** that does not have dipoles aligned in the same direction. Therefore, favoured migration of the α-fluoro substituent during the oxidation of the *cis* isomer demonstrated that the primary stereoelectronic effect are more important than the classical migratory aptitude of substituents.

Noyori and co-workers also used rigid bicyclic ketones to study how important the secondary stereoelectronic effects were during the Baeyer-Villiger oxidation (migrating substituent being antiperiplanar to a non-bonding electron pair of the hydroxyl group). In their investigations five bicyclic ketones (**3.57**) with different *γ*-substituents were oxidised to examine how varying degrees of steric hinderance in the Criegee intermediate would impact regioselectivity (Table 18).[237]

Table 18: The effect substituents hindering the formation of the Criegee intermediate.[237]

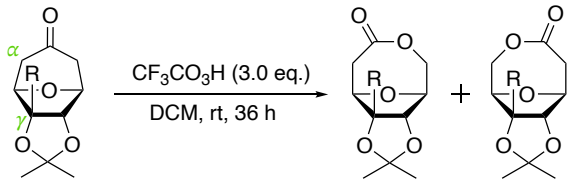

3.57 **3.58a** **3.58b**

Entry	R	Conversion of **3.57** to **3.58** / %	Ratio of **3.58a**:**3.58b**
1	H	100	-
2	CH_3	62	67:33
3	*n*-C_4H_{11}	48	75:25
4	$CH_2OCH_2C_6H_5$	32	77:23
5	*t*-C_4H_9	0	-

The oxidation of the parent bicyclic ketone (R=H) with trifluoroperacetic acid proceeded smoothly, with full conversion to the product reported (Table 18, entry 1). However, the introduction of bulkier substituents at the gamma position reduced the consumption of

the ketone (entry 2-4), with the *tert*-butyl derivative remaining unreactive under the reaction conditions (entry 5). For entries 2-4, the ratio of the two lactones was approximately the same, with a preference for migration to proceed via conformer **3.58a'** (Figure 26). The observed regiochemical outcomes can be attributed to the relative stability of the reactive conformers of the Criegee intermediate and the assumption that similar steric demands are present in the product determining transition states. In conformer **3.58a'**, the authors proposed that there is reduced steric hinderance between the hydroxyl hydrogen and the *γ*-substituent in comparison to conformer **3.58b'**. As a result, conformer **3.58a'** preferentially leads to the formation of regioisomer **3.58a**. The spatial arrangement of the hydroxyl hydrogen and the non-bonding electrons in the Criegee intermediate therefore plays a significant role in governing the regioselectivity of the Baeyer-Villiger oxidation.

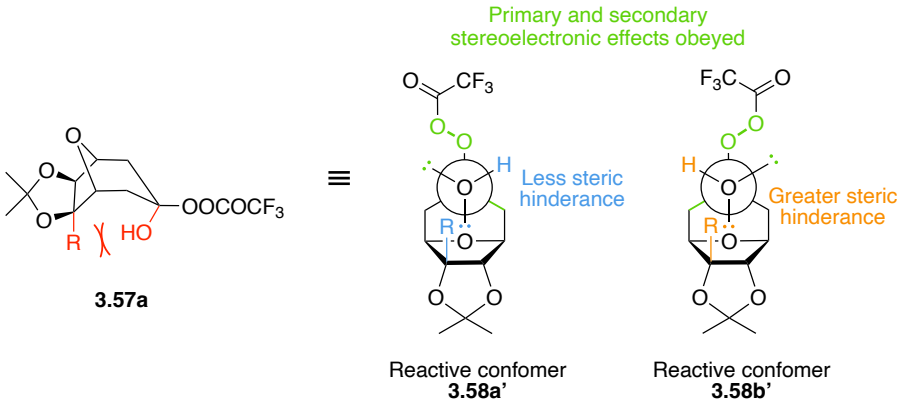

Figure 26: The two reactive conformers of the Criegee intermediate for ketone **3.57**.[237]

Vil' and co-workers postulated that if the primary and secondary stereoelectronic effects were supressed, the Criegee intermediate would be too deactivated to undergo the rearrangement step (Scheme 71).[241] This would offer further evidence that the Baeyer-Villiger oxidation cannot proceed in the absence of these two stereoelectronic effects. In their study, various ketoesters (**3.59**) were reacted with hydrogen peroxide in the presence of boron trifluoride etherate, resulting in the formation of 5-membered peroxy-Criegee intermediates (**3.60**) that were sufficiently stable to be isolated and characterised. The ability to isolate these pseudo-Criegee intermediates was attributed to the disruption of both stereoelectronic effects: (a) the loss of an antiperiplanar

alignment between the C-R_m bond and the O-O bond, and (b) weakening the donation of electron density from the hydroxy group's lone pair, achieved by substituting the hydrogen of the hydroxyl group with an OH group creating an inverse α-effect. To demonstrate that supressing the secondary stereoelectronic effect does influence the stability of the Criegee intermediate, the exocyclic hydroperoxide moiety (**3.60**) was treated with triphenyl phosphine to unmask the classical Criegee intermediate (**3.61a**). Given the reactivity normally associated with the Criegee intermediate, the authors happily reported yields ranging from modest to excellent for the isolation of several Criegee intermediates. It was observed that when the migrating centre of R_1 was a secondary or a tertiary centre, such as a *i*-propyl group (**3.61aa**) or an adamantane ring (**3.61ab**), the Criegee intermediate was not detected. In contrast, when R_1 was a primary centred *n*-propyl group the Criegee intermediate was isolated in a yield of 28% (**3.61ac**). Notably, derivatives where R_1 was a methyl group (**3.61ad**), which has a lower migratory aptitude compared to tertiary, secondary and other primary centred groups, the Criegee intermediates were isolated in higher yields. Under these reaction conditions, the trend in the stability of the Criegee intermediate is therefore consistent with the trend for the migratory aptitudes of substituents in the Baeyer-Villiger oxidation.

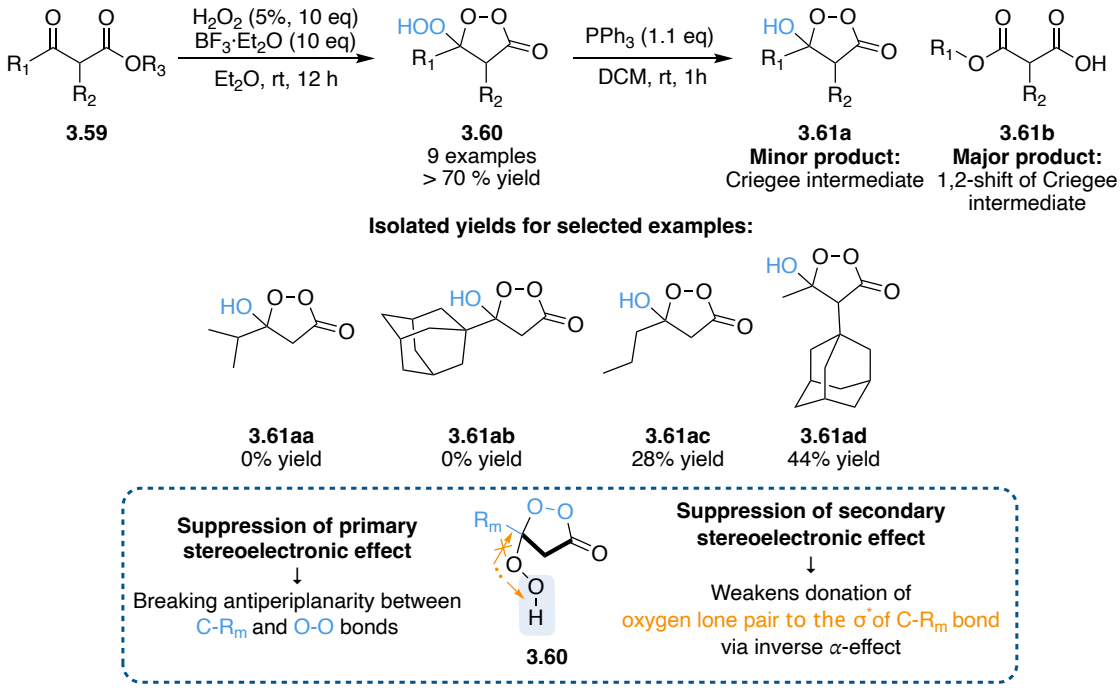

Scheme 71: Isolation of Criegee intermediate by suppressing the primary stereoelectronic effect.[241]

Structural characterisation of a non-cyclic Criegee intermediate has never been reported for the Baeyer-Villiger oxidation, due to its low stability and high reactivity.[241, 242] However similar to the work of Vil' and co-workers[241, 242], other protected derivates of the Criegee intermediate have been isolated and characterised. Instead of protecting the hydroxyl with a hydroperoxide moiety to supress the secondary stereoelectronic effects, Fox and co-workers protected the hydroxyl of the Criegee intermediate by forming the sodium salt (Scheme 72).[243] This was achieved by performing the Baeyer-Villiger oxidation of hexafluoroacetone with the sodium salt of trifluoroperacetic acid (**3.63**). The addition of the sodium salt of trifluoroperacetic acid to the ketone occurred rapidly to afford the sodium salt of the Criegee intermediate (**3.64**), which was characterised by elemental analysis and ^{19}F NMR to confirm its identity. Unfortunately, yields were not provided for any of the steps in Scheme 72, making it challenging to comment on the stability of the protected Criegee intermediate **3.64**.

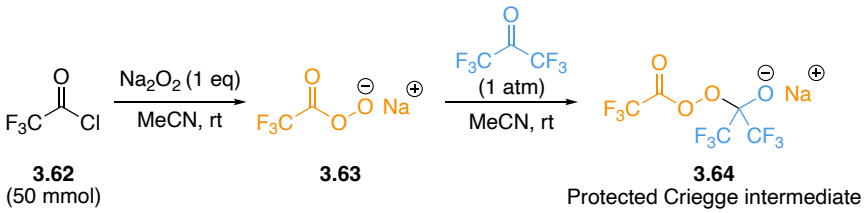

Scheme 72: Isolation of a protected Criegee intermediate during the BV oxidation of hexafluoroacetone.

3.1.5 Migratory aptitude trends

The migratory preference of substituents during the Baeyer-Villiger oxidation of an unsymmetrical ketone or an aldehyde generally follows the trend: tertiary alkyl > secondary alkyl > benzyl > phenyl > H > primary alkyl > methyl.[232, 244-246] Doering and Speers were the first to investigate the Baeyer-Villiger oxidation of unsymmetrical ketones.[247] The study focussed on treating a series of unsymmetrical benzophenones (**3.65**) with peracetic acid, to examine how different *para*-substituents on one of the phenyl rings would affect the regioselectivity of the ester products (Table 19). *Para*-substituted phenyl rings bearing electron donating groups were found to migrate in preference over the un-substituted phenyl ring (entry 1-2). However, the migration

preference was reversed when the *para*-substituent was an electron withdrawing group, which favoured migration of the un-substituted phenyl ring (entry 4-5).

Table 19: The electronic influence that different *para*-substituted benzophenones have on the Baeyer-Villiger oxidation using peracetic acid.[247]

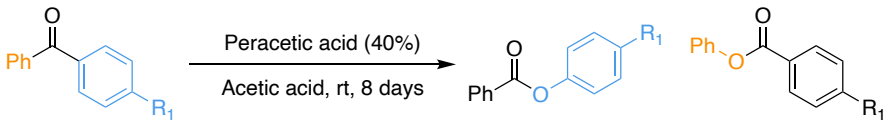

3.65 **3.66a** **3.66b**

Entry	R_1	Recovered 3.65 / %[a]	3.66a yield / %[a]	3.66b yield / %[a]
1	OCH_3	0	86	0
2	CH_3	39	47[b]	0
3	H	46	45[b]	
4	Cl	74	2	20
5	NO_2	0	0	100

[a]Isolated yield of the ester. [b]Isolated yield of the phenol after hydrolysis of the ester.

The regioselectivity reported by Doering and Speers for the oxidation of *para*-substituted benzophenones (Table 19) aligns with the kinetic studies on the Baeyer-Villiger oxidation of substituted acetophenones (Table 20).[248-251] For instance, Hawthorne and Emmons performed rate measurements on a series of *para*-substituted acetophenones oxidised with trifluoroperacetic acid (Table 20).[248] A Hammett plot of the Log(k_3) versus the Hammett constant (σ_p) for each of the *para*-substituted acetophenones was then used to calculate the Hammett reaction constant (ρ) as -1.5.[248, 252] The negative ρ value indicates that electrons are flowing out of the transition state, resulting in the development of a positive charge in the transition state. Consequently, the Baeyer-Villiger oxidation of the *para*-substituted acetophenones was accelerated by electron donating aryl groups. This reasoning similarly helps explain the Doering and Speers experimental results (Table 19), which showed a preference for the migration of electron donating aryl groups in the oxidation of *para*-substituted benzophenones.[247]

Table 20: Rate data for the Baeyer-Villiger oxidation of *para*-substituted acetophenones, using trifluoroperacetic acid in DCM at 30 °C.[248]

Entry	R	Hammett constant (σ)[252]	k_3 / L^2 mol^{-2} s^{-1}	Log(k_3)
1	*para*-CH_3	-0.17	2.9×10^{-3}	-2.54
2	*para*-H	0	1.7×10^{-3}	-2.77
3	*para*-Cl	0.23	5.3×10^{-4}	-3.28
4	*para*-Br	0.23	7.7×10^{-4}	-3.11
5	*para*-NO_2	0.78	1.1×10^{-4}	-3.96

The observed regioselectivity in the oxidation of *para*-substituted aryl ketones, where the migratory aptitude coincidentally mirrors with the trend of carbocation stability, has led to the common misconception that the regioselectivity in other ketones can be predicted solely based on the substituents ability to stabilise the partial positive charge in the transition state. Aforementioned, when predicting or explaining the regioselectivity of the Baeyer-Villiger oxidation, first all the conformations of the Criegee intermediate that fulfils the anti-periplanar alignments (primary and secondary stereoelectronic effects) should be considered.[253] The principal product typically results from the lowest energy conformer, the steric effects of which translate to the respective transition states, being mindful of the Curtin-Hammett principle.[253] When considering the energy of the transition state both structural stability, such as dipole interactions and steric repulsion, and kinetic stability, such as cation stability in the transition state are factors to consider.[253] Consequently, predicting the regioselectivity of Baeyer-Villiger oxidations for unsymmetrical ketones or aldehydes can be highly challenging without the aid of computational studies. Fortunately, a substantial body of literature exists that has documented the regioselectivity of Baeyer-Villiger oxidations since its discovery 125 years ago, allowing organic chemists to make educated predictions.

Hawthorne and co-workers investigated the Baeyer-Villiger oxidation of various alkyl phenyl ketones (**3.67**) with trifluoroperoxyacetic acid, to compare the migratory aptitude of primary, secondary and tertiary alkyl groups relative to a phenyl ring (Table 21).[232] To ensure an accurate comparison between the migratory ability of different substituents,

the authors performed the oxidations under conditions that did not encourage transesterification of the products generated. The authors achieved this by adding disodium acid phosphate to the reaction, which acted as an acid scavenger to the trifluoroacetic acid being generated. Under the conditions described in Table 21, the oxidation of acetophenone resulted in phenyl migration without measurable migration of the methyl group (entry 1). This result was not unexpected, as prior to this publication it has been reported that all functional groups migrate in preference to a methyl group.[244, 249] As a result, the Baeyer-Villiger oxidation of methyl ketones can be used as a convenient method to acquire the respective acetates, which has become a good synthetic tool to shorten the carbon chain by two units (Scheme 73).[254, 255]

Table 21: The relative migratory aptitudes of alkyl groups during the oxidation of phenyl alkyl ketones using trifluoroperacetic acid.[232]

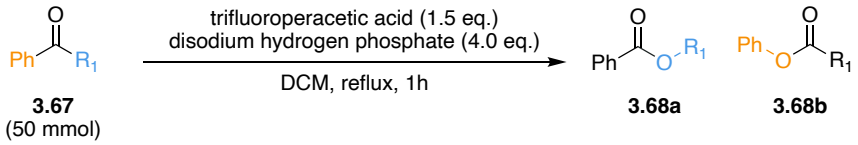

3.67 (50 mmol) **3.68a** **3.68b**

Entry	R_1	Recovered 3.67 / %[a]	3.68a yield / %[a]	3.68b yield / %[a]
1	methyl	0	-	90
2	ethyl	0	6	87
3	*n*-propyl	0	6	85
4	benzyl	0	51	39
5	*i*-propyl	0	63	33
6	cyclohexyl	0	75	25
7	*t*-butyl	11	77	2

[a]*Yields was calculated by quantitative infrared analysis of the reaction mixtures.*

Lengthening the alkyl chain to an ethyl or *n*-propyl group resulted in a loss of regioselectivity, affording **3.68a** in a 6 % yield for both substrates, due to migration of the alkyl groups. Substituting the alkyl chain to a benzyl group reversed the regioselectivity (entry 4), with benzyl migration becoming the major product in a yield of 51 %. Introducing bulkier secondary alkyl groups, such as *i*-propyl and cyclohexyl (entry 5-6), further increased the yield of ester **3.68a** to 63 % and 75 % respectively. Notably,

ketones that are excessively bulky can hinder the nucleophilic attack of the peracid to the carbonyl, resulting in incomplete consumption of the ketone, as demonstrated by the recovery of the *t*-butyl substituted ketone in a yield of 11 % (entry 7).

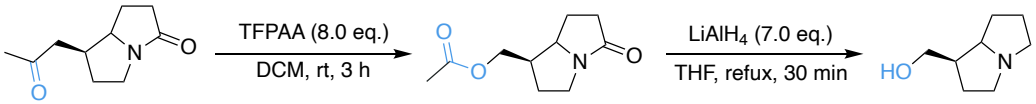

3.69 (0.54 mmol) **3.70** (56 %) **3.71** (86 %)

Scheme 73: Baeyer-Villiger oxidation of a methyl ketone to shorten the carbon chain.[255]

To further demonstrate how steric bulk proximal to the ketone can hinder the Baeyer-Villiger oxidation, Saunders oxidised a series of *ortho*-substituted benzophenones (**3.72**) with peroxyacetic acid (Table 22).[256] For each oxidation a low mass balance of the products were reported, particularly for 2-methylbenzophenone (entry 3). When Saunders resubjected the phenylbenzonate esters to the reaction conditions the esters were recovered in yields exceeding 95 %, demonstrating their stability to the reaction conditions. Therefore, the discrepancy in the mass balance was attributed to the incomplete consumption of the ketones due to the increase in steric hinderance surrounding the carbonyl.

Table 22: The steric and electronic influence of different *ortho*-substituted benzophenones have on the Baeyer-Villiger oxidation using peracetic acid.[256]

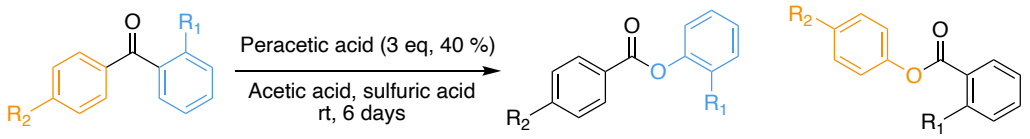

3.72 (10 mmol) **3.73a** **3.73b**

Entry	R_1	R_2	3.73a yield / %[a]	3.73b yield / %[a]
1	Cl	H	0	71
2	Cl	Cl	0	80
3	CH_3	H	12	38
4	OCH_3	H	82	0

[a] *Isolated yield of the respective acids after the hydrolysis of the ester products.*

In the oxidation of the *ortho*-chlorophenyl ketone, no migration of the *ortho*-chlorophenyl was observed (Table 22, entry 1). This result was consistent with the findings of Doering and Speers, that reported when 4-chlorobenzophenone was treated with peracetic acid only migration of the unsubstituted phenyl ring was observed (Table 19, entry 4). Direct comparison between migration of *para*-chlorophenyl and *ortho*-chlorophenyl saw only the *para*-substituted chlorophenyl migrate under these conditions (Table 22, entry 2). The regioselectivity could be attributed to: (a) an unfavourable dipole interaction between the *ortho*-Cl group and the carboxylate leaving group in the transition state, and/or (b) the *ortho*-Cl group interfering with the ability of the *ortho*-chlorophenyl to rotate to the required conformation to obey the primary and secondary stereoelectronic factors. The addition of a methyl group at the *ortho* position activated this ring relative to the chloro-substrate, which promoted the *ortho*-methylphenyl group to migrate in a yield of 12 % (entry 3). The introduction of *ortho*-methoxyphenyl, a stronger electron donating group compensated for the *ortho*-steric interference resulting in no migration of the unsubstituted phenyl group (entry 4).

Having discussed the relative migratory aptitude of aryl and alkyl groups in the Baeyer-Villiger oxidation, the final aspect to review is the migratory aptitude of a hydrogen atom, which can be examined by the oxidation of aldehydes. Lehtinen and co-workers oxidised a series of primary and secondary aliphatic aldehydes with *m*-CPBA (Table 23).[245] The primary aliphatic aldehydes were mostly oxidised to the carboxylic acid by *m*-CPBA, resulting from the migration of the hydrogen atom (entry 1-2). Although, if the α-carbon of the aldehyde was secondary the formation of the formate was favoured over the carboxylic acid under the same conditions (entry 3-5).

Table 23: Oxidation of primary and secondary aldehydes (13 mmol) with *m*-CPBA (1.2 eq) in DCM at room temperature for 2 hours.[245]

Entry	Aldehyde	Recovered aldehyde / %[a]	Formate / %[a]	Carboxylic acid / %[a]
1	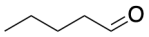	-	-	100
2	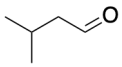	22	-	78
3	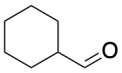	1	55	44
4	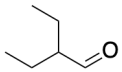	4	73	23
5[b]	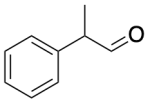	-	96	2

[a] *Yields for the oxidation products were determined by GC-MS equipped with EI and CI.* [b] *By-products formation was reported.*

Tertiary aldehydes can also be oxidised using *m*-CPBA, as evidenced by the work of DeBoer and Ellwanger studying the oxidation of aldehyde lactones (Scheme 74).[257] When the aldehyde **3.74** (1:1 mixture of diastereomers) was subjected to the reaction conditions, the formate **3.75** was isolated in a 85 % yield. Unfortunately, during the work-up of the reaction the authors performed a base wash, therefore there was no way to conclude if the carboxylic acid was generated. Nevertheless, even if the carboxylic acid was produced the fact the formate was isolated with an 85 % yield demonstrates the tertiary carbon centre had a greater migratory ability under these reaction conditions.

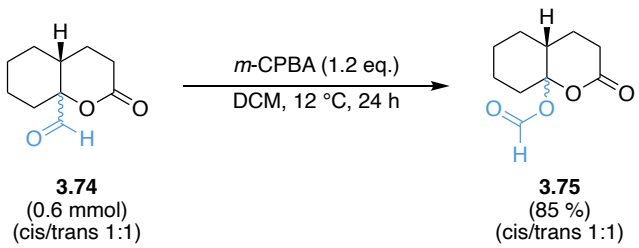

3.74
(0.6 mmol)
(cis/trans 1:1)

3.75
(85 %)
(cis/trans 1:1)

Scheme 74: Oxidation of a tertiary aldehyde (1:1 mixture of diastereomers) with *m*-CPBA.[257]

3.1.6 Impact of reagent selection

When selecting a peracid for the oxidation, there are a range of reagents to choose from with varying oxidising strengths. The reactivity of the oxidising agent is related to the acidity of the conjugate acid of the leaving group, therefore the strength order of common peracids is TFPAA > *m*-CPBA > peracetic acid > hydrogen peroxide. Predicting the regioselectivity of the Baeyer-Villiger reaction is not trivial, as using different peracids on the same substrate can change the regioselectivity of the oxidation. One study compared the percentage of phenyl migration when phenyl cyclohexyl ketone (**3.76**) was oxidised with peroxyacetic acid verses trifluoroperoxyacetic acid (Table 24).[232] When using the weaker peracid 10 % phenyl migration was reported (entry 2), versus 20 % phenyl migration for the stronger peracid (entry 1). The authors reported that when using the oxidant trifluoroperacetic acid, it is likely the Criegee intermediate was more reactive. As a consequence, the effect of the migrating groups on the energies of the transition state was reduced, resulting in lower regioselectivity when using a stronger oxidant.

Table 24: Impact on regioselectivity when employing different strength peracids.

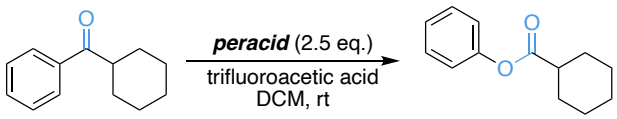

3.76
(0.2 mmol)

3.77

Entry	Peroxyacid	Phenyl migration (3.77) / %
1	Trifluoroperoxyacetic acid	20
2	Peroxyacetic acid	10

The choice of solvent can also have a significant effect of the regioselectivity. If the oxidation of a ketone/aldehyde leads to conformations of the Criegee intermediate where there are unfavourable dipole/dipole interactions (Scheme 70), using a more polar solvent can be used as a technique to stabilise the dipole moments and alter the regioselectivity of the reaction.[238] This is demonstrated in Table 25 where the selectivity of the oxidation of the equatorial substrate (**3.78**$_{eq}$), that suffers with unfavourable

dipole/dipole interactions (**3.79a** versus **3.79b**), decreases in more polar solvents (entry 1-5). Whereas the regioselectivity of the axial substrate (**3.82**$_{ax}$), which does not have unfavourable dipole/dipole interactions (**3.83a** and **3.83b**), is mostly unaffected in different solvents (entry 6-10).

Table 25: The effect of solvent polarity on the regioselectivity for the oxidation of 3.78$_{eq}$ and 3.82$_{aq}$.[238]

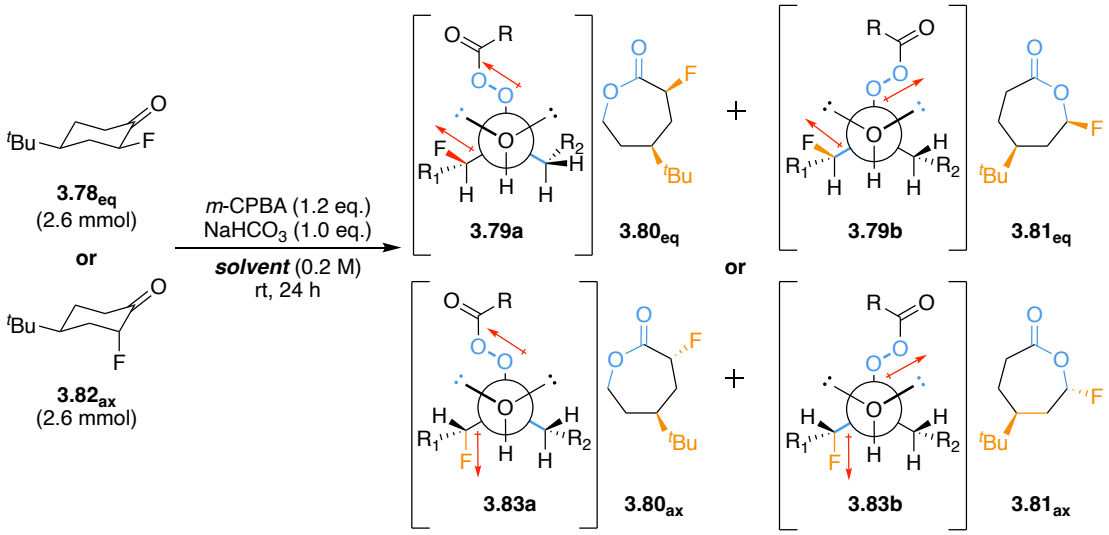

Entry	Ketone	Solvent	Ratio of 3.80 : 3.81
1	**3.78**$_{eq}$	CCl_4	1 : 13.6
2	**3.78**$_{eq}$	$CHCl_3$	1 : 9.3
3	**3.78**$_{eq}$	DCM	1 : 7.2
4	**3.78**$_{eq}$	MeCN	1 : 5.5
5	**3.78**$_{eq}$	Sulfolane	1 : 5.1
6	**3.82**$_{ax}$	CCl_4	1.3 : 1
7	**3.82**$_{ax}$	$CHCl_3$	2.4 : 1
8	**3.82**$_{ax}$	DCM	2.5 : 1
9	**3.82**$_{ax}$	MeCN	2.6 : 1
10	**3.82**$_{ax}$	Sulfolane	2.5 : 1

3.1.7 Migratory aptitude of strained hydrocarbons

There has been a substantial amount of research on the oxidation of ketones and aldehydes over the last 125 years, however, there is limited amount of data about the

behaviour of strained hydrocarbon systems during this transformation. For the oxidation cyclopropyl systems with trifluoroperacetic acid and *m*-CPBA, the migratory sequence reported was phenyl ~ secondary alkyl > primary alkyl > cyclopropyl > methyl (Table 26, entry 1-4).[258] Interestingly entry 4, where phenyl migrated preferentially to cyclopropane, directly contradicted an earlier study on the same substrate, in which the cyclopropyl group migrated preferentially (entry 5).[259] The main difference between the two reactions was entry 5 used a weaker oxidising agent perbenzoic acid. Again, this is another example where the choice of peracid can alter the regioselectivity of the reaction.

Table 26: The migratory aptitude of different cyclopropyl ketones.[258]

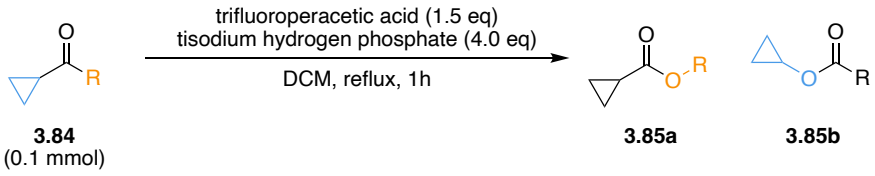

3.84 (0.1 mmol) **3.85a** **3.85b**

Entry	R	3.93a Yield / %	3.93b Yield / %
1	CH_3	4	96
2	*n*-C_2H_5	79	21
3	*i*-C_3H_7	94	6
4	C_6H_5	97	3
5[a]	C_6H_5	11	57

[a]*Ketone was treated with perbenzoic acid (1.0 eq) in $CHCl_3$ at 35 °C for 8 days.*[259]

The first Baeyer-Villiger oxidation of a cubyl ketone was reported by Eaton and co-workers, who treated a cubyl phenyl ketone (**3.6f**) with trifluoroperacetic acid (Scheme 75a).[191] The authors reported the reaction proceeded with exclusive migration of the phenyl group, although the yield of cubyl benzoate (**3.7f**) was not reported. However, in the doctoral thesis written by Millikan, it was reported that the crude product mixture from the BV oxidation of **3.6f** was directly hydrolysed using sodium hydroxide to obtain the respective di-carboxylic acid, which was subsequently treated with ethereal diazomethane to give the methyl ester **3.86** in 85 % yield over three steps (Scheme 75a).[260] Eaton continued to further explore cubane chemistry and used the Baeyer-

Villiger oxidation as a synthetic route to study the solvolysis of 4-substituted mesylate and triflate cubanes (Scheme 75b).[169] Both methyl-4-(trimethylsilyl)cubyl ketone (**3.6a**) and methyl-4-(trimethylstannyl)cubyl ketone (**3.6b**) were treated with *m*-CPBA, with the corresponding acetates being isolated in a 98 % and 71 % yield respectively. Unfortunately, only the reagents used for the oxidation and the melting point of the acetates were reported, no further experimental or analytical data was included to conclusively prove that no other by-products were formed under these reaction conditions.

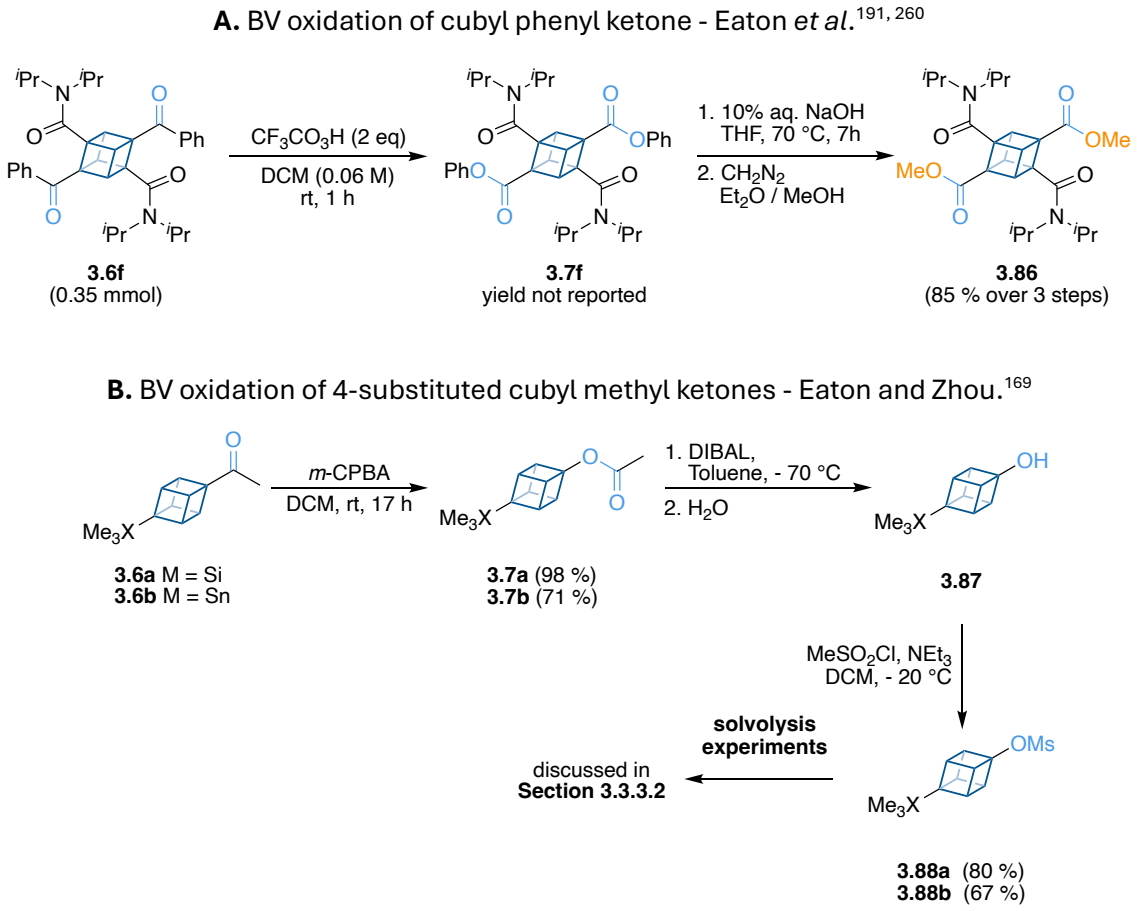

Scheme 75: Eaton literature examples for BV oxidations of cubyl ketones.

Della and Head investigated how the ^{19}F chemical shifts vary with different 4-substituted fluorocubanes (Scheme 76a).[190] One of the substrates included in the study was 4-fluorocubane acetate (**3.7c**), which was synthesised by treating methyl-4-fluorocubane ketone (**3.6c**) with *m*-CPBA. Similarly to Eaton[169], it was reported that only

the acetate was formed under these conditions, which was verified with ^{1}H NMR analysis and elemental analysis of the crude product.[190] The last example for the oxidation of a cubyl ketone was a year later by Choi and co-workers, which used the Baeyer-Villiger oxidation to synthesise authentic references for their studies on the hydroxylation of methyl cubanes (Scheme 76b).[109] Once again, the Baeyer-Villiger oxidations in this study was of substituted methyl cubyl ketones (**3.6d-e**) and the corresponding cubane acetates were formed (**3.7d-e**). In all four of these papers the authors have made no reference to whether the substituted cubane ketones were fully consumed and how they determined there was exclusive migration of one substituent in each instance. In addition, most of the examples are for the oxidation of methyl ketones, in which we are aware that a methyl group almost never migrates during the Baeyer-Villiger oxidation. Currently, no study has attempted to look at the migratory behaviour of cubane against different functional groups for this reaction.

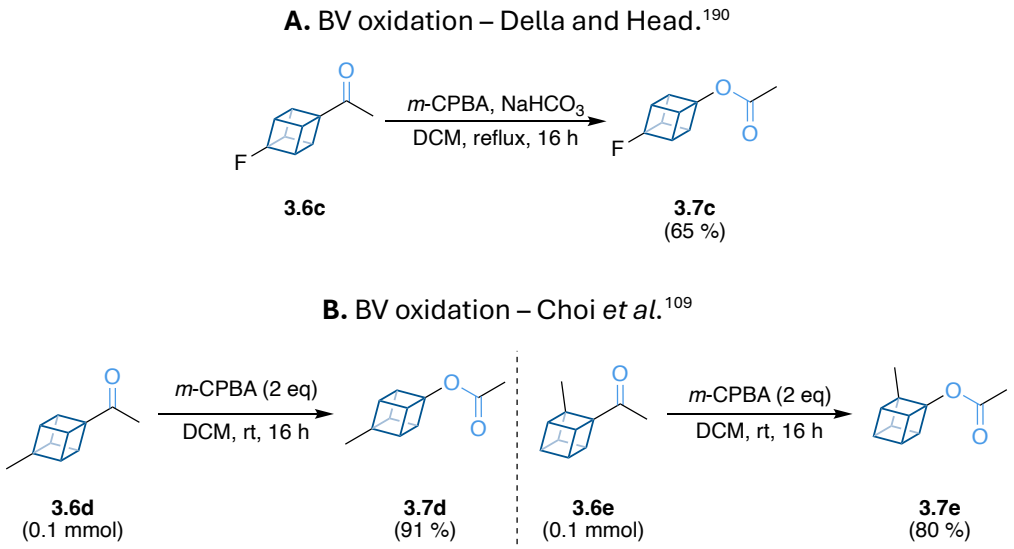

Scheme 76: Further examples of the Baeyer-Villiger oxidation of cubyl ketones.

The migratory tendencies of other polycyclic bridgeheads have been examined by measuring the kinetics of the Beckmann rearrangement of methyl ketoxime picrates (**3.89**, Table 27).[261] In the Beckmann rearrangement the group that is *anti* to the leaving group will always migrate (Scheme 77).[262] Therefore, the oximes in Table 27 were prepared in a way that ensured the polycyclic bridgeheads were *anti* to the picrate

leaving group. The kinetic data showed that the rate of the rearrangement was higher for the class of polycyclic bridgeheads that had less ring strain. Although, the most noteworthy result was the cubane oxime migrating faster than the *tert*-butyl oxime (entry 1 versus entry 4), potentially indicating that the migratory aptitude of cubane in the Baeyer-Villiger oxidation could be comparable to that of a *tert*-butyl group.

Table 27: Comparison of the rate of the Beckmann rearrangement of polycyclic bridgehead oximes.[261]

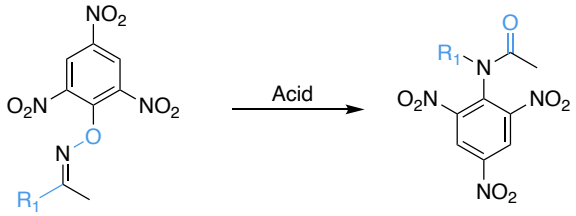

3.89 **3.90**

Entry	R_1	$10^5 \cdot k_{80°C}$ / s^{-1}
1		60
2		5
3		88
4		126
5		192
6		520
7		4580

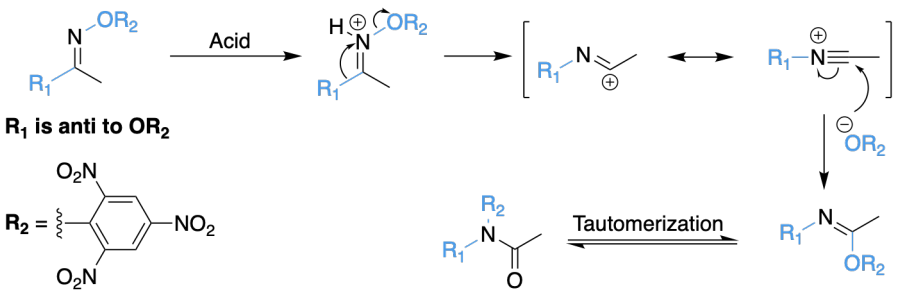

Scheme 77: Mechanism of the Beckmann rearrangement.

Given the limited number of reports on the Baeyer-Villiger oxidation of cubyl ketones, we believe it is important to perform a systematic examination of the Baeyer-Villiger oxidation of a series of functionalised unsymmetric cubyl ketones to investigate how steric and electronic factors influence the migratory aptitude of cubane, thus allowing us to determine where cubane is positioned in the BV migratory aptitude series. The cubyl ester products in which the cubane has migrated could then be used to access cubanols, a synthetic intermediate we had earlier identified as being critical for the synthesis of our most complicated cubyl tamoxifen analogue (Chapter 4).

3.2 Results and discussion

The work described in this chapter has been published.[263]

3.2.1 Preparation of substrate for BV optimisation studies

To examine the migratory aptitude of cubane in the Baeyer-Villiger (BV) oxidation of unsymmetrical cubyl ketones, we began by synthesising phenyl-4-phenylcubyl ketone (**3.91a**) for the optimisation studies. In the BV oxidation the migratory aptitude of a phenyl ring in acyclic ketones normally lies in the middle of the trend (Figure 27), therefore, the initial preliminary studies on the BV rearrangement of **3.91a** should provide valuable information regarding the migratory aptitude of cubane.[232, 244] The phenyl ring on the γ-carbon on the cubyl framework was selected to increase the molecular mass of the optimisation substrate, ensuring the ester products of the BV rearrangement were not volatile or prone to sublimation.

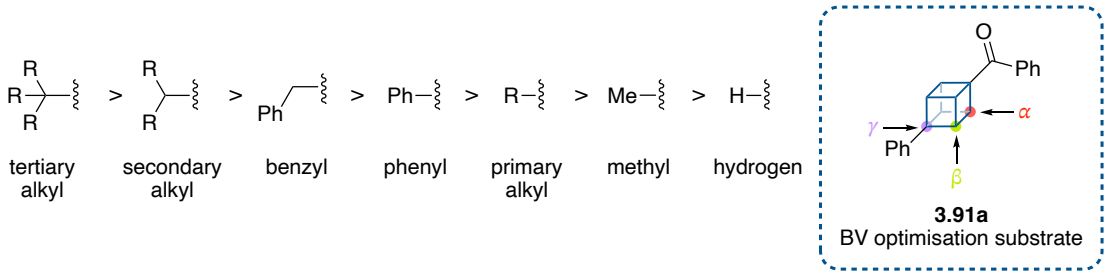

Figure 27: General migratory aptitude trend in the BV rearrangement and cubyl ketone 3.91a selected for BV optimisation studies.

Ketone **3.91a** was synthesised in five steps in an overall yield of 28 %, starting with the commercially available material 4-methoxycarbonylcubanecarboxylic acid (**2.8**) (Scheme 78 & 79). To introduce the phenyl ring onto the cubane framework, a C-C cross-coupling reaction was utilised (Scheme 78). The metal-mediated cross coupling arylations of cubane redox-active ester that have been reported include: Ni-mediated by the Senge group,[163] Fe-mediated by the Baran group[162] and Cu-mediated by the MacMillan group[88]. These cross-coupling reactions for cubane rely on activating the carboxylic acid as their redox-active ester derivatives, either as the *N*-hydroxyphthalimide (**2.9**) or the *N*-hydroxy-tetrachlorophthalimide (**2.9a**). We opted to use the Ni-based cross coupling system to synthesise **2.55** based on the superior yields and broad substrate scope reported.[163] To begin with the commercially available **2.8** was treated with oxalyl chloride (1.2 eq) in DCM with a catalytic quantity of DMF (10 mol %) at rt, after 1.5 hours this produced the acid chloride. Direct addition of the acid chloride to a solution of *N*-hydroxyphthalimide (1.2 eq) and triethylamine (2.5 eq) in DCM for 2 hours at rt gave **2.9** as a yellow solid. It was found that the phthalimide **2.9** was slightly unstable to silica gel column chromatography. Therefore, we opted to purify the crude product by washing the impure solid with hexane several times, this gave pure **2.9** in 94 % yield. The next step was the Ni-mediated cross-coupling between **2.9** and an arylzinc reagent. Preparation of the arylzinc reagent was achieved by the addition of bromobenzene (1 eq) to magnesium turnings (1.2 eq) in the presence of lithium chloride (1 eq) in THF at room temperature, followed by the addition of the Grignard to a solution of anhydrous $ZnCl_2$ in THF. An excess of the freshly prepared arylzinc reagent (3.5 eq) was subsequently added to a solution of **2.9** (1 eq), $NiCl_2$-glyme (1 eq) and

dimethyl 2,2'-bipyridine-4,4'-dicarboxylate (2 eq) in DMF at room temperature to give **2.55** in 53 % yield after purification by silica gel column chromatography. Pleasingly, we found the Ni-mediated cross-coupling to be reliable, with no reduction in yield when scaling the reaction from 0.1 to 2 mmol of **2.9** (49 % and 53 % isolated yield respectively).

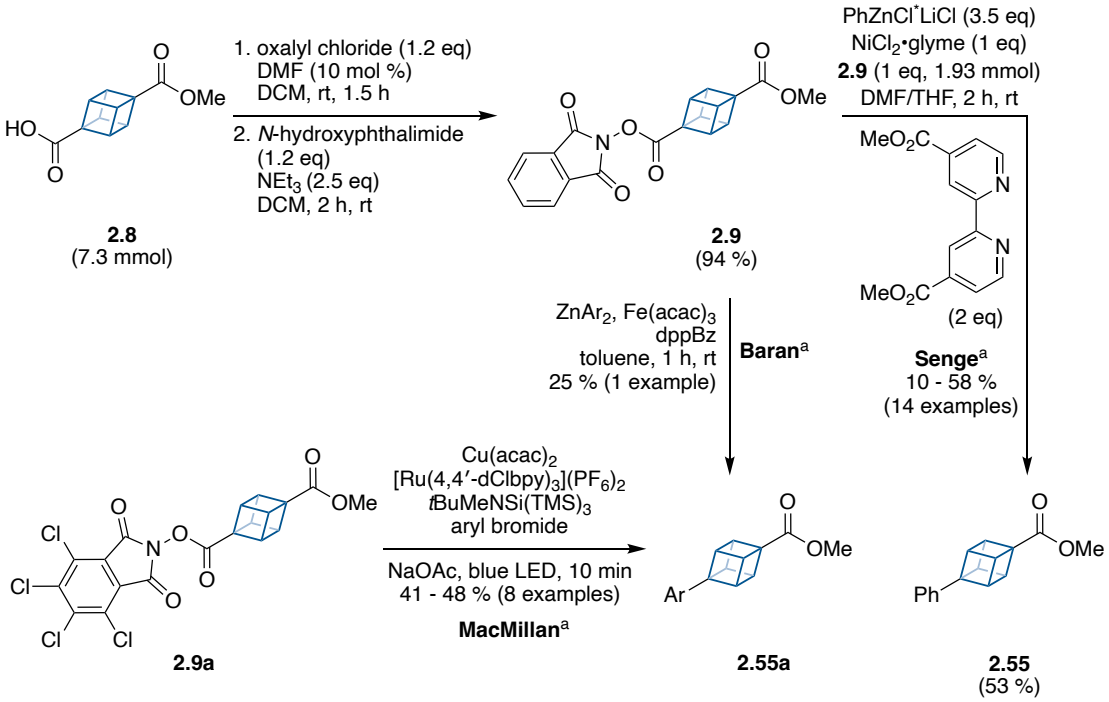

Scheme 78: Synthesis of 2.3 via a Ni-mediated cross-coupling.

[a] *Literature methods for metal-mediated C-C cross-coupling arylations for cubane.*[88, 162, 163]

With the aryl group now installed, we then turned our attention to the opposite side of the cubane scaffold. The direct synthesis of a ketone from a carboxylic acid derivative, for example from a methyl ester, is often not efficient due to the newly formed ketone being highly susceptible to attack from any remaining organometallic reagent in the reaction. To avoid the tertiary alcohol being formed as a by-product we opted to proceed via the Weinreb amide.[147] Preparation of the Weinreb amide **3.93** began with the hydrolysis of the methyl ester **2.55** (1 eq) with lithium hydroxide (2.5 eq) in THF:MeOH:H_2O (3:3:1, 0.34 M) at room temperature, which gave the carboxylic acid **3.92** in a yield of 95 % (Scheme 79). Following a protocol similar to that described previously the carboxylic acid moiety was converted to the acid chloride with oxalyl

chloride, which when treated directly with *N,O*-dimethylhydroxylamine (1.4 eq) and triethylamine (2.5 eq) afforded the Weinreb amide **3.93** in 81 % yield after purification by silica gel column chromatography. Addition of the Grignard phenylmagnesium bromide (1.5 eq, 1 M in THF) to the Weinreb amide **3.93**, gave the desired ketone **3.91a**. As expected, in the crude product no over addition of the Grignard to form the tertiary alcohol side product was detected by TLC or ^{1}H NMR analysis, with **3.91a** isolated in a 74 % yield after purification by silica gel column chromatography.

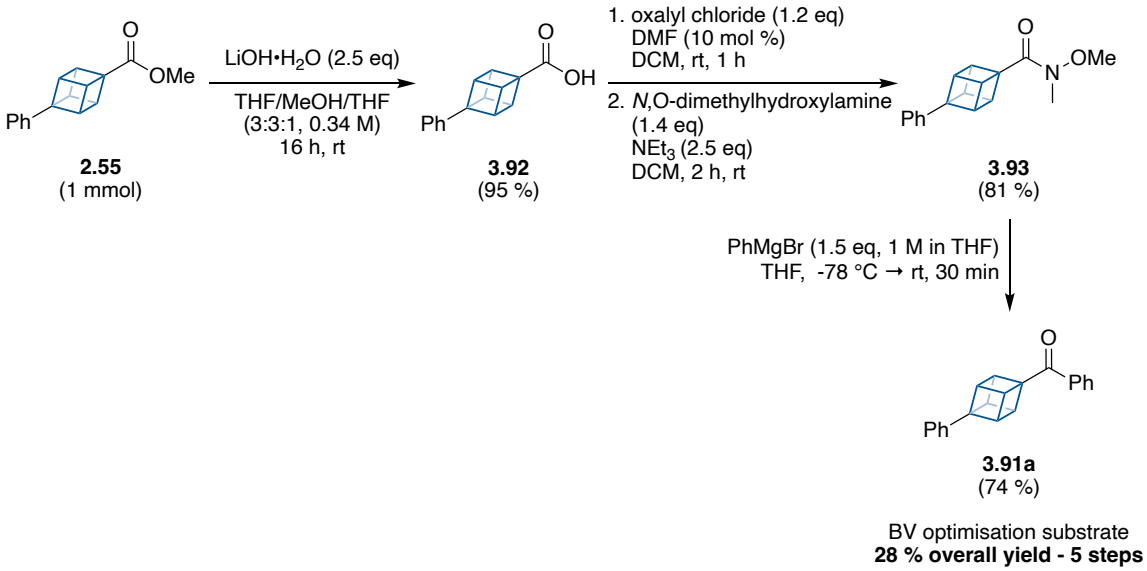

Scheme 79: Continued synthesis of BV optimisation substrate **3.91a** via the Weinreb amide.

Overall, the BV optimisation substrate **3.91a** was synthesised in 5 steps from commercially available 4-methoxycarbonylcubanecarboxylic acid (**2.8**) in a combined yield of 28 %.

3.2.2 Baeyer-Villiger optimisation

Our initial experiments for the BV oxidation of phenyl-4-phenylcubyl ketone (**3.91a**) were inspired by the previous literature, which in most instances performed the rearrangement of cubyl ketones with *m*-CPBA in DCM at room temperature.[109, 169, 190, 191] Treatment of **3.91a** with 2 equivalents of ≤ 77 % *m*-CPBA in DCM at room temperature for 24 hours resulted in 35 % consumption of **3.91a**, with preferential formation of ester **3.94a** resulting from migration of the cubyl group in a NMR yield of 20 % (Table 28, entry

1). Performing the reaction in $CHCl_3$ under the same reaction conditions slightly decreased the consumption of **3.91a** to 31 %, while the formation of ester **3.94a** increased to 30 % (entry 2). Increasing the quantity of *m*-CPBA to 4 equivalents in both DCM and $CHCl_3$ led to an increased consumption of ketone **3.91a** (66 % versus 74 %) and formation of ester **3.94a** (42 % versus 46 %) (entries 3-4). Small quantities of **3.95a** were observed in DCM (3 %) and $CHCl_3$ (4 %), resulting from the migration of the phenyl ring under these conditions (entries 3-4).

Table 28: Screening of peracid loading in dichloromethane and chloroform.

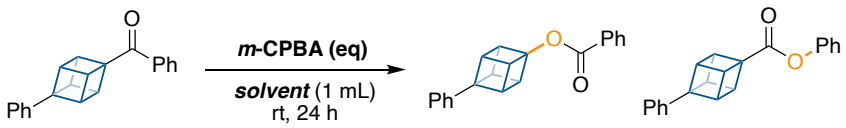

3.91a (0.1 mmol) **3.94a** **3.95a**

Entry	*m*-CPBA / equiv[b]	Solvent	NMR Yield[a] / %		
			3.91a (% consumption)	3.94a	3.95a
1	2	DCM	35	20	0
2	2	$CHCl_3$	31	30	0
3	4	DCM	66	42	3
4	4	$CHCl_3$	74	46	4
5	8	DCM	86	63	3
6	8	$CHCl_3$	90	72	5

[a] NMR yields were determined by ^1H NMR analysis using the internal standard durene. [b] The equivalents of m-CPBA have not taken into account its purity.

Identifying the trend that using more equivalents of *m*-CPBA was enhancing both the consumption of **3.91a** and formation of **3.94a** in DCM and $CHCl_3$, the experiments were repeated with using 8 equivalents of *m*-CPBA (entries 5-6). Using such a large excess of the peracid resulted in nearly full consumption of **3.91a** in both DCM (86 %) and $CHCl_3$ (90 %), whilst increasing the formation of **3.94a** to yields of 63 % and 72 % respectively. The quantity of **3.95a** also increased in both solvents when using 8 equivalents of *m*-CPBA, indicating that large excess of peracid was promoting phenyl migration to a small extent (entries 5-6). Notably, for each experiment screening the quantity of peracid to use, $CHCl_3$ outperformed DCM. From a practical perspective given the modest increase

in yield we deemed using 8 equivalents of *m*-CPBA in $CHCl_3$ as non-optimal from both an atom economy and a safety stance. Therefore, to increase the extent of consumption of **3.91a** without requiring 8 equivalents of *m*-CPBA, we opted to investigate the use of a Lewis acid catalyst and varying temperatures to promote the BV oxidation.[264-266]

To explore if using a Lewis acid would increase the consumption of **3.91a**, we began with the conditions outlined in Table 28, entry 4. Performing the BV oxidation using those conditions with the addition of the Lewis acid $Sc(OTf)_3$ (10 mol%) resulted in a decreased consumption of **3.91a** (74 % versus 65 %), but with an increased formation of ester **3.94a** (46 % versus 51 %) (Table 98, entries 1-2). Once more, small quantities of ester **3.95a** (3 %, entry 2) were formed when using the Lewis acid $Sc(OTf)_3$ over a period of 24 hours. Notably, when the reaction time was decreased from 24 to 6 hours, no measurable quantity of **3.95a** was detected by ^{1}H NMR analysis (entry 3). Although, this reduction in reaction time caused a reduction in both consumption of ketone **3.91a** (35 %) and formation of ester **3.94a** (19 %) (entry 3).

Table 29: Screening of catalyst, temperature and time.

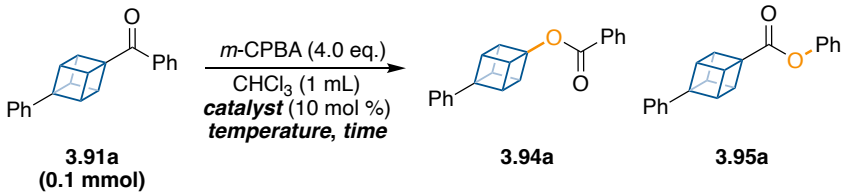

3.91a (0.1 mmol) **3.94a** **3.95a**

Entry	Catalyst	Temperature / °C	Time / h	NMR Yield[a] / %		
				3.91a consumption	3.94a	3.95a
1	-	rt	24	74	46	4
2	$Sc(OTf)_3$	rt	24	65	51	3
3	$Sc(OTf)_3$	rt	6	35	19	0
4[b]	$Sc(OTf)_3$	50	6	87	51	3
5	$BF_3{\cdot}OEt_2$	50	6	84	51	3
6	$Sc(OTf)_3$	50	3	65	46	3

[a] *NMR yields were determined by ^{1}H NMR analysis using the internal standard durene.*
[b] *Optimised reaction conditions.*

Fortunately, increasing the temperature from room temperature (20 °C) to 50 °C for 6 hours produced ester **3.94a** in 51 % yield (entry 4), the same result observed when performing the oxidation at room temperature for 24 hours (51 %, entry 2). Changing the Lewis acid to $BF_3{\cdot}OEt_2$ (10 mol %) had minor impact on the consumption of starting material and yields of the ester products (entry 5). Given the yield of **3.94a** was identical for both Lewis acids, we chose to use $Sc(OTf)_3$ in the further screening experiments due to its ease of handling. Reducing the reaction time to from 6 to 3 hours at 50 °C using $Sc(OTf)_3$ (10 mol %) (entry 4 and 6) only slightly decreased the yield of **3.94a** (46 %), however, the shorter reaction time significantly lowered the consumption of **3.91a** (65 %). Since the substrate scope was likely to include cubyl ketones that could be less reactive towards the BV rearrangement than our model substrate **3.91a**, the conditions in Table 28, entry 4, with the longer reaction time of 6 hours were selected for studying the relative migratory aptitudes.

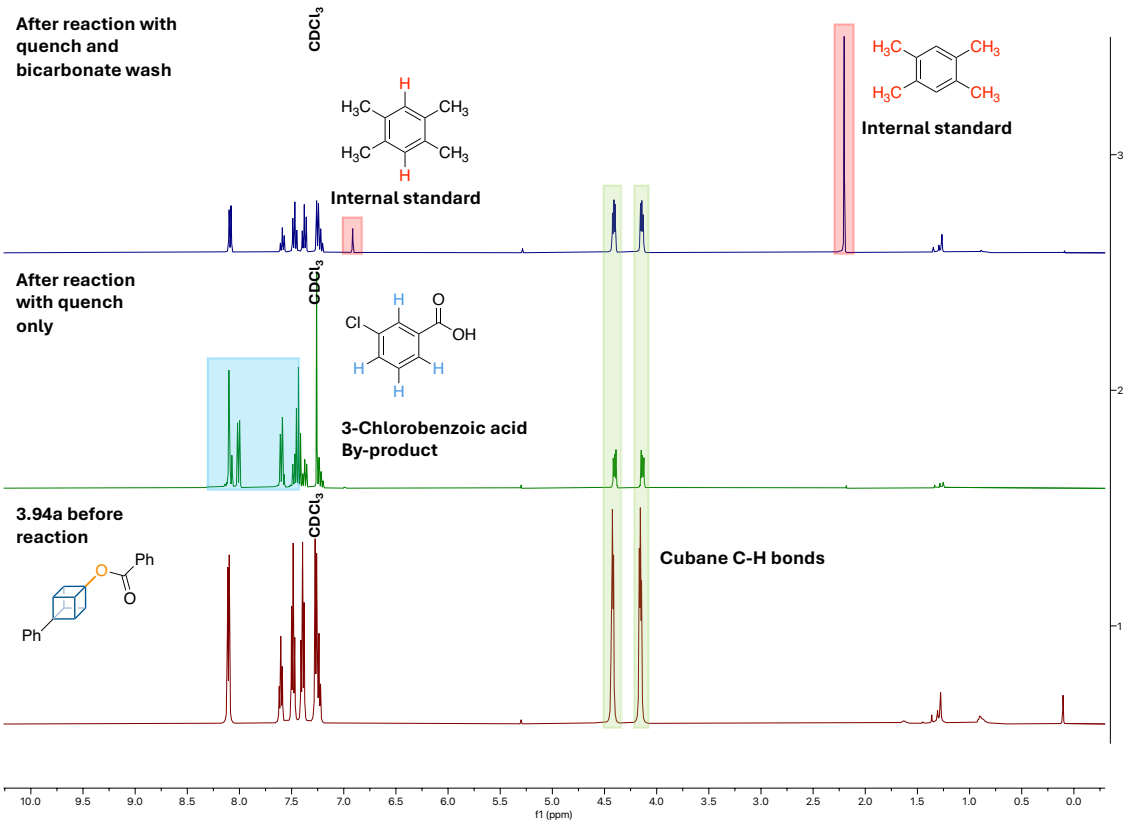

Figure 28: Stacked ^{1}H NMR for **3.94a** being resubjected to the optimised reaction conditions (Table 29, entry 4). After quench and bicarbonate work up **3.94a** was re-isolated in a 73 % yield.

To verify that the yields in Table 28 and 29 were an accurate representation of the migratory aptitude of cubane rather than the stability of the two ester products (**3.94a** and **3.95a**) under the reaction conditions, each ester was independently subjected to the optimised reaction conditions in Table 28, entry 4. Both esters were re-isolated in yields > 70 %, confirming that the yields were a good indication of the relative migratory aptitude of the cubyl group versus a phenyl ring and hydrolysis was not significant factor in the observed yields of products (Figure 28 and 29). The overlays in Figures 28 and 29 each include: (1) ^{1}H NMR of the ester before being resubmitted to the optimised reaction conditions, (2) ^{1}H NMR of the re-isolated ester after quenching the oxidation with sodium bisulfite solution and (3) ^{1}H NMR of the re-isolated esters after quenching with sodium bisulfite solution, followed by washing with saturated aqueous bicarbonate solution.

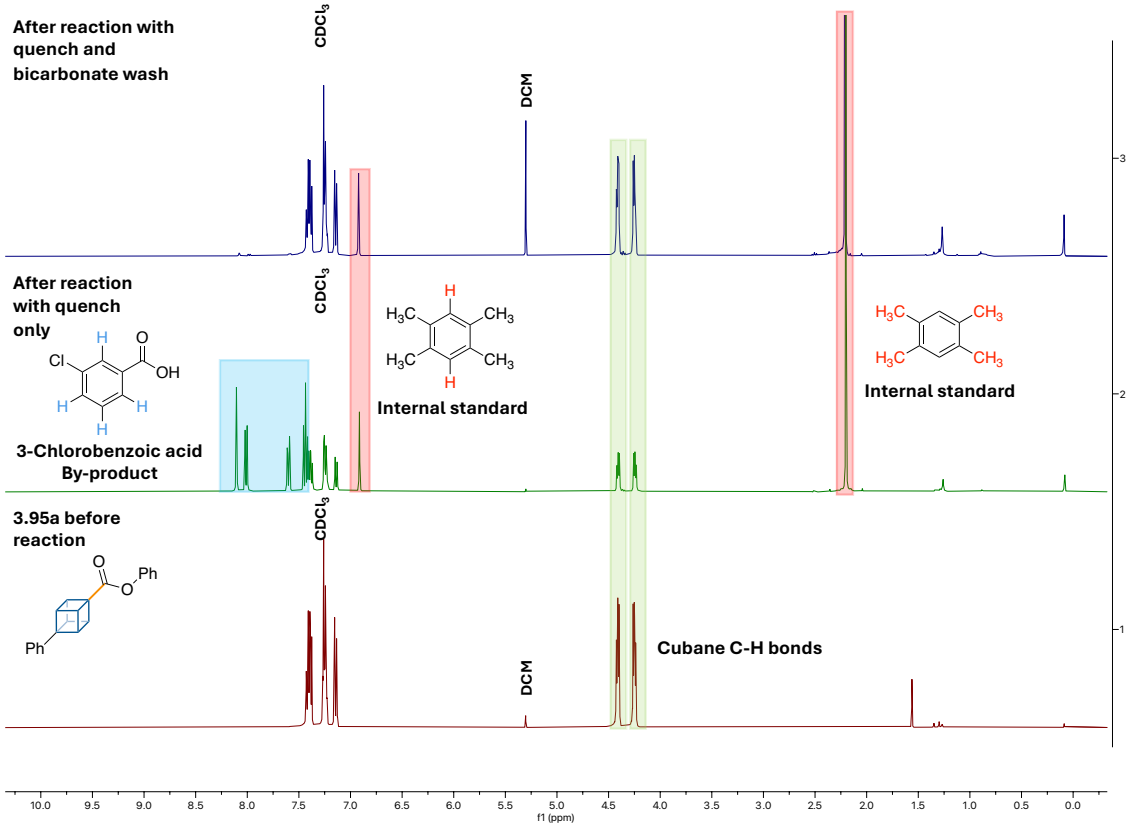

Figure 29: Stacked ^{1}H NMR for **3.95a** being resubjected to the optimised reaction conditions (Table 29, entry 4). After quench, **3.95a** was re-isolated in a 76 % yield. After quench with a bicarbonate work up **3.95a** was re-isolated in a 72 % yield.

Overall, the ^{1}H NMR overlays for the re-isolated **3.94a** (Figure 28) and **3.95a** (Figure 29) confirm that when these esters were independently subjected to the optimised reaction conditions no additional cubyl or rearranged cubyl species were formed. Furthermore, these control experiments demonstrate that the esters remained stable to the work-up conditions.

During the optimisation studies for the BV oxidation of **3.91a**, the major product observed was **3.94a**, resulting from the preferential migration of the cubyl group over the phenyl ring. Interestingly, Eaton observed the opposite regioselectivity for the BV rearrangement of **3.6f** (1 eq) with trifluoroperacetic acid (2 eq) in DCM at rt, in which exclusive migration of the phenyl ring was observed (Scheme 80a).[191] As the migratory aptitude in the BV rearrangement can be dependent on the reaction conditions used, we treated **3.91a** to the same conditions as described in the Eaton study.[191] Surprisingly, we observed extensive cubyl decomposition, with 66 % of **3.91a** consumed and only trace amounts of **3.94a** (3 %) detected (Scheme 80b). In contrast to Eaton's study, ester **3.95a** or the corresponding cubyl carboxylic acid (**3.92**, formed via the hydrolysis of **3.95a**) were not observed by ^{1}H NMR analysis.

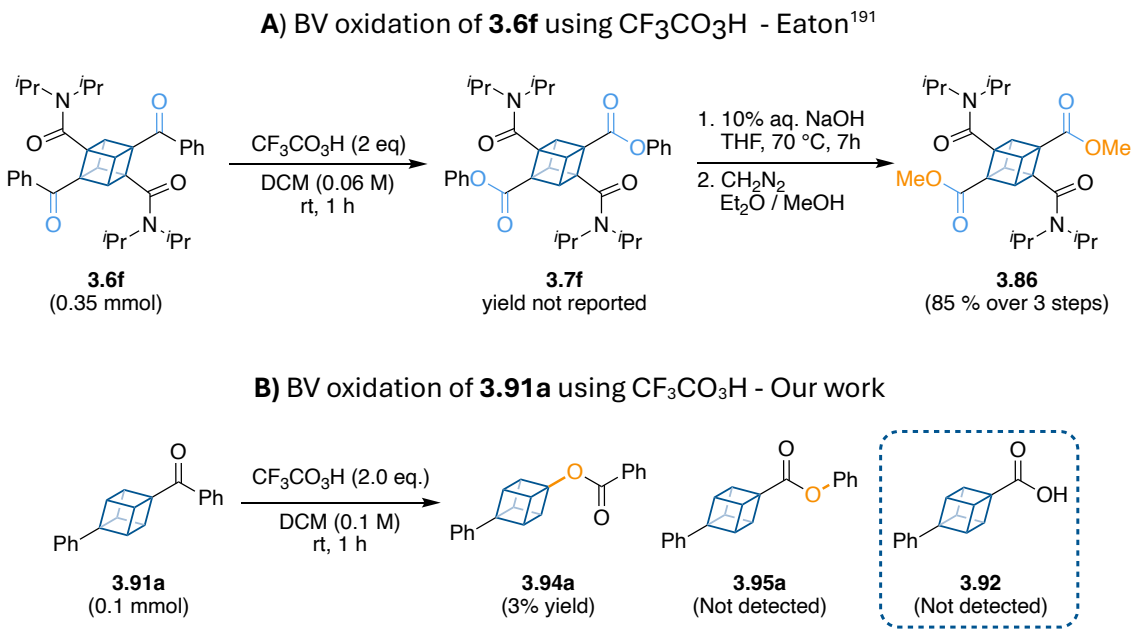

Scheme 80: Comparison of migratory aptitude of cubane versus phenyl for **3.6f** and **3.91a** with comparable reaction conditions

3.2.3 Substrate scope

3.2.3.1 Migratory aptitude of cubane

Having established optimised reaction conditions for the BV rearrangement of **3.91a** (Table 29, entry 4), our studies began by exploring the migratory aptitude of cubane in a range of unsymmetrical cubyl ketones, in addition to the cubyl aldehyde (Table 30). Details regarding the synthesis of all the cubyl substrates in Table 30 can be found at the end of this chapter (**Section 3.3.1 – Substrate scope synthesis**).

For the BV oxidation of the unsymmetrical cubyl ketone bearing a methyl substituent (**3.91b**) the ester **3.94b**, resulting from cubyl migration, was formed in a 79 % yield (Table 30, entry 1). By ^{1}H NMR there was no evidence of methyl migration under these reaction conditions, which is consistent with the previous reports for the BV rearrangement of cubyl methyl ketones (Scheme 81).[109, 169, 190] Increasing the carbon chain length to an ethyl substituent (**3.91c**) gave a similar result, with only **3.94c** being formed in a 87 % yield (entry 2).

Table 30: Migratory aptitude of cubane in the Baeyer-Villiger oxidation

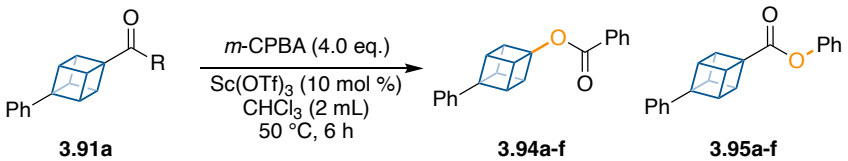

3.91a (0.2 mmol) | **3.94a-f** | **3.95a-f**

Entry	Substrate	R	Conversion (%)	Yield 3.94a-f[a] (%)	Yield 3.95a-f[a] (%)	Ratio[b] (3.94:3.95)
1	**3.91b**	Me	100	79 (86)	0 (n.d)	>99:1
2	**3.91c**	Et	100	87 (76)	0 (n.d)	>99:1
3	**3.91a**	Ph	87	51(50)	3 (n.d)	17:1
4	**3.91d**	H	100	55 (50)	28 (n.d)	2:1
5	**3.91e**	*i*-Pr	100	58 (62)	25 (27)	2:1
6	**3.91f**	*t*-Bu	36	0 (n.d)	8 (n.d)	1: >99

[a] NMR yields determined by ^{1}H NMR using durene as an internal standard, isolated yields are in parentheses and n.d = isolated yield not determined .[b] Product ratios determined using ^{1}H NMR yields.

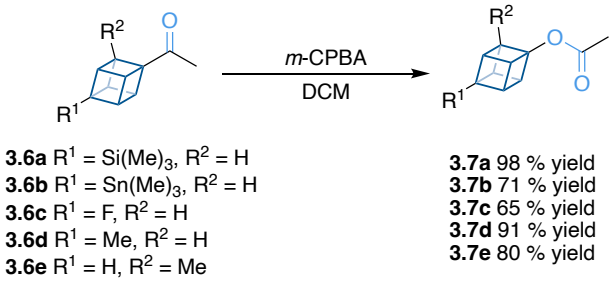

3.6a $R^1 = Si(Me)_3$, $R^2 = H$
3.6b $R^1 = Sn(Me)_3$, $R^2 = H$
3.6c $R^1 = F$, $R^2 = H$
3.6d $R^1 = Me$, $R^2 = H$
3.6e $R^1 = H$, $R^2 = Me$

3.7a 98 % yield
3.7b 71 % yield
3.7c 65 % yield
3.7d 91 % yield
3.7e 80 % yield

Scheme 81: Previous reports on the BV rearrangement of cubyl methyl ketones.[109, 169, 190]

Treating 1-phenyl cubyl aldehyde (**3.91d**) under the optimised conditions resulted in a lower regioselectivity, affording a 2:1 mixture of the formate **3.94d** (55 %) and the carboxylic acid **3.95d** (28 %) (Table 30, entry 4). Attempts to isolate the carboxylic acid **3.95d** via silica gel column chromatography were unsuccessful, due to the by-product 3-chlorobenzoic acid (a result of quenching the excess *m*-CPBA) co-eluting during the purification. The 2:1 product ratio of the formate **3.94d** and the carboxylic acid **3.95d** was consistent with the reported literature for the BV rearrangement of tertiary substituted aldehydes, with the formation of the formate being favoured due to preferential migration of the tertiary cubyl group over hydrogen.[257] In this instance the regioselectivity can be explained by comparing the steric hinderance associated with a cubyl group versus a hydrogen atom. Assuming the product-determining transition state has a similar steric demand to the Criegee intermediate, it is likely that more sterically demanding cubyl substituent will adopt an antiperiplanar arrangement to the O-O bond of the carboxylate leaving group and migrate preferentially, over the sterically smaller hydrogen (to obey the primary and secondary stereoelectronic effects).[232, 236-238, 253] However, this is not always the case, and the Curtin-Hammett principle must be considered.[267, 268] If the interconversion of conformers of the Criegee intermediate is faster than the migration step in the BV mechanism, the regioselectivity is determined by the relative energies of the two product-determining transition states and not the lowest energy conformer of the Criegee intermediate.[246, 253] This principle is particularly relevant in the BV rearrangement of aldehydes with primary alkyl substituents, where preferential migration of the hydrogen over the larger alkyl chain substituent has been reported in the literature.[245, 269]

Preferential migration of the cubyl group remained during the BV oxidation of the cubyl ketone bearing a sterically bulkier *i*-propyl substituent (**3.91e**), with formation of the two esters **3.94e** and **3.95e** in a 58 % and 25 % yield respectively (Table 30, entry 5). Further increasing the steric bulk of the substituent to a *t*-butyl group (**3.91f**) led to only 36 % consumption of the cubyl ketone **3.91f**. This is likely due to the ketone bearing two bulky tertiary substituents, which significantly hindered the nucleophilic attack of the peracid to the carbonyl centre. ^{1}H NMR analysis of the crude product revealed trace quantities of one cubyl ester forming in the reaction. Based on the chemical shift of the three CH_3 protons in the *tert*-butyl group, a shift from 1.23 ppm for **3.91f** to 1.50 ppm (Figure 30), allowed us to tentatively assign that migration of the *t*-butyl (**3.95f**) had occurred (8 % NMR yield).

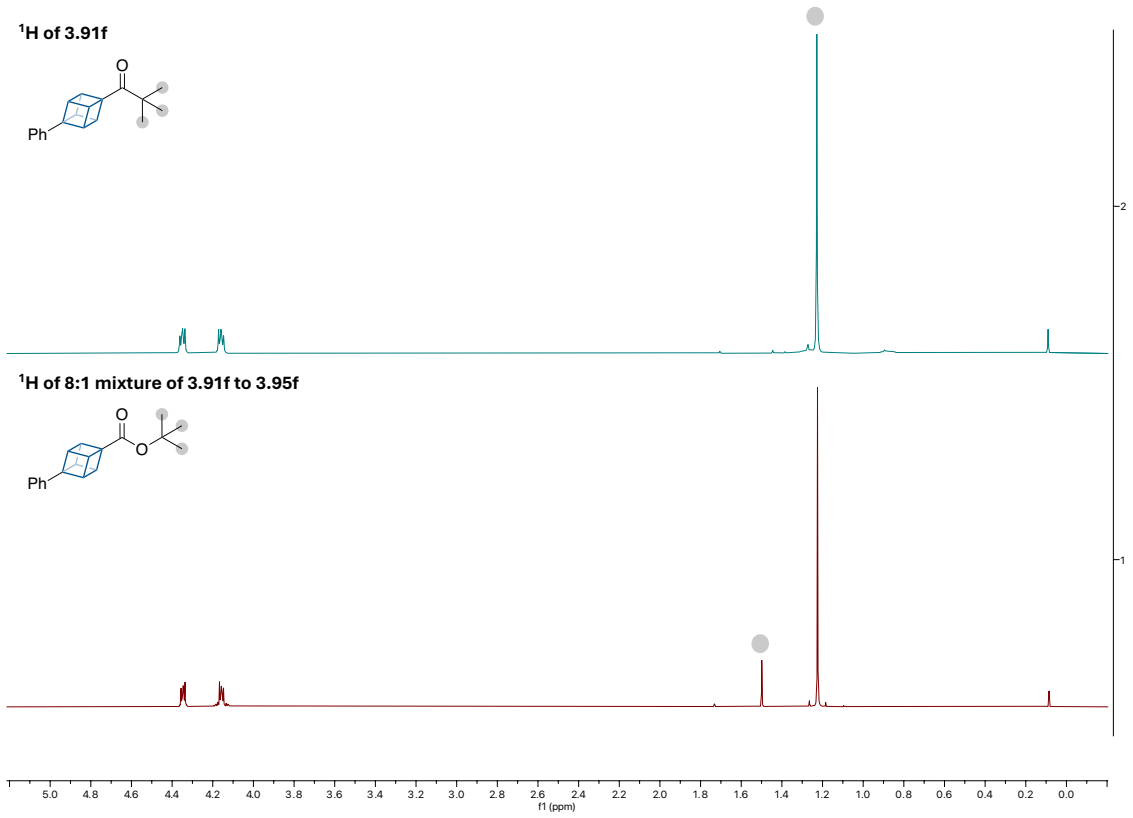

Figure 30: Stacked ^{1}H NMR of ketone **3.91f** (top) and 8:1 mixture of **3.91f** to **3.95a** from BV rearrangement of **3.91f** after silica gel chromatography (bottom).

Unfortunately attempts to isolate **3.95f** were unsuccessful, with the best outcome obtained being an 8:1 mixture of the ketone **3.91f** with the ester we tentatively assigned

as **3.95f**. ^{13}C NMR analysis of this mixture supported that the ester **3.95f** was formed, with tertiary carbon of the **C**Me_3 group shifting from 44.5 ppm in **3.91f** to 80.2 ppm, which is consistent with migration of the *t*-butyl group rather than the cubyl group (Figure 31). It is important to clarify that we are not ruling out the possibility of cubyl migration under these conditions; however, due to poor consumption of ketone **3.91f** and the detection limits of ^{1}H and ^{13}C NMR, it is not possible to draw a conclusion.

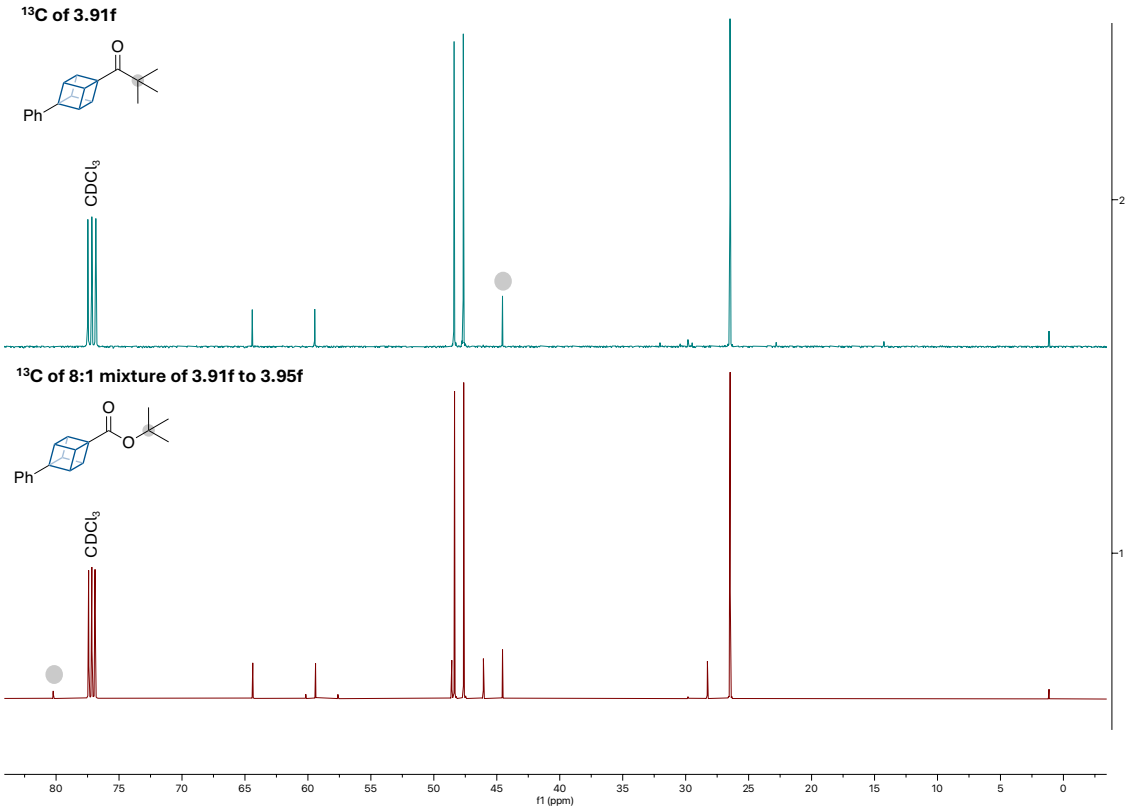

Figure 31: Stacked ^{13}C NMR of ketone **3.91f** (top) and 8:1 mixture of **3.91f** to **3.95a** from BV rearrangement of **3.91f** after silica gel chromatography (bottom).

Overall, the migratory aptitude of the alkyl groups in this study are consistent with previous reports.[232, 246, 248, 258] Under the conditions outlined in this study, cubane can be positioned in the BV migratory aptitude series as follows:

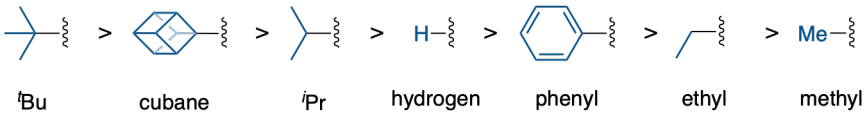

According to the primary stereoelectronic effect for the BV rearrangement and assuming the product determining transition state has a similar steric demand to the Criegee intermediate, the lowest energy conformer places the more sterically demanding group antiperiplanar to the O-O bond. [232, 236-238, 253, 267, 268] Our calculations found that for substrate **3.91e** the Criegee intermediate was 2.9 kJ/mol lower in free energy when the cubyl group was antiperiplanar to the O-O bond compared to the *i*-propyl group, leading to a 77/23 Boltzmann weighting. This is in line with the observed 2:1 regioselectivity for the formation of **3.94e** over **3.95e** in our experiments (Table 30, entry 5). All computational calculations were performed by Dr James Platts, Cardiff University.

3.2.3.2 Effect of cubyl substituents on cubyl migratory aptitude

Having established where cubane fits in the BV migratory aptitude series, we were next interested if different substituents on the cubyl framework would influence the relative migratory aptitude of the cubyl group. Based on the migratory aptitude data presented in Table 30, we decided to prepare a series of functionalised cubyl *i*-propyl ketones due to the similar migratory aptitude observed between the *i*-propyl and cubyl groups (ratio of ester products **3.94e**:**3.95e** = 2:1). We hypothesised that this study would allow us to observe the influence of electronic factors on the relative migratory aptitude of the cubyl group, whilst providing cubyl esters that could be used to prepare structurally complex cubanols. Details regarding the synthesis of the functionalised cubyl *i*-propyl ketones can be found at the end of this chapter (**3.3.2 – Substrate scope synthesis**).

The BV rearrangement of the trimethylsilyl substituted cubane (**3.91g**), performed under the optimised conditions detailed in Table 30, resulted in a 65 % and 9 % NMR yield of **3.94g** from cubyl migration, and **3.95g** from *i*-propyl migration respectively (**3.94g**:**3.95g** = 7:1) (Table 31, entry 1). Comparing this ratio of products to that of the model substrate **3.91e** (**3.94e**:**3.95e** = 2:1 Table 31, entry 4), demonstrated that the migratory aptitude of the trimethylsilyl substituted cubyl group was significantly greater than the phenyl substituted compound. With the parent unsubstituted cubyl framework (**3.91h**) the two esters **3.94h** and **3.95h** were formed in a 44 % and 15 % NMR yield respectively

(**3.94h**:**3.95h** = 3:1 entry 2). Despite a lower migratory aptitude of the cubyl component relative to trimethylsilyl substrate **3.91g** (**3.94g**:**3.95g** = 7:1), the migratory aptitude of cubane for the unsubstituted substrate **3.91h** remained greater than the model substrate **3.91e** (**3.7e**:**3.8e** = 2:1) (entry 2 and 4). A similar result was observed for the alkyl substituted cubane **3.91i**, yielding **3.94i** in 44 % and **3.95i** in 15 % in a ratio of 3:1 (entry 3).

Table 31: Effect of cubyl substituents on migratory aptitude

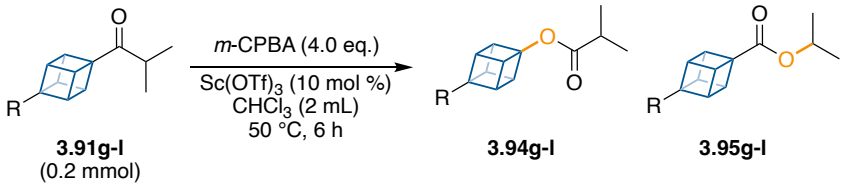

3.91g-l (0.2 mmol) **3.94g-l** **3.95g-l**

Entry	Substrate	R	Conversion (%)	Yield 3.94g-l[a] (%)	Yield 3.95g-l[a] (%)	Ratio[b] (3.94:3.95)
1	**3.91g**	$SiMe_3$	100	65 (61)	9 (10)	7:1
2	**3.91h**	H	100	44 (46)	15 (22)	3:1
3	**3.91i**	CH_2OMe	100	44 (42)	15 (8)	3:1
4	**3.91e**	Ph	100	58 (62)	25 (27)	2:1
5	**3.91j**	$C(O)N(iPr)_2$	100	25 (22)	29 (9)	1:1
6	**3.91k**	Br	100	12 (9)	50 (46)	1:4
7	**3.91l**	F	100	11 (10)	49 (39)	1:4

[a]NMR yields determined by ^{1}H NMR using durene as an internal standard, isolated yields are in parentheses. [b] Product ratios determined using NMR yields.

It was found that the addition of electron-withdrawing substituents onto the cubane framework decreased the migratory aptitude of cubane versus the *i*-propyl group. For instance, a 1:1 ratio of **3.94j**:**3.95j** was observed for the *N*,*N*-diisopropylamide substituted cubane (**3.91j**), with a yield of 25 % and 29 % respectively (Table 31, entry 5). Notably, halogens had a profound effect on the migratory aptitude of cubane, favouring the migration of *i*-propyl group over the cubyl group (entry 5-6). In the case of the bromo- and fluoro-substituted cubanes (**3.91k** and **3.91l**), a similar product ratio of 1:4 of **3.94k**:**3.95k** and **3.94l**:**3.95l** was observed with preferential migration of the *i*-propyl

group over the cubane, in stark contrast to our model substrate the phenyl-substituted cubane **3.91e**.

The variation in the ratio of cubyl versus *i*-propyl migration for the isopropyl cubyl ketones examined in our study (Table 31) demonstrates that there is an electronic component influencing the migratory aptitude of groups, as noted in previous studies on the BV rearrangement of substituted arenes.[247, 248] The presence of the trimethylsilyl group at the γ-position on the cubane ring increased the migratory aptitude of the cubyl group over the *i*-propyl under our reaction condition (Table 31, entry 1), presumably by providing stabilisation to the positive charge that forms on the cubane core in the transition state (Scheme 82a).

A) The transition state in the BV rearrangement

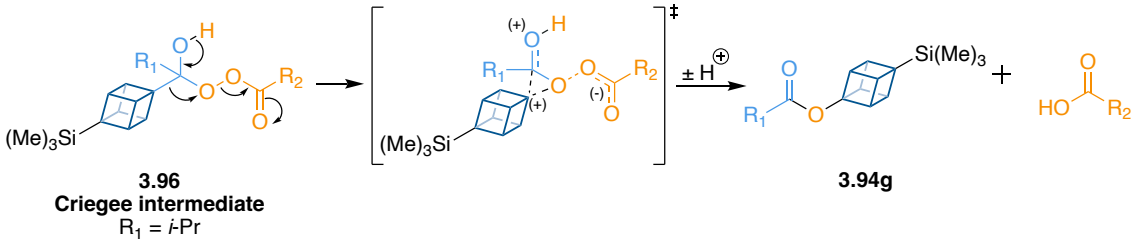

B) Charge distribution in a cubyl carbocation through hyperconjugation

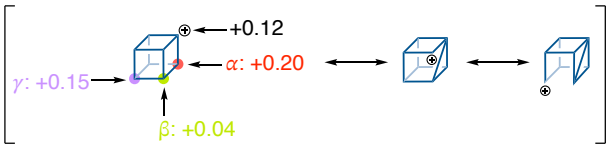

Scheme 82: Rationale behind the observed regioselectivity in our BV studies.[270]

Della and Schiesser have performed *ab initio* MP2/6-31G** calculations on cubyl cations to examine how charge was distributed amongst the cubyl framework.[270] Population analysis revealed that a charge of +0.12 was present at the cationic centre, with extensive charge delocalisation at the α-carbons (+0.20) and the γ-carbon (+0.15), with minimal build up at the β-carbons (+0.04) (Scheme 82b). Della and Schiesser's proposal that charge delocalisation in a cubyl cation occurs through hyperconjugation of the α-β and β-γ cubane C–C bonds is consistent with separate experimental studies

by Eaton, Kevill, and Moriarty, which examined the varying rates of solvolysis of 4-substituted cubyl triflates.[169, 270-272] For instance, Kevill *et al* compared the rate of solvolysis of 4-substituted cubyl triflates and found the presence of electron withdrawing substituents on the γ-carbon significantly decreased the rate of solvolysis relative to the unsubstituted species (Table 32).[272]

Table 32: Rate of solvolysis of 4-substituted cubyl triflates – Kevill *et al*.[272]

	Rate of solvolysis / 10^6 k/s^{-1}	
4-Substituent	**63 °C**	**75 °C**
I	6.47	18.8
CO_2Me	4.15	12.5
Br	1.10	2.97
Cl	0.53	1.29
H	10760[a]	

[a] *Rate of solvolysis at 25 °C*

Based on the computational data by Della and Schiesser and the independent experimental data on the solvolysis rate of four 4-substituted cubyl triflates, it can be inferred that any functional group on the γ-carbon that can destabilise a cubyl cation and thus raise the energy of the corresponding transition state, will consequently reduce cubyl migration in the Baeyer-Villiger oxidation. Our experimental results in Table 31 support this notion. To provide further evidence, we performed our own computational calculations of the relative stability of 4-substituted cubyl cations. We found that the presence of an electron donating trimethylsilyl group at the γ-carbon stabilised the cubyl cation by 22.8 kJ/mol relative to the unsubstituted species (**3.97b**), whereas the electron withdrawing fluorine destabilised the cubyl cation by 52.1 kJ/mol (**3.97c**) (Figure 32). All computational calculation was performed by Dr James Platts, Cardiff University. Overall, our computational data alongside our experimental work was in agreement with the proposal by Della and Schiesser, that stabilisation of cubyl cations occur via hyperconjugation of the α-β and β-γ C–C bonds (Scheme 82b).[228, 270]

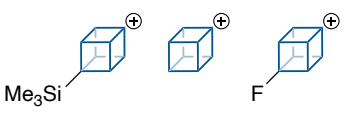

3.97a **3.97b** **3.97c**

Figure 32: 4-substituted cubyl cations.

Now considering the factors that can influence cubyl cation stabilisation, Eaton's observation of exclusive migration of the phenyl group during the BV oxidation of the di-amide-substituted cubyl phenyl ketone (**3.6f**) is in line with the expected experimental outcome (Scheme 83a). In the computational studies by Della and Schiesser, the largest partial positive charge build up was on the α-carbon of the cubyl core (Scheme 82b).[270] Consequently, the BV oxidation of **3.6f** in Eaton's study resulted in exclusive migration of the phenyl ring, presumably due to the presence of the two electron-withdrawing amides at the α-carbons sufficiently destabilising the cubyl carbocation thereby preventing any cubyl migration. Whereas, when employing Eaton's conditions to our model substrate **3.91a** we observed no phenyl migration and only trace quantities of cubyl migration (3 %), demonstrating greater stabilisation of the cubyl cation in our model substrate versus Eaton's study (Scheme 83b). Overall, our work alongside Eaton's shows that the variations in the substituents and their positioning on the cubyl framework plays an important role in controlling the regioselectivity of the BV rearrangement of cubyl ketones and aldehydes.

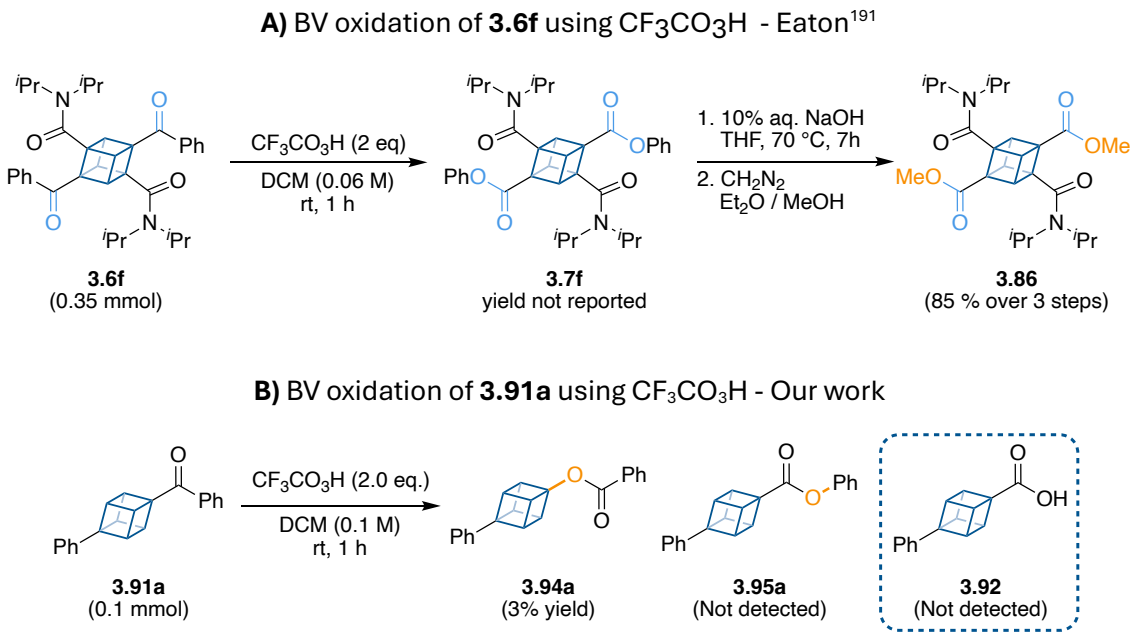

Scheme 83: Migratory aptitude of cubane verses phenyl in **3.6f** and **3.91a** under comparable reaction conditions.

3.3 Substrate scope synthesis

An overview of the synthesis of the BV substrates studied in **Section 3.2** are summarised in this section.

3.3.1 Synthesis of 4-phenyl substituted cubyl ketones

The phenyl substituted cubyl ketones (**3.91b-c** and **3.91e**) were prepared by the addition of the relevant commercially available Grignard (between 2-3 eq) to a solution of the Weinreb amide **3.93** (1 eq) in THF, with yields exceeding 70 % for each ketone (Scheme 84). Overall, we found all the Grignard reagents employed reacted cleanly with the cubyl Weinreb amide **3.93**, with no side product formation observed by TLC or ^{1}H NMR analysis.

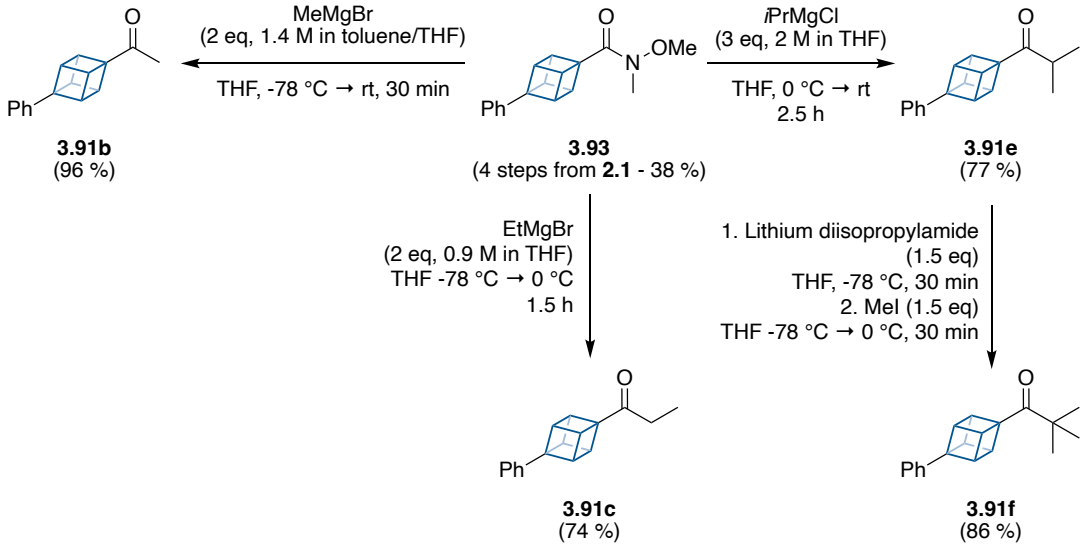

Scheme 84: Synthesis of the cubyl ketones (**3.91b-c** and **3.91e**) used in Section 3.2.3.1 (Table 29) for studying the migratory aptitude of cubane.

As anticipated, the addition of *tert*-butylmagnesium chloride (1.2 eq, 2 M in Et_2O) to a solution of the Weinreb amide **3.93** (1 eq) at room temperature for 2 hours resulted in no formation of the desired cubyl *t*-butyl ketone **3.91f**, likely due to the Grignard reagent acting a strong base rather than a nucleophile. Therefore, we opted to synthesise **3.91f** via the alkylation of the *i*-propyl ketone (**3.91e**, Scheme 84). We prepared the lithium

enolate of ketone **3.91e** using lithium diisopropylamide (1.5 eq) at - 78 °C in THF, freshly generated by the addition of *n*-BuLi (1.4 eq, 1.6 M in hexanes) to a solution of diisopropylamide (1.5 eq) also cooled to - 78 °C in THF. Subsequent addition of the methylating agent iodomethane (1.5 eq) to the lithium enolate of ketone **3.91e**, followed by warming the reaction to 0 °C afforded the desired ketone **3.91f** in an 86 % yield after silica gel column chromatography.

Finally, the cubyl aldehyde (**3.91d**) was prepared in two steps from the cubyl carboxylic acid **3.92** (Scheme 85). In the first step, the carboxylic acid moiety in **3.92** (1 eq) was reduced to the primary alcohol using borane dimethyl sulfide (1.6 eq, 1 M in 2-MeTHF) within 5 hours at room temperature. Without purification, the crude alcohol was directly added to a solution of oxalyl chloride (1.2 eq) and DMSO (2.7 eq) in DCM at - 78 °C. Subsequent addition of triethylamine (5.4 eq) and warming the Swern reaction to room temperature gave the aldehyde **3.91d** in 68 % yield, after purification by silica gel column chromatography.

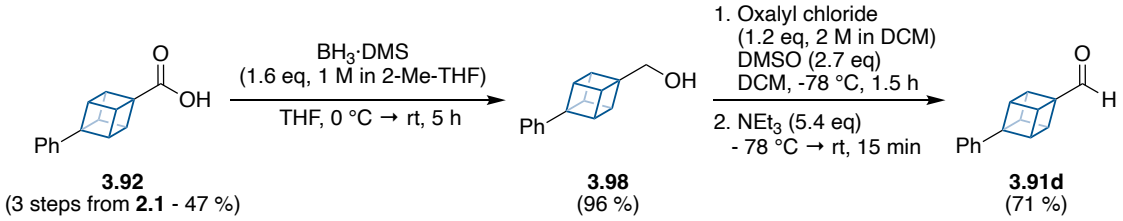

3.92
(3 steps from **2.1** - 47 %)

3.98
(96 %)

3.91d
(71 %)

Scheme 85**:** Synthesis of cubyl aldehyde **3.91d** used **in Section 3.2.3.1** (Table 29) for studying the migratory aptitude of cubane.

3.3.2 Synthesis of the 4-substituted cubyl *i*-propyl ketones

3.3.2.1 Trimethylsilyl substituted BV substrate (3.91g):

The retrosynthetic analysis of trimethylsilyl substituted cubyl *i*-propyl ketone (**3.91g**) is described in Scheme 86. Several protocols to introduce a trimethylsilyl group onto the cubane framework have been published. [158, 169, 190, 191, 273] However, only one paper by Eaton and Zhou have reported the synthesis of 4-(trimethylsilyl)cubyl ester **3.100**, a key intermediate we identified in our retrosynthetic analysis towards cubyl ketone **3.91g**.[169]

Eaton and Zhou reported that **3.100** was prepared in two steps from cubane **2.8**, with second step involving the addition of *t*-BuLi to a solution of cubyl iodide **3.99** in THF at -78 °C, promoting a halogen-lithium exchange reaction. The subsequent addition of trimethylsilyl chloride provided **3.100**.[169] Although the authors did not include details on reagent quantities or timings, we believed based on the information included we could replicate this work.[169]

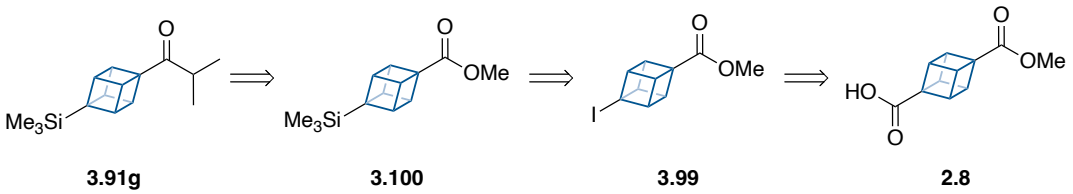

Scheme 86: Retrosynthetic analysis of trimethylsilyl substituted cubyl *i*-propyl ketone (**3.91g**), based on the published work by Eaton and Zhou on silylation of cubanes.[169]

We began preparing the cubyl iodide **3.99** by an iododecarboxylation of 4-methoxycarbonylcubanecarboxylic acid (**2.8**, 1 eq) with 1,3-diiodo-5,5-dimethylhydantoin (DIH, 1.2 eq) in refluxing DCE, a protocol previously reported by Kulbitski and co-workers (Scheme 87).[274] Instead of using a tungsten lamp as reported by Kulbitski *et al* we opted to irradiate the mixture with a blue LED light source for 5 hours. After purification by silica gel column chromatography the cubyl iodide **3.99** was isolated in 85 % yield, consistent with the reported literature yield of 93 % yield when employing a tungsten lamp.[274] With the cubyl iodide **3.99** in hand we next focussed our attention to the halogen-lithium exhange reaction. Treatment of **3.99** with *t*-BuLi (2.2 eq, 1.9 M in pentanes) in THF at - 78 °C, followed by the addition of chlorotrimethylsilane (4 eq) after 10 minutes did not yield the desired product **3.100** (Scheme 87). Instead, ^{1}H NMR analysis revealed mostly decomposition of the starting material **3.99**, with only 16 % of **3.99** recovered from the reaction after silica gel column chromatography. In addition, when increasing the timeframe between addition of *t*-BuLi and the electrophile chlorotrimethylsilane from 10 to 30 minutes, we observed full consumption of the starting material **3.99** and no formation of the desired product **3.100** was detected by ^{1}H NMR.

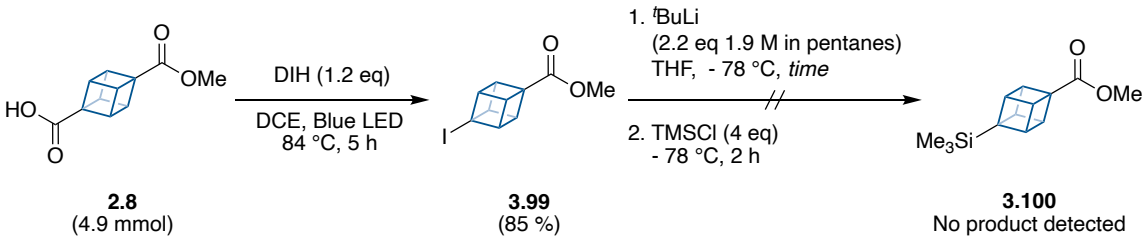

Scheme 87: Iododecarboxylation of **2.8** using blue LED light source and lithium-halogen exhange of cubyl iodide **3.99**.

We were unable to replicate the work by Eaton and Zhou, which was particularly surprising when considering Della and Head, and Plunkett *et al* have reported the introduction of the trimethylsilyl moiety onto the cubane framework with the 4-susbtituted cubyl iodides **3.101a** and **3.101b** under similar conditions (Scheme 88a-b).[158, 190] Based on these literature results, we hypothesised that the methyl ester moiety in **3.99** may be unstable to the reaction conditions we described in Scheme 87.

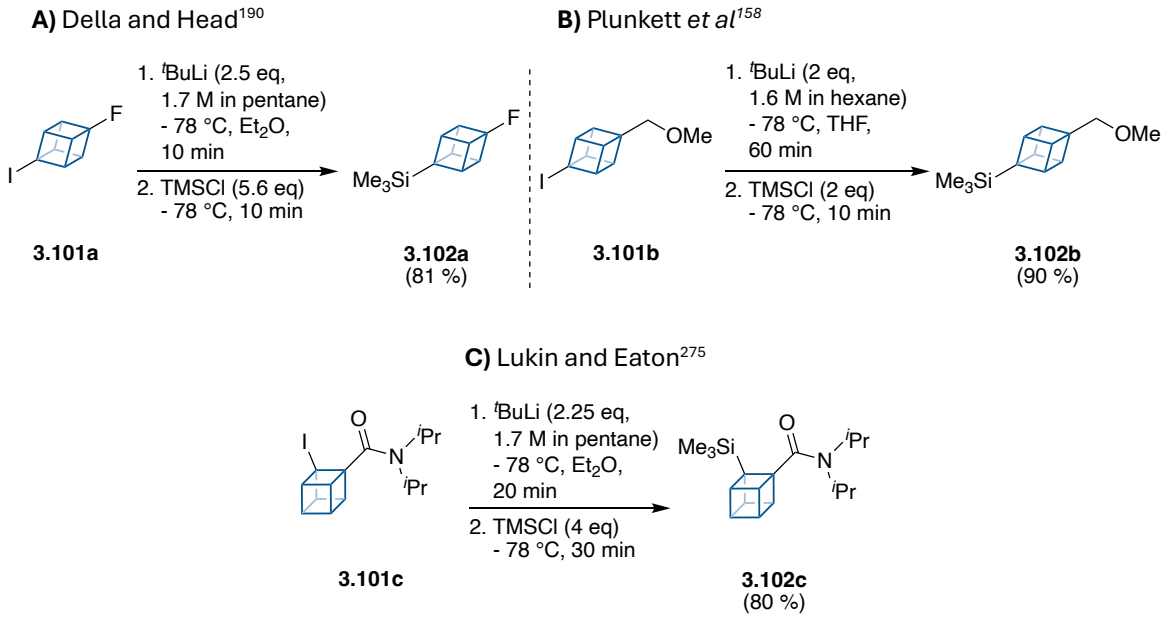

Scheme 88: Literature examples of lithium-halogen exhange of substituted cubyl iodides followed by addition of chlorotrimethylsilane.

When reviewing the literature, we found Lukin and Eaton had later reported the silylation of substrate 1-((diisopropylamino)carbonyl)-2-iodocubane **3.101c**, by performing the metallation at - 78 °C in THF with *t*-BuLi (2.25 eq, 1.7 M in pentanes) followed by the

addition of 4 equivalents of chlorotrimethylsilane after 20 minutes (Scheme 88c).[275] At the time we were undecided if the *ortho* relationship between the metallation site and the diisopropyl amide was necessary for a successful silylation, or if the diisopropyl amide group in **3.101c** was inert compared to the methyl ester group in **3.99**, thus reducing side reactions and decomposition of the cubyl framework. Pleasingly, we found the latter was true and when employing the Lukin and Eaton reaction conditions to the cubyl iodide **3.104**, which was prepared from the cubyl iodide **3.99** in two-steps via a hydrolysis followed by amide formation via an acid chloride, we successfully isolated **3.105** in an excellent yield of 94 % after purification by silica gel column chromatography (Scheme 89).

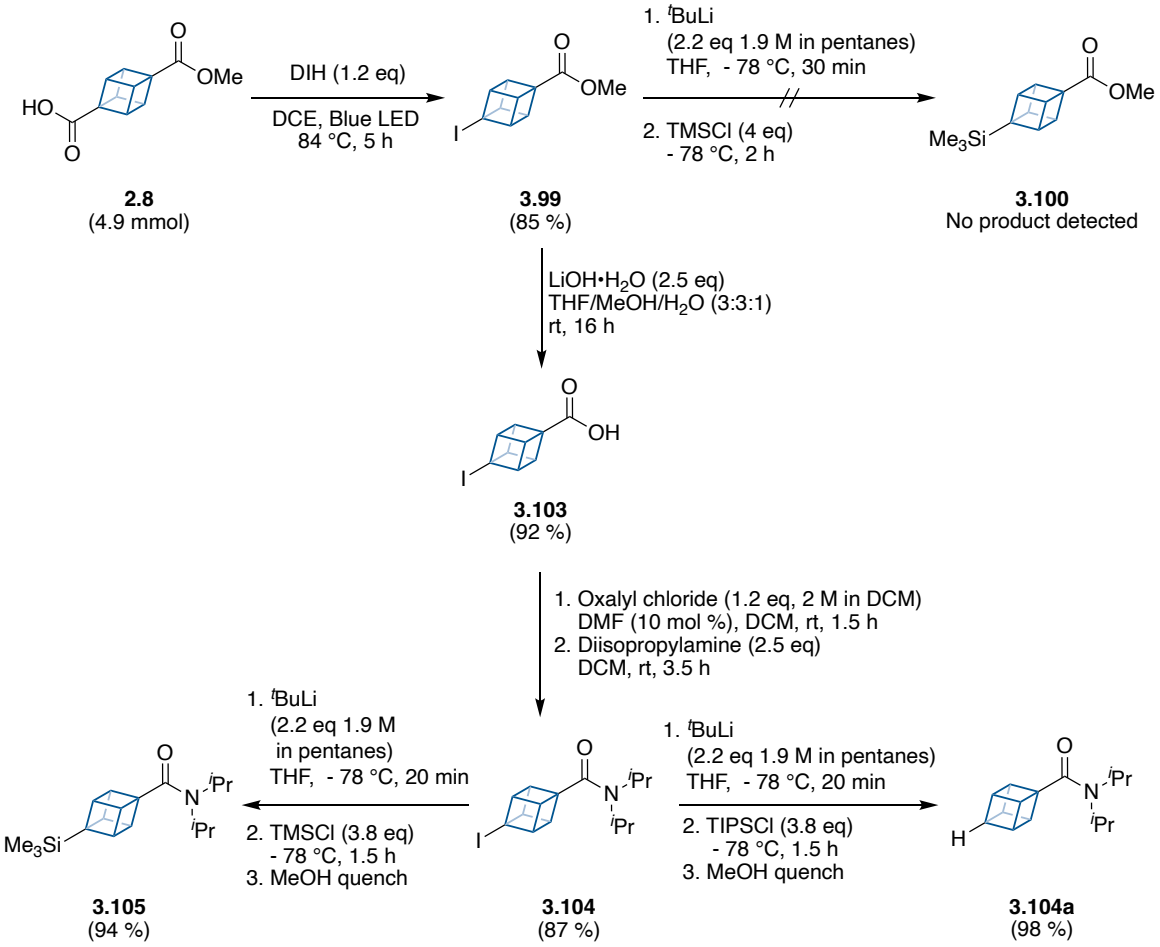

Scheme 89: Protocol for silylation of cubane towards the synthesis of trimethylsilyl cubyl ketones **3.91g**.

For our own knowledge we repeated the reaction with the bulkier silylation agent triisopropylsilyl chloride (TIPSCl, 4 eq). Unfortunately, the only cubyl species isolated was cubyl diisopropyl amide **3.104a** in 98 % yield, formed by the lithiated cubyl species of **3.104** being quenched with methanol (Scheme 89). Having synthesised **3.105**, we next sought to remove the diisopropylamide group which in essence acted as a protecting group (Scheme 90). The diisopropylamide **3.105** was converted to the carboxylic acid **3.107** using an established two-step protocol reported by Lukin and Eaton.[275] In the first step the amide **3.105** was reduced to amine **3.106** in a yield of 97 %, by refluxing the amide (1 eq) with lithium aluminium hydride (1.5 eq) for 1 hour. In the next step the crude amine **3.106** (1 eq) was dissolved in acetone and heated to reflux. Potassium permanganate (4.5 eq) in H_2O:acetone (1:5 ratio) was slowly added to the refluxing solution until the mixture remained a deep purple colour, indicating the presence of excess potassium permanganate in the reaction. After an acid/base work up, the carboxylic **3.107** was isolated in 88 % yield.

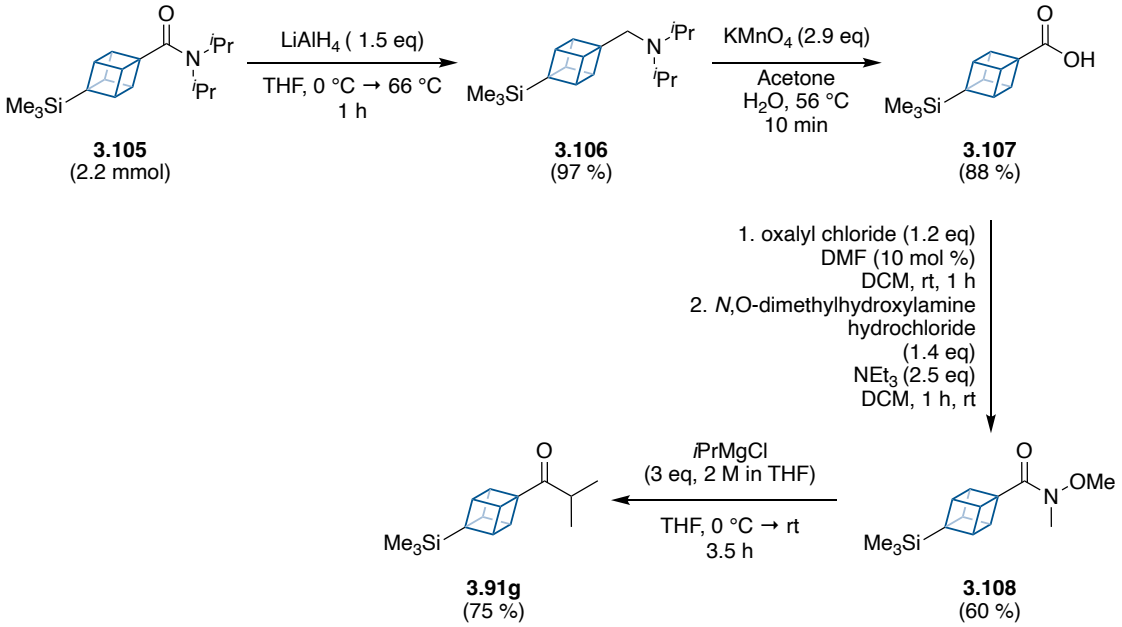

Scheme 90: Final steps in the synthesis towards **3.91g** for our study on the migratory aptitude of cubane (**Section 3.2.3.2**, Table 30).

The final steps in the synthesis included converting the carboxylic acid **3.107** to the Weinreb amide via an acid chloride (60 % yield), which was subsequently treated with

the Grignard isopropyl magnesium chloride to afford the trimethylsilyl substituted cubyl ketone **3.91g** (75 % yield). Overall, trimethylsilyl substituted cubyl *i*-propyl ketone (**3.91g**) was synthesised in 8-steps in a yield of 25 %.

3.3.2.2 Mono-substituted BV substrate (3.91h):

The synthesis of **3.91h** commenced by converting 4-methoxycarbonylcubanecarboxylic acid **2.8** to the Weinreb amide **2.12** in 4 steps (30 % overall yield,). The details of this were previously discussed in **Section 2.2.1.2.2**, with an overview of the conditions displayed in Scheme 91.

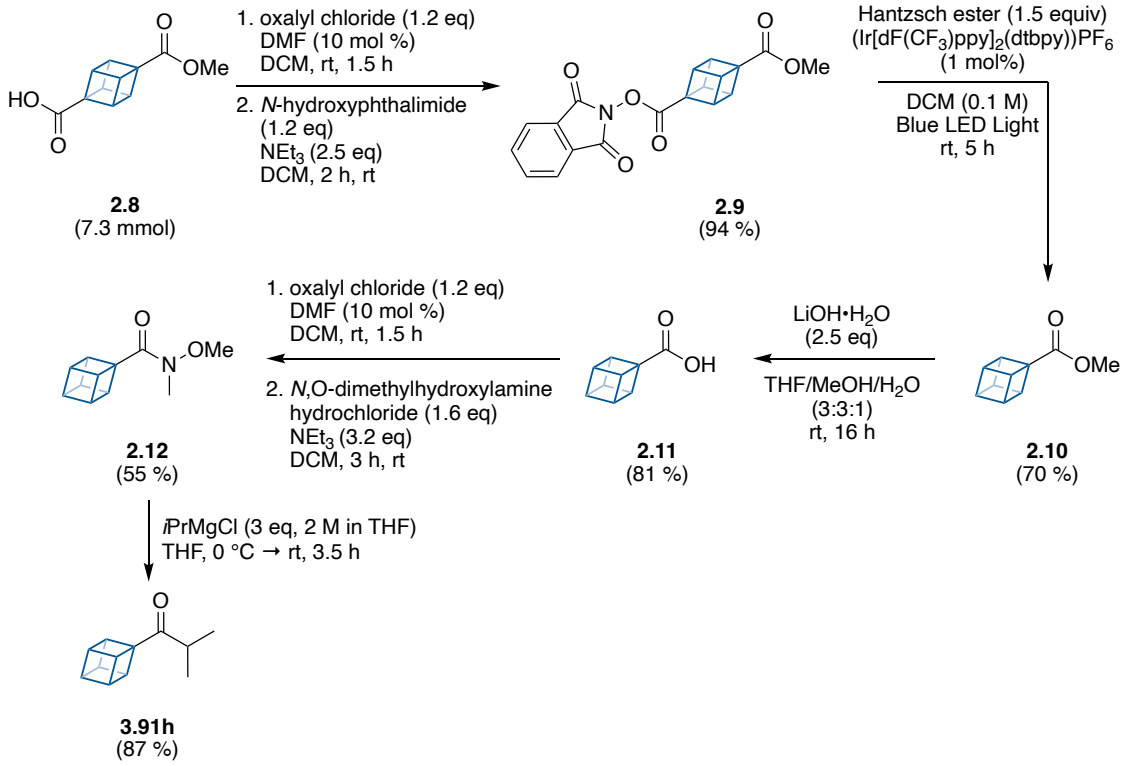

Scheme 91: Synthesis of **3.91h** for our study on the migratory aptitude of cubane (**Section 3.3.3.2**, Table 30).

In the final step, an excess of the Grignard isopropyl magnesium chloride (3 eq, 2 M in THF) was added to a solution of Weinreb amide **2.12** in THF at 0 °C, after 3.5 hours we observed full consumption of the starting material by TLC. Purification of the crude product mixture by silica gel column chromatography gave the final product cubyl isopropyl ketone **3.91h** in 67 %, with an overall yield of 20 % over 5 steps.

3.3.2.3 Alkyl substituted BV substrate (3.91i):

When considering synthetic routes towards **3.91i**, we opted to follow the retrosynthetic analysis described in Scheme 92a. The methylation of cubylmethanol **3.109** was unknown in the literature, although recently, the Linclau group had reported the benzylation of **3.109** by the addition of NaH (2 eq) and benzyl bromide (1.5 eq), which provided the product **3.110b** in 29 % yield (Scheme 92c).[164] Furthermore, based on our group's previous work on the alkylation of alcohol **3.109** with 2-(bromomethyl)naphthalene, we were aware that using the base NaH to deprotonate the alcohol would also lead to the hydrolysis of the methyl ester moiety in **3.109**. However, given that carboxylic acid **3.110** was the next target in our synthetic sequence we were not concerned about this side reaction and thus chose to proceed with the retrosynthetic route.

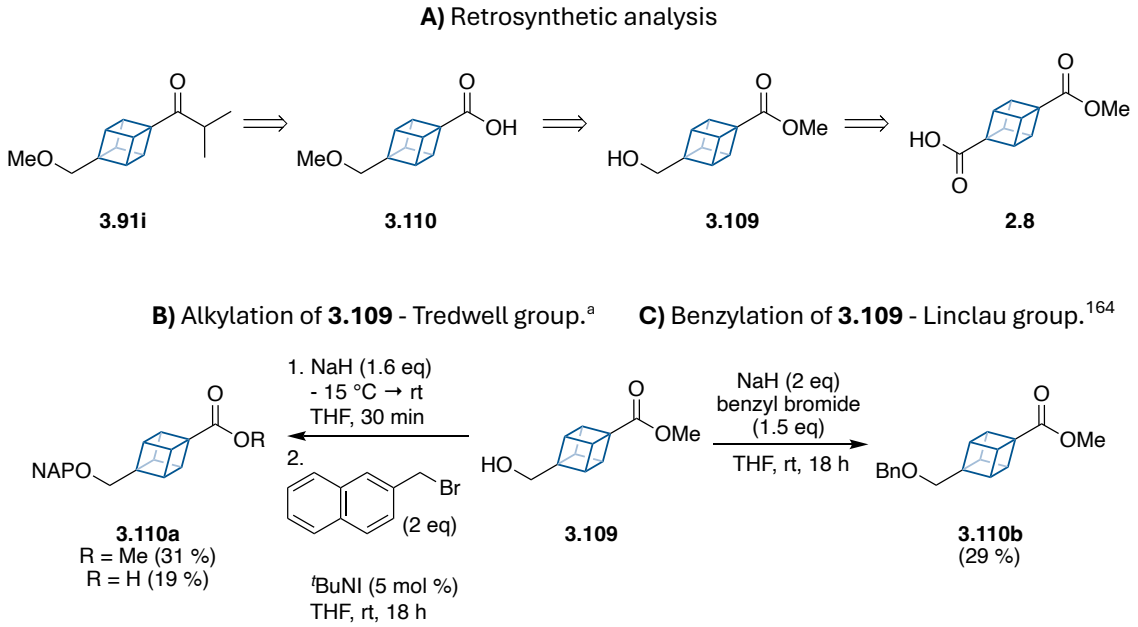

Scheme 92: Retrosynthetic analysis of the alkyl substituted cubyl ketone **3.91i** and reported protocols for the alkylation and benzylation of cubylmethanols.

[a] *Unreported work by Annika Burget, Tredwell group.*

To begin with the carboxylic acid in **2.8** was selectively reduced using borane dimethyl sulfide (1.7 eq, 1 M in 2-MeTHF), affording alcohol **3.109** in 96 % yield after 4.5 hours at room temperature (Scheme 93). When treating **3.109** (1 eq) with NaH (2 eq, 60 %

dispersion in mineral oil) followed by the addition of methyl iodide (3 eq) at room temperature for 6 hours, as predicted a mixture of products were formed. After purification of the crude mixture by silica gel column chromatography, **3.110** (16 %) and **3.111** (26 %) were isolated, along with recovered starting material **3.109** (7 %). During the purification process there were several unknown side products eluting with fractions of both **3.110** and **3.111**, which likely contributed to the poor isolated yields of these products. However, based on the quantity of **3.110** and **3.111** isolated we believed we had sufficient material to reach the end of our synthetic sequence, therefore, we did not attempt to re-purify the contaminated fractions containing **3.110** and **3.111**.

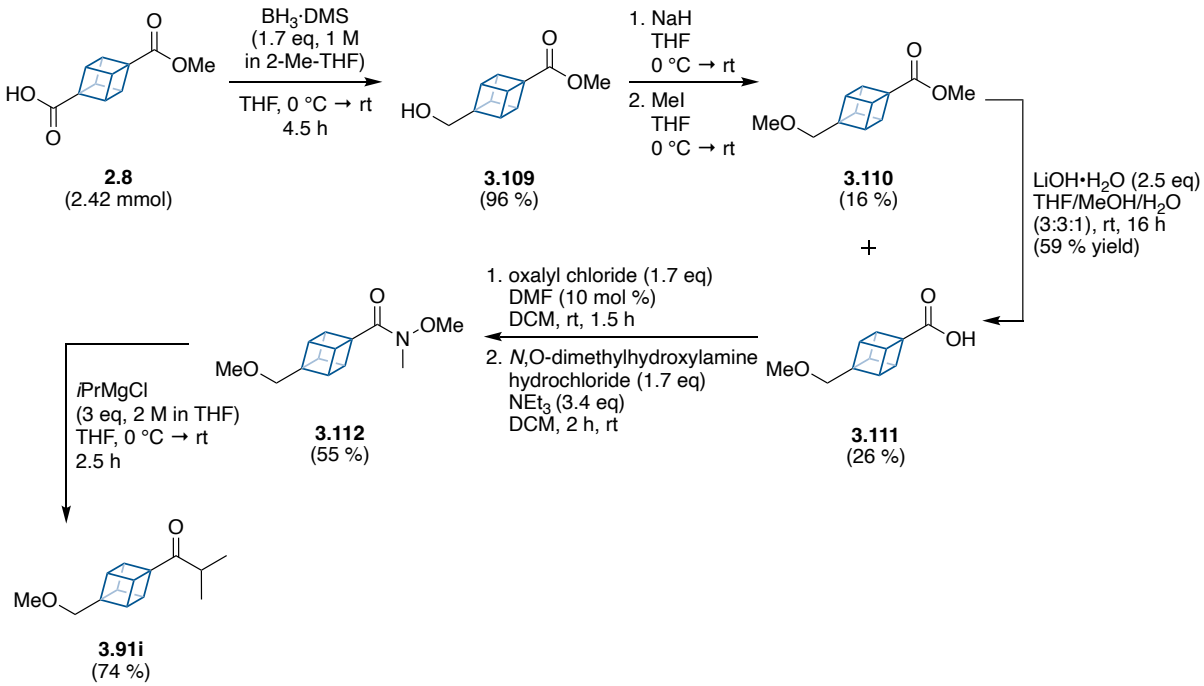

Scheme 93: Synthesis of **3.91i** for our study on the migratory aptitude of cubane (**Section 3.2.3.2**, Table 30).

The ester moiety in intermediate **3.110** was then subjected to our standard hydrolysis protocol, using lithium hydroxide (2.5 eq) in THF:MeOH:H_2O (3:3:1 ratio, 0.34 M) at room temperature, yielding pure carboxylic acid **3.111** after workup (Scheme 93). The carboxylic acid **3.111** from the hydrolysis reaction was combined with the carboxylic acid **3.111** from the ether synthesis, resulting in an overall yield of 36 % over two-steps. Next, the carboxylic acid **3.111** was converted into the Weinreb amide in a moderate

yield of 55 %, by using our usual protocol via the acid chloride followed by the addition of the amine *N*,O-dimethylhydroxylamine hydrochloride. Subsequent addition of isopropylmagnesium chloride (3 eq, 2 M in THF) to a solution of the Weinreb amide **3.112** (1 eq) gave the final product **3.91i** in 74 % yield. Overall, the alkyl substituted cubyl ketone **3.91i** was synthesised in 5-steps in a yield of 14 % (Scheme 93).

3.3.2.4 Amide substituted BV substrate (3.91j):

The synthesis of **3.91j** began with the formation on an acyl chloride, by treating **2.8** (1 eq) with oxalyl chloride (1.7 eq, 2 M in DCM and DMF (10 mol %) at room temperature. After 1.5 hours, 2.5 equivalents of diisopropylamine was added to the reaction mixture to afford the amide **3.113** in 95 % yield (Scheme 94). Intermediate **3.113** was subjected to hydrolysis conditions using 1.1 equivalents of lithium hydroxide in THF:MeOH:H_2O (3:3:1 ratio, 0.34 M) at room temperature, providing the desired product **3.114** in a good yield of 88 %. Importantly, under those hydrolysis conditions the bulky diisopropylamide remained intact.

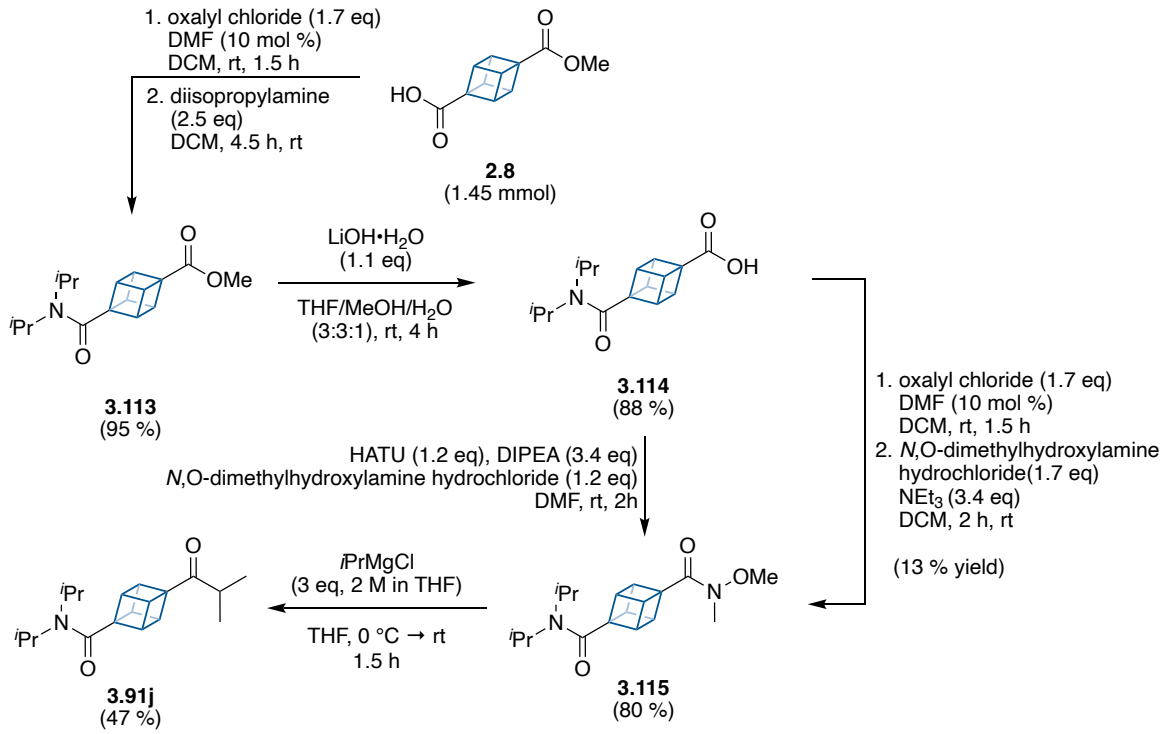

Scheme 94: Synthesis of **3.91j** for our study on the migratory aptitude of cubane (**Section 3.2.3.2**, Table 30).

Initially, we attempted to synthesise the Weinreb amide **3.115** via the acid chloride, again using the combination of oxalyl chloride and DMF. However, we observed significant decomposition in the crude product NMR, with the desired product **3.115** isolated in a poor yield of 13 % after silica gel column chromatography. Eaton *et al* have also reported the same issue when using thionyl chloride in the presence of cubyl diisopropylamides, but mentioned decomposition can be avoided using an excess of TMEDA in the acid chloride formation step.[276] Instead of repeating the reaction with TMEDA, we opted to use the coupling agent HATU (1.2 eq) in the presence of DIPEA (3.4 eq) and *N*,O-dimethylhydroxylamine hydrochloride (1.2 eq) for the amide bond formation, which gave **3.115** in a much improved yield of 80 %. Finally, the addition of 3 equivalents of the Grignard reagent isopropylmagnesium chloride (2 M in THF) to the Weinreb amide **3.115** gave the ketone **3.91j** in a moderate yield of 47 % after silica gel column chromatography. In total, the amide-substituted cubyl ketone **3.91j** was synthesised over 4-steps in an overall yield of 32 % (Scheme 94).

3.3.2.5 Bromo substituted BV substrate (3.91k):

The bromodecarboxylation of **2.8** was achieved following a procedure reported by Watanabe and co-workers.[277] A solution of **2.8** (1 eq), (diacetoxyiodo)benzene (1.5 eq) and potassium bromide (1.8 eq) in DCM under air was irradiated with the standard fluorescent light fittings located in the fume hood. After 24 hours at room temperature the crude product mixture was purified by silica gel column chromatography to afford the bromide **3.116** in 48 % yield, which was consistent with the reported literature yield of 53 % (Scheme 95).[277] The subsequent steps to afford the bromo substituted cubyl ketone **3.91k** for our BV studies proceeded with no issues, using the standard conditions previously discussed to install the isopropyl ketone group. Overall, **3.91k** was synthesised in 4 steps in a total yield of 19 %.

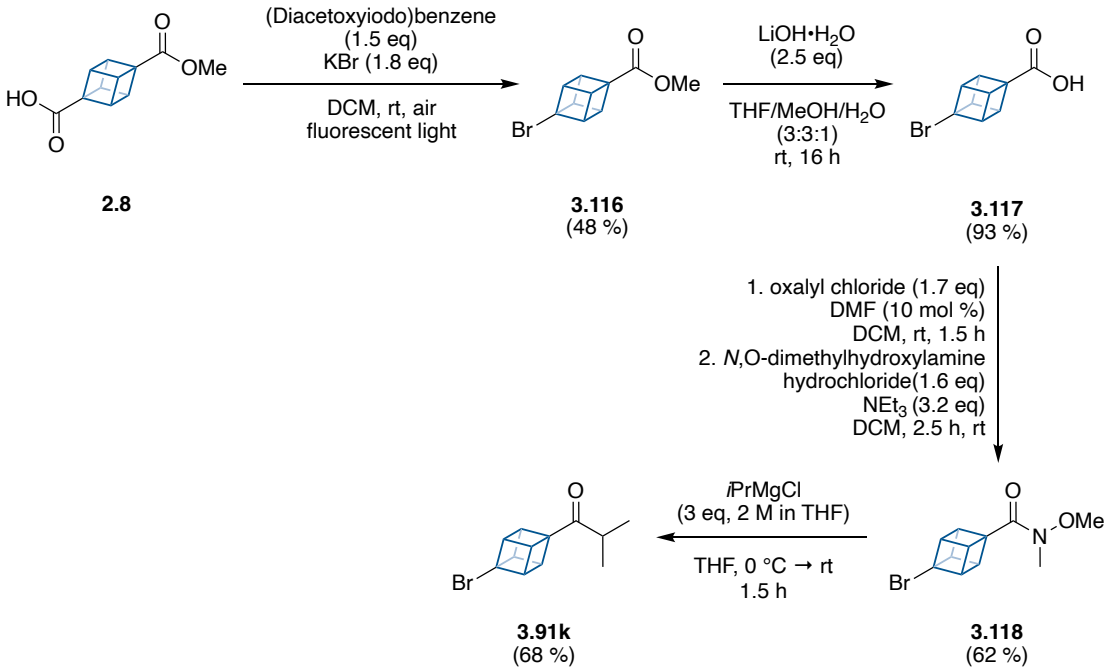

Scheme 95: Synthesis of **3.91k** for our study on the migratory aptitude of cubane (**Section 3.2.3.2**, Table 30).

3.3.2.6 Fluoro substituted BV substrate (3.91l):

Della and Head were the first to synthesise 4-fluorocubane-1-carboxylate **3.119** by using the fluorinating reagent xenon difluoride (1.5 eq) (Scheme 96a-b).[278] Two methodologies were described: (1) the fluorodecarboxylation of the carboxylic acid **2.8** to give **3.119** in DCM at room temperature overnight (Scheme 96a) or (2) the fluorodeiodination of iodo **3.99** to give **3.119** in DCM at reflux for 6.5 hours (Scheme 96b).[278] In both examples the fluoride product was contaminated with chloro-cubane **3.120**, a result of the cubyl cation abstracting a chloride atom from the DCM solvent. In addition, for the fluorodecarboxylation of the carboxylic acid **2.8** a significant quantity of methyl-cubanecarboxylate **2.10** was observed by GC/MS analysis (Scheme 96a). In a subsequent study Della and Head reported that yield for the fluorodeiodination of **3.99** to afford **3.119** could be increased to 80 %, by performing the fluorination reaction in a sealed vessel at an elevated temperature of 70 - 80 °C.[190] For this improved procedure the authors did not comment on whether the chloro contaminant **3.120** was formed under these conditions, although, we suspect it did as shortly after Della *et al* published a new method that replaced the chlorinated solvent DCM for hexane.[166] Thus,

preventing the formation of the chloro contaminant **3.120** during the fluorodeiodination reaction (Scheme 96c).[166]

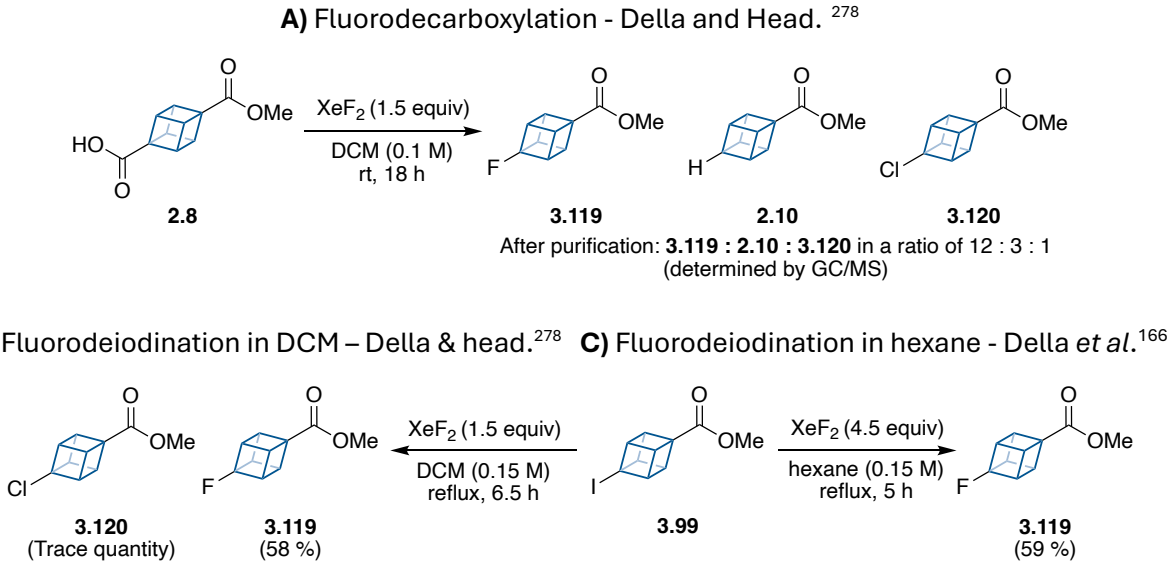

Scheme 96: Literature repots for the synthesis of fluorocubanes.

Based on the existing literature towards the synthesis of fluorocubanes, we opted to begin with the fluorination of the cubyl iodide **3.99** with xenon difluoride in hexane. We choose to use the cubyl iodide **3.99** over the carboxylic acid **2.8**, as we anticipated that **2.8** would not be soluble in hexane even at elevated temperatures. Unfortunately, in contrast to the success Della *et al* reported, in our hands the fluorination was largely unsuccessful in hexane. We found the addition of xenon difluoride (1.5 eq) to a solution of iodide **3.99** (1 eq, 0.5 mmol) in hexane (0.15 M) at room temperature (behind a blast shield) resulted in only 15 % conversion of the iodo **3.99** to fluoride **3.119** after 6 hours at reflux (determined by ^{1}H NMR, Scheme 97). As expected, separation of the desired fluoride product from the iodide starting material would be extremely challenging by silica gel column chromatography, therefore, no attempt to isolate **3.119** was made on this occasion as the yield for the reaction was too low.

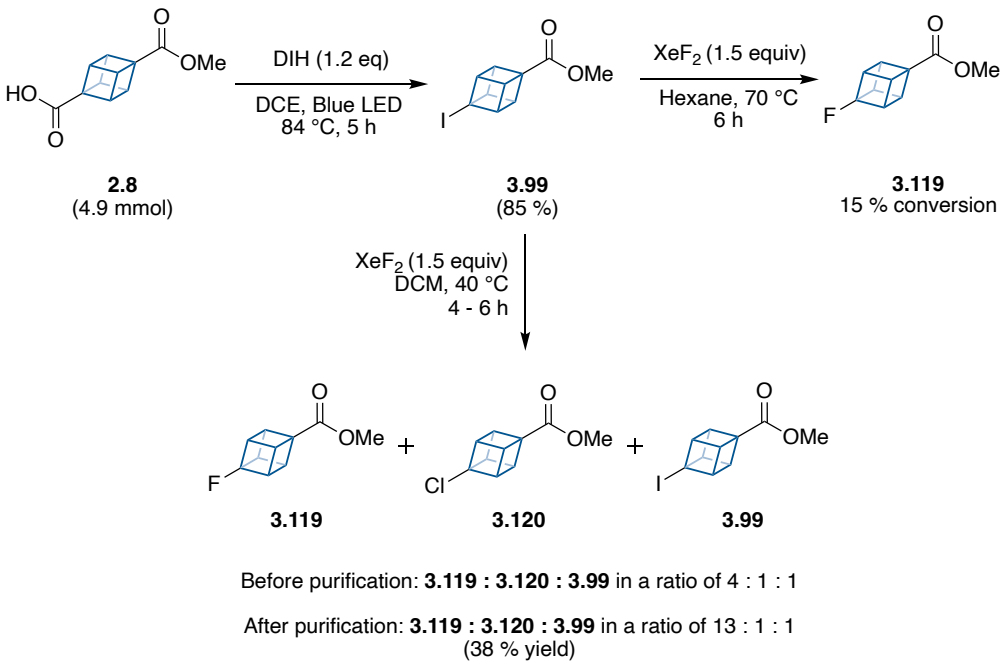

Scheme 97: Fluorodeiodination of **3.99** using xenon difluoride in hexane and DCM.

With hexane not being a suitable solvent, we had no option but to attempt the fluorination of the cubyl iodide **3.99** in the chlorinated solvent DCM, knowing the chlorinated cubane by-product **3.120** would make the purification of the fluorinated product even more challenging. Subjecting the iodide **3.99** (1 eq, 0.5 mmol) to xenon difluoride (1.5 eq) in DCM (0.15 M) for 4 hours at reflux resulted in a 4:1:1 ratio of **3.119** : **3.120** : **3.99** in the crude mixture (Scheme 97). By ^{1}H NMR analysis we were able determine the ratio each cubyl species by comparing the chemical shifts of the cubane multiplets to authentic samples of **3.120** and **3.99** we had previously synthesised (Figure 33), in addition to the ^{1}H NMR data reported by Della and Head for fluoride **3.119**.[278]

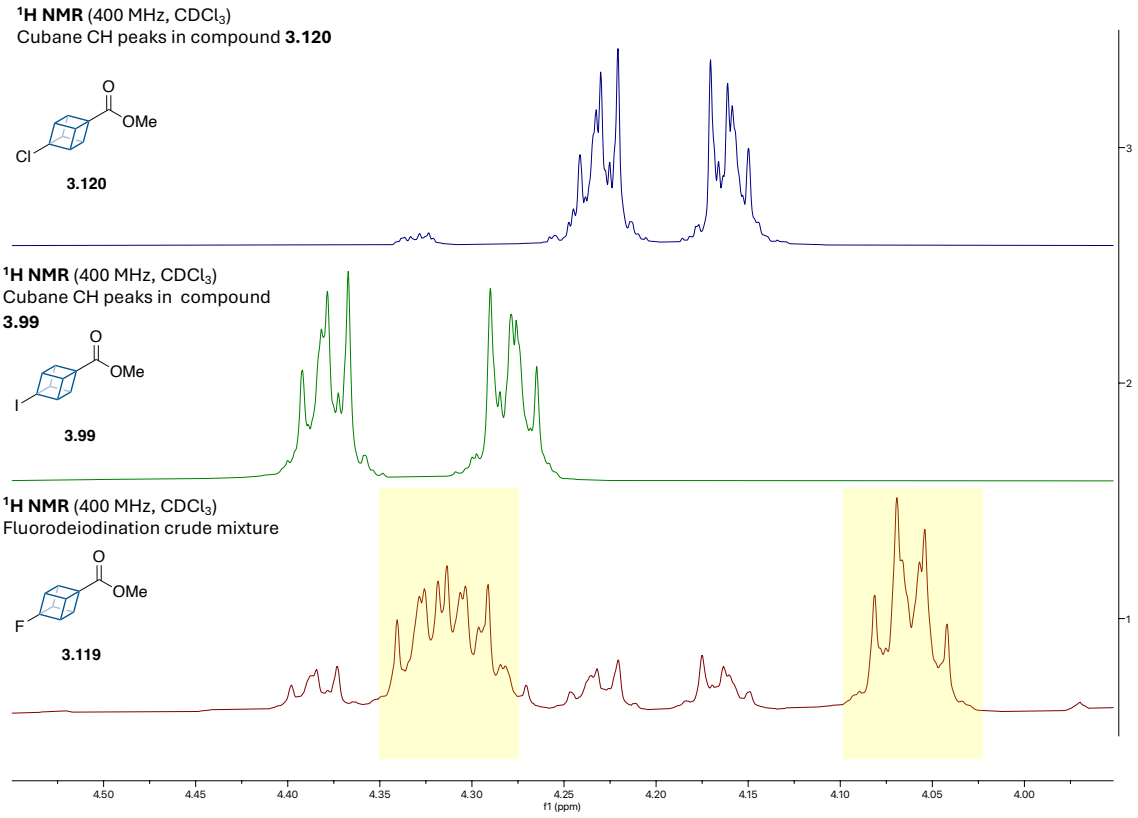

Figure 33: Stacked ^{1}H NMR spectra of crude mixture containing fluorocubane **3.119** (highlighted in yellow).

Due to safety concerns with using large quantities of xenon difluoride, the fluorination in DCM was repeated in an additional 4 batches, each using 0.5 mmol of cubyl iodide **3.99** (Scheme 97). The reaction time was also increased to 6 hours to try and enhance the consumption of the iodide starting material **3.99**. The crude product from each batch was combined and ^{1}H NMR analysis revealed the ratio of **3.119** : **3.120** : **3.99** remained the same (4:1:1), despite increasing the reaction time from 4 to 6 hours. Pleasingly, after one challenging round of purification via silica gel column chromatography the ratio of **3.119** : **3.120** : **3.99** was improved to 13:1:1 in a yield of 38 % (Figure 34), albeit lower than the reported literature yield of 58 % under similar conditions (Scheme 96b).[278]

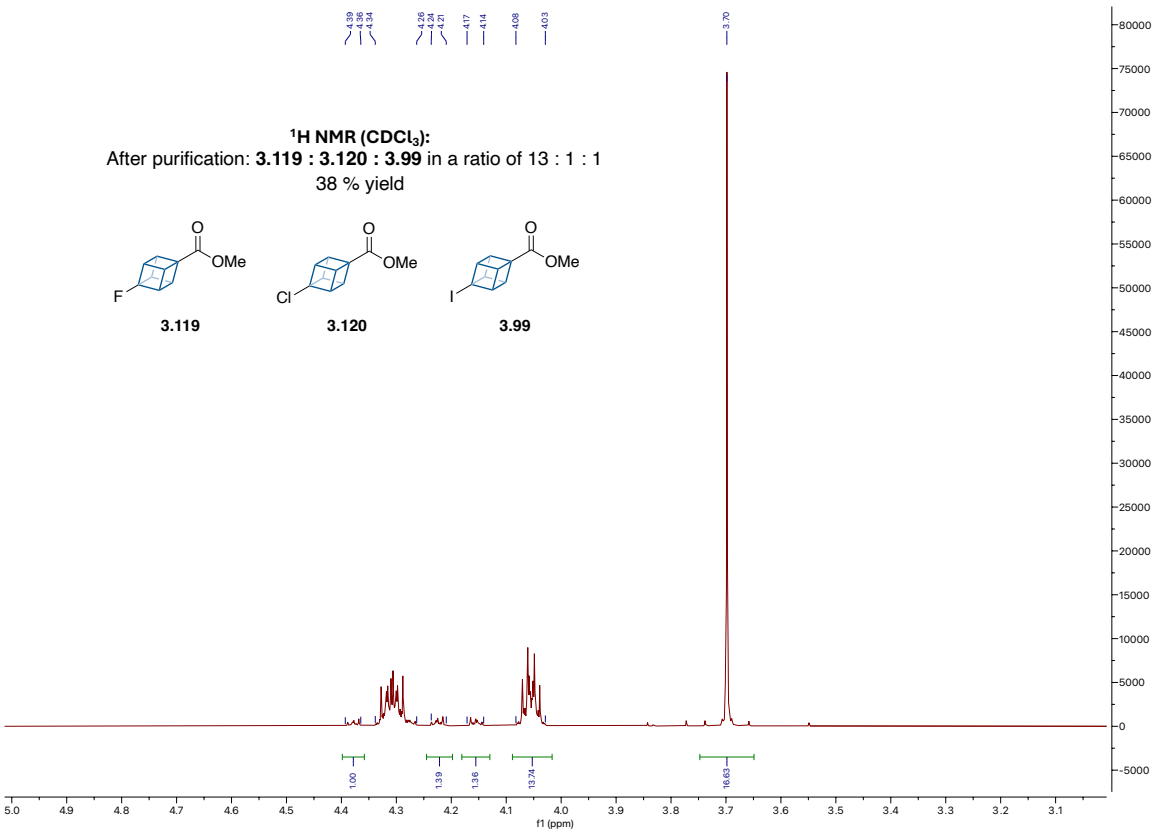

Figure 34: ^{1}H NMR of **3.119** : **3.120** : **3.99** in a ratio of 13:1:1 after purification by silica gel column chromatography.

Despite Della and Head reporting the synthesis of **3.119** over 30 years ago, to the best of our knowledge the literature does not contain ^{19}F NMR data of any fluorocubane species.[278] We can report that in the ^{19}F{^{1}H}NMR (471 MHz, $CDCl_3$) of 4-fluorocubane-1-carboxylate **3.119**, a singlet at -140.36 ppm was observed (see appendix for ^{19}F NMR spectrum).

At this stage, we decided to use the halogen mixture in the next step of the synthesis, with the thought that purification may be easier on a different substrate later in the synthetic sequence (Scheme 98). Continuing with the synthetic sequence, the 13:1:1 mixture of **3.119** : **3.120** : **3.99** was hydrolysed with lithium hydroxide (2.5 eq) in THF:MeOH:H_2O (3:3:1 ratio, 0.34 M) at room temperature, affording **3.121** in 94 % yield. As a result of the crude product not requiring purification by silica gel column chromatography the ratio of halo contaminants remained unchanged (13:1:1 ratio of fluoro : chloro : iodo determined by ^{1}H NMR). Employing the peptide coupling reagent

HATU (1.2 eq) in the presence of DIPEA (3.5 eq) and *N*,O-dimethylhydroxylamine hydrochloride (1.2 eq) in DMF, the carboxylic acid moiety in **3.121** was converted into the Weinreb amide **3.122** within 2 hours at room temperature. One round of purification by silica gel column chromatography gave **3.122** in 62 % yield, with an improved ratio of the fluoro : chloro : iodo products to 59:4:1 respectively.

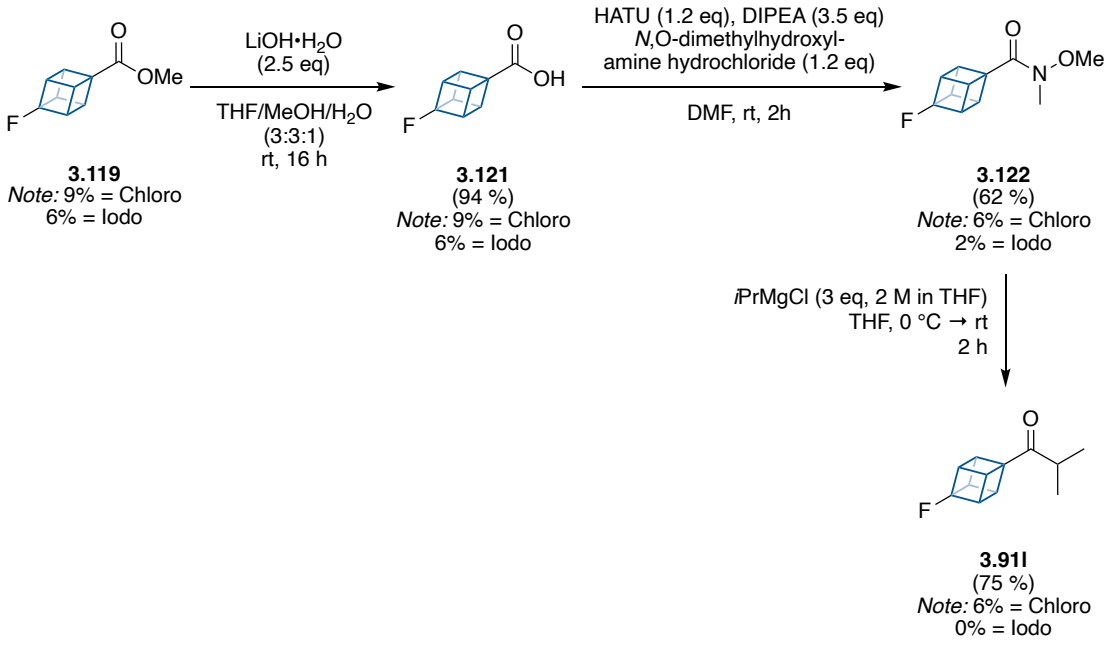

Scheme 98: Continued synthesis of **3.91l** for our study on the migratory aptitude of cubane (**Section 3.2.3.2**, Table 30).

Finally, the Weinreb amide **3.122** (1 eq) was treated with isopropylmagnesium chloride (3 eq, 2 M in THF) in THF at room temperature for 2 hours, followed by one round of silica gel column chromatography to afford the final product **3.91l** in 75 % yield (14:1 of fluoro:chloro). During the purification, we were able to completely remove the iodo impurity, although the ratio of the fluoro:chloro remained largely unchanged. The difficulty associated with removing the chloro cubane impurity highlights the importance of finding an alternative solvent for the fluorination reaction, although, more importantly the development of a novel fluorination method compatible to cubane. Overall, we were able to successfully synthesise fluoro substituted cubyl ketone **3.91l** in 17 % yield over 5 steps, with **3.91l** having a purity of 94 % (determined by ^{1}H NMR).

3.4 Summary

To summarise this chapter has focused on examining the Baeyer-Villiger oxidation of cubyl ketones as a method to acquire cubyl esters, which we propose could act as a useful synthetic building block to access cubanols. At the start of this chapter, we identified that cubanol **3.3** could be an important synthetic intermediate towards the cubyl tamoxifen **1.19** (Scheme 99). With a method for the Baeyer-Villiger oxidation of cubyl ketones now established, the next chapter will focus on the method development for the transformation of the cubyl esters to cubanols via a hydrolysis reaction.

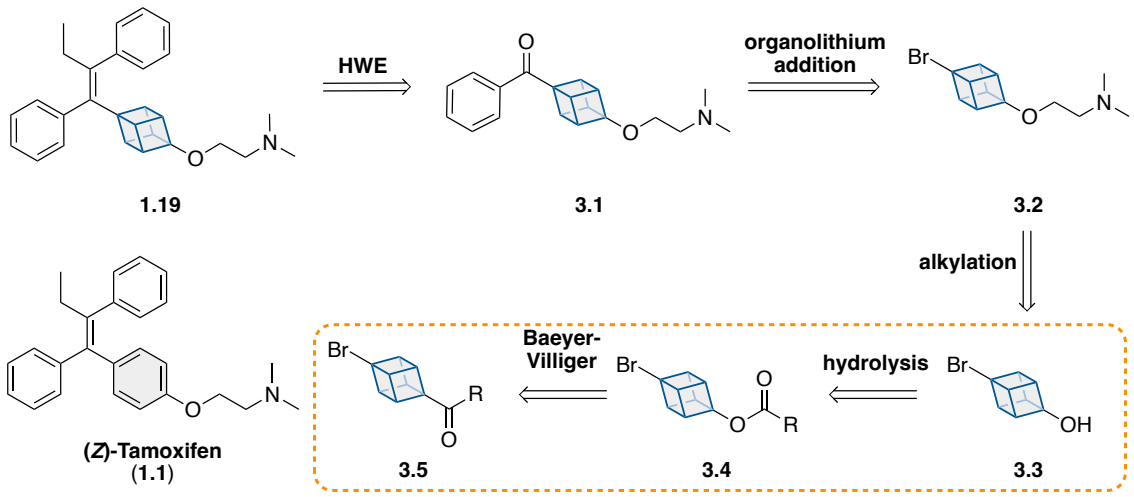

Scheme 99: Retrosynthetic analysis towards cubyl tamoxifen **1.19**, incorporating the Baeyer-Villiger oxidation of cubyl ketones (Chapter 3) followed by hydrolysis of the resulting cubyl esters to afford cubanols (Chapter 4).

Chapter 4 Cubanol

4.1 Introduction

The recent interest around strained hydrocarbon cages, such as 1,4-substituted cubanes acting as bioisosteres for *para*-substituted phenyl rings, has driven the advancement of novel chemical methods to incorporate these strained scaffolds into complex molecules. Despite phenols being commonly found in pharmaceuticals and natural products, literature reports on the synthesis of cubanols are limited and their stability and synthetic utility as intermediates are inconclusive (Figure 35). [112, 167, 169, 189, 190, 279]

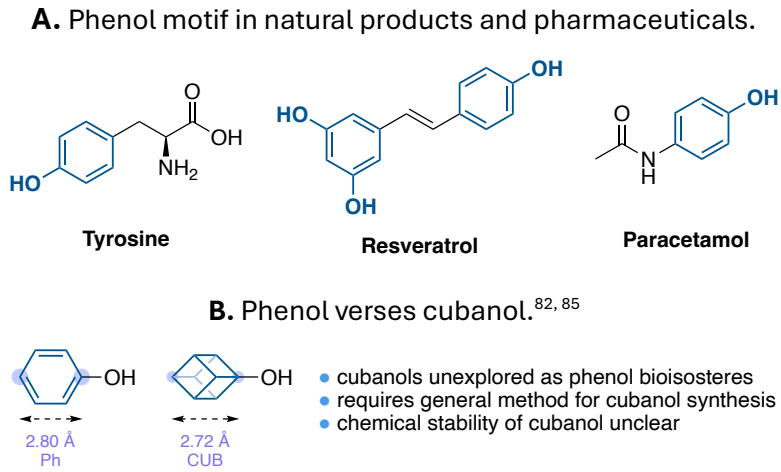

Figure 35: Cubanol as a phenol bioisostere.

Eaton and Zhou reported that cubanols could be accessed by the reduction of cubyl acetates using DIBAL at -70 °C (Scheme 100a).[169] The crude mixture was then directly treated with methanesulfonyl chloride in the presence of triethylamine at - 20 °C to afford the mesylate **3.88a** and **3.88b** in 80 % and 67 % yield respectively.[169] Unfortunately, Eaton and Zhou omitted experimental information and analytical data for the DIBAL reduction and subsequent mesylate formation.

A. DIBAL reduction of cubyl acetate - Eaton and Zhou.[169]

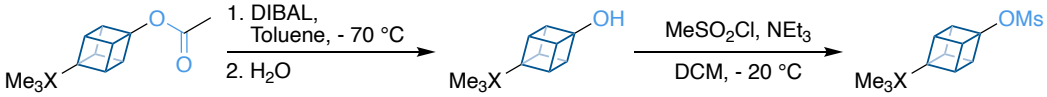

3.7a M = Si
3.7b M = Sn

3.87

3.88a (80 %)
3.88b (67 %)

B. Acid and base catalysed hydrolysis of homocubyl acetates - Klunder and Zwanenburg.[167, 168]

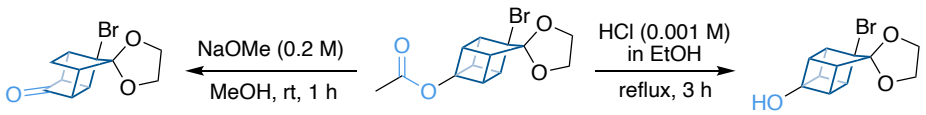

4.3 (95 %)

4.1 (1.6 mmol)

4.2 (87 %)

C. Deamination - Klunder and Zwanenburg.[167]

D. Deamination - Della and head.[190]

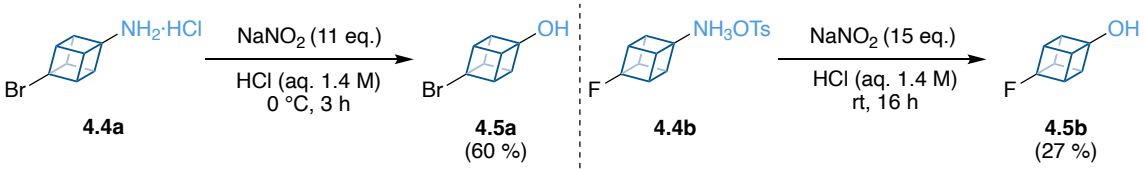

4.4a

4.5a (60 %)

4.4b

4.5b (27 %)

Scheme 100: Synthetic routes to cubyl and homocubyl alcohols.

Unlike Eaton and Zhou, Klunder and Zwanenburg provided a detailed experimental section for their work on the synthesis of cubanols and homocubanols (a ring expanded analogue of cubane).[167, 168] The synthesis of homocubyl alcohol **4.2** was achieved by acid catalysed hydrolysis of the homocubyl acetate **4.1** in refluxing 0.001 M HCl in ethanol for 3 hours (87 % yield, Scheme 100b).[167] Conversely, the treatment of **4.1** with sodium methoxide (0.2 M) in methanol at room temperature for 1 hour led to the rearrangement of the polycyclic system, affording ketone **4.3** in a 95 % yield.[168] Based on these two experiments, Klunder and Zwanenburg suggested to avoid decomposition of the homocubyl alcohol only acidic conditions should be employed. Despite the acid catalysed hydrolysis method affording the homocubanol in a yield of 87 %, Klunder and Zwanenburg did not indicate whether this protocol could be applied to cubyl acetates to yield cubanols. Instead, the authors synthesised the cubyl alcohol **4.5a** via a diazonium salt, implying the acid catalysed hydrolysis of cubyl acetates could be more challenging than homocubyl acetates (Scheme 100c).[167] Klunder and Zwanenburg reported that

treating cubyl amine **4.4a** (1 eq) with $NaNO_2$ (1.1 eq) in dilute aqueous HCl (5 %) at 0 °C for 3 hours gave **4.5a** in 60 % yield, with decomposition of the product only observed at temperatures exceeding 100 °C.[167] Under similar conditions Della and Head reported the deamination of the amine **4.4b** only gave 4-fluorocubanol in 27 % yield (Scheme 100d).[190] The poor isolated yield for **4.5b** could be attributed to Della and Head leaving the reaction at room temperature for a prolonged period of time (16 hours), which may have promoted some decomposition of the cubanol product.

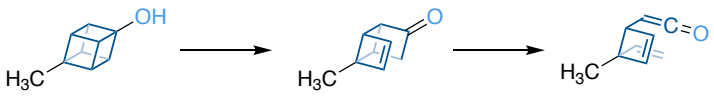

4.5c **4.6** **4.7**

Scheme 101: Cubane ring-opening by homoketonisation - Eaton.[105]

In a review published by Eaton on advances in cubane chemistry, the stability of cubanol was briefly discussed. Eaton reported that cubanols can be fragile, stating they can be isolated but are susceptible to ring opening by homoketonisation and rearranging to vinylcyclobutenylketene (**4.7**) (Scheme 101).[105] In addition to these synthetic methodologies, there are several enzymatic literature reports towards cubanols. Enzymatic approaches for the C-H oxidations of the cubane core to yield cubanols were previously discussed in **Chapter 1, Section 1.2.2.2.4**, with an example included in Table 33.[111]

Table 33: Enzymatic oxidation of methylcubane.[111]

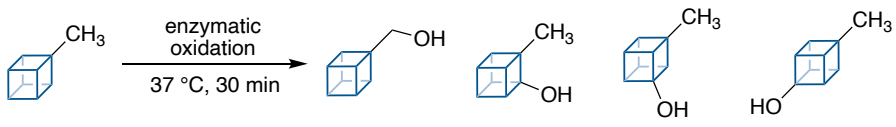

1.14 **1.14a** **1.14b** **1.14c** **1.14d**

	Yield[a] / %			
	1.14a	**1.14b**	**1.14c**	**1.14d**
Rat CYP2B1	62	12	19	7
Rat CYP2B4	88	4	1	7
Rat CYP2E1	55	13	16	10

[a] *The percentage yields represent product distribution not isolated yields. Overall yield was not reported.*

Overall, all the enzymatic approaches currently reported for the synthesis of cubanol are generally low yielding, on biological scale and reported poor regioselectivity.[109, 111, 112, 279] Similar to the synthetic methodologies, no reference to the cubanols stability were made in any of the studies.

As a result of the limited reports on cubanols in general, we became interested in developing a general method towards cubanols to evaluate their suitability as useful synthetic intermediate and a potential (bio)isostere for phenol. We envisaged that a useful transformation for the esters formed in our BV rearrangements, in the cases where cubane migrated, would be their conversion into cubanols (Scheme 102a). Once a reliable method for accessing cubanols has been developed, the synthesis and alkylation of cubanol **3.3**, using 2-chloro-*N*,*N*'-dimethylethylamine as the alkylating agent, would be of considerable interest to us. As this transformation could provide a route to prepare the most challenging cubyl analogue of the oncology drug (*Z*)-tamoxifen **1.19** (Scheme 102b).

A. Two-step protocol to prepare cubanols from cubyl ketones/aldehyde.

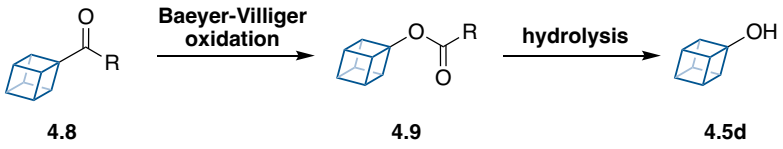

B. Synthesis cubyl-tamoxifen **1.19**.

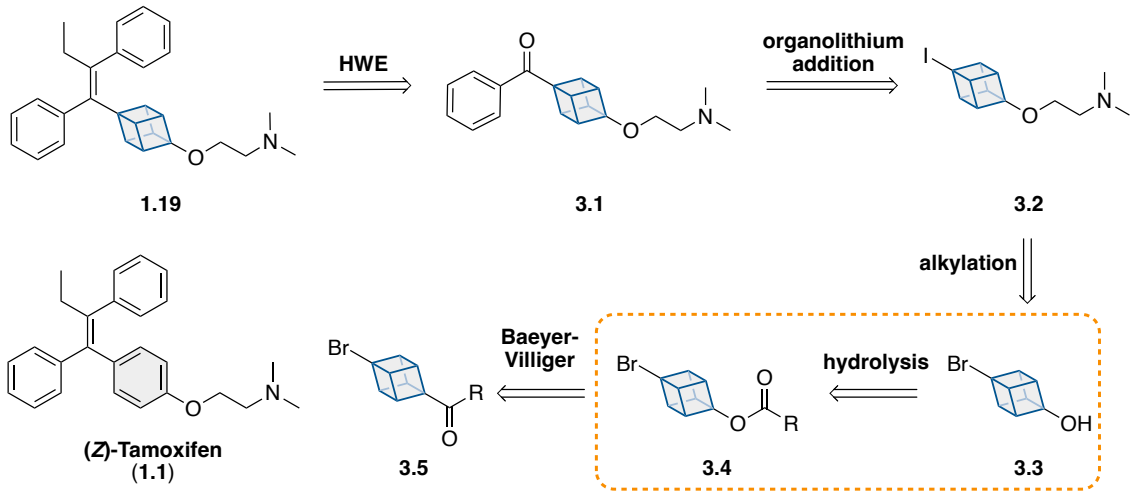

Scheme 102: Proposed synthetic approach towards cubanols and its derivatisation into cubyl-tamoxifen **1.19**.

4.2. Result and discussion

The work described in this chapter has been published.[263]

4.2.1 Hydrolysis optimisation

The conversion of cubyl esters into cubanols has only been reported by Eaton and Zhou, by a DIBAL reduction (Scheme 100a).[169] Therefore, based on the literature we elected to begin our cubanol studies with the DIBAL reduction of cubyl ester **4.10** (where R = Ph), prepared via a Bayer-Villiger oxidation (Chapter 3). In our hands we found no reduction took place when treating ester **4.10** (1 eq) in THF with DIBAL (1.1 eq, 1 M in toluene) at -78 °C for 2 hours. Instead, the starting material was fully recovered (Table 34, entry 1). When performing the reaction at room temperature under similar reaction conditions, the only identifiable compound in the crude ^{1}H NMR was the starting material **4.10**, with the presence of numerous signals that presumably belonged to decomposition products (entry 2). The fact decomposition signals were observed made us consider that cubanol formation under the conditions in entry 2 may have taken place, although **4.11** may have been unstable in the basic reaction conditions at room temperature. Due to incomplete consumption of ester **4.10** despite performing the DIBAL reduction at room temperature (entry 2), led us to question whether **4.10** was the best substrate for this reaction optimisation.

Table 34: Synthesis of cubanol **4.11** under basic conditions.

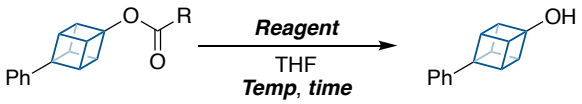

4.10 **4.11**

Entry	R	Reagent / equiv	Temp / °C	Time / h	Conversion of 4.10 to 4.11[a] / %	Major products in crude ^{1}H NMR
1	Ph	DIBAL / 1.1	-78	2	0	**4.10**
2	Ph	DIBAL / 1.1	rt	2	0	**4.10** + decomposition
3	H	DIBAL / 1.5	-78	2	0	decomposition
4	Ph	$LiAlH_4$ / 2.0	0	0.25	0	decomposition
5[b]	Ph	LiOH / 2.5	Rt	24	0	**4.10** + decomposition

[a] Conversion calculated by integration of relevant peaks in ^{1}H NMR of the crude material. [b] 3:1:1 solvent ratio of THF/MeOH/H_2O.

We decided to revisit the conditions in Table 34 entry 1, but with the sterically less hindered formate (where R = H) (entry 3). We were pleased to find that the formate was fully consumed at - 78 °C, demonstrating how much more reactive the cubyl formate was compared to cubyl benzoate. To our surprise, cubanol **4.11** was not observed in the crude ^{1}H NMR, instead signals belonging to an unidentified side product which was likely a mixture of cubane ring-opened by-products. Attempts to isolate the side products by silica gel column chromatography to characterise them were unsuccessful. In addition to the DIBAL reduction, we also explored a reduction of **4.10** (R = Ph, 1 eq) with lithium aluminium hydride (2 eq) in THF at 0 °C and a hydrolysis using lithium hydroxide (2.5 eq) in a solvent system of THF: MeOH:H_2O (3:3:1 ratio) (entries 4-5). Unfortunately, cubanol formation was not observed in both conditions, with peaks only relating to extensive decomposition visible in the crude product ^{1}H NMR.

Given the lack of success in synthesising cubanol through basic conditions, our next experiments focused on exploring acidic conditions to promote this transformation and thus avoiding the potential formation of the unstable deprotonated cubanol . Unlike Klunder and Zwanenburg, when we refluxed the ester **4.10** (R = Me) with HCl in ethanol (0.001 M) for 3 hours, we only observed starting material and slight decomposition in the crude ^{1}H NMR (Table 35, entry 1) . Extending the reaction time to 6 hours only increased decomposition (entry 2). The concentration of HCl in ethanol used in entry 1 and entry 2 was very low, therefore we suspected the decomposition was a result of heating the reaction at 78 °C rather than the concentration of the acid. To our delight, when running the hydrolysis at room temperature and using a more concentrated solution of HCl in ethanol (1.25 M), **4.10** was fully converted into cubanol **4.11** within 3 hours and no decomposition products were observed by ^{1}H NMR (entry 3). Pleasingly, the same result occurred when extending the reaction time to 18 hours, demonstrating that cubanol was stable to the reaction conditions (entry 4). Interestingly, when treating the ester **4.10** (R = Ph) under the same conditions only 6 % conversion of ester **4.10** to cubanol **4.11** was observed, which further demonstrated that the cubyl benzoate was a poor substrate for accessing cubanols (entry 5) .

Table 35: Synthesis cubanol **4.11** under acidic conditions.

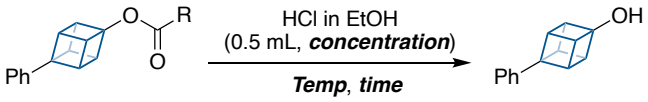

4.10 **4.11**

Entry	R	*Conc. of HCl in EtOH / M*	Temp / °C	Time / h	Conversion of **4.10** to **4.11**[a] / %	Major products in crude ^{1}H NMR
1	Me	0.001	78	3	0	**4.10** + decomposition
2	Me	0.001	78	6	0	decomposition
3[b]	Me	1.25	rt	3	100	**4.11**
4	Me	1.25	rt	18	100	**4.11**
5	Ph	1.25	rt	18	6	**4.10** + **4.11**

[a] *Conversion calculated by integration of relevant peaks in ^{1}H NMR of the crude material.*
[b] *Optimised conditions.*

Initially inspection of crude ^{1}H NMR from the hydrolysis reaction revealed the reaction proceeded cleanly, with the only impurity present being residual ethanol (Table 35, entry 3-4 and Figure 36 bottom spectrum). When the crude mixture was left under high vacuum for extensive time periods (5 days), the trace quantities of what we tentatively assigned as ethanol via ^{1}H and ^{13}C NMR analysis remained. Attempts to remove this impurity using trituration and ethanol azeotropes were unsuccessful. Additionally, 2D-TLC analysis indicated that the cubanol was unstable to normal phase silica gel column chromatography, preventing us removing this impurity by this method. Instead, we discovered this impurity could be removed by a liquid-liquid extraction, using ethyl acetate and a solution saturated ammonium chloride. Washing the organic layer several times with the slightly acidic solution over a time frame of 5 minutes resulted in no decomposition of the cubanol and complete removal of the impurity. It is important to note, when we used water at pH 7, instead of saturated ammonium chloride, we observed some decomposition of cubanol **4.11**.

NMR analysis of cubanol **4.11** also provided greater insight into its stability. We found that cubanol **4.11** began to decompose in $CDCl_3$ after 1 hour at room temperature (20 °C) via ^{1}H NMR monitoring, shown by the intensity of the cubyl C-H peaks decreasing

and decomposition peaks increasing over time (Figure 36, top spectrum). From our optimisation studies we learnt that cubanol was stable in acidic ethanol solution for at least 18 hours, we therefore believed acetic acid-d_3 may be a more suitable NMR solvent. As proposed, we observed no decomposition of cubanol **4.11** in acetic acid-d_3 after 24 hours at room temperature (20 °C) via ^{1}H NMR monitoring (*see appendix*).

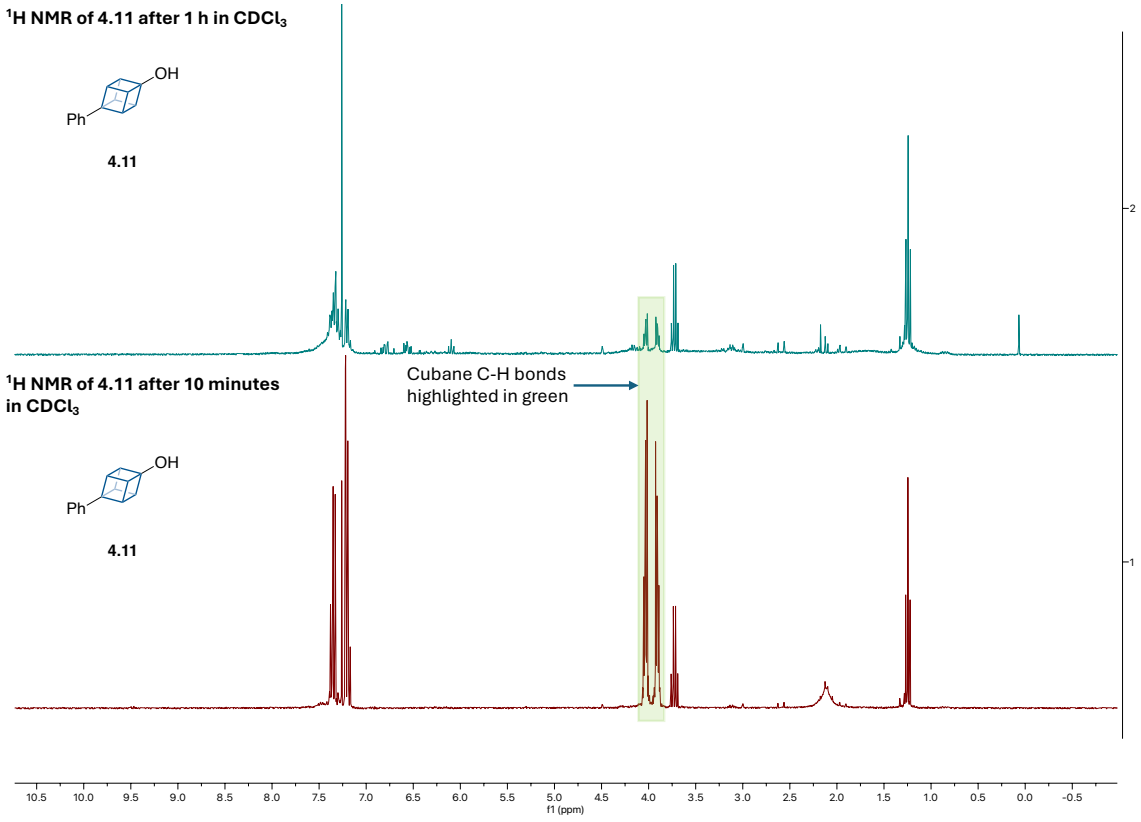

Figure 36: Decomposition of cubanol **4.11** in NMR solvent $CDCl_3$ after 1 hour.

To examine the synthetic utility of this hydrolysis method to generate cubanols, we originally wanted to apply our BV and hydrolysis protocols towards the synthesis of the cubyl tamoxifen **1.19**. However, due to time constraints associated with the project and the complexity of that target, we instead opted to test the usefulness of our method by synthesising cubyl derivatives of resveratrol, a phenol containing biologically active compound.

4.2.2 Application to complex molecule synthesis

4.2.2.1 Overview of cubyl-resveratrol

The two cubyl analogues of the biologically active compound resveratrol (**4.12**) we set out to synthesise are displayed in Figure 37. In achieving this target, we would demonstrate that the ester products of the BV rearrangement of cubyl ketones, in which cubane migrates, are a useful precursor to cubanol a potential phenol bioisostere. Traditionally, resveratrol can be found in certain plant species and red wines; although, more recently it has been sold as a nutritional supplement due to its wide range of biological properties including antioxidant, anticancer, anti-inflammatory and antiaging.[280] However, its use beyond a nutritional supplement has been restricted due to its poor bioavailability resulting from extensive first-pass metabolism.[280] An approach which is becoming more popular to reduce phenyl ring related drug metabolism includes utilising phenyl bioisosteres that could have an improved metabolic stability, such as cubane. This, in conjunction with the breadth of chemistry needed to synthesise the two cubyl analogues of resveratrol (**4.13a and 4.13b**), made us believe this was an ideal substrate to demonstrate the general applicability of our BV and hydrolysis protocol.

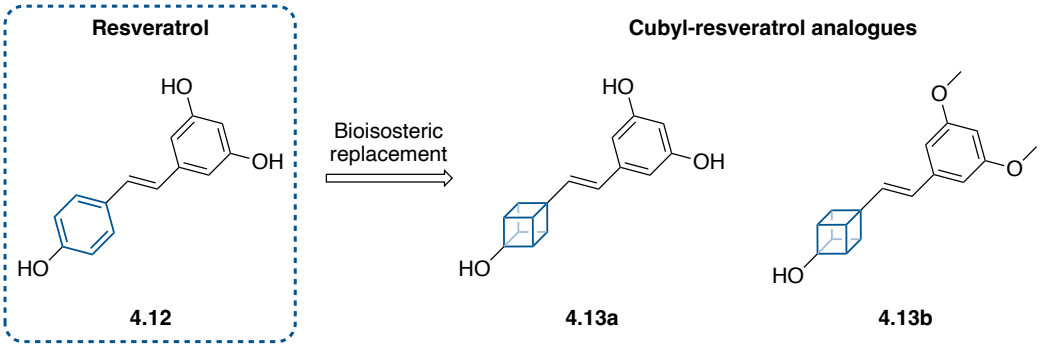

Figure 37: Resveratrol (**4.12**) and cubyl-resveratrol analogues **4.13a** and **4.13b.**

Recently, Goh and co-workers synthesised bicyclo[1.1.1]pentane-resveratrol and evaluated several of its pharmacokinetic properties against the parent aromatic compound.[281] In the first instance we opted to follow a similar synthetic strategy. The retrosynthetic analysis for the two cubyl-resveratrol analogues are outlined in Scheme

103. The target cubanol **4.13a** and **4.13b** would be revealed by hydrolysis of the acetate ester in **4.26a** and **4.26b**, with this moiety installed in an earlier step by the BV rearrangement of the cubyl methyl ketone (**4.17**). Given the ease of access of carbonyl functionalised cubanes, we planned to prepare the alkene moiety in **4.26a** and **4.26b** by a Wittig reaction with the cubyl aldehyde **4.20**. The intermediate **4.20** would be accessed using the same Weinreb amide strategy we previously employed in our optimisation of the BV reaction. However, as under our optimised BV conditions (*m*-CPBA (4 eq), $Sc(OTf)_3$ (10 mol%), $CHCl_3$ (0.1 M), 50 °C, 6h) both ketones and aldehydes are expected to rearrange, it would be necessary to introduce a protecting group at the start of synthetic sequence.

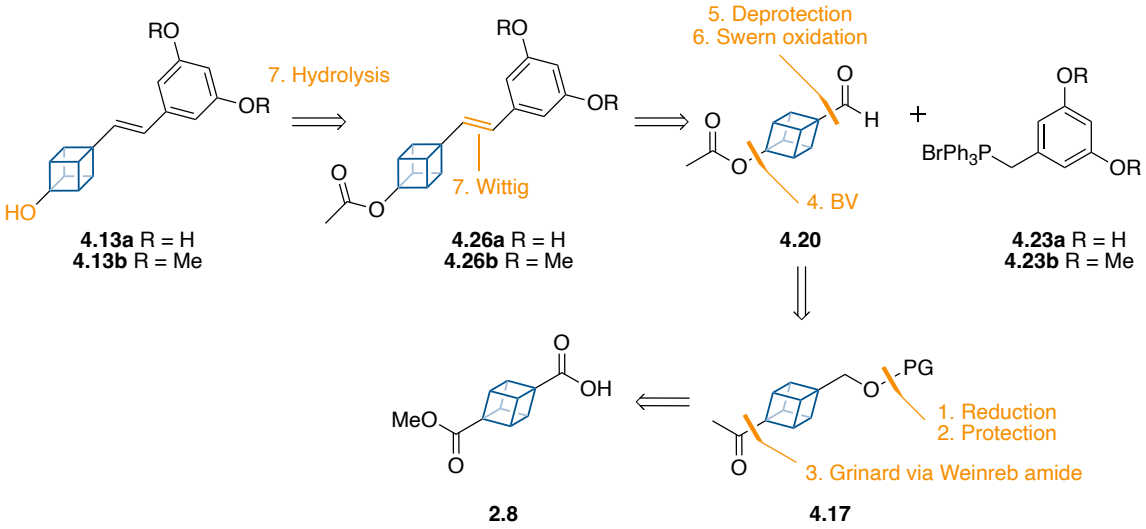

Scheme 103: Retrosynthetic analysis of cubyl-resveratrol analogues **4.13a** and **4.13b** via the BV rearrangement of the cubyl methyl ketone **4.17**. PG = *tert*-butyldimethylsilyl protecting group.

4.2.2.2 Synthesis of cubyl-resveratrol

The synthesis commenced with the reduction of the carboxylic acid moiety in the commercially available material 4-methoxycarbonylcubanecarboxylic acid (**2.8**). To ensure the selective reduction of the carboxylic acid over the methyl ester in **2.8,** we opted to reduce **2.8** (1 eq) in THF with borane-dimethyl sulfide (1.7 eq), which gave the primary alcohol **3.109** in a 98 % yield after 6 hours at room temperature (Scheme 104). For the protection of the primary alcohol we elected to follow Goh's approach of

performing a TBS-protection with *tert*-butyldimethylsilyl chloride, as we predicted the stability of the protecting group between bicyclo[1.1.1]pentane and cubane substrates would be comparable.[281] Protection of the primary alcohol **3.109** (1 eq) with *tert*-butyldimethylsilyl chloride (1.2 eq) in the presence of imidazole (2.5 eq) in DCM gave **4.14** in a 92 % yield, after purification by silica gel column chromatography (Scheme 104). With installation of the protecting group complete, the focus was now switched to the opposite side of the cubyl framework, synthesis of the methyl ketone moiety in **4.17**. The first step towards this goal was the hydrolysis of the methyl ester in **4.14** (1 eq) using lithium hydroxide in a solution of THF:MeOH:H_2O (0.5 M, ratio of 3:3:1), which gave rise to the carboxylic acid **4.15** in a yield of 93 %, after only 3 hours at room temperature. As the TBS protecting group is suspectable to cleave under acidic conditions, we chose to avoid synthesising the Weinreb amide via the acid chloride. Instead, we opted to access the Weinreb amide through a peptide coupling reaction.

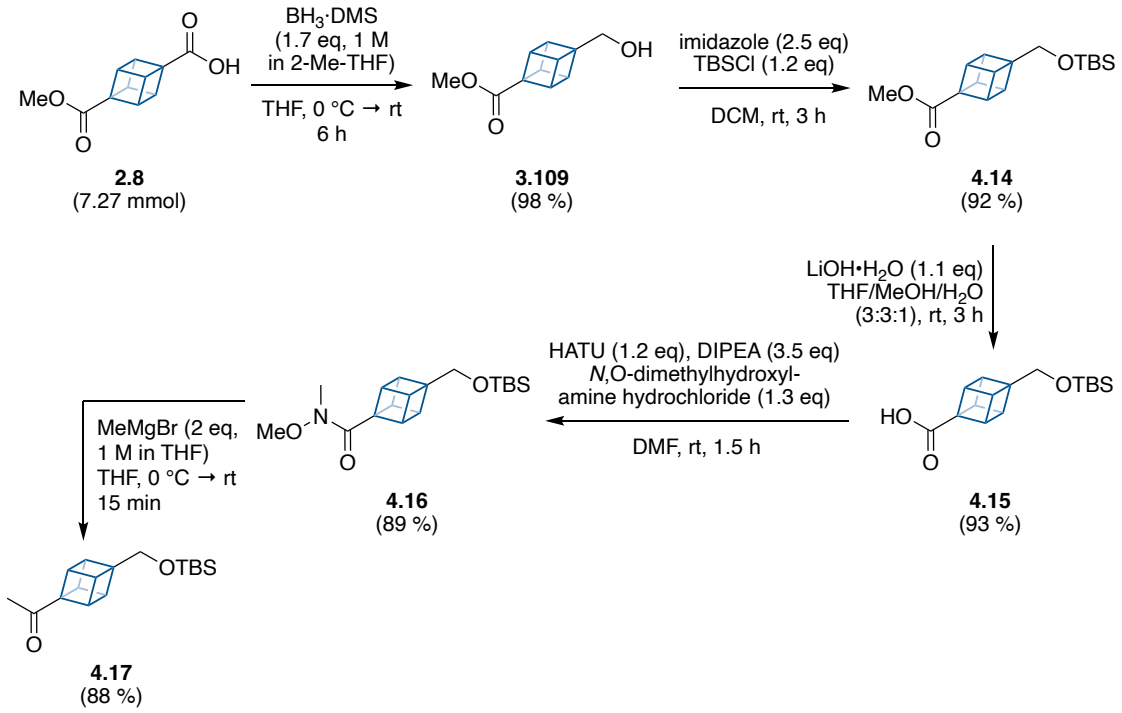

Scheme 104: Synthetic sequence towards precursor **4.17** for the BV rearrangement step.

TBS = tert-butyldimethylsilyl.

Treatment of carboxylic acid **4.15** (1 eq) with HATU (1.2), *N*,*N*-diisopropylethylamine (3.5 eq) and *N*,O-dimethylhydroxylamine hydrochloride (1.3 eq) in DMF at room temperature

provided the Weinreb amide **4.16** in an excellent yield of 89 %, after purification by silica gel column chromatography (Scheme 104). The cubyl methyl ketone **4.17** was then prepared by the addition of the commercially available Grignard reagent methylmagnesium bromide (2 eq, 1 M in THF) to a solution of the Weinreb amide **4.16** (1 eq) in THF, with full consumption of starting material observed by TLC analysis within 15 minutes at room temperature. The reaction mixture was quenched with a saturated aqueous solution of ammonium chloride and purified by silica gel column chromatography, affording the cubyl methyl ketone **4.17** in 88 % yield.

When submitting the ketone **4.17** under our optimised BV reaction conditions (*m*-CPBA (4 eq), $Sc(OTf)_3$ (10 mol%), $CHCl_3$ (0.1 M), 50 °C, 6 h) we observed by TLC analysis that the ketone was fully consumed within 3 hours, although more than one product was formed (Scheme 105, conditions A). Purification of by silica gel column chromatography allowed us to isolate two main compounds: (1) the desired product **4.18** in a 23 % isolated yield and (2) the deprotected alcohol **4.19** in a 35 % isolated yield. At first, we believed the low mass balance for this reaction might be attributed to the *in-situ* cleavage of the TBS-protecting group forming the cubyl methyl alcohol **4.19**, which has been reported to be fragile and can rearrange to the homocubyl system with ease (**4.19a**, Scheme 105).[105] However, of the fractions collected none included the homocubyl product **4.19a**.

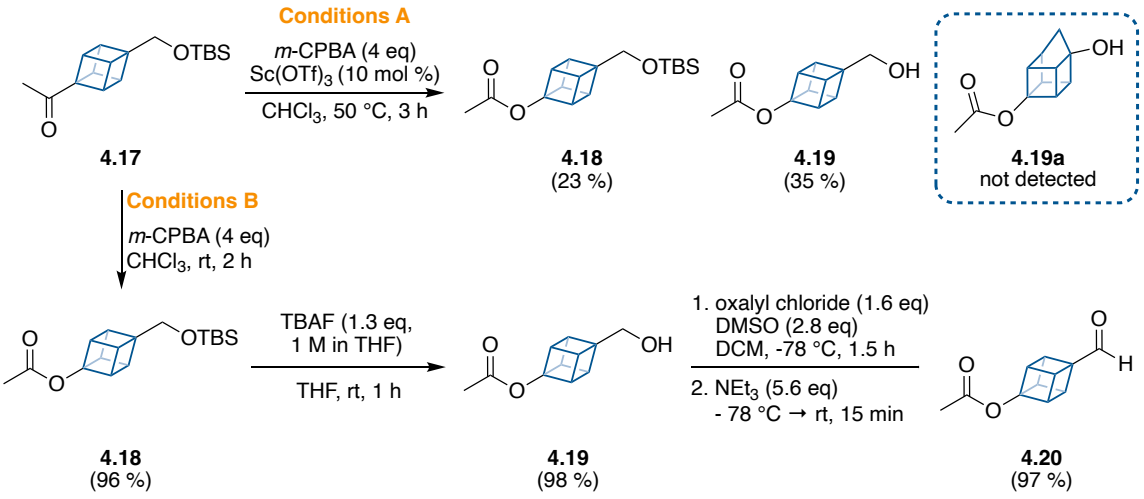

Scheme 105: BV rearrangement (A) under our optimised reaction conditions (B) under our adapted reaction conditions, towards precursor **4.20** for the Wittig reaction.

To avoid the cleavage of the TBS protecting group we opted to use milder BV reaction conditions. When treating **4.17** (1 eq) with *m*-CPBA (4 eq, ≤ 77 % purity) in $CHCl_3$ (0.1 M) at room temperature we observed fully consumption of the ketone within 2 hours, with no cleave of the TBS-protecting group visible by TLC analysis (Scheme 105, conditions B). After quenching the excess oxidant with aqueous sodium bisulfite and washing the organic layer with saturated bicarbonate solution, cubyl acetate **4.18** was obtained in a 98 % yield without requiring purification. As expected, the BV rearrangement of **4.17** was regioselective, with only migration of cubane observed by ^{1}H NMR analysis. Pleasingly, cleavage of the TBS-protecting group in **4.18** (1 eq) with TBAF (1.3 eq, 1 M in THF) at room temperature cleanly gave the product **4.19** in 1 hour, with a 98 % yield achieved after purification by silica gel column chromatography. Finally, a Swern oxidation of the primary alcohol **4.21** (1 eq) using oxalyl chloride (1.6 eq, 2 M in DCM), DMSO (2.8 eq) in DCM at -78 °C, followed by the addition of triethylamine (5.6 eq) gave the desired aldehyde **4.20** in a 97 % yield without requiring purification.

Our synthetic strategy outlined earlier in Scheme 103, next required us to synthesise the two phosphonium salts **4.23a** and **4.23b** for the proposed Wittig reactions (Scheme 106). For the phosphonium salt **4.23a** we began with the bromination of 3,5-dihydroxybenzyl alcohol (**4.21a**) via the Appel reaction. Bromination of the primary alcohol in **4.21a** (1 eq) on a 1 mmol scale, when using tetrabromomethane (1.2 eq) and triphenylphosphine oxide (1.2 eq), allowed desired product **4.22a** to be separated from the by-product triphenylphosphine oxide by silica gel column chromatography. Unfortunately, when scaling the bromination of **4.21a** to 10.7 mmol, the product **4.22a** and triphenylphosphine oxide were inseparable by silica gel column chromatography. As we suspected the product mixture containing triphenylphosphine oxide as an impurity would not drastically affect the next step, we directly treated the mixture with triphenylphosphine (1.4 eq respective to **4.21a**) in MeCN under refluxing conditions for 5 hours (Scheme 106). Based on reported protocols towards the synthesis of **4.23a** the salt should have crushed out of solution when the reaction mixture was cooled to 0 °C, with the precipitate collected by filtration and washed with ice-cold MeCN to remove impurities. In contrast to the literature **4.23a** did not precipitate at 0 °C when we performed the reaction, despite performing the reaction at a higher concentration. As

we discovered the product was soluble in ice-cold MeCN, we deviated from the literature purification protocol. We found the phosphonium salt **4.23a** could be purified by trituration with DCM, as the impurities triphenylphosphine and triphenylphosphine oxide were readily soluble in this solvent compared to **4.23a**, which allowed us to isolate the phosphonium salt in a 24 % yield over the two steps.

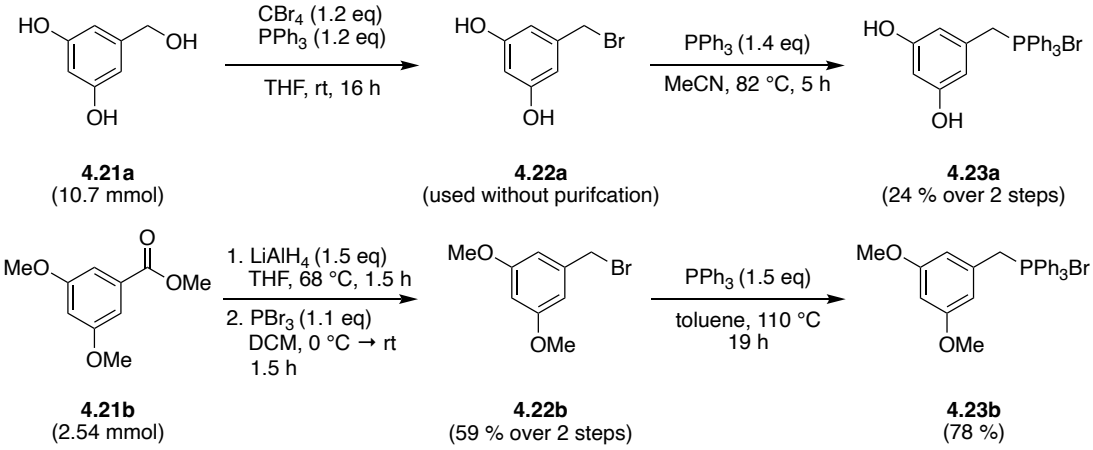

Scheme 106: Preparation of the phosphonium salts **4.23a-b** for the Wittig reactions.

The phosphonium salt **4.23b** was synthesised in a similar manner over three steps, beginning with the commercially available methyl 3,5-dimethoxybenzoate (**4.21b**) (Scheme 106). Reduction of the ester **4.21b** (1 eq) using lithium aluminium hydride (1.5 eq) in refluxing THF for 1.5 hours gave the primary alcohol in 98 % isolated yield, without the need for purification by silica gel column chromatography. Bromination of the alcohol (1 eq) with phosphorous tribromide (1.1 eq) in DCM at room temperature did not achieve full conversion to the bromide **4.22b** after 2 hours. Therefore, the crude was quickly passed through a short-pad of silica gel to isolate the desired bromide **4.22b** in 60 % yield. For the phosphine alkylation of **4.22b**, we chose to use toluene instead of MeCN, with the latter used in the synthesis of the previous phosphonium salt **4.23a**. This decision was based on the bromide **4.22b** having good solubility in toluene, with the expectation that precipitation of the desired product **4.23b** would be easier in toluene compared to the more polar solvent MeCN. When refluxing the bromide **4.22b** (1 eq) with triphenylphosphine (1.5 eq) in toluene, within 30 minutes a white precipitate began to form. The precipitate was filtered, washed with hexane and dried to give the

phosphonium salt **4.23b** in 78 % yield. Overall, **4.23b** was synthesised in 46 % yield over three steps, a higher overall yield than the over phosphonium salt **4.23a** (24 % yield over two steps).

With both the cubyl aldehyde **4.20** and the phosphonium salts **4.23a** and **4.23b** in hand, we next examined the Wittig reaction. To initially test the Wittig reaction, we opted to use the cubyl aldehyde **4.24** over **4.20**, as the former could be prepared quickly in two steps from the commercially available 4-methoxycarbonylcubanecarboxylic acid (**2.8**) compared to the latter which took 7 steps to synthesise and thus was a more valuable precursor. Following the protocol developed by Goh and co-workers, we prepared our ylide by treating a solution of the phosphonium salt **4.23b** (1.4 eq) in THF with 1.5 eq of lithium bis(trimethylsilyl)amide (1 M in THF) at -78 °C. After 30 minutes the aldehyde **4.24** (1 eq) was added and warmed to room temperature for 1.5 hours, yielding a 2:3 *E*/*Z* mixture of **4.25** in a 43 % yield after purification by silica gel column chromatography (Scheme 107). The *E*/*Z* ratio was determined by analysis of the coupling constants of the olefin protons in the ^{1}H NMR spectrum, with the major isomer having a coupling constant consistent with the geometry of the *Z*-isomer ($^{3}J_{Ha\text{-}Hb}$ = 11.7 Hz) and the minor consistent with the *E*-isomer ($^{3}J_{Ha\text{-}Hb}$ = 15.7 Hz).

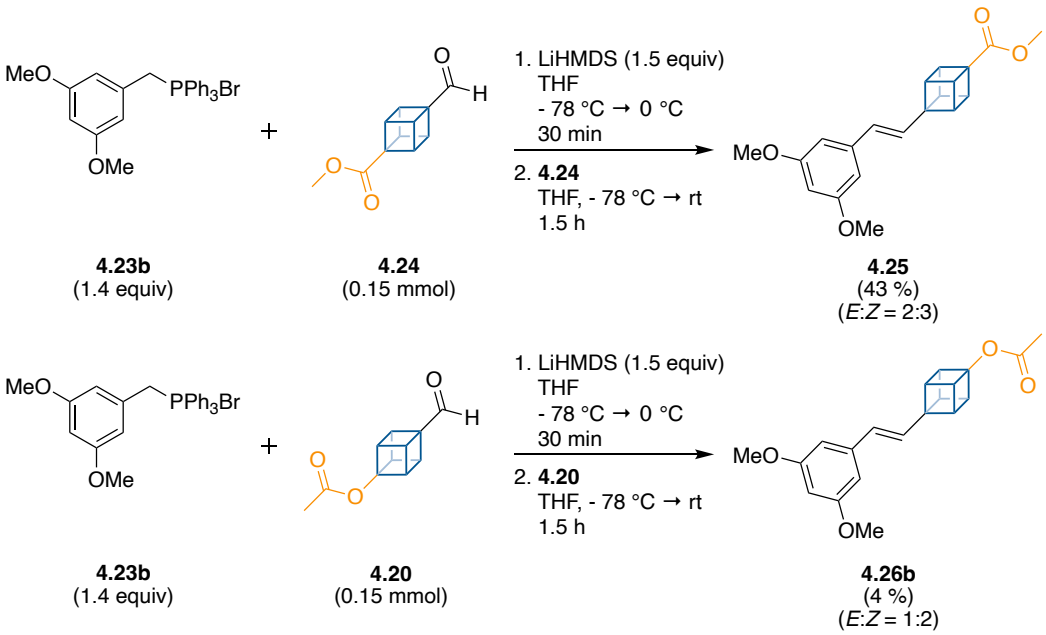

Scheme 107: Outcome of room temperature Wittig reaction for aldehyde **4.24** and **4.20** with phosphonium salt **4.23b**.

Having established conditions for the Wittig reaction with our test cubyl aldehyde **4.24**, these conditions were then applied to the cubyl aldehyde **4.20** included in our original retrosynthetic analysis of cubyl-resveratrol (Scheme 105 and 107). When employing the same conditions for the Wittig reaction using aldehyde **4.20** with phosphonium salt **4.23b**, the olefin **4.26b** was only isolated in trace quantities (4 % yield) in a *E*/*Z* ratio of 1:2 (Scheme 107). Initially we suspected the poor yield of **4.26b** was the result of aldehyde **4.20** being less reactive than aldehyde **4.24**. Therefore, to test this hypothesis we extended the reaction time at room temperature from 1.5 to 24 hours. Analysis of the crude mixture by ^{1}H NMR revealed both the product **4.26b** and the aldehyde **4.20** were not present, which led us to believe the acetate moiety in aldehyde **4.20** and/or the olefin product could be decomposing under the reaction conditions. To minimise decomposition, we first ensured the base (LiHMDS) was fully consumed before the addition of aldehyde **4.20** by using less equivalents of LiHMDS (1.1 eq) in respect to the phosphonium salt **4.23b** (1.4 eq). Secondly, following the addition of the aldehyde **4.20** the temperature was maintained at -78 °C. By implementing these changes, we observed full consumption of aldehyde **4.20** within 10 minutes (via TLC analysis). Purification of the crude by silica gel column chromatography afforded a 1:2 *E*/*Z* mixture of **4.26b** in a 71 % yield (Scheme 108). Attempts to convert **4.26b** directly to **4.26a** by ether cleavage with BBr_3 were unsuccessful, leading to decomposition of **4.26b**.

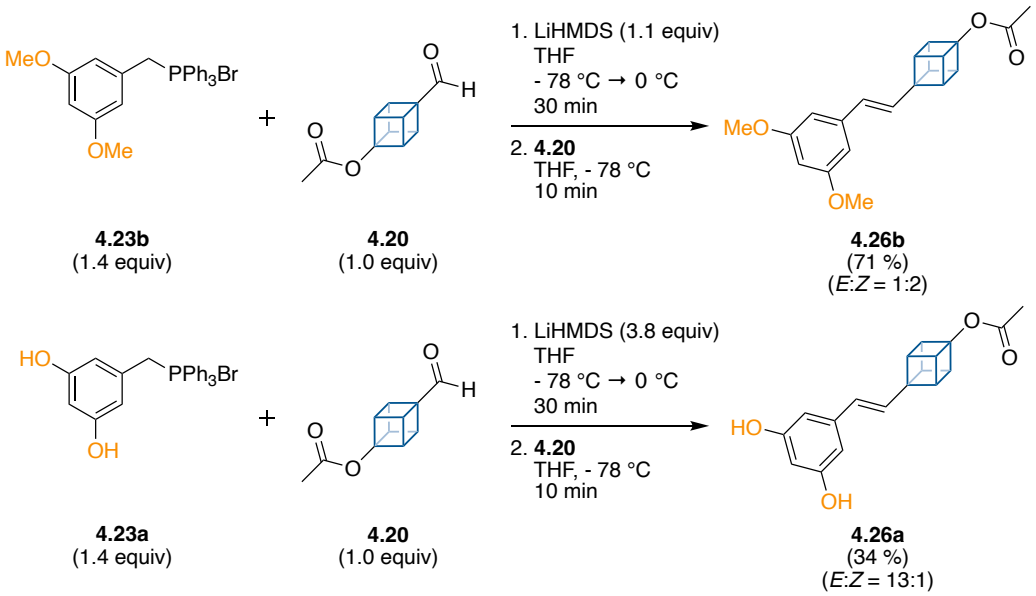

Scheme 108: Stereoselectivity of Wittig reaction between phosphonium salts **4.23a** and **4.23b** with cubyl aldehyde **4.20**.

The olefin **4.26a** was then synthesised by a Wittig reaction using the phosphonium salt **4.23a** (Scheme 108). Preparation of the ylide was achieved by treating **4.35a** with 3.8 equivalents of LiHMDS. Increased equivalents of base were necessary to account for the two phenol moieties in the phosphonium salt **4.23a** which would be deprotonated by LiHMDS. However, it is noteworthy that the equivalents of base used were still lower than the theoretical requirement of 4.2 equivalents required for full deprotonation of all three labile deprotonation sites in **4.23a**. Addition of the aldehyde **4.20** to the freshly prepared ylide at -78 °C resulted in full consumption of **4.20** within 20 minutes, affording a 13:1 *E*/*Z* mixture of **4.26a** in a 34 % yield after purification by silica gel column chromatography (Scheme 108). Interestingly, for the Wittig reaction between phosphonium salts **4.23a** and the aldehyde **4.20** we observed a complete reversal in the stereochemistry, compared to the Wittig reaction that used the phosphonium salts **4.23b** (**4.26a**: 13:1 *E*/*Z* and **4.26b**: 1:2 *E*/*Z*) (Scheme 108). Notably, the stereoselectivity and yield for **4.26a** are comparable to those reported for the BCP analogue of **4.26a** by Goh and co-workers (19:1 *E*/*Z*, 31 % yield).[281]

The final step in our synthetic sequence towards two cubanol analogues resveratrol (**4.13a** and **4.13b**), was to apply our hydrolysis conditions to cleave the cubyl acetate in **4.26a** and **4.26b** to unmask the desired cubanols (Scheme 109). Treating each of the acetates (0.04 mmol) with anhydrous HCl (0.5 mL, 1.25 M in ethanol) at room temperature facilitated the acid-catalysed transesterification, affording the cubanols **4.13a** and **4.13b** in an NMR yield of 38 % (13:1 *E*/*Z*) and 49 % (1:2 *E*/*Z*) respectively. Notably, the reaction time for the hydrolysis of **4.26a** and **4.26b** were considerably different, 3 hours verses 24 hours respectively. We attributed the longer reaction time required for cubyl acetate **4.26b** to it only being sparingly soluble in the HCl ethanol solution, with the acetate not fully dissolved 8 hours into the reaction. In the future, potentially using HCl in a solvent **4.26b** has greater solubility in would increase the reaction rate. As we wanted to observe the cubanol OH peak in the ^{1}H NMR analysis we opted to use DMSO-d_6 as the NMR solvent. Pleasingly, we found the cubanol moiety in the two cubyl-resveratrol analogues **4.13a** and **4.13b** were stable in DMSO-d_6 for over 48 hours at room temperature (20 °C), with successful recovery of the cubanols possible using the optimised work-up protocol previously discussed in **Section 4.2.1**.

Importantly, ^{1}H NMR analysis of the coupling constants of the olefin protons revealed that the ratio of the stereoisomers remained unchanged and no hydrohalogenation of the olefin was observed in the ^{1}H NMR analysis of the crude product under our hydrolysis reaction conditions. To the best of our knowledge, these are the first two examples of cubanols that have been isolated and characterised.

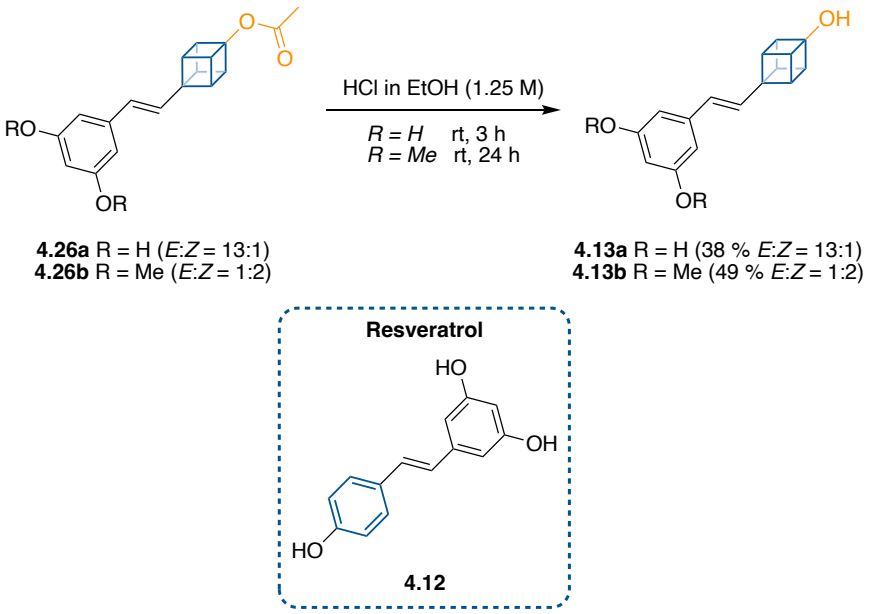

Scheme 109: Hydrolysis of cubyl acetates to prepare two cubanol analogues of the natural product resveratrol.

In conclusion, we have successfully demonstrated that the BV rearrangement of cubyl ketones serves as an effective synthetic strategy for accessing cubanols, illustrated by our synthesis of two cubanol analogues of the natural product resveratrol **4.12**. The first cubanol **4.13a** was synthesised in an overall yield of 8 % over 10 steps and the second **4.13b** was made in an overall yield of 21 % in 11 steps. Future work will explore the synthetic utility of cubanols as an intermediate towards the preparation more complex cubane-containing compounds, particularly the preparation of cubyl tamoxifen **1.19**.

5.1 General information

General information: ^{1}H, ^{13}C and ^{19}F NMR spectra were obtained on either a Bruker Avance 300 (300 MHz ^{1}H, 75 MHz ^{13}C), Bruker Avance 400 (400 MHz ^{1}H, 101 MHz ^{13}C, 376 MHz ^{19}F) or a Bruker Avance 500 (500 MHz ^{1}H, 126 MHz ^{13}C, 471 MHz ^{19}F) spectrometer at rt in the solvent stated. Chemical shifts (δ) for protons and carbons are reported in parts per million (ppm) relative to the residual deuterated solvent signal. Data has been reported as follows: chemical shift, multiplicity (s = singlet, brs = broad singlet, d = doublet, t = triplet, q = quartet, m = multiplet), coupling constants (Hz) and integration. High resolution mass spectrometry (HRMS, m/z) data was acquired at Cardiff University. ES/EI/CI HRMS data was collected on a Thermo Scientific Exactive GC machine with an orbitrap mass analyser or a Waters Xevo G2XS. TLC analysis was performed on commercially prepared 60 F_{254} silica gel plates and visualized by ultraviolet light (254 nm), followed by staining with 1% aqueous $KMnO_4$ solution. Flash chromatography used silica gel 60 (230-400 mesh) in the solvent system stated. IUPAC names were obtained using the ChemDraw service. Weighing was performed with a 4 or 5 decimal place balance. All reagents were used directly as obtained commercially unless otherwise noted. For reactions that required heating a heating mantle was used. The blue LED photoreactor (Aldrich® Micro Photochemical Reactor blue LED (ALDKIT001) were purchased from Merck. The irradiation vessel material was borosilicate glass and the distance of irradiation vessel from light source was 5 cm. Unless otherwise stated, all glassware was dried in a 125 °C oven before use and all reactions were performed under an atmosphere of nitrogen. All anhydrous solvents were purchased from Fisher Scientific, over molecular sieves in Acroseal bottles. All cubanol compounds were under an atmosphere of nitrogen and stored in the freezer (- 5 °C).

5.2 Chapter 2 experimental

5.2.1 Route 1: McMurry approach

5.2.1.1 Synthesis of (*Z*/*E*)-tamoxifen (1.1)

General scheme:

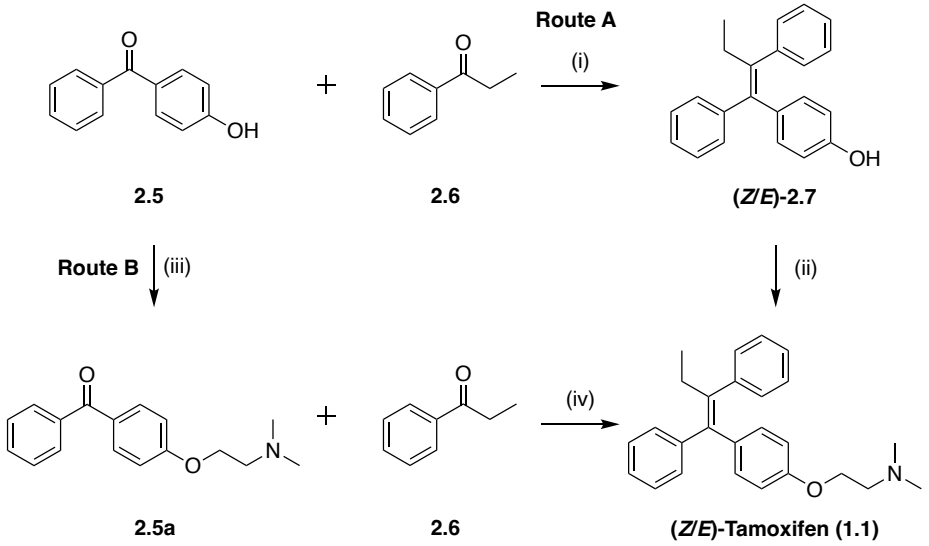

Conditions: (i) 1. Zn, $TiCl_4$, THF, reflux, 2 h; 2. **2.5**, **2.6**, THF, reflux, 2 h, 34 % (*Z*/*E* = 5:4); (ii) 1. K_2CO_3, acetone, 0 °C → rt; 2. 2-chloro-*N*,*N*'-dimethylethylamine hydrochloride, rt → 60 °C, 16 h, 35 % (*Z*/*E* = 1:1); (iii) 1. K_2CO_3, acetone, 0 °C → rt, 10 min; 2. 2-chloro-*N*,*N*'-dimethylethylamine hydrochloride, rt → 60 °C, 6 h, 48 %; (iv) 1. Zn, $TiCl_4$, THF, reflux, 2 h; 2. **2.5a**, **2.6**, THF, reflux, 2 h, 18 % (*Z*/*E* = 5:2).

Route A:

(*Z*/*E*)-4-(1,2-diphenylbut-1-en-1-yl)phenol (2.7)

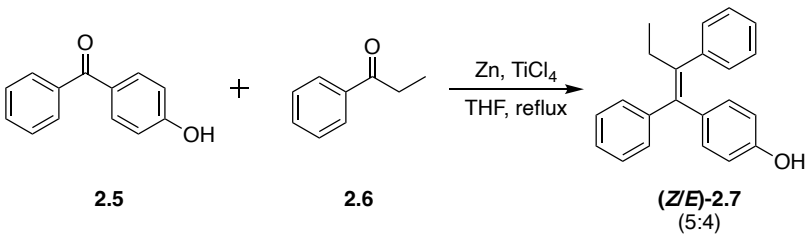

Titanium tetrachloride (2.95 mL, 5.9 equiv., 1 M in toluene) was added dropwise to a solution of zinc powder (440 mg, 13.3 equiv., 6.7 mmol) in anhydrous THF (5 mL) at -5 °C. After the addition, the mixture was heated at reflux for 2 hours. The reaction mixture was cooled to 0 °C and a solution of 4-hydroxybenzophenone (**2.5a**) (100 mg, 1.0 equiv.,

0.50 mmol) and propiophenone (**2.6**) (0.2 mL, 3.0 equiv., 1.5 mmol) in anhydrous THF (5 mL) was added dropwise. Following the addition the reaction mixture was heated to reflux for 2 hours. The mixture was cooled to 0 °C and quenched with sat. $brine_{(aq)}$ (5 mL) and filtered through a pad of celite. The aqueous layer was extracted with EtOAc (3 x 15 mL) and the combined organic layers were washed with sat. $brine_{(aq)}$ (10 mL), dried over $MgSO_4$, filtered and concentrated *in vacuo* to afford the crude (*Z*/*E* = 5:4). Purification by silica gel column chromatography (7:93 EtOAc/hexane) gave the title compound as a 5:4 ratio of (*Z*)-**2.7** : (*E*)-**2.7** (51 mg, 34 %) as a white solid.

^{1}H NMR (400 MHz, $CDCl_3$) *δ* 7.40 – 7.32 (m, 2H, *Z*-isomer), 7.32 – 7.23 (m, 4.1H, *Z*/*E*-isomer), 7.22 – 7.06 (m, 11.3H, *Z*/*E*-isomer), 7.06 – 6.94 (m, 2.7H, *Z*/*E*-isomer), 6.92 – 6.85 (m, 1.7H, *Z*/*E*-isomer), 6.85 – 6.78 (m, 1.7H, *Z*/*E*-isomer), 6.78 – 6.71 (m, 2H, *Z*-isomer), 6.52 – 6.43 (m, 2H, *Z*-isomer), 4.79 (s, 0.8H, *E*-isomer), 4.56 (s, 1H, *Z*-isomer), 2.57 – 2.41 (m, 3.8H, *Z*/*E*-isomer), 0.99 – 0.89 (m, 5.8H, *Z*/*E*-isomer); **^{13}C NMR** (101 MHz, $CDCl_3$) *δ* 154.3, 153.5, 143.9, 143.4, 142.5, 142.5, 142.1, 141.6, 138.4, 138.3, 136.4, 135.9, 132.2, 130.9, 129.8, 129.6, 128.3, 128.0, 127.9, 127.4, 126.7, 126.2, 125.8, 115.1, 114.4, 29.1, 13.7; **HRMS (ESI$^+$)** m/z: $[M+H]^+$ Calcd. for $C_{22}H_{21}O$ 301.1587; Found 301.1591. All spectroscopic data were in accordance with the literature.[282]

(*Z*/*E*)-Tamoxifen (1.1)

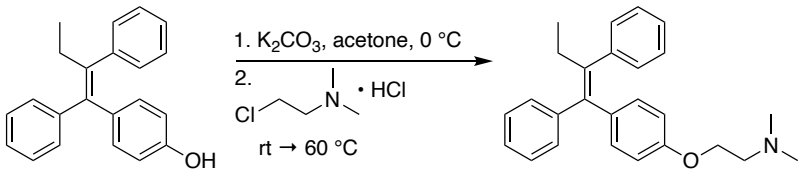

(*Z*/*E*)-2.7 (5:4)

(*Z*/*E*)-Tamoxifen (1.1) (1:1)

Anhydrous K_2CO_3 (47 mg, 2 equiv., 0.34 mmol) was added to a solution of (*Z*/*E*)-4-(1,2-diphenylbut-1-en-1-yl)phenol (**2.7**, *Z*/*E* ratio 5:4) (51 mg, 1 equiv., 0.17 mmol) in acetone (2.5 mL) at 0 °C. The reaction mixture was warmed to rt and after 5 minutes 2-chloro-*N*,*N*'-dimethylethylamine hydrochloride (30 mg, 1.2 equiv., 0.2 mmol) was added. Following the addition the mixture was heated to 60 °C for 16 hours. After cooling to rt the mixture was concentrated *in vacuo* to remove the acetone. 1 M $HCl_{(aq)}$ (3 mL) was added to the mixture and the aqueous layer was washed with EtOAc (10 mL), and the organic layer was extracted further with 1 M $HCl_{(aq)}$ (3 x 5 mL). The combined aqueous

layers were basified using 2.5 M $NaOH_{(aq)}$ to pH 9 and extracted with EtOAc (3 x 10 mL). The combined organic layers were washed with sat. $brine_{(aq)}$ (10 mL), dried over $MgSO_4$, filtered and concentrated *in vacuo* to afford the crude (*Z*/*E* = 1:1). Purification by silica gel column chromatography (3:7 EtOAc/hexane + 2% NEt_3) gave the title compound as a 1:1 ratio of (*Z*)-**1.1** : (*E*)-**1.1** (22 mg, 35 %) as a colourless oil.

^{1}H NMR (300 MHz, $CDCl_3$) δ 7.42 – 7.33 (m, 2H, *Z*-isomer), 7.32 – 7.24 (m, 3H, *Z*/*E*-isomer), 7.23 – 7.07 (m, 12H, *Z*/*E*-isomer), 7.06 – 6.98 (m, 3H, *Z*/*E*-isomer), 6.96 – 6.87 (m, 4H, *Z*/*E*-isomer), 6.84 – 6.75 (m, 2H, *Z*-isomer), 6.64 – 6.54 (m, 2H, *Z*-isomer), 4.12 (t, *J* = 5.8 Hz, 2H, *E*-isomer), 3.96 (t, *J* = 5.8 Hz, 2H, *Z*-isomer), 2.79 (t, *J* = 5.8 Hz, 2H, *E*-isomer), 2.69 (t, *J* = 5.8 Hz, 2H, *Z*-isomer), 2.61 – 2.43 (m, 4H, *Z*/*E*-isomer), 2.39 (s, 6H, *E*-isomer), 2.32 (s, 6H, *Z*-isomer), 1.02 – 0.90 (m, 6H, *Z*/*E*-isomer); **HRMS (ESI$^+$)** m/z: $[M+H]^+$ Calcd. for $C_{26}H_{30}NO$ 372.2322; Found 372.2325. All spectroscopic data were in accordance with the literature.[283]

Route B:

(4-(2-(Dimethylamino)ethoxy)phenyl)(phenyl)methanone (2.5a)

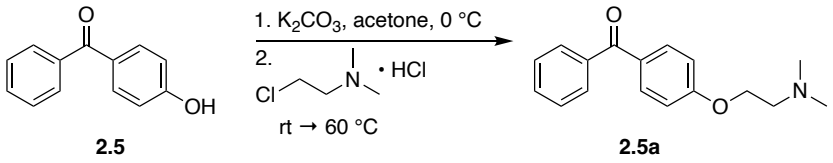

2.5 **2.5a**

Anhydrous K_2CO_3 (1.7 g, 2.4 equiv., 12 mmol) was added to a solution of 4-hydroxybenzophenone (**2.5**) (1 g, 1 equiv., 5 mmol) in acetone (20 mL) at 0 °C. The reaction mixture was warmed to rt and after 5 minutes 2-chloro-*N*,*N*'-dimethylethylamine hydrochloride (870 mg, 1.2 equiv., 6 mmol) was added. Following the addition the mixture was heated to 60 °C for 6 hours. After cooling to rt the mixture was concentrated *in vacuo* to remove the acetone. 1 M $HCl_{(aq)}$ (5 mL) was added to the mixture and the aqueous layer was washed with EtOAc (10 mL), and the organic layer was extracted further with 1 M $HCl_{(aq)}$ (3 x 10 mL). The combined aqueous layers were basified using 2.5 M $NaOH_{(aq)}$ to pH 9 and extracted with EtOAc (3 x 20 mL). The combined organic layers were washed with sat. $brine_{(aq)}$ (20 mL), dried over $MgSO_4$, filtered and concentrated *in vacuo* to afford the crude. Purification by silica gel column

chromatography (3:7 EtOAc/hexane → 3:7 EtOAc/hexane + 2% NEt_3 → 1:1 EtOAc/hexane + 2% NEt_3) gave the title compound **2.5a** (654 mg, 48 %) as a colourless oil.

^{1}H NMR (400 MHz, $CDCl_3$) δ 7.85 – 7.79 (m, 2H), 7.78 – 7.72 (m, 2H), 7.59 – 7.52 (m, 1H), 7.50 – 7.43 (m, 2H), 7.02 – 6.94 (m, 2H), 4.15 (t, *J* = 5.7 Hz, 2H), 2.76 (t, *J* = 5.7 Hz, 2H), 2.35 (s, 6H); **^{13}C NMR** (101 MHz, $CDCl_3$) δ 195.7, 162.7, 138.4, 132.7, 132.0, 130.3, 129.9, 128.3, 114.2, 66.4, 58.3, 46.1; **HRMS (ESI$^+$)** m/z: $[M+H]^+$ Calcd. for $C_{17}H_{20}NO_2$ 270.1489; Found 270.1495. All spectroscopic data were in accordance with the literature.[284]

(*Z*/*E*)-Tamoxifen (1.1)

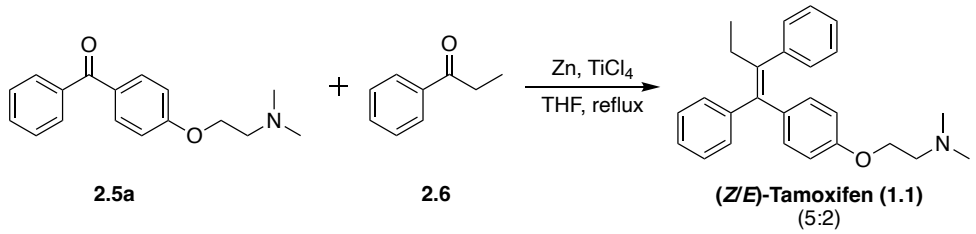

2.5a **2.6** **(*Z*/*E*)-Tamoxifen (1.1)** (5:2)

Titanium tetrachloride (2.1 mL, 5.9 equiv., 1 M in toluene) was added dropwise to a solution of zinc powder (304 mg, 13.3 equiv., 4.7 mmol) in anhydrous THF (5 mL) at -5 °C, followed by being heated at reflux for 2 hours. The reaction mixture was cooled to 0 °C and a solution of (4-(2-(dimethylamino)ethoxy)phenyl)(phenyl)methanone (**2.5a**) (94 mg, 1.0 equiv., 0.35 mmol) and propiophenone (**2.6**) (0.14 mL, 3.0 equiv., 1.1 mmol) in anhydrous THF (5 mL) was added dropwise. After the addition, the reaction mixture was heated to reflux for 2 hours. The mixture was cooled to 0 °C, quenched with sat. $brine_{(aq)}$ (5 mL) and filtered through a pad of celite. The aqueous layer was extracted with EtOAc (3 x 15 mL) and the combined organic layers were washed with sat. $brine_{(aq)}$ (10 mL), dried over $MgSO_4$, filtered and concentrated *in vacuo* to afford the crude (*Z*/*E* = 5:2). Purification by silica gel column chromatography (7:93 EtOAc/hexane) gave the title compound as a 5:2 ratio of (*Z*)-**1.1** : (*E*)-**1.1** (23 mg, 18 %) as a colourless oil.

^{1}H NMR (400 MHz, $CDCl_3$) δ 7.39 – 7.31 (m, 2H, *Z*-isomer), 7.31 – 7.21 (m, 4.3H, *Z*/*E*-isomer), 7.21 – 7.05 (m, 7.5H, *Z*/*E*-isomer), 7.02 – 6.96 (m, 0.9H, *Z*/*E*-isomer), 6.93 – 6.86 (m, 1.5H, *Z*/*E*-isomer), 6.79 – 6.73 (m, 2H, *Z*-isomer), 6.58 – 6.52 (m, 2H, *Z*-isomer), 4.10

(t, *J* = 5.8 Hz, 0.7H, *E*-isomer), 3.95 (t, *J* = 5.8 Hz, 2H, *Z*-isomer), 2.78 (t, *J* = 5.8 Hz, 0.7H, *E*-isomer), 2.68 (t, *J* = 5.8 Hz, 2H, *Z*-isomer), 2.55 – 2.41 (m, 2.6H, *Z*/*E*-isomer), 2.38 (s, 2.1H, *E*-isomer), 2.31 (s, 6H, *Z*-isomer), 0.97 – 0.90 (m, 4H, *Z*/*E*-isomer). **HRMS (ESI$^+$)** m/z: $[M+H]^+$ Calcd. for $C_{26}H_{30}NO$ 372.2322; Found 372.2325. All spectroscopic data were in accordance with the literature.[283]

5.2.1.2 Synthesis towards (*Z*/*E*)-cubyl-tamoxifen (1.18)

General scheme:

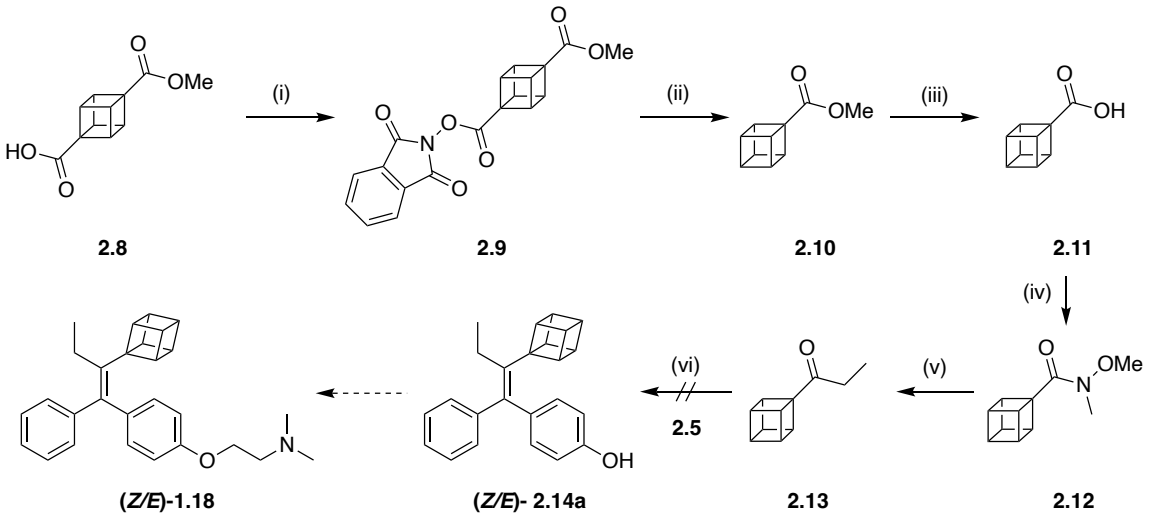

Conditions: (i) 1. oxalyl chloride (2 M in DCM), DMF, DCM, rt, 1.5 h; 2. *N*-hydroxyphthalimide, NEt_3, DCM, rt, 2 h, 94 %; (ii) hantzsch ester, $(Ir[dF(CF_3)ppy]_2(dtbpy))PF_6$, DCM, blue LED lights, rt, 5 h, 70 %; (iii) LiOH, THF:MeOH:H_2O in 3:1:1 ratio, rt, overnight, 81 %; (iv) 1. oxalyl chloride (2 M in DCM), DMF, DCM, rt, 1.5 h; 2. *N*,O-dimethylhydroxylamine hydrochloride, NEt_3, DCM, rt, 3 h, 55 %; (v) EtMgBr (0.9 M in THF), THF, -78 °C → rt, 30 min, 71 %; (vi) 1. Zn, $TiCl_4$, THF, reflux, 2 h; 2. **2.13**, **2.5**, THF, reflux, 2 h, 0 %.

1-(1,3-Dioxoisoindolin-2-yl) 4-methyl-cubane-1,4-dicarboxylate (2.9)

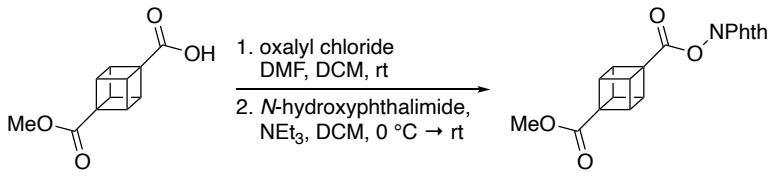

To a solution of 4-(methoxycarbonyl)cubane-1-carboxylic acid (**2.8**) (1.5 g, 1.0 equiv., 7.27 mmol) in anhydrous DCM (30 mL) was added oxalyl chloride (4.36 mL, 1.2 equiv., 2 M in DCM) at rt. Anhydrous DMF (55 mL, 10 mol%) was then added and the reaction

mixture was allowed to stir at rt for 1.5 hours. The mixture was concentrated *in vacuo* to afford the acid chloride as a light-yellow solid.

The acid chloride was dissolved in anhydrous DCM (15 mL) and added dropwise to a solution of *N*-hydroxyphthalimide (1.4 g, 1.2 equiv., 8.73 mmol) and triethylamine (2.53 mL, 2.5 equiv., 18.2 mmol) in anhydrous DCM (15 mL) at 0 °C. After the addition, the reaction mixture was warmed to rt and stirred for a further 2 hours. The reaction was quenched with sat. $NH_4Cl_{(aq)}$ (15 mL) and diluted with DCM (20 mL). The organic layer was washed with H_2O (4 x 20 mL), dried over $MgSO_4$, filtered, and concentrated *in vacuo* to give the crude. The beige solid was washed with hexane (3 x 5 mL) to afford the title compound **2.9** (2.39 g, 94 %) as a white solid.

^{1}H NMR (400 MHz, $CDCl_3$) δ = 7.94 – 7.85 (m, 2H), 7.85 – 7.75 (m, 2H), 4.52 – 4.44 (m, 3H), 4.41 – 4.33 (m, 3H), 3.73 (s, 3H); **^{13}C NMR** (101 MHz, $CDCl_3$) δ = 171.6, 167.0, 162.1, 134.9, 129.1, 124.1, 55.9, 53.1, 51.9, 47.8, 47.7; **HRMS (ESI$^+$)** m/z: $[M+H]^+$ Calcd. for $C_{19}H_{14}NO_6$ 352.0816; Found 352.0823. All spectroscopic data were in accordance with the literature.

Methyl-cubane-1-carboxylate (2.10)

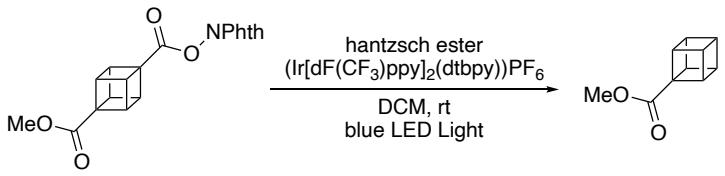

2.9 **2.10**

1-(1,3-Dioxoisoindolin-2-yl) 4-methyl-cubane-1,4-dicarboxylate (**2.9**) (500 mg, 1.0 equiv., 1.42 mmol), hantzsch ester (540 mg, 1.5 equiv., 0.09 mmol) and $(Ir[dF(CF_3)ppy]_2(dtbpy))PF_6$ (2.2 mg, 0.13 mol %) were combined in anhydrous DCM (15 mL). The mixture was irradiated with blue LED light at rt for 5 hours (Aldrich® micro photochemical reactor blue LED (ALDKIT001) was used as the blue LED light source). The reaction mixture was concentrated *in vacuo* and purification of the crude yellow solid by silica gel column chromatography (2:98 EtOAc/hexane) gave the title compound **2.10** (162 mg, 70 %) as a white solid.

^{1}H NMR (400 MHz, $CDCl_3$) δ 4.30 – 4.20 (m, 3H), 4.06 – 3.94 (m, 4H), 3.70 (s, 3H); **^{13}C NMR** (101 MHz, $CDCl_3$) δ 173.0, 55.8, 51.6, 49.6, 48.0, 45.3; **HRMS (ESI$^+$)** m/z: $[M+H]^+$ Calcd. for $C_{10}H_{11}O_2$ 163.0754; Found 163.0759. All spectroscopic data were in accordance with the literature.[141]

Cubane-1-carboxylic acid (2.11)

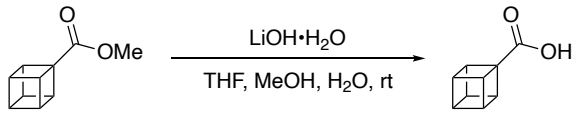

2.10 **2.11**

To a solution of methyl-cubane-1-carboxylate (**2.10**) (411 mg, 1.0 equiv., 2.53 mmol) in 3:3:1 ratio of THF:MeOH:H_2O (7.9 mL) was added lithium hydroxide monohydrate (266 mg, 2.5 equiv., 6.34 mmol) in one-portion at rt. The mixture was allowed to stir at rt overnight. The mixture was acidified with 2 M $HCl_{(aq)}$, and the aqueous layer was extracted with EtOAc (3 x 15 mL). The combined organic layers were washed sat. $brine_{(aq)}$ (15 mL), dried with anhydrous $MgSO_4$, filtered, and concentrated *in vacuo* to afford the crude. The solid was washed with hexane (3 x 5 mL) to afford the title compound **2.11** (305 mg, 81 %) as a white solid.

^{1}H NMR (400 MHz, $CDCl_3$) δ 11.69 (br s, 1H), 4.37 – 4.25 (m, 3H), 4.11 – 3.94 (m, 4H); **^{13}C NMR** (101 MHz, $CDCl_3$) δ 178.9, 55.6, 49.6, 48.0, 45.3; **HRMS (CI$^-$)** m/z: $[M-H]^-$ Calcd. for $C_9H_7O_2$ 147.0451; Found 147.0441. All spectroscopic data were in accordance with the literature.[285]

***N*-Methoxy-*N*-methylcubane-1-carboxamide (2.12)**

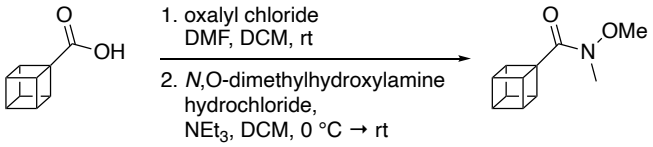

2.11 **2.12**

To a solution of cubane-1-carboxylic acid (**2.11**) (237 mg, 1.0 equiv., 1.60 mmol) in anhydrous DCM (5 mL) was added oxalyl chloride (0.96 mL, 1.2 equiv., 2 M in DCM) dropwise at rt. Anhydrous DMF (12 mL, 10 mol%) was then added and the reaction

mixture was allowed to stir at rt for 1.5 hours. The mixture was concentrated *in vacuo* to afford the acid chloride as a yellow solid.

The acid chloride was dissolved in anhydrous DCM (2 mL) and added dropwise to a solution of *N*,O-dimethylhydroxylamine hydrochloride (250 mg, 1.6 equiv., 2.56 mmol) and triethylamine (0.71 mL, 3.2 equiv., 2.07 mmol) in anhydrous DCM (2 mL) at 0 °C. The mixture was warmed to rt and stirred for 3 hours. The mixture was quenched with sat. $NH_4Cl_{(aq)}$ (5 mL) and diluted with DCM (10 mL). The organic layer was washed with 1 M $HCl_{(aq)}$ (10 mL), sat. $brine_{(aq)}$ (10 mL), dried with anhydrous $MgSO_4$, and concentrated *in vacuo* to afford the crude. Purification by silica gel column chromatography (1:3 EtOAc/petroleum ether) gave the title compound **2.12** (167 mg, 55 %) as a white solid.

^{1}H NMR (500 MHz, $CDCl_3$) δ 4.28 – 4.20 (m, 3H), 4.00 – 3.91 (m, 4H), 3.68 (s, 3H), 3.15 (s, 3H); **^{13}C NMR** (126 MHz, $CDCl_3$) δ 173.9, 61.6, 57.5, 49.7, 47.4, 45.1, 32.8; **HRMS (CI$^+$)** m/z: $[M+H]^+$ Calcd. for $C_{11}H_{14}O_2N$ 192.1019; Found 192.1017. All spectroscopic data were in accordance with the literature.[130]

1-(Cuban-1-yl)propan-1-one (2.13)

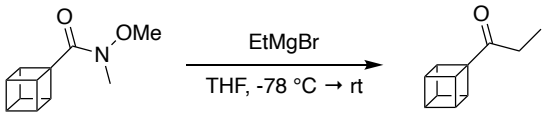

2.12 **2.13**

To a solution of *N*-methoxy-*N*-methylcubane-1-carboxamide (**2.12**) (54 mg, 1.0 equiv., 0.28 mmol) in anhydrous THF (2.5 mL) at -78 °C was added ethylmagnesium bromide (0.63 mL, 2.0 equiv., 0.9 M in THF) dropwise. The mixture was stirred at -78 °C for 30 minutes and then allowed to warm to rt. After 30 minutes, the mixture was quenched with 1 M $HCl_{(aq)}$ (5 mL) at 0 °C. The aqueous was extracted with Et_2O (3 x 10 mL) and the combined organic layers were washed with sat. $brine_{(aq)}$ (10 mL), dried with anhydrous $MgSO_4$, filtered, and concentrated *in vacuo* to afford the crude orange oil. Purification by silica gel column chromatography (01:99 EtOAc/petroleum ether) gave the title compound **2.13** (32 mg, 71 %) as a colourless oil.

^{1}H NMR (500 MHz, $CDCl_3$) δ 4.30 – 4.22 (m, 3H), 4.05 – 3.93 (m, 4H), 2.44 (q, *J* = 7.4 Hz, 2H), 1.06 (t, *J* = 7.4 Hz, 3H); **^{13}C NMR** (126 MHz, $CDCl_3$) δ 209.6, 63.2, 49.8, 48.1, 44.9, 31.0, 7.7; **HRMS (APCl$^+$)** m/z: $[M+H]^+$ Calcd. for $C_{11}H_{13}O$ 161.0961; Found 161.0966.

1-Chloro-9-ethylpentacyclo[4.3.0.0^{2,5}.0^{3,8}.0^{4,7}]nonan-9-ol (2.14b)

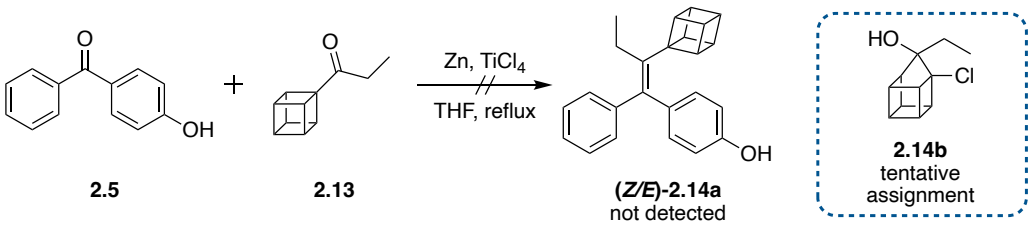

2.5 **2.13** (***Z/E***)**-2.14a** not detected **2.14b** tentative assignment

Titanium tetrachloride (1.1 mL, 5.8 equiv., 1 M in toluene) was added dropwise to a solution of zinc (167 mg, 13.4 equiv., 2.6 mmol) in anhydrous THF (2.5 mL) at -5 °C. After the addition, the mixture was heated at reflux for 2 hours. The reaction mixture was cooled to 0 °C and a solution of 4-hydroxybenzophenone (**2.5**) (100 mg, 1.0 equiv., 0.50 mmol) and 1-(cuban-1-yl)propan-1-one (**2.13**) (30 mg, 1 equiv., 0.19 mmol) in anhydrous THF (3 mL) was added dropwise. After the addition, the reaction mixture was heated to reflux for 2 hours. The mixture was cooled to 0 °C and quenched with sat. $brine_{(aq)}$ (5 mL) and filtered through a pad of celite. The aqueous layer was extracted with EtOAc (3 x 15 mL) and the combined organic layers were washed with sat. $brine_{(aq)}$ (10 mL), dried over $MgSO_4$, filtered and concentrated *in vacuo* to afford the crude. Purification by silica gel column chromatography (5:95 EtOAc/hexane) gave a compound we have tentatively assigned as **2.14b** (13 mg, 36 %) as a colourless oil.

^{1}H NMR (500 MHz, $CDCl_3$) δ 3.65 – 3.53 (m, 2H), 3.47 – 3.31 (m, 3H), 3.27 – 3.21 (m, 1H), 3.15 – 3.09 (m, 1H), 1.52 – 1.29 (m, 3H), 0.98 (t, *J* = 7.5 Hz, 3H); **^{13}C NMR** (126 MHz, $CDCl_3$) δ 93.2, 79.6, 51.5, 49.5, 46.1, 43.0, 41.1, 40.3, 39.7, 21.2, 8.8; **LRMS (Cl$^+$)** m/z: $[M-H]^+$ Calcd. for $C_{11}H_{12}ClO$ 195.06; Found 195.06.

5.2.2 Route 2: Organometallic approach

5.2.2.1 Synthesis towards (*Z*/*E*)-cubyl-tamoxifen (1.17)

General scheme:

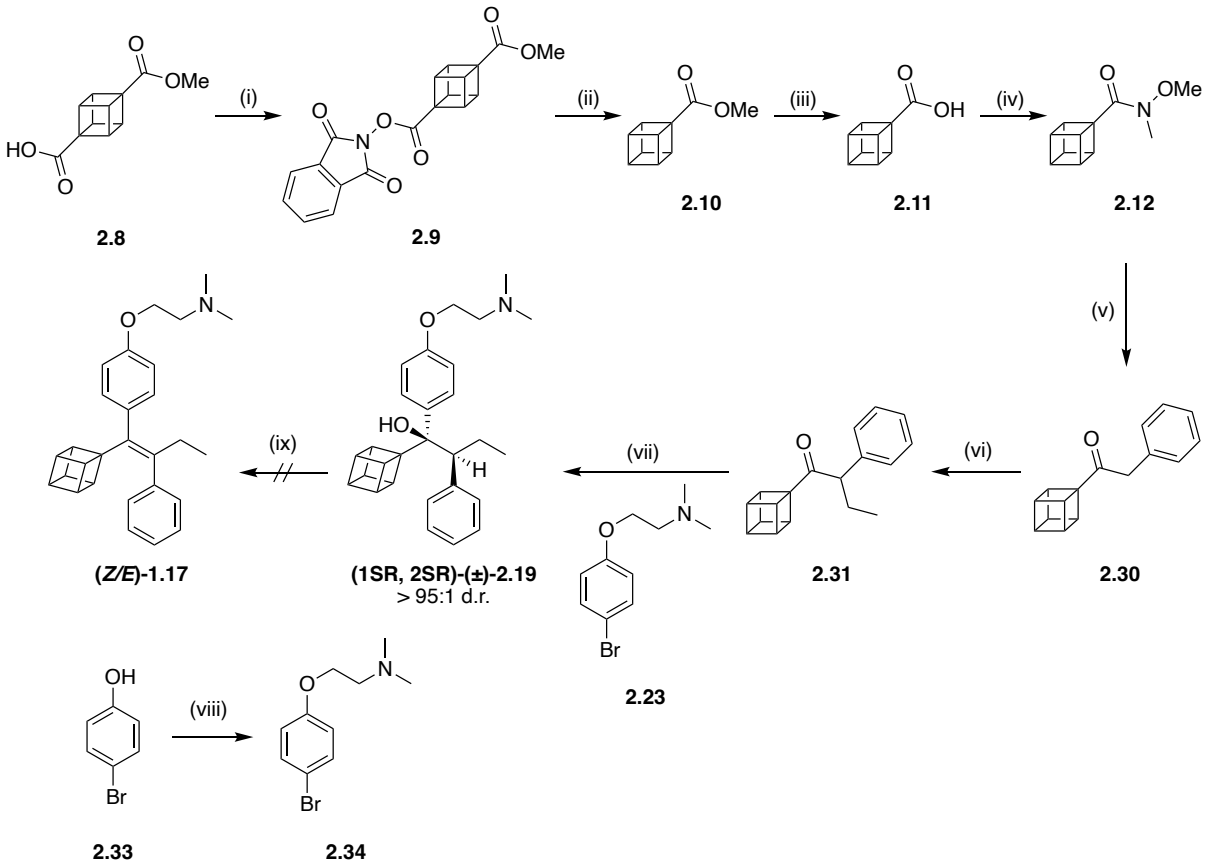

Conditions: (i) 1. oxalyl chloride (2 M in DCM), DMF, DCM, rt, 1.5 h; 2. *N*-hydroxyphthalimide, NEt_3, DCM, rt, 2 h, 94 %; (ii) hantzsch ester, $(Ir[dF(CF_3)ppy]_2(dtbpy))PF_6$, DCM, blue LED lights, rt, 5 h, 70 %; (iii) LiOH, THF:MeOH:H_2O in 3:1:1 ratio, rt, overnight, 81 %; (iv) 1. oxalyl chloride (2 M in DCM), DMF, DCM, rt, 1.5 h; 2. *N*,O-dimethylhydroxylamine hydrochloride, NEt_3, DCM, rt, 3 h, 55 %; (v) 1. Mg, I_2, benzyl bromide, Et_2O, 0 °C; 2. **2.12**, Et_2O 0 °C → rt, 30 min, 74 %; (vi) 1. K^tBuO, THF, 0 °C, 20 min; 2. EtI, 0 °C, 30 min, 72 %; (vii) 1. **2.34**, *n*-BuLi (1.6 M in hexanes), THF, -78 °C, 30 min; 2. **2.31**, THF, -78 °C → 0 °C, 20 min, 98 %; (viii) 4-bromophenol (**2.33**), K_2CO_3, 2-chloro-*N*,*N*'-dimethylethylamine hydrochloride, acetone, 0 °C, 8 h, 48 %; (ix) see **Table 36**.

*Experimental procedure and analytical data for **2.9**-**2.12** was previously described in **Section 5.2.1.2**.*

1-(Cuban-1-yl)-2-phenylethan-1-one (2.30)

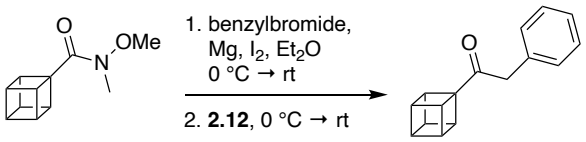

2.12 **2.30**

A mixture of magnesium turnings (140 mg, 3.81 equiv., 5.74 mmol) and iodine (41 mg, 0.11 equiv., 0.16 mmol) were stirred and heated to 40 °C for 5 minutes. The mixture was cooled to 0 °C and anhydrous diethyl ether (1 mL) was added. To the stirred solution, benzyl bromide (0.59 mL, 3.3 equiv., 5 mmol) was added dropwise over 20 minutes at 0 °C. The freshly prepared benzylmagnesium bromide (1 mL, 1.1 equiv., 1.6 M) was subsequently added dropwise to a solution of *N*-methoxy-*N*-methylcubane-1-carboxamide (**2.12**) (288 mg, 1.0 equiv., 1.51 mmol) in anhydrous Et_2O (1 mL) at 0 °C. The mixture was allowed to warm to rt and after 30 minutes was quenched with sat. $NH_4Cl_{(aq)}$ (5 mL). The aqueous was extracted with EtOAc (3 x 10 mL) and the combined organic layers were washed with sat. $brine_{(aq)}$ (10 mL), dried with anhydrous $MgSO_4$, filtered and concentrated *in vacuo* to afford the crude. Purification by silica gel column chromatography (04:96 EtOAc/hexane) gave the title compound **2.30** (249 mg, 74 %) as a colourless oil.

^{1}H NMR (500 MHz, $CDCl_3$) δ 7.34 – 7.27 (m, 2H), 7.26 – 7.21 (m, 3H), 4.21 – 4.14 (m, 3H), 3.97 – 3.92 (m, 1H), 3.92 – 3.88 (m, 3H), 3.73 (s, 2H); **^{13}C NMR** (126 MHz, $CDCl_3$) δ 206.0, 134.3, 129.7, 128.7, 127.0, 63.8, 50.2, 47.9, 46.1, 45.0; **HRMS (Cl$^+$)** m/z: $[M+H]^+$ Calcd. for $C_{16}H_{15}O$ 223.1117; Found 223.1117.

1-(Cuban-1-yl)-2-phenylbutan-1-one (2.31)

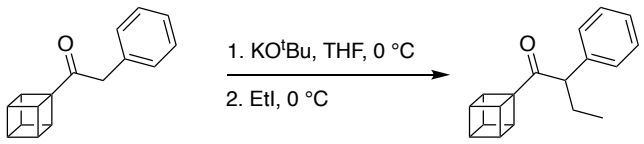

2.30 **2.31**

1-(Cuban-1-yl)-2-phenylethan-1-one (**2.30**) (249 mg, 1.0 equiv., 1.12 mmol) in anhydrous THF (1 mL) was added dropwise to a solution of potassium *tert*-butoxide (144 mg, 1.2 equiv., 1.28 mmol) in anhydrous THF (1 mL) at 0 °C. After 20 minutes ethyl iodide (90 μL,

1.0 equiv., 1.12 mmol) was added dropwise and stirred for 30 minutes at 0 °C. The reaction mixture was quenched with 1 M $HCl_{(aq)}$ (5 mL) and the aqueous layer was extracted with EtOAc (3 x 10 mL). The combined organic layers were washed with sat. $brine_{(aq)}$ (10 mL), dried with anhydrous $MgSO_4$, filtered and concentrated *in vacuo* to afford the crude. Purification by silica gel column chromatography (03:97 EtOAc/hexane) gave the title compound **2.31** (201 mg, 72 %) as a colourless oil.

^{1}H NMR (500 MHz, $CDCl_3$) δ 7.32 – 7.27 (m, 2H), 7.25 – 7.20 (m, 3H), 4.10 – 4.02 (m, 3H), 3.93 – 3.87 (m, 1H), 3.87 – 3.81 (m, 3H), 3.70 (t, *J* = 7.4 Hz, 1H), 2.12 – 2.00 (m, 1H), 1.79 – 1.66 (m, 1H), 0.83 (t, *J* = 7.4 Hz, 3H); **^{13}C NMR** (126 MHz, $CDCl_3$) δ 208.2, 139.2, 128.7, 128.7, 127.1, 64.1, 56.6, 50.3, 47.8, 44.9, 25.8, 12.3; **HRMS (ESI$^+$)** m/z: $[M+H]^+$ Calcd. for $C_{18}H_{19}O$ 251.1430; Found 251.1440.

2-(4-Bromophenoxy)-*N*,*N*-dimethylethan-1-amine (2.34)

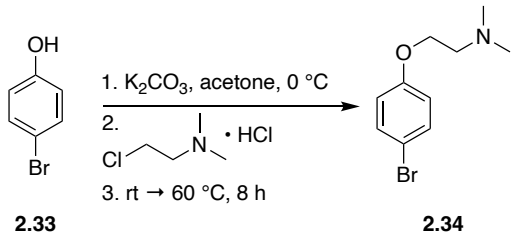

2.33 **2.34**

Anhydrous K_2CO_3 (1.76 g, 2.2 equiv., 12.7 mmol) was added to a solution of 4-bromophenol (**2.33**) (1 g, 1 equiv., 5.8 mmol) in acetone (20 mL) at 0 °C. The reaction mixture was warmed to room temperature and after 5 minutes 2-chloro-*N*,*N*'-dimethylethylamine hydrochloride (2.20 g, 2.6 equiv., 15.2 mmol) was added. Following the addition the mixture was heated to 60 °C for 8 hours. The mixture was concentrated *in vacuo* to remove the acetone. 1 M $HCl_{(aq)}$ (10 mL) was added to the mixture and the aqueous layer was washed with EtOAc (10 mL), and the organic layer was extracted further with 1 M $HCl_{(aq)}$ (3 x 5 mL). The combined aqueous layers were basified using 2.5 M $NaOH_{(aq)}$ to pH 9 and extracted with EtOAc (3 x 25 mL). The combined organic layers were washed with sat. $brine_{(aq)}$ (10 mL), dried over $MgSO_4$, filtered and concentrated *in vacuo* to afford compound **2.34** (675 mg, 48 %) as a light-yellow oil.

^{1}H NMR (500 MHz, $CDCl_3$) δ 7.44 – 7.31 (m, 2H), 6.90 – 6.70 (m, 2H), 4.02 (t, *J* = 5.7 Hz, 2H), 2.71 (t, *J* = 5.7 Hz, 2H), 2.33 (s, 6H); **^{13}C NMR** (126 MHz, $CDCl_3$) δ 158.1, 132.3,

116.5, 113.0, 66.4, 58.3, 46.0; **HRMS (CI$^+$)** m/z: $[M+H]^+$ Calcd. for $C_{10}H_{15}NO^{79}Br$ 244.0332; Found 244.0327.

(1SR, 2SR)-(±)-1-(Cuban-1-yl)-1-(4-(2-(dimethylamino)ethoxy)phenyl)-2-phenylbutan-1-ol (2.19)

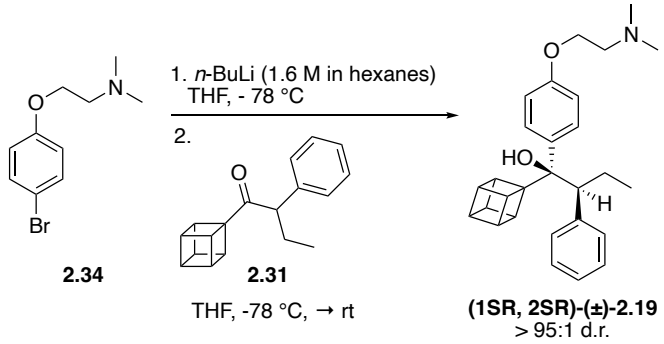

n-BuLi (0.27 mL, 1.5 equiv., 1.6 M in hexanes) was added dropwise to a solution of 2-(4-bromophenoxy)-*N*,*N*-dimethylethan-1-amine (**2.34**) (107 mg, 1.5 equiv., 0.44 mmol) in anhydrous THF (1 mL) at -78 °C. After 30 minutes a solution of 1-(cuban-1-yl)-2-phenylbutan-1-one (**2.31**) (62 mg, 1.0 equiv., 0.25 mmol) in anhydrous THF (1 mL) was added dropwise. The mixture was stirred at - 78 °C for 30 minutes and then warmed to 0 °C. After 20 minutes the mixture was quenched with H_2O (5 mL). The aqueous layer was extracted with EtOAc (3 x 10 mL) and the combined organic layers were washed with sat. $brine_{(aq)}$ (10 mL), dried with anhydrous $MgSO_4$, filtered, and concentrated *in vacuo* to afford the crude. Purification by silica gel column chromatography (1:4 EtOAc/hexane + 2% NEt_3) gave the title compound as a >95:1 ratio of (1SR, 2SR)-(±)-**2.19** : (1SR, 2RS)-(±)-**2.19** (101 mg, 98 %) as a colourless oil. Crystals were obtained by slow evaporation of DCM over 1 week and X-ray crystal structure collected by Dr Benson Kariuki (Cardiff University).

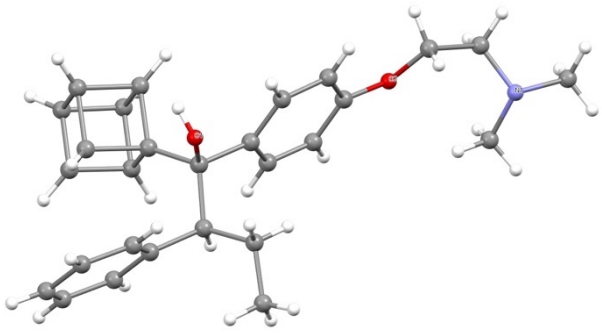

Major diastereomer* (1SR, 2SR)-(±)-**2.19**: **^{1}H NMR** (500 MHz, $CDCl_3$) δ 7.43 – 7.38 (m, 2H), 7.38 – 7.34 (m, 2H), 7.34 – 7.29 (m, 2H), 7.28 – 7.23 (m, 1H), 6.94 – 6.90 (m, 2H), 4.09 (t, *J* = 5.9 Hz, 2H), 3.72 – 3.66 (m, 1H), 3.52 – 3.45 (m, 3H), 3.34 – 3.27 (m, 3H), 3.09 (dd, *J* = 11.9, 3.2 Hz, 1H), 2.75 (t, *J* = 5.8 Hz, 2H), 2.35 (s, 6H),

1.81 – 1.67 (m, 1H), 1.34 – 1.23 (m, 1H), 0.53 (t, *J* = 7.4 Hz, 3H); **^{13}C NMR** (126 MHz, $CDCl_3$) δ 157.4, 141.7, 141.7, 136.0, 129.4, 128.5, 126.8, 125.9, 114.1, 78.8, 66.0, 64.8, 58.6, 54.5, 47.7, 47.1, 46.1, 43.6, 22.1, 12.2; **HRMS (ESI$^+$)** m/z: $[M+H]^+$ Calcd. for $C_{28}H_{34}NO_2$ 416.2584; Found 416.2589.

The diastereomeric ratio was determined by ^{1}H NMR integration of the -CH_2CH_2N $(CH_3)_2$** in the product*: Major diastereomer (1SR, 2SR)-(±)-**2.19** = 2.35 (s, 5.7H); minor diastereomer (1SR, 2RS)-(±)-**2.19** = 2.34 (s, 0.30H).[121, 153, 172]

(*Z*/*E*)-Cubyl-tamoxifen (1.17)

Table 36: Screening of elimination conditions

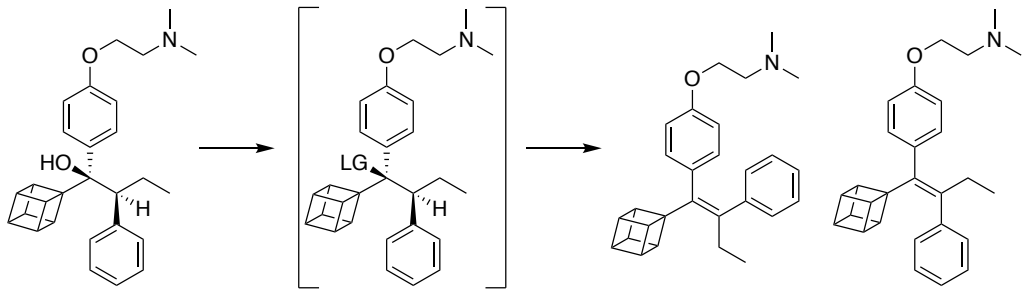

(1SR, 2SR)-(±)-2.19
> 95:1 d.r.
(0.06 mmol)

2.38a

(*Z*)-1.17

(*E*)-1.17

Entry	Conditions	Major product in crude[b]	Products detected in ESI$^+$ mass spec[c]
1	diphenyl phosphoryl chloride (2.0 eq), NaHMDS (3 eq), 1,4-dioxane (0.35 mL), 45 °C, 3 h	**2.19** + decom.	**2.19** $[M+H]^+$; **2.38a** $[M+H]^+$; **1.17** $[M+H]^+$
2	*n*-BuLi (1.1 eq, 1.6 M in hexanes), -78 °C → rt, THF (1 mL), then trifluoroacetic anhydride (2 eq), 1 h	**2.19** + decom.	**2.19** $[M+H]^+$; **2.38a** $[M+H]^+$; **1.17** $[M+H]^+$
3	PPh_3 (2 eq), CBr_4 (2 eq), DCM (2 mL), rt, 30 min	decom.	**2.19** $[M+H]^+$; **2.38a** $[M+H]^+$; **1.17** $[M+H]^+$
4[a]	PPh_3 (2 eq), CBr_4 (2 eq), pyridine (2.5 eq), DCM (2 mL), rt, 30 min	**2.19**	**2.19** $[M+H]^+$
5	PBr_3 (2 eq), Et_2O (0. 5 mL), -20 °C, 1.5 h	decom.	-
6	PBr_3 (2 eq), Et_2O (0. 2 mL), THF (0.5 mL), rt, 2 h	**2.19** + decom.	**2.19** $[M+H]^+$; **2.38a** $[M+H]^+$; **1.17** $[M+H]^+$
7	PBr_3 (2 eq), DCM (0.4 mL), rt	**2.19** + decom.	**2.19** $[M+H]^+$; **2.38a** $[M+H]^+$; **1.17** $[M+H]^+$
8	$SOCl_2$ (1.5 eq), DMF (0.1 eq), DCM (0.5 mL), 0 °C, 30 min	decomp.	-
9	DAST (1.1 eq), pyridine (2.5 eq), DCM (1 mL), -78 °C, 1 h	**2.19**	n.d
10	Conc. HCl (0.02 mL, 37 %), MeOH (0.2 mL), 68 °C, 30 mins	decomp.	**2.18** $[M+H]^+$; **1.17** $[M+H]^+$

[a] After an aqueous workup the crude was treated with K^{t}BuO (2 eq) in THF (0.5 mL) at rt for 1 hour, which resulted in decomposition. [b] via ^{1}H NMR analysis. [c] ***(Z/E)-1.17*** *could not be isolated. n.d = not determined; LG = leaving group; decom. = decomposition*

5.2.2.2 Synthesis of (*Z*/*E*)-tamoxifen (1.1)

General scheme:

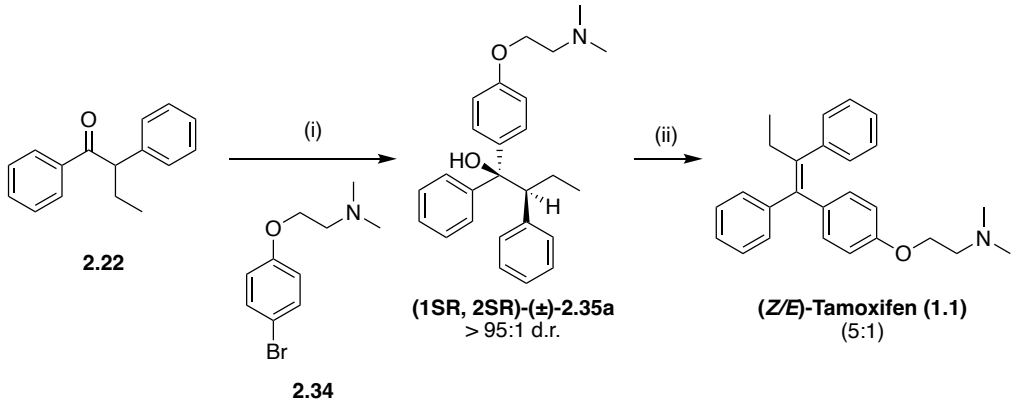

Conditions: (i) 1. **2.34**, *n*-BuLi (1.6 M in hexanes), THF, -78 °C, 30 min; 2. **2.22**, -78 °C → rt, 1 h, 52 %; (iii) *n*-BuLi (1.6 M in hexanes), THF, -78 °C → rt, 15 min; 2. trifluoroacetic anhydride, 4 h, 60 %.

(1SR, 2SR)-(±)-1-(4-(2-(Dimethylamino)ethoxy)phenyl)-1,2-diphenylbutan-1-ol (2.35a)

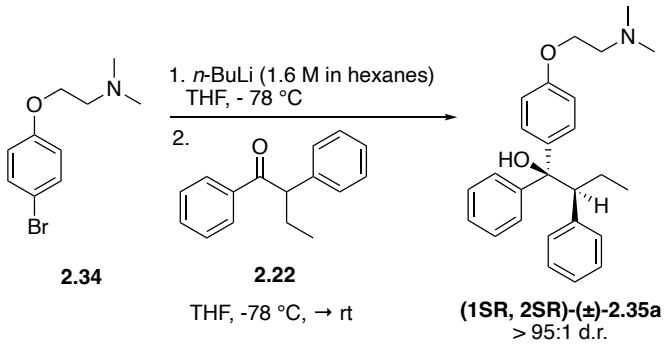

n-BuLi (0.84 mL, 1.1 equiv., 1.6 M in hexanes) was added dropwise to a solution of 2-(4-bromophenoxy)-*N,N*-dimethylethan-1-amine (**2.34**) (326 mg, 1.1 equiv., 1.34 mmol) in anhydrous THF (2 mL) at -78 °C. After 30 minutes a solution of 1,2-diphenylbutan-1-one (**2.22**) (272 mg, 1.0 equiv., 1.21 mmol) in anhydrous THF (1.5 mL) was added dropwise. The mixture was stirred at - 78 °C for 30 minutes and then warmed to rt. After 1 hour the mixture was quenched with H_2O (5 mL). The aqueous layer was extracted with EtOAc (3 x 10 mL) and the combined organic layers were washed with sat. $brine_{(aq)}$ (10 mL), dried with anhydrous $MgSO_4$, filtered, and concentrated *in vacuo* to afford the crude. Purification by silica gel column chromatography (20:80 EtOAc/hexane + 2% NEt_3) gave the title compound **(1SR, 2SR)-(±)-2.35a** (245 mg, 52 %) as a white solid.

Major diastereomer* (1SR, 2SR)-(±)-**2.35a**: **^{1}H NMR** (500 MHz, $CDCl_3$) δ 7.50 – 7.43 (m, 2H), 7.22 – 7.16 (m, 2H), 7.15 – 7.04 (m, 7H), 7.04 – 6.97 (m, 1H), 6.94 – 6.87 (m, 2H), 4.07 (t, J = 5.8 Hz, 2H), 3.55 (dd, J = 10.8, 3.5 Hz, 1H), 2.73 (t, J = 5.8 Hz, 2H), 2.43 (br s, 1H), 2.34 (s, 6H, 5.9H, major diastereoisomer), 2.29 (s, 0.1H, minor diastereoisomer), 1.89 – 1.75 (m, 2H), 0.76 (t, J = 7.3 Hz, 3H); **^{13}C NMR** (126 MHz, $CDCl_3$) δ 157.7, 146.8, 140.0, 138.4, 130.3, 127.8, 127.7, 127.6, 126.4, 126.2, 125.9, 114.2, 80.8, 66.1, 58.5, 56.5, 46.1, 23.5, 12.7; **HRMS (ESI^{+})** m/z: $[M+H]^{+}$ Calcd. for $C_{26}H_{32}NO_2$ 390.2433; Found 390.2439. All spectroscopic data were in accordance with the literature. [121, 153, 172]

The diastereomeric ratio was determined by ^{1}H NMR integration of the -CH_2CH_2N $(CH_3)_2$** in the product*: Major diastereomer (1SR, 2SR)-(±)-**2.35a** = 2.34 (s, 5.9H); minor diastereomer (1SR, 2RS)-(±)-**2.35b**= 2.29 (s, 0.1H). [121, 153, 172]

(*Z*/*E*)-Tamoxifen (1.1)

Table 37: Screening of elimination conditions

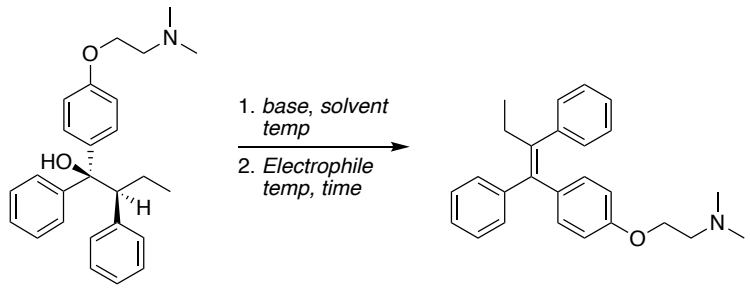

(1SR, 2SR)-(±)-2.35a
> 95:1 d.r.
(0.13 mmol)

(*Z*/*E*)-Tamoxifen
(1.1)

Entry	Base (eq)	Electrophile (eq)	Solvent	Temp / °C	Time / h	Yield of 1.1 / %[b]	(*Z*/*E*) ratio[c]
1	NaHMDS[d] (3)	diphenyl phosphoryl chloride (1.5)	1,4-dioxane	40	16	15	3:1
2	NaHMDS[d] (3)	tosyl chloride (1.5)	1,4-dioxane	40	16	0	-
3	NaH[e] (1.2)	tosyl chloride (1.2)	THF	40	5	0	-
4	pyridine (1.2)	tosyl chloride (1.2)	DCM	rt	5	0	-
5[a]	*n*-BuLi[f] (1.1)	TFAA[g] (2)	THF	-78 to rt	1	60	5:1
6	*n*-BuLi[f] (1.1)	Ac_2O[h] (2)	THF	-78 to rt	1	35	2:1
7	*n*-BuLi[f] (1.1)	benzyl chloride (2)	THF	-78 to rt	4	4	1:1
8	pyridine (20)	mesyl chloride (1.2)	pyridine	rt	5	3	2:1
9	DMAP (1.1)	Ac_2O[h] (2)	-	80	1.5	6	2:1
10	PPh_3 (2)	CBr_4 (2)	DCM	rt	16	67	3:1

[a]Optimised reaction conditions. [b]Isolated yield. [c]Determined by ^1H NMR. [d]Sodium bis(trimethylsilyl) amide (2 M in THF). [e]Sodium hydride (60 % dispersion in mineral oil). [f]n-Butyl lithium (1.6 M in hexanes). [g]Trifluoroacetic anhydride. [h]Acetic anhydride.

Full experimental details for the synthesis of (*Z*/*E*)-tamoxifen (**1.1**) using the conditions described in **Table 37, entry 5** (highest Z-selectivity in a good yield) are described below:

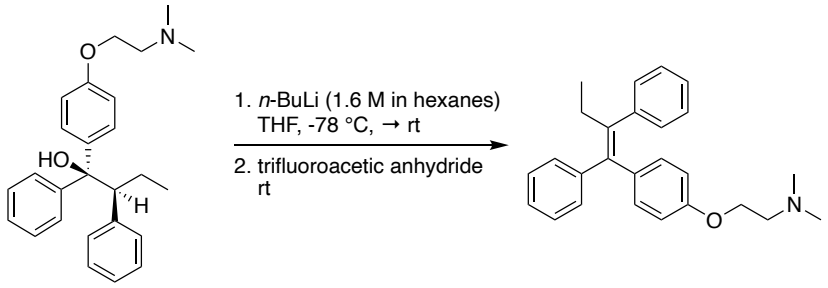

(1SR, 2SR)-(±)-2.35a
> 95:1 d.r.

(*Z*/*E*)-Tamoxifen (1.1)
(5:1)

n-BuLi (0.1 mL, 1.1 equiv., 1.6 M in hexanes) was added dropwise to a solution of (1SR, 2SR)-(±)-1-(4-(2-(dimethylamino)ethoxy)phenyl)-1,2-diphenylbutan-1-ol (**2.35a**, 50 mg, 1.0 equiv., 0.13 mmol) in anhydrous THF (1 mL) at - 78 °C. Following the addition the reaction mixture was warmed to rt and after 15 minutes trifluoroacetic anhydride (36 μL, 2.0 equiv., 0.26 mmol) was added. The reaction mixture was stirred at rt for 4 hours and quenched with H_2O (2 mL). The aqueous layer was extracted with EtOAc (3 x 5 mL) and the combined organic layers were washed with sat. $brine_{(aq)}$ (10 mL), dried with anhydrous $MgSO_4$, filtered, and concentrated *in vacuo* to afford the crude. Purification by silica gel column chromatography (3:7 EtOAc/hexane + 2% NEt_3) gave the title compound as a 5:1 ratio of (*Z*)-**1.1** : (*E*)-**1.1** (30 mg, 60 %) as a colourless oil.

^{1}H NMR (300 MHz, $CDCl_3$) δ 7.39 – 7.30 (m, 2.2H, *Z*/*E*-isomer), 7.30 – 7.21 (m, 3.5H, *Z*/*E*-isomer), 7.21 – 7.07 (m, 6.5H, *Z*/*E*-isomer), 7.02 – 6.96 (m, 0.6H, *E*-isomer), 6.93 – 6.85 (m, 0.8H, *E*-isomer), 6.81 – 6.73 (m, 2H, *Z*-isomer), 6.60 – 6.52 (m, 2H, *Z*-isomer), 4.09 (t, *J* = 5.8 Hz, 0.4H, *E*-isomer), 3.93 (t, *J* = 5.8 Hz, 2H, *Z*-isomer), 2.76 (t, *J* = 5.8 Hz, 0.4H, *E*-isomer), 2.66 (t, *J* = 5.8 Hz, 2H, *Z*-isomer), 2.58 – 2.39 (m, 2H, *Z*/*E*-isomer), 2.36 (s, 1.2H, *E*-isomer), 2.30 (s, 6H, *Z*-isomer), 0.98 – 0.89 (m, 3.6H, *Z*/*E*-isomer); **HRMS (ESI$^+$)** m/z: $[M+H]^+$ Calcd. for $C_{26}H_{30}NO$ 372.2322; Found 372.2325. All spectroscopic data were in accordance with the literature.[283, 286, 287]

5.2.2.3 Synthesis towards (*Z*/*E*)-cubyl-tamoxifen (1.18)

General scheme:

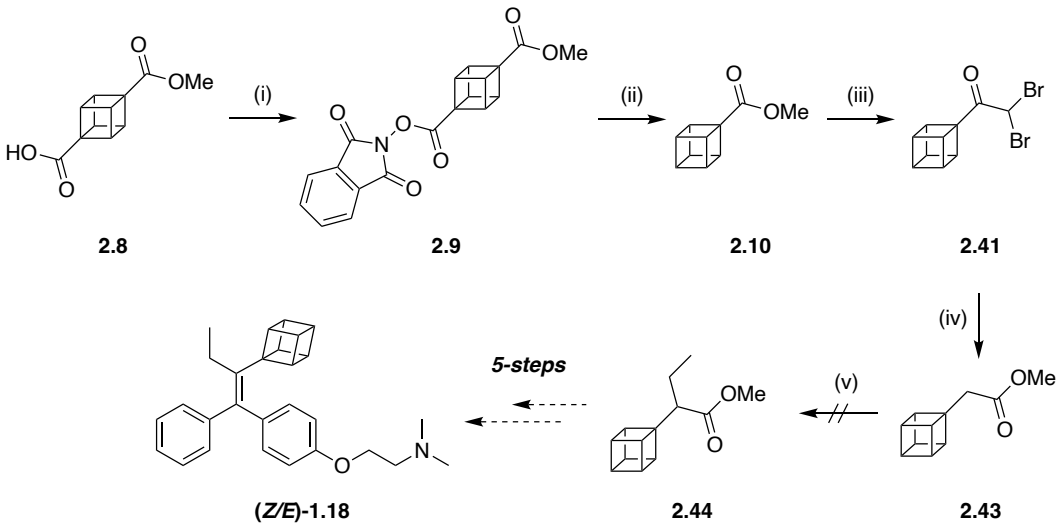

Conditions: (i) 1. oxalyl chloride (2 M in DCM), DMF, DCM, rt, 1.5 h; 2. *N*-hydroxyphthalimide, NEt_3, DCM, rt, 2 h, 94 %; (ii) hantzsch ester, $(Ir[dF(CF_3)ppy]_2(dtbpy))PF_6$, DCM, blue LED lights, rt, 5 h, 70 %; (iii) 1. **2.10**, THF, -78 °C, 5 min; 2. dibromomethane, -78 °C, 5 min; 3. *n*-BuLi (1.6 M in hexanes), 2,2,6,6-tetramethylpiperidine, THF, -78 °C, 20 min, 99 %; (iv) 1. LiHMDS (1 M in THF), THF, -78 °C, 30 min; 2. *n*-BuLi (1.6 M in hexanes), -78 °C → 0 °C, 30 min, 94 %; (v) LDA, THF -78 °C, 5 min; 2. EtI, - 78 °C, 30 min, 0 %.

*Experimental procedure and analytical data for **2.9**-**2.10** was previously described in* **Section 5.2.1.2**.

2,2-Dibromo-1-(cuban-1-yl)ethan-1-one (2.41)

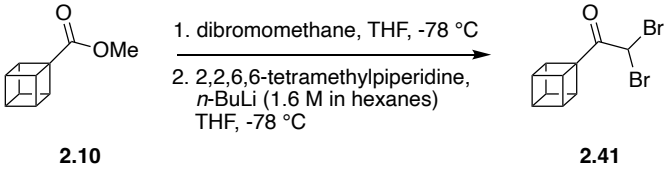

To a solution of 2,2,6,6-tetramethylpiperidine (0.26 mL, 2.0 equiv., 1.54 mmol) in anhydrous THF (2.6 mL), *n*-BuLi (0.87 mL, 1.8 equiv., 1.6 M) was added dropwise at -78 °C. Separately, **2.10** (124 mg, 1.0 equiv., 0.76 mmol) was dissolved in anhydrous THF (2.6 mL), when reaching -78 °C dibromomethane (0.1 mL, 1.9 equiv., 1.44 mmol) was added dropwise. After 5 minutes this reaction mixture was added to the freshly prepared lithium tetramethylpiperidide solution at -78 °C. The reaction mixture was stirred at -78 °C for 20 minutes and poured into a solution of 1 M $HCl_{(aq)}$ (15 mL) at 0 °C. The aqueous layer was extracted with EtOAc (3 x 15 mL) and the combined organic

layers were washed with sat. brine$_{(aq)}$ (10 mL), dried with anhydrous $MgSO_4$, filtered, and concentrated *in vacuo* to afford the title compound **2.41** (234 mg, 99 %) as an orange oil.

^{1}H NMR (300 MHz, $CDCl_3$) δ 5.90 (s, 1H), 4.52 – 4.41 (m, 3H), 4.14 – 4.05 (m, 3H), 4.05 – 3.99 (m, 1H). **HRMS (EI$^+$)** m/z: $[M]^{+\bullet}$ Calcd. for $C_{10}H_8{}^{79}Br_2O$ 301.8936; Found 301.8937. All spectroscopic data were in accordance with the literature.[174]

Methyl 2-(cuban-1-yl)acetate (2.43)

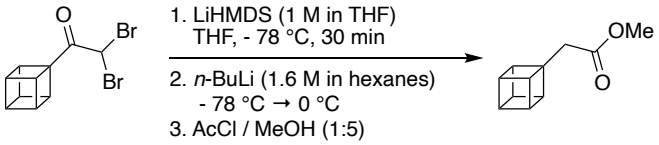

2.41 **2.43**

Lithium bis(trimethylsilyl)amide (0.85 mL, 1.1 equiv., 1.0 M in THF) was added dropwise to a solution of 2,2-dibromo-1-(cuban-1-yl)ethan-1-one (**2.41**) (234 mg, 1.0 equiv., 0.77 mmol) in anhydrous THF (3 mL) at -78 °C. After 30 minutes *n*-BuLi (1.0 mL, 2.1 equiv., 1.6 M in hexanes) was added dropwise and warmed to -50 °C for 20 minutes. The reaction mixture was then warmed to 0 °C and stirred at this temperature for 20 minutes before being quenched with acidic methanol (6 mL) at 0 °C (acidic methanol was prepared by slow addition of acetyl chloride to ice-cooled dry methanol (1:5 ratio/vol). The aqueous layer was extracted with Et_2O (3 x 10 mL) and the combined organic layers were washed with sat. brine$_{(aq)}$ (10 mL), dried with anhydrous $MgSO_4$, filtered, and concentrated *in vacuo* to afford the crude as a brown oil. Purification by silica gel column chromatography (3:7 DCM/hexane) gave the title compound **2.43** (128 mg, 94 %) as a colourless oil.

^{1}H NMR (400 MHz, $CDCl_3$) δ 4.05 – 3.99 (m, 1H), 3.95 – 3.87 (m, 3H), 3.87 – 3.80 (m, 3H), 3.66 (s, 3H), 2.64 (s, 2H); **^{13}C NMR** (101 MHz, $CDCl_3$) δ 172.1, 54.5, 51.5, 49.1, 48.5, 44.5, 38.3; **HRMS (EI$^+$)** m/z: $[M]^{+\bullet}$ Calcd. for $C_{11}H_{12}O_2$ 176.0832; Found 176.0828.

5.2.3 Route 3: Cross-coupling approach

5.2.3.1 Synthesis of methyl (*Z*)-4-(1-(4-methoxyphenyl)-2-phenylbut-1-en-1-yl)cubane-1-carboxylate (2.65)

General scheme:

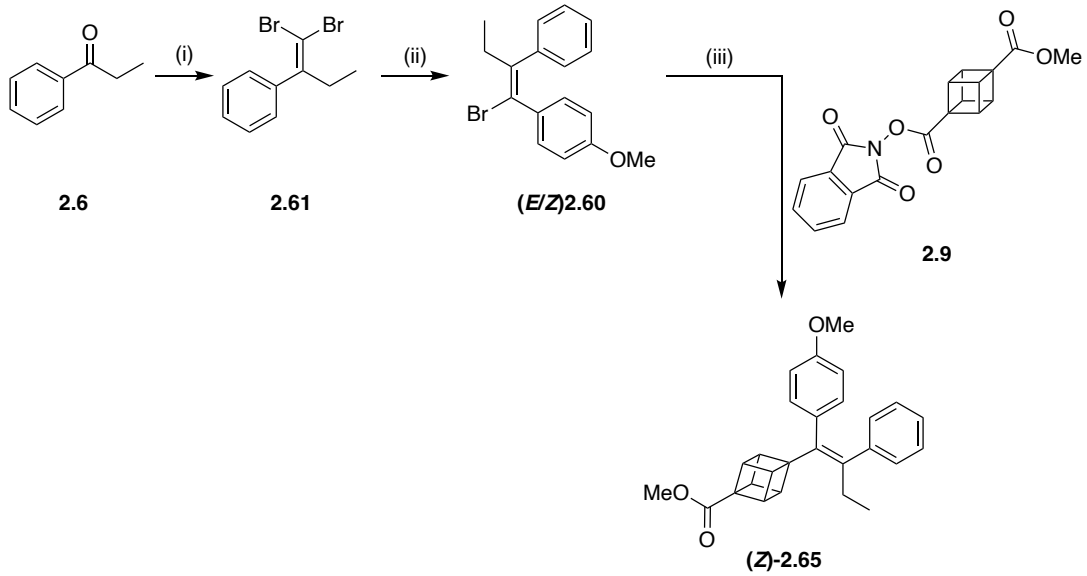

Conditions: (i) PPh_3, CBr_4, toluene, 110 °C, 24 h, 61 %; (ii) 4-methoxyphenyl boronic acid, bis(dibenzylideneacetone) palladium, tri(2-furyl)- phosphine, cesium carbonate, THF:H_20 (3:1), 70 °C, 6 h, 36 %; iii) 1. Mg, I_2, LiCl, THF, rt → 60 °C, 4 h; 2. **2.9**, $NiCl_2$-glyme, dimethyl 2,2'-bipyridine-4,4'-dicarboxylate, DMF, rt, 2 h, 2 %.

(1,1-Dibromobut-1-en-2-yl)benzene (2.61)

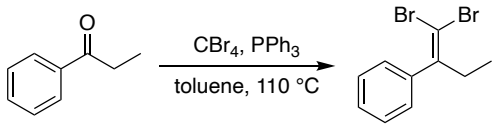

Triphenylphosphine (1.57 g, 4.0 equiv., 6 mmol) and tetrabromomethane (1.0 g, 2.0 equiv., 3 mmol) were stirred in anhydrous toluene (11.5 mL) at 110 °C for 15 minutes. The reaction mixture was cooled to rt and propiophenone (**2.6**, 0.2 mL, 1.0 equiv., 1.5 mmol) in anhydrous toluene (2 mL) was added dropwise. After the addition the reaction mixture was heated at 110 °C for 24 hours. After cooling the mixture was added to hexane (20 mL), filtered through a pad of celite, and concentrated *in vacuo* to afford the crude. Purification by silica gel column chromatography (100 % hexane) gave the title compound **2.61** (260 mg, 61 %) as a colourless oil.

^{1}H NMR (500 MHz, $CDCl_3$) δ 7.42 – 7.35 (m, 2H), 7.35 – 7.30 (m, 1H), 7.21 – 7.13 (m, 2H), 2.61 (q, *J* = 7.5 Hz, 2H), 0.99 (t, *J* = 7.5 Hz, 3H); **^{13}C NMR** (126 MHz, $CDCl_3$) δ 149.0, 141.0, 128.5, 128.0, 127.8, 87.7, 32.9, 11.5; **HRMS (EI$^+$)** m/z: $[M]^{+\bullet}$ Calcd. for $C_{10}H_{10}{}^{79}Br_2$ 287.9144; Found 287.9144. All spectroscopic data were in accordance with the literature.[288]

(*Z*/*E*)-1-(1-Bromo-2-phenylbut-1-en-1-yl)-4-methoxybenzene (2.60)

Table 38: Screening of Suzuki-Miyaura cross-coupling conditions

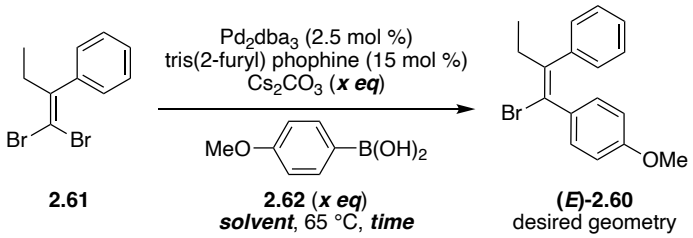

2.61 | **2.62** (***x eq***) ***solvent***, 65 °C, ***time*** | (***E***)-**2.60** desired geometry

Entry	2.61 (mmol)	2.62 (eq)	Base (eq)	Solvent (ratio/concentration)	Time / h	Ratio of *Z*/*E*-**2.47**[a]	(*Z*/*E*)-2.60 yield[a] / %
1	0.35	1.05	2	THF: H_2O (7:3/0.15 M)	16	2:1	28
2	0.35	1.05	2	Et_2O:THF:H_2O (2:1:1/ 0.1 M)	16	2:1	32
3	0.35	1.05	2	Et_2O:THF:H_2O (2:1:1/ 0.01 M)	5	3:2	26
4	0.35	1.05	2	THF:H_2O (3:1/0.1 M)	5	3:2	27
5	0.35	1.3	2	THF:H_2O (3:1/0.1 M)	16	2:1	28
6	0.35	1.3[b]	2	THF:H_2O (3:1/0.1 M)	16[c]	2:1	23
7	0.35	1.05	1.1	THF:H_2O (3:1/0.1 M)	5	3:2	27
8[d]	3.3	1.05	1.1	THF:H_2O (3:1/0.1 M)	6	3:2	36

[a] after silica-gel chromatography. [b] dropwise addition over 40 minutes. [c] reaction at 45 °C. [d] conditions chosen when repeating the cross-coupling.

Full experimental details for the synthesis of **(*Z*/*E*)-2.60** using the conditions described in **Table 38, Entry 8** are described below:

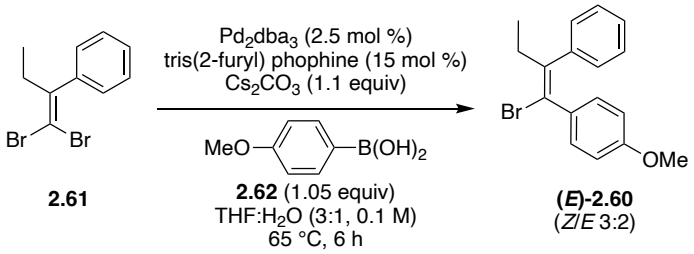

2.61

2.62 (1.05 equiv)
THF:H_2O (3:1, 0.1 M)
65 °C, 6 h

(*E*)-2.60
(*Z*/*E* 3:2)

A Schlenk tube was charged with (1,1-dibromobut-1-en-2-yl)benzene (**2.61**) (958 mg, 1.0 equiv., 3.3 mmol), 4-methoxyphenyl boronic acid (**2.62**, 527 mg, 1.05 equiv., 3.5 mmol), bis(dibenzylideneacetone) palladium (95 mg, 5 mol %), tri(2-furyl)- phosphine (115 mg, 15 mol %). Degassed THF (15 mL) was added, followed by a degassed solution of cesium carbonate (1.2 g, 1.1 equiv., 3.6 mmol) in H_2O (5 mL). The mixture was heated at 70 °C for 6 hours. The reaction mixture was cooled to rt and diluted with H_2O (5 mL) and the aqueous layer was extracted with EtOAc (3 x 15 mL). The combined organic layers were washed with sat. $brine_{(aq)}$ (10 mL), dried over $MgSO_4$, filtered and concentrated *in vacuo* to afford the crude. Purification by silica gel column chromatography (3:7 toluene/hexane) gave the title compound as a 3:2 ratio of **(*Z*)-2.60** : **(*E*)-2.60** (377 mg, 36 %) as a yellow solid.

^{1}H NMR (300 MHz, $CDCl_3$) δ 7.46 – 7.27 (m, 7H, *Z*/*E*-isomer), 7.20 – 7.00 (m, 5H, *Z*/*E*-isomer), 6.96 – 6.90 (m, 2H, *Z*-isomer), 6.69 – 6.59 (m, 1.4H, *E*-isomer), 3.85 (s, 3H, *Z*-isomer), 3.72 (s, 2H, *E*-isomer), 2.81 (q, *J* = 7.5 Hz, 1.4H, *E*-isomer), 2.38 (q, *J* = 7.4 Hz, 2H, *Z*-isomer), 1.06 (t, *J* = 7.5 Hz, 2.3H, *E*-isomer), 0.89 (t, *J* = 7.4 Hz, 3H, *Z*-isomer); **^{13}C NMR** (75 MHz, $CDCl_3$) δ 159.4, 158.7, 144.6, 143.8, 142.7, 140.8, 133.6, 133.4, 131.6, 130.4, 129.3, 128.4, 128.3, 128.1, 127.2, 126.7, 120.9, 119.0, 113.8, 113.1, 55.4, 55.2, 33.4, 29.6, 13.2, 11.8; **HRMS (CI$^+$)** m/z: $[M]^{+\bullet}$ Calcd. for $C_{17}H_{17}O^{79}Br$ 316.0457; Found 316.0455.

The Z/E ratio was determined by ^{1}H NMR integration of the ArH** ortho to the OMe group:* Major isomer **(*Z*)-2.60** = 6.96 – 6.90 (m, 2H); minor isomer **(*E*)-2.60** = 6.69 – 6.59 (m, 1.4H).[121, 153, 172]

Methyl (*Z*)-4-(1-(4-methoxyphenyl)-2-phenylbut-1-en-1-yl)cubane-1-carboxylate (2.65)

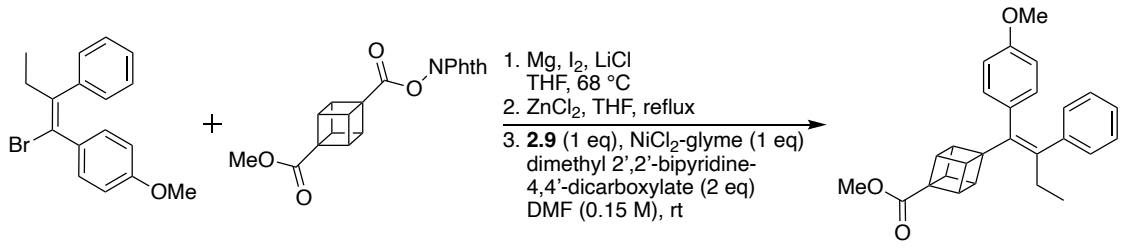

(*E*)-2.60 (*Z*/*E* 3:2) **2.9** **(*Z*)-2.65**

Following an adapted procedure reported by Senge *et al*.[163] To a solution of magnesium turnings (55 mg, 1.8 equiv., 2.4 mmol) and LiCl (85 mg, 1.5 equiv., 2 mmol) in anhydrous THF (1.5 mL), was added 1 pellet of iodine. To this mixture **(*Z*/*E*)-2.60** (3:2) (418 mg, 1.0 equiv., 1.32 mmol) in anhydrous THF (0.5 mL) was added dropwise. After the addition was complete, the mixture was heated to 68 °C for 4 hours. The newly formed Grignard was cooled to rt and added dropwise to a solution of $ZnCl_2$ (1.1 g, 1.0 equiv., 8 mmol) in anhydrous THF (1.5 mL) and was stirred for 15 minutes at rt.

All of the organozinc mixture (3.5 mL, 3 equiv., 2.4 mmol) was added to a solution of **2.9** (155 mg, 1.0 equiv., 0.44 mmol), $NiCl_2$-glyme (95 mg, 1.0 equiv., 0.44 mmol), dimethyl 2,2'-bipyridine-4,4'-dicarboxylate (122 mg, 2.0 equiv., 0.88 mmol) in anhydrous DMF (3 mL) in one quick addition. The purple mixture was stirred at rt for 2 hours and quenched with 1 M $HCl_{(aq)}$ (10 mL). To the mixture was added EtOAc (30 mL) and the organic layer was washed with H_2O (3 x 15 mL), sat. $brine_{(aq)}$ (3 x 15 mL), dried with anhydrous $MgSO_4$, filtered, and concentrated *in vacuo* to afford the crude. Purification by silica gel column chromatography (100 % hexane → 1:5 EtOAc/hexane) gave the title compound **(*Z*)-2.65** (3 mg, 2 %) as a yellow solid.

^{1}H NMR (300 MHz, $CDCl_3$) δ 7.24 – 7.09 (m, 5H), 7.05 – 6.98 (m, 2H), 6.66 – 6.60 (m, 2H), 4.37 – 4.26 (m, 6H), 3.73 (s, 3H), 3.71 (s, 3H), 2.46 (q, *J* = 7.5 Hz, 2H), 0.96 (t, *J* = 7.5 Hz, 3H); **HRMS (ESI$^+$)** m/z: $[M+H]^+$ Calcd. for $C_{27}H_{27}O_3$ 399.1955; Found 399.1953.

*Tentatively assign the stereochemistry as **(*Z*)-2.65** based on the chemical shift of the Ar***H*** ortho to the OMe group δ 6.66 – 6.60 (m, 2H) in the ^{1}H NMR being consistent with the *Z*-stereochemistry.[121, 153, 172]

5.2.4 Route 4: Horner-Wadsworth-Emmons

5.2.4.1 Synthesis towards (*Z*/*E*)-cubyl-tamoxifen (1.18)

General scheme:

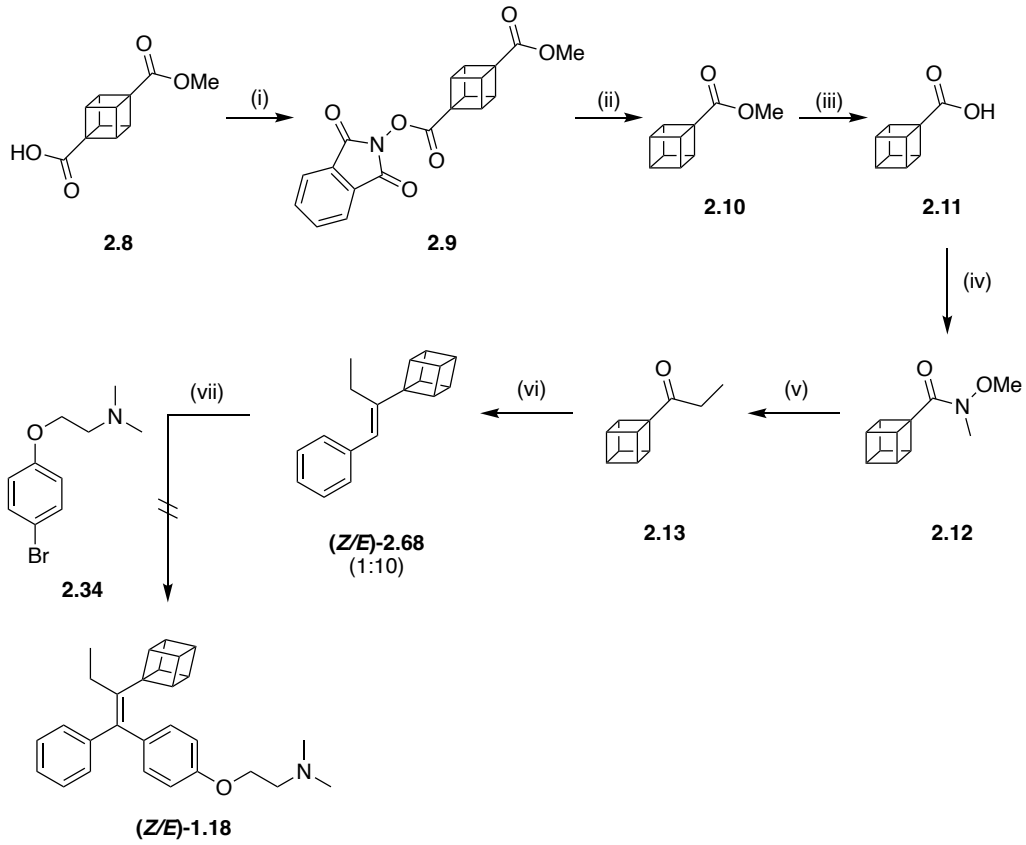

Conditions: (i) 1. oxalyl chloride (2 M in DCM), DMF, DCM, rt, 1.5 h; 2. *N*-hydroxyphthalimide, NEt_3, DCM, rt, 2 h, 94 %; (ii) hantzsch ester, $(Ir[dF(CF_3)ppy]_2(dtbpy))PF_6$, DCM, blue LED lights, rt, 5 h, 70 %; (iii) LiOH, THF:MeOH:H_2O in 3:1:1 ratio, rt, overnight, 81 %; (iv) 1. oxalyl chloride (2 M in DCM), DMF, DCM, rt, 1.5 h; 2. *N,*O-dimethylhydroxylamine hydrochloride, NEt_3, DCM, rt, 3 h, 55 %; (v) EtMgBr (0.9 M in THF), THF, -78 °C → rt, 30 min, 71 %; (vi) diethyl benzylphosphonate, K^{t}BuO, THF, 0 °C, 30 min; 2. **2.13**, THF, 0 °C, 15 min, 52 %; (vii) **2.34**, $Pd(OAc)_2$, PPh_3, Na_2CO_3, DME, reflux, 5 h, 0 %.

*Experimental procedure and analytical data for **2.9**-**2.13** was previously described in **Section 5.2.1.2**. The experimental procedure and analytical data for **2.34** was previously described in **Section 5.2.2.1**.*

(*Z*/*E*)-1-(1-Phenylbut-1-en-2-yl)cubane (2.68)

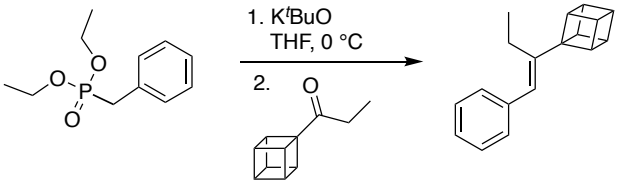

2.67 **2.13** THF, 0 °C **(*Z*/*E*)-2.68** (1:10)

Diethyl benzylphosphonate (**2.67**, 0.16 mL, 2.1 equiv., 0.77 mmol) was added dropwise to a solution of potassium *tert*-butoxide (84 mg, 2.0 equiv., 0.75 mmol) in anhydrous THF (1 mL) at 0 °C. After 30 minutes, a solution of 1-(cuban-1-yl)propan-1-one (**2.13**, 60 mg, 1.0 equiv., 0.37 mmol) in anhydrous THF (1 mL) was added dropwise. The blue mixture was stirred at 0 °C for 15 minutes and then quenched with sat. $NH_4Cl_{(aq)}$ (5 mL). The aqueous layer was extracted with EtOAc (3 x 10 mL) and the combined organic layers were washed with sat. $brine_{(aq)}$ (10 mL), dried with anhydrous $MgSO_4$, filtered and concentrated *in vacuo* to afford the crude (*Z*/*E* 1:4). Purification by silica gel column chromatography (100 % hexane) gave the title compound as a 1:10 ratio of (*Z*)-**2.68** : (*E*)-**2.68** (45 mg, 52 %) as a colourless oil.

^{1}H NMR (500 MHz, $CDCl_3$) δ 7.35 – 7.30 (m, 2H, *Z/E*-isomer), 7.30 – 7.26 (m, 2H, *Z/E*-isomer), 7.21 – 7.17 (m, 1H, *Z/E*-isomer), 7.11 – 7.07 (m, 0.2H, *Z*-isomer), 6.35 (s, 0.1H, *Z*-isomer), 6.13 (s, 1H, *E*-isomer), 4.15 – 4.10 (m, 3H, *E*-isomer), 4.10 – 4.06 (m, 1H, *E*-isomer), 3.99 – 3.94 (m, 3H, *E*-isomer), 3.94 (s, 0.1H, *Z*-isomer), 3.91 – 3.87 (m, 0.3H, *Z*-isomer), 3.87 – 3.83 (m, 0.3H, *Z*-isomer), 2.40 (qd, *J* = 7.6, 0.8 Hz, 2H, *E*-isomer), 2.25 (qd, *J* = 7.5, 1.4 Hz, 0.2H, *Z*-isomer), 1.10 (t, *J* = 7.6 Hz, 3H, *E*-isomer), 1.09 (t, *J* = 7.5 Hz, 0.3H, *Z*-isomer); **NOESY ($CDCl_3$)**: Correlation between the peak at δ 6.13 (s, 1H, C=C**H**) and peak at δ 4.15 – 4.10 (m, 3H, three C-H bonds in cubane) confirmed **(*E*)-2.68** as the major geometric-isomer; **^{13}C NMR** (126 MHz, $CDCl_3$) δ 144.7 (*Z*-isomer), 144.3 (*E*-isomer), 139.3 (*Z*-isomer), 138.6 (*E*-isomer), 128.8 (*E*-isomer), 128.6 (*Z*-isomer), 128.2 (*E*-isomer), 127.6 (*Z*-isomer), 126.1 (*E*-isomer + *Z*-isomer), 124.0 (*Z*-isomer), 122.6 (E-isomer), 64.0 (*E*-isomer), 61.0 (*Z*-isomer), 51.3 (*Z*-isomer), 50.5 (*E*-isomer), 48.2 (*E*-isomer), 46.5 (*Z*-isomer), 44.1 (*Z*-isomer), 43.9 (*E*-isomer), 22.8 (*Z*-isomer), 21.9 (*E*-isomer), 14.3 (*Z*-isomer), 13.7 (*E*-isomer); **HRMS (CI$^+$)** m/z: $[M]^{+\bullet}$ Calcd. for $C_{18}H_{18}$ 234.1403; Found 234.1402.

5.2.4.2 Synthesis towards (*Z*/*E*)-tamoxifen (1.1)

General scheme:

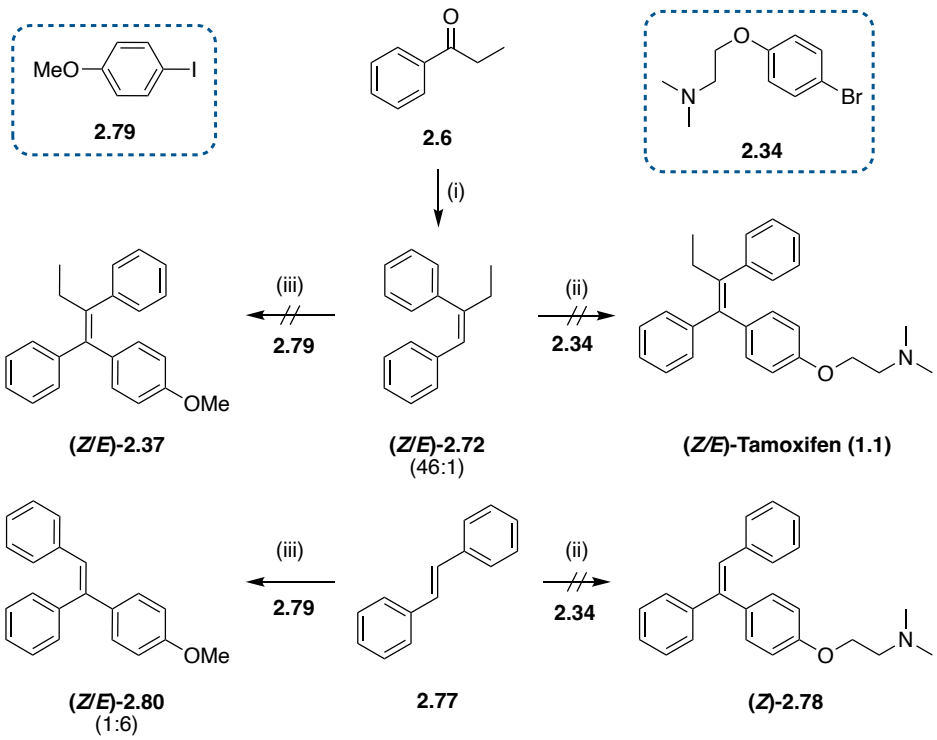

Conditions: (i) diethyl benzylphosphonate, K^{t}BuO, THF, 0 °C, 30 min; 2. **2.6**, THF, rt, 2 h, 94 %; (ii) **2.34**, $Pd(OAc)_2$, PPh_3, Na_2CO_3, DME, reflux, 5 h, 0 % for (*Z*/*E*)-**1.1** and (*Z*/*E*)-**2.78**; (iii) **2.79**, $Pd(OAc)_2$, K_2CO_3, *n*-Et_4NBr, KBr, DMF, 80 °C, 5 h, 30 % for (*Z*/*E*)-**2.80** (1:6 ratio) and 0 % for (*Z*/*E*)-**2.37**.

(*Z*/*E*)-But-1-ene-1,2-diyldibenzene (2.72)

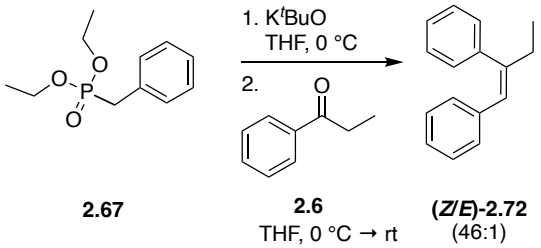

Diethyl benzylphosphonate (**2.67**, 0.33 mL, 2.1 equiv., 1.58 mmol) was added dropwise to a solution of potassium *tert*-butoxide (168 mg, 2.0 equiv., 1.5 mmol) in anhydrous THF (2 mL) at 0 °C. After 30 minutes, propiophenone (**2.6**, 0.1 mL, 1.0 equiv., 0.75 mmol) was added dropwise. The mixture was stirred at rt for 2 hours and then quenched with sat. $NH_4Cl_{(aq)}$ (10 mL) at 0 °C. The aqueous layer was extracted with EtOAc (3 x 10 mL) and the combined organic layers were washed with sat. $brine_{(aq)}$ (10 mL). The organic

layer was dried with anhydrous $MgSO_4$, filtered, and concentrated *in vacuo* to afford the crude (*Z*/*E* 10:1). Purification by silica gel column chromatography (100 % hexane) gave the title compound as a 46:1 ratio of (*Z*)-**2.72** : (*E*)-**2.72** (147 mg, 94 %) as a colourless oil.

^{1}H NMR (300 MHz, $CDCl_3$) δ 7.37 – 7.24 (m, 3H), 7.22 – 7.16 (m, 2H), 7.15 – 7.06 (m, 3H), 6.99 – 6.92 (m, 2H), 6.46 (s, 1H), 2.55 (qd, *J* = 7.4, 1.4 Hz, 2H), 1.11 (t, *J* = 7.4 Hz, 3H); **HRMS (CI$^+$)** m/z: $[M]^{+\bullet}$ Calcd. for $C_{16}H_{16}$ 208.1247; Found 208.1245. All spectroscopic data were in accordance with the literature.[289]

The Z/E ratio was determined by ^{1}H NMR integration of the* $C\boldsymbol{H_2}CH_3$ protons: Major isomer (*Z*)-2.72** = δ 2.55 (qd, *J* = 7.4, 1.4 Hz, 2H); minor isomer (*E*)-**2.72** = δ 2.79 (q, *J* = 8.0 Hz, 0.04H).

(*Z*/*E*)-(1-(4-methoxyphenyl)ethene-1,2-diyl)dibenzene (2.80)

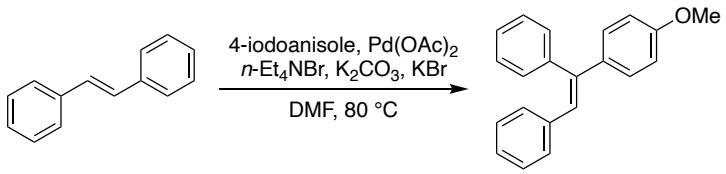

2.77 **(*Z*/*E*)-2.80** (1:6)

Trans-stilbene (**2.77**, 50 mg, 0.28 mmol, 1 eq), 4-iodoanisole (78 mg, 0.33 mmol, 1.2 eq), $Pd(OAc)_2$ (2 mg, 3 mol %), potassium carbonate (58 mg, 0.42 mmol, 1.5 eq), *n*-tetraethylammonium bromide (117 mg, 0.55 mmol, 2 eq) and KBr (40 mg, 0.33 mmol, 1.2 eq) in degassed DMF (2 mL) was heated at 80 °C for 5 hours. The reaction mixture was cooled to rt and quenched with 1 M $HCl_{(aq)}$ (1 mL) and diluted with EtOAc (15 mL). The organic layer was washed with H_2O (3 x 5 mL), sat. $brine_{(aq)}$ (10 mL), dried with anhydrous $MgSO_4$, filtered, and concentrated *in vacuo* to afford the crude (*Z*/*E* 1:6). Purification by silica gel column chromatography (1:99 EtOAc/hexane) gave the title compound as a 1:6 ratio of (*Z*)-**2.80** : (*E*)-**2.80** (24 mg, 30 %) as a colourless oil.

^{1}H NMR (300 MHz, $CDCl_3$) δ 7.34 – 7.29 (m, 3.8H, *E*/*Z*-isomer), 7.28 – 7.23 (m, 2.5H, *E*/*Z*-isomer), 7.23 – 7.17 (m, 2H, *E*/*Z*-isomer), 7.16 – 7.04 (m, 4.2H, *E*/*Z*-isomer), 7.03 – 6.98 (m, 2H, *E*/*Z*-isomer), 6.90 (s, 0.2H, *Z*-isomer), 6.89 (s, 1H, *E*-isomer), 6.88 – 6.81 (m, 2.5H, *E*/*Z*-isomer),3.83 (s, 0.5H, *Z*-isomer), 3.81 (s, 3H, *E*-isomer). **HRMS (CI$^+$)** m/z: $[M]^{+\bullet}$

Calcd. for $C_{21}H_{18}O$ 286.1352; Found 286.1253. All spectroscopic data were in accordance with the literature.[290]

The Z/E ratio was determined by ^1H NMR integration of the* OC*H₃*** protons: Major isomer (*E*)-**2.80** = δ 3.81 (s, 3H); minor isomer (*Z*)-**2.80** = δ 3.83 (s, 0.5H)

5.2.4.3 Synthesis towards (*Z*/*E*)-cubyl-tamoxifen (1.17)

General scheme:

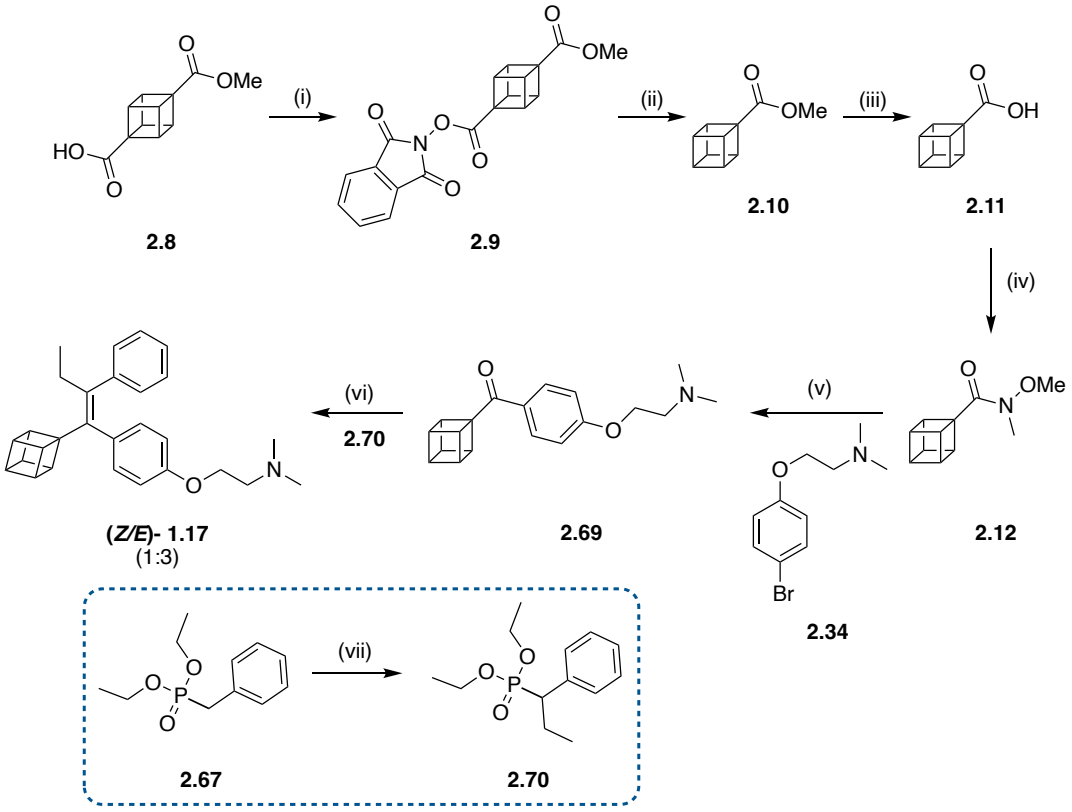

Conditions: (i) 1. oxalyl chloride (2 M in DCM), DMF, DCM, rt, 1.5 h; 2. *N*-hydroxyphthalimide, NEt_3, DCM, rt, 2 h, 94 %; (ii) hantzsch ester, $(Ir[dF(CF_3)ppy]_2(dtbpy))PF_6$, DCM, blue LED lights, rt, 5 h, 70 %; (iii) LiOH, THF:MeOH:H_2O in 3:1:1 ratio, rt, overnight, 81 %; (iv) 1. oxalyl chloride (2 M in DCM), DMF, DCM, rt, 1.5 h; 2. *N,O*-dimethylhydroxylamine hydrochloride, NEt_3, DCM, rt, 3 h, 55 %; (v) 1. **2.34**, *n*-BuLi (1.6 M in hexanes), THF, -78 °C, 15 min; 2. **2.12**, THF, -78 °C, 2 h, 77 %; (vi) **2.70**, *n*-BuLi (1.6 M in hexanes), THF, -78 °C, 15 min; 2. **2.69**, THF, - 78 °C → 50 °C, 21 h, 40 %; (vii) *n*-BuLi (1.6 M in hexanes), THF, -78 °C, 10 min; 2. EtI, - 78 °C → rt, 30 min, 84 %.

Experimental procedure and analytical data for ***2.9****-****2.12*** *was previously described in* ***Section 5.2.1.2****. The experimental procedure and analytical data for* ***2.34*** *was previously described in* ***Section 5.2.2.1.***

(Cuban-1-yl)(4-(2-(dimethylamino)ethoxy)phenyl)methanone (2.69)

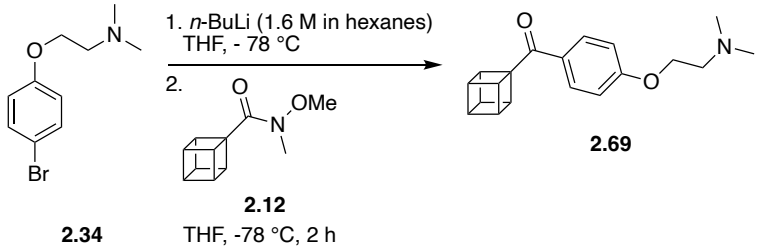

n-BuLi (0.48 mL, 1.5 equiv., 1.6 M in hexanes) was added dropwise to a solution of 2-(4-bromophenoxy)-*N*,*N*-dimethylethan-1-amine (**2.34**) (185 mg, 1.5 equiv., 0.76 mmol) in anhydrous THF (2 mL) at -78 °C. After 15 minutes, *N*-methoxy-*N*-methylcubane-1-carboxamide (**2.12**) (97 mg, 1.0 equiv., 0.50 mmol) in anhydrous THF (0.8 mL) was added dropwise to the yellow solution. The mixture was stirred at -78 °C for 2 hours, then quenched with H_2O (5 mL). 1 M $NaOH_{(aq)}$ (10 mL) was added to the mixture and the aqueous layer was extracted with EtOAc (3 x 10 mL). The combined organic layers were washed with sat. $brine_{(aq)}$ (10 mL), dried with anhydrous $MgSO_4$, filtered, and concentrated *in vacuo* to afford the crude. Purification by silica gel column chromatography (3:7 EtOAc/hexane + 2% NEt_3 → 1:1 EtOAc/hexane + 2% NEt_3) gave the title compound **2.69** (114 mg, 77 %) as a pink solid.

^{1}H NMR (400 MHz, $CDCl_3$) δ 7.83 – 7.74 (m, 2H), 6.99 – 6.91 (m, 2H), 4.48 – 4.38 (m, 3H), 4.16 – 4.06 (m, 6H), 2.76 (t, *J* = 5.7 Hz, 2H), 2.34 (s, 6H); **^{13}C NMR** (101 MHz, $CDCl_3$) δ 197.3, 162.6, 130.3, 128.3, 114.5, 66.2, 63.1, 58.2, 51.0, 47.1, 46.0, 45.3; **HRMS (ESI$^+$)** m/z: $[M+H]^+$ Calcd. for $C_{19}H_{22}NO_2$ 296.1645; Found 296.1648.

Diethyl (1-phenylpropyl)phosphonate (2.70)

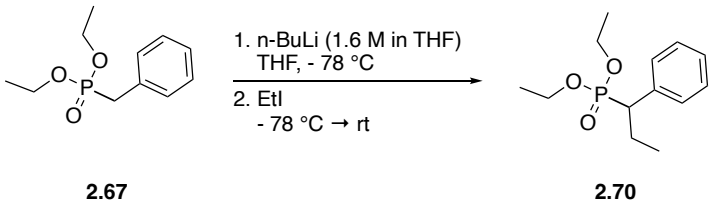

n-BuLi (1.64 mL, 1.2 equiv., 1.6 M in hexanes) was added dropwise to a solution of diethyl benzylphosphonate (**2.67**, 0.46 mL, 1.0 equiv., 2.20 mmol) in anhydrous THF (10 mL) at -78 °C. After 10 minutes iodoethane (0.21 mL, 1.2 equiv., 2.63 mmol) was added dropwise to the yellow solution. The mixture was stirred at -78 °C for 5 minutes, then

warmed to rt. After 30 minutes the reaction was quenched with H_2O (10 mL) and diluted with EtOAc (20 mL). The organic layer was washed with H_2O (2 x 10 mL), sat. $brine_{(aq)}$ (10 mL), dried with anhydrous $MgSO_4$, filtered and concentrated *in vacuo* to afford the title compound **2.70** (488 mg, 84 %) as a light orange oil.

^{1}H NMR (400 MHz, $CDCl_3$) δ 7.34 – 7.28 (m, 4H), 7.28 – 7.21 (m, 1H), 4.14 – 3.97 (m, 2H), 3.95 – 3.80 (m, 1H), 3.78 – 3.62 (m, 1H), 2.88 (ddd, *J* = 22.2, 11.2, 4.1 Hz, 1H), 2.24 – 2.06 (m, 1H), 2.03 – 1.88 (m, 1H), 1.27 (td, *J* = 7.1, 0.5 Hz, 3H), 1.09 (td, *J* = 7.1, 0.6 Hz, 3H), 0.84 (td, *J* = 7.4, 1.0 Hz, 3H); **^{13}C NMR** (101 MHz, $CDCl_3$) δ 136.2 (d, *J* = 6.6 Hz), 129.4 (d, *J* = 6.9 Hz), 128.5 (d, *J* = 2.5 Hz), 127.1 (d, *J* = 3.2 Hz), 62.5 (d, *J* = 7.0 Hz), 61.8 (d, *J* = 7.1 Hz), 46.6 (d, *J* = 136.8 Hz), 23.3 (d, *J* = 3.4 Hz), 16.6 (d, *J* = 6.0 Hz), 16.4 (d, *J* = 5.9 Hz), 12.6 (d, *J* = 16.2 Hz); **^{31}P NMR** (162 MHz, $CDCl_3$) δ 29.0; **HRMS (ESI$^+$)** m/z: $[M+H]^+$ Calcd. for $C_{13}H_{22}PO_3$ 257.1301; Found 257.1306. All spectroscopic data were in accordance with the literature.[291]

(*Z*)-Cubyl-tamoxifen (1.17) and (*E*)-cubyl-tamoxifen (1.17)

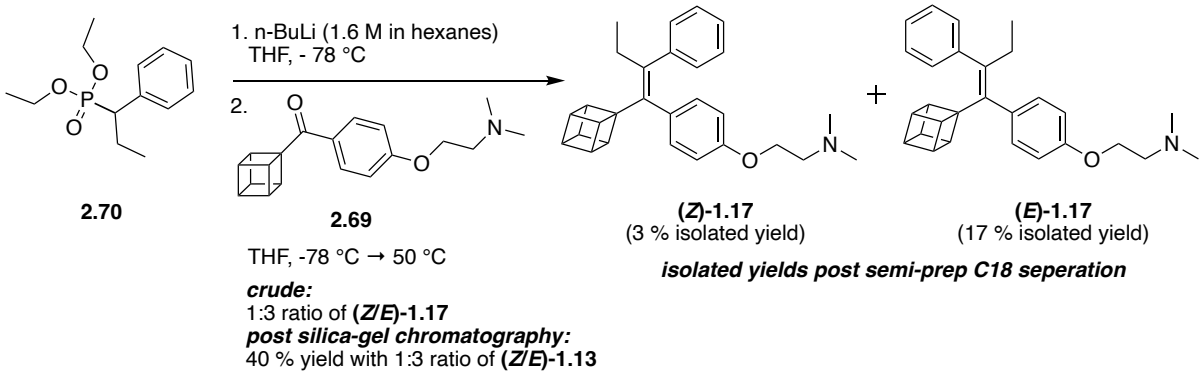

n-BuLi (0.47 mL, 3.0 equiv., 1.6 M in hexanes) was added dropwise to a solution of diethyl (1-phenylpropyl)phosphonate (**2.70**) (198 mg, 3.1 equiv., 0.51 mmol) in anhydrous THF (5 mL) at -78 °C. After 15 minutes, phenyl(4-phenylcuban-1-yl)methanone (**2.69**) (70 mg, 1.0 equiv., 0.24 mmol) in anhydrous THF (1 mL) was added dropwise to the beige solution. The mixture was stirred at -78 °C for 2 minutes, then heat at 50 °C for 21 hours. The reaction mixture was quenched with sat. $NH_4Cl_{(aq)}$ (5 mL) and the aqueous layer was extracted with EtOAc (3 x 10 mL). The combined organic layers were washed with sat. brine (10 mL), dried with anhydrous $MgSO_4$, filtered and concentrated *in vacuo* to afford the crude (*Z*/*E* = 1:3). Purification by silica gel column

chromatography (80:20 EtOAc/hexane → 20:80 EtOAc/hexane + 2% NEt_3) gave the title compound (*Z*/*E*)-**1.17** (38 mg, 40 %, *Z*/*E* 1:3) as a colourless oil.

Purification of (*Z*/*E*)-**1.17** (38 mg, *Z*/*E* 1:3) by reverse phase (C18) chromatography:

Instrument:

Agilent 1260 infinity system with DAD detector and temperature controlled autosampler/column compartment.

HPLC Conditions A: Isocratic gradient and eluent (3:1 MeCN/H_2O with 0.1 % TFA); flow rate (2 mL/min); column (Agilent Eclipse XBD-C18 5 μm 9.4 x 250 mm); wavelength (254 nm).

Sample preparation: Dissolve entire sample in MeCN (1 mL), sonicate to dissolve. Then for each reverse phase run place 100 μL of the dissolved sample into a HPLC vial, add 50 μL of H_2O containing 0.1 % TFA followed by sonication.

Retention time: (*E*)-**1.17** = 10.3 – 11.4 min**;** (*Z*)-**1.17** = 11.8 – 13.3 min. *Note: Separation is not ideal and there is slight overlap between the two geometric isomer.*

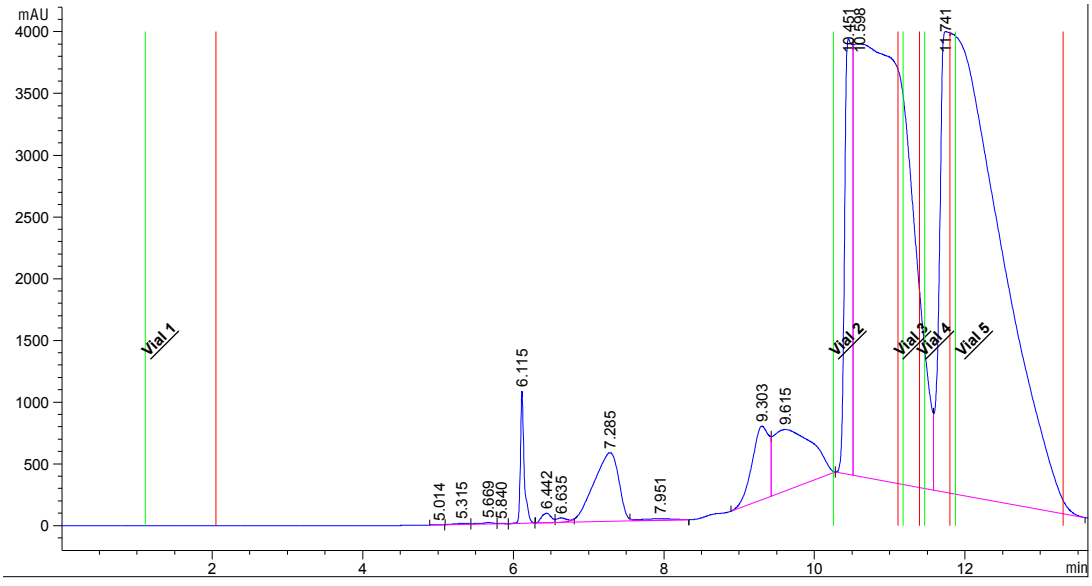

Figure 38: HPLC trace of semi-preparative separation of (*Z*/*E*)-**1.17**.

Following the semi-preparation runs (all done in day to minimise the time each product was in aqueous solution), the fractions for (*E*)-**1.17** and (*Z*)-**1.17** were combined

separately and concentration *in vacuo* to remove the bulk of MeCN and H_2O. To each geometric isomer diethylether (10 mL) was added and the organic layer was washed with 1 M $NaOH_{(aq)}$ (3 x 5 mL), sat. $brine_{(aq)}$ (10 mL), dried with anhydrous $MgSO_4$, filtered and concentrated *in vacuo* to afford the crude. Each crude was separately passed through a short-silica gel plug (5 cm heigh, 2 cm diameter) (30:70 EtOAc/hexane + 2% NEt_3) which gave the title compounds (*E*)-**1.17** (16 mg, 17 %, white solid) and (*Z*)-**1.17** (3 mg, 3 %, white solid).

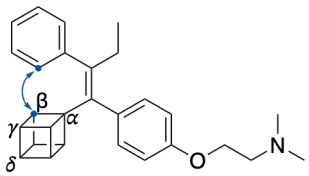

(*E*)-S11

(*E*)-**1.17**: **^{1}H NMR** (400 MHz, $CDCl_3$) δ 7.35 – 7.26 (m, 3H), 7.23 – 7.19 (m, 2H), 7.10 – 7.04 (m, 2H), 6.96 – 6.90 (m, 2H), 4.10 (t, *J* = 5.8 Hz, 2H), 3.79 – 3.72 (m, 1H), 3.61 – 3.54 (m, 3H), 3.45 – 3.39 (m, 3H), 2.77 (t, *J* = 5.8 Hz, 2H), 2.37 (s, 6H), 2.23 (q, *J* = 7.5 Hz, 2H), 0.73 (t, *J* = 7.5 Hz, 3H); **^{13}C NMR** (101 MHz, $CDCl_3$) δ 157.3, 143.1, 139.3, 138.0, 133.3, 129.5, 128.7, 127.6, 126.5, 114.1, 66.0, 61.4, 58.6, 51.6, 47.1, 46.1, 43.6, 28.7, 13.5.; **NOESY ($CDCl_3$)**: Correlation between the peak at δ 3.45 – 3.39 (m, 3H, β-hydrogens of cubane) and 7.23 – 7.19 (m, 2H, *ortho*-hydrogens of unsubstituted phenyl ring) confirmed the *E*-stereochemistry; **HRMS (ESI$^+$)** m/z: $[M+H]^+$ Calcd. for $C_{28}H_{32}NO$ 398.2478; Found 398.2482.

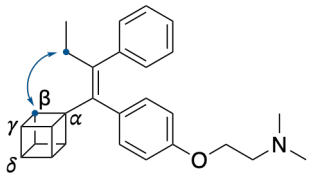

(*Z*)-S11

(*Z*)-**1.17**: ^{1}H NMR (300 MHz, $CDCl_3$) δ 7.10 – 6.96 (m, 3H), 6.93 – 6.88 (m, 2H), 6.71 – 6.64 (m, 2H), 6.64 – 6.58 (m, 2H), 4.08 – 3.89 (m, 9H), 2.67 (t, *J* = 5.8 Hz, 2H), 2.45 (q, *J* = 7.4 Hz, 2H), 2.31 (s, 6H), 0.91 (t, *J* = 7.4 Hz, 3H); **^{13}C NMR** (101 MHz, $CDCl_3$) δ 156.4, 141.0, 138.7, 134.0, 130.5, 129.7, 127.5, 125.4, 113.4, 65.6, 61.1, 58.3, 52.8, 47.1, 45.9, 44.0, 27.5, 13.5. ***Note:*** *One quaternary carbon is missing around 143 ppm*; **NOESY ($CDCl_3$)**: Correlation between the peak at δ 2.45 (q, *J* = 7.4 Hz, 2H, C=CC***H*$_2$**CH_3) and δ 4.06 – 4.01 (m, 3H, β-hydrogens of cubane) confirmed the *Z*-stereochemistry.

5.2.5 Log *P*

5.2.5.1 HPLC Methods

Instrument:

Agilent 1260 infinity system with DAD detector and temperature controlled autosampler/column compartment

HPLC Conditions B:

Solvent A: 50 mM aqueous triethylammonium bicarbonate buffer at pH 7.4

Solvent B: MeCN

Flow rate (1 mL/min); column (Agilent pursuit-C18 5 μm 200 Å, 3 x 100 mm); wavelength (254 nm).

Gradient:

0 – 1 min: 10 % solvent B (isocratic); 1 – 11 min: 10 % solvent B to 100 % solvent B (linear increase); 11 – 13 min: 100 % solvent B (isocratic); 13 – 14 min: 100 % solvent B to 10 % solvent B (linear decrease); 14 – 15 min: 10 % solvent B (isocratic).

5.2.5.2 Log *P* calibration plot

Valko C-18 test mix purchased from Bio-Mimetic Chromatography (Bio-Mimetic Chromatography Ltd., Stevenage, UK).

Table 39: Raw data for calibration plot using Valko C-18 test mix using HPLC conditions B. Literature CHI values obtained from Valko.[188]

	Retention time at pH 7.4 / min					
Valko test mix c18	**t_r 1**	**t_r 2**	**t_r 3**	**t_r 4**	**Average**	**CHI values at pH 7.4**
Theophylline	0.95	0.96	0.959	0.961	0.95775	**18.40**
Phenyltetrazole	1.06	1.034	1.046	1.034	1.04425	**23.60**
Benzimidazole	2.79	2.778	2.792	2.778	2.78525	**34.30**
Colchicine	2.96	2.934	2.917	2.934	2.93525	**42.00**
Phenyltheophylline	4.89	4.885	4.894	4.885	4.88825	**51.20**
Acetophenone	5.22	5.216	5.218	5.216	5.217	**65.10**
indole	6.22	6.226	6.223	6.226	6.22475	**71.50**
propiophenone	6.47	6.465	6.464	6.464	6.4645	**77.40**
butyrophenone	7.37	7.367	7.368	7.367	7.367	**87.50**
valerophenone	8.15	8.151	8.154	8.151	8.15175	**96.20**

Table 40: Log *P* raw data.

Compound	Retention time at pH 7.4 / min				
	t_r 1	t_r 2	Average	CHI	CHI log *P*
(*Z*)-Tamoxifen (**1.1**)	10.60	10.62	10.61	119	5.0
(*E*)-Cubyl-tamoxifen (**1.17**)	12.40	12.40	12.40	138	6.0
1:3 mixture of (*Z*/*E*)-Cubyl-tamoxifen (**1.17**, peak 1)	12.21	12.22	12.21	136	5.9
1:3 ratio of (*Z*/*E*)-Cubyl-tamoxifen (**1.17**, peak 2)	12.39	12.36	12.39	138	6.0

5.3 Chapter 3 experimental

5.3.1 Synthesis of Baeyer-Villiger oxidation substrates

5.3.1.1 Synthesis of 3.91a-f

Methyl-4-phenylcubane-1-carboxylate (2.55)

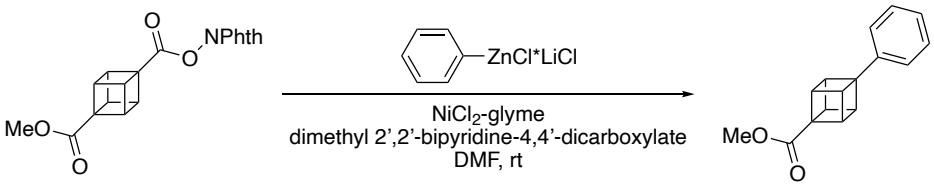

2.9 **2.55**

Following the procedure of Bernhard and co-workers.[163] To a solution of magnesium turnings (235 mg, 1.25 equiv., 10 mmol) and LiCl (425 mg, 1.25 equiv., 10 mmol) in anhydrous THF (2 mL), was added 1 pellet of iodine. To this mixture bromobenzene (0.84 mL, 1.0 equiv., 8 mmol) in anhydrous THF (6 mL) was added dropwise. After the addition was complete, the black mixture was left to stir at rt for 30 minutes. The newly formed Grignard was then added dropwise to a solution of $ZnCl_2$ (1.1 g, 1.0 equiv., 8 mmol) in anhydrous THF (8 mL) and was stirred for 15 minutes at rt.

The organozinc mixture (13.5 mL, 3.5 equiv., 6.76 mmol) was added to a solution of **2.9** (678 mg, 1.0 equiv., 1.93 mmol), $NiCl_2$-glyme (425 mg, 1.0 equiv., 1.93 mmol), dimethyl 2,2'-bipyridine-4,4'-dicarboxylate (1.05 g, 2.0 equiv., 3.86 mmol) in anhydrous DMF (13.8 mL) in one quick addition. The purple mixture was stirred at rt for 2 hours and quenched with 1 M $HCl_{(aq)}$ (10 mL). To the mixture was added EtOAc (30 mL) and the organic layer was washed with H_2O (3 x 15 mL), sat. $brine_{(aq)}$ (3 x 15 mL), dried with

anhydrous $MgSO_4$, filtered, and concentrated *in vacuo* to afford the crude. Purification by silica gel column chromatography (02:98 EtOAc/hexane) gave the title compound **2.55** (244 mg, 53 %) as a yellow solid.

^{1}H NMR (500 MHz, $CDCl_3$) δ 7.40 – 7.32 (m, 2H), 7.25 – 7.17 (m, 3H), 4.28 – 4.21 (m, 3H), 4.20 – 4.12 (m, 3H), 3.74 (s, 3H); **HRMS (APCI$^+$)** m/z: $[M+H]^+$ Calcd. for $C_{16}H_{15}O_2$ 239.1067; Found 239.1067. All spectroscopic data were in accordance with the literature.[162]

4-Phenylcubane-1-carboxylic acid (3.92)

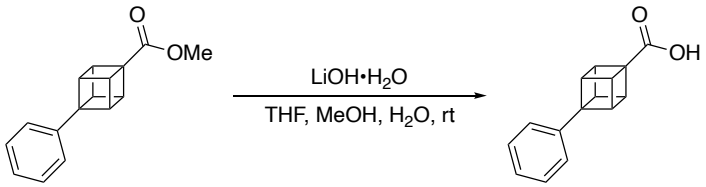

2.55 **3.92**

To a solution of methyl-4-phenylcubane-1-carboxylate (**2.55**, 244 mg, 1.0 equiv., 1.0 mmol) in 3:3:1 ratio of THF:MeOH:H_2O (11.3 mL), was added lithium hydroxide monohydrate (230 mg, 9.6 mmol) in one-portion at 0 °C . The mixture was warmed to rt and stirred overnight. The mixture was acidified with 2 M $HCl_{(aq)}$, and the aqueous layer was extracted with EtOAc (3 x 15 mL). The combined organic layers were washed sat. $brine_{(aq)}$ (15 mL), dried with anhydrous $MgSO_4$, filtered, and concentrated *in vacuo* to afford the crude. The crude solid was washed with hexane (3 x 5 mL) to afford the title compound **3.92** (218 mg, 95 %) as a white solid.

^{1}H NMR (500 MHz, $CDCl_3$) δ 11.89 (br s, 1H), 7.42 – 7.34 (m, 2H), 7.25 – 7.19 (m, 3H), 4.36 – 4.27 (m, 3H), 4.24 – 4.16 (m, 3H); **^{13}C NMR** (126 MHz, $CDCl_3$) δ 178.8, 142.0, 128.6, 126.4, 124.9, 60.4, 56.3, 48.9, 46.2. All spectroscopic data were in accordance with the literature.[278]

_N_-Methoxy-_N_-methyl-4-phenylcubane-1-carboxamide (3.93)

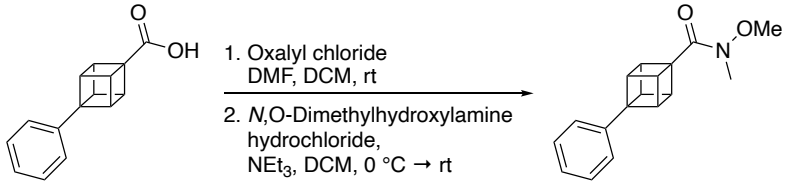

3.92 **3.93**

To a solution of 4-phenylcubane-1-carboxylic acid (**3.92**) (218 mg, 1.0 equiv., 0.97 mmol) in anhydrous DCM (5 mL) was added oxalyl chloride (0.58 mL, 1.2 equiv., 2 M in DCM) at rt. Anhydrous DMF (7.5 mL, 10 mol%) was then added and the reaction mixture was allowed to stir at rt for 1.5 hours. The mixture was concentrated *in vacuo* to afford the acid chloride as a yellow solid.

The acid chloride was dissolved in anhydrous DCM (2 mL) and added dropwise to a solution of *N*,O-dimethylhydroxylamine hydrochloride (130 mg, 1.4 equiv., 1.33 mmol) and triethylamine (0.34 mL, 2.5 equiv., 2.43 mmol) in anhydrous DCM (2 mL) at 0 °C. The mixture was warmed to rt and stirred for 3 hours. The mixture was quenched with sat. $NH_4Cl_{(aq)}$ (5 mL) and diluted with DCM (10 mL). The organic layer was washed with 1 M $HCl_{(aq)}$ (10 mL), sat. $brine_{(aq)}$ (10 mL), dried with anhydrous $MgSO_4$, and concentrated *in vacuo* to afford the crude. Purification by silica gel column chromatography (1:3 EtOAc/hexane) gave the title compound **3.93** (210 mg, 81 %) as a white solid.

^{1}H NMR (500 MHz, $CDCl_3$) δ 7.40 – 7.32 (m, 2H), 7.25 – 7.17 (m, 3H), 4.30 – 4.23 (m, 3H), 4.18 – 4.10 (m, 3H), 3.75 (s, 3H), 3.22 (s, 3H); **^{13}C NMR** (126 MHz, $CDCl_3$) δ 173.8, 142.5, 128.5, 126.1, 124.9, 61.8, 59.8, 58.4, 48.8, 46.3, 32.8; **HRMS (CI$^+$)** m/z: $[M+H]^+$ Calcd. for $C_{17}H_{18}O_2N$ 268.1332; Found 268.1333.

Phenyl(4-phenylcuban-1-yl)methanone (3.91a)

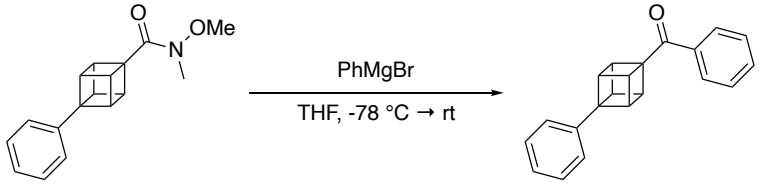

3.93 **3.91a**

To a solution of *N*-methoxy-*N*-methyl-4-phenylcubane-1-carboxamide (**3.93**) (264 mg, 1.0 equiv., 0.99 mmol) in anhydrous THF (5 mL) at -78 °C was added phenylmagnesium bromide (1.48 mL, 1.5 equiv., 1M in THF) dropwise. The mixture was stirred at -78 °C for 30 minutes and then allowed to warm to rt. After 30 minutes, the mixture was quenched with 1 M $HCl_{(aq)}$ (5 mL) at 0 °C. The aqueous was extracted with EtOAc (3 x 10 mL) and the combined organic layers were washed with sat. $brine_{(aq)}$ (10 mL), dried with anhydrous $MgSO_4$, filtered, and concentrated *in vacuo* to afford the crude. Purification by silica gel column chromatography (03:97 EtOAc/hexane) gave the title compound **3.91a** (206 mg, 74 %) as a white solid.

^{1}H NMR (400 MHz, $CDCl_3$) δ 7.93 – 7.85 (m, 2H), 7.63 – 7.55 (m, 1H), 7.54 – 7.47 (m, 2H), 7.45 – 7.36 (m, 2H), 7.31 – 7.20 (m, 3H), 4.52 – 4.42 (m, 3H), 4.38 – 4.26 (m, 3H); **^{13}C NMR** (101 MHz, $CDCl_3$) δ 198.4, 142.2, 135.0, 133.2, 128.9, 128.7, 128.1, 126.4, 125.0, 64.1, 59.5, 49.0, 47.7; **HRMS (CI$^+$)** m/z: $[M+H]^+$ Calcd. for $C_{21}H_{17}O$ 285.1274; Found 285.1274.

1-(4-Phenylcuban-1-yl)ethan-1-one (3.91b)

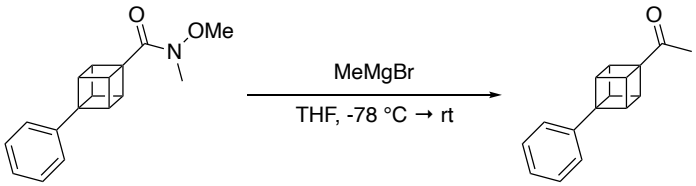

3.93 **3.91b**

To a solution of *N*-methoxy-*N*-methyl-4-phenylcubane-1-carboxamide (**3.93**) (75 mg, 1.0 equiv., 0.28 mmol) in anhydrous THF (3 mL) at -78 °C, was added methylmagnesium bromide (0.4 mL, 2.0 equiv., 1.4 M in toluene/THF) dropwise. The mixture was stirred at -78 °C for 30 minutes before being warmed to rt. After stirring for 30 minutes at rt, the mixture was quenched with 1 M $HCl_{(aq)}$ (5 mL) at 0 °C. The aqueous was extracted with

EtOAc (3 x 10 mL) and the combined organic layers were washed with sat. $brine_{(aq)}$ (10 mL), dried with anhydrous $MgSO_4$, filtered, and concentrated *in vacuo* to afford the crude. Purification by silica gel column chromatography (05:95 EtOAc/petroleum ether) gave the title compound **3.91b** (60 mg, 96 %) as a white solid.

^{1}H NMR (500 MHz, $CDCl_3$) δ 7.41 – 7.33 (m, 2H), 7.26 – 7.18 (m, 3H), 4.31 – 4.24 (m, 3H), 4.18 – 4.11 (m, 3H), 2.19 (s, 3H); **^{13}C NMR** (126 MHz, $CDCl_3$) δ 206.7, 142.1, 128.6, 126.3, 124.9, 64.5, 60.7, 48.4, 46.3, 24.9; **HRMS (ESI$^+$)** m/z: $[M+H]^+$ Calcd. for $C_{16}H_{15}O$ 223.1117; Found 223.1126.

1-(4-Phenylcuban-1-yl)propan-1-one (3.91c)

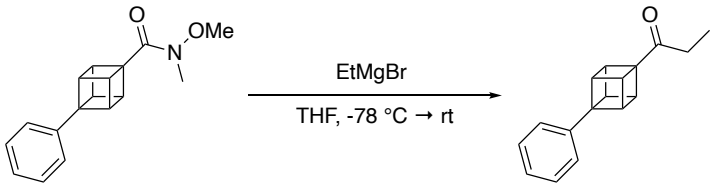

3.93 **3.91c**

To a solution of *N*-methoxy-*N*-methyl-4-phenylcubane-1-carboxamide (**3.93**) (81 mg, 1.0 equiv., 0.3 mmol) in anhydrous THF (3 mL) at -78 °C was added ethylmagnesium bromide (0.67 mL, 2.0 equiv., 0.9 M in THF) dropwise. The mixture was stirred at - 78 °C for 30 minutes and then allowed to warm to rt. After 90 minutes, the mixture was quenched with 1 M $HCl_{(aq)}$ (5 mL) at 0 °C. The aqueous was extracted with EtOAc (3 x 10 mL) and the combined organic layers were washed with sat. $brine_{(aq)}$ (10 mL), dried with anhydrous $MgSO_4$, filtered, and concentrated *in vacuo* to afford the crude orange oil. Purification by silica gel column chromatography (05:95 EtOAc/petroleum ether) gave the title compound **3.91c** (53 mg, 74 %) as a white solid.

^{1}H NMR (500 MHz, $CDCl_3$) δ 7.41 – 7.34 (m, 2H), 7.26 – 7.19 (m, 3H), 4.31 – 4.23 (m, 3H), 4.18 – 4.11 (m, 3H), 2.53 (q, J = 7.4 Hz, 2H), 1.13 (t, J = 7.4 Hz, 3H); **^{13}C NMR** (126 MHz, $CDCl_3$) δ 209.5, 142.1, 128.6, 126.3, 124.8, 63.9, 60.5, 48.5, 46.4, 31.1, 7.7; **HRMS (EI$^+$)** m/z: $[M]^{+\bullet}$ Calcd. for $C_{17}H_{16}O$ 236.1196; Found 236.1194.

(4-Phenylcuban-1-yl)methanol (3.98)

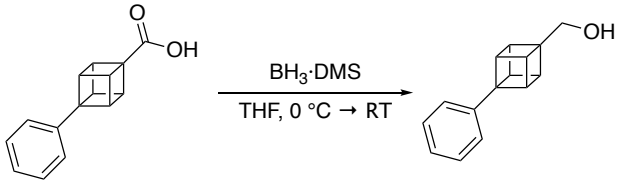

3.92 **3.98**

Borane dimethyl sulfide (0.77 mL, 1.6 equiv., 1M in 2-methyltetrahydrofuran) was added dropwise to a solution of 4-phenylcubane-1-carboxylic acid (**3.92**) (107 mg, 1.0 equiv., 0.48 mmol) in anhydrous THF (5 mL) at 0 °C. The mixture was stirred at 0 °C for 20 minutes and then allowed to warm to rt. After 5 hours the mixture was quenched with H_2O (5 mL) at 0 °C. The mixture was diluted with EtOAc (10 mL) and the organic layer was washed with sat. $NaHCO_{3(aq)}$ (3 x 10 mL), sat. $brine_{(aq)}$ (10 mL), dried with anhydrous $MgSO_4$, filtered, and concentrated *in vacuo* to afford the title compound **3.98** (97 mg, 96%) as a white solid.

^{1}H NMR (400 MHz, $CDCl_3$) δ 7.43 – 7.33 (m, 2H), 7.30 – 7.18 (m, 3H), 4.15 – 4.04 (m, 3H), 3.95 – 3.89 (m, 3H), 3.87 (s, 2H), 1.60 (br s, 1H); **^{13}C NMR** (101 MHz, $CDCl_3$) δ 143.1, 128.5, 125.9, 124.8, 64.0, 60.9, 59.5, 48.1, 43.4; **HRMS (CI$^+$)** m/z: $[M-H_2O]^+$ Calcd. for $C_{15}H_{12}$ 192.0933; Found 192.0941.

4-Phenylcubane-1-carbaldehyde (3.91d)

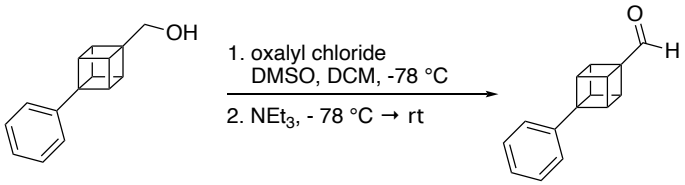

3.98 **3.91d**

DMSO (87 µL, 2.7 equiv., 1.24 mmol) was added to a solution of oxalyl chloride (0.28 mL, 1.2 equiv., 2 M in DCM) in anhydrous DCM (3.5 mL) at -78 °C. After 20 minutes a solution of (4-phenylcuban-1-yl)methanol (**3.98**) (97 mg, 1.0 equiv., 0.46 mmol) in anhydrous DCM (1.5 mL) was added dropwise, and the mixture stirred at -78 °C for a further 1.5 hours. Triethylamine (0.34 mL, 5.4 equiv., 2.47 mmol) was then added and the mixture was allowed to warm to rt over 15 minutes. The mixture was quenched with H_2O (5 mL) and the aqueous layer was extracted with DCM (3 x 10 mL). The combined organic layer was washed sat. $brine_{(aq)}$ (10 mL), dried with anhydrous $MgSO_4$, filtered,

and concentrated *in vacuo* to afford the crude. Purification by silica gel column chromatography (05:95 EtOAc/hexane) gave the title compound **3.91d** (68 mg, 71 %) as a light-yellow oil.

^{1}H NMR (400 MHz, $CDCl_3$) δ 9.82 (s, 1H), 7.43 – 7.33 (m, 2H), 7.26 – 7.18 (m, 3H), 4.44 – 4.34 (m, 3H), 4.23 – 4.13 (m, 3H); **^{13}C NMR** (101 MHz, $CDCl_3$) δ 198.4, 141.9, 128.6, 126.4, 124.9, 63.5, 60.7, 48.9, 45.0; **HRMS (EI$^+$)** m/z: $[M]^{+\bullet}$ Calcd. for $C_{15}H_{12}O$ 208.0883; Found 208.0882.

2-Methyl-1-(4-phenylcuban-1-yl)propan-1-one (3.91e)

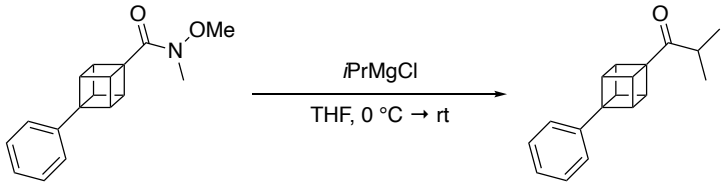

3.93 **3.91e**

To a solution of *N*-methoxy-*N*-methyl-4-phenylcubane-1-carboxamide (**3.93**) (250 mg, 1.0 equiv., 0.94 mmol) in anhydrous THF (5 mL) at 0 °C was added isopropylmagnesium chloride (1.4 mL, 3.0 equiv., 2 M in THF) dropwise. The mixture was stirred at 0 °C for 5 minutes and then allowed to warm to rt. After 2.5 hours, the mixture was quenched with 1 M $HCl_{(aq)}$ (5 mL) at 0 °C. The aqueous was extracted with EtOAc (3 x 10 mL) and the combined organic layers were washed with sat. $brine_{(aq)}$ (10 mL), dried with anhydrous $MgSO_4$, filtered, and concentrated *in vacuo* to afford the crude. Purification by silica gel column chromatography (03:97 EtOAc/petroleum ether) gave the title compound **3.91e** (179 mg, 77 %) as a white solid.

^{1}H NMR (400 MHz, $CDCl_3$) δ 7.41 – 7.32 (m, 2H), 7.25 – 7.19 (m, 3H), 4.31 – 4.25 (m, 3H), 4.19 – 4.11 (m, 3H), 2.85 (hept, *J* = 6.9 Hz, 1H), 1.15 (d, *J* = 6.9 Hz, 6H); **^{13}C NMR** (101 MHz, $CDCl_3$) δ 212.4, 142.2, 128.6, 126.3, 124.9, 63.9, 60.2, 48.5, 46.8, 37.7, 18.1; **HRMS (ESI$^+$)** m/z: $[M+H]^+$ Calcd. for $C_{18}H_{19}O$ 251.1431; Found 251.1443.

2,2-Dimethyl-1-(4-phenylcuban-1-yl)propan-1-one (3.91f)

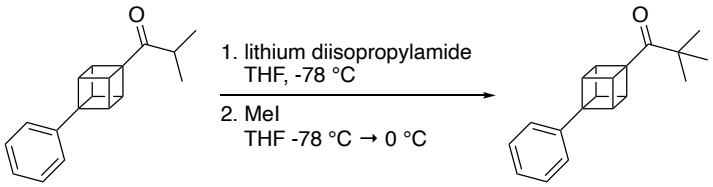

3.91e **3.91f**

To a solution of diisopropylamine (105 mL, 1.5 equiv., 0.75 mmol) in anhydrous THF (5 mL) was added *n*-BuLi (0.44 mL, 1.4 equiv., 1.6 M in hexanes) dropwise at -78 °C. After 10 minutes, a solution of 2-methyl-1-(4-phenylcuban-1-yl)propan-1-one (**3.91e**) (126 mg, 1 equiv., 0.5 mmol) in anhydrous THF (1 mL) was added dropwise to the freshly prepared lithium diisopropylamide solution. The mixture was stirred at -78 °C for a further 30 minutes, then methyl iodide (47 mL, 1.5 equiv., 0.75 mmol) was added dropwise. The reaction was allowed to stir for 10 minutes before being allowed to warm to 0 °C. After 30 minutes at 0 °C the mixture was quenched with H_2O (5 mL) and diluted with EtOAc (15 mL). The organic layer was washed with 1 M $NaOH_{(aq)}$ (1 x 15 mL), sat. $brine_{(aq)}$ (10 mL), dried with anhydrous $MgSO_4$, filtered, and concentrated *in vacuo* to afford the crude. Purification by silica gel column chromatography (02:98 EtOAc/petroleum ether) gave the title compound **3.91f** (114 mg, 86 %) as a white solid.

^{1}H NMR (400 MHz, $CDCl_3$) δ 7.42 – 7.32 (m, 2H), 7.25 – 7.19 (m, 3H), 4.39 – 4.30 (m, 3H), 4.21 – 4.12 (m, 3H), 1.23 (s, 9H); **^{13}C NMR** (101 MHz, $CDCl_3$) δ 213.1, 142.2, 128.6, 126.2, 124.9, 64.4, 59.5, 48.4, 47.7, 44.5, 26.5; **HRMS (ESI$^+$)** m/z: $[M+H]^+$ Calcd. for $C_{19}H_{21}O$ 265.1587; Found 265.1591.

5.3.1.2 Synthesis of 3.91g

Methyl-4-iodocubane-1-carboxylate (3.99)

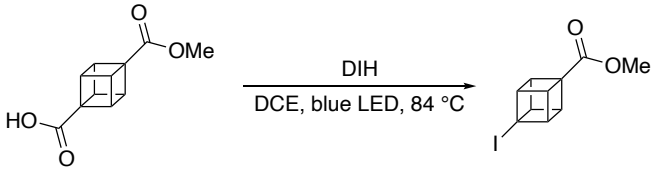

2.8 **3.99**

Following an adapted procedure of Kulbitski and co-workers.[274] A solution of the commercially available 4-(methoxycarbonyl)cubane-1-carboxylic acid (**2.8**) (1.0 g, 1.0 equiv., 4.85 mmol) and 1,3-diiodo-5,5-dimethylhydantoin (DIH) (2.2 g, 1.2, equiv., 5.82 mmol) in anhydrous DCE (30 mL) was heated at 84 °C under blue light irradiation for 5

hours (Aldrich® micro photochemical reactor blue LED (ALDKIT001)). The mixture was cooled to rt and quenched with 1 M sodium thiosulfate$_{(aq)}$ (15 mL) and diluted with DCM (15 mL). The organic layer was washed with 1 M sodium thiosulfate$_{(aq)}$ (2 x 15 mL), dried with anhydrous $MgSO_4$, filtered, and concentrated *in vacuo* to afford the crude. Purification by silica gel column chromatography (03:97 EtOAc/petroleum ether) gave the title compound **3.99** (1.2 g, 85 %) as a white solid.

^{1}H NMR (400 MHz, $CDCl_3$) δ 4.42 – 4.34 (m, 3H), 4.33 – 4.22 (m, 3H), 3.70 (s, 3H). **^{13}C NMR** (101 MHz, $CDCl_3$) δ 172.0, 56.2, 55.0, 51.8, 50.4, 36.3; **HRMS (EI$^+$)** m/z: $[M-H]^+$ Calcd. for $C_{10}H_8O_2{}^{127}I$ 286.9564; Found 286.9561. All spectroscopic data were in accordance with the literature.[274]

4-Iodocubane-1-carboxylic acid (3.103)

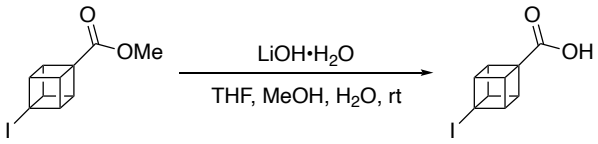

3.99 **3.103**

To a solution of methyl-4-iodocubane-1-carboxylate (**3.99**) (1.2 g, 1.0 equiv., 4.17 mmol) in 3:3:1 ratio of THF:MeOH:H_2O (10 mL) was added lithium hydroxide monohydrate (437 mg, 2.5 equiv., 10.4 mmol) in one-portion at rt. The mixture was allowed to stir at rt overnight. The mixture was diluted with 1 M $NaOH_{(aq)}$ (2 mL) and the aqueous layer was washed with EtOAc (2 x 10 mL). The aqueous layer was acidified with 2 M $HCl_{(aq)}$, and the aqueous layer was extracted with EtOAc (3 x 15 mL). The combined organic layers were washed sat. brine$_{(aq)}$ (15 mL), dried with anhydrous $MgSO_4$, filtered, and concentrated *in vacuo* to afford the title compound **3.103** (1.1 g, 92 %) as a cream solid.

^{1}H NMR (300 MHz, DMSO-d_6): δ 12.52 (br, 1H), 4.34-4.25 (m, 6H); **HRMS (ESI$^-$)** m/z: $[M-H]^-$ Calcd. for $C_9H_6{}^{127}IO_2$ 272.9418; Found 272.9407. All spectroscopic data were in accordance with the literature.[274]

4-Iodo-*N*,*N*-diisopropylcubane-1-carboxamide (3.104)

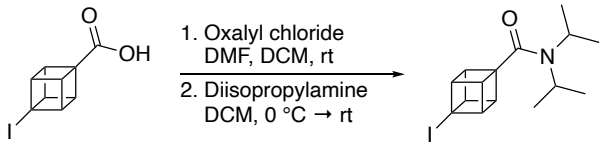

3.103 **3.104**

To a solution of 4-iodocubane-1-carboxylic acid (**3.103**) (765 mg, 1.0 equiv., 2.79 mmol) in anhydrous DCM (15mL) was added oxalyl chloride (2.37 mL, 1.7 equiv., 2 M in DCM) at rt. Anhydrous DMF (22 mL, 10 mol%) was then added and the reaction mixture was allowed to stir at rt for 1.5 hours. The mixture was concentrated *in vacuo* to afford the acid chloride as a yellow solid.

The acid chloride was dissolved in anhydrous DCM (7.5 mL) and added dropwise to a solution of diisopropylamine (0.98 mL, 2.5 equiv., 6.98 mmol) in anhydrous DCM (7.5 mL) at 0 °C. The mixture was warmed to rt and stirred for 3.5 hours. The mixture was quenched with sat. $NH_4Cl_{(aq)}$ (5 mL) and diluted with DCM (15 mL). The organic layer was washed with 1 M $HCl_{(aq)}$ (10 mL), sat. $brine_{(aq)}$ (10 mL), dried with anhydrous $MgSO_4$, filtered and concentrated *in vacuo* to afford the crude. Purification by silica gel column chromatography (1:5 EtOAc/petroleum ether) gave the title compound **3.104** (868 mg, 87 %) as a white solid.

^{1}H NMR (400 MHz, $CDCl_3$) δ 4.35 – 4.28 (m, 3H), 4.28 – 4.21 (m, 3H), 3.35 (hept, *J* = 6.7 Hz, 1H), 3.29 (hept, *J* = 6.8 Hz, 1H), 1.39 (d, *J* = 6.8 Hz, 6H), 1.18 (d, *J* = 6.7 Hz, 6H); **^{13}C NMR** (101 MHz, $CDCl_3$) δ 169.9, 59.9, 54.3, 50.3, 48.5, 46.1, 36.2, 21.1, 20.6; **HRMS (EI$^+$)** m/z: $[M-H]^+$ Calcd. for $C_{15}H_{19}ON^{127}I$ 356.0506; Found 356.0493. All spectroscopic data were in accordance with the literature.[292]

4-Iodo-*N*,*N*-diisopropylcubane-1-carboxamide (3.105)

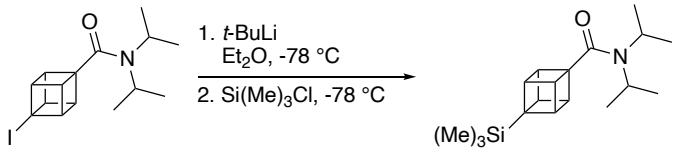

3.104 **3.105**

Following an adapted procedure of Lukin and Eaton.[275] To a solution of 4-iodo-*N*,*N*-diisopropylcubane-1-carboxamide (**3.104**) (868 mg, 1.0 equiv., 2.43 mmol) in anhydrous

diethyl ether (20 mL) was added *tert*-butyl lithium (2.74 mL, 2.15 equiv., 1.9 M in pentanes) dropwise over 5 minutes at -78 °C. After 20 minutes, chlorotrimethylsilane (1.17 mL, 3.8 equiv., 9.22 mmol) was added dropwise and the mixture was stirred for a further 1.5 hours at - 78 °C. The mixture was quenched with methanol (1 mL) and then allowed to warm to 0 °C. After, H_2O (5 mL) was added dropwise to the mixture and allowed to warm to rt. The aqueous layer was extracted with Et_2O (3 x 15 mL) and the combined organic layers were washed with sat. $brine_{(aq)}$ (10 mL), dried with anhydrous $MgSO_4$, filtered and concentrated *in vacuo* to afford the crude. Purification by silica gel column chromatography (7:93 EtOAc/petroleum ether) gave the title compound **3.105** (660 mg, 94 %) as a white solid.

^{1}H NMR (400 MHz, $CDCl_3$) δ 4.23 – 4.13 (m, 3H), 3.84 – 3.75 (m, 3H), 3.52 (hept, *J* = 6.6 Hz, 1H), 3.28 (hept, *J* = 6.8 Hz, 1H), 1.41 (d, *J* = 6.8 Hz, 6H), 1.17 (d, *J* = 6.6 Hz, 6H), -0.06 (s, 9H); **^{13}C NMR** (101 MHz, $CDCl_3$) δ 171.2, 59.6, 49.7, 48.3, 47.4, 45.9, 43.1, 21.1, 20.7, -4.7; **HRMS (ESI$^+$)** m/z: $[M+H]^+$ Calcd. for $C_{18}H_{30}NOSi$ 304.2091; Found 304.2089. All spectroscopic data were in accordance with the literature.[293]

***N*-Isopropyl-*N*-(4-(trimethylsilyl)cuban-1-yl)methyl)propan-2-amine (3.106)**

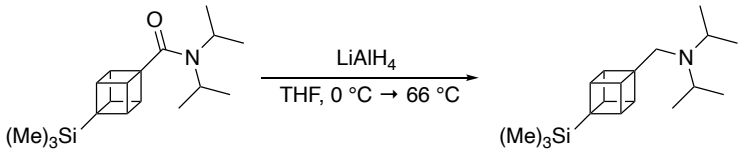

3.105 **3.106**

Following an adapted procedure of Lukin and Eaton.[275] To a solution of lithium aluminum hydride (124 mg, 1.5 equiv., 3.26 mmol) in anhydrous THF (15 mL) was added 4-iodo-*N*,*N*-diisopropylcubane-1-carboxamide (**3.105**) (660 mg, 1.0 equiv., 2.17 mmol) in anhydrous THF (2 mL) dropwise at 0 °C. After the addition the mixture was heated to 66 °C for 1 hour and then cooled to 0 °C. The mixture was quenched with H_2O (1 mL), 1 M $NaOH_{(aq)}$ (1 mL) and H_2O (2 mL) dropwise. The aqueous layer was extracted with Et_2O (3 x 15 mL) and the combined organic layers were washed with sat. $brine_{(aq)}$ (10 mL), dried with anhydrous $MgSO_4$, filtered and concentrated *in vacuo* to afford the title compound **3.106** (609 mg, 97 %) as a light-yellow oil.

^{1}H NMR (400 MHz, $CDCl_3$) δ 3.83 – 3.76 (m, 3H), 3.75 – 3.66 (m, 3H), 2.93 (hept, *J* = 6.6 Hz, 2H), 2.63 (s, 2H), 0.97 (d, *J* = 6.6 Hz, 12H), -0.06 (s, 9H); **^{13}C NMR** (101 MHz, $CDCl_3$) δ 59.4, 48.8, 48.7, 47.9, 46.8, 43.2, 21.0, -4.7; **HRMS (ESI$^+$)** m/z: $[M+H]^+$ Calcd. for $C_{18}H_{32}NSi$ 290.2299; Found 290.2302.

4-(Trimethylsilyl)cubane-1-carboxylic acid (3.107)

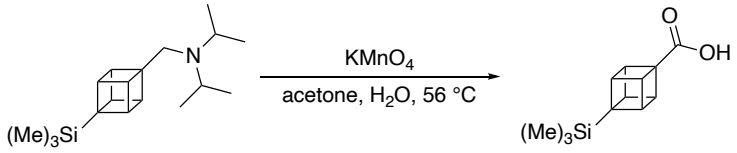

3.106 **3.107**

Following an adapted procedure of Lukin and Eaton.[275] To a solution of *N*-isopropyl-*N*-(4-(trimethylsilyl)cuban-1-yl)methyl)propan-2-amine (**3.106**) (609 mg, 1.0 equiv., 2.1 mmol) in acetone (18 mL) at 56 °C was added 32 mL of a solution of $KMnO_4$ (1.5 g, 4.5 equiv., 9.26 mmol) dissolved in acetone (42 mL) and H_2O (8.4 mL), resulting in a deep purple colour. After 5 minutes, the mixture was cooled to rt and quenched with the addition of solid sodium bisulfite till a grey solid precipitate formed. The mixture was filtered through a pad of celite and the solid was washed with acetone (50 mL). The filtrate was concentrated *in vacuo* and the residue was diluted with 1 M $NaOH_{(aq)}$ (5 mL) and the aqueous layer was washed with EtOAc (2 x 10 mL). The aqueous layer was acidified with 2 M $HCl_{(aq)}$, and the aqueous layer was extracted with EtOAc (3 x 15 mL). The combined organic layers were washed sat. $brine_{(aq)}$ (15 mL), dried with anhydrous $MgSO_4$, filtered, and concentrated *in vacuo* to afford the title compound **3.107** (406 mg, 88 %) as a white solid.

^{1}H NMR (500 MHz, $CDCl_3$) δ 4.34 – 4.23 (m, 3H), 3.92 – 3.79 (m, 3H), -0.04 (s, 9H); **^{13}C NMR** (126 MHz, $CDCl_3$) δ 178.3, 55.8, 49.9, 49.1, 44.2, -4.7; **HRMS (ESI$^+$)** m/z: $[M+H]^+$ Calcd. for $C_{12}H_{17}O_2Si$ 221.0992; Found 221.0992.

_N_-Methoxy-_N_-methyl-4-(trimethylsilyl)cubane-1-carboxamide (3.108)

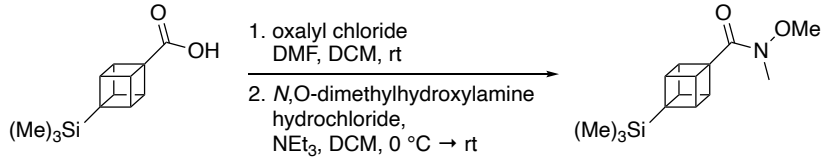

3.107 **3.108**

To a solution of 4-(trimethylsilyl)cubane-1-carboxylic acid (**3.107**) (236 mg, 1.0 equiv., 1.07 mmol) in anhydrous DCM (5 mL) was added oxalyl chloride (0.91 mL, 1.7 equiv., 2 M in DCM) at rt. Anhydrous DMF (8 mL, 10 mol%) was then added and the reaction mixture was allowed to stir at rt for 1.5 hours. The mixture was concentrated *in vacuo* to afford the acid chloride as a yellow solid.

The acid chloride was dissolved in anhydrous DCM (2.5 mL) and added dropwise to a solution of *N*,O-dimethylhydroxylamine hydrochloride (167 mg, 1.6 equiv., 1.71 mmol) and triethylamine (0.47 mL, 3.2 equiv., 3.39 mmol) in anhydrous DCM (2.5 mL) at 0 °C. The mixture was warmed to rt and stirred for 1 hour. The mixture was quenched with sat. $NH_4Cl_{(aq)}$ (5 mL) and diluted with DCM (10 mL). The organic layer was washed with 1 M $HCl_{(aq)}$ (10 mL), sat. $brine_{(aq)}$ (10 mL), dried with anhydrous $MgSO_4$, and concentrated *in vacuo* to afford the crude. Purification by silica gel column chromatography (1:4 EtOAc/petroleum ether) gave the title compound **3.108** (167 mg, 60 %) as a light-yellow solid.

^{1}H NMR (500 MHz, $CDCl_3$) δ 4.31 – 4.23 (m, 3H), 3.88 – 3.79 (m, 3H), 3.69 (s, 3H), 3.17 (s, 3H), -0.05 (s, 9H); **^{13}C NMR** (126 MHz, $CDCl_3$) δ 173.8, 61.7, 57.9, 50.0, 48.2, 44.0, 32.8, -4.7; **HRMS (ESI$^+$)** m/z: $[M+H]^+$ Calcd. for $C_{14}H_{22}NO_2Si$ 264.1414; Found 264.1410.

2-Methyl-1-(4-(trimethylsilyl)cuban-1-yl)propan-1-one (3.91g)

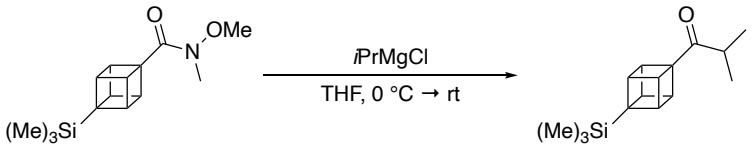

3.108 **3.91g**

To a solution of *N*-methoxy-*N*-methyl-4-(trimethylsilyl)cubane-1-carboxamide (**3.108**) (141 mg, 1.0 equiv., 0.54 mmol) in anhydrous THF (3 mL) at 0 °C was added isopropylmagnesium chloride (0.80 mL, 3.0 equiv., 2 M in THF) dropwise. The mixture

was stirred at 0 °C for 5 minutes and allowed to warm to rt. After 3.5 hours, the mixture was quenched with 1 M $HCl_{(aq)}$ (5 mL) at 0 °C. The aqueous was extracted with EtOAc (3 x 10 mL) and the combined organic layers were washed with sat. $brine_{(aq)}$ (10 mL), dried with anhydrous $MgSO_4$, filtered, and concentrated *in vacuo* to afford the crude orange oil. Purification by silica gel column chromatography (02:98 EtOAc/petroleum ether) gave the title compound **3.91g** (99 mg, 75 %) as a colourless oil.

^{1}H NMR (400 MHz, $CDCl_3$) δ 4.34 – 4.24 (m, 3H), 3.88 – 3.78 (m, 3H), 2.78 (hept, *J* = 6.9 Hz, 1H), 1.09 (d, *J* = 6.9 Hz, 6H), -0.05 (s, 9H); **^{13}C NMR** (101 MHz, $CDCl_3$) δ 212.2, 63.4, 50.5, 48.9, 43.8, 37.6, 18.1, -4.7; **HRMS (ESI$^+$)** m/z: $[M+H]^+$ Calcd. for $C_{15}H_{23}OSi$ 247.1513; Found 247.1515.

5.3.1.3 Synthesis of 3.91h:

*Experimental procedure and analytical data for the 4-step method to synthesise **2.12** was previously described in **Section 5.2.1.2**.*

1-(Cuban-1-yl)-2-methylpropan-1-one (3.91h)

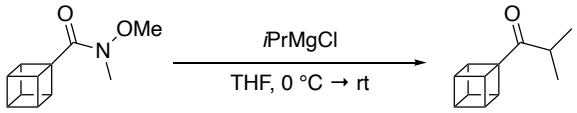

2.12 **3.91h**

To a solution of *N*-methoxy-*N*-methylcubane-1-carboxamide (**2.12**) (146 mg, 1.0 equiv., 0.76 mmol) in anhydrous THF (5 mL) at 0 °C was added isopropylmagnesium chloride (1.15 mL, 3.0 equiv., 2 M in THF) dropwise. The mixture was stirred at 0 °C for 5 minutes and allowed to warm to rt. After 3.5 hours, the mixture was quenched with 1 M $HCl_{(aq)}$ (5 mL) at 0 °C. The aqueous was extracted with EtOAc (3 x 10 mL) and the combined organic layers were washed with sat. $brine_{(aq)}$ (10 mL), dried with anhydrous $MgSO_4$, filtered, and concentrated *in vacuo* to afford the crude. Purification by silica gel column chromatography (02:98 EtOAc/petroleum ether) gave the title compound **3.91h** (89 mg, 67 %) as a white solid.

^{1}H NMR (400 MHz, $CDCl_3$) δ 4.33 – 4.22 (m, 3H), 4.05 – 3.92 (m, 4H), 2.77 (hept, *J* = 6.9 Hz, 1H), 1.08 (d, *J* = 6.9 Hz, 6H); **^{13}C NMR** (101 MHz, $CDCl_3$) δ 212.5, 63.1, 50.2, 47.9, 44.9, 37.6, 18.1; **HRMS (EI$^+$)** m/z: $[M]^{+\bullet}$ Calcd. for $C_{12}H_{14}O$ 174.1039; Found 174.1040.

5.3.1.4 Synthesis of 3.91i

Methyl-4-(hydroxymethyl)cubane-1-carboxylate (3.109)

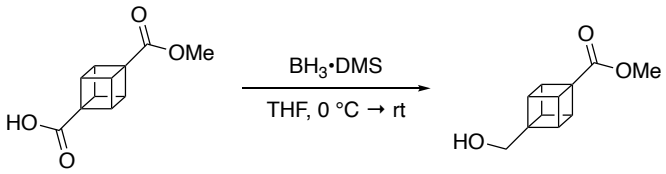

2.8 **3.109**

To a solution of the commercially available 4-(methoxycarbonyl)cubane-1-carboxylic acid (**2.8**) (500 mg, 1.0 equiv., 2.42 mmol) in anhydrous THF (10 mL) was added borane dimethyl sulfide (4.12 mL, 1.7 equiv., 1 M in 2-methyltetrahydrofuran) dropwise at 0 °C. After the addition the mixture was stirred at rt for 4.5 hours. The mixture was quenched with H_2O (2 mL) at 0 °C and diluted with EtOAc (20 mL). The organic layer was washed with sat. $NaHCO_{3(aq)}$ (2 x 10 mL), sat. $brine_{(aq)}$ (20 mL), dried with anhydrous $MgSO_4$, filtered, and concentrated *in vacuo* to afford the title compound **3.109** (449 mg, 96 %) as a white solid.

^{1}H NMR (400 MHz, $CDCl_3$) δ 4.18 – 4.11 (m, 3H), 3.92 – 3.86 (m, 3H), 3.77 (s, 2H), 3.70 (s, 3H); **HRMS (EI$^+$)** m/z: $[M-H_2O]^+$ Calcd. for $C_{11}H_{10}O_2$ 174.0675; Found 174.0674. All spectroscopic data were in accordance with the literature.[294]

Methyl-4-(methoxymethyl)cubane-1-carboxylate (3.110)

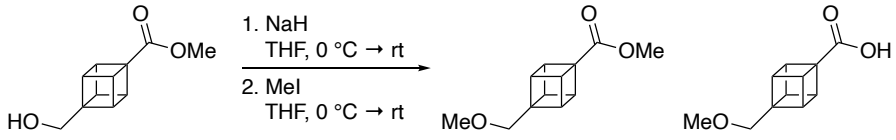

3.109 **3.110** **3.111**

To a solution of sodium hydride (60% dispersion in mineral oil) (161 mg, 2.0 equiv., 3.98 mmol) in anhydrous THF (10 mL) was added methyl-4-(hydroxymethyl)cubane-1-carboxylate (**3.109**) (383 mg, 1.0 equiv., 1.99 mmol) in anhydrous THF (5 mL) dropwise at 0 °C and then stirred at rt for 15 minutes. The mixture was re-cooled to 0 °C and iodomethane (0.37 mL, 3.0 equiv., 3.98 mmol) was added dropwise, after 10 minutes the mixture was warmed to rt. After 6 hours the mixture was cooled to 0 °C , quenched with H_2O (5 mL) and allowed to stir at rt for 15 minutes. The basic aqueous layer* was washed with EtOAc (2 x 15 mL) and the combined organic layers were washed with sat.

brine$_{(aq)}$ (20 mL), dried with anhydrous $MgSO_4$, filtered, and concentrated *in vacuo* to afford the crude containing **3.110**. Purification by silica gel column chromatography (1:9 EtOAc/petroleum ether) gave the title compound **3.110** (66 mg, 16 %) as a white solid.

^{1}H NMR (400 MHz, $CDCl_3$) δ 4.19 – 4.09 (m, 3H), 3.92 – 3.81 (m, 3H), 3.69 (s, 3H), 3.52 (s, 2H), 3.36 (s, 3H); **^{13}C NMR** (101 MHz, $CDCl_3$) δ 172.9, 73.2, 59.4, 57.6, 56.3, 51.6, 46.7, 45.2; **HRMS (EI$^+$)** m/z: $[M-H]^+$ Calcd. for $C_{12}H_{13}O_3$ 205.0859; Found 205.0857.

*To isolate **3.111**, the basic aqueous layer was acidified with 2 M $HCl_{(aq)}$, and the aqueous layer was extracted with EtOAc (3 x 15 mL). The combined organic layers were washed sat. brine$_{(aq)}$ (15 mL), dried with anhydrous $MgSO_4$, filtered, and concentrated *in vacuo* to afford the title compound **3.111** (101 mg, 26 %) as a white solid.

^{1}H NMR (400 MHz, $CDCl_3$) δ 4.23 – 4.16 (m, 3H), 3.93 – 3.86 (m, 3H), 3.54 (s, 2H), 3.38 (s, 3H); **^{13}C NMR** (101 MHz, $CDCl_3$) δ 178.4, 73.1, 59.4, 57.7, 56.1, 46.7, 45.3; **HRMS (ESI$^-$)** m/z: $[M-H]^-$ Calcd. for $C_{11}H_{11}O_3$ 191.0713; Found 191.0710.

4-(Methoxymethyl)cubane-1-carboxylic acid (3.111)

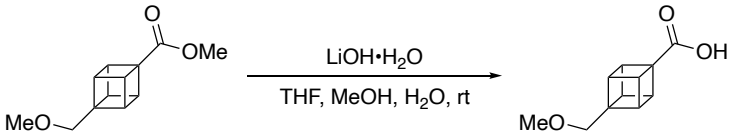

3.110 **3.111**

To a solution of methyl-4-(methoxymethyl)cubane-1-carboxylate (**3.110**) (66 mg, 1.0 equiv., 0.32 mmol) in 3:3:1 ratio of THF:MeOH:H_2O (1 mL) was added lithium hydroxide monohydrate (34 mg, 2.5 equiv., 0.8 mmol) in one-portion at rt. The mixture was allowed to stir at rt overnight. The mixture was diluted with 1 M $NaOH_{(aq)}$ (2 mL) and the aqueous layer was washed with EtOAc (2 x 10 mL). The aqueous layer was acidified with 2 M $HCl_{(aq)}$, and the aqueous layer was extracted with EtOAc (3 x 10 mL). The combined organic layers were washed sat. brine$_{(aq)}$ (10 mL), dried with anhydrous $MgSO_4$, filtered, and concentrated *in vacuo* to afford the title compound **3.111** (36 mg, 59 %) as a cream solid.

^{1}H NMR (400 MHz, $CDCl_3$) δ 4.23 – 4.16 (m, 3H), 3.93 – 3.86 (m, 3H), 3.54 (s, 2H), 3.38 (s, 3H); **^{13}C NMR** (101 MHz, $CDCl_3$) δ 178.4, 73.1, 59.4, 57.7, 56.1, 46.7, 45.3; **HRMS (ESI$^-$)** m/z: $[M-H]^-$ Calcd. for $C_{11}H_{11}O_3$ 191.0713; Found 191.0710.

_N_-Methoxy-4-(methoxymethyl)-_N_-methylcubane-1-carboxamide (3.112)

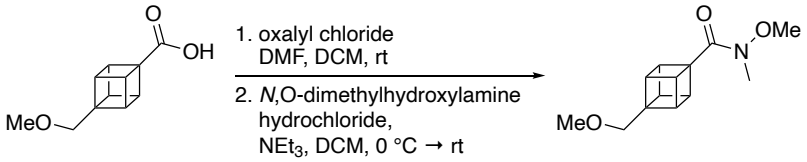

3.111 **3.112**

To a solution of 4-(methoxymethyl)cubane-1-carboxylic acid (**3.111**) (137 mg, 1.0 equiv., 0.71 mmol) in anhydrous DCM (3 mL) was added oxalyl chloride (0.61 mL, 1.7 equiv., 2 M in DCM) at rt. Anhydrous DMF (6 mL, 10 mol %) was then added and the reaction mixture was allowed to stir at rt for 1.5 hours. The mixture was concentrated *in vacuo* to afford the acid chloride as a yellow solid.

The acid chloride was dissolved in anhydrous DCM (1.5 mL) and added dropwise to a solution of *N*,O-dimethylhydroxylamine hydrochloride (117 mg, 1.7 equiv., 1.20 mmol) and triethylamine (0.33 mL, 3.4 equiv., 2.41 mmol) in anhydrous DCM (1.5 mL) at 0 °C. The mixture was warmed to rt and stirred for 2 hours. The mixture was quenched with sat. $NH_4Cl_{(aq)}$ (5 mL) and diluted with DCM (10 mL). The organic layer was washed with 1 M $HCl_{(aq)}$ (10 mL), sat. $brine_{(aq)}$ (10 mL), dried with anhydrous $MgSO_4$, and concentrated *in vacuo* to afford the crude. Purification by silica gel column chromatography (1:1 EtOAc/petroleum ether) gave the title compound **3.112** (93 mg, 55 %) as a white solid.

^{1}H NMR (400 MHz, $CDCl_3$) δ 4.19 – 4.08 (m, 3H), 3.87 – 3.77 (m, 3H), 3.66 (s, 3H), 3.50 (s, 2H), 3.34 (s, 3H), 3.14 (s, 3H); **^{13}C NMR** (101 MHz, $CDCl_3$) δ 173.8, 73.2, 61.6, 59.3, 58.1, 57.0, 46.7, 45.1, 32.7; **HRMS (EI$^+$)** m/z: $[M\text{-}OMe]^+$ Calcd. for $C_{12}H_{14}O_2N$ 204.1019; Found 204.1016.

1-(4-(Methoxymethyl)cuban-1-yl)-2-methylpropan-1-one (3.91i)

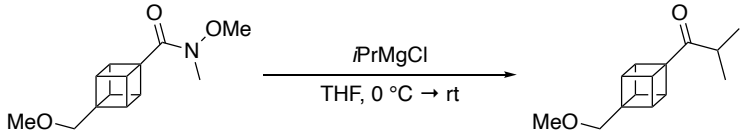

3.112 **3.91i**

To a solution of *N*-methoxy-4-(methoxymethyl)-*N*-methylcubane-1-carboxamide (**3.112**) (93 mg, 1.0 equiv., 0.40 mmol) in anhydrous THF (2.5 mL) at 0 °C was added isopropylmagnesium chloride (0.6 mL, 3.0 equiv., 2 M in THF) dropwise. The mixture was stirred at 0 °C for 5 minutes and allowed to warm to rt. After 2.5 hours, the mixture was

quenched with 1 M $HCl_{(aq)}$ (5 mL) at 0 °C. The aqueous was extracted with EtOAc (3 x 10 mL) and the combined organic layers were washed with sat. $brine_{(aq)}$ (10 mL), dried with anhydrous $MgSO_4$, filtered, and concentrated *in vacuo* to afford the crude. Purification by silica gel column chromatography (15:85 EtOAc/petroleum ether) gave the title compound **3.91i** (64 mg, 74 %) as a colourless oil.

^{1}H NMR (400 MHz, $CDCl_3$) δ 4.23 – 4.14 (m, 3H), 3.91 – 3.82 (m, 3H), 3.54 (s, 2H), 3.38 (s, 3H), 2.79 (hept, *J* = 6.9 Hz, 1H), 1.09 (d, *J* = 6.9 Hz, 6H); **^{13}C NMR** (101 MHz, $CDCl_3$) δ 212.5, 73.2, 63.7, 59.4, 57.6, 47.4, 44.9, 37.6, 18.1; **HRMS (EI$^+$)** m/z: $[M]^{+\bullet}$ Calcd. for $C_{14}H_{18}O_2$ 218.1301; Found 218.1296.

5.3.1.5 Synthesis of 3.91j Methyl-4-(diisopropylcarbamoyl)cubane-1-carboxylate (3.113)

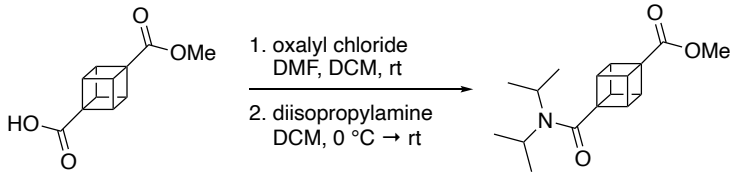

2.8 **3.113**

To a solution of the commercially available 4-(methoxycarbonyl)cubane-1-carboxylic acid (**2.8**) (300 mg, 1.0 equiv., 1.45 mmol) in anhydrous DCM (5mL) was added oxalyl chloride (1.24 mL, 1.7 equiv., 2 M in DCM) at rt. Anhydrous DMF (12 mL, 10 mol %) was then added and the reaction mixture was allowed to stir at rt for 1.5 hours. The mixture was concentrated *in vacuo* to afford the acid chloride as a yellow solid.

The acid chloride was dissolved in anhydrous DCM (2.5 mL) and added dropwise to a solution of diisopropylamine (0.51 mL, 2.5 equiv., 3.63 mmol) in anhydrous DCM (2.5 mL) at 0 °C. The mixture was warmed to rt and stirred for 4.5 hours. The mixture was quenched with sat. $NH_4Cl_{(aq)}$ (5 mL) and diluted with DCM (10 mL). The organic layer was washed with 1 M $HCl_{(aq)}$ (10 mL), sat. $brine_{(aq)}$ (10 mL), dried with anhydrous $MgSO_4$, filtered and concentrated *in vacuo* to afford the title compound **3.113** (401 mg, 95 %) as a yellow solid.

^{1}H NMR (400 MHz, $CDCl_3$) δ 4.23 – 4.14 (m, 6H), 3.70 (s, 3H), 3.46 (hept, *J* = 6.6 Hz, 1H), 3.30 (hept, *J* = 6.8 Hz, 1H), 1.41 (d, *J* = 6.8 Hz, 6H), 1.20 (d, *J* = 6.6 Hz, 6H); **HRMS (EI$^+$)**

m/z: $[M]^{+\bullet}$ Calcd. for $C_{17}H_{23}O_3N$ 289.1673; Found 289.1665. All spectroscopic data were in accordance with the literature.[164]

4-(Diisopropylcarbamoyl)cubane-1-carboxylic acid (3.114)

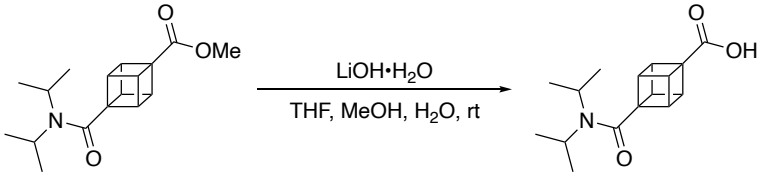

3.113 **3.114**

To a solution of methyl-4-(diisopropylcarbamoyl)cubane-1-carboxylate (**3.113**) (401 mg, 1.0 equiv., 1.39 mmol) in 3:3:1 ratio of THF:MeOH:H_2O (4.1 mL) was added lithium hydroxide monohydrate (69 mg, 1.2 equiv., 1.64 mmol) in one-portion at rt. The mixture was allowed to stir at rt for 4 hours. The mixture was diluted with 1 M $NaOH_{(aq)}$ (2 mL) and the aqueous layer was washed with EtOAc (2 x 10 mL). The aqueous layer was acidified with 2 M $HCl_{(aq)}$, and the aqueous layer was extracted with EtOAc (3 x 15 mL). The combined organic layers were washed sat. $brine_{(aq)}$ (15 mL), dried with anhydrous $MgSO_4$, filtered, and concentrated *in vacuo* to afford the title compound **3.114** (335 mg, 88 %) as a white solid.

^{1}H NMR (400 MHz, $CDCl_3$) δ 10.83 (br s, 1H), 4.26 – 4.14 (m, 6H), 3.46 (hept, *J* = 6.7 Hz, 1H), 3.31 (hept, *J* = 6.9 Hz, 1H), 1.40 (d, *J* = 6.9 Hz, 6H), 1.20 (d, *J* = 6.7 Hz, 6H); **HRMS (ESI$^+$)** m/z: $[M+H]^+$ Calcd. for $C_{16}H_{22}NO_3$ 276.1594; Found 276.1600. All spectroscopic data were in accordance with the literature.[164]

***N*^{1},*N*^{1}-Diisopropyl-*N*^{4}-methoxy-*N*^{4}-methylcubane-1,4-dicarboxamide (3.115)**

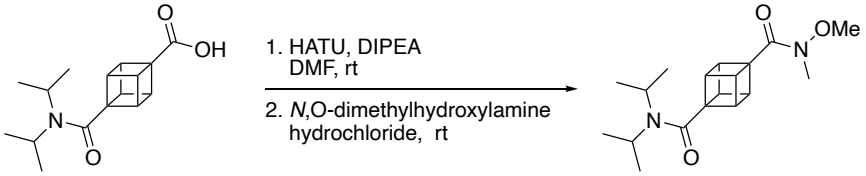

3.114 **3.115**

To a solution of 4-(diisopropylcarbamoyl)cubane-1-carboxylic acid (**3.114**) (335 mg, 1.0 equiv., 1.22 mmol) and HATU (560 mg, 1.2 equiv., 1.47 mmol) in anhydrous DMF (10 mL) was added *N*,*N*-diisopropylethylamine (DIPEA) (0.72 mL, 3.4 equiv., 4.2 mmol) at rt. After 5 minutes, *N*,O-dimethylhydroxylamine hydrochloride (144 mg, 1.2 equiv., 1.48

mmol) was added in one portion and the reaction mixture was allowed to stir at rt for 2 hours. The mixture was quenched with H_2O (3 mL) and diluted with EtOAc (20 mL). The organic layer was washed with H_2O (3 x 15 mL), sat. $brine_{(aq)}$ (15 mL), dried with anhydrous $MgSO_4$, filtered, and concentrated *in vacuo* to afford the crude. Purification by silica gel column chromatography (70:30 EtOAc/petroleum ether) gave the title compound **3.115** (309 mg, 80 %) as a white solid.

^{1}H NMR (500 MHz, $CDCl_3$) δ 4.21 – 4.15 (m, 3H), 4.15 – 4.09 (m, 3H), 3.68 (s, 3H), 3.47 (hept, *J* = 6.6 Hz, 1H), 3.28 (hept, *J* = 6.8 Hz, 1H), 3.16 (s, 3H), 1.38 (d, *J* = 6.8 Hz, 6H), 1.18 (d, *J* = 6.6 Hz, 6H); **^{13}C NMR** (126 MHz, $CDCl_3$) δ 173.2, 170.5, 61.8, 58.9, 56.5, 48.5, 46.9, 46.4, 45.9, 32.6, 21.1, 20.6; **HRMS (ESI$^+$)** m/z: $[M+H]^+$ Calcd. for $C_{18}H_{27}N_2O_3$ 319.2016; Found 319.2017.

4-Isobutyryl-*N*,*N*-diisopropylcubane-1-carboxamide (3.91j)

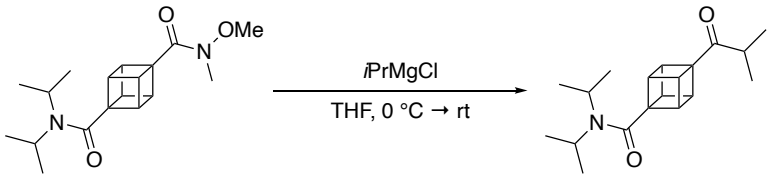

3.115 **3.91j**

To a solution of *N*^{1},*N*^{1}-diisopropyl-*N*^{4}-methoxy-*N*^{4}-methylcubane-1,4-dicarboxamide (**3.115**) (280 mg, 1.0 equiv., 0.88 mmol) in anhydrous THF (5 mL) at 0 °C was added isopropylmagnesium chloride (1.32 mL, 3.0 equiv., 2 M in THF) dropwise. The mixture was stirred at 0 °C for 5 minutes and allowed to warm to rt. After 1.5 hours, the mixture was quenched with 1 M $HCl_{(aq)}$ (5 mL) at 0 °C. The aqueous was extracted with EtOAc (3 x 10 mL) and the combined organic layers were washed with sat. $brine_{(aq)}$ (10 mL), dried with anhydrous $MgSO_4$, filtered and concentrated *in vacuo* to afford the crude. Purification by silica gel column chromatography (1:3 EtOAc/petroleum ether) gave the title compound **3.91j** (142 mg, 47 %) as a white solid.

^{1}H NMR (400 MHz, $CDCl_3$) δ 4.25 – 4.18 (m, 3H), 4.18 – 4.12 (m, 3H), 3.47 (hept, *J* = 6.6 Hz, 1H), 3.30 (hept, *J* = 6.8 Hz, 1H), 2.78 (hept, *J* = 6.9 Hz, 1H), 1.40 (d, *J* = 6.8 Hz, 6H), 1.19 (d, *J* = 6.6 Hz, 6H), 1.09 (d, *J* = 6.9 Hz, 6H); **^{13}C NMR** (101 MHz, $CDCl_3$) δ 211.9, 170.2, 61.9, 59.4, 48.6, 46.9, 46.7, 46.0, 37.7, 21.1, 20.6, 18.0; **HRMS (ESI$^+$)** m/z: $[M+H]^+$ Calcd. for $C_{19}H_{28}NO_2$ 302.2115; Found 302.2122.

5.3.1.6 Synthesis of 3.91k

Methyl-4-(bromocarbonyl)cubane-1-carboxylate (3.116)

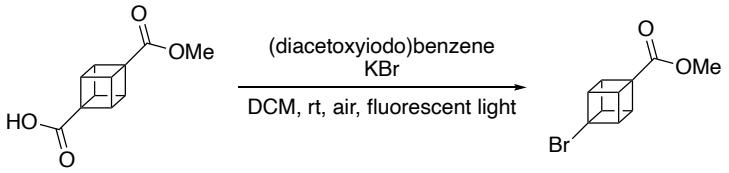

2.8 **3.116**

Following the procedure of Watanabe and co-workers.[277] To a solution of the commercially available 4-(methoxycarbonyl)cubane-1-carboxylic acid (**2.8**) (300 mg, 1.0 equiv., 1.45 mmol) and (diacetoxyiodo)benzene (701 mg,1.5 equiv., 2.18 mmol) in anhydrous DCM (2.9 mL) was added potassium bromide (310 mg, 1.8 equiv., 2.61 mmol) at rt under air in the presence of the standard fluorescent light fitting in the fume hood. After 24 hours the reaction mixture was filtered through a pad of celite and the solid was washed with DCM (15 mL) and the filtrate was concentrated *in vacuo* to afford the crude. Purification by silica gel column chromatography (02:98 EtOAc/petroleum ether) gave the title compound **3.116** (167 mg, 48 %) as a white solid.

^{1}H NMR (300 MHz, $CDCl_3$) δ 4.35 – 4.28 (m, 3H), 4.28 – 4.20 (m, 3H), 3.70 (s, 3H); **HRMS (EI$^+$)** m/z: $[M\text{-}OMe]^+$ Calcd. for $C_9H_6O^{79}Br$ 208.9597; Found 208.9593. All spectroscopic data were in accordance with the literature.[277]

4-Bromocubane-1-carboxylic acid (3.117)

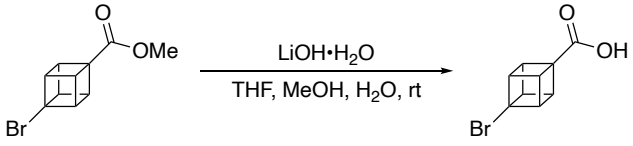

3.116 **3.117**

To a solution of methyl-4-(bromocarbonyl)cubane-1-carboxylate (**3.116**) (150 mg, 1.0 equiv., 0.62 mmol) in 3:3:1 ratio of THF:MeOH:H_2O (1 mL) was added lithium hydroxide monohydrate (65 mg, 2.5 equiv., 1.55 mmol) in one-portion at rt. The mixture was allowed to stir at rt overnight. The mixture was diluted with H_2O (5 mL) and the aqueous layer was washed with EtOAc (10 mL). The aqueous layer was acidified with 2 M $HCl_{(aq)}$, and the aqueous layer was extracted with EtOAc (3 x 10 mL). The combined organic layers were washed sat. $brine_{(aq)}$ (10 mL), dried with anhydrous $MgSO_4$, filtered, and

concentrated *in vacuo* to afford the crude. The solid was washed with hexane (3 x 5 mL) to afford the title compound **3.117** (131 mg, 93 %) as a white solid.

^{1}H NMR (400 MHz, $CDCl_3$) δ 4.40 – 4.32 (m, 3H), 4.32 – 4.24 (m, 3H); **HRMS (ESI$^+$)** m/z: $[M+H]^+$ Calcd. for $C_9H_8O_2{}^{79}Br$ 226.9702; Found 226.9710. All spectroscopic data were in accordance with the literature.[295]

4-Bromo-N-methoxy-N-methylcubane-1-carboxamide (3.118)

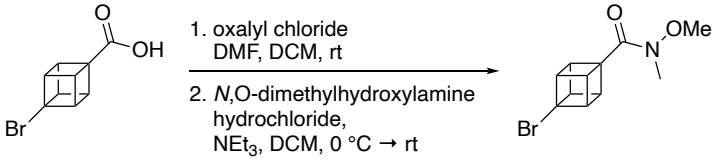

3.117 **3.118**

To a solution of 4-bromocubane-1-carboxylic acid (**3.117**) (125 mg, 1.0 equiv., 0.55 mmol) in anhydrous DCM (3 mL) was added oxalyl chloride (0.47 mL, 1.7 equiv., 2 M in DCM) at rt. Anhydrous DMF (5 mL, 10 mol %) was then added and the reaction mixture was allowed to stir at rt for 1.5 hours. The mixture was concentrated *in vacuo* to afford the acid chloride as a yellow solid.

The acid chloride was dissolved in anhydrous DCM (1.5 mL) and added dropwise to a solution of *N*,O-dimethylhydroxylamine hydrochloride (86 mg, 1.6 equiv., 0.88 mmol) and triethylamine (0.24 mL, 3.2 equiv., 1.76 mmol) in anhydrous DCM (1.5 mL) at 0 °C. The mixture was warmed to rt and stirred for 2.5 hours. The mixture was quenched with sat. $NH_4Cl_{(aq)}$ (5 mL) and diluted with DCM (10 mL). The organic layer was washed with 1 M $HCl_{(aq)}$ (10 mL), sat. $brine_{(aq)}$ (10 mL), dried with anhydrous $MgSO_4$, filtered and concentrated *in vacuo* to afford the crude. Purification by silica gel column chromatography (1:3 EtOAc/petroleum ether) gave the title compound **3.118** (93 mg, 62 %) as a white solid.

^{1}H NMR (400 MHz, $CDCl_3$) δ 4.37 – 4.28 (m, 3H), 4.26 – 4.19 (m, 3H), 3.69 (s, 3H), 3.17 (s, 3H); **^{13}C NMR** (101 MHz, $CDCl_3$) δ 172.6, 63.3, 61.7, 58.1, 54.7, 47.9, 32.6; **HRMS (ESI$^+$)** m/z: $[M+H]^+$ Calcd. for $C_{11}H_{13}NO_2{}^{79}Br$ 270.0124; Found 270.0133.

1-(4-Bromocuban-1-yl)-2-methylpropan-1-one (3.91k)

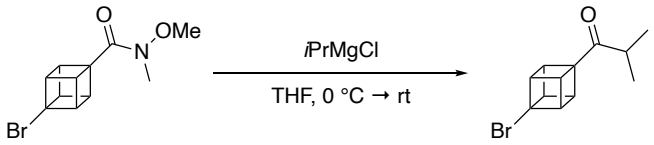

3.118 **3.91k**

To a solution of 4-bromo-*N*-methoxy-*N*-methylcubane-1-carboxamide (**3.118**) (93 mg, 1.0 equiv., 0.34 mmol) in anhydrous THF (3 mL) at 0 °C was added isopropylmagnesium chloride (0.52 mL, 3.0 equiv., 2 M in THF) dropwise. The mixture was stirred at 0 °C for 5 minutes and allowed to warm to rt. After 1.5 hours, the mixture was quenched with 1 M $HCl_{(aq)}$ (5 mL) at 0 °C. The aqueous was extracted with EtOAc (3 x 10 mL) and the combined organic layers were washed with sat. $brine_{(aq)}$ (10 mL), dried with anhydrous $MgSO_4$, filtered and concentrated *in vacuo* to afford the crude. Purification by silica gel column chromatography (03:97 EtOAc/petroleum ether) gave the title compound **3.91k** (59 mg, 68 %) as a colourless oil.

^{1}H NMR (500 MHz, $CDCl_3$) δ 4.35 – 4.30 (m, 3H), 4.27 – 4.18 (m, 3H), 2.74 (hept, *J* = 6.9 Hz, 1H), 1.07 (d, *J* = 6.9 Hz, 6H); **^{13}C NMR** (126 MHz, $CDCl_3$) δ 211.4, 63.3, 63.2, 54.3, 48.3, 37.8, 18.0; **HRMS (ESI$^+$)** m/z: $[M+H]^+$ Calcd. for $C_{12}H_{14}O^{79}Br$ 253.0223; Found 253.0231.

5.3.1.7 Synthesis of 3.91l

*Experimental procedure and analytical data for **3.99** was previously described in **Section 5.3.1.2**.*

Methyl-4-fluorocubane-1-carboxylate (3.119)

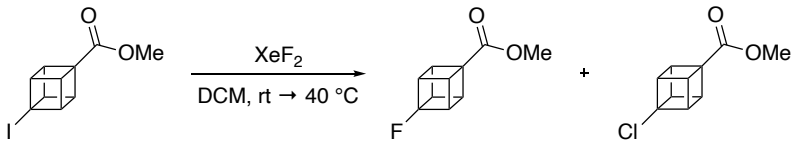

3.99 **3.119** **3.120**

Following the procedure of Della and Head.[278] To a solution of methyl-4-iodocubane-1-carboxylate (**3.99**) (150 mg, 1.0 equiv., 0.52 mmol) in anhydrous DCM (3.5 mL) was added xenon difluoride (130 mg, 1.5 equiv., 0.78 mmol) in two portions at rt. The mixture was heated to 40 °C for 6 hours behind a blast shield. After cooling to rt, the mixture was carefully quenched by dropwise addition of 1 M $sodium\ thiosulfate_{(aq)}$ (5 mL),

followed by the addition of sat. $NaHCO_{3(aq)}$ (1 mL). The aqueous layer was extracted with DCM (1 x 15 mL), followed by the organic layer being washed with $NaHCO_{3(aq)}$ (2 x 5 mL), dried with anhydrous $MgSO_4$, filtered and concentrated *in vacuo* to afford the crude. *The reaction was repeated a further three times on the same scale and the crude for each was combined for the purification step.* ***Note:*** *^{1}H NMR of the combined crude material had a ratio of* ***3.119*** *:* ***3.120*** *:* ***3.99*** *of 4:1:1 before purification.* Purification by silica gel column chromatography (02:98 EtOAc: petroleum ether) gave a mixture of **3.119** : **3.120** : **3.99** in a ratio of 13:1:1 (142 mg, 38 %) as a white solid.

3.119 **^{1}H NMR** (500 MHz, $CDCl_3$) δ 4.34 – 4.28 (m, 3H), 4.11 – 4.00 (m, 3H), 3.70 (s, 3H); **^{19}F{^{1}H}NMR** (471 MHz, $CDCl_3$) δ -140.36; **^{13}C NMR** (126 MHz, $CDCl_3$) δ 172.5 (d, *J* = 7.2 Hz), 103.0 (d, *J* = 328.1 Hz), 56.7 (d, *J* = 13.8 Hz), 54.2 (d, *J* = 25.5 Hz), 51.7, 42.4 (d, *J* = 5.5 Hz); **HRMS (EI$^+$)** m/z: $[M\text{-}OMe]^+$ Calcd. for C_9H_6OF 149.0397; Found 149.0396.

Towards the synthesis of **3.91l** compound **3.120** was synthesised and fully characterised following an adapted procedure of Candish and co-workers:[296]

Methyl-4-chlorocubane-1-carboxylate (3.120)

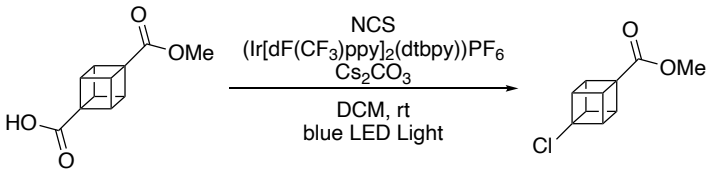

2.8 **3.120**

N_2 gas was bubbled through a solution of the commercially available 4-(methoxycarbonyl)cubane-1-carboxylic acid (**2.8**) (50 mg, 1.0 equiv., 0.24 mmol), $(Ir[dF(CF_3)ppy]_2(dtbpy))PF_6$ (4.9 mg, 2 mol %), *N*-chlorosuccinimide (64 mg, 2.0 equiv., 0.48 mmol), cesium carbonate (78 mg, 1.0 equiv., 0.24 mmol) in anhydrous DCM (4.8 mL) for 5 minutes. The reaction mixture was then stirred at rt for 16 hours whilst being irradiated with blue LED light (Aldrich® micro photochemical reactor blue LED (ALDKIT001) was used as the blue LED light source). The reaction mixture was filtered through a pad of celite and the solid was washed with DCM (15 mL) and the filtrate was concentrated *in vacuo* to afford the crude. Purification by silica gel column chromatography (05:95 EtOAc/petroleum ether) gave the title compound **3.120** (13 mg, 28 %) as a white solid.

^{1}H NMR (500 MHz, $CDCl_3$) δ 4.25 – 4.20 (m, 3H), 4.19 – 4.12 (m, 3H), 3.71 (s, 3H); **^{13}C NMR** (126 MHz, $CDCl_3$) δ 172.1, 72.2, 56.5, 54.2, 51.8, 46.0; **HRMS (EI$^+$)** m/z: $[M\text{-}OMe]^+$ Calcd. for C_9H_6OCl 165.0102; Found 165.0100.All spectroscopic data were in accordance with the literature.[106, 295]

4-Fluorocubane-1-carboxylic acid (3.121)

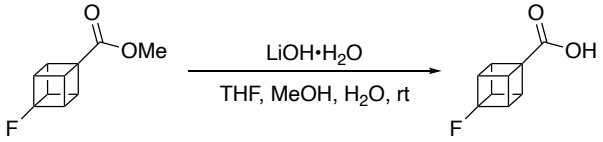

3.119 **3.121**

To a mixture of **3.119 : 3.120 : 3.99** in a ratio of 13:1:1 (142 mg, 1.0 equiv., 0.79 mmol) in 3:3:1 ratio of THF:MeOH:H_2O (1 mL) was added lithium hydroxide monohydrate (83 mg, 2.5 equiv., 1.97 mmol) in one-portion at rt. The mixture was allowed to stir at rt overnight. The aqueous layer was acidified with 2 M $HCl_{(aq)}$, and the aqueous layer was extracted with EtOAc (3 x 10 mL). The combined organic layers were washed sat. $brine_{(aq)}$ (10 mL), dried with anhydrous $MgSO_4$, filtered and concentrated *in vacuo* to afford the title compound **3.121** (123 mg, 94 %) as a white solid.

^{1}H NMR (400 MHz, $CDCl_3$) δ 11.39 (s, 1H), 4.39 – 4.29 (m, 3H), 4.15 – 4.06 (m, 3H); **^{19}F{^{1}H}NMR** (376 MHz, $CDCl_3$) δ -140.41; **^{13}C NMR** (101 MHz, $CDCl_3$) δ 178.6 (d, *J* = 7.2 Hz), 102.8 (d, *J* = 328.1 Hz), 56.4 (d, *J* = 13.7 Hz), 54.1 (d, *J* = 25.7 Hz), 42.4 (d, *J* = 5.5 Hz); **HRMS (EI$^+$)** m/z: $[M]^{+\bullet}$ Calcd. for $C_9H_7O_2F$ 166.0425; Found 166.0421.

***Note:** ^{1}H NMR shows that the product contains 9% of 4-chlorocubane-1-carboxylic acid and 6% of 4-iodocubane-1-carboxylic acid.*

4-Fluoro-*N*-methoxy-*N*-methylcubane-1-carboxamide (3.122)

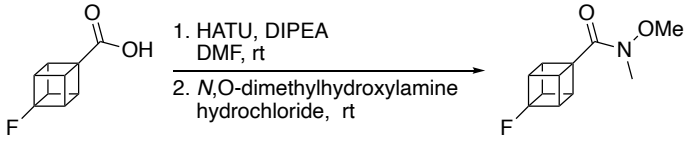

3.121 **3.122**

To a solution of 4-fluorocubane-1-carboxylic acid (**3.121**) (119 mg, 1.0 equiv., 0.72 mmol) and HATU (326 mg, 1.2 equiv., 0.86 mmol) in anhydrous DMF (5 mL) was added *N*,*N*-diisopropylethylamine (DIPEA) (0.43 mL, 3.5 equiv., 2.52 mmol) at rt. After 5 minutes, *N*,O-dimethylhydroxylamine hydrochloride (83 mg, 1.2 equiv., 0.86 mmol) was

added in one portion and the reaction mixture was allowed to stir at rt for 2 hours. The mixture was quenched with H_2O (3 mL) and diluted with EtOAc (20 mL). The organic layer was washed with H_2O (3 x 15 mL), sat. $brine_{(aq)}$ (15 mL), dried with anhydrous $MgSO_4$, filtered and concentrated *in vacuo* to afford the crude. Purification by silica gel column chromatography (30:70 EtOAc/petroleum ether) gave the title compound **3.122** (93 mg, 62 %) as a cream solid.

^{1}H NMR (500 MHz, $CDCl_3$) δ 4.30fh – 4.22 (m, 3H), 4.08 – 4.02 (m, 3H), 3.68 (s, 3H), 3.15z (s, 3H); **^{19}F{^{1}H}NMR** (471 MHz, $CDCl_3$) δ -141.11; **^{13}C NMR** (126 MHz, $CDCl_3$) δ 173.3, 102.8 (d, *J* = 328.3 Hz), 61.8, 58.5 (d, *J* = 14.6 Hz), 54.0 (d, *J* = 25.2 Hz), 42.5 (d, *J* = 5.5 Hz), 32.7; **HRMS (EI$^+$)** m/z: $[M\text{-}OMe]^+$ Calcd. for $C_{10}H_9FNO$ 178.0663; Found 178.0661.

Note: *^{1}H NMR shows that the product contains 6% of 4-chloro-N-methoxy-N-methylcubane-1-carboxamide and 2% of 4-iodo-N-methoxy-N-methylcubane-1-carboxamide.*

1-(4-Fluorocuban-1-yl)-2-methylpropan-1-one (3.91l)

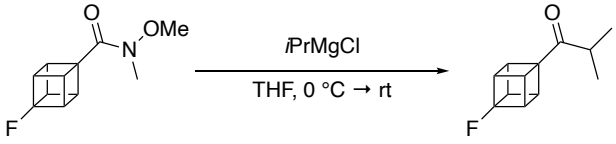

3.122 **3.91l**

To a solution of 4-fluoro-*N*-methoxy-*N*-methylcubane-1-carboxamide (**3.122**) (88 mg, 1.0 equiv., 0.42 mmol) in anhydrous THF (2.5 mL) at 0 °C was added isopropylmagnesium chloride (0.63 mL, 3.0 equiv., 2 M in THF) dropwise. The mixture was stirred at 0 °C for 5 minutes and allowed to warm to rt. After 2 hours, the mixture was quenched with 1 M $HCl_{(aq)}$ (5 mL) at 0 °C. The aqueous was extracted with EtOAc (3 x 10 mL) and the combined organic layers were washed with sat. $brine_{(aq)}$ (10 mL), dried with anhydrous $MgSO_4$, filtered and concentrated *in vacuo* to afford the crude orange solid. Purification by silica gel column chromatography (02:98 EtOAc/petroleum ether) gave the title compound **3.91l** (61 mg, 75 %) as a white solid.

^{1}H NMR (400 MHz, $CDCl_3$) δ 4.35 – 4.27 (m, 3H), 4.12 – 4.04 (m, 3H), 2.76 (hept, *J* = 6.9 Hz, 1H), 1.09 (d, *J* = 6.9 Hz, 6H); **^{19}F{^{1}H}NMR** (376 MHz, $CDCl_3$) δ -140.25; **^{13}C NMR** (101 MHz, $CDCl_3$) δ 212.2 (d, *J* = 6.3 Hz), 102.8 (d, *J* = 329.0 Hz), 63.9 (d, *J* = 13.3 Hz), 53.8 (d, *J*

= 25.4 Hz), 43.0 (d, *J* = 5.5 Hz), 37.8, 18.0; **HRMS (EI$^+$)** m/z: $[M]^{+\bullet}$ Calcd. for $C_{12}H_{13}OF$ 192.0945; Found 192.0942.

Note: *^{1}H NMR shows that the product contains 6% of 4-chloro-N-methoxy-N-methylcubane-1-carboxamide*

5.3.2 Baeyer-Villiger studies

5.3.2.1 Baeyer-Villiger general procedure

A 3 mL reaction vial was charged with cubane carbonyl (1.0 eq., 0.2 mmol), scandium (III) triflate (10 mg, 0.1 eq., 0.02 mmol) and 3-chloroperbenzoic acid (172 mg, 4.0 equiv., 0.77 mmol) and then flushed with N_2. The mixture was dissolved in anhydrous chloroform (2 mL) and stirred at 50 °C for 6 hours. After cooling to rt, the reaction mixture was quenched with sodium bisulfite (0.5 mL).

Workup 1: The reaction mixture was diluted with DCM (5 mL) and the organic layer was washed further with sodium bisulfite (10 mL). The aqueous layer was then re-extracted with DCM (3 x 5 mL) and the combined organic layers were dried with anhydrous $MgSO_4$, filtered and concentrated *in vacuo* to afford the crude. By ^{1}H NMR ($CDCl_3$) the crude material contains 3-chlorobenzoic acid as a by-product (highlighted in blue).

Workup 2: The crude from workup 1 was dissolved in DCM (15 mL) and washed with sat. $NaHCO_3$ (3 x 5 mL), dried with anhydrous $MgSO_4$, filtered, and concentrated *in vacuo* to afford the crude. The entire sample of the crude was dissolved in $CDCl_3$ (0.7 mL), added to a known mass of 1,2,4,5-tetramethylbenzene (internal standard) and transferred to an NMR tube for ^{1}H NMR ($CDCl_3$) analysis to determine % yield of products and unreacted starting material. By ^{1}H NMR the crude material will contain the internal standard (highlighted in red).

$$\%\, Yield = \frac{nIS * (rP/rIS)}{nSM}$$

Where:
P = Product
*n*IS = mmol of internal standard (1,2,4,5-tetramethylbenzene)
*n*SM = mmol of cubane starting material

$$rP/rIS = \frac{Integral\ of\ P\ /\ no.of\ protons}{Integral\ of\ IS\ /\ no.of\ protons}$$

5.3.2.2 Baeyer-Villiger substrate scope

Baeyer-Villiger of phenyl(4-phenylcuban-1-yl)methanone (3.91a)

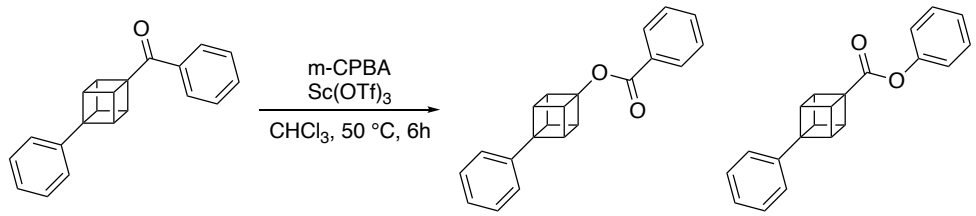

3.91a **3.94a** **3.95a**

The reaction was performed using the **general procedure** with phenyl(4-phenylcuban-1-yl)methanone (**3.91a**) (57 mg, 1.0 eq., 0.20 mmol), scandium (III) triflate (10.1 mg, 0.1 eq., 0.02 mmol), 3-chloroperbenzoic acid (170 mg, 4.0 equiv., 0.73 mmol) and $CHCl_3$ (2.0 mL). Purification by silica column chromatography (30:70 DCM/petroleum ether → 50:50 DCM/petroleum ether) gave the title compound **3.94a** (35 mg, 58 %) as a white solid.

^{1}H NMR (500 MHz, $CDCl_3$) δ 8.13 – 8.08 (m, 2H), 7.64 – 7.57 (m, 1H), 7.52 – 7.45 (m, 2H), 7.43 – 7.36 (m, 2H), 7.29 – 7.20 (m, 3H), 4.47 – 4.38 (m, 3H), 4.20 – 4.11 (m, 3H); **^{13}C NMR** (126 MHz, $CDCl_3$) δ 165.2, 142.6, 133.3, 129.9, 129.8, 128.6, 128.6, 126.2, 124.9, 89.2, 60.1, 51.6, 45.9; **HRMS (EI$^+$)** m/z: $[M\text{-}C_7H_5O]^+$ Calcd. for $C_{14}H_{11}O$ 195.0804; Found 195.0804.

Note: *The isolated yield of **3.95a** was not determined as it was not found during the purification process. However, **3.95a** was synthesised separately and fully characterised:*

NMR yield of **3.91a** / %	NMR yield of **3.94a** / %	NMR yield of **3.95a** / %	Isolated yield of **3.91a** / %	Isolated yield of **3.94a** / %	Isolated yield of **3.95a** / %
13	51	3	10	58	n.d

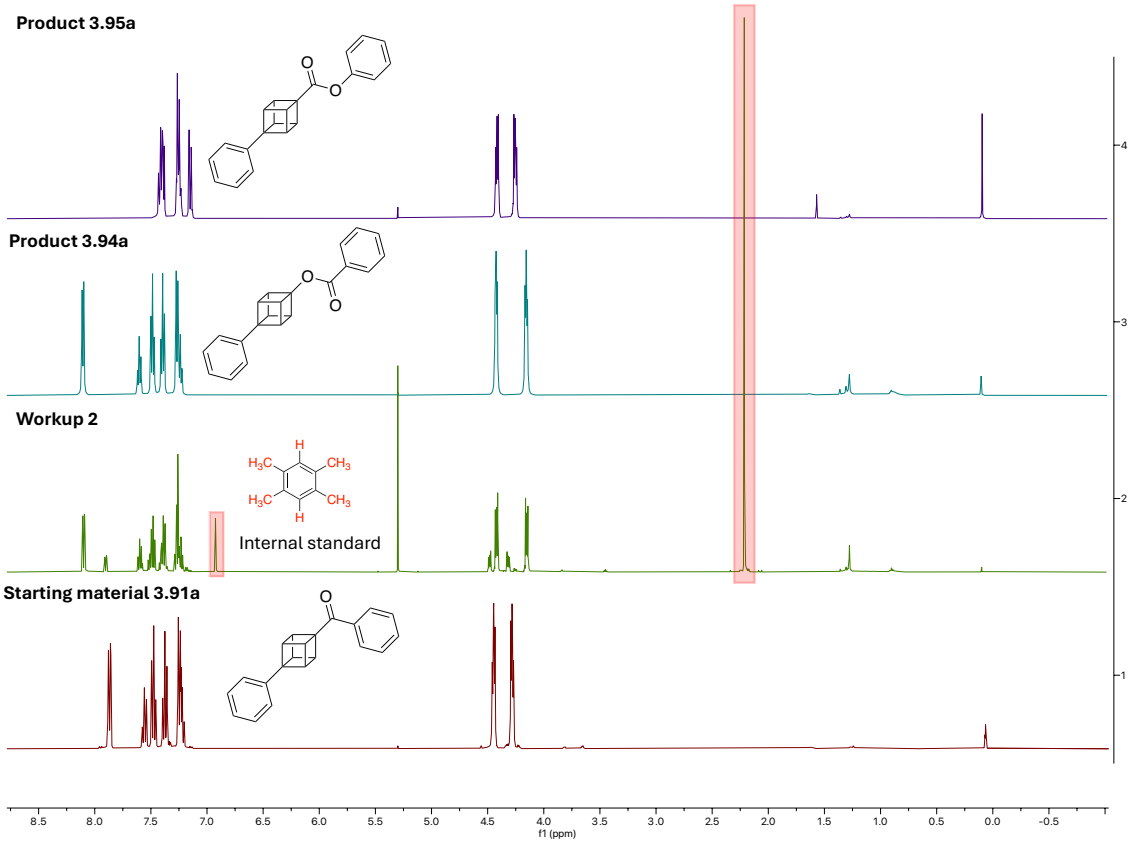

Phenyl-4-phenylcubane-1-carboxylate (3.95a)

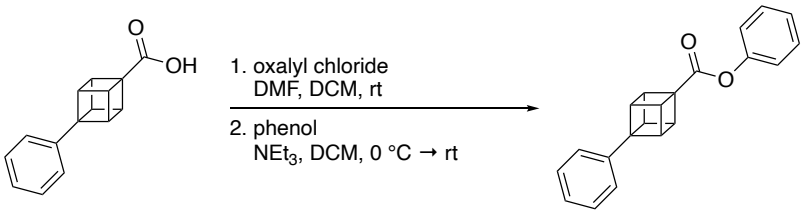

3.92 **3.95a**

To a solution of 4-phenylcubane-1-carboxylic acid (**3.92**) (100 mg, 1.0 equiv., 0.45 mmol) in anhydrous DCM (3 mL) was added oxalyl chloride (0.38 mL, 1.7 equiv., 2 M in DCM) at rt. Anhydrous DMF (4 mL, 10 mol %) was then added and the reaction mixture was allowed to stir at rt for 1.5 hours. The mixture was concentrated *in vacuo* to afford the acid chloride as a yellow solid.

The acid chloride was dissolved in anhydrous DCM (1.5 mL) and added dropwise to a solution of phenol (68 mg, 1.6 equiv., 0.72 mmol) and triethylamine (0.2 mL, 3.2 equiv., 1.44 mmol) in anhydrous DCM (1.5 mL) at 0 °C. The mixture was warmed to rt and stirred for 2.5 hours. The mixture was quenched with sat. $NH_4Cl_{(aq)}$ (5 mL) and diluted

with DCM (10 mL). The organic layer was washed with 1 M $HCl_{(aq)}$ (10 mL), sat. $brine_{(aq)}$ (10 mL), dried with anhydrous $MgSO_4$, filtered and concentrated *in vacuo* to afford the crude. Purification by silica gel column chromatography (1:9 EtOAc/petroleum ether) gave the title compound **3.95a** (128 mg, 95 %) as a white solid.

^{1}H NMR (400 MHz, $CDCl_3$) δ 7.46 – 7.35 (m, 4H), 7.29 – 7.20 (m, 4H), 7.19 – 7.11 (m, 2H), 4.46 – 4.36 (m, 3H), 4.30 – 4.21 (m, 3H); **^{13}C NMR** (101 MHz, $CDCl_3$) δ 170.7, 150.8, 142.0, 129.5, 128.6, 126.4, 125.9, 124.9, 121.7, 60.4, 56.6, 49.0, 46.4; **HRMS (ESI$^+$)** m/z: $[M+H]^+$ Calcd. for $C_{21}H_{17}O_2$ 301.1229; Found 301.1241.

Baeyer-Villiger of 1-(4-phenylcuban-1-yl)ethan-1-one (3.91b)

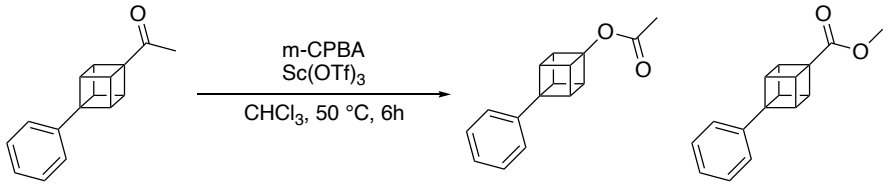

3.91b **3.94b** **3.95b**

The reaction was performed using the **general procedure** with 1-(4-phenylcuban-1-yl)ethan-1-one (**3.91b**) (45 mg, 1.0 eq., 0.2 mmol), scandium (III) triflate (10 mg, 0.1 eq., 0.02 mmol), 3-chloroperbenzoic acid (172 mg, 4.0 equiv., 0.77 mmol) and $CHCl_3$ (2 mL). Purification by silica gel column chromatography (30:70 DCM/petroleum ether) gave the title compound **3.94b** (42 mg, 86 %) as a colourless oil.

^{1}**H NMR** (400 MHz, $CDCl_3$) δ 7.41 – 7.31 (m, 2H), 7.24 – 7.17 (m, 3H), 4.33 – 4.22 (m, 3H), 4.12 – 4.00 (m, 3H), 2.12 (s, 3H); **^{13}C NMR** (101 MHz, $CDCl_3$) δ 169.6, 142.7, 128.6, 126.2, 124.9, 88.7, 60.1, 51.4, 45.8, 21.2; **HRMS** (EI$^+$) m/z: $[M]^{+\bullet}$ Calcd. for $C_{16}H_{14}O_2$ 238.0988; Found 238.0988.

NMR yield of **3.91b** / %	NMR yield of **3.94b** / %	NMR yield of **3.95b** / %	Isolated yield of **3.91b** / %	Isolated yield of **3.94b** / %	Isolated yield of **3.95b** / %
0	79	0	0	86	0

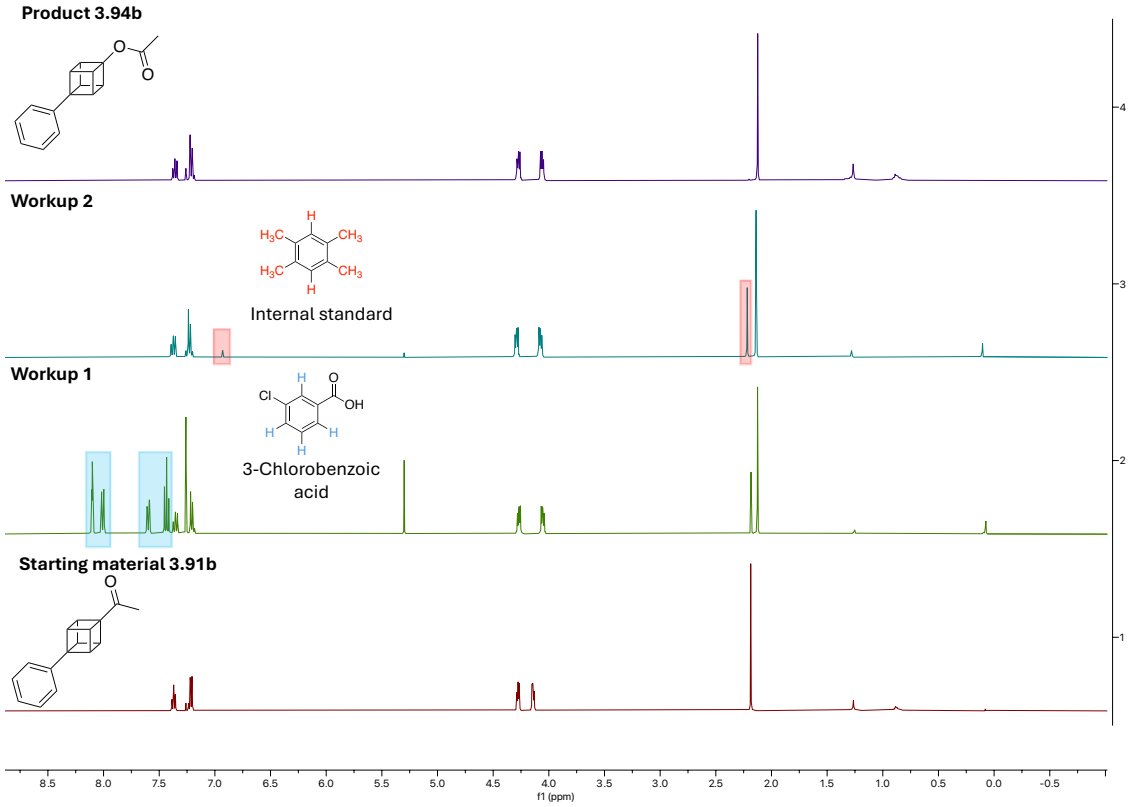

Baeyer-Villiger of 1-(4-phenylcuban-1-yl)propan-1-one (3.91c)

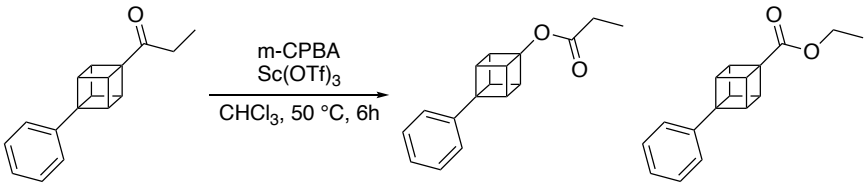

3.91c **3.94c** **3.95c**

The reaction was performed using the **general procedure** with 1-(4-phenylcuban-1-yl)propan-1-one (**3.91c**) (45 mg, 1.0 eq., 0.19 mmol), scandium (III) triflate (10 mg, 0.1 eq., 0.02 mmol), 3-chloroperbenzoic acid (163 mg, 4.0 equiv., 0.73 mmol) and $CHCl_3$ (1.9 mL). Purification by silica gel column chromatography (30:70 DCM/petroleum ether) gave the title compound **3.94c** (36 mg, 76 %) as a white solid.

^{1}H NMR (400 MHz, $CDCl_3$) δ 7.40 – 7.33 (m, 2H), 7.25 – 7.18 (m, 3H), 4.34 – 4.23 (m, 3H), 4.13 – 4.02 (m, 3H), 2.42 (q, *J* = 7.6 Hz, 2H), 1.19 (t, *J* = 7.6 Hz, 3H); **^{13}C NMR** (101 MHz, $CDCl_3$) δ 173.1, 142.6, 128.5, 126.1, 124.9, 88.7, 60.1, 51.4, 45.7, 27.6, 9.0; **HRMS** (Cl^+) m/z: $[M-H]^+$ Calcd. for $C_{17}H_{15}O_2$ 251.1067; Found 251.1065.

NMR yield of **3.91c** / %	NMR yield of **3.94c** / %	NMR yield of **3.95c** / %	Isolated yield of **3.91c** / %	Isolated yield of **3.94c** / %	Isolated yield of **3.95c** / %
0	87	0	0	76	0

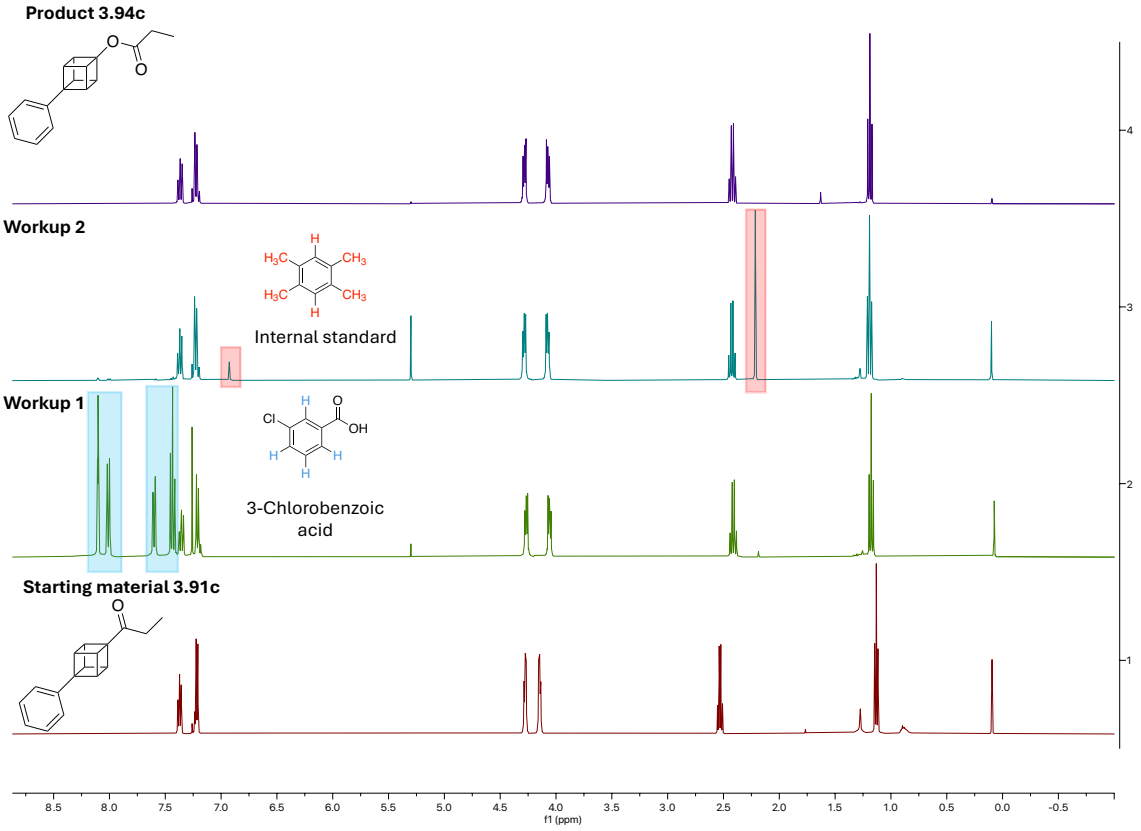

Baeyer-Villiger of 4-phenylcubane-1-carbaldehyde (3.91d)

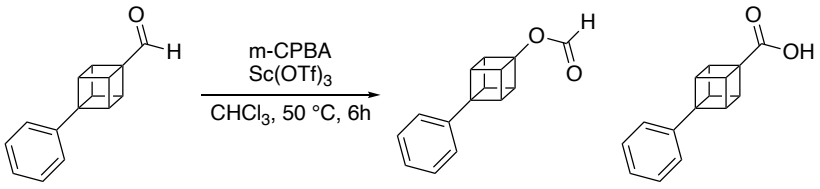

3.91d **3.94d** **3.95d**

The reaction was performed using the **general procedure** (workup 2 not used for this substrate) with 4-phenylcubane-1-carbaldehyde (**3.91d**) (41.4 mg, 1.0 eq., 0.20 mmol), scandium (III) triflate (9.9 mg, 0.1 eq., 0.02 mmol), 3-chloroperbenzoic acid (174 mg, 4.0 equiv., 0.73 mmol) and $CHCl_3$ (2.0 mL). Purification by silica column chromatography

(3:97 EtOAc/petroleum ether → 1:1 EtOAc/petroleum ether) gave the title compound **3.94d** (29 mg, 65 %) as a white solid.

^{1}H NMR (400 MHz, $CDCl_3$) δ 8.07 (s, 1H), 7.42 – 7.32 (m, 2H), 7.25 – 7.18 (m, 3H), 4.38 – 4.26 (m, 3H), 4.15 – 4.04 (m, 3H); **^{13}C NMR** (101 MHz, $CDCl_3$) δ 159.3, 142.4, 128.6, 126.3, 124.9, 89.0, 60.1, 51.5, 45.9; **HRMS (EI$^+$)** m/z: $[M\text{-}COH]^+$ Calcd. for $C_{14}H_{11}O$ 195.0804; Found 195.0803.

Note: *The isolated yield of* ***3.95d*** *was not determined, as it was not possible to separate product* ***3d*** *with the by-product 3-chlorobenzoic acid during the purification.*

NMR yield of **3.91d** / %	NMR yield of **3.94d** / %	NMR yield of **3.95d** / %	Isolated yield of **3.91d** / %	Isolated yield of **3.94d** / %	Isolated yield of **3.95d** / %
0	55	28	0	65	n.d

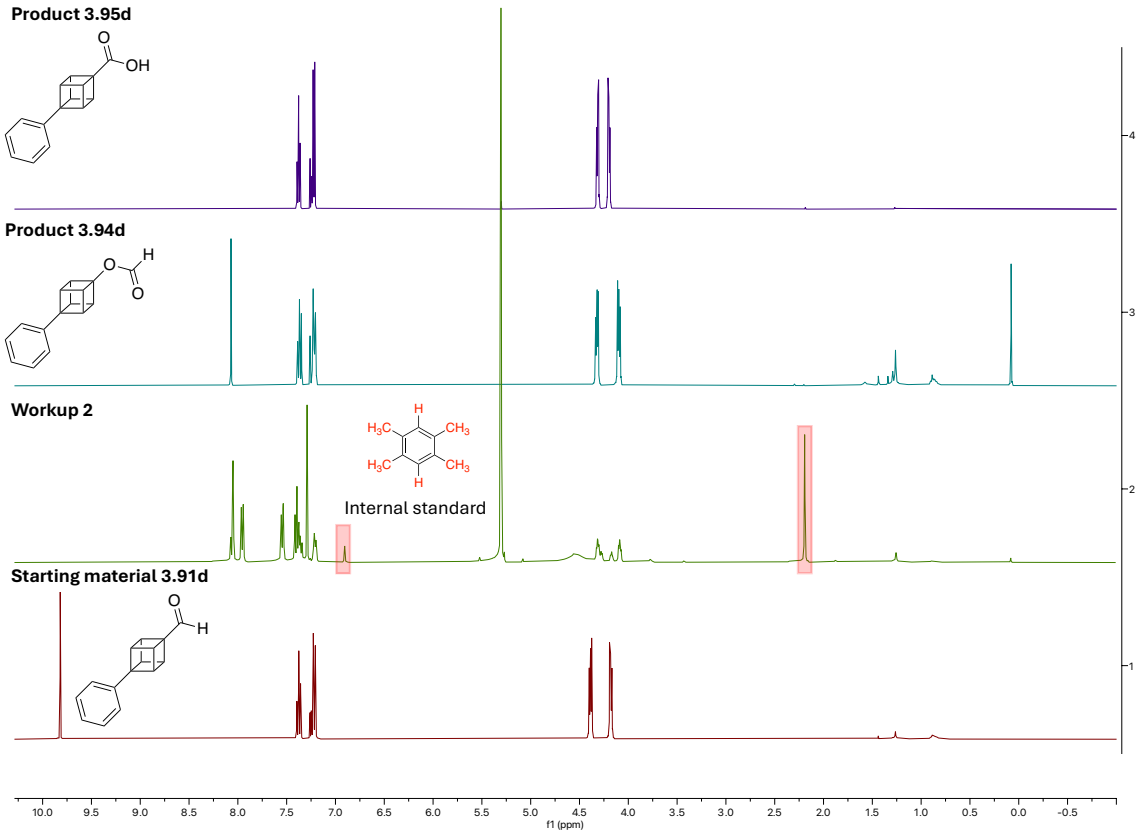

Baeyer-Villiger of 2-methyl-1-(4-phenylcuban-1-yl)propan-1-one (3.91e)

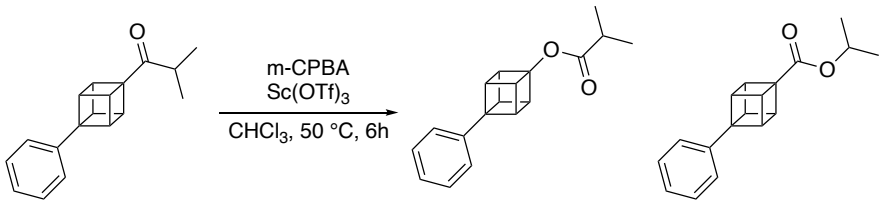

3.91e **3.94e** **3.95e**

The reaction was performed using the **general procedure** with 2-methyl-1-(4-phenylcuban-1-yl)propan-1-one (**3.91e**) (50 mg, 1.0 eq., 0.20 mmol), scandium (III) triflate (10.1 mg, 0.1 eq., 0.02 mmol), 3-chloroperbenzoic acid (174 mg, 4.0 equiv., 0.73 mmol) and $CHCl_3$ (2.0 mL). Purification by silica gel column chromatography (30:70 DCM/petroleum ether → 50:50 DCM/petroleum ether) gave the title compound **3.94e** (33 mg, 62 %) as a white solid and **3.95e** (14 mg, 27%) as a white solid.

3.94e: **^{1}H NMR** (400 MHz, $CDCl_3$) δ 7.40 – 7.33 (m, 2H), 7.25 – 7.18 (m, 3H), 4.33 – 4.21 (m, 3H), 4.13 – 4.02 (m, 3H), 2.62 (hept, *J* = 7.0 Hz, 1H), 1.23 (d, *J* = 7.0 Hz, 6H); **^{13}C NMR** (101 MHz, $CDCl_3$) δ 175.9, 142.7, 128.5, 126.1, 124.9, 88.7, 60.0, 51.4, 45.7, 34.0, 19.0; **HRMS (EI$^+$)** m/z: $[M]^{+\bullet}$ Calcd. for $C_{18}H_{18}O_2$ 266.1301; Found 266.1301.

3.95e: **^{1}H NMR** (400 MHz, $CDCl_3$) δ 7.40 – 7.33 (m, 2H), 7.24 – 7.19 (m, 3H), 5.06 (hept, *J* = 6.3 Hz, 1H), 4.24 – 4.18 (m, 3H), 4.18 – 4.10 (m, 3H), 1.27 (d, *J* = 6.3 Hz, 6H); **^{13}C NMR** (101 MHz, $CDCl_3$) δ 172.2, 142.4, 128.6, 126.2, 124.9, 67.5, 60.3, 56.9, 48.8, 46.1, 22.0; **HRMS (EI$^+$)** m/z: $[M]^{+\bullet}$ Calcd. for $C_{18}H_{18}O_2$ 266.1301; Found 266.1303.

NMR yield of **3.91e** / %	NMR yield of **3.94e** / %	NMR yield of **3.95e** / %	Isolated yield of **3.91e** / %	Isolated yield of **3.94e** / %	Isolated yield of **3.95e** / %
0	58	25	0	62	27

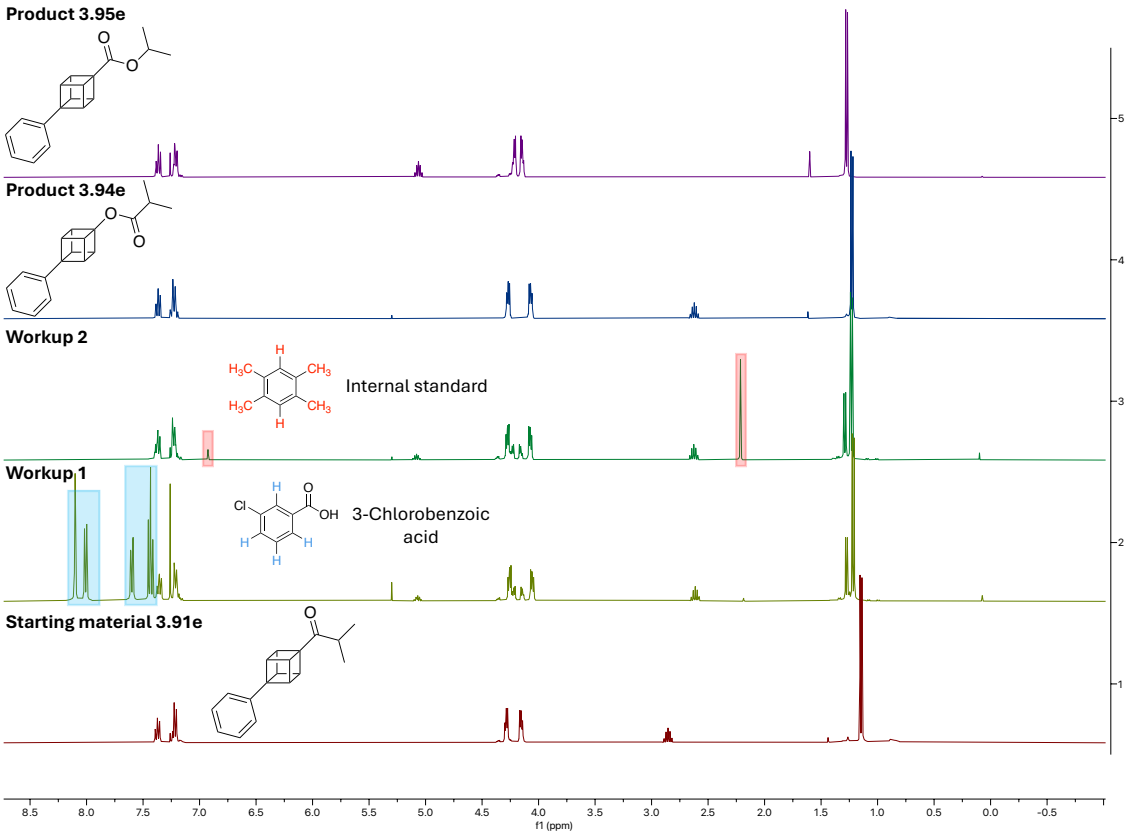

Baeyer-Villiger of 2,2-dimethyl-1-(4-phenylcuban-1-yl)propan-1-one (3.91f)

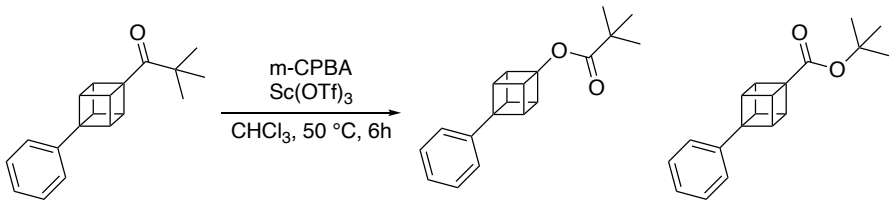

3.91f **3.94f** **3.95f**

The reaction was performed using the **general procedure** with 2,2-dimethyl-1-(4-phenylcuban-1-yl)propan-1-one (**3.91f**) (54 mg, 1.0 eq., 0.20 mmol), scandium (III) triflate (10.3 mg, 0.1 eq., 0.02 mmol), 3-chloroperbenzoic acid (173 mg, 4.0 equiv., 0.73 mmol) and $CHCl_3$ (2.0 mL). Purification by column chromatography (30:70 DCM/petroleum ether → 50:50 DCM/petroleum ether) gave a mixture of **3.91f**:**3.95f** in a ratio of 9:1 as a white solid (42 mg).

3.95f: **^{1}H NMR** (500 MHz, $CDCl_3$) δ 7.40 – 7.35 (m, 2H), 7.25 – 7.19 (m, 3H), 4.21 – 4.10 (m, 6H), 1.50 (s, 9H); **^{13}C NMR** (126 MHz, $CDCl_3$) δ 172.2, 142.4, 128.5, 126.1, 124.9,

80.2, 60.2, 57.6, 48.6, 46.1, 28.3; HRMS (EI$^+$) m/z: $[M\text{-}OC_4H_9]^+$ Calcd. for $C_{15}H_{11}O$ 207.0805; Found 207.0802.

NMR yield of **3.91f** / %	NMR yield of **3.94f** / %	NMR yield of **3.95f** / %	Isolated yield of **3.91f** / %	Isolated yield of **3.94f** / %	Isolated yield of **3.95f** / %
64	0	8	69	0	9

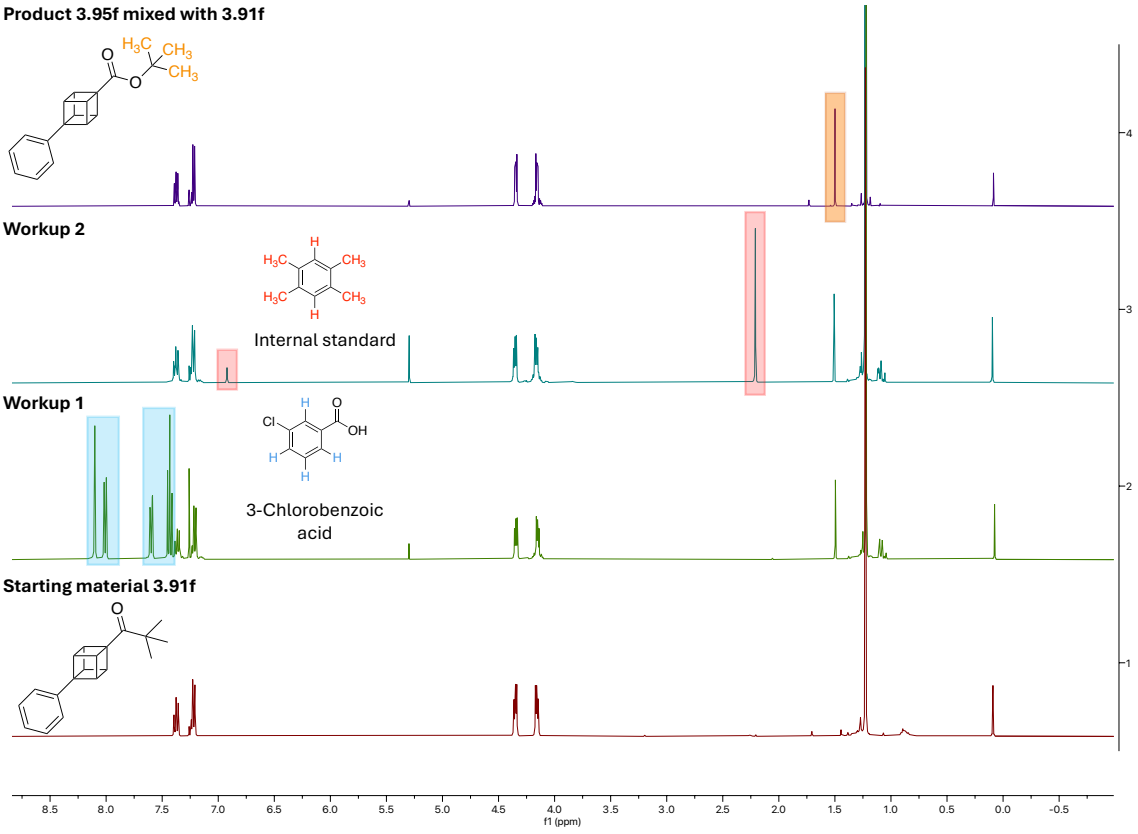

Baeyer-Villiger of 2-methyl-1-(4-(trimethylsilyl)cuban-1-yl)propan-1-one (3.91g)

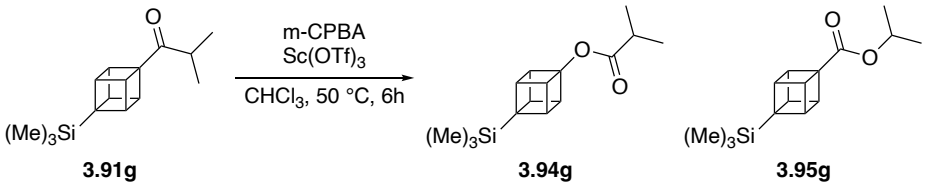

The reaction was performed using the **general procedure** with 2-methyl-1-(4-(trimethylsilyl)cuban-1-yl)propan-1-one (**3.91g**) (50 mg, 1.0 eq., 0.20 mmol), scandium (III) triflate (9.6 mg, 0.1 eq., 0.02 mmol), 3-chloroperbenzoic acid (177 mg, 4.0 equiv.,

0.73 mmol) and $CHCl_3$ (2.0 mL). Purification by column chromatography (30:70 DCM/petroleum ether → 50:50 DCM/petroleum ether) gave the title compound **3.94g** (32 mg, 61 %) as a colourless oil and impure **3.95g**. Further purification of **3.95g** by silica gel column chromatography (02:98 EtOAc/petroleum ether) gave the title compound **3.95g** (5 mg, 10 %) as a colourless oil.

3.94g: **^{1}H NMR** (400 MHz, $CDCl_3$) δ 4.30 – 4.21 (m, 3H), 3.79 – 3.69 (m, 3H), 2.57 (hept, *J* = 7.0 Hz, 1H), 1.18 (d, *J* = 7.0 Hz, 6H), -0.05 (s, 9H); **^{13}C NMR** (101 MHz, $CDCl_3$) δ 175.8, 88.4, 55.2, 48.4, 40.9, 34.0, 19.0, -4.7; **HRMS (EI$^+$)** m/z: $[M\text{-}CH_3]^+$ Calcd. for $C_{14}H_{19}O_2{}^{28}Si$ 247.1149; Found 247.1145.

3.95g: **^{1}H NMR** (400 MHz, $CDCl_3$) δ 5.02 (hept, *J* = 6.2 Hz, 1H), 4.25 – 4.19 (m, 3H), 3.85 – 3.79 (m, 3H), 1.24 (d, *J* = 6.2 Hz, 6H), -0.05 (s, 9H); **^{13}C NMR** (126 MHz, $CDCl_3$) δ 172.1, 67.3, 56.5, 49.8, 48.9, 44.1, 22.0, -4.7; **HRMS (EI$^+$)** m/z: $[M\text{-}C_3H_7]^+$ Calcd. for $C_{12}H_{15}O_2{}^{28}Si$ 219.0836; Found 219.0839.

NMR yield of **3.91g** / %	NMR yield of **3.94g** / %	NMR yield of **3.95g** / %	Isolated yield of **3.91g** / %	Isolated yield of **3.94g** / %	Isolated yield of **3.95g** / %
0	65	9	0	61	10

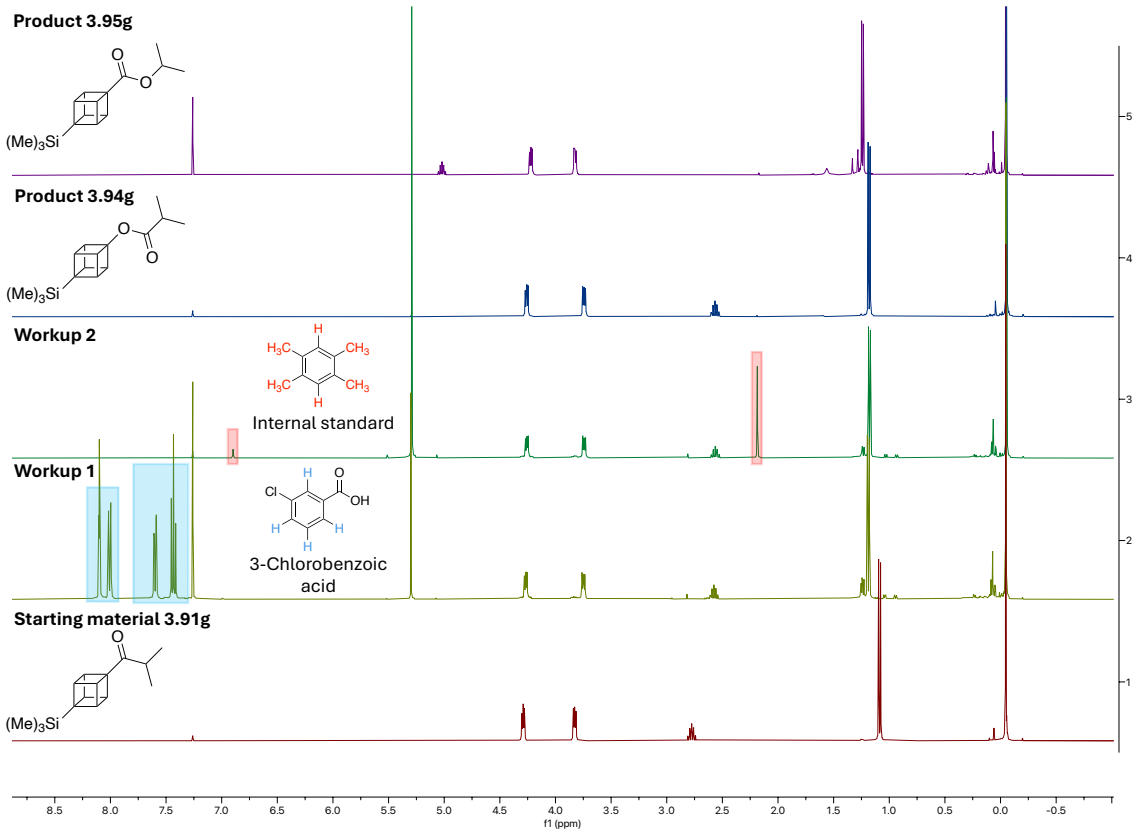

Baeyer-Villiger of 1-(cuban-1-yl)-2-methylpropan-1-one (3.91h)

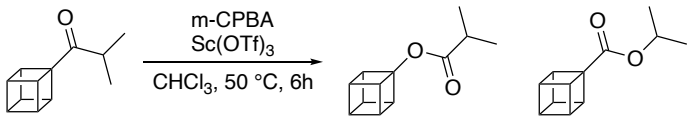

3.91h **3.94h** **3.95h**

The reaction was performed using the **general procedure** with 1-(cuban-1-yl)-2-methylpropan-1-one (**3.91h**) (34.5 mg, 1.0 eq., 0.20 mmol), scandium (III) triflate (10.1 mg, 0.1 eq., 0.02 mmol), 3-chloroperbenzoic acid (172 mg, 4.0 equiv., 0.73 mmol) and $CHCl_3$ (2.0 mL). Purification by silica gel column chromatography (30:70 DCM/petroleum ether → 50:50 DCM/petroleum ether) gave the title compound **3.94h** (18 mg, 46 %) as a white solid and impure **3.95h**. Further purification of **3.95h** by silica gel column chromatography (3:97 EtOAc/petroleum ether) gave the title compound **3.95h** (8 mg, 22 %) as a colourless oil.

3.94h: **^{1}H NMR** (400 MHz, $CDCl_3$) δ 4.30 – 4.21 (m, 3H), 3.96 – 3.87 (m, 4H), 2.57 (hept, *J* = 7.0 Hz, 1H), 1.18 (d, *J* = 7.0 Hz, 6H); **^{13}C NMR** (101 MHz, $CDCl_3$) δ 176.0, 88.2, 54.8,

47.7, 42.0, 34.0, 19.0; **HRMS (EI$^+$)** m/z: $[M-H]^+$ Calcd. for $C_{12}H_{13}O_2$ 189.0910; Found 189.0909.

3.95h: **^{1}H NMR** (500 MHz, $CDCl_3$) δ 5.02 (hept, *J* = 6.3 Hz, 1H), 4.25 – 4.18 (m, 3H), 4.03 – 3.95 (m, 4H), 1.24 (d, *J* = 6.3 Hz, 6H); **^{13}C NMR** (126 MHz, $CDCl_3$) δ 172.3, 67.3, 56.1, 49.5, 47.9, 45.2, 22.0; **HRMS (EI$^+$)** m/z: $[M]^{+\cdot}$ Calcd. for $C_{12}H_{14}O_2$ 190.0988; Found 190.0988.

NMR yield of **3.91h** / %	NMR yield of **3.94h** / %	NMR yield of **3.95h** / %	Isolated yield of **3.91h** / %	Isolated yield of **3.94h** / %	Isolated yield of **3.95h** / %
0	44	15	0	46	22

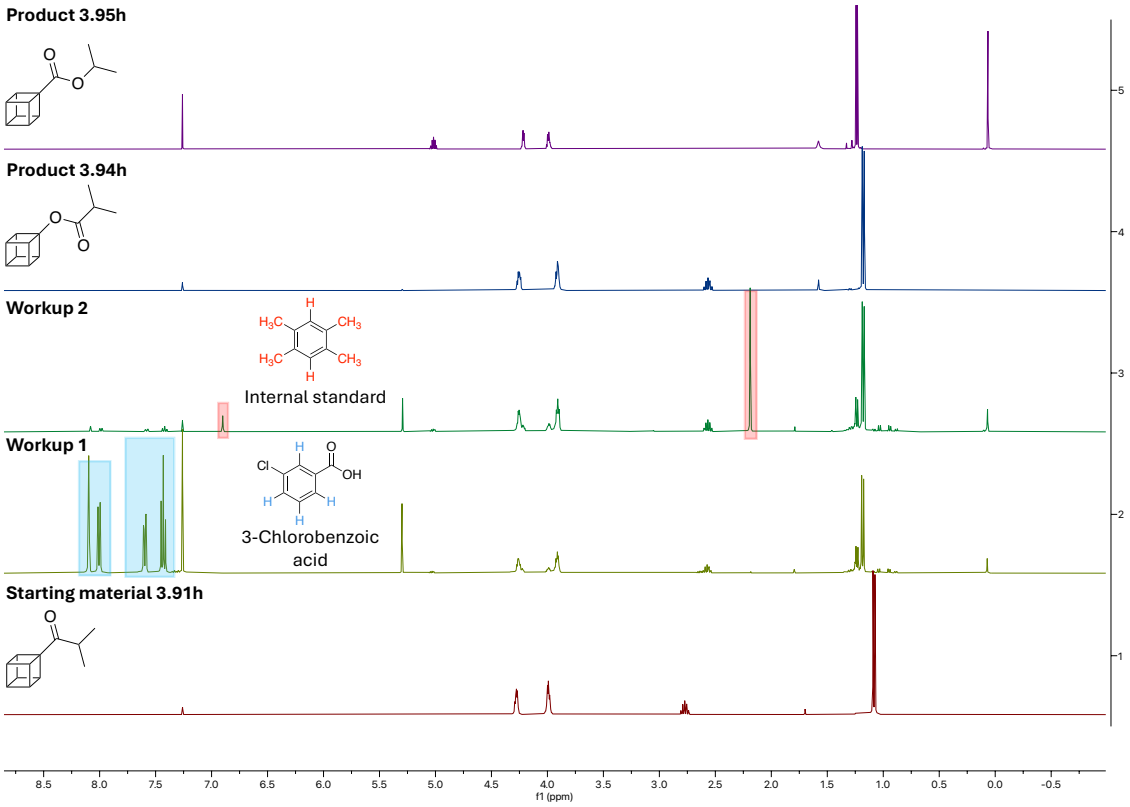

Baeyer-Villiger of 1-(4-(methoxymethyl)cuban-1-yl)-2-methylpropan-1-one (3.91i)

3.91i **3.94i** **3.95i**

The reaction was performed using the **general procedure** with 1-(4-(methoxymethyl)cuban-1-yl)-2-methylpropan-1-one (**3.91i**) (44 mg, 1.0 eq., 0.20 mmol), scandium (III) triflate (9.9 mg, 0.1 eq., 0.02 mmol), 3-chloroperbenzoic acid (173 mg, 4.0 equiv., 0.73 mmol) and $CHCl_3$ (2.0 mL). Purification by silica gel column chromatography (07:93 EtOAc/petroleum ether) gave the title compound **3.94i** (20 mg, 42 %) as a white solid and **3.95i** (4 mg, 8 %) as a white solid.

3.94i: **^{1}H NMR** (500 MHz, $CDCl_3$) δ 4.19 – 4.13 (m, 3H), 3.81 – 3.74 (m, 3H), 3.54 (s, 2H), 3.37 (s, 3H), 2.56 (hept, *J* = 6.9 Hz, 1H), 1.18 (d, *J* = 6.9 Hz, 6H); **^{13}C NMR** (126 MHz, $CDCl_3$) δ 175.8, 88.5, 73.6, 59.4, 57.4, 52.0, 42.1, 33.9, 19.0; **HRMS (ESI$^+$)** m/z: $[M+H]^+$ Calcd. for $C_{14}H_{19}O_3$ 235.1329; Found 235.1326.

3.95i: **^{1}H NMR** (500 MHz, $CDCl_3$) δ 5.02 (hept, *J* = 6.3 Hz, 1H), 4.15 – 4.09 (m, 3H), 3.89 – 3.84 (m, 3H), 3.53 (s, 2H), 3.38 (s, 3H), 1.24 (d, *J* = 6.3 Hz, 6H); **^{13}C NMR** (126 MHz, $CDCl_3$) δ 172.2, 73.3, 67.5, 59.4, 57.6, 56.7, 46.7, 45.2, 22.0; **HRMS (EI$^+$)** m/z: $[M-C_3H_7]^+$ Calcd. for $C_{11}H_{11}O_3$ 191.0703; Found 191.0701.

NMR yield of **3.91i** / %	NMR yield of **3.94i** / %	NMR yield of **3.95i** / %	Isolated yield of **3.91i** / %	Isolated yield of **3.94i** / %	Isolated yield of **3.95i** / %
0	44	15	0	42	8

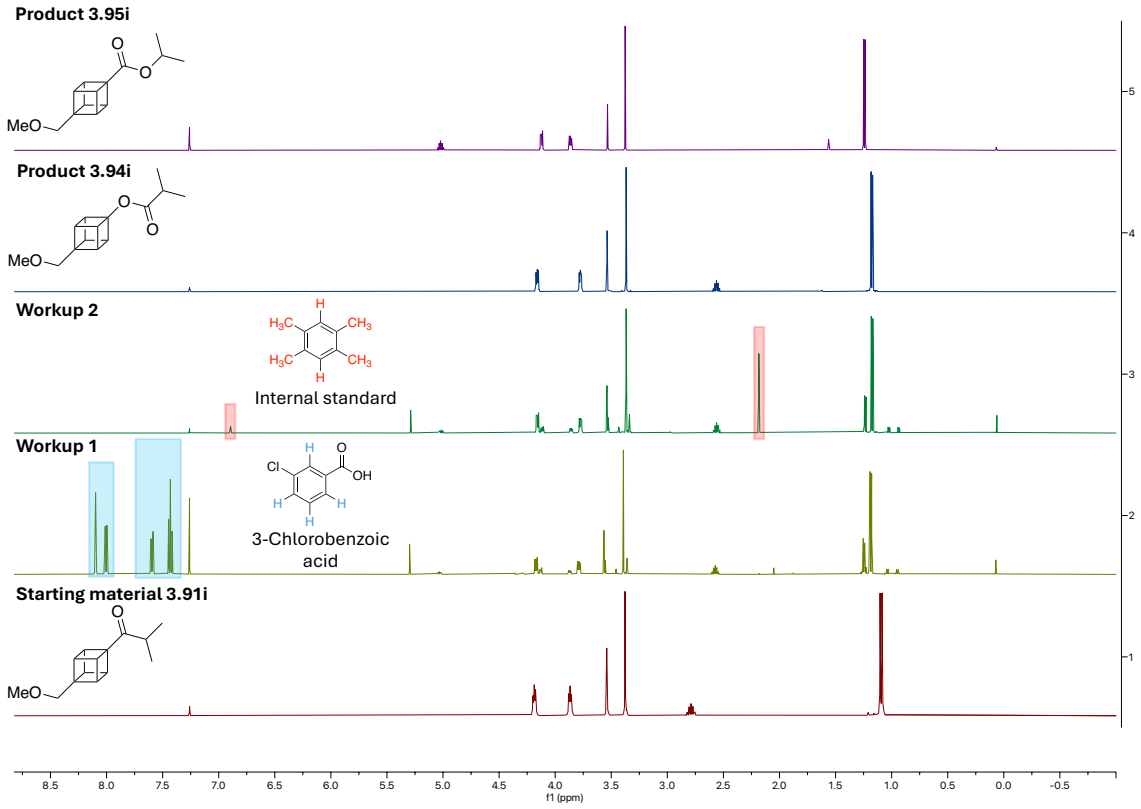

Baeyer-Villiger of 4-isobutyryl-*N*,*N*-diisopropylcubane-1-carboxamide (3.91j)

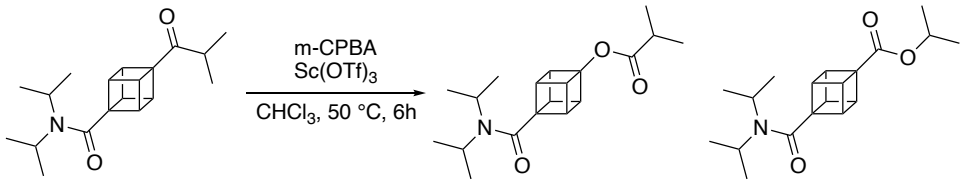

3.91j **3.94j** **3.95j**

The reaction was performed using the **general procedure** with 4-isobutyryl-N,N-diisopropylcubane-1-carboxamide (**3.91j**) (61 mg, 1.0 eq., 0.20 mmol), scandium (III) triflate (9.7 mg, 0.1 eq., 0.02 mmol), 3-chloroperbenzoic acid (175 mg, 4.0 equiv., 0.73 mmol) and $CHCl_3$ (2.0 mL). Purification by silica gel column chromatography (15:75 EtOAc/petroleum ether) separated **3.94j** from **3.95j**, but both compounds were still impure**.** Further purification of **3.94j** by silica gel column chromatography (15:75 EtOAc/toluene) gave the title compound **3.94j** (14 mg, 22 %) as a white solid. Further purification of **3.95j** by silica gel column chromatography (15:75 EtOAc/toluene) gave the title compound **3.95j** (11 mg, 9 %) as a white solid.

3.94j: **^{1}H NMR** (500 MHz, $CDCl_3$) δ 4.23 – 4.18 (m, 3H), 4.11 – 4.05 (m, 3H), 3.47 (hept, *J* = 6.6 Hz, 1H), 3.29 (hept, *J* = 6.7 Hz, 1H), 2.57 (hept, *J* = 7.0 Hz, 1H), 1.41 (d, *J* = 6.7 Hz, 6H), 1.19 (d, *J* = 6.6 Hz, 6H), 1.18 (d, *J* = 7.0 Hz, 6H); **^{13}C NMR** (126 MHz, $CDCl_3$) δ 176.0, 170.9, 86.8, 59.3, 51.6, 48.4, 46.0, 44.1, 33.9, 21.1, 20.6, 19.0; **HRMS (ESI$^+$)** m/z: $[M+H]^+$ Calcd. for $C_{19}H_{28}NO_3$ 318.2064; Found 318.2066.

3.95j: **^{1}H NMR** (500 MHz, $CDCl_3$) δ 5.02 (hept, *J* = 6.3 Hz, 1H), 4.17 (s, 6H), 3.47 (hept, *J* = 6.6 Hz, 1H), 3.30 (hept, *J* = 6.7 Hz, 1H), 1.41 (d, *J* = 6.7 Hz, 6H), 1.24 (d, *J* = 6.3 Hz, 6H), 1.20 (d, *J* = 6.6 Hz, 6H); **^{13}C NMR** (126 MHz, $CDCl_3$) δ 171.7, 170.4, 67.7, 59.4, 55.1, 48.6, 47.0, 46.3, 46.0, 22.0, 21.1, 20.6; **HRMS (ESI$^+$)** m/z: $[M+H]^+$ Calcd. for $C_{19}H_{28}NO_3$ 318.2069; Found 318.2065.

NMR yield of **3.91j** / %	NMR yield of **3.94j** / %	NMR yield of **3.95j** / %	Isolated yield of **3.91j** / %	Isolated yield of **3.94j** / %	Isolated yield of **3.95j** / %
0	25	29	0	22	9

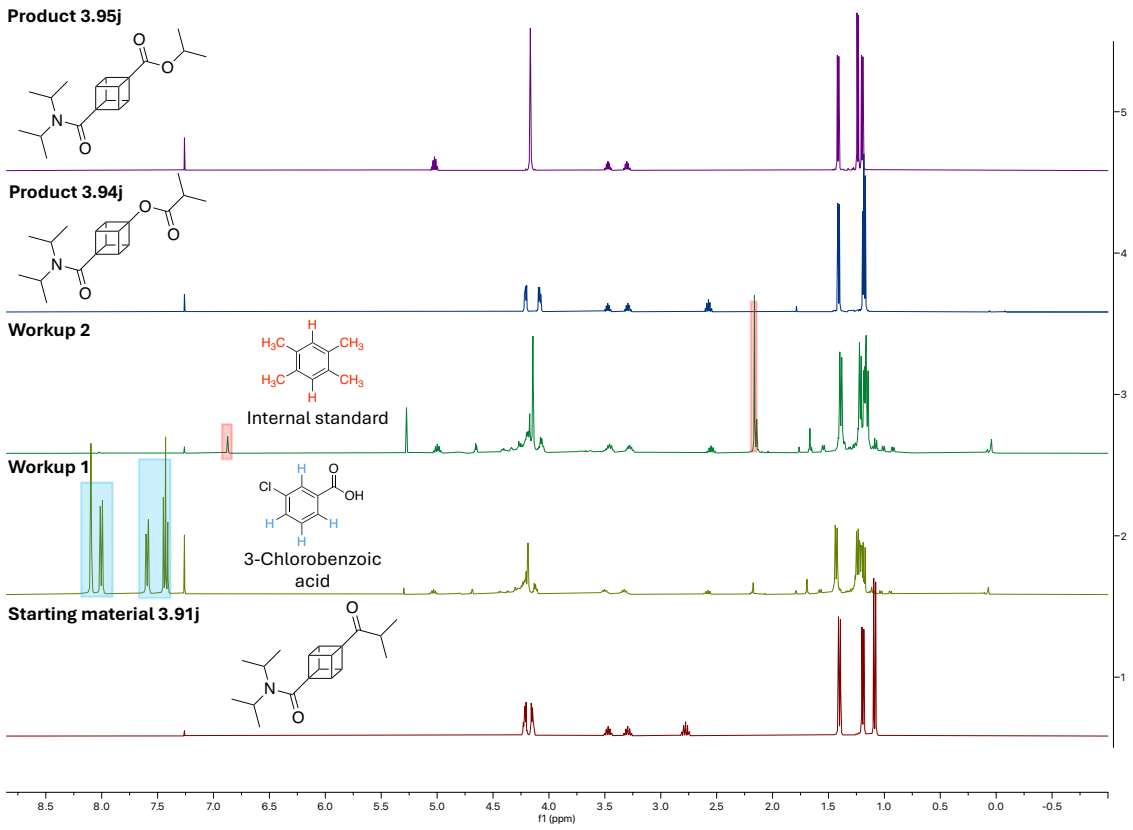

Baeyer-Villiger of 1-(4-bromocuban-1-yl)-2-methylpropan-1-one (3.91k)

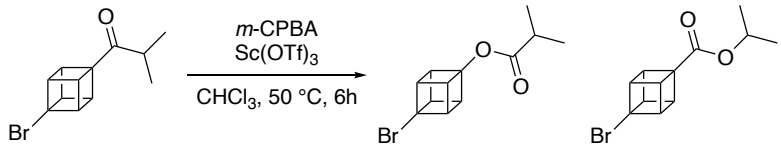

3.91k **3.94k** **3.95k**

The reaction was performed using the **general procedure** with 1-(4-bromocuban-1-yl)-2-methylpropan-1-one (**3.91k**) (51 mg, 1.0 eq., 0.20 mmol), scandium (III) triflate (9.8 mg, 0.1 eq., 0.02 mmol), 3-chloroperbenzoic acid (173 mg, 4.0 equiv., 0.73 mmol) and $CHCl_3$ (2.0 mL). Purification by silica gel column chromatography (2:98 EtOAc/petroleum ether) gave an impure **3.94k** and the title compound **3.95k** (25 mg, 46 %) as a white solid. Further purification of **3.94k** by silica gel column chromatography (30:70 DCM/petroleum ether) gave the title compound **3.94k** (5 mg, 9 %) as a white solid.

3.94k: **^{1}H NMR** (500 MHz, $CDCl_3$) δ 4.35 – 4.28 (m, 3H), 4.18 – 4.11 (m, 3H), 2.57 (hept, *J* = 7.0 Hz, 1H), 1.18 (d, *J* = 7.0 Hz, 6H); **^{13}C NMR** (126 MHz, $CDCl_3$) δ 175.8, 88.4, 64.6, 52.7, 51.4, 33.9, 18.9; **HRMS (EI$^+$)** m/z: $[M\text{-}CH_3]^+$ Calcd. for $C_{11}H_{10}O_2{}^{79}Br$ 252.9859; Found 252.9856.

3.95k: **^{1}H NMR** (400 MHz, $CDCl_3$) δ 5.02 (hept, *J* = 6.3 Hz, 1H), 4.31 – 4.20 (m, 6H), 1.23 (d, *J* = 6.3 Hz, 6H); **^{13}C NMR** (101 MHz, $CDCl_3$) δ 171.2, 67.9, 63.4, 56.7, 54.7, 47.7, 22.0; **HRMS (EI$^+$)** m/z: $[M\text{-}C_3H_7]^+$ Calcd. for $C_9H_6O_2{}^{79}Br$ 224.9545; Found 224.9539.

NMR yield of **3.91k** / %	NMR yield of **3.94k** / %	NMR yield of **3.95k** / %	Isolated yield of **3.91k** / %	Isolated yield of **3.94k** / %	Isolated yield of **3.95k** / %
0	12	50	0	9	46

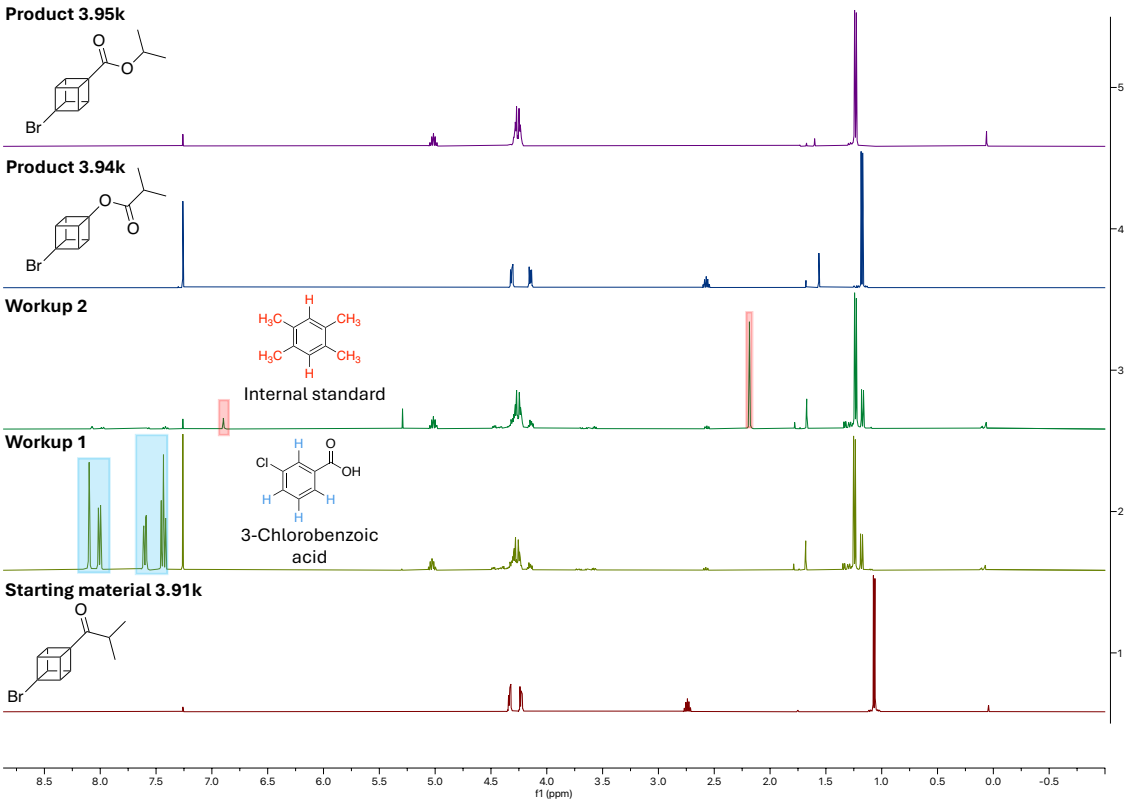

Baeyer-Villiger of 1-(4-fluorocuban-1-yl)-2-methylpropan-1-one (3.91l)

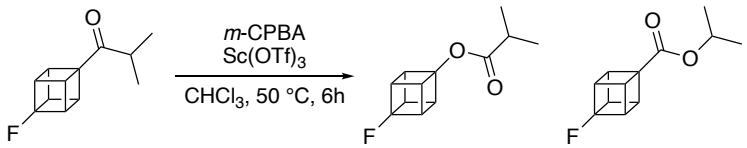

3.91l **3.94l** **3.95l**

The reaction was performed using the **general procedure** with 1-(4-fluorocuban-1-yl)-2-methylpropan-1-one (**3.91l**) (39 mg, 1.0 eq., 0.20 mmol), scandium (III) triflate (10.3 mg, 0.1 eq., 0.02 mmol), 3-chloroperbenzoic acid (171 mg, 4.0 equiv., 0.73 mmol) and $CHCl_3$ (2.0 mL). Purification by silica gel column chromatography (02:98 EtOAc/petroleum ether) gave the title compound **3.94l** (4 mg, 10 %) as a white solid and **3.95l** (16 mg, 39 %) as a white solid.

3.94l: **^{1}H NMR** (500 MHz, $CDCl_3$) δ 4.26 – 4.17 (m, 3H), 4.10 – 4.03 (m, 3H), 2.57 (hept, *J* = 6.9 Hz, 1H), 1.18 (d, *J* = 6.9 Hz, 6H). **^{19}F{^{1}H}NMR** (471 MHz, $CDCl_3$) δ -142.94. **^{13}C NMR** (126 MHz, $CDCl_3$) δ 175.7, 104.1 (d, *J* = 322.5 Hz), 89.0 (d, *J* = 21.7 Hz), 50.8 (d, *J* = 25.8

Hz), 47.4 (d, *J* = 6.5 Hz), 33.9, 18.9; **HRMS (EI$^+$)** m/z: $[M\text{-}CH_3]^+$ Calcd. for $C_{11}H_{10}O_2F$ 193.0659; Found 193.0657.

3.95l: **^{1}H NMR** (400 MHz, $CDCl_3$) δ 5.02 (hept, *J* = 6.3 Hz, 1H), 4.36 – 4.25 (m, 3H), 4.08 – 3.97 (m, 3H), 1.24 (d, *J* = 6.3 Hz, 6H); **^{19}F{^{1}H}NMR** (376 MHz, $CDCl_3$) δ -140.42; **^{13}C NMR** (101 MHz, $CDCl_3$) δ 171.8 (d, *J* = 7.2 Hz), 103.1 (d, *J* = 328.0 Hz), 67.8, 57.1 (d, *J* = 13.8 Hz), 54.1 (d, *J* = 25.3 Hz), 42.3 (d, *J* = 5.6 Hz), 22.0; **HRMS (EI$^+$)** m/z: $[M\text{-}C_3H_7]^+$ Calcd. for $C_9H_6O_2F$ 165.0346; Found 165.0344.

NMR yield of **3.91l** / %	NMR yield of **3.94l** / %	NMR yield of **3.95l** / %	Isolated yield of **3.91l** / %	Isolated yield of **3.94l** / %	Isolated yield of **3.95l** / %
0	11	49	0	10	39

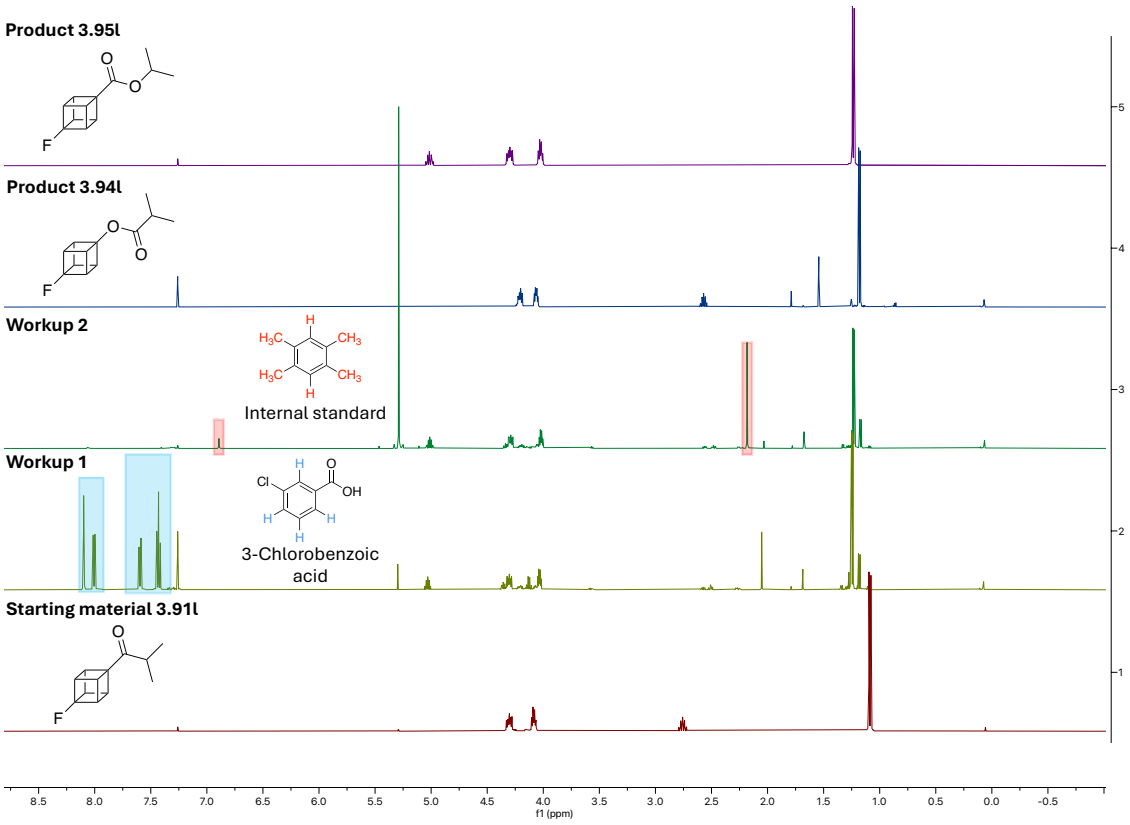

5.3.3 Computational Details

DFT calculations were carried out at PBE0/def2-TZVP-D3BJ level[19,20,21] in CPCM model of $CHCl_3$,[22] using Orca v6.0.[5] All species were fully optimised without any symmetry constraints, and confirmed as minima through harmonic frequency calculation, from which enthalpy and entropy corrections were extracted.

Optimised Cartesian Coordinate

[cubane]+

C	-0.644726	1.043429	-1.176080
H	-0.339143	1.724583	-1.960549
C	-1.446034	1.433046	0.112495
H	-1.731704	2.454686	0.340678
C	-0.524536	0.580324	1.050464
H	-0.129630	0.899951	2.006798
C	0.102230	0.165969	-0.234175
C	-0.611742	-1.119951	-0.463994
H	-0.279928	-2.125599	-0.690479
C	-1.532329	-0.233651	-1.370859
H	-1.890740	-0.558059	-2.342334
C	-2.333793	0.173353	-0.101834
C	-1.414463	-0.687693	0.810533
H	-1.674096	-1.379416	1.605248
H	-3.415587	0.176579	-0.042316

[4F-cubane]+

C	-0.629255	1.047692	-1.181835
H	-0.304056	1.724319	-1.962056
C	-1.428486	1.443511	0.113649
H	-1.735689	2.458860	0.341982
C	-0.508463	0.581814	1.055523
H	-0.093813	0.899938	2.003803
C	0.093104	0.166176	-0.233692
C	-0.596036	-1.125933	-0.465591
H	-0.243822	-2.124360	-0.692506
C	-1.515263	-0.237009	-1.382004
H	-1.895180	-0.559621	-2.345899
C	-2.302277	0.172996	-0.103386
C	-1.396676	-0.695416	0.818023
H	-1.681610	-1.381998	1.608509
F	-3.628701	0.176582	-0.030925

[3F-cubane]+

C	-0.630525	1.035171	-1.159042
H	-0.351430	1.672458	-1.990584
C	-1.434397	1.431271	0.111860
F	-1.825544	2.665028	0.388971

C	-0.512180	0.579946	1.030529
H	-0.135808	0.838272	2.013951
C	0.115771	0.147102	-0.238756
C	-0.605556	-1.155834	-0.471446
H	-0.258408	-2.154974	-0.697158
C	-1.527832	-0.258036	-1.351511
H	-1.869465	-0.529503	-2.345004
C	-2.340939	0.155148	-0.105150
C	-1.412465	-0.701819	0.782707
H	-1.655572	-1.352848	1.616078
H	-3.421870	0.176169	-0.041849

[2F-cubane]+

C	-0.667148	1.048841	-1.181044
F	-0.287612	1.873679	-2.129482
C	-1.448313	1.413585	0.100015
H	-1.702218	2.427734	0.395250
C	-0.523777	0.536193	1.051812
H	-0.158156	0.945392	1.986454
C	0.135404	0.145850	-0.212893
C	-0.608567	-1.114757	-0.420282
H	-0.315078	-2.110365	-0.732215
C	-1.532886	-0.219291	-1.354226
H	-1.860646	-0.612438	-2.312396
C	-2.335067	0.162349	-0.089651
C	-1.422572	-0.717171	0.845749
H	-1.722296	-1.401580	1.630490
H	-3.417289	0.169528	-0.033984

[4-$SiMe_3$-cubane]+

C	-0.706479	1.047828	-1.157517
H	-0.415786	1.740659	-1.937603
C	-1.512513	1.428377	0.121947
H	-1.787696	2.452134	0.355726
C	-0.606708	0.568209	1.056060
H	-0.238443	0.881607	2.025186
C	0.059141	0.165904	-0.222280
C	-0.681353	-1.111307	-0.466298
H	-0.371263	-2.122873	-0.697823
C	-1.586935	-0.222162	-1.373155
H	-1.922376	-0.539706	-2.355522
C	-2.417794	0.174178	-0.109167
C	-1.488557	-0.692886	0.801330
H	-1.743449	-1.394913	1.589177
Si	-4.307957	0.176591	-0.021691
C	-4.766479	0.746880	1.693440
H	-5.854301	0.765860	1.802590
H	-4.363971	0.074768	2.455477
H	-4.391346	1.754659	1.888453
C	-4.907657	1.357882	-1.334032
H	-4.585498	1.042158	-2.329504

H	-6.000456	1.395851	-1.330857
H	-4.535946	2.370001	-1.155412
C	-4.862055	-1.573803	-0.348004
H	-4.459931	-2.261940	0.399835
H	-5.953113	-1.634004	-0.307525
H	-4.543588	-1.913715	-1.336717

5.4 Chapter 4 experimental

5.4.1 Cubanol

Synthesis of phenylcuban-1-ol (4.11)

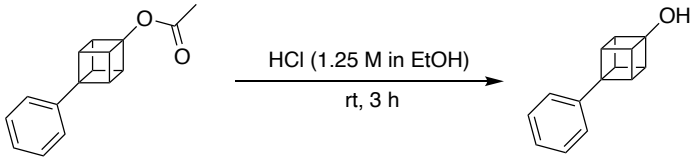

3.94b **4.11**

4-Phenylcuban-1-yl acetate (**3.94b**) (10 mg, 1.0 equiv., 0.04 mmol) in a solution of anhydrous HCl in ethanol (0.5 mL, 1.25 M) was stirred at rt for 3 hours. The reaction mixture was concentrated *in vacuo* to remove bulk of the ethanol to afford a white solid.

^{1}H NMR (300 MHz, $CDCl_3$) δ 7.39 – 7.31 (m, 2H), 7.24 – 7.16 (m, 3H), 4.08 – 3.98 (m, 3H), 3.96 – 3.87 (m, 3H); **^{1}H NMR** (400 MHz, acetic acid-d_3) δ 7.35 – 7.28 (m, 2H), 7.22 – 7.11 (m, 3H), 4.08 – 3.98 (m, 3H), 3.95 – 3.84 (m, 3H).). **HRMS (EI$^+$)** m/z: $[M]^{+\bullet}$ Calcd. for $C_{14}H_{12}O$ 196.0882; Found 196.0881.

5.4.2 Synthesis of cubyl-resveratrol 4.13a and 4.13b

5.4.2.1 Synthesis of cubyl aldehyde 4.20

The synthesis of cubyl-resveratrol followed the general synthetic methodology reported by Yi Ling Goh and co-workers for the synthesis of BCP-resveratrol.[281]

Synthetic scheme

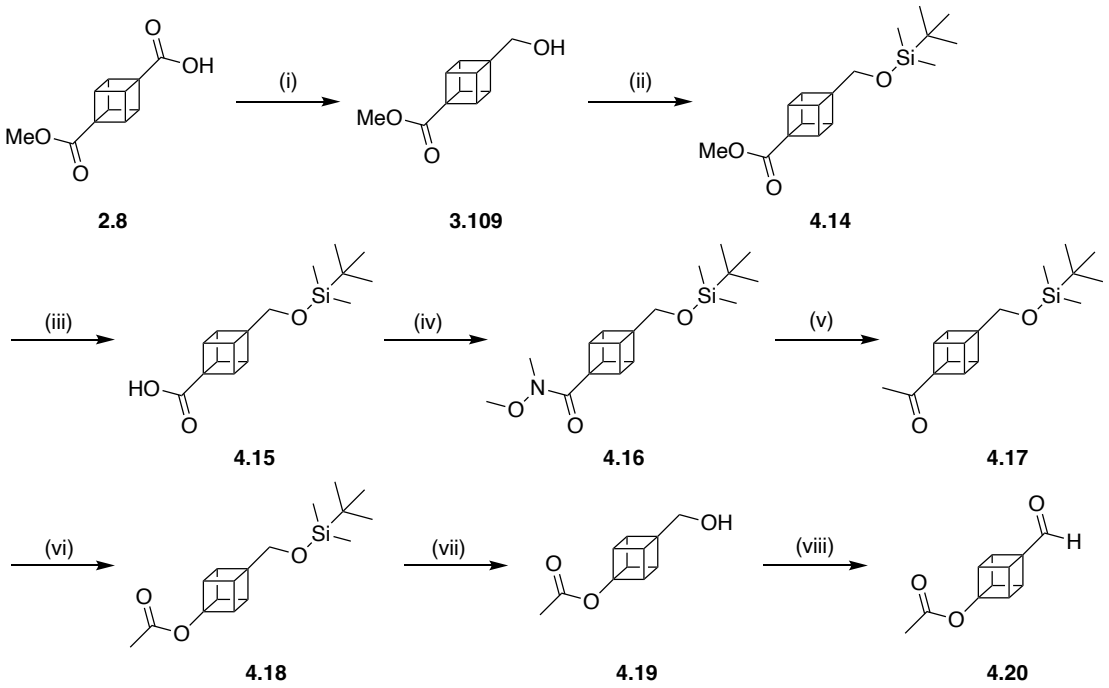

Conditions: (i) BH_3·DMS (1 M in 2-MeTHF), THF, 0 °C → rt, 6 h, 98 % (ii) imidazole, TBSCl, DCM, rt, 3 h, 92 % (iii) LiOH, THF/MeOH/H_2O (3:1:1), rt, 3 h, 93 % (iv) HATU, DIPEA, CH_3ONHCH_3·HCl, DMF, rt, 1.5 h, 89 % (v) MeMgBr (1 M in THF), THF, 0 °C → rt, 15 min, 88 % (vi) *m*-CPBA, $CHCl_3$, rt, 2 h, 96 % (vii) TBAF (1 M in THF), THF, rt, 1 h, 98 % (viii) oxalyl chloride (2 M in DCM), DMSO, DCM, -78 °C, 1.5 h; NEt_3, -78 °C → rt, 15 min, 97 %.

*Experimental procedure and analytical data for **3.109** was previously described in **Section 5.3.1.4**.*

Methyl-4-(((tert-butyldimethylsilyl)oxy)methyl)cubane-1-carboxylate (4.14)

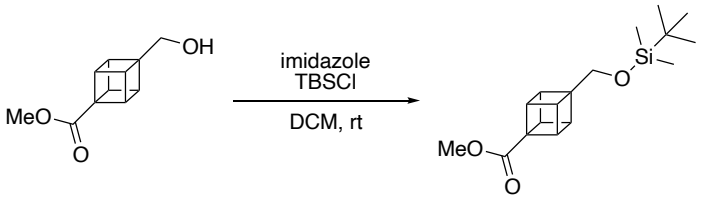

To a solution of methyl-4-(hydroxymethyl)cubane-1-carboxylate (**3.109**) (1.37 g, 1.0 equiv., 7.13 mmol) in anhydrous DCM (32 mL) was added imidazole (1.2 g, 2.5 equiv., 17.8 mmol) in one portion at rt. After 10 minutes *tert*-butyldimethylsilyl chloride (TBSCl) (1.3 g, 1.2 equiv., 8.56 mmol) was added in one portion and the cloudy white mixture was stirred at rt for 3 hours. The mixture was quenched with H_2O (5 mL) and the organic layer was washed with H_2O (3 x 15 mL), dried with anhydrous $MgSO_4$, filtered and

concentrated *in vacuo* to afford the crude. Purification by silica gel column chromatography (05:95 EtOAc/petroleum ether) gave the title compound **4.14** (2.0 g, 92 %) as a colourless oil.

^{1}H NMR (400 MHz, $CDCl_3$) δ 4.14 – 4.07 (m, 3H), 3.85 – 3.79 (m, 3H), 3.73 (s, 2H), 3.70 (s, 3H), 0.88 (s, 9H), 0.04 (s, 6H); **^{13}C NMR** (101 MHz, $CDCl_3$) δ 173.0, 63.6, 59.1, 56.5, 51.6, 46.5, 44.8, 26.0, 18.6, -5.0; **HRMS (ESI$^+$)** m/z: $[M+H]^+$ Calcd. for $C_{17}H_{27}O_3Si$ 307.1724; Found 307.1730.

4-(((tert-Butyldimethylsilyl)oxy)methyl)cubane-1-carboxylic acid (4.15)

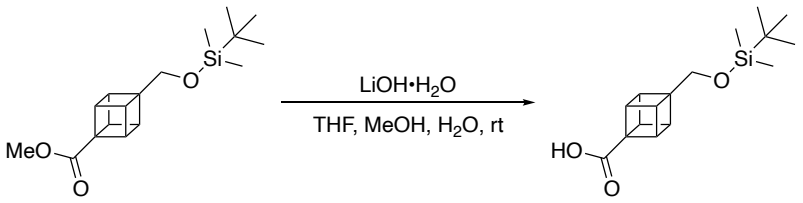

4.14 **4.15**

To a solution of methyl-4-(((*tert*-butyldimethylsilyl)oxy)methyl)cubane-1-carboxylate (**4.14**) (2.0 g, 1.0 equiv., 6.56 mmol) in 3:3:1 ratio of THF:MeOH:H_2O (13 mL) was added lithium hydroxide monohydrate (302 mg, 1.1 equiv., 7.22 mmol) in one-portion at rt. The mixture was allowed to stir at rt for 3 hours. The mixture was diluted with 1 M $NaOH_{(aq)}$ (2 mL) and the aqueous layer was washed with EtOAc (1 x 20 mL). The aqueous layer was acidified with 2 M $HCl_{(aq)}$ and the aqueous layer was extracted with EtOAc (3 x 20 mL). The combined organic layers were washed sat. $brine_{(aq)}$ (10 mL), dried with anhydrous $MgSO_4$, filtered and concentrated *in vacuo* to afford the title compound **4.15** (1.77 g, 93%) as a white solid.

^{1}H NMR (400 MHz, $CDCl_3$) δ 11.36 (Br s, 1H), 4.18 – 4.12 (m, 3H), 3.89 – 3.81 (m, 3H), 3.74 (s, 2H), 0.88 (s, 9H), 0.05 (s, 6H); **^{13}C NMR** (101 MHz, $CDCl_3$) δ 178.6, 63.5, 59.2, 56.2, 46.5, 44.9, 26.0, 18.6, -5.0; **HRMS (ESI$^-$)** m/z: $[M-H]^-$ Calcd. for $C_{16}H_{23}O_3Si$ 291.1421; Found 291.1409.

4-(((tert-Butyldimethylsilyl)oxy)methyl)-N-methoxy-N-methylcubane-1-carboxamide (4.16)

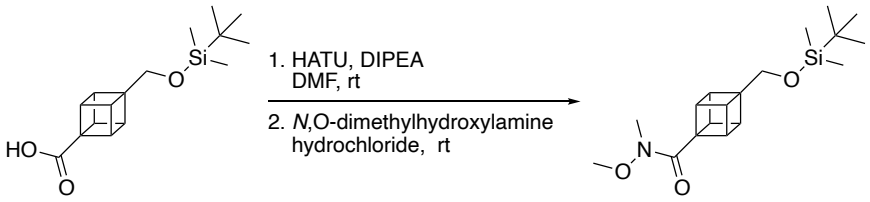

4.15 **4.16**

To a solution of 4-(((*tert*-butyldimethylsilyl)oxy)methyl)cubane-1-carboxylic acid (**4.15**) (1.77 g, 1.0 equiv., 6.07 mmol) and HATU (2.77 g, 1.2 equiv., 7.29 mmol) in anhydrous DMF (30 mL) was added *N*,*N*-diisopropylethylamine (DIPEA) (3.6 mL, 3.5 equiv., 21.2 mmol) at rt. After 5 minutes, *N*,O-dimethylhydroxylamine hydrochloride (770 mg, 1.3 equiv., 7.89 mmol) was added in one portion and the reaction mixture was allowed to stir at rt for 1.5 hour. The mixture was quenched with H_2O (10 mL) and diluted with EtOAc (20 mL). The organic layer was washed with H_2O (3 x 20 mL), sat. $brine_{(aq)}$ (15 mL), dried with anhydrous $MgSO_4$, filtered and concentrated *in vacuo* to afford the crude. Purification by silica gel column chromatography (1:3 EtOAc/petroleum ether) gave the title compound **4.16** (1.81 g, 89 %) as a colourless oil.

^{1}H NMR (500 MHz, $CDCl_3$) δ 4.15 – 4.09 (m, 3H), 3.82 – 3.77 (m, 3H), 3.73 (s, 2H), 3.70 (s, 3H), 3.17 (s, 3H), 0.88 (s, 9H), 0.04 (s, 6H); **^{13}C NMR** (126 MHz, $CDCl_3$) δ 174.0, 63.7, 61.7, 58.5, 58.3, 46.6, 44.7, 32.8, 26.0, 18.5, -5.1; **HRMS (ESI$^+$)** m/z: $[M+H]^+$ Calcd. for $C_{18}H_{30}O_3NSi$ 336.1989; Found 336.2002.

1-(4-(((tert-Butyldimethylsilyl)oxy)methyl)cuban-1-yl)ethan-1-one (4.17)

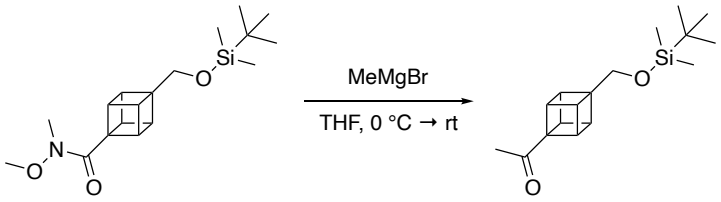

4.16 **4.17**

To a solution of 4-(((*tert*-butyldimethylsilyl)oxy)methyl)-*N*-methoxy-*N*-methylcubane-1-carboxamide (**4.16**) (1.81 g, 1.0 equiv., 5.40 mmol) in anhydrous THF (20 mL) at 0 °C was added methylmagnesium bromide (10.8 mL, 2.0 equiv., 1 M in THF) dropwise. The mixture was stirred at 0 °C for 5 minutes and allowed to warm to rt. After 15 minutes, the

mixture was quenched with 1 M $HCl_{(aq)}$ (5 mL) at 0 °C. The aqueous was extracted with EtOAc (3 x 10 mL) and the combined organic layers were washed with sat. $brine_{(aq)}$ (10 mL), dried with anhydrous $MgSO_4$, filtered and concentrated *in vacuo* to afford the crude. Purification by silica gel column chromatography (07:93 EtOAc/petroleum ether) gave the title compound **4.17** (1.34 g, 88 %) as a colourless oil.

^{1}H NMR (400 MHz, $CDCl_3$) δ 4.17 – 4.07 (m, 3H), 3.83 – 3.76 (m, 3H), 3.73 (s, 2H), 2.12 (s, 3H), 0.88 (s, 9H), 0.05 (s, 6H); **^{13}C NMR** (101 MHz, $CDCl_3$) δ 206.9, 64.4, 63.5, 59.4, 46.6, 44.3, 26.0, 24.8, 18.5, -5.1; **HRMS (ESI$^+$)** m/z: $[M+H]^+$ Calcd. for $C_{17}H_{27}O_2Si$ 291.1775; Found 291.1788.

4-(((tert-Butyldimethylsilyl)oxy)methyl)cuban-1-yl acetate (4.18)

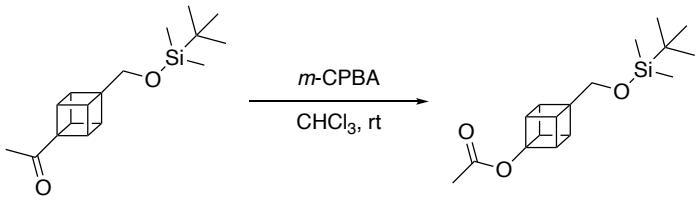

4.17 **4.18**

To a solution of 1-(4-(((*tert*-butyldimethylsilyl)oxy)methyl)cuban-1-yl)ethan-1-one (**4.17**) (580 mg, 1.0 equiv., 2.0 mmol) in anhydrous chloroform (20 mL) was added 3-chloroperbenzoic acid (1.73 g, 4.0 equiv., 9 mmol) in one portion at 0 °C. After 5 minutes, the reaction mixture was stirred at rt for 2 hours and quenched with sodium $bisulfite_{(aq)}$ (10 mL). The organic layer was washed further with sodium $bisulfite_{(aq)}$ (10 mL), sat. $NaHCO_{3(aq)}$ (2 x 10 mL), dried with anhydrous $MgSO_4$, filtered and concentrated *in vacuo* to afford the title compound **4.18** (585 mg, 96 %) as a colourless oil.

^{1}H NMR (500 MHz, $CDCl_3$) δ 4.16 – 4.10 (m, 3H), 3.75 – 3.70 (m, 3H), 3.73 (s, 2H), 2.08 (s, 3H), 0.88 (s, 9H), 0.04 (s, 6H); **^{13}C NMR** (126 MHz, $CDCl_3$) δ 169.5, 88.7, 63.9, 58.9, 51.7, 41.7, 26.0, 21.2, 18.6, -5.1; **HRMS (ESI$^+$)** m/z: $[M+H]^+$ Calcd. for $C_{17}H_{27}O_3Si$ 307.1724; Found 307.1736.

4-(Hydroxymethyl)cuban-1-yl acetate (4.19)

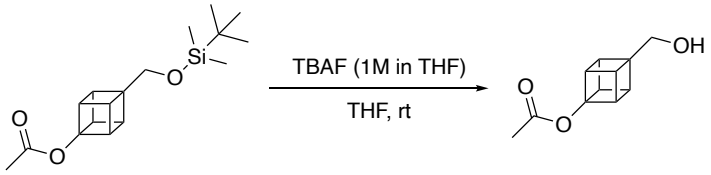

4.18 **4.19**

To a solution of 4-(((*tert*-butyldimethylsilyl)oxy)methyl)cuban-1-yl acetate (**4.18**) (585 mg, 1.0 equiv., 1.91 mmol) in anhydrous THF (9.5 mL) was added TBAF (2.5 mL, 1.3 equiv., 1 M in THF) dropwise at rt. After 1 hour, the reaction mixture was quenched with H_2O (3 mL) and diluted with EtOAc (30 mL). The organic layer was washed with sat. $NaHCO_{3(aq)}$ (2 x 10 mL), sat. $brine_{(aq)}$ (20 mL), dried with anhydrous $MgSO_4$, filtered and concentrated *in vacuo* to afford the crude. Purification by silica gel column chromatography (4:6 EtOAc/petroleum ether) gave the title compound **4.19** (357 mg, 98 %) as a colourless oil.

^{1}H NMR (400 MHz, $CDCl_3$) δ 4.19 – 4.11 (m, 3H), 3.80 – 3.73 (m, 3H), 3.76 (s, 2H) 2.07 (s, 3H), 1.94 (br s, 1H); **^{13}C NMR** (101 MHz, $CDCl_3$) δ 169.6, 88.5, 63.7, 58.7, 51.7, 41.5, 21.1; **HRMS (EI$^+$)** m/z: $[(M - {}^{\cdot}C(O)OCH_3]^+$ Calcd. for C_9H_9O 133.0648; Found 133.0647.

4-Formylcuban-1-yl acetate (4.20)

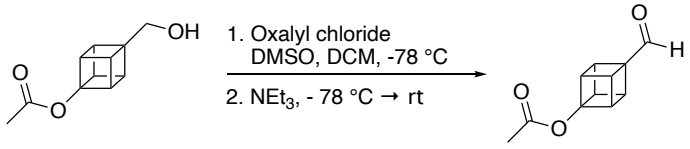

4.19 **4.20**

DMSO (0.37 mL, 2.8 equiv., 5.27 mmol) was added to a solution of oxalyl chloride (1.5 mL, 1.6 equiv., 2 M in DCM) in anhydrous DCM (10 mL) at -78 °C. After 20 minutes a solution of 4-(hydroxymethyl)cuban-1-yl acetate (**4.19**) (357 mg, 1.0 equiv., 1.86 mmol) in anhydrous DCM (5 mL) was added dropwise, and the mixture stirred at -78 °C for a further 1.5 hours. Triethylamine (1.45 mL, 5.6 equiv., 10.5 mmol) was then added and the mixture was allowed to warm to rt over 15 minutes. The mixture was quenched with H_2O (10 mL) and the aqueous layer was extracted with DCM (3 x 15 mL). The combined organic layer was washed sat. $brine_{(aq)}$ (20 mL), dried with anhydrous $MgSO_4$, filtered and concentrated *in vacuo* to afford the title compound **4.20** (342 mg, 97 %) as a light-yellow solid.

^{1}H NMR (400 MHz, $CDCl_3$) δ 9.75 (s, 1H), 4.25 (s, 6H), 2.07 (s, 3H); **^{13}C NMR** (101 MHz, $CDCl_3$) δ 198.4, 169.4, 87.2, 62.6, 52.5, 43.0, 21.0; **HRMS (EI$^+$)** m/z: $[M\text{-}CHO]^+$ Calcd. for $C_{10}H_9O_2$ 161.0597; Found 161.0594.

5.4.2.2 Synthesis of cubyl aldehyde 4.24

*Experimental procedure and analytical data for **3.109** was previously described in **Section 5.3.1.4**.*

Methyl-4-formylcubane-1-carboxylate (4.24)

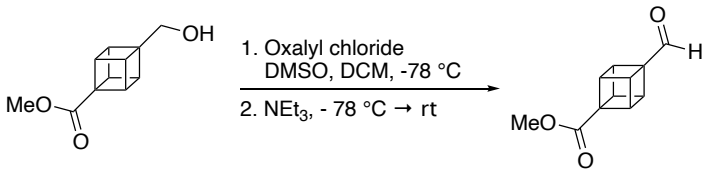

3.109 **4.24**

DMSO (0.25 mL, 2.7 equiv., 3.51 mmol) was added to a solution of oxalyl chloride (0.98 mL, 1.5 equiv., 2 M in DCM) in anhydrous DCM (7 mL) at -78 °C. After 20 minutes a solution of methyl-4-(hydroxymethyl)cubane-1-carboxylate (**3.109**) (250 mg, 1.0 equiv., 1.3 mmol) in anhydrous DCM (5 mL) was added dropwise, and the mixture stirred at -78 °C for a further 1.5 hours. Triethylamine (0.97 mL, 5.4 equiv., 7.1 mmol) was then added and the mixture was allowed to warm to rt over 15 minutes. The mixture was quenched with H_2O (10 mL) and the aqueous layer was extracted with DCM (3 x 15 mL). The combined organic layer was washed sat. $brine_{(aq)}$ (20 mL), dried with anhydrous $MgSO_4$, filtered and concentrated *in vacuo* to afford the title compound **4.24** (236 mg, 95 %) as a light-yellow solid.

^{1}H NMR (300 MHz, $CDCl_3$) δ 9.74 (s, 1H), 4.41 – 4.33 (m, 3H), 4.29 – 4.22 (m, 3H), 3.72 (s, 3H); **HRMS (EI$^+$)** m/z: $[M]^{+\bullet}$ Calcd. for $C_{11}H_{10}O_3$ 190.0624; Found 190.0623. All spectroscopic data were in accordance with the literature.[174]

5.4.2.3 Synthesis of phosphonium salt 4.23a

5-(Bromomethyl)benzene-1,3-diol (4.22a)

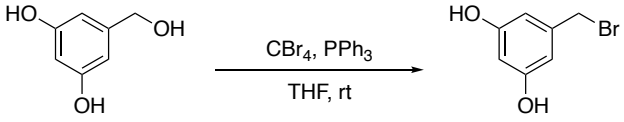

4.21a **4.22a**

To a solution of tetrabromomethane (4.26 g, 1.2 equiv., 12.8 mmol) and triphenylphosphine (3.38 g, 1.2 equiv., 12.8 mmol) in anhydrous THF (20 mL), 3,5-dihydroxybenzyl alcohol (**4.21a**) (1.50 g, 1.0 equiv., 10.7 mmol) in anhydrous THF (10 mL) was added dropwise at rt. The reaction mixture was stirred at rt for 16 hours before being quenched with H_2O (20 mL). The aqueous was extracted with EtOAc (3 x 20 mL) and the combined organic layers were washed with sat. $brine_{(aq)}$ (10 mL), dried with anhydrous $MgSO_4$, filtered, and concentrated *in vacuo* to afford the crude. Purification by column chromatography (40:60 EtOAc/petroleum ether) gave a mixture of the title compound **4.22a** and triphenylphosphine oxide in a 2:1 ratio (2.77 g) as a light-yellow sticky solid. The mixture was used in the next step without further purification.
Note: 100 mg of the mixture was purified by column chromatography (40:60 EtOAc/petroleum ether) to afford pure **4.22a** (56 mg) as a light-yellow solid for full data analysis.

^{1}H NMR (400 MHz, acetone-d_6) δ 8.34 (s, 2H), 6.43 (d, *J* = 2.2 Hz, 2H), 6.30 (t, *J* = 2.2 Hz, 1H), 4.46 (s, 2H); **^{13}C NMR** (101 MHz, acetone-d_6) δ 159.5, 141.0, 108.5, 103.5, 34.6; **HRMS (EI$^+$)** m/z: $[M]^{+\bullet}$ Calcd. for $C_7H_7O_2{}^{79}Br$ 201.9624; Found 201.9624. All spectroscopic data were in accordance with the literature.[297]

(3,5-Dihydroxybenzyl)triphenylphosphonium bromide (4.23a)

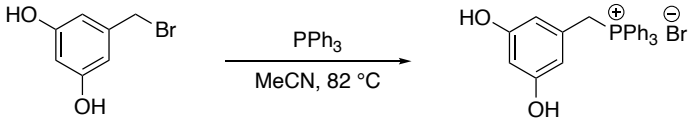

4.22a **4.23a**

To a solution of a 2:1 mixture of 5-(bromomethyl)benzene-1,3-diol (**4.22a**):triphenylphosphine oxide (2.67 g) in anhydrous MeCN (30 mL) was added triphenylphosphine (3.93 g, 15 mmol) in one portion at rt. The reaction mixture was heated to 82 °C for 5 hours then concentrated *in vacuo* to remove the MeCN. Et_2O (10

mL) was added to promote the product and triphenylphosphine oxide to precipitate out. The Et_2O was decanted off and the solid residue was washed further with Et_2O (2 x 10 mL). The solid was then washed with DCM (3 x 2 mL) to remove triphenylphosphine oxide impurity. The remaining solid was dried under vacuum to afford the title compound **4.23a** (1.21 g, 24 % yield over two steps) as a white solid.

^{1}H NMR (500 MHz, DMSO-d_6) δ 9.31 (s, 2H), 7.94 – 7.86 (m, 3H), 7.79 – 7.69 (m, 6H), 7.67 – 7.61 (m, 6H), 6.14 (q, *J* = 2.2 Hz, 1H), 5.85 (t, *J* = 2.2 Hz, 2H), 4.92 (d, *J* = 15.6 Hz, 2H); **^{13}C NMR** (126 MHz, DMSO-d_6) δ 158.5 (d, *J* = 3.1 Hz), 135.0 (d, *J* = 3.0 Hz), 134.0 (d, *J* = 9.8 Hz), 130.0 (d, *J* = 12.4 Hz), 129.4 (d, *J* = 8.4 Hz), 118.1 (d, *J* = 85.6 Hz), 109.0 (d, *J* = 5.7 Hz), 102.4 (d, *J* = 3.7 Hz), 28.2 (d, *J* = 46.7 Hz); **^{31}P{^{1}H}NMR** (162 MHz, DMSO-d_6) δ 22.67; **HRMS (ESI$^+$)** m/z: $[M\text{-}Br]^+$ Calcd. for $C_{25}H_{22}O_2P$ 385.1352; Found 385.1359.

5.4.2.4 Synthesis of phosphonium salt 4.23b

(3,5-Dimethoxyphenyl)methanol (4.21b')

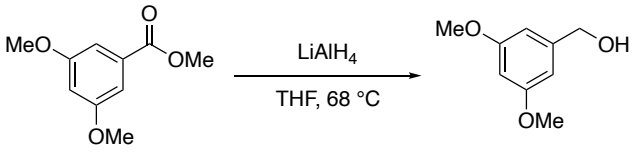

4.21b **4.21b'**

To a solution of lithium aluminium hydride (145 mg, 1.5 equiv., 3.82 mmol) in anhydrous THF (10 mL), methyl 3,5-dimethoxybenzoate (**4.21b**) (500 mg, 1.0 equiv., 2.54 mmol) in anhydrous THF (2 mL) was added dropwise at 0 °C and then heated to 68 °C for 1.5 hours. The reaction mixture was cooled to 0 °C and slowly quenched with H_2O (1 mL), 1 M $NaOH_{(aq)}$ (1 mL) and H_2O (2 mL) dropwise. The aqueous layer was extracted with Et_2O (3 x 15 mL) and the combined organic layers were washed with sat. $brine_{(aq)}$ (15 mL), dried with anhydrous $MgSO_4$, and concentrated *in vacuo* to afford the title compound **4.21b'** (419 mg, 98 %) as a colourless oil.

^{1}H NMR (300 MHz, $CDCl_3$) δ 6.53 (d, *J* = 2.3 Hz, 2H), 6.39 (t, *J* = 2.3 Hz, 1H), 4.64 (d, *J* = 0.5 Hz, 2H), 3.80 (s, 6H), 1.69 (br s, 1H); **HRMS (EI$^+$)** m/z: $[M]^{+\bullet}$ Calcd. for $C_9H_{12}O_3$ 168.0781; Found 168.0777. All spectroscopic data were in accordance with the literature.[298]

1-(Bromomethyl)-3,5-dimethoxybenzene (4.22b)

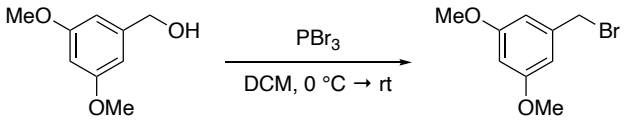

4.21b' **4.22b**

To a solution of (3,5-dimethoxyphenyl)methanol (**4.21b'**) (419 mg, 1.0 equiv., 2.49 mmol) in anhydrous DCM (5 mL), phosphorus tribromide (0.26 mL, 1.1 equiv., 2.74 mmol) was added dropwise at 0 °C. The reaction mixture stirred at rt for 1.5 hours, cooled to 0 °C and quenched with H_2O (3 mL). The aqueous layer was extracted with DCM (3 x 10 mL) and the combined organic layers were washed with sat. $brine_{(aq)}$ (20 mL), dried with anhydrous $MgSO_4$, filtered, and concentrated *in vacuo* to afford the crude. The crude was passed through a short pad of silica-gel pad (20:80 EtOAc/petroleum ether). The filtrate was concentrated *in vacuo* to afford the title compound **4.22b** (347 mg, 60%) as a colourless oil.

^{1}H NMR (400 MHz, $CDCl_3$) δ 6.54 (d, *J* = 2.3 Hz, 2H), 6.39 (t, *J* = 2.3 Hz, 1H), 4.42 (s, 2H), 3.79 (s, 6H); **HRMS (ESI$^+$)** m/z: $[M]^{+\bullet}$ Calcd. for $C_9H_{11}O_2{}^{79}Br$ 229.9937; Found 229.9935. All spectroscopic data were in accordance with the literature.[299]

(3,5-Dimethoxybenzyl)triphenylphosphonium bromide (4.23b)

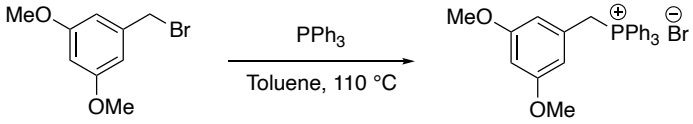

4.22b **4.23b**

A solution of 1-(bromomethyl)-3,5-dimethoxybenzene (**4.22b**) (347 mg, 1.0 equiv., 1.50 mmol) and triphenylphosphine (590 mg, 1.5 equiv., 2.25 mmol) in anhydrous toluene (5 mL) was heated at 110 °C for 19 hours. The reaction mixture was cooled to 0 °C, filtered and the white solid was washed with petroleum ether (20 mL). The solid was dried under vacuum to afford the title compound **4.23b** (579 mg, 78%) as a white solid.

^{1}H NMR (400 MHz, $CDCl_3$) δ 7.77 – 7.66 (m, 9H), 7.60 (m, 6H), 6.29 (t, *J* = 2.3 Hz, 2H), 6.24 (q, *J* = 2.3 Hz, 1H), 5.23 (d, *J* = 14.4 Hz, 2H), 3.48 (s, 6H); **^{13}C NMR** (101 MHz, $CDCl_3$) δ 160.7 (d, *J* = 3.4 Hz), 135.0 (d, *J* = 3.1 Hz), 134.5 (d, *J* = 9.7 Hz), 130.1 (d, *J* = 12.6 Hz), 129.1 (d, *J* = 8.6 Hz), 117.8 (d, *J* = 85.8 Hz), 109.2 (d, *J* = 5.5 Hz), 101.4 (d, *J* = 3.8 Hz), 55.6, 31.0 (d, *J* = 46.9

Hz); **^{31}P NMR** (162 MHz, $CDCl_3$) δ 23.23. All spectroscopic data were in accordance with the literature.[300]

5.4.2.5 Wittig reactions

Methyl-4-((*E*/*Z*)-3,5-dimethoxystyryl)cubane-1-carboxylate (4.25)

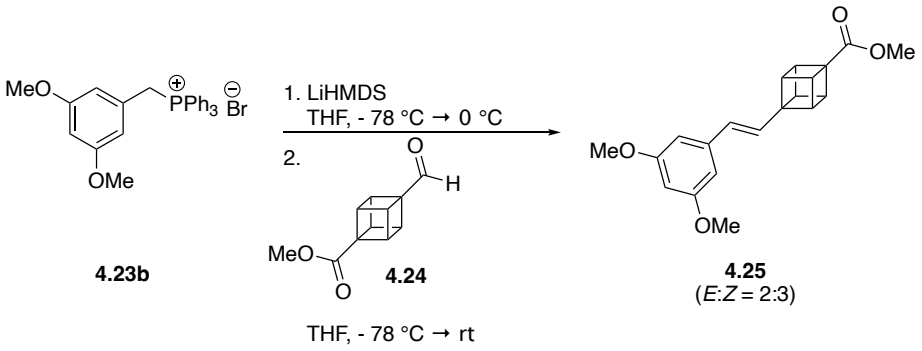

To a suspension of (3,5-dihydroxybenzyl)triphenylphosphonium bromide (**4.23b**) (272 mg, 1.4 equiv., 0.55 mmol) in anhydrous THF (2.5 mL) was added lithium bis(trimethylsilyl)amide (0.6 mL, 1.5 equiv., 1 M in THF) dropwise at -78 °C. After the addition, the mixture was stirred at 0 °C for 30 minutes in which time the suspension turned red. The reaction mixture was re-cooled to -78 °C and a solution of methyl-4-formylcubane-1-carboxylate (**4.24**) (75 mg, 1.0 equiv., 0.39 mmol) in anhydrous THF (0.5 mL) was added dropwise. The reaction mixture was stirred at rt for 1.5 hours and then quenched with 1 M $HCl_{(aq)}$ (2 mL) at 0 °C. The aqueous was extracted with EtOAc (3 x 10 mL) and the combined organic layers were washed with sat. $brine_{(aq)}$ (10 mL), dried with anhydrous $MgSO_4$, filtered and concentrated *in vacuo* to afford the crude (*E*/*Z* = 2:3). Purification by silica gel column chromatography (20:80 EtOAc/DCM) gave the title compound **4.25** (55 mg, 43 %, *E*/*Z* = 2:3) as a colourless oil.

^{1}H NMR (400 MHz, $CDCl_3$) δ 6.54 (d, *J* = 2.2 Hz, 0.8H, *E*-isomer), 6.45 (d, *J* = 16.0 Hz, 0.4H, *E*-isomer), 6.42 (d, *J* = 11.6 Hz, 0.6H, *Z*-isomer), 6.35 (q, *J* = 2.5 Hz, 1H, *Z*-isomer and *E*-isomer), 6.27 (d, *J* = 2.3 Hz, 1.2H, *Z*-isomer), 6.20 (d, *J* = 16.0 Hz, 0.4H, *E*-isomer), 5.83 (d, *J* = 11.6 Hz, 0.6H, *Z*-isomer), 4.21 – 4.11 (m, 6H, *Z*-isomer and *E*-isomer), 4.06 – 4.00 (m, 1.3H, *E*-isomer), 3.88 – 3.83 (m, 2H, *Z*-isomer), 3.79 (s, 2.4H, *E*-isomer), 3.78 (s, 3.6H, *Z*-isomer), 3.72 (s, 1.3H, *E*-isomer), 3.69 (s, 2.7H, *Z*-isomer); **^{13}C NMR** (101 MHz, $CDCl_3$) δ 172.8 (*Z*-isomer), 172.8 (*E*-isomer), 161.0 (*E*-isomer), 160.5 (*Z*-isomer), 139.7 (*Z*-isomer), 139.4 (*E*-isomer), 132.1 (*Z*-isomer), 130.2 (*Z*-isomer), 129.8 (*E*-isomer), 128.3

(*E*-isomer), 106.7 (*Z*-isomer), 104.3 (*E*-isomer), 99.7 (*E*-isomer), 99.1 (*Z*-isomer), 59.7 (*E*-isomer), 57.7 (*Z*-isomer), 56.4 (*E*-isomer), 55.4 (*E*-isomer), 55.4 (*Z*-isomer), 55.2 (*Z*-isomer), 51.6 (*E*-isomer), 51.6 (*Z*-isomer), 49.2 (*Z*-isomer), 47.8 (*E*-isomer), 46.1 (*E*-isomer), 46.1 (*Z*-isomer); **HRMS (EI$^+$)** m/z: $[M]^{+\bullet}$ Calcd. for $C_{20}H_{20}O_4$ 324.1356; Found 324.1355.

4-((*E*/*Z*)-3,5-dihydroxystyryl)cuban-1-yl acetate (4.26a)

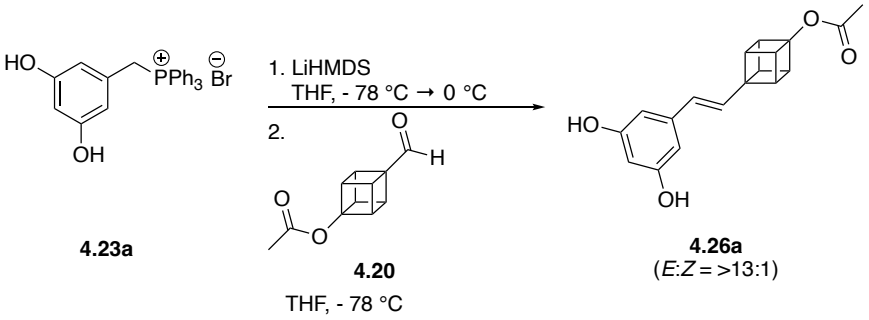

4.23a **4.20** THF, - 78 °C **4.26a** (*E*:*Z* = >13:1)

To a suspension of (3,5-dihydroxybenzyl)triphenylphosphonium bromide (**4.23a**) (517 mg, 1.4 equiv., 1.11 mmol) in anhydrous THF (5 mL) was added lithium bis(trimethylsilyl)amide (3 mL, 3.8 equiv., 1 M in THF) dropwise at -78 °C. After the addition, the mixture was stirred at 0 °C for 30 minutes in which time the suspension turned red. The reaction mixture was re-cooled to -78 °C and a solution of 4-formylcuban-1-yl acetate (**4.20**) (150 mg, 1.0 equiv., 0.79 mmol) in anhydrous THF (1 mL) was added dropwise. After stirring at -78 °C for 20 minutes the mixture was quenched with 1 M $HCl_{(aq)}$ (2 mL) at -78 °C and allowed to warm to rt. The aqueous was extracted with EtOAc (3 x 10 mL) and the combined organic layers were washed with sat. $brine_{(aq)}$ (10 mL), dried with anhydrous $MgSO_4$, filtered and concentrated *in vacuo* to afford the crude (*E*/*Z* = >13:1). Purification by silica gel column chromatography (20:80 EtOAc/DCM) gave the title compound **4.26a** (80 mg, 34 %, *E*/*Z* = >13:1) as a light-yellow solid.

(*E*)-**4.26a:** **^{1}H NMR** (500 MHz, DMSO-d_6) δ 9.16 (s, 2H), 6.36 (d, *J* = 15.8 Hz, 1H), 6.26 (d, *J* = 2.2 Hz, 2H), 6.13 (d, *J* = 15.8 Hz, 1H), 6.09 (t, *J* = 2.2 Hz, 1H), 4.16 – 4.10 (m, 3H), 3.92 – 3.86 (m, 3H), 2.07 (s, 3H); **^{13}C NMR** (126 MHz, DMSO-d_6) δ 168.9, 158.4, 138.6, 128.8, 128.3, 104.3, 101.8, 87.4, 58.8, 50.5, 43.9, 20.7; **HRMS (ESI$^+$)** m/z: $[M+H]^+$ Calcd. for $C_{18}H_{17}O_4$ 297.1121; Found 297.1121.

4-((*E*/*Z*)-3,5-dimethoxystyryl)cuban-1-yl acetate (4.26b)

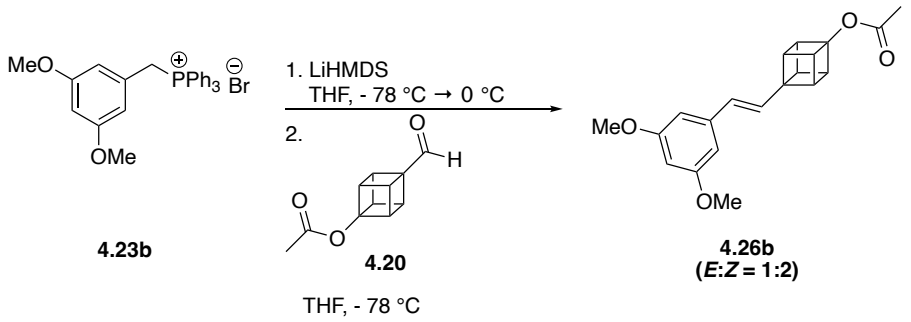

To a suspension of (3,5-dimethoxybenzyl)triphenylphosphonium bromide (**4.23b**) (100 mg, 1.4 equiv., 0.20 mmol) in anhydrous THF (1 mL), lithium bis(trimethylsilyl)amide (0.15 mL, 1.0 equiv., 1 M in THF) was added dropwise at -78 °C. After the addition, the mixture was stirred at 0 °C for 30 minutes in which time the suspension turned orange. The reaction mixture was re-cooled to -78 °C and a solution of 4-formylcuban-1-yl acetate (**4.20**) (28 mg, 1.0 equiv., 0.15 mmol) in anhydrous THF (0.5 mL) was added dropwise. After stirring at -78 °C for 20 minutes the mixture was quenched with 1 M $HCl_{(aq)}$ (2 mL) at -78 °C and allowed to warm to rt. The aqueous was extracted with EtOAc (3 x 10 mL) and the combined organic layers were washed with sat. $brine_{(aq)}$ (10 mL), dried with anhydrous $MgSO_4$, filtered, and concentrated *in vacuo* to afford the crude (*E*/*Z* = 1:2). Purification by silica gel column chromatography (10:90 EtOAc/petroleum ether) gave the title compound **4.26b** (34 mg, 71%, *E*/*Z* = 1:2) as a white solid.

^{1}H NMR (400 MHz, $CDCl_3$) δ 6.54 (d, *J* = 2.3 Hz, 0.8H, *E* isomer), 6.48 (d, *J* = 15.7 Hz, 0.5H, *E* isomer), 6.41 (d, *J* = 11.7 Hz, 1H, *Z* isomer), 6.34 (m, 1.5H, *Z*/*E* isomer), 6.27 (d, *J* = 2.3 Hz, 1H, *Z*-isomer), 6.21 (d, *J* = 15.7 Hz, 0.4H, *E*-isomer), 5.87 (d, *J* = 11.7 Hz, 1H, *Z*-isomer), 4.24 – 4.12 (m, 4.5H, *Z*/*E* isomer), 3.96 – 3.90 (m, 1.3H, *E*-isomer), 3.80 – 3.74 (m, 3H, *Z*-isomer), 3.79 (s, 2.3H, *E*-isomer), 3.78 (s, 6H, *Z*-isomer), 2.10 (s, 1.2H, *E*-isomer), 2.07 (s, 3H, *Z*-isomer); **^{13}C NMR** (101 MHz, $CDCl_3$) δ 169.5 (*Z*/*E*-isomer), 161.0 (*Z*-isomer), 160.5 (*E*-isomer), 139.7 (*Z*-isomer), 139.5 (*E*-isomer), 132.5 (*Z*-isomer), 130.4 (*E*-isomer), 130.0 (*Z*-isomer), 128.1 (*E*-isomer), 106.7 (*Z*-isomer), 104.2 (*E*-isomer), 99.7 (*E*-isomer), 99.1 (*Z*-isomer), 88.4 (*E*-isomer), 87.5 (*Z*-isomer), 59.5 (*E*-isomer), 57.3 (*Z*-isomer), 55.4 (*E*-isomer), 55.4 (*Z*-isomer), 51.4 (*E*-isomer), 51.3 (*Z*-isomer), 46.1 (*Z*-isomer), 44.8 (*E*-isomer), 21.2 (*E*-isomer), 21.1 (*Z*-isomer); **HRMS (ESI$^+$)** m/z: $[M+H]^+$ Calcd. for $C_{20}H_{21}O_4$ 325.1434; Found 325.1436.

5.4.2.5 Cubanols

5-((*E*/*Z*)-2-(4-Hydroxycuban-1-yl)vinyl)benzene-1,3-diol (4.13a)

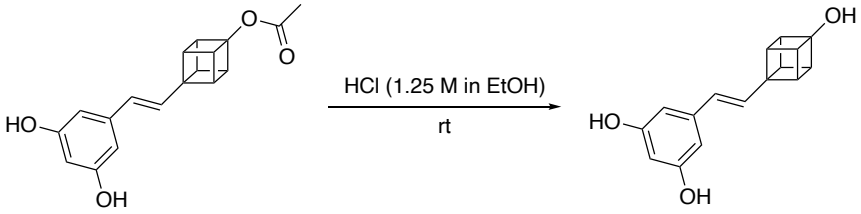

4.26a
(*E*:*Z* = >13:1)

4.13a
(*E*:*Z* = >13:1)

4-((*E*/*Z*)-3,5-Dihydroxystyryl)cuban-1-yl acetate (**4.26a**) (10 mg, 1.0 equiv., 0.04 mmol, *E*/*Z* = 13:1) in a solution of HCl in ethanol (0.5 mL, 1.25 M) was stirred at rt for 3 h. The reaction mixture was concentrated *in vacuo* to remove bulk of the ethanol to afford a brown sticky solid. The sample was triturated with Et_2O (1 mL) to afford a light brown solid which still contained ethanol. Removal of ethanol was achieved by dissolving the sample in EtOAc (10 mL) and washing the organic layer quickly with sat. $NH_4Cl_{(aq)}$ (4 x 5 mL), dried with anhydrous $MgSO_4$, filtered and concentrated *in vacuo* to afford the title compound **4.13a** (3 mg, 32 %, *E*/*Z* = >13:1) as a light brown solid. NMR yield = 38 % when using durene as internal standard.

^{1}H NMR (500 MHz, DMSO-d_6) δ 9.15 (s, 2H), 6.36 (d, *J* = 15.8 Hz, 1H), 6.36 (s, 1H), 6.25 (d, *J* = 2.2 Hz, 2H), 6.08 (t, *J* = 2.2 Hz, 1H), 6.08 (d, *J* = 15.8 Hz, 1H), 3.84 – 3.78 (m, 3H), 3.73 – 3.67 (m, 3H); **^{13}C NMR** (126 MHz, DMSO-d_6) δ 158.4, 138.7, 129.6, 127.7, 104.2, 101.7, 86.7, 60.0, 51.8, 42.1; **HRMS (ESI$^-$)** m/z: $[M-H]^-$ Calcd. for $C_{16}H_{13}O_3$ 253.0870; Found 253.0863.

4-((*E*/*Z*)-3,5-dimethoxystyryl)cuban-1-ol (4.13b)

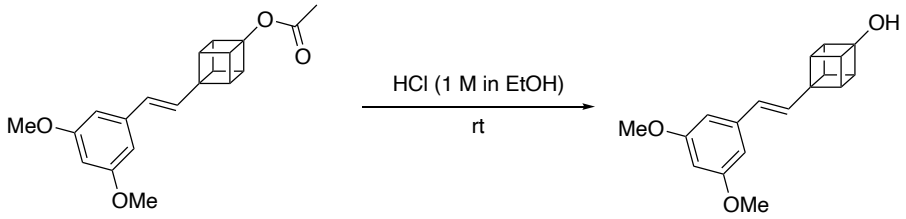

4.26b
(*E*:*Z* = 1:2)

4.13b
(*E*:*Z* = 1:2)

4-((*E*/*Z*)-3,5-dimethoxystyryl)cuban-1-yl acetate (**4.26b**) (20.1 mg, 1.0 equiv., 0.06 mmol, *E*/*Z* = 1:2) in a solution of HCl in ethanol (0.5 mL, 1.25 M) was stirred at rt for 24 hours.

Over the course of the reaction **4.26b** slowly dissolved, with progress monitored via TLC. After full consumption (24 hours), the reaction mixture was concentrated *in vacuo* and placed under high vacuum to remove bulk of the ethanol to afford a brown sticky solid. NMR yield = 49 % when using durene as internal standard.

^{1}H NMR (400 MHz, DMSO-d_6) δ 6.62 (d, *J* = 15.8 Hz, 0.45H, *E*-isomer), 6.60 (d, *J* = 2.3 Hz, 0.9H, *E*-isomer), 6.40 (t, *J* = 2.3 Hz, 1H, *Z*-isomer), 6.36 (d, *J* = 11.8 Hz, 1H, *Z*-isomer), 6.33 (t, *J* = 2.3 Hz, 0.45H, *E*-isomer), 6.27 (d, *J* = 2.3 Hz, 2H, *Z*-isomer), 6.22 (d, *J* = 15.8 Hz, 0.45H, *E*-isomer), 5.87 (d, *J* = 11.8 Hz, 1H, *Z*-isomer), 3.85 – 3.77 (m, 6H, *Z*-isomer and *E*-isomer), 3.76 - 3.71 (m, 1.4 H), 3.73 (s, 6H), 3.73 (s, 2.7H, *E*-isomer), 3.58 – 3.53 (m, 3H, *Z*-isomer); **HRMS (ESI$^+$)** m/z: $[M+H]^+$ Calcd. for $C_{18}H_{19}O_3$ 283.1329; Found 283.1328.

References

(1) Jordan, V. C. Tamoxifen: a most unlikely pioneering medicine. *Nat. rev. Drug discov.* **2003**, *2* (3), 205-213.
(2) Quirke, V. Imperial Chemical Industries and Craig Jordan,"the First Tamoxifen Consultant," 1960s–1990s. *Ambix* **2020**, *67* (3), 289-307.
(3) Harper, M.; Walpole, A. A new derivative of triphenylethylene: effect on implantation and mode of action in rats. *Reproduction* **1967**, *13* (1), 101-119.
(4) Klopper, A.; Hall, M. New synthetic agent for the induction of ovulation: preliminary trials in women. *Br. Med. J.* **1971**, *1* (5741), 152-154.
(5) Ingle, J. N.; Ahmann, D. L.; Green, S. J.; Edmonson, J. H.; Bisel, H. F.; Kvols, L. K.; Nichols, W. C.; Creagan, E. T.; Hahn, R. G.; Rubin, J. Randomized clinical trial of diethylstilbestrol versus tamoxifen in postmenopausal women with advanced breast cancer. *N. Engl. J. of Med.* **1981**, *304* (1), 16-21.
(6) Cole, M. P.; Jones, C.; Todd, I. A new anti-oestrogenic agent in late breast cancer: an early clinical appraisal of ICI46474. *Br. J. Cancer* **1971**, *25* (2), 270-275.
(7) Allen, K. E.; Clark, E.; Jordan, V. Evidence for the metabolic activation of non-steroidal antioestrogens: a study of structure-activity relationships. *Br. J. Pharmacol* **1980**, *71* (1), 83-91.
(8) Belachew, E. B.; Sewasew, D. T. Molecular mechanisms of endocrine resistance in estrogen-receptor-positive breast cancer. *Front. Endocrinol* **2021**, *12*, 599586.
(9) Patel, R.; Klein, P.; Tiersten, A.; Sparano, J. A. An emerging generation of endocrine therapies in breast cancer: a clinical perspective. *npj Breast Cancer* **2023**, *9* (1), 20.
(10) Patel, H. K.; Bihani, T. Selective estrogen receptor modulators (SERMs) and selective estrogen receptor degraders (SERDs) in cancer treatment. *Pharmacology & therapeutics* **2018**, *186*, 1-24.
(11) Jordan, V. Effect of tamoxifen (ICI 46,474) on initiation and growth of DMBA-induced rat mammary carcinomata. *European Journal of Cancer* **1976**, *12* (6), 419-424.
(12) Group, E. B. C. T. C. Effects of adjuvant tamoxifen and of cytotoxic therapy on mortality in early breast cancer. *N. Eng. J. Med* **1988**, *319* (26), 1681-1692.
(13) Early-Breast-Cancer-Trialists'-Collaborative-Group. Tamoxifen for early breast cancer: an overview of the randomised trials. *The Lancet* **1998**, *351* (9114), 1451-1467.
(14) Fisher, B.; Costantino, J. P.; Wickerham, D. L.; Redmond, C. K.; Kavanah, M.; Cronin, W. M.; Vogel, V.; Robidoux, A.; Dimitrov, N.; Atkins, J. Tamoxifen for prevention of breast cancer: report of the National Surgical Adjuvant Breast and Bowel Project P-1 Study. *JNCI* **1998**, *90* (18), 1371-1388.
(15) Bray, F.; Laversanne, M.; Sung, H.; Ferlay, J.; Siegel, R. L.; Soerjomataram, I.; Jemal, A. Global cancer statistics 2022: GLOBOCAN estimates of incidence and mortality worldwide for 36 cancers in 185 countries. *CA: A Cancer Cournal for Clinicians* **2024**, *74* (3), 229-263.
(16) Will, M.; Liang, J.; Metcalfe, C.; Chandarlapaty, S. Therapeutic resistance to anti-oestrogen therapy in breast cancer. *Nat. Rev. Cancer* **2023**, *23* (10), 673-685.
(17) *NICE. BNF. Treatment summaries. Breast Cancer*. 2025. (accessed 2025 13 April).
(18) Howell, A.; Howell, S. J. Tamoxifen evolution. *Br. J. Cancer* **2023**, *128* (3), 421-425.
(19) Buckley, M. M.-T.; Goa, K. L. Tamoxifen: a reappraisal of its pharmacodynamic and pharmacokinetic properties, and therapeutic use. *Drugs* **1989**, *37*, 451-490.

(20) Katzenellenbogen, B. S.; Norman, M. J.; Eckert, R. L.; Peltz, S. W.; Mangel, W. F. Bioactivities, estrogen receptor interactions, and plasminogen activator-inducing activities of tamoxifen and hydroxytamoxifen isomers in MCF-7 human breast cancer cells. *Cancer Res.* **1984**, *44* (1), 112-119.
(21) Lien, E. A.; Solheim, E.; Lea, O. A.; Lundgren, S.; Kvinnsland, S.; Ueland, P. M. Distribution of 4-hydroxy-N-desmethyltamoxifen and other tamoxifen metabolites in human biological fluids during tamoxifen treatment. *Cancer Res.* **1989**, *49* (8), 2175-2183.
(22) Fromson, J. M.; Pearson, S.; Bramah, S. The metabolism of tamoxifen (ICI 46,474) Part II: In female patients. *Xenobiotica* **1973**, *3* (11), 711-714.
(23) Jordan, V. C. Metabolites of tamoxifen in animals and man: identification, pharmacology, and significance. *Breast Cancer Res. Tr* **1982**, *2*, 123-138.
(24) Jordan, V. C. Chemoprevention of breast cancer with selective oestrogen-receptor modulators. *Nat. Rev. Cancer* **2007**, *7* (1), 46-53.
(25) Jordan, V. C. New insights into the metabolism of tamoxifen and its role in the treatment and prevention of breast cancer. *Steroids* **2007**, *72* (13), 829-842.
(26) Maximov, P. Y.; McDaniel, R. E.; Fernandes, D. J.; Bhatta, P.; Korostyshevskiy, V. R.; Curpan, R. F.; Jordan, V. C. Pharmacological relevance of endoxifen in a laboratory simulation of breast cancer in postmenopausal patients. *JNCI* **2014**, *106* (10), 1-10.
(27) Watanabe, M.; Watanabe, N.; Maruyama, S.; Kawashiro, T. Comparative metabolic study between two selective estrogen receptor modulators, toremifene and tamoxifen, in human liver microsomes. *DMPK* **2015**, *30* (5), 325-333.
(28) Kiyotani, K.; Mushiroda, T.; Zembutsu, H.; Nakamura, Y. Important and critical scientific aspects in pharmacogenomics analysis: lessons from controversial results of tamoxifen and CYP2D6 studies. *J. Hum Genet* **2013**, *58* (6), 327-333.
(29) Jin, Y.; Desta, Z.; Stearns, V.; Ward, B.; Ho, H.; Lee, K.-H.; Skaar, T.; Storniolo, A. M.; Li, L.; Araba, A. CYP2D6 genotype, antidepressant use, and tamoxifen metabolism during adjuvant breast cancer treatment. *JNCI* **2005**, *97* (1), 30-39.
(30) Lien, E. A.; Solheim, E.; Ueland, P. M. Distribution of tamoxifen and its metabolites in rat and human tissues during steady-state treatment. *Cancer Res.* **1991**, *51* (18), 4837-4844.
(31) Sanchez-Spitman, A.; Swen, J.; Dezentje, V.; Moes, D.; Gelderblom, H.; Guchelaar, H. Clinical pharmacokinetics and pharmacogenetics of tamoxifen and endoxifen. *Expert Rev Clin. Pharmacol* **2019**, *12* (6), 523-536.
(32) Schroth, W.; Goetz, M. P.; Hamann, U.; Fasching, P. A.; Schmidt, M.; Winter, S.; Fritz, P.; Simon, W.; Suman, V. J.; Ames, M. M. Association between CYP2D6 polymorphisms and outcomes among women with early stage breast cancer treated with tamoxifen. *JAMA* **2009**, *302* (13), 1429-1436.
(33) Lammers, L.; Mathijssen, R.; van Gelder, T.; Bijl, M.; de Graan, A.-J.; Seynaeve, C.; van Fessem, M.; Berns, E.; Vulto, A.; van Schaik, R. The impact of CYP2D6-predicted phenotype on tamoxifen treatment outcome in patients with metastatic breast cancer. *Br. J. Cancer* **2010**, *103* (6), 765-771.
(34) Sanchez-Spitman, A.; Dezentjé, V.; Swen, J.; Moes, D. J. A.; Böhringer, S.; Batman, E.; van Druten, E.; Smorenburg, C.; van Bochove, A.; Zeillemaker, A. Tamoxifen pharmacogenetics and metabolism: results from the prospective CYPTAM study. *J. Clin Oncol* **2019**, *37* (8), 636-646.

(35) Goetz, M. P.; Suman, V. J.; Reid, J. M.; Northfelt, D. W.; Mahr, M. A.; Ralya, A. T.; Kuffel, M.; Buhrow, S. A.; Safgren, S. L.; McGovern, R. M. First-in-human phase I study of the tamoxifen metabolite Z-endoxifen in women with endocrine-refractory metastatic breast cancer. *J. Clin Oncol* **2017**, *35* (30), 3391-3400.
(36) Jayaraman, S.; Reid, J. M.; Hawse, J. R.; Goetz, M. P. Endoxifen, an estrogen receptor targeted therapy: from bench to bedside. *Endocrinology* **2021**, *162* (12), bqab191.
(37) Jayaraman, S.; Reid, J. M.; Hawse, J. R.; Goetz, M. P. Endoxifen, an estrogen receptor targeted therapy: from bench to bedside. *Endocrinology* **2021**, *162* (12), 1-12.
(38) Fiorito, E.; Katika, M. R.; Hurtado, A. Cooperating transcription factors mediate the function of estrogen receptor. *Chromosoma* **2013**, *122*, 1-12.
(39) Todd, A.; Groundwater, P. W.; Gill, J. H. *Anticancer therapeutics: from drug discovery to clinical applications*; John Wiley & Sons, 2018.
(40) Jordan, V. C. Antiestrogens and selective estrogen receptor modulators as multifunctional medicines. 1. Receptor interactions. *J. Med. Chem.* **2003**, *46* (6), 883-908.
(41) Ahmed, N. S.; Samec, M.; Liskova, A.; Kubatka, P.; Saso, L. Tamoxifen and oxidative stress: an overlooked connection. *Discov. Onc.* **2021**, *12* (17), 1-15.
(42) Osborne, C. K.; Wiebe, V. J.; McGuire, W. L.; Ciocca, D. R.; DeGregorio, M. W. Tamoxifen and the isomers of 4-hydroxytamoxifen in tamoxifen-resistant tumors from breast cancer patients. *J. Clin. Oncol* **1992**, *10* (2), 304-310.
(43) Narendra, G.; Choudhary, S.; Raju, B.; Verma, H.; Silakari, O. Role of genetic polymorphisms in drug-metabolizing enzyme-mediated toxicity and pharmacokinetic resistance to anti-cancer agents: a review on the pharmacogenomics aspect. *Clin. Pharmacokinet.* **2022**, *61* (11), 1495-1517.
(44) Jordan, V. C. Molecular mechanisms of antiestrogen action in breast cancer. *Breast Cancer Res. Tr* **1994**, *31*, 41-52.
(45) Crewe, H. K.; Notley, L. M.; Wunsch, R. M.; Lennard, M. S.; Gillam, E. M. Metabolism of tamoxifen by recombinant human cytochrome P450 enzymes: formation of the 4-hydroxy, 4'-hydroxy and N-desmethyl metabolites and isomerization of trans-4-hydroxytamoxifen. *Drug Metab. Dispos.* **2002**, *30* (8), 869-874.
(46) Williams, M.; Lennard, M.; Martin, I.; Tucker, G. Interindividual variation in the isomerization of 4-hydroxytamoxifen by human liver microsomes: involvement of cytochromes P450. *Carcinogenesis* **1994**, *15* (12), 2733-2738.
(47) Wolf, D. M.; Langan-Fahey, S. M.; Parker, C. J.; McCague, R.; Jordan, V. C. Investigation of the mechanism of tamoxifen-stimulated breast tumor growth with nonisomerizable analogues of tamoxifen and metabolites. *JNCI* **1993**, *85* (10), 806-812.
(48) Katzenellenbogen, J. A.; Carlson, K. E.; Katzenellenbogen, B. S. Facile geometric isomerization of phenolic non-steroidal estrogens and antiestrogens: limitations to the interpretation of experiments characterizing the activity of individual isomers. *J. Steroid Biochem.* **1985**, *22* (5), 589-596.
(49) Gao, L.; Tu, Y.; Wegman, P.; Wingren, S.; Eriksson, L. A. A mechanistic hypothesis for the cytochrome P450-catalyzed cis–trans isomerization of 4-hydroxytamoxifen: an unusual redox reaction. *J. Chem. Inf. Model* **2011**, *51* (9), 2293-2301.
(50) Yu, D. D.; Forman, B. M. Simple and efficient production of (Z)-4-hydroxytamoxifen, a potent estrogen receptor modulator. *J. Org. Chem.* **2003**, *68* (24), 9489-9491.

(51) Brockdorff, B. L.; Skouv, J.; Reiter, B. E.; Lykkesfeldt, A. E. Increased expression of cytochrome p450 1A1 and 1B1 genes in anti-estrogen–resistant human breast cancer cell lines. *Int. J Cancer* **2000**, *88* (6), 902-906.
(52) Widschwendter, M.; Siegmund, K. D.; Müller, H. M.; Fiegl, H.; Marth, C.; Müller-Holzner, E.; Jones, P. A.; Laird, P. W. Association of breast cancer DNA methylation profiles with hormone receptor status and response to tamoxifen. *Cancer Res.* **2004**, *64* (11), 3807-3813.
(53) Mürdter, T.; Schroth, W.; Bacchus-Gerybadze, L.; Winter, S.; Heinkele, G.; Simon, W.; Fasching, P.; Fehm, T.; Tamoxifen, G.; Group, A. C.; et al. Activity levels of tamoxifen metabolites at the estrogen receptor and the impact of genetic polymorphisms of phase I and II enzymes on their concentration levels in plasma. *Clin. Pharmacol. Ther* **2011**, *89* (5), 708-717.
(54) Lloyd, D. G.; Hughes, R. B.; Zisterer, D. M.; Williams, D. C.; Fattorusso, C.; Catalanotti, B.; Campiani, G.; Meegan, M. J. Benzoxepin-derived estrogen receptor modulators: a novel molecular scaffold for the estrogen receptor. *J. Med. Chem.* **2004**, *47* (23), 5612-5615.
(55) Chiacchio, M. A.; Legnani, L.; Campisi, A.; Paola, B.; Giuseppe, L.; Iannazzo, D.; Veltri, L.; Giofrè, S.; Romeo, R. 1, 2, 4-Oxadiazole-5-ones as analogues of tamoxifen: Synthesis and biological evaluation. *Org. Biomol. Chem* **2019**, *17* (19), 4892-4905.
(56) Palacios, S. Selective estrogen receptor modulators (SERMs): State of the art. In: Pérez-López, F. (eds). *Postmenopausal Diseases and Disorders Springer, Cham*. **2019**, 349-366.
(57) Beer, M. L.; Lemon, J.; Valliant, J. F. Preparation and evaluation of carborane analogues of tamoxifen. *J. Med. Chem.* **2010**, *53* (22), 8012-8020.
(58) Valliant, J. F.; Schaffer, P.; Stephenson, K. A.; Britten, J. F. Synthesis of Boroxifen, AN ido-Carborane Analogue of Tamoxifen. *J. Org. Chem.* **2002**, *67* (2), 383-387.
(59) Top, S.; Dauer, B.; Vaissermann, J.; Jaouen, G. Facile route to ferrocifen, 1-[4-(2-dimethylaminoethoxy)]-1-(phenyl-2-ferrocenyl-but-1-ene), first organometallic analogue of tamoxifen, by the McMurry reaction. *J. Organomet. Chem.* **1997**, *541* (1-2), 355-361.
(60) Malo-Forest, B.; Landelle, G.; Roy, J.-A.; Lacroix, J.; Gaudreault, R. C.; Paquin, J.-F. Synthesis and growth inhibition activity of fluorinated derivatives of tamoxifen. *Bioorg. Med. Chem. Lett.* **2013**, *23* (6), 1712-1715.
(61) Subbaiah, M. A.; Meanwell, N. A. Bioisosteres of the phenyl ring: recent strategic applications in lead optimization and drug design. *J. Med. Chem.* **2021**, *64* (19), 14046-14128.
(62) Taylor, R. D.; MacCoss, M.; Lawson, A. D. Rings in drugs: Miniperspective. *J. Med. Chem.* **2014**, *57* (14), 5845-5859.
(63) Shearer, J.; Castro, J. L.; Lawson, A. D.; MacCoss, M.; Taylor, R. D. Rings in clinical trials and drugs: present and future. *J. Med. Chem.* **2022**, *65* (13), 8699-8712.
(64) Galloway, W. R.; Isidro-Llobet, A.; Spring, D. R. Diversity-oriented synthesis as a tool for the discovery of novel biologically active small molecules. *Nat. Commun.* **2010**, *1* (80), 1-13.
(65) Lovering, F.; Bikker, J.; Humblet, C. Escape from flatland: Increasing saturation as an approach to improving clinical success. *J. Med. Chem.* **2009**, *52* (21), 6752-6756.
(66) Mykhailiuk, P. K. Saturated bioisosteres of benzene: where to go next? *Org. Biomol. Chem.* **2019**, *17* (11), 2839-2849.

(67) Tsien, J.; Hu, C.; Merchant, R. R.; Qin, T. Three-dimensional saturated C (sp 3)-rich bioisosteres for benzene. *Nat. Rev. Chem.* **2024**, *8*, 605-627.
(68) Fang, Z.; Xu, Q.; Lu, X.; Wan, N.; Yang, W.-L. The Application of Bicyclo [1.1. 1] pentane as a Bioisostere of the Phenyl Ring in Pharmaceutical Chemistry. *Synthesis* **2024**, *57* (6), 1171-1179.
(69) Diepers, H. E.; Walker, J. C. L. (Bio) isosteres of ortho-and meta-substituted benzenes. *Beilstein J. Org. Chem.* **2024**, *20*, 859-890.
(70) Meanwell, N. A. Synopsis of some recent tactical application of bioisosteres in drug design. *J. Med. Chem.* **2011**, *54* (8), 2529-2591.
(71) Langmuir, I. Isomorphism, Isosterism and Covalence. *J. Am. Chem. Soc.* **1919**, *41* (10), 1543-1559.
(72) Brown, N. *Bioisosterism in medicinal chemistry*; Brown, N., Ed.; Vol. 54; Wiley-VCH, 2012.
(73) Friedman, H. L. *Influence of isosteric replacements upon biological activity.*; First Symposium on Chemical-Biological Correlation, National Research Council, 1951.
(74) Thornber, C. Isosterism and molecular modification in drug design. *Chem. Soc. Rev.* **1979**, *8* (4), 563-580.
(75) Patani, G. A.; LaVoie, E. J. Bioisosterism: A rational approach in drug design. *Chem. Rev.* **1996**, *96* (8), 3147-3176.
(76) Meanwell, N. A. Fluorine and fluorinated motifs in the design and application of bioisosteres for drug design. *J. Med. Chem.* **2018**, *61* (14), 5822-5880.
(77) Longley, D. B.; Harkin, D. P.; Johnston, P. G. 5-fluorouracil: mechanisms of action and clinical strategies. *Nat. Rev. Cancer* **2003**, *3*, 330-338.
(78) Schann, S.; Bruban, V.; Pompermayer, K.; Feldman, J.; Pfeiffer, B.; Renard, P.; Scalbert, E.; Bousquet, P.; Ehrhardt, J.-D. Synthesis and biological evaluation of pyrrolinic isosteres of rilmenidine. Discovery of cis-/trans-dicyclopropylmethyl-(4, 5-dimethyl-4, 5-dihydro-3 H-pyrrol-2-yl)-amine (LNP 509), an I_1 imidazoline receptor selective ligand with hypotensive activity. *J. Med. Chem.* **2001**, *44* (10), 1588-1593.
(79) Counsell, R.; Klimstra, P.; Nysted, L.; Ranney, R. Hypocholesterolemic agents. V. Isomeric azacholesterols. *J. Med. Chem.* **1965**, *8*, 45-48.
(80) Barnes, M. J.; Conroy, R.; Miller, D. J.; Mills, J. S.; Montana, J. G.; Pooni, P. K.; Showell, G. A.; Walsh, L. M.; Warneck, J. B. Trimethylsilylpyrazoles as novel inhibitors of p38 MAP kinase: A new use of silicon bioisosteres in medicinal chemistry. *Bioorg. Med. Chem. Lett.* **2007**, *17* (2), 354-357.
(81) Ritchie, T. J.; Macdonald, S. J. F. The impact of aromatic ring count on compound developability – are too many aromatic rings a liability in drug design? *Drug Discov. Today* **2009**, *14* (21-22), 1011-1020.
(82) Hedberg, L.; Hedberg, K.; Eaton, P. E.; Nodari, N.; Robiette, A. G. Bond lengths and quadratic force field for cubane. *J. Am. Chem. Soc.* **1991**, *113* (5), 1514-1517.
(83) Ermer, O.; Dunitz, J. Conformation of the bicyclo [2, 2, 2]octane system. *Chem. Commun.* **1968**, (10), 567-568.
(84) Almenningen, A.; Andersen, B.; Nyhus, B. On the Molecular Structure of Bicyclo (lll) pentane in the Vapour Phase Determined by Electron Diffraction. *Acta. Chem. Scand* **1971**, *25* (4), 1217-1223.
(85) Stepan, A. F.; Subramanyam, C.; Efremov, I. V.; Dutra, J. K.; O'Sullivan, T. J.; DiRico, K. J.; McDonald, W. S.; Won, A.; Dorff, P. H.; Nolan, C. E.; et al. Application of the bicyclo

[1.1. 1]pentane motif as a nonclassical phenyl ring bioisostere in the design of a potent and orally active γ-secretase inhibitor. *J. Med. Chem.* **2012**, *55* (7), 3414-3424.
(86) Frank, N.; Nugent, J.; Shire, B. R.; Pickford, H. D.; Rabe, P.; Sterling, A. J.; Zarganes-Tzitzikas, T.; Grimes, T.; Thompson, A. L.; Smith, R. C.; et al. Synthesis of meta-substituted arene bioisosteres from [3.1. 1] propellane. *Nature* **2022**, *611*, 721-726.
(87) Reinhold, M.; Steinebach, J.; Golz, C.; Walker, J. C. Synthesis of polysubstituted bicyclo [2.1. 1] hexanes enabling access to new chemical space. *Chemical Science* **2023**, *14* (36), 9885-9891.
(88) Wiesenfeldt, M. P.; Rossi-Ashton, J. A.; Perry, I. B.; Diesel, J.; Garry, O. L.; Bartels, F.; Coote, S. C.; Ma, X.; Yeung, C. S.; Bennett, D. J.; et al. General access to cubanes as benzene bioisosteres. *Nature* **2023**, *618*, 513-518.
(89) Zhao, J.-X.; Chang, Y.-X.; He, C.; Burke, B. J.; Collins, M. R.; Del Bel, M.; Elleraas, J.; Gallego, G. M.; Montgomery, T. P.; Mousseau, J. J.; et al. 1,2-Difunctionalized bicyclo [1.1. 1]pentanes: Long–sought-after mimetics for ortho/meta-substituted arenes. *PNAS* **2021**, *118* (28), e2108881118.
(90) Denisenko, A.; Garbuz, P.; Shishkina, S. V.; Voloshchuk, N. M.; Mykhailiuk, P. K. Saturated bioisosteres of ortho-substituted benzenes. *Angew. Chem.* **2020**, *132* (46), 20696-20702.
(91) Ishikawa, M.; Hashimoto, Y. Improvement in aqueous solubility in small molecule drug discovery programs by disruption of molecular planarity and symmetry. *J. Med. Chem.* **2011**, *54* (6), 1539-1554.
(92) Li, H.; Gao, Y.; Ma, J. Advances in nonclassical phenyl bioisosteres for drug structural optimization. *Fut. Med. Chem.* **2022**, *14* (22), 1681-1692.
(93) Xia, K. Recent Advances in Bridged Structures as 3D Bioisosteres of *ortho*-Phenyl Rings in Medicinal Chemistry Applications. *Chem. Commun.* **2025**, *61* (35), 6417-6425.
(94) Garry, O. L.; Heilmann, M.; Chen, J.; Liang, Y.; Zhang, X.; Ma, X.; Yeung, C. S.; Bennett, D. J.; MacMillan, D. W. Rapid access to 2-substituted bicyclo [1.1. 1]pentanes. *J. Am. Chem. Soc.* **2023**, *145* (5), 3092-3100.
(95) Yang, L.; Shao, Y.; Han, H.-K. Improved pH-dependent drug release and oral exposure of telmisartan, a poorly soluble drug through the formation of drug-aminoclay complex. *Int. J Pharm.* **2014**, *471* (1-2), 258-263.
(96) Almeida, A. S.; Guedes de Pinho, P.; Remião, F.; Fernandes, C. Metabolomics as a tool for unraveling the impact of enantioselectivity in cellular metabolism. *Crit. Rev. Anal. Chem.* **2025**, 1-21.
(97) Levterov, V. V.; Panasyuk, Y.; Pivnytska, V. O.; Mykhailiuk, P. K. Water-soluble non-classical benzene mimetics. *Angew. Chem.* **2020**, *132* (18), 7228-7234.
(98) Garrido-García, P.; Quirós, I.; Milán-Rois, P.; Ortega-Gutiérrez, S.; Martín-Fontecha, M.; Campos, L. A.; Somoza, Á.; Fernández, I.; Rigotti, T.; Tortosa, M. Enantioselective photocatalytic synthesis of bicyclo [2.1. 1]hexanes as *ortho*-disubstituted benzene bioisosteres with improved biological activity. *Nat. Chem.* **2025**, *17*, 734-745.
(99) Li, Y.-J.; Wu, Z.-L.; Gu, Q.-S.; Fan, T.; Duan, M.-H.; Wu, L.; Wang, Y.-T.; Wu, J.-P.; Fu, F.-L.; Sang, F.; et al. Catalytic intermolecular asymmetric [2π+ 2σ] cycloadditions of bicyclo[1.1. 0]butanes: Practical synthesis of enantioenriched highly substituted bicyclo [2.1. 1]hexanes. *J. Am. Chem. Soc.* **2024**, *146* (50), 34427-34441.
(100) Fu, Q.; Cao, S.; Wang, J.; Lv, X.; Wang, H.; Zhao, X.; Jiang, Z. Enantioselective [2π+ 2σ] cycloadditions of bicyclo[1.1.0]butanes with vinylazaarenes through asymmetric photoredox catalysis. *J. Am. Chem. Soc.* **2024**, *146* (12), 8372-8380.

(101) Villani, A.; Fabbrocini, G.; Costa, C.; Scalvenzi, M. Sonidegib: Safety and efficacy in treatment of advanced basal cell carcinoma. *Dermat. Ther.* **2020**, *10*, 401-412.
(102) Aguilar, A.; Lu, J.; Liu, L.; Du, D.; Bernard, D.; McEachern, D.; Przybranowski, S.; Li, X.; Luo, R.; Wen, B.; et al. Discovery of 4-((3'*R*, 4'*S*, 5'*R*)-6"-Chloro-4'-(3-chloro-2-fluorophenyl)-1'-ethyl-2"-oxodispiro[cyclohexane-1,2'-pyrrolidine-3',3"-indoline]-5'-carboxamido)bicyclo[2.2. 2] octane-1-carboxylic acid (AA-115/APG-115): A potent and orally active murine double minute 2 (MDM2) inhibitor in clinical development. *J. Med. Chem.* **2017**, *60* (7), 2819-2839.
(103) Ambrose, M.; Lee, J.; Syed, A.; Ahmed, Z.; Peng, G. Non-enzymatic protein targeting agents as a promising strategy for cancer treatment. *Front. Drug Discov.* **2025**, *5*, 1-19.
(104) Eaton, P. E.; Cole, T. W. Cubane. *J. Am. Chem. Soc.* **1964**, *86* (15), 3157-3158.
(105) Eaton, P. E. Cubanes: Starting Materials for the Chemistry of the 1990s and the New Century. *Angew. Chem. Int. Ed.* **1992**, *31* (11), 1421-1436.
(106) Chalmers, B. A.; Xing, H.; Houston, S.; Clark, C.; Ghassabian, S.; Kuo, A.; Cao, B.; Reitsma, A.; Murray, C. E. P.; Stok, J. E.; et al. Validating Eaton's hypothesis: Cubane as a benzene bioisostere. *Angew. Chem. Int. Ed.* **2016**, *55* (11), 3580-3585.
(107) Lipinski, C. A.; Lombardo, F.; Dominy, B. W.; Feeney, P. J. Experimental and computational approaches to estimate solubility and permeability in drug discovery and development settings. *Advan. Drug Deliv. Rev.* **1997**, *23* (1-3), 3-25.
(108) Houston, S. D.; Fahrenhorst-Jones, T.; Xing, H.; Chalmers, B. A.; Sykes, M. L.; Stok, J. E.; Farfan Soto, C.; Burns, J. M.; Bernhardt, P. V.; De Voss, J. J.; et al. The cubane paradigm in bioactive molecule discovery: further scope, limitations and the cyclooctatetraene complement. *Org. Biomol. Chem.* **2019**, *17* (28), 6790-6798.
(109) Choi, S.-Y.; Eaton, P. E.; Hollenberg, P. F.; Liu, K. E.; Lippard, S. J.; Newcomb, M.; Putt, D. A.; Upadhyaya, S. P.; Xiong, Y. Regiochemical variations in reactions of methylcubane with *tert*-butoxyl radical, cytochrome P-450 enzymes, and a methane monooxygenase system. *J. Am. Chem. Soc.* **1996**, *118* (28), 6547-6555.
(110) Eaton, P. E.; Cole, T. W. The cubane system. *J. Am. Chem. Soc.* **1964**, *86* (5), 962-964.
(111) Newcomb, M.; Shen, R.; Choi, S.-Y.; Toy, P. H.; Hollenberg, P. F.; Vaz, A. D.; Coon, M. J. Cytochrome P450-catalyzed hydroxylation of mechanistic probes that distinguish between radicals and cations. Evidence for cationic but not for radical intermediates. *J. Am. Chem. Soc.* **2000**, *122* (12), 2677-2686.
(112) Tse, E. G.; Houston, S. D.; Williams, C. M.; Savage, G. P.; Rendina, L. M.; Hallyburton, I.; Anderson, M.; Sharma, R.; Walker, G. S.; Obach, R. S.; et al. Nonclassical phenyl bioisosteres as effective replacements in a series of novel open-source antimalarials. *J. Med. Chem.* **2020**, *63* (20), 11585-11601.
(113) Barborak, J. C.; Watts, L.; Pettit, R. A convenient synthesis of the cubane system. *Journal of the American Chemical Society* **1966**, *88* (6), 1328-1329.
(114) Fiedorczuk, K.; Chen, J. Mechanism of CFTR correction by type I folding correctors. *Cell* **2022**, *185* (1), 158-168.
(115) Sirachainan, E.; Jaruhathai, S.; Trachu, N.; Panvichian, R.; Sirisinha, T.; Ativitavas, T.; Ratanatharathorn, V.; Chamnanphon, M.; Sukasem, C. CYP2D6 polymorphisms influence the efficacy of adjuvant tamoxifen in Thai breast cancer patients. *Pharmacogenomics and Personalized Medicine* **2012**, *5*, 149-153.

(116) Auberson, Y. P.; Brocklehurst, C.; Furegati, M.; Fessard, T. C.; Koch, G.; Decker, A.; La Vecchia, L.; Briard, E. Improving nonspecific binding and solubility: Bicycloalkyl groups and cubanes as *para*-phenyl bioisosteres. *ChemMedChem* **2017**, *12* (8), 590-598.
(117) Tandon, N.; Luxami, V.; Tandon, R.; Paul, K. Recent advances in the synthesis of tamoxifen and analogues in medicinal chemistry. *Asian J. Org. Chem.* **2020**, *9* (10), 1432-1465.
(118) M Kasiotis, K.; A Haroutounian, S. Tamoxifen: A synthetic overview. *Curr. Org. Chem.* **2012**, *16* (3), 335-352.
(119) Coe, P. L.; Scriven, C. E. Crossed coupling of functionalised ketones by low valent titanium (the McMurry reaction): a new stereoselective synthesis of tamoxifen. *J. Chem. Soc., Perkin Trans.1* **1986**, 475-477.
(120) Harper, M. J.; Richardson, D. N.; Walpole, A. L. Alkene derivatives. United States, Patent number 4,536,516, Imperial Chemical Industries PLC, 1985.
(121) McCague, R. Stereoselective olefin formation from the dehydration of 1-(*p*-alkoxyphenyl)-1,2-diphenylbutan-1-ols: Application to the synthesis of tamoxifen. *J. Chem. Soc., Perkin Trans.1* **1987**, 1011-1015.
(122) Katzenellenbogen, J.; Robertson, D. Synthesis of the *E* and *Z* isomers of the antiestrogen tamoxifen and its metabolite, hydroxytamoxifen, in tritium-labeled form. *J. Org. Chem* **1982**, *47* (12), 2387-2393.
(123) Chang, M.-Y.; Cheng, Y.-C.; Sun, P.-P. Pd $(OAc)_2$-catalyzed desulfinative cross-coupling of sodium sulfinates with β-bromostyrenes: Synthesis of tamoxifen. *Synthesis* **2017**, *49* (11), 2411-2422.
(124) Potter, G. A.; McCague, R. Highly stereoselective access to an (*E*)-vinyl bromide from an aryl ketone leads to short syntheses of (*Z*)-tamoxifen and important substituted derivatives. *J. Org. Chem.* **1990**, *55* (25), 6184-6187.
(125) Pandey, R. K.; Wakharkar, R.; Kumar, P. Wittig–Horner approach for the synthesis of tamoxifen. *Synth. Commun.* **2005**, *35*, 2795-2800.
(126) Carroll, V. M.; Harpp, D. N.; Priefer, R. Thermo-cage opening of 4-iodo-1-vinylcubane to a novel styrene derivative. *Tetrahedron Lett.* **2008**, *49* (17), 2677-2680.
(127) Xing, H.; Houston, S. D.; Chen, X.; Ghassabian, S.; Fahrenhorst-Jones, T.; Kuo, A.; Murray, C. E. P.; Conn, K. A.; Jaeschke, K. N.; Jin, D. Y.; et al. Cyclooctatetraene: a bioactive cubane paradigm complement. *Chem. - Eur. J.* **2019**, *25* (11), 2729-2734.
(128) Churches, Q. I.; Mulder, R. J.; White, J. M.; Tsanaktsidis, J.; Duggan, P. J. The synthesis of a cubane-substituted dipeptide. *Australian J. Chem.* **2012**, *65* (6), 690-693.
(129) Wu, X. D., Wei; Chen, Dongmei; Mao, Haibin; Lin, Dong; Zhao, Tanfeng; Yang, Yingying; Zheng, Shansong; Fu, Jianmin; Zhang, Xue. Indoleamine 2,3-dioxygenase inhibitor. China, CN112062717 A, Qilu Pharmaceutical co Ltd, 2020.
(130) Wlochal, J.; Davies, R. D.; Burton, J. Synthesis of novel amino acids containing cubane. *Synlett* **2016**, *27* (06), 919-923.
(131) Nicolaou, K.; Härter, M. W.; Gunzner, J. L.; Nadin, A. The Wittig and related reactions in natural product synthesis. *Liebigs Annalen* **1997**, *1997* (7), 1283-1301.
(132) Vedejs, E.; Meier, G.; Snoble, K. Low-temperature characterization of the intermediates in the Wittig reaction. *J. Am. Chem. Soc.* **1981**, *103* (10), 2823-2831.
(133) Li, Y.; Shao, Q.; He, H.; Zhu, C.; Xue, X.-S.; Xie, J. Highly selective synthesis of all-carbon tetrasubstituted alkenes by deoxygenative alkenylation of carboxylic acids. *Nat. Commun.* **2022**, *13* (1), 1-8.

(134) Flynn, A. B.; Ogilvie, W. W. Stereocontrolled synthesis of tetrasubstituted olefins. *Chem. Rev.* **2007**, *107* (11), 4698-4745.
(135) McMurry, J. E.; Fleming, M. P.; Kees, K. L.; Krepski, L. R. Titanium-induced reductive coupling of carbonyls to olefins. *J. Org. Chem.* **1978**, *43* (17), 3255-3266.
(136) McMurry, J. E.; Fleming, M. P. New method for the reductive coupling of carbonyls to olefins. Synthesis of β-carotene. *J. Am. Chem. Soc.* **1974**, *96* (14), 4708-4709.
(137) Bongso, A.; Roswanda, R.; Syah, Y. M. Recent advances of carbonyl olefination via McMurry coupling reaction. *RSC Adv.* **2022**, *12* (25), 15885-15909.
(138) Kurti, L.; Czakó, B. *Strategic applications of named reactions in organic synthesis*; Elsevier, 2005.
(139) Jiang, Q.; Zhong, Q.; Zhang, Q.; Zheng, S.; Wang, G. Boron-based 4-hydroxytamoxifen bioisosteres for treatment of de novo tamoxifen resistant breast cancer. *ACS Med. Chem. Lett.* **2012**, *3* (5), 392-396.
(140) Lv, W.; Liu, J.; Skaar, T. C.; Flockhart, D. A.; Cushman, M. Design and synthesis of norendoxifen analogues with dual aromatase inhibitory and estrogen receptor modulatory activities. *J. Med. Chem.* **2015**, *58* (6), 2623-2648.
(141) Ko, E. J.; Savage, G. P.; Williams, C. M.; Tsanaktsidis, J. Reducing the cost, smell, and toxicity of the Barton reductive decarboxylation: Chloroform as the hydrogen atom source. *Org. Lett.* **2011**, *13* (8), 1944-1947.
(142) Qin, T.; Malins, L. R.; Edwards, J. T.; Merchant, R. R.; Novak, A. J.; Zhong, J. Z.; Mills, R. B.; Yan, M.; Yuan, C.; Eastgate, M. D.; et al. Nickel-catalyzed Barton decarboxylation and Giese reactions: A practical take on classic transforms. *Angew. Chem. Int. Ed.* **2017**, *56* (1), 260-265.
(143) Okada, K.; Okubo, K.; Morita, N.; Oda, M. Reductive decarboxylation of *N*-(acyloxy) phthalimides via redox-initiated radical chain mechanism. *Tetrahedron Lett.* **1992**, *33* (48), 7377-7380.
(144) Johnston, C. P.; Smith, R. T.; Allmendinger, S.; MacMillan, D. W. Metallaphotoredox-catalysed sp^3–sp^3 cross-coupling of carboxylic acids with alkyl halides. *Nature* **2016**, *536*, 322-325.
(145) Chan, A. Y.; Perry, I. B.; Bissonnette, N. B.; Buksh, B. F.; Edwards, G. A.; Frye, L. I.; Garry, O. L.; Lavagnino, M. N.; Li, B. X.; Liang, Y.; et al. Metallaphotoredox: The merger of photoredox and transition metal catalysis. *Chem. Rev.* **2021**, *122* (2), 1485-1542.
(146) Wang, P.-Z.; Chen, J.-R.; Xiao, W.-J. Hantzsch esters: An emerging versatile class of reagents in photoredox catalyzed organic synthesis. *Org. Biomol. Chem.* **2019**, *17* (29), 6936-6951.
(147) Nahm, S.; Weinreb, S. M. *N*-Methoxy-*N*-methylamides as effective acylating agents. *Tetrahedron Lett.* **1981**, *22* (39), 3815-3818.
(148) Takebe, H.; Matsubara, S. Scaffold editing of cubanes into homocubanes, homocuneanes via cuneanes. *Chem. -Eur. J.* **2024**, *30* (9), e202303063.
(149) Luh, T.-Y. The chemistry of cubane. The University of Chicago, 1974.
(150) Harper, M. J.; Walpole, A. L. Contrasting endocrine activities of *cis* and *trans* isomers in a series of substituted triphenylethylenes. *Nature* **1966**, *212* (5057), 87.
(151) Collins, D.; Hobbs, J.; Emmens, C. Antiestrogenic and antifertility compounds. 4. 1,1,2-triarylalkan-1-ols and 1,1,2-triarylalk-1-enes containing basic ether groups. *J. Med. Chem.* **1971**, *14* (10), 952-957.
(152) Bedford, G.; Richardson, D. Preparation and identification of *cis* and *trans* isomers of a substituted triarylethylene. *Nature* **1966**, *212* (5063), 733-734.

(153) Olier-Reuchet, C.; Aitken, D. J.; Bucourt, R.; Husson, H.-P. Synthesis of tamoxifen and 4-hydroxytamoxifen using super-base-metalated propylbenzene. *Tetrahedron Lett.* **1995**, *36* (45), 8221-8224.
(154) McCague, R.; Leclercq, G.; Legros, N.; Goodman, J.; Blackburn, G. M.; Jarman, M.; Foster, A. B. Derivatives of tamoxifen. Dependence of antiestrogenicity on the 4-substituent. *J. Med. Chem.* **1989**, *32* (12), 2527-2533.
(155) Smith, B. J.; Tsanaktsidis, J. Cubylcarbinyl cation: Fact or fiction? *J. Org. Chem.* **1997**, *62* (17), 5709-5712.
(156) WINSTON JR, T. The Synthesis and Chemistry of Cubane. The University of Chicago, 1966.
(157) Lim, N.-K.; Weiss, P.; Li, B. X.; McCulley, C. H.; Hare, S. R.; Bensema, B. L.; Palazzo, T. A.; Tantillo, D. J.; Zhang, H.; Gosselin, F. Synthesis of highly stereodefined tetrasubstituted acyclic all-carbon olefins via a syn-elimination approach. *Org. Lett.* **2017**, *19* (22), 6212-6215.
(158) Plunkett, S.; Flanagan, K. J.; Twamley, B.; Senge, M. O. Highly strained tertiary sp^3 scaffolds: Synthesis of functionalized cubanes and exploration of their reactivity under Pd (II) catalysis. *Organometallics* **2015**, *34* (7), 1408-1414.
(159) Cassar, L.; Eaton, P. E.; Halpern, J. Catalysis of symmetry-restricted reactions by transition metal compounds. Valence isomerization of cubane. *J. Am. Chem. Soc.* **1970**, *92* (11), 3515-3518.
(160) Eaton, P. E.; Cassar, L.; Halpern, J. Silver (I)-and palladium (II)-catalyzed isomerizations of cubane. Synthesis and characterization of cuneane. *J. Am. Chem. Soc.* **1970**, *92* (21), 6366-6368.
(161) Le, C.; Chen, T. Q.; Liang, T.; Zhang, P.; MacMillan, D. W. A radical approach to the copper oxidative addition problem: Trifluoromethylation of bromoarenes. *Science* **2018**, *360* (6392), 1010-1014.
(162) Fumihiko, T.; Josep, C.; Laurin, W.; Tie-Gen, C.; Gardner, C.; Baran, P. S. Redox-active esters in Fe-catalyzed C–C coupling. *J. Am. Chem. Soc.* **2016**, *138* (35), 11132-11135.
(163) Bernhard, S. S.; Locke, G. M.; Plunkett, S.; Meindl, A.; Flanagan, K. J.; Senge, M. O. Cubane cross-coupling and cubane–porphyrin qrrays. *Chem. -Eur. J.* **2018**, *24* (5), 1026-1030.
(164) Collin, D. E.; Folgueiras-Amador, A. A.; Pletcher, D.; Light, M. E.; Linclau, B.; Brown, R. C. Cubane electrochemistry: Direct conversion of cubane carboxylic acids to alkoxy cubanes using the Hofer–Moest reaction under flow conditions. *Chem. -Eur. J.* **2020**, *26* (2), 374-378.
(165) Reddy, D. S.; Sollott, G. P.; Eaton, P. E. Photolysis of cubyl iodides: Access to the cubyl cation. *J. Org. Chem.* **1989**, *54*, 722-723.
(166) Irngartinger, H.; Strack, S.; Gredel, F.; Dreuw, A.; Della, E. W. The cubane cage – A sensitive probe for assessing substituent effects on a four-membered ring, part II. *Eur. J. Org. Chem.* **1999**, *1999* (5), 1253-1257.
(167) Klunder, A.; Zwanenburg, B. Chemistry of strained polycyclic compounds—III: Synthesis of cubane and homocubane alcohols. *Tetrahedron* **1972**, *28* (15), 4131-4138.
(168) Klunder, A.; Zwanenburg, B. Homoketonization in a homocubane system. *Tetrahedron Lett.* **1971**, *12* (20), 1721-1724.
(169) Eaton, P. E.; Zhou, J. P. The nature of the cubyl cation. *J. Am. Chem. Soc.* **1992**, *114* (8), 3118-3120.

(170) Kadam, A.; Nguyen, M.; Kopach, M.; Richardson, P.; Gallou, F.; Wan, Z.-K.; Zhang, W. Comparative performance evaluation and systematic screening of solvents in a range of Grignard reactions. *Green Chem.* **2013**, *15* (7), 1880-1888.
(171) Job, G. E.; Buchwald, S. L. Copper-catalyzed arylation of β-amino alcohols. *Org. Lett.* **2002**, *4* (21), 3703-3706.
(172) Sohar, P.; Schneider, G.; Abraham, G.; Horvath, T.; Mehesfalvi, Z. Determination of the configuration of diastereomeric ethane derivatives by 1H NMR and 13C NMR spectroscopy. *Acta Chim. Acad. Sci. Hung.* **1980**, *105* (3), 201-207.
(173) Murray, P. R.; Browne, D. L.; Pastre, J. C.; Butters, C.; Guthrie, D.; Ley, S. V. Continuous flow-processing of organometallic reagents using an advanced peristaltic pumping system and the telescoped flow synthesis of (*E*/*Z*)-tamoxifen. *Org. Process Res. Dev.* **2013**, *17* (9), 1192-1208.
(174) Wlochal, J.; Davies, R. D.; Burton, J. Cubanes in medicinal chemistry: synthesis of functionalized building blocks. *Org. Lett.* **2014**, *16* (16), 4094-4097.
(175) Kowalski, C. J.; Reddy, R. E. Ester homologation revisited: A reliable, higher yielding and better understood procedure. *J. Org. Chem.* **1992**, *57* (26), 7194-7208.
(176) Gray, D.; Concellón, C.; Gallagher, T. Kowalski ester homologation. Application to the synthesis of β-amino esters. *J. Org. Chem.* **2004**, *69* (14), 4849-4851.
(177) Klunder, A.; Zwanenburg, B. Chemistry of strained polycyclic compounds—VII: A base induced homoallylic rearrangement in the homocubane and cubane system. *Tetrahedron* **1975**, *31* (11-12), 1419-1426.
(178) Yip, Y. C. Cubycarbinyl radical and cubycarbinyl anion. The University of Chicago, 1993.
(179) Edward, J. T.; Farrell, P. G.; Langford, G. E. Proton magnetic resonance spectra of cubane derivatives. I. Syntheses and spectra of mono-and 1,4-disubstituted cubanes. *J. Am. Chem. Soc.* **1976**, *98* (11), 3075-3085.
(180) Potter, G. A.; McCague, R. Coupling of low-order organocopper complexes with organoiron cations; synthesis of tamandron, a novel potentially antiandrogenic analogue of tamoxifen. *J. Chem. Soc., Chem. Commun.* **1992**, *1992* (8), 635-637.
(181) Dieudonné-Vatran, A.; Azoulay, M.; Florent, J.-C. A new access to 3-substituted-1(2H)-isoquinolone by tandem palladium-catalyzed intramolecular aminocarbonylation annulation. *Org. Biomol. Chem.* **2012**, *10* (13), 2683-2691.
(182) Iwasaki, M.; Araki, Y.; Iino, S.; Nishihara, Y. Synthesis of multisubstituted triphenylenes and phenanthrenes by cascade reaction of *o*-iodobiphenyls or (*Z*)-β-halostyrenes with *o*-bromobenzyl alcohols through two sequential C–C bond formations catalyzed by a palladium complex. *J. Org. Chem.* **2015**, *80* (18), 9247-9263.
(183) Ziegler, D. S.; Wei, B.; Knochel, P. Improving the halogen–magnesium exchange by using new turbo-Grignard reagents. *Chem. - Eur. J.* **2019**, *25* (11), 2695-2703.
(184) Wadsworth, W. S.; Emmons, W. D. The utility of phosphonate carbanions in olefin synthesis. *J. Am. Chem. Soc.* **1961**, *83* (7), 1733-1738.
(185) Maryanoff, B. E.; Reitz, A. B. The Wittig olefination reaction and modifications involving phosphoryl-stabilized carbanions. Stereochemistry, mechanism, and selected synthetic aspects. *Chem. Rev.* **1989**, *89* (4), 863-927.
(186) Eaton, P. E.; Stossel, D. Synthesis of alkynylcyclooctatetraenes and alkynylcubanes. *J. Org. Chem.* **1991**, *56* (17), 5138-5142.
(187) Tsuji, J. *Palladium reagents and catalysts: New perspectives for the 21st century*; John Wiley & Sons, 2006.

(188) Valkó, K. L. Lipophilicity and biomimetic properties measured by HPLC to support drug discovery. *J. Pharm. Biomed. Anal.* **2016**, *130*, 35-54.
(189) Scott, K. A.; Cox, P. B.; Njardarson, J. T. Phenols in pharmaceuticals: Analysis of a recurring motif. *J. Med. Chem.* **2022**, *65* (10), 7044-7072.
(190) Della, E. W.; Head, N. J. Synthesis and ^{19}F and ^{13}C NMR studies of a series of 4-substituted fluorocubanes: Resonance dependence of ^{19}F chemical shifts in a saturated system. *J. Org. Chem.* **1995**, *60* (16), 5303-5313.
(191) Eaton, P. E.; Higuchi, H.; Millikan, R. Synthesis of zinc, cadmium, tin, and silicon derivatives of cubane. *Tetrahedron Lett.* **1987**, *28* (10), 1055-1058.
(192) Eaton, P. E.; Cunkle, G. T. Oxidative deiodination of cubyl iodides: A tactic for the nucleophilic introduction of substituents onto the cubane framework. *Tetrahedron Lett.* **1986**, *27* (50), 6055-6058.
(193) Moriarty, R. M.; Khosrowshahi, J. S.; Penmasta, R. Functionalized cubanes. Oxidative displacement upon methyl 4-iodocubane carboxylate using hypervalent iodine reagents. *Tetrahedron Lett.* **1989**, *30* (7), 791-794.
(194) Nagasawa, S.; Hosaka, M.; Iwabuchi, Y. *ortho*-C–H Acetoxylation of cubane enabling access to cubane analogues of pharmaceutically relevant scaffolds. *Organic Lett.* **2021**, *23* (22), 8717-8721.
(195) Baeyer, A.; Villiger, V. Einwirkung des caro'schen reagens auf ketone. *Ber. Dtsch. Chem. Ges.* **1899**, *32* (3), 3625-3633.
(196) Krow, G. R. *The Baeyer–Villiger oxidation of ketones and aldehydes*; Wiley, 1993.
(197) Alcaide, B.; Aly, M. F.; Sierra, M. A. Stereoselective synthesis of 3-substituted 4-(formyloxy)-2-azetidinones by the unusual Baeyer− Villiger reaction of β-lactam aldehydes. Scope and synthetic applications. *J. Org. Chem.* **1996**, *61* (25), 8819-8825.
(198) Ten Brink, G.-J.; Arends, I.; Sheldon, R. The Baeyer−Villiger reaction: New developments toward greener procedures. *Chem. Rev.* **2004**, *104* (9), 4105-4124.
(199) Demnitz, F. J.; Philippini, C.; Raphael, R. A. Unexpected rearrangement in the peroxytrifluoroacetic acid- ediated Baeyer-Villiger oxidation of *trans*-3β-hydroxy-4,4,10β-trimethyl-9-decalone forming a 7-oxabicyclo[2.2.1]heptane. Structure proof and total yynthesis of (±)-farnesiferol-C[1]. *J. Org. Chem.* **1995**, *60* (16), 5114-5120.
(200) Chandler, C. L.; Phillips, A. J. A total synthesis of (±)-trans-kumausyne. *Org. Lett.* **2005**, *7* (16), 3493-3495.
(201) Jung, M. E.; Zeng, L.; Peng, T.; Zeng, H.; Le, Y.; Su, J. Total synthesis of Bao Gong Teng A, a natural antiglaucoma compound. *J. Org. Chem.* **1992**, *57* (13), 3528-3530.
(202) Thompson, M. J.; Mandava, N.; Flippen-Anderson, J. L.; Worley, J. F.; Dutky, S. R.; Robbins, W. E.; Lusby, W. Synthesis of brassino steroids: New plant-growth-promoting steroids. *J. Org. Chem* **1979**, *44* (26), 5002-5004.
(203) Kierstead, R. W.; Faraone, A. 16-Oxa Steroids. *J. Org. Chem* **1967**, *32* (3), 704-708.
(204) Bose, A. K.; Steinberg, N. G. Steroids. VIII. A-Nor steroids via pinacol-type rearrangement. *J. Org. Chem* **1971**, *36* (17), 2400-2402.
(205) Laurent, M.; Cérésiat, M.; Marchand-Brynaert, J. Regioselective Baeyer−Villiger oxidation in 4-carbonyl-2-azetidinone series: A revisited route toward carbapenem precursor. *J. Org. Chem* **2004**, *69* (9), 3194-3197.
(206) Deng, W.; Overman, L. E. Enantioselective total synthesis of either enantiomer of the antifungal antibiotic preussin (L-657,398) from (*S*)-phenylalanine. *J. Am. Chem. Soc.* **1994**, *116* (25), 11241-11250.

(207) Shing, T. K.; Lee, C. M.; Lo, H. Y. Synthesis of the CD ring in taxol from (*S*)-(+)-carvone. *Tetrahedron Lett.* **2001**, *42* (47), 8361-8363.
(208) Gibson, M.; Nur-e-alam, M.; Lipata, F.; Oliveira, M. A.; Rohr, J. Characterization of kinetics and products of the Baeyer– Villiger oxygenase MtmOIV, the key enzyme of the biosynthetic pathway toward the natural product anticancer drug mithramycin from streptomyces argillaceus. *J. Am. Chem. Soc.* **2005**, *127* (50), 17594-17595.
(209) Chadha, N.; Batcho, A.; Tang, P.; Courtney, L.; Cook, C.; Wovkulich, P.; Uskokovic, M. R. Synthesis of tetrahydrolipstatin. *J. Org. Chem* **1991**, *56* (15), 4714-4718.
(210) Roush, W. R.; D'Ambra, T. E. Synthesis of a bicyclic precursor to verrucarol: Application of a trimethylsilyl-controlled Diels-Alder reaction and Wagner-Meerwein rearrangement sequence. *J. Org. Chem* **1981**, *46* (24), 5045-5047.
(211) Suryawanshi, S.; Fuchs, P. Bruceantin support studies. 10. Use of an axial .alpha.-face control element in intramolecular conjugate additions: Synthesis of an ABCD tetracyclic bruceantin precursor. *J. Org. Chem* **1986**, *51* (6), 902-921.
(212) Kane, V. V.; Doyle, D. L. Total synthesis of (±) zoapatanol: A stereospecific synthesis of a key intermediate. *Tetrahedron Lett.* **1981**, *22* (32), 3027-3030.
(213) Lee, T. V.; Toczek, J.; Roberts, S. M. The total synthesis of (±)-boonein. *J. Chem. Soc., Chem. Commun.* **1985**, *1985* (6), 371-372.
(214) Rakhit, S.; Gut, M. 17-Oxa-5α-androstan-3-one. *J. Org. Chem* **1964**, *29* (1), 229-231.
(215) Narasaka, K.; Sakakura, T.; Uchimaru, T.; Guedin-Vuong, D. Total synthesis of a macrocyclic pyrrolizidine alkaloid,(±)-integerrimine, utilizing an activable protecting group. *J. Am. Chem. Soc.* **1984**, *106* (10), 2954-2961.
(216) Shiozaki, M.; Ishida, N.; Maruyama, H.; Hiraoka, T. Stereocontrolled syntheses of chiral and racemic key intermediates to thienamycin from D-allo-threonine and *trans*-crotonic acid. *Tetrahedron* **1983**, *39* (14), 2399-2407.
(217) Weissermel, K.; Arpe, H.-J. Components for Polyamides. In *Industrial Organic Chemistry*, Wiley, 2003; pp 239-266.
(218) Katiyar, V.; Gupta, R.; Ghosh, T. Sustainable routes for synthesis of poly(ε-caprolactone): Prospects in chemical industries. In *Advances in Sustainable Polymers*, Springer, 2019; pp 21-33.
(219) Labet, M.; Thielemans, W. Synthesis of polycaprolactone: a review. *Chem. Soc. Rev.* **2009**, *38* (12), 3484-3504.
(220) Albertsson, A.-C.; Varma, I. K. Recent developments in ring opening polymerization of lactones for biomedical applications. *Biomacromolecules* **2003**, *4* (6), 1466-1486.
(221) Snead, D. R.; Wang, Y.; Liu, S.; Lin, L. Access to cyclopropanol via supply-centered synthesis. *Org. Process Res. Dev.* **2024**, *28* (5), 1830-1837.
(222) Doraghi, F.; Pegah Aledavoud, S.; Fakhrioliaei, A.; Larijani, B.; Mahdavi, M. Ring-opening cross-coupling/cyclization reaction of cyclopropanols with organic compounds. *ChemistrySelect* **2023**, *8* (32), e202301438.
(223) McDonald, T. R.; Mills, L. R.; West, M. S.; Rousseaux, S. A. Selective carbon–carbon bond cleavage of cyclopropanols. *Chem. Rev.* **2020**, *121* (1), 3-79.
(224) Cai, X.; Liang, W.; Dai, M. Total syntheses via cyclopropanols. *Tetrahedron* **2019**, *75* (2), 193-208.

(225) Kingsbury, J. S.; Corey, E. Enantioselective total synthesis of isoedunol and β-araneosene featuring unconventional strategy and methodology. *J. Am. Chem. Soc.* **2005**, *127* (40), 13813-13815.
(226) Smith, C. R.; Aranda, R.; Bobinski, T. P.; Briere, D. M.; Burns, A. C.; Christensen, J. G.; Clarine, J.; Engstrom, L. D.; Gunn, R. J.; Ivetac, A.; et al. Fragment-based discovery of MRTX1719, a synthetic lethal inhibitor of the PRMT5•MTA complex for the treatment of *MTAP*-deleted cancers. *J. Med. Chem.* **2022**, *65* (3), 1749-1766.
(227) Achmatowicz, M.; Scattolin, T.; Snead, D. R.; Paymode, D. J.; Roshandel, S.; Xie, C.; Chen, G.; Chen, C.-y. Scalable atroposelective synthesis of MRTX1719: An inhibitor of the PRMT5/MTA Complex. *Org. Process Res. Dev.* **2023**, *27* (5), 954-971.
(228) Criegee, R. Die Umlagerung der Dekalin-peroxydester als Folge von kationischem Sauerstoff. *Liebigs Ann. Chem.* **1948**, *560* (1), 127-135.
(229) Wittig, G.; Pieper, G. Über das monomere fluorenon-peroxyd. *Ber. Dtsch. Chem. Ges. (A and B series)* **1940**, *73* (4), 295-297.
(230) Doering, W. v. E.; Dorfman, E. Mechanism of the peracid ketone—ester conversion. Analysis of organic compounds for oxygen-18. *J. Am. Chem. Soc.* **1953**, *75* (22), 5595-5598.
(231) Ochiai, M.; Yoshimura, A.; Miyamoto, K.; Hayashi, S.; Nakanishi, W. Hypervalent λ^3-bromane strategy for Baeyer− Villiger oxidation: Selective transformation of primary aliphatic and aromatic aldehydes to formates, which is missing in the classical Baeyer−Villiger oxidation. *J. Am. Chem. Soc.* **2010**, *132* (27), 9236-9239.
(232) Hawthorne, M. F.; Emmons, W. D.; McCallum, K. A re-examination of the peroxyacid cleavage of ketones. I. Relative migratory aptitudes. *J. Am. Chem. Soc.* **1958**, *80* (23), 6393-6398.
(233) Turner, R. B. Stereochemistry of the peracid oxidation of ketones. *J. Am. Chem. Soc.* **1950**, *72* (2), 878-882.
(234) Mislow, K.; Brenner, J. Stereospecificity of the Baeyer-Villiger rearrangement. *J. Am. Chem. Soc.* **1953**, *75* (10), 2318-2322.
(235) Abe, Y.; Hirakawa, T.; Nakajima, S.; Okano, N.; Hayase, S.; Kawatsura, M.; Hirose, Y.; Itoh, T. Remarkable activation of an enzyme by (*R*)-pyrrolidine-substituted imidazolium alkyl PEG sulfate. *Adv. Synth. Catal.* **2008**, *350* (13), 1954-1958.
(236) Chandrasekhar, S.; Roy, C. D. Evidence for a stereoelectronic effect in the Baeyer-Villiger reaction: Introducing the intramolecular reaction. *Tetrahedron Lett.* **1987**, *28* (50), 6371-6372.
(237) Noyori, R.; Kobayashi, H.; Sato, T. Remote substituent effects in the Baeyer-Villiger oxidation. II. Regioselection based on the hydroxyl group orientation in the tetrahedral intermediate. *Tetrahedron Lett.* **1980**, *21* (26), 2573-2576.
(238) Crudden, C. M.; Chen, A. C.; Calhoun, L. A. A demonstration of the primary stereoelectronic effect in the Baeyer–Villiger oxidation of *α*-fluorocyclohexanones. *Angew. Chem.* **2000**, *112* (16), 2973-2977.
(239) Grein, F.; Chen, A. C.; Edwards, D.; Crudden, C. M. Theoretical and experimental studies on the Baeyer− Villiger oxidation of ketones and the effect of *α*-halo substituents. *J. Org. Chem* **2006**, *71* (3), 861-872.
(240) Brady, W. T.; Cheng, T. C. Some reactions of chlorotrialkyl-1,3-cyclobutanediones. *J. Org. Chem* **1976**, *41* (11), 2036-2038.
(241) Vil', V. A.; dos Passos Gomes, G.; Bityukov, O. V.; Lyssenko, K. A.; Nikishin, G. I.; Alabugin, I. V.; Terent'ev, A. O. Interrupted Baeyer–Villiger rearrangement: Building a

stereoelectronic trap for the Criegee intermediate. *Angew. Chem. Int. Ed.* **2018**, *57* (13), 3372-3376.
(242) Vil, V. A.; Barsegyan, Y. A.; Kuhn, L.; Ekimova, M. V.; Semenov, E. A.; Korlyukov, A. A.; Terent'ev, A. O.; Alabugin, I. V. Synthesis of unstrained Criegee intermediates: Inverse *α*-effect and other protective stereoelectronic forces can stop Baeyer–Villiger rearrangement of γ-hydroperoxy-γ-peroxylactones. *Chem. Sci.* **2020**, *11* (20), 5313-5322.
(243) Anderson, L.; Young, D.; Young, W. Fluorinated peroxides derived from hexafluoroacetone. II. Insertion of $(CF_3)_2CO$ into alkali-metal peroxides and subsequent reaction with active halogen compounds. *J. Fluor. Chem* **1976**, *7* (5), 491-500.
(244) Emmons, W. D.; Lucas, G. B. Peroxytrifluoroacetic acid. V. The oxidation of ketones to esters. *J. Am. Chem. Soc.* **1955**, *77* (8), 2287-2288.
(245) Lehtinen, C.; Nevalainen, V.; Brunow, G. Experimental and computational studies on substituent effects in reactions of peracid–aldehyde adducts. *Tetrahedron* **2000**, *56* (47), 9375-9382.
(246) Winnik, M. A.; Stoute, V. Steric effects in the Baeyer–Villiger reaction of simple ketones. *Canadian J. Chem.* **1973**, *51* (16), 2788-2793.
(247) Doering, W. v. E.; Speers, L. The Peracetic acid cleavage of unsymmetrical ketones. *J. Am. Chem. Soc.* **1950**, *72* (12), 5515-5518.
(248) Hawthorne, M. F.; Emmons, W. D. A re-examination of the peroxyacid cleavage of ketones. II. Kinetics of the Baeyer-Villiger reaction. *J. Am. Chem. Soc.* **1958**, *80* (23), 6398-6404.
(249) Friess, S.; Soloway, A. Reactions of peracids. V. The reaction of substituted acetophenones with perbenzoic Acid. *J. Am. Chem. Soc.* **1951**, *73* (8), 3968-3972.
(250) Palmer, B. W.; Fry, A. Variation of carbon-14 isotope effect with substituent and the mechanism of the *m*-chloroperbenzoic acid oxidation of laeled *para*-substituted acetophenones. *J. Am. Chem. Soc.* **1970**, *92* (8), 2580-2581.
(251) Ogata, Y.; Tomizawa, K.; Ikeda, T. Kinetics of the Baeyer-Villiger reaction of acetophenones with permonophosphoric acid. *J. Org. Chem* **1978**, *43* (12), 2417-2419.
(252) Hansch, C.; Leo, A.; Taft, R. A survey of Hammett substituent constants and resonance and field parameters. *Chem. Rev.* **1991**, *91* (2), 165-195.
(253) Itoh, Y.; Yamanaka, M.; Mikami, K. Theoretical study on the regioselectivity of Baeyer–Villiger reaction of *α*-Me-,-F-,-CF_3-cyclohexanones. *J. Org. Chem* **2013**, *78* (1), 146-153.
(254) Pearlman, B. A. A total synthesis of reserpine. *J. Am. Chem. Soc.* **1979**, *101* (21), 6404-6408.
(255) Hart, D. J.; Tsai, Y. M. *α*-Acylamino radical cyclizations: Syntheses of isoretronecanol. *J. Am. Chem. Soc.* **1984**, *106* (26), 8209-8217.
(256) Saunders Jr, W. H. Steric effects on migration aptitudes. Reaction of some *o*-substituted benzophenones with peroxyacetic acid. *J. Am. Chem. Soc.* **1955**, *77* (17), 4679-4681.
(257) DeBoer, A.; Ellwanger, R. E. Baeyer-Villiger oxidation of $\Delta^{1(9)}$-octalone-2 and $\Delta^{1(8)}$-indanone-2. *J. Org. Chem* **1974**, *39* (1), 77-83.
(258) Sauers, R.; Ubersax, R. Baeyer—Villiger oxidation of cyclopropyl ketones. *J. Org. Chem* **1965**, *30* (11), 3939-3941.

(259) Yukawa, Y.; Yokoyama, T. Studies on the peroxyoxidation of ketone II. Peroxybenzoic acid oxidation of cyclophenylketones. *J. Chem. Soc. Japan* **1956**, *13* (171), 190-193.
(260) Millikan, R. *Cubanes as starting materials: Addition reactions and new routes to tetrasubstituted cubane derivatives*; The University of Chicago, 1985.
(261) Langhals, H.; Rüchardt, C. Wanderungstendenzen cyclischer, polycyclischer und methylverzweigter Alkylreste bei der Beckmann-Umlagerung. *Chem. Ber.* **1981**, *114* (12), 3831-3854.
(262) Nguyen, M. T.; Vanquickenborne, L. G. Mechanism of the Beckmann rearrangement of formaldehyde oxime and formaldehyde hydrazone in the gas phase. *J. Chem. Soc., Perkin Trans.2* **1993**, *1993* (10), 1969-1972.
(263) Hind, J.; Fallis, I. A.; Platts, J. A.; Tredwell, M. The Baeyer–Villiger oxidation of cubyl ketones: A synthetic route to functionalized cubanols. *Org. Lett.* **2025**, *27* (33), 9218-9222.
(264) Kotsuki, H.; Arimura, K.; Araki, T.; Shinohara, T. Sc $(OTf)_3$-and TfOH-catalyzed Baeyer-Villiger oxidation of carbonyl compounds with *m*-chloroperbenzoic acid. *Synlett* **1999**, *1999* (4), 462-464.
(265) Latos, P.; Siewniak, A.; Sitko, M.; Chrobok, A. The Baeyer–Villiger rearrangement with metal triflates: New developments toward mechanism. *RSC Adv.* **2020**, *10* (36), 21382-21386.
(266) Macias-Alonso, M.; Morzycki, J. W.; Iglesias-Arteaga, M. A. Studies on the $BF_3{\cdot}Et_2O$ catalyzed Baeyer–Villiger reaction of spiroketalic steroidal ketones. *Steroids* **2011**, *76* (3), 317-323.
(267) Curtin, D. Y. Stereochemical control of organic reactions differences in behaviour of diastereoisomers. *Rec. Chem. Prog* **1954**, *15*, 110-128.
(268) Andraos, J. The contributions of Solomon F. Acree (1875–1957) and the centennial anniversary of the discovery of the Acree–Curtin–Hammett Principle. *Chem. Educator* **2008**, *13*, 170-178.
(269) Sato, K.; Hyodo, M.; Takagi, J.; Aoki, M.; Noyori, R. Hydrogen peroxide oxidation of aldehydes to carboxylic acids: an organic solvent-, halide-and metal-free procedure. *Tetrahedron Lett.* **2000**, *41* (9), 1439-1442.
(270) Della, E. W.; Schiesser, C. H. Hyperconjugation in strained bridgehead cyclobutyl cations: an *ab initio* study of bicyclo[1.1. 1]pent-1-yl cubyl and norcubyl cations. *J. Chem. Soc., Chem. Commun.* **1994**, *1994* (4), 417-419.
(271) Eaton, P. E.; Yang, C. X.; Xiong, Y. Cubyl cation. *J. Am. Chem. Soc.* **1990**, *112* (8), 3225-3226.
(272) Kevill, D. N.; D'Souza, M. J.; Moriarty, R. M.; Tuladhar, S. M.; Penmasta, R.; Awasthi, A. K. Solvolysis of cubyl trifluoromethanesulphonate: Solvent and remote substituent effects. *J. Chem. Soc., Chem. Commun.* **1990**, *1990* (8), 623-624.
(273) Della, E. W.; Tsanaktsidis, J. Synthesis of some bridgehead (trimethylsilyl) polycycloalkanes. Silicon-29 NMR chemical shifts and silicon-29-carbon-13 coupling constants. *Organometallics* **1988**, *7* (5), 1178-1182.
(274) Kulbitski, K.; Nisnevich, G.; Gandelman, M. Metal-free efficient, general and facile iododecarboxylation method with biodegradable co-products. *Adv. Synth. Catal.* **2011**, *353* (9), 1438-1442.
(275) Lukin, K.; Eaton, P. E. Dimerization of cubene. 1-Iodoadamantane as a probe for radical intermediates. *J. Am. Chem. Soc.* **1995**, *117* (29), 7652-7656.

(276) Eaton, P. E.; Xiong, Y.; Zhou, J. P. Systematic substitution on the cubane nucleus: Steric and electronic effects. *J. Org. Chem.* **1992**, *57* (15), 4277-4281.
(277) Watanabe, A.; Koyamada, K.; Miyamoto, K.; Kanazawa, J.; Uchiyama, M. Decarboxylative bromination of sterically hindered carboxylic acids with hypervalent iodine (III) reagents. *Org. Process Res. Dev.* **2020**, *24* (7), 1328-1334.
(278) Della, E. W.; Head, N. J. Synthesis of bridgehead fluorides by fluorodeiodination. *J. Org. Chem.* **1992**, *57* (10), 2850-2855.
(279) Annese, C.; D'Accolti, L.; Fusco, C.; Gandolfi, R.; Eaton, P. E.; Curci, R. Oxyfunctionalization of non-natural targets by dioxiranes. 6. On the selective hydroxylation of cubane. *Org. Lett.* **2009**, *11* (16), 3574-3577.
(280) Keylor, M. H.; Matsuura, B. S.; Stephenson, C. R. Chemistry and biology of resveratrol-derived natural products. *Chem. Rev.* **2015**, *115* (17), 8976-9027.
(281) Goh, Y. L.; Cui, Y. T.; Pendharkar, V.; Adsool, V. A. Toward resolving the resveratrol conundrum: Synthesis and *in vivo* pharmacokinetic evaluation of BCP–resveratrol. *ACS Med. Chem. Lett.* **2017**, *8* (5), 516-520.
(282) Sirindil, F.; Pertschi, R.; Naulin, E.; Hatey, D.; Weibel, J.-M.; Pale, P.; Blanc, A. *trans*-Dichlorobis (XPhos)palladium(II) precatalyst for Suzuki–Miyaura Cross-Coupling reactions of aryl/vinyl sulfonates/halides: Scope, mechanistic study, and synthetic applications. *ACS Omega* **2021**, *7* (1), 1186-1196.
(283) Chen, Z.; So, C. M. Pd-Catalyzed cross-coupling of highly sterically congested enol carbamates with Grignard reagents via C–O bond activation. *Org. Lett.* **2020**, *22* (10), 3879-3883.
(284) Meegan, M. J.; Hughes, R. B.; Lloyd, D. G.; Williams, D. C.; Zisterer, D. M. Flexible estrogen receptor modulators: design, synthesis, and antagonistic effects in human MCF-7 breast cancer cells. *J. Med. Chem.* **2001**, *44* (7), 1072-1084.
(285) Eaton, P. E.; Nordari, N.; Tsanaktsidis, J.; Upadhyaya, S. P. Barton decarboxylation of cubane-1, 4-dicarboxylic acid: Optimized procedures for cubanecarboxylic acid and cubane. *Synthesis* **1995**, *1995* (5), 501-502.
(286) Zhu, Z.; Chen, S.; Qiu, D.; Li, B. Q. Metal-free visible light-promoted synthesis of 1,2,2-triarylethanones and 2,2-diarylethanones: Route towards tamoxifen. *Eur. J. Org. Chem.* **2023**, *26* (36), e202300534.
(287) Zhang, K.; Huang, J.; Zhao, W. Rh-Catalyzed coupling of aldehydes with allylboronates enables facile access to ketones. *Chem. - Eur. J.* **2022**, *28* (15), e202103851.
(288) Zhao, L.-M.; Jin, H.-S.; Liu, J.; Skaar, T. C.; Ipe, J.; Lv, W.; Flockhart, D. A.; Cushman, M. A new Suzuki synthesis of triphenylethylenes that inhibit aromatase and bind to estrogen receptors α and β. *Bioorg. Med. Chem.* **2016**, *24* (21), 5400-5409.
(289) Tanaka, R.; Sanjiki, H.; Urabe, H. Yttrium-mediated conversion of vinyl Grignard reagent to a 1,2-dimetalated ethane and its synthetic application. *J. Am. Chem. Soc.* **2008**, *130* (10), 2904-2905.
(290) Aukland, M. H.; Talbot, F. J.; Fernández-Salas, J. A.; Ball, M.; Pulis, A. P.; Procter, D. J. An interrupted pummerer/nickel-catalysed cross-coupling sequence. *Angew. Chem.* **2018**, *130* (31), 9933-9937.
(291) Strotman, N. A.; Sommer, S.; Fu, G. C. Hiyama reactions of activated and unactivated secondary alkyl halides catalyzed by a nickel/norephedrine complex. *Angew. Chem. Int. Ed.* **2007**, *46* (19), 3556-3558.

(292) Oi, M.; Takita, R.; Kanazawa, J.; Muranaka, A.; Wang, C.; Uchiyama, M. Organocopper cross-coupling reaction for C–C bond formation on highly sterically hindered structures. *Chem. Sci.* **2019**, *10* (24), 6107-6112.
(293) Kato, Y.; Williams, C. M.; Uchiyama, M.; Matsubara, S. A protocol for an iodine–metal exchange reaction on cubane using lithium organozincates. *Org. Lett.* **2019**, *21* (2), 473-475.
(294) Nicolaou, K. C.; Vourloumis, D.; Totokotsopoulos, S.; Papakyriakou, A.; Karsunky, H.; Fernando, H.; Gavrilyuk, J.; Webb, D.; Stepan, A. F. Synthesis and biopharmaceutical evaluation of imatinib analogues featuring unusual structural motifs. *ChemMedChem* **2016**, *11* (1), 31-37.
(295) Kuduva, S. S.; Craig, D. C.; Nangia, A.; Desiraju, G. R. Cubanecarboxylic acids. Crystal engineering considerations and the role of C−H···O hydrogen bonds in determining O−H···O networks. *J. Am. Chem. Soc.* **1999**, *121* (9), 1936-1944.
(296) Candish, L.; Standley, E. A.; Gómez-Suárez, A.; Mukherjee, S.; Glorius, F. Catalytic access to alkyl bromides, chlorides and iodides via visible light-rromoted decarboxylative halogenation. *Chem. - Eur. J.* **2016**, *22* (29), 9971-9974.
(297) Harmalkar, D. S.; Lu, Q.; Lee, K. Total synthesis of gramistilbenoids A, B, and C. *J. Nat. Prod.* **2018**, *81* (4), 798-805.
(298) Lesch, B.; Toräng, J.; Nieger, M.; Braese, S. The Diels-Alder approach towards cannabinoids. *Synthesis* **2005**, *2005* (11), 1888-1900.
(299) Snyder, S. A.; Breazzano, S. P.; Ross, A. G.; Lin, Y.; Zografos, A. L. Total synthesis of diverse carbogenic complexity within the resveratrol class from a common building block. *J. Am. Chem. Soc.* **2009**, *131* (5), 1753-1765.
(300) Gabriele, B.; Benabdelkamel, H.; Plastina, P.; Fazio, A.; Sindona, G.; Di Donna, L. *trans*-Resveratrol-d_4, a molecular tracer of the wild-type ohytoalexin; Synthesis and spectroscopic properties. *Synthesis* **2008**, *2008* (18), 2953-2956.

Appendix - NMR Spectra: ^{1}H NMR (500 MHz, $CDCl_3$) of 2.13

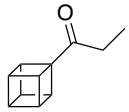

2.13

^{13}C NMR (126 MHz, $CDCl_3$) of 2.13

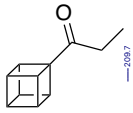

2.13

^{1}H NMR (500 MHz, $CDCl_3$) of 2.14b

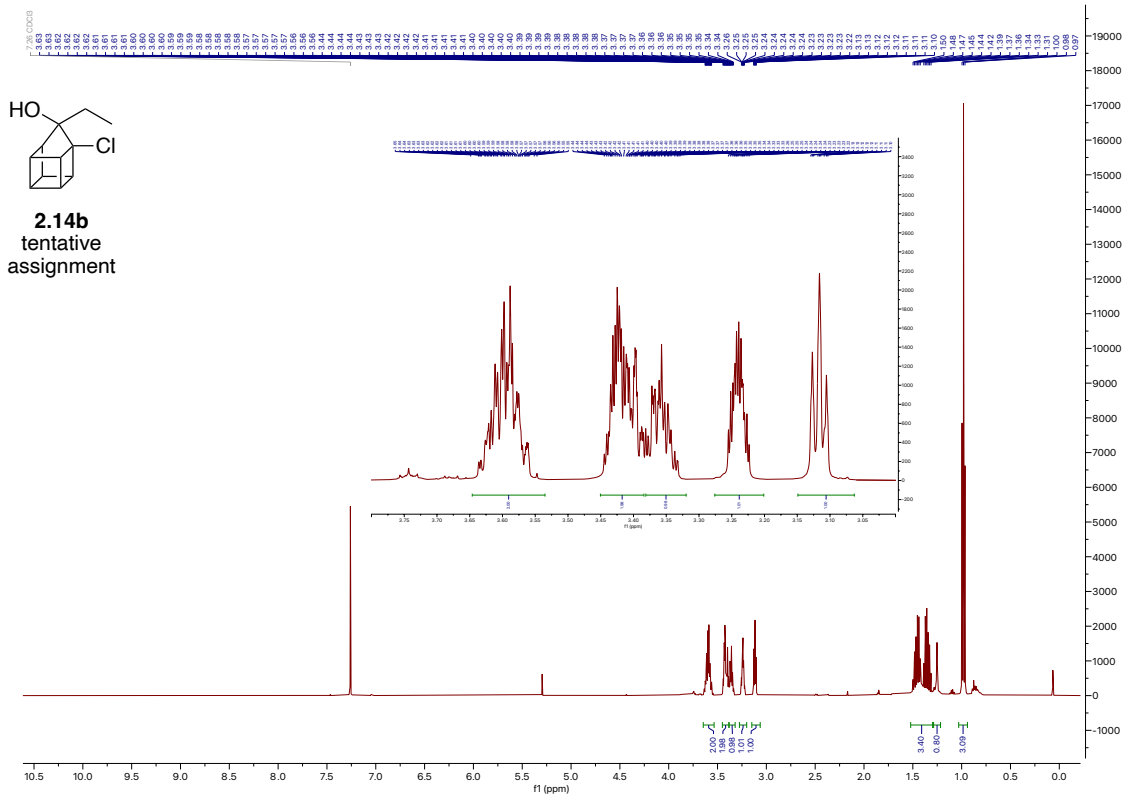

^{13}C NMR (126 MHz, $CDCl_3$) of 2.14b

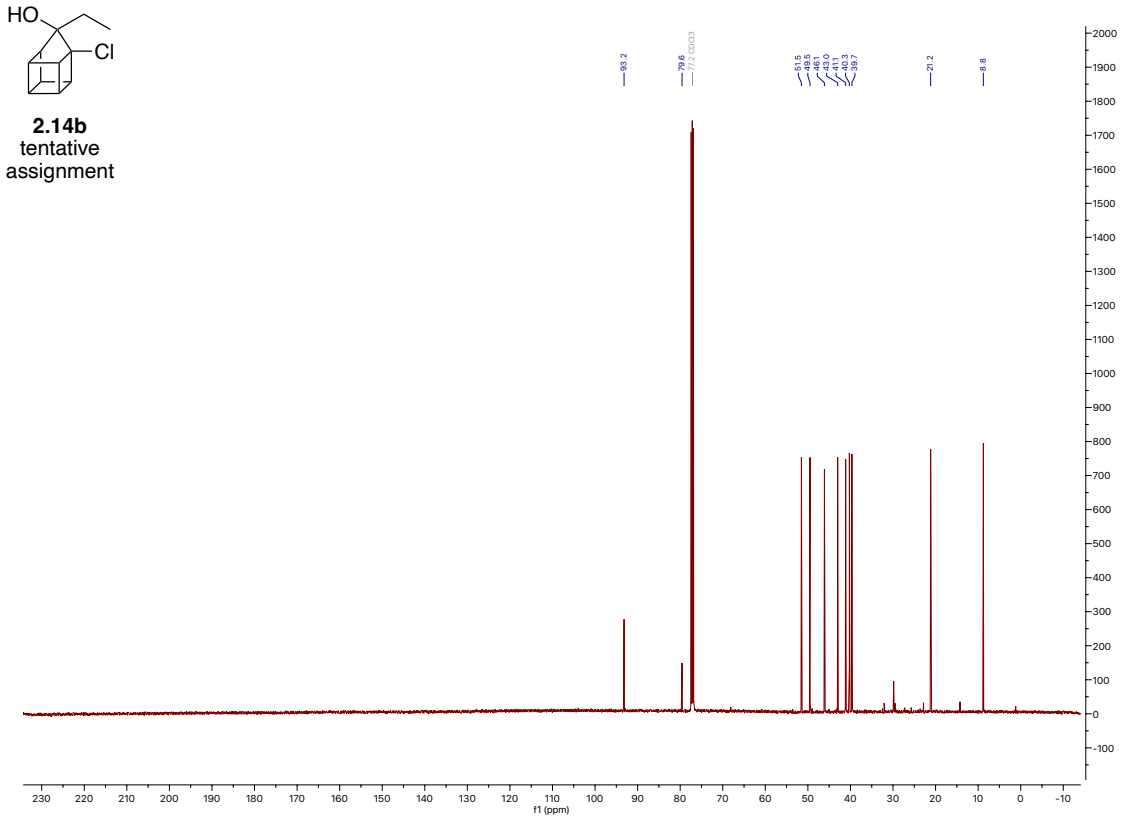

^{1}H COSY NMR (500 MHz, $CDCl_3$) of 2.14b

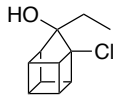

2.14b
tentative
assignment

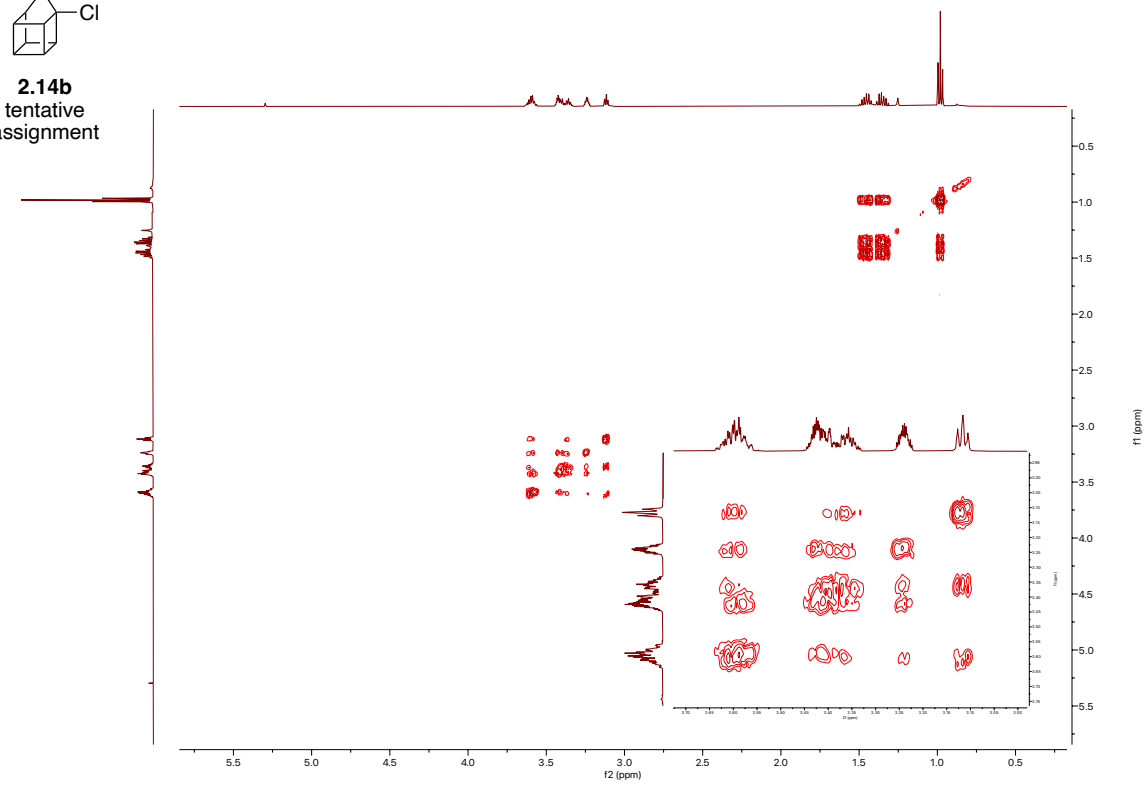

HSQC NMR (500 MHz, $CDCl_3$) of 2.14b

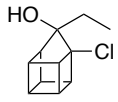

2.14b
tentative
assignment

^{1}H NMR (500 MHz, $CDCl_3$) of 2.30

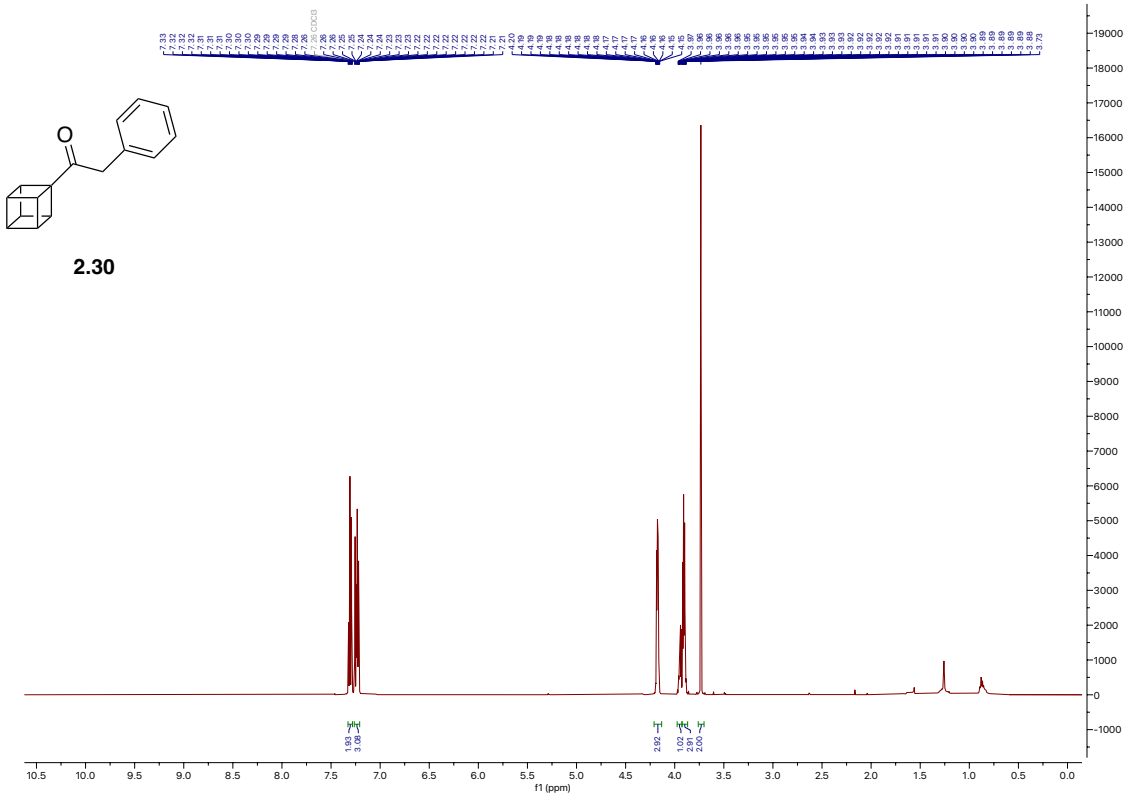

^{13}C NMR (126 MHz, $CDCl_3$) of 2.30

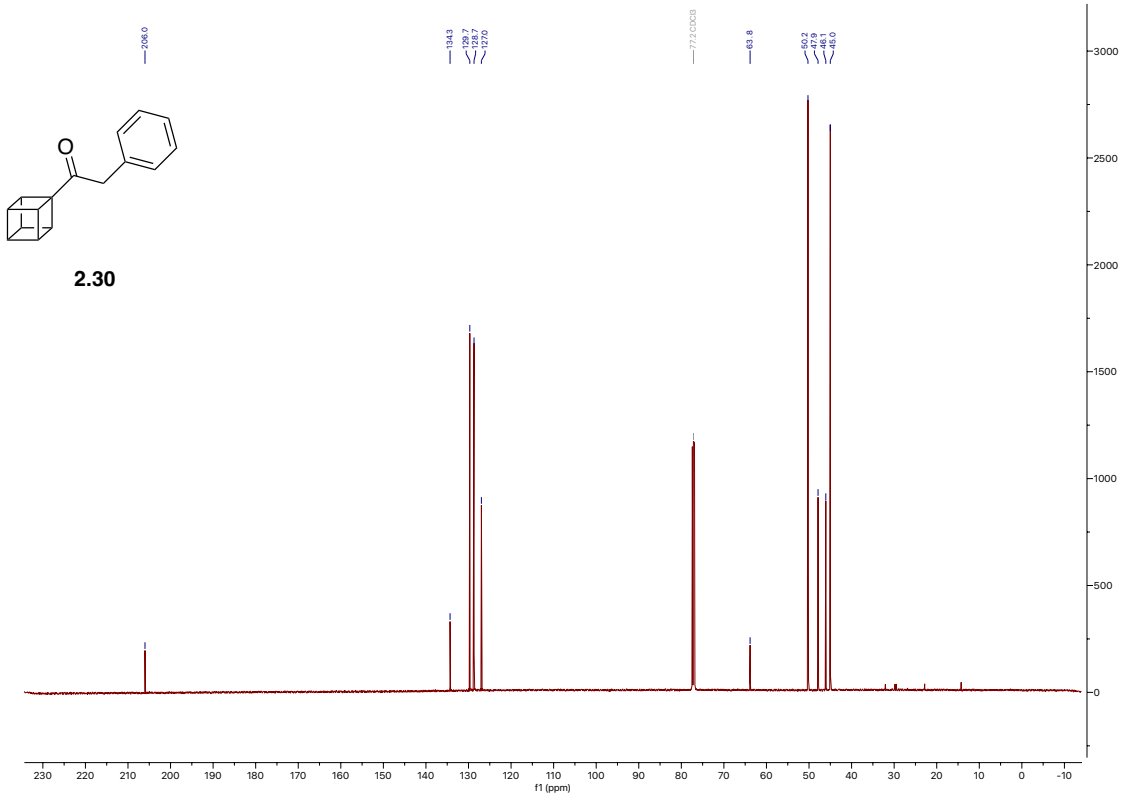

^{1}H NMR (500 MHz, $CDCl_3$) of 2.31

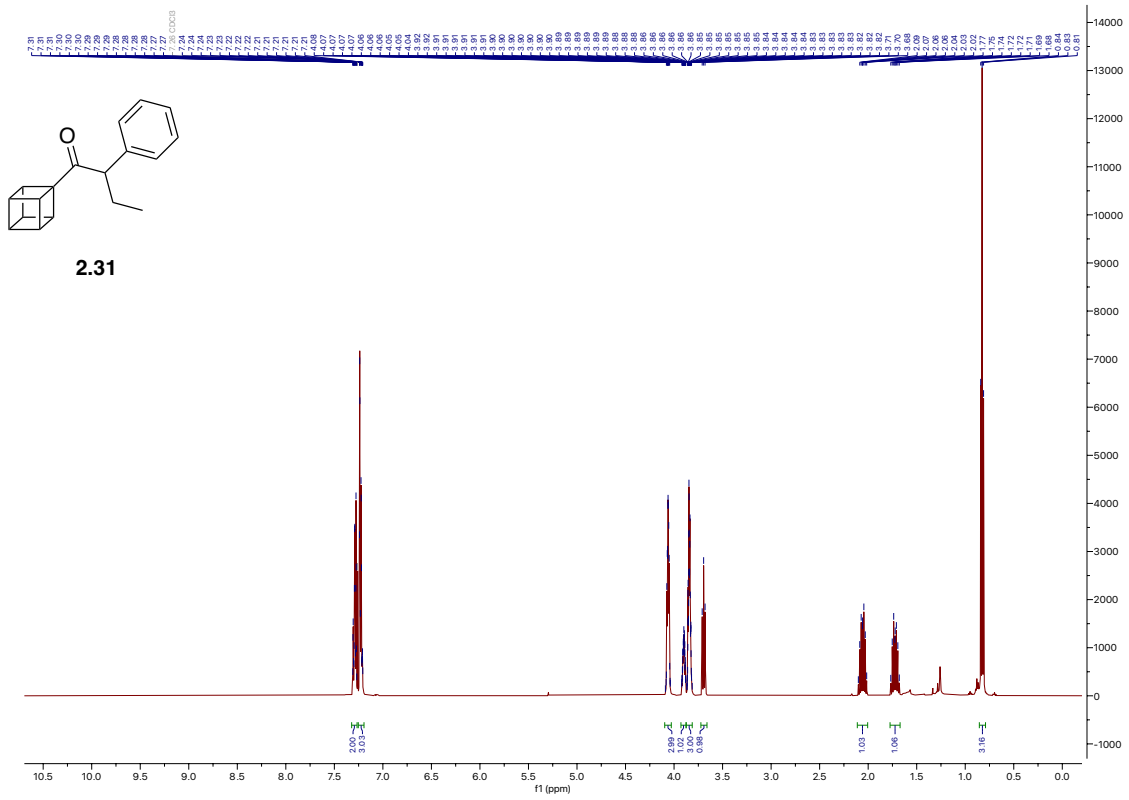

2.31

^{13}C NMR (126 MHz, $CDCl_3$) of 2.31

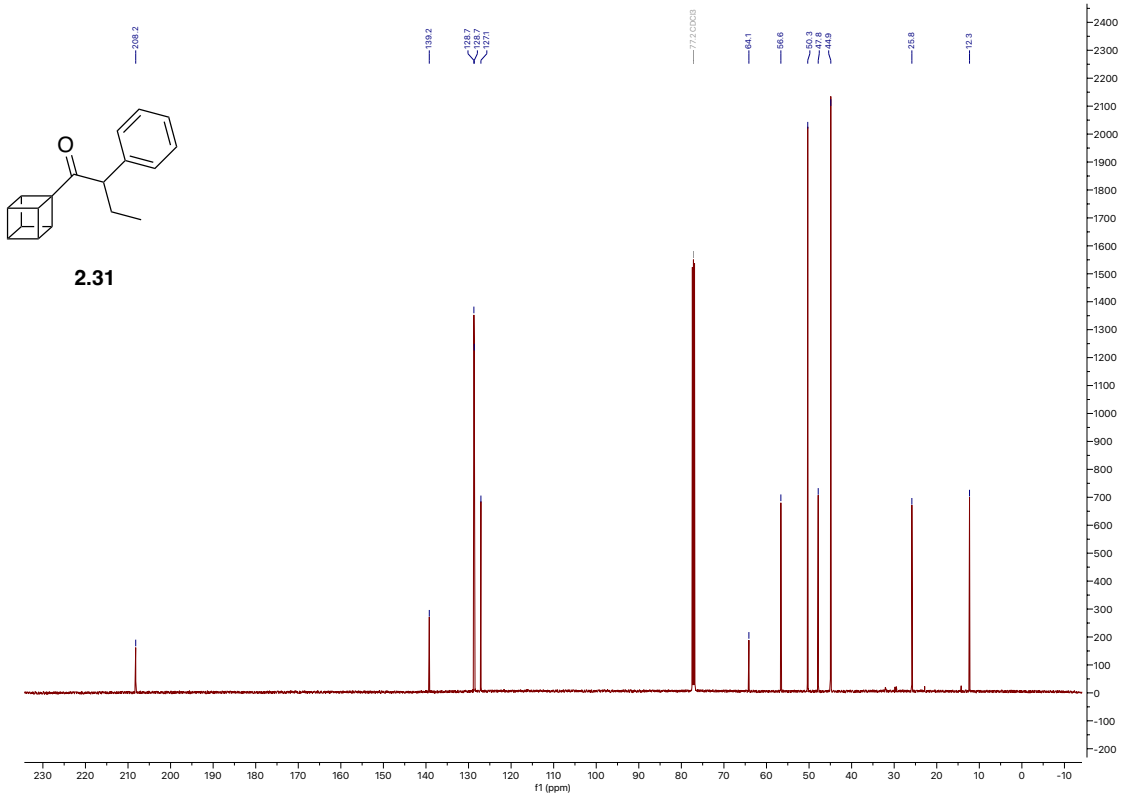

2.31

^{1}H NMR (500 MHz, $CDCl_3$) of 2.34

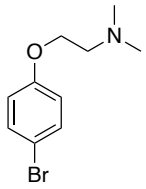

2.34

^{13}C NMR (126 MHz, $CDCl_3$) of 2.34

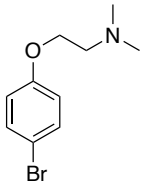

2.34

^{1}H NMR (500 MHz, $CDCl_3$) of (1SR,2SR)-(±)2.19

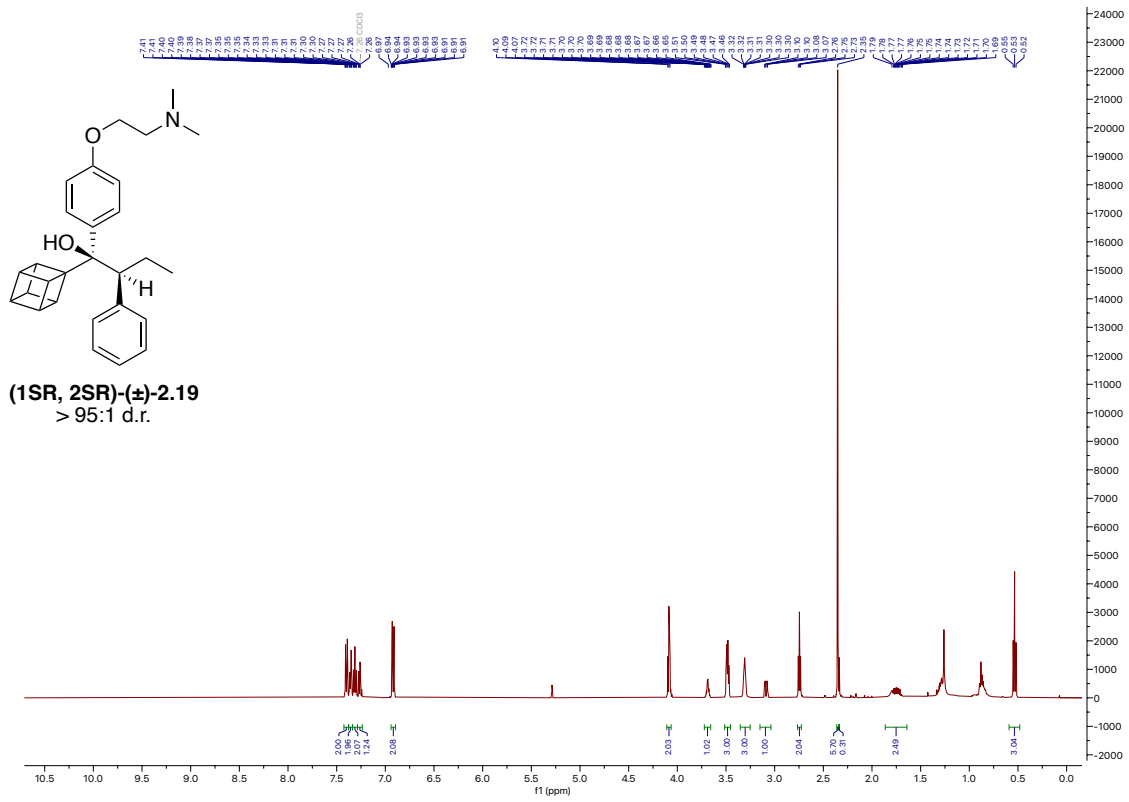

(1SR, 2SR)-(±)-2.19
> 95:1 d.r.

^{13}C NMR (126 MHz, $CDCl_3$) of (1SR, 2SR)-(±)-2.19

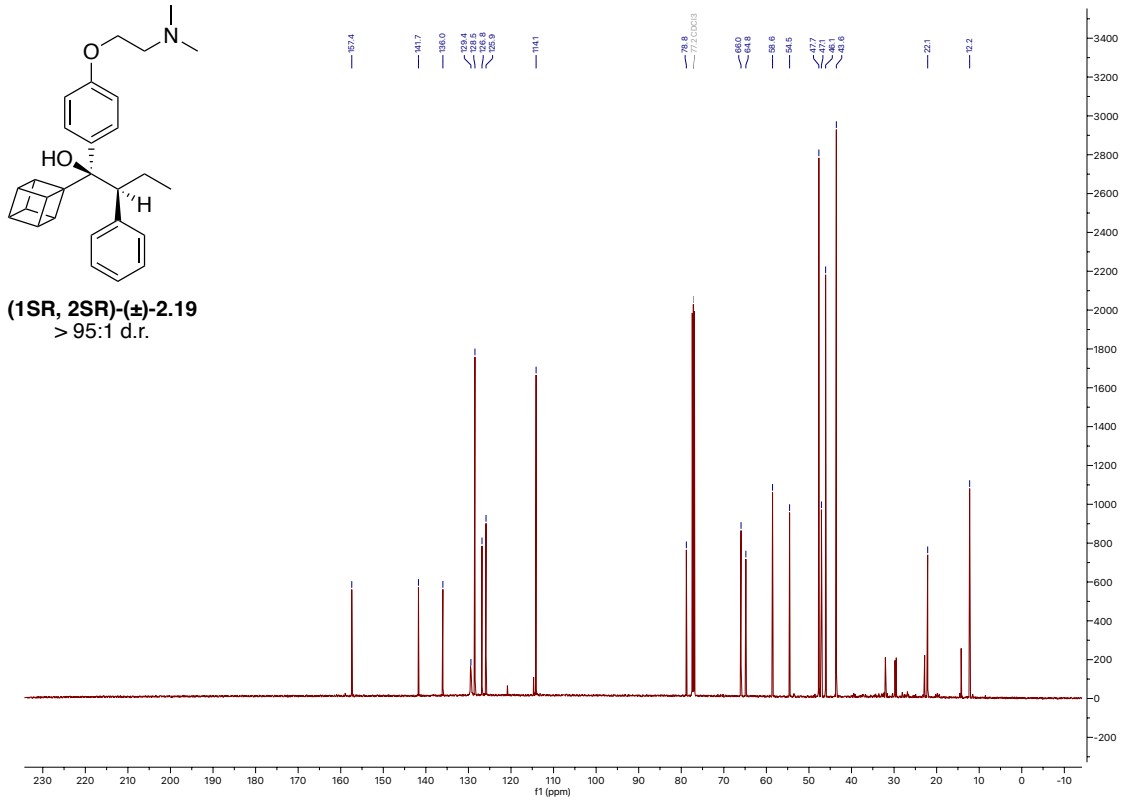

(1SR, 2SR)-(±)-2.19
> 95:1 d.r.

^{1}H COSY NMR (500 MHz, $CDCl_3$) of (1SR, 2SR)-(±)-2.19

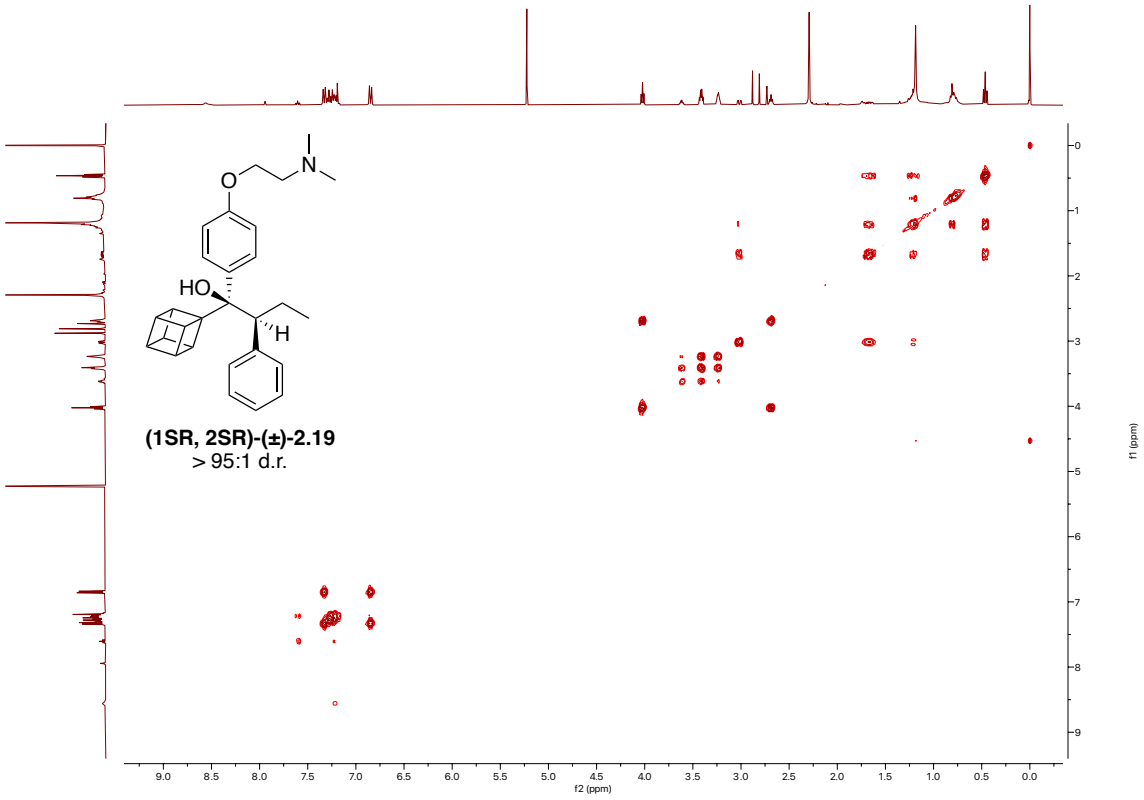

HSQC NMR (500 MHz, $CDCl_3$) of (1SR, 2SR)-(±)-2.19

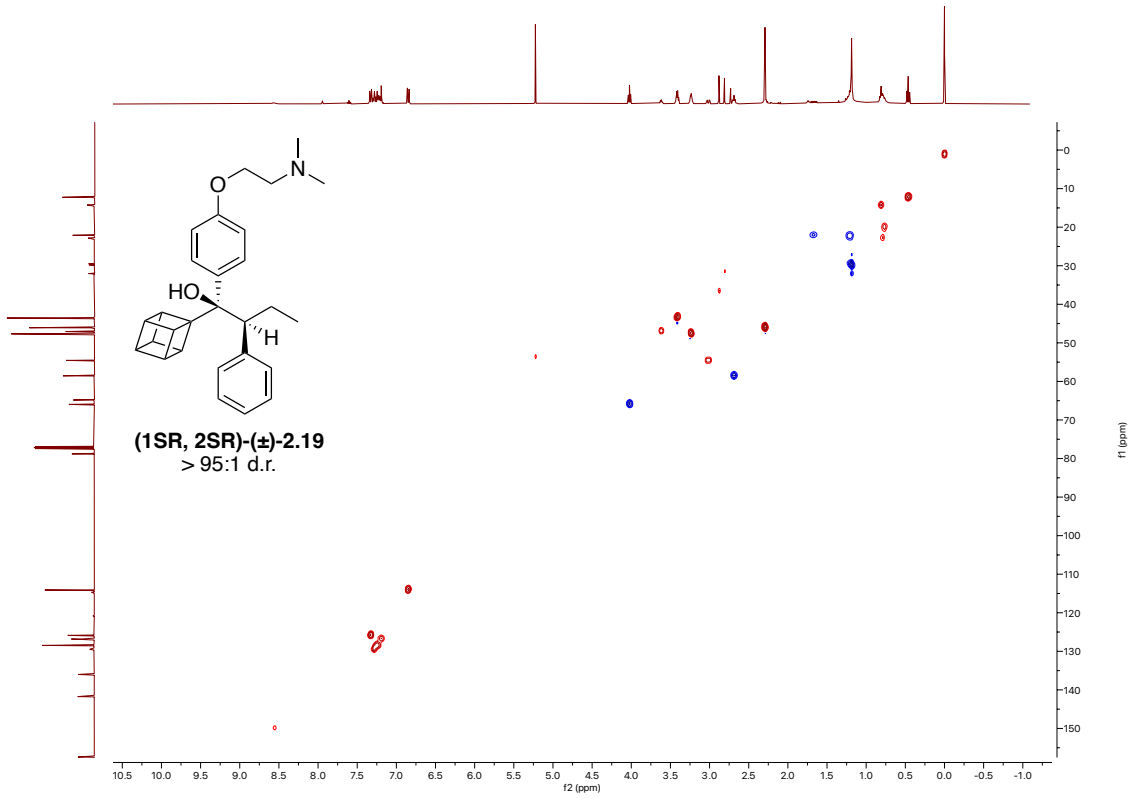

^{1}H NOESY NMR (500 MHz, $CDCl_3$) of (1SR, 2SR)-(±)-2.19

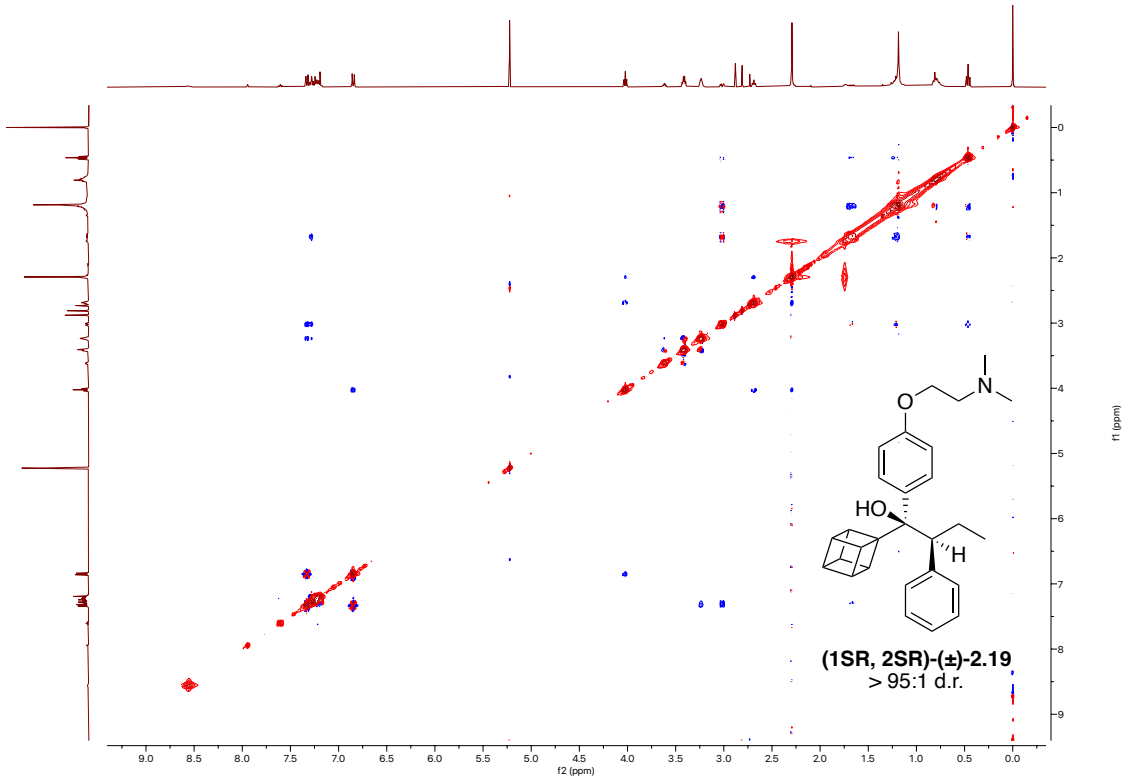

^{1}H NMR (500 MHz, $CDCl_3$) of (1SR, 2SR)-(±)-2.35a

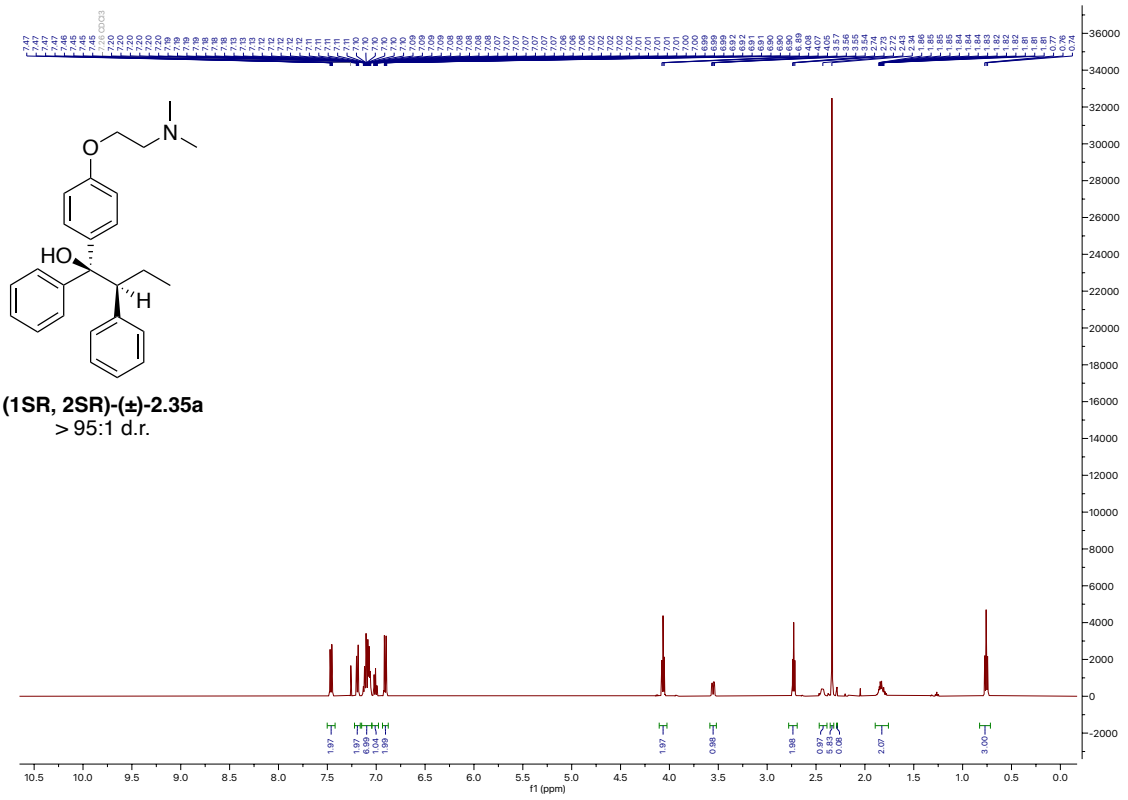

^{13}C NMR (126 MHz, $CDCl_3$) of (1SR, 2SR)-(±)-2.35a

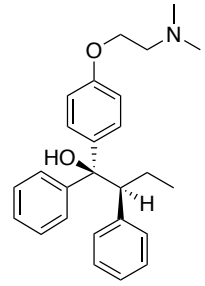

(1SR, 2SR)-(±)-2.35a
> 95:1 d.r.

^{1}H NMR (300 MHz, $CDCl_3$) of 1.1

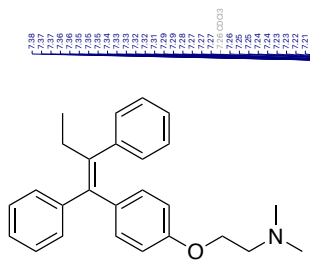

(*Z*/*E*)-Tamoxifen (1.1)
(5:1)

^{1}H NMR (400 MHz, $CDCl_3$) of 2.43

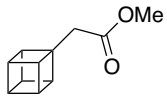

2.43

^{13}C NMR (101 MHz, $CDCl_3$) of 2.43

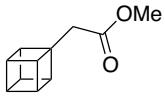

2.43

^{1}H COSY NMR (400 MHz, $CDCl_3$) of 2.43

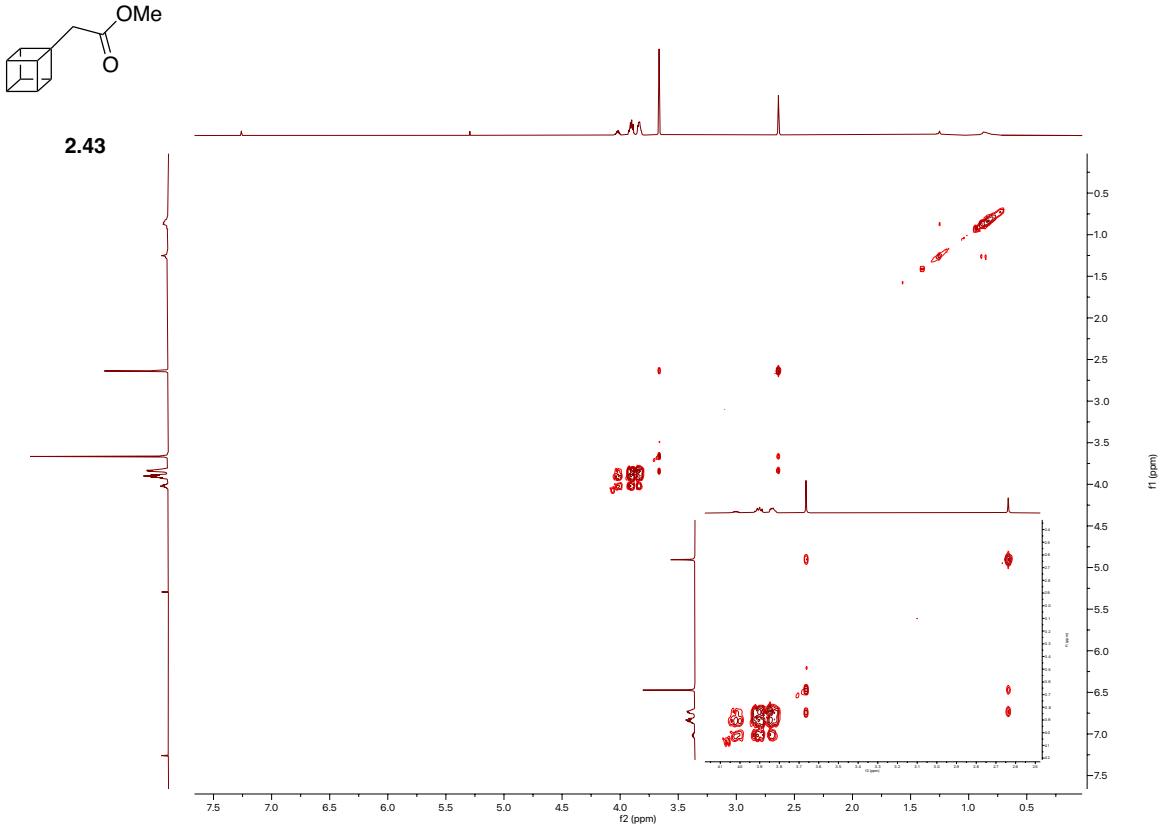

HSQC NMR (400 MHz, $CDCl_3$) of 2.43

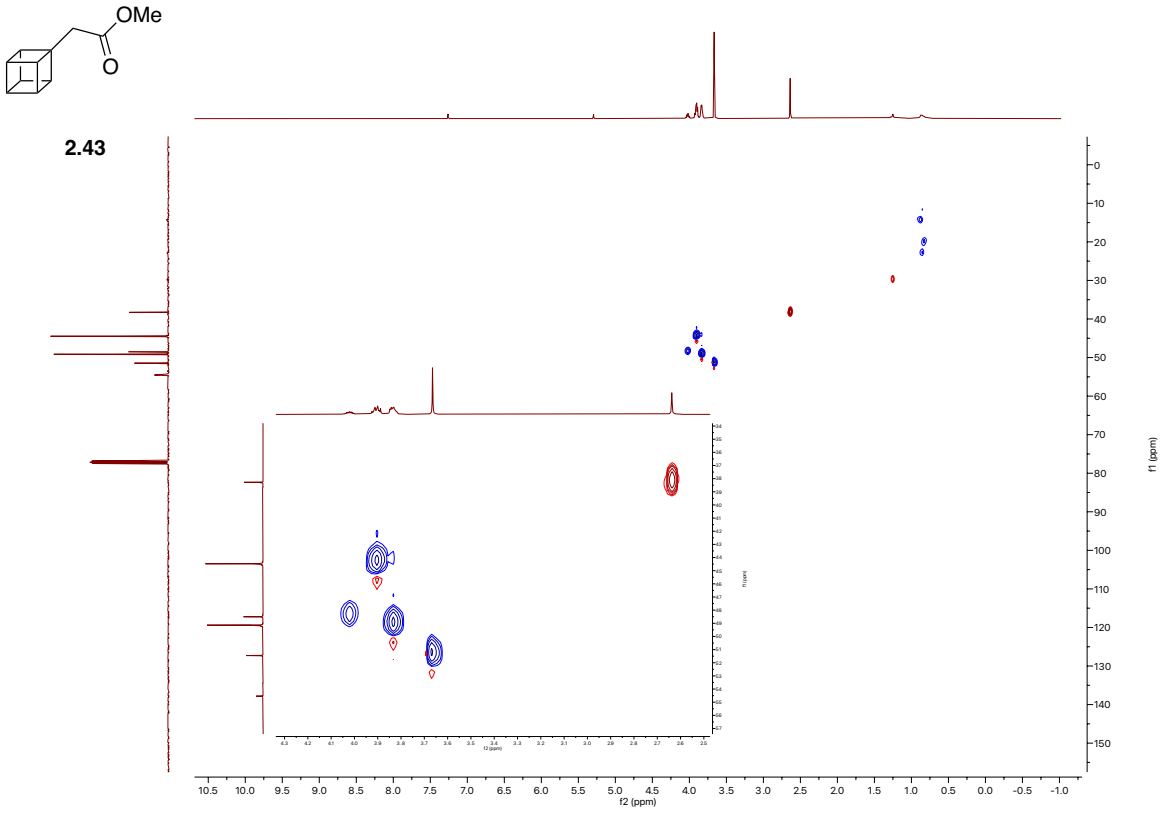

^{1}H NMR (300 MHz, $CDCl_3$) of (*Z*/*E*)-2.60

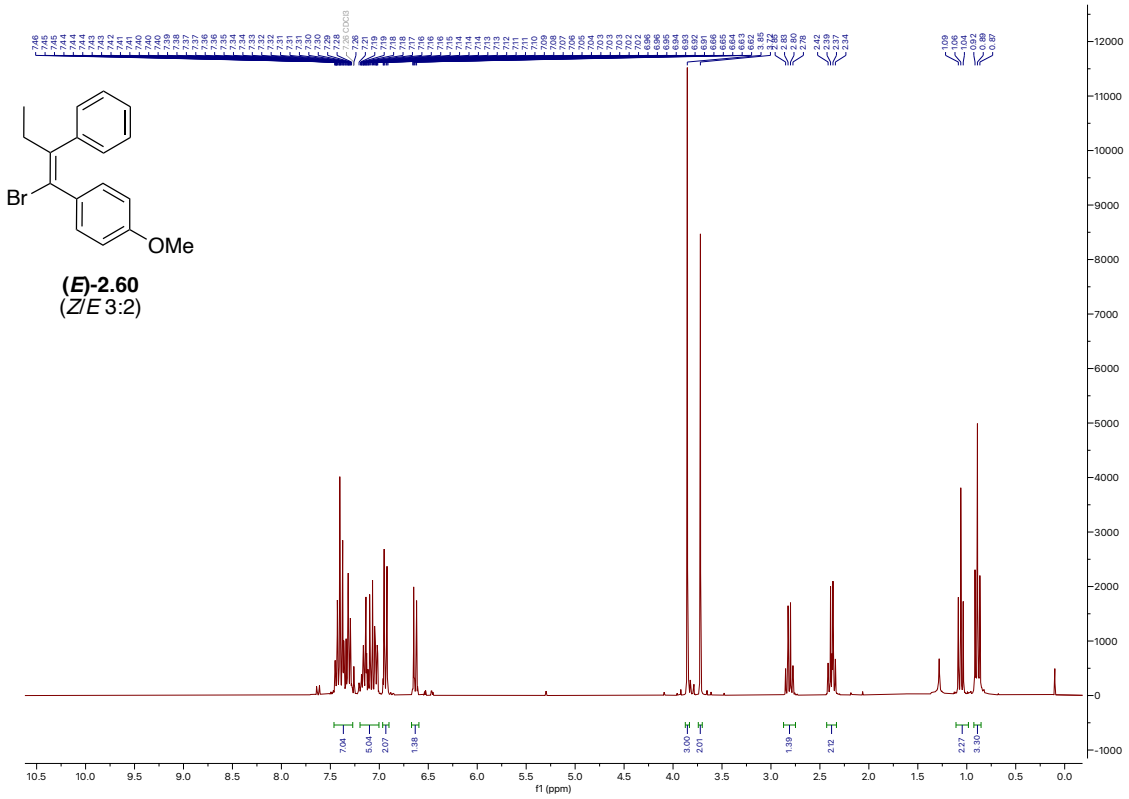

^{13}C NMR (75 MHz, $CDCl_3$) of (*Z*/*E*)-2.60

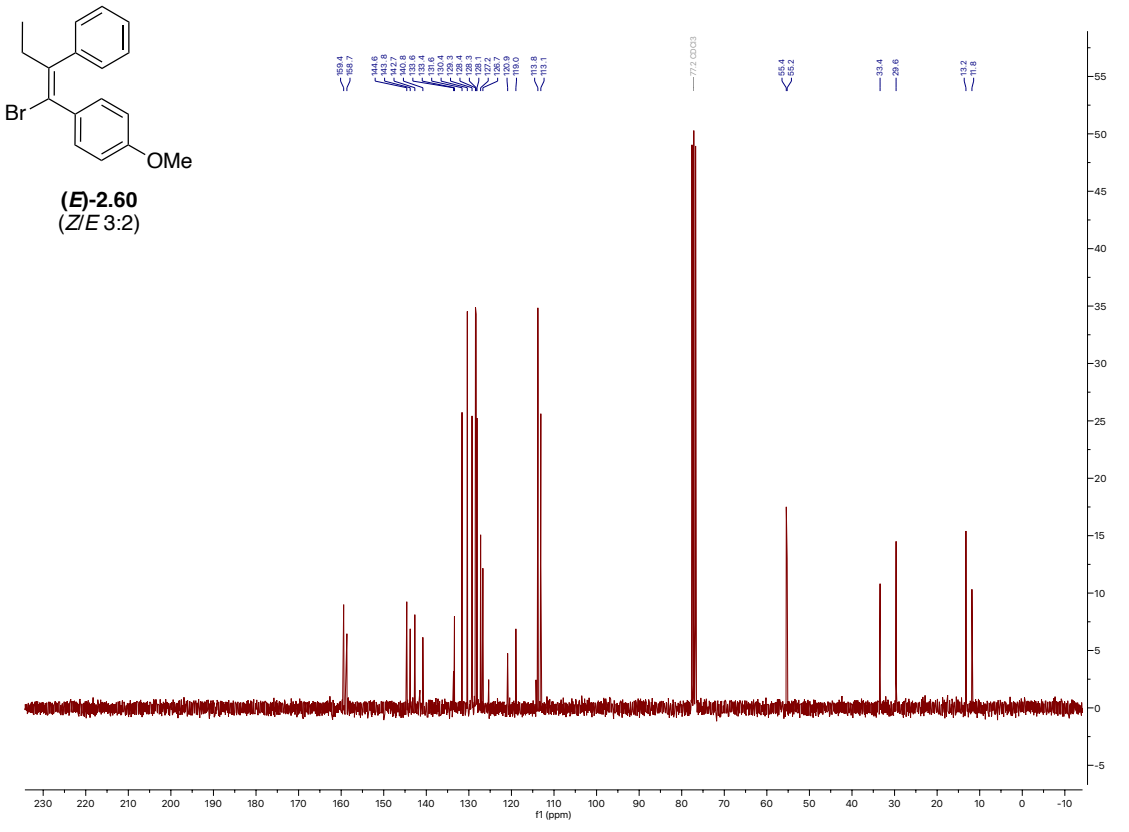

^{1}H NMR (300 MHz, $CDCl_3$) of (*Z*)-2.65

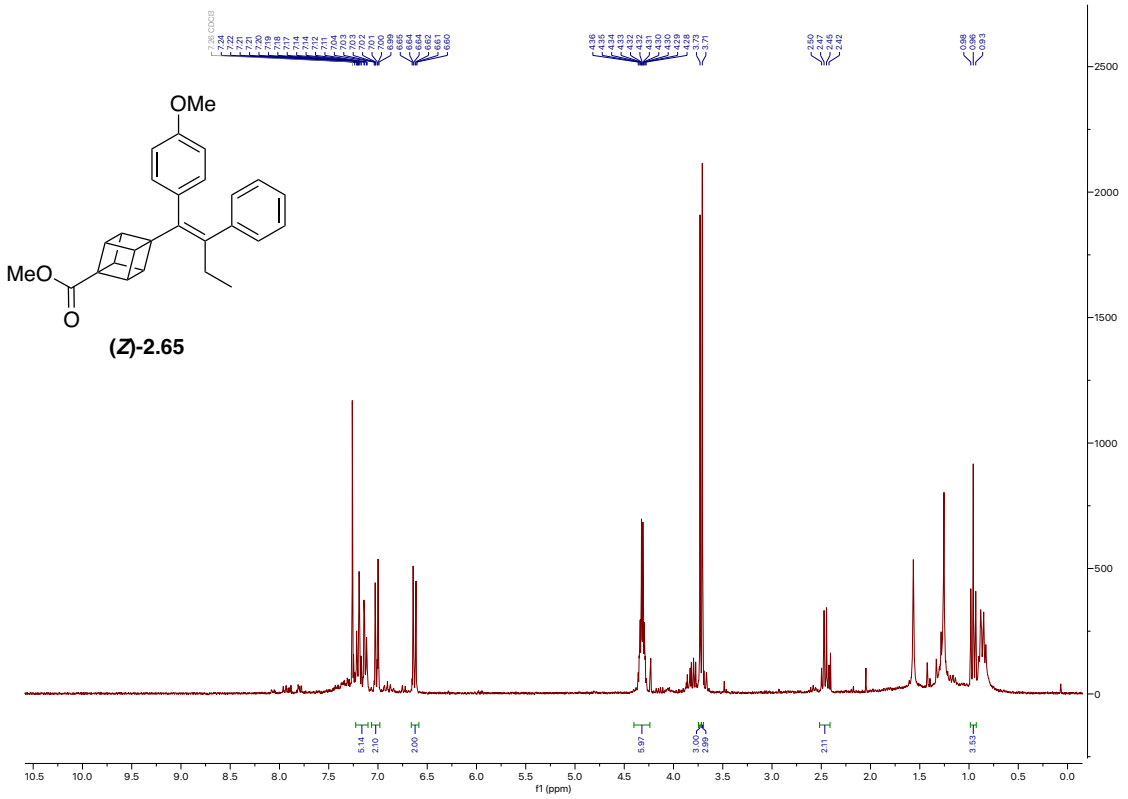

^{1}H NMR (500 MHz, $CDCl_3$) of (*Z*/*E*)-2.68

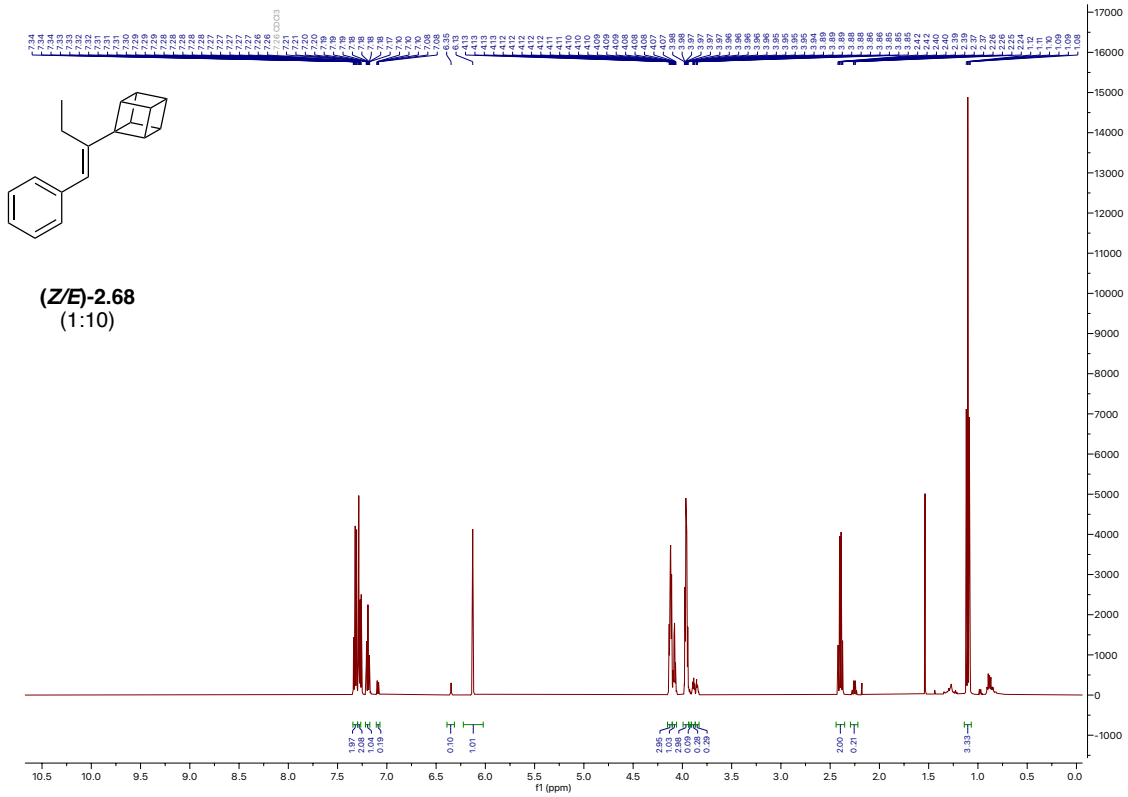

^{13}C NMR (126 MHz, $CDCl_3$) of (*Z*/*E*)-2.68

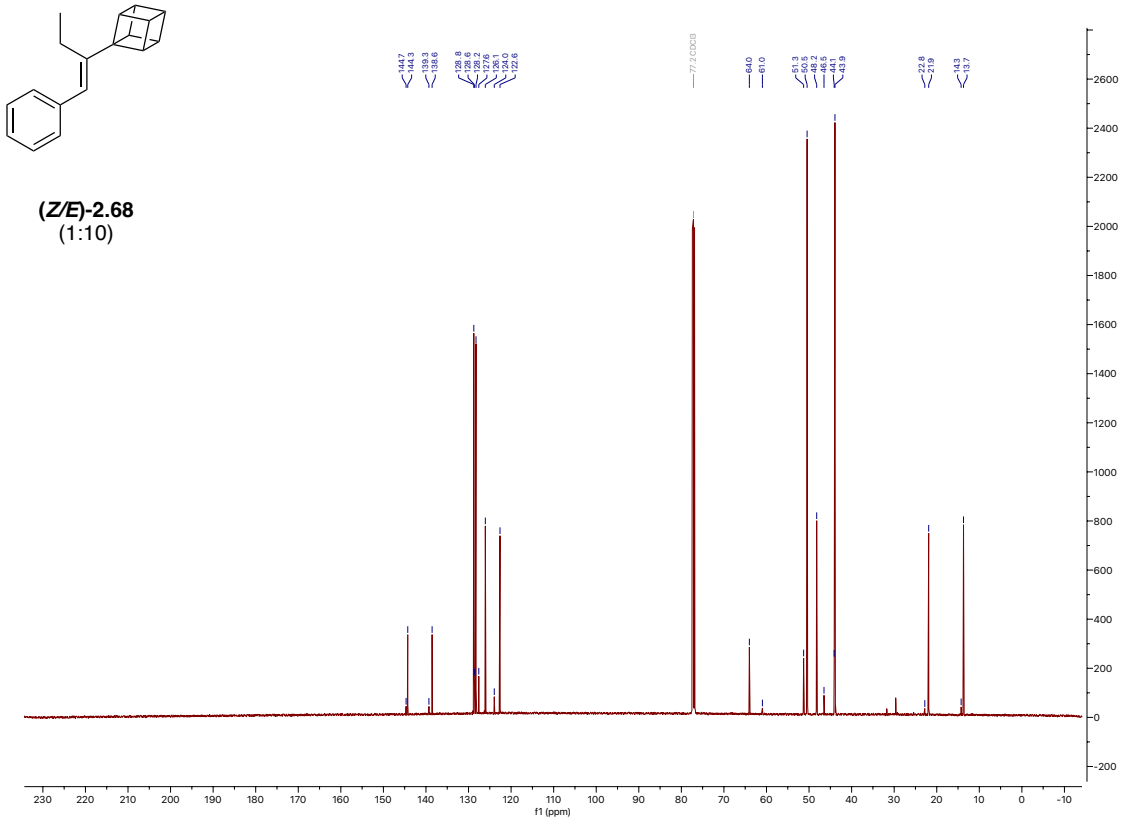

^{1}H NOESY NMR (500 MHz, $CDCl_3$) of (*Z*/*E*)-2.68

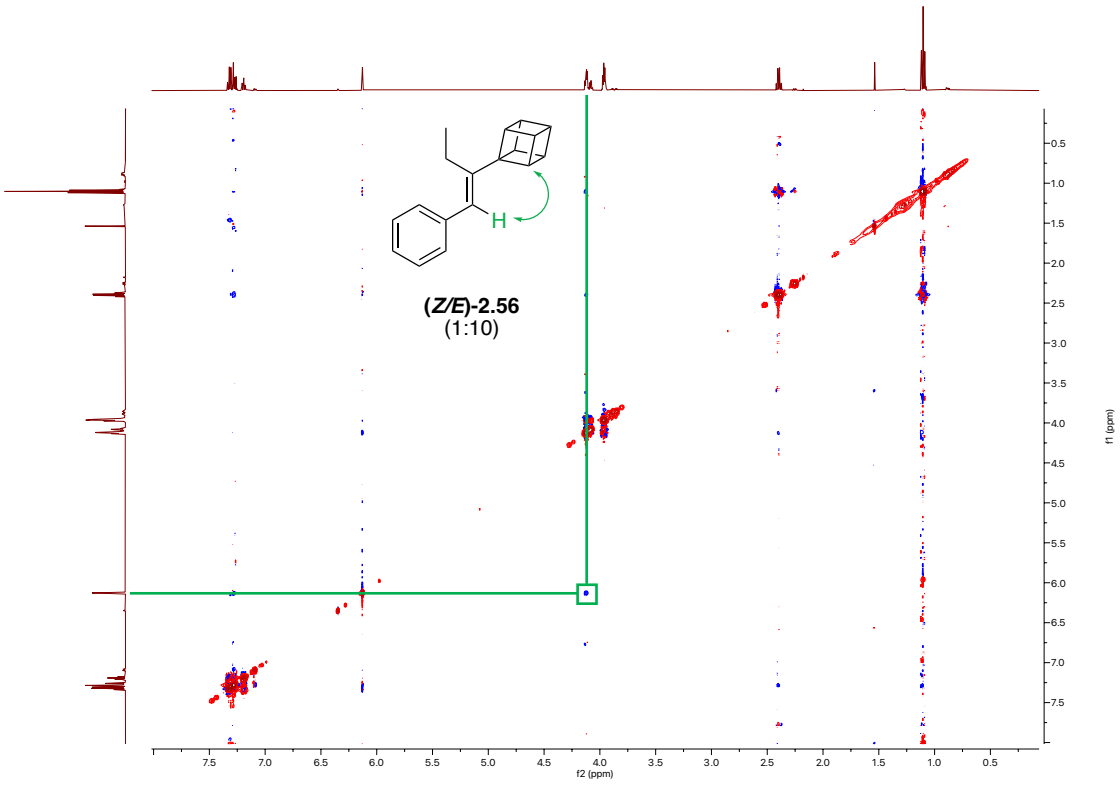

^{1}H NMR (300 MHz, $CDCl_3$) of (*Z*/*E*)-2.72

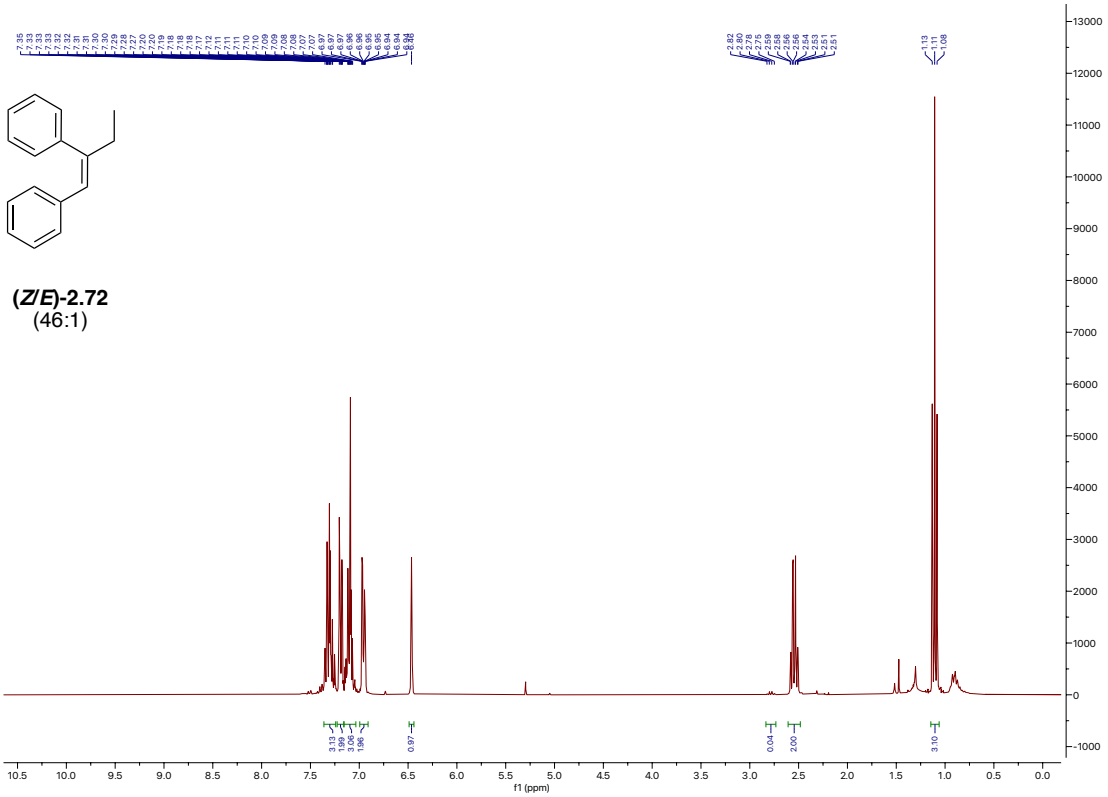

^{1}H NMR (400 MHz, $CDCl_3$) of 2.69

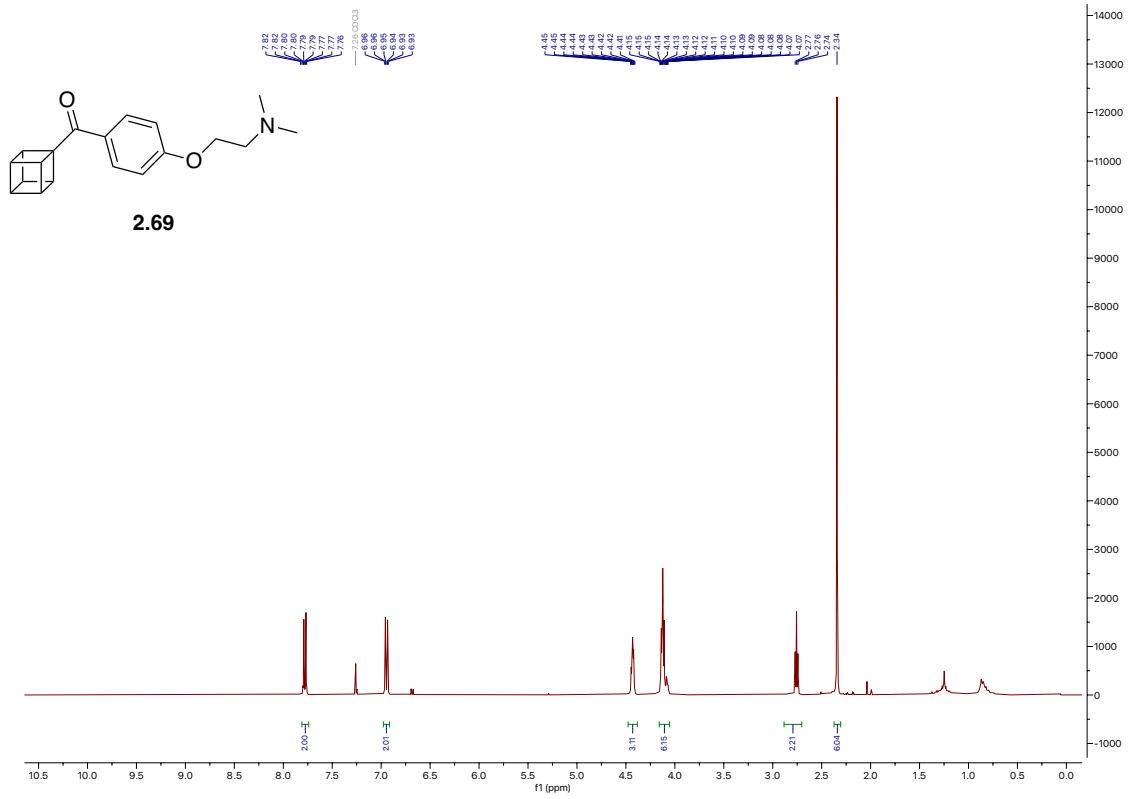

^{13}C NMR (101 MHz, $CDCl_3$) of 2.69

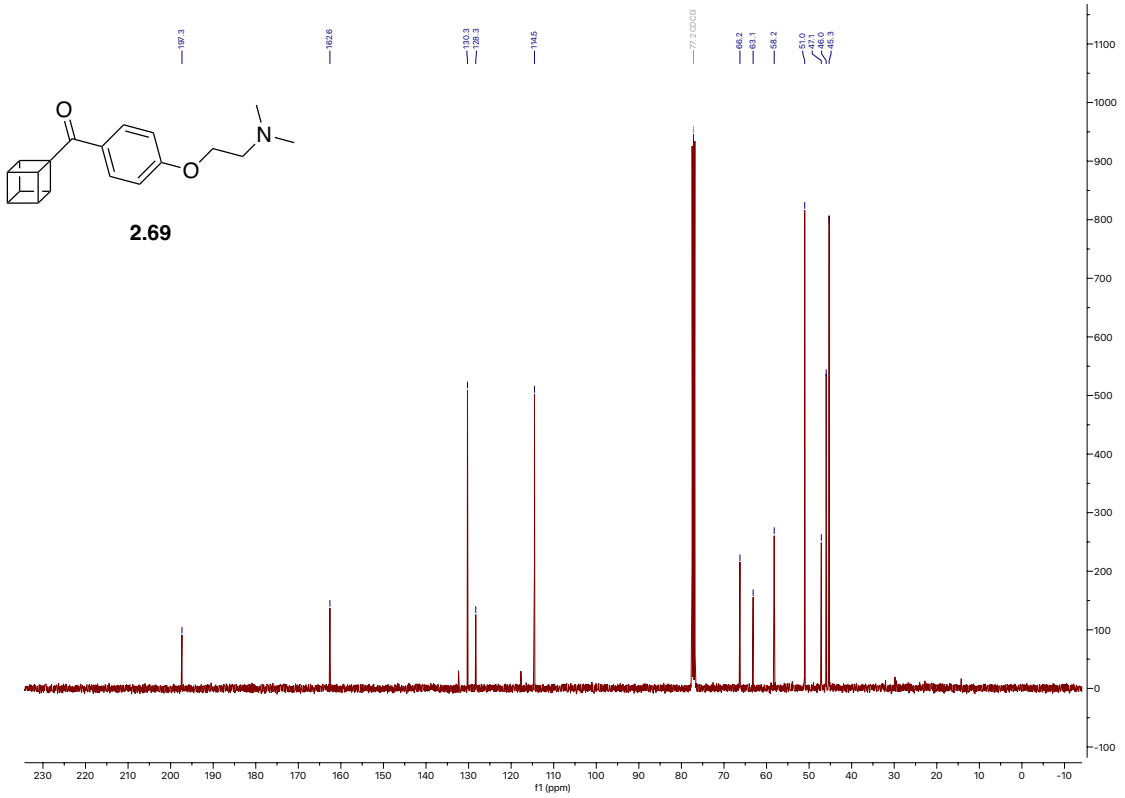

2.69

^{1}H NMR (400 MHz, $CDCl_3$) of (*Z*/*E*)-1.17 mixture

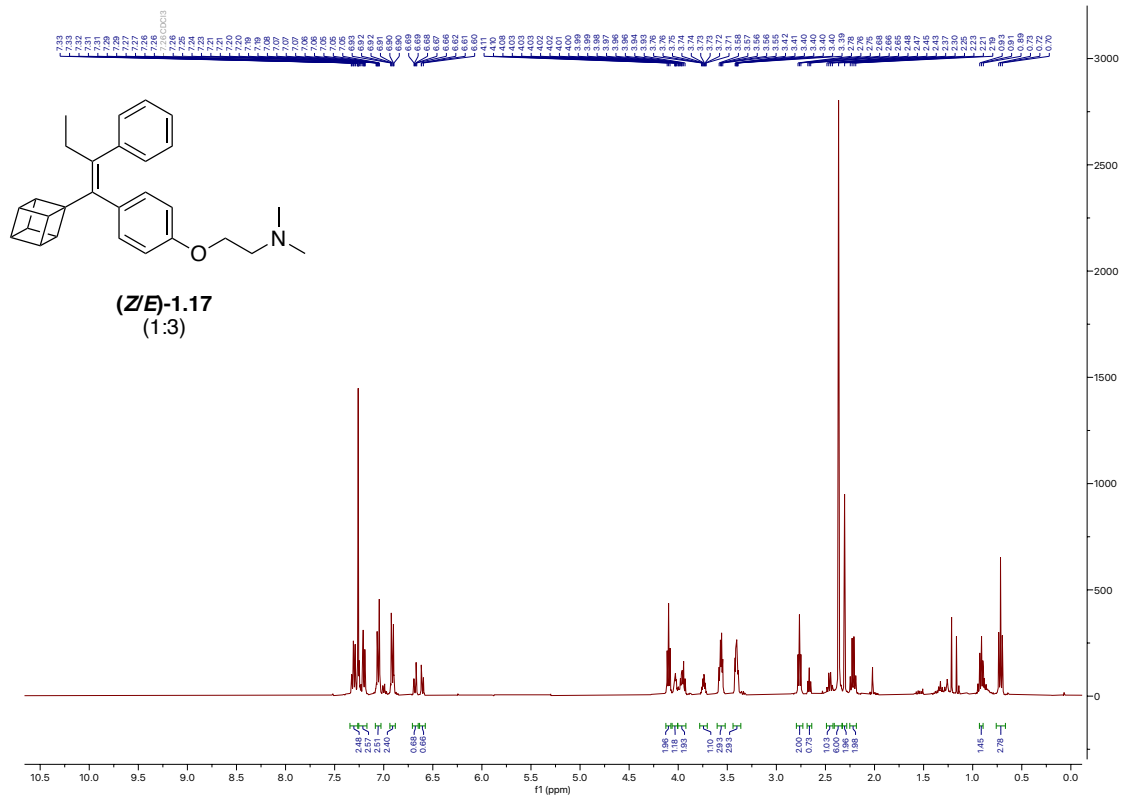

(*Z*/*E*)-1.17
(1:3)

^{1}H NMR (400 MHz, $CDCl_3$) of (*E*)-1.17

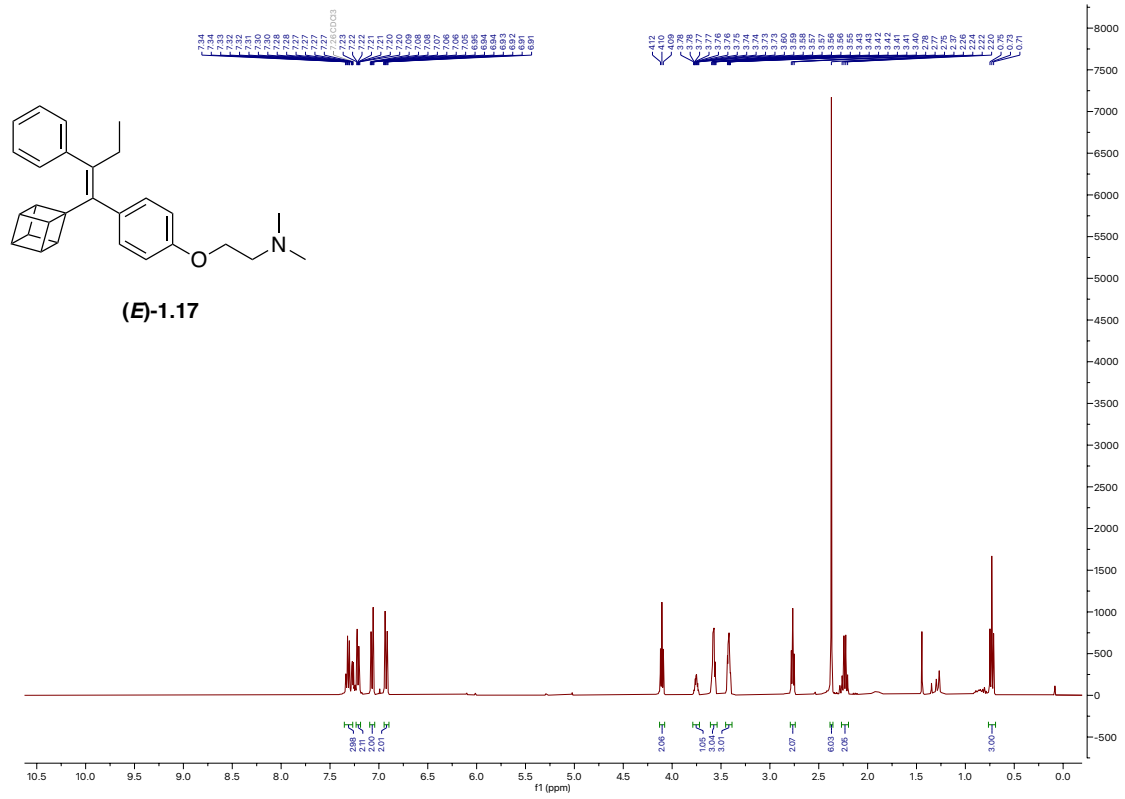

(*E*)-1.17

^{13}C NMR (101 MHz, $CDCl_3$) of (*E*)-1.17

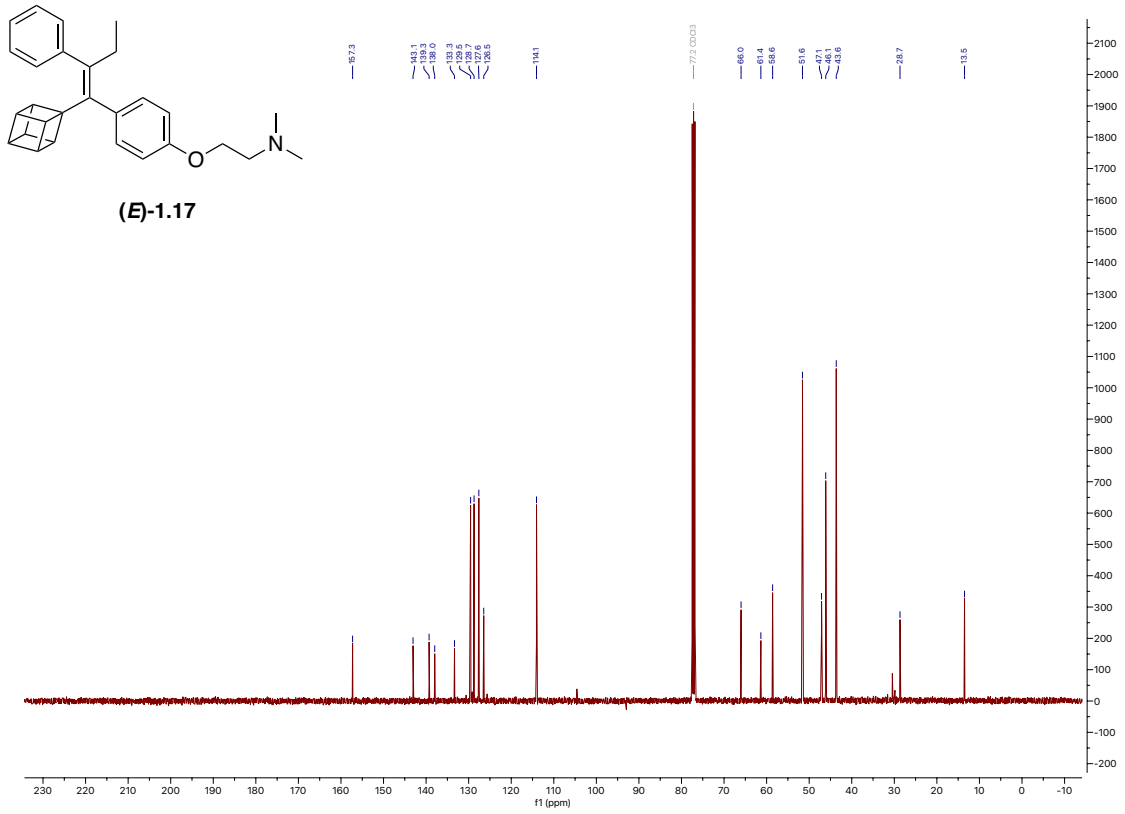

(*E*)-1.17

^{1}H COSY NMR (400 MHz, $CDCl_3$) of (*E*)-1.17

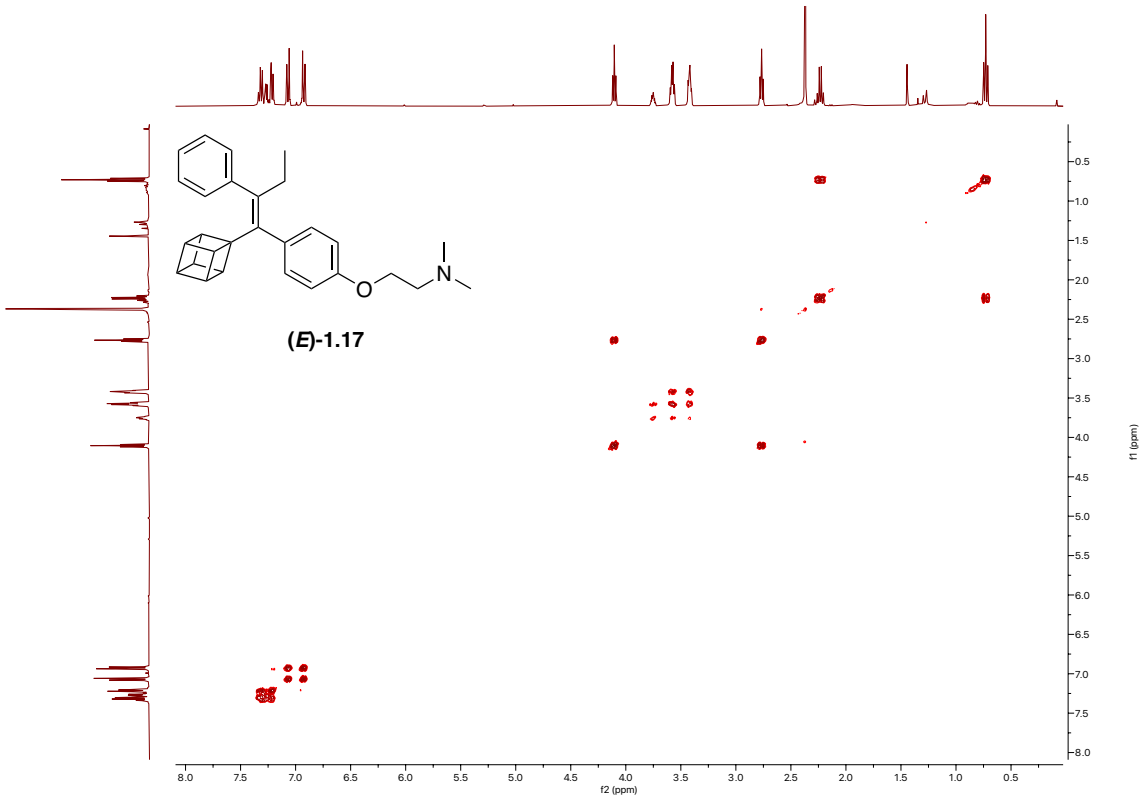

^{1}H NOESY NMR (400 MHz, $CDCl_3$) of (*E*)-1.17

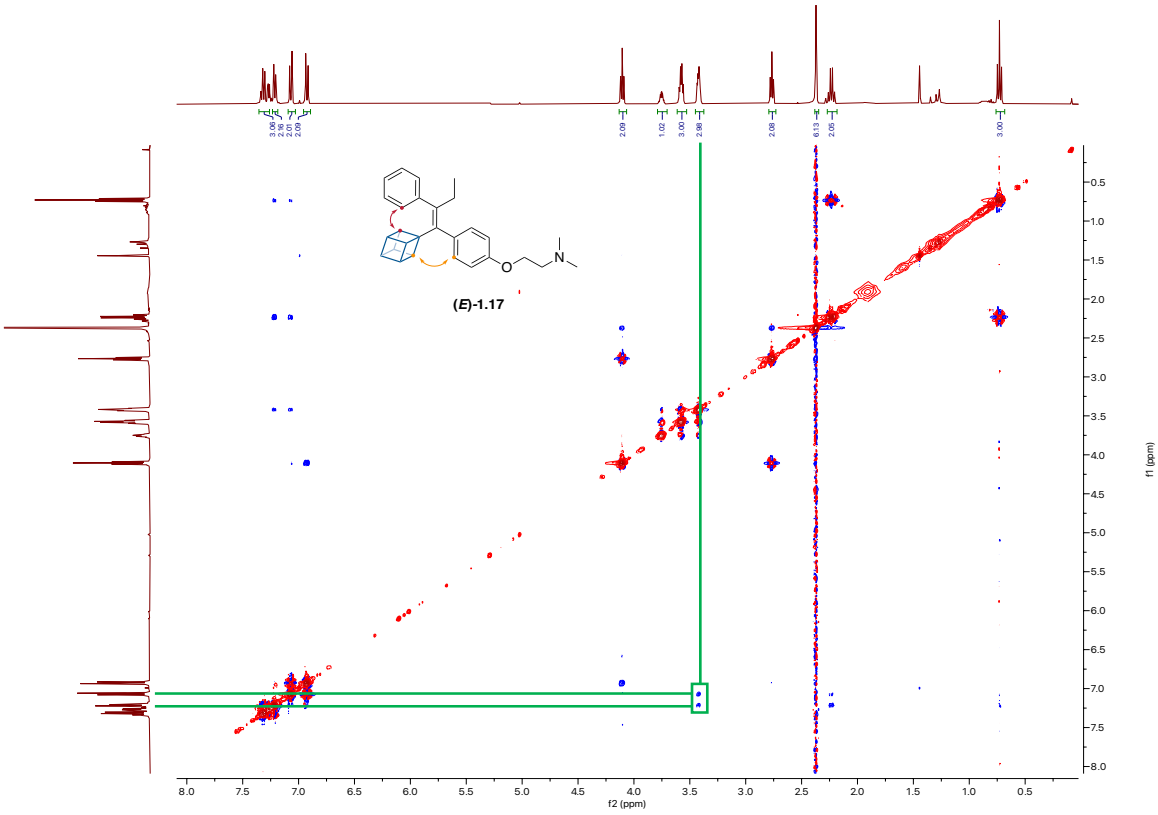

HSQC NMR (400 MHz, $CDCl_3$) of (*E*)-1.17

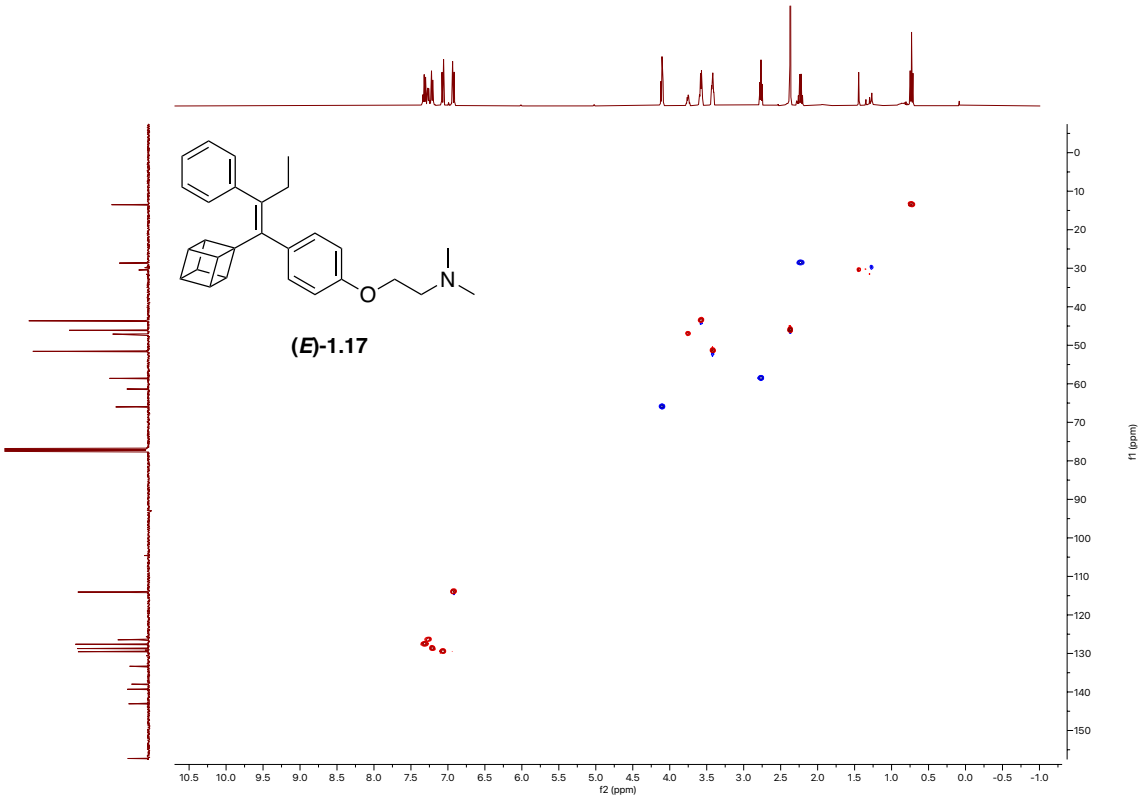

^{1}H NMR (300 MHz, $CDCl_3$) of (*Z*)-1.17

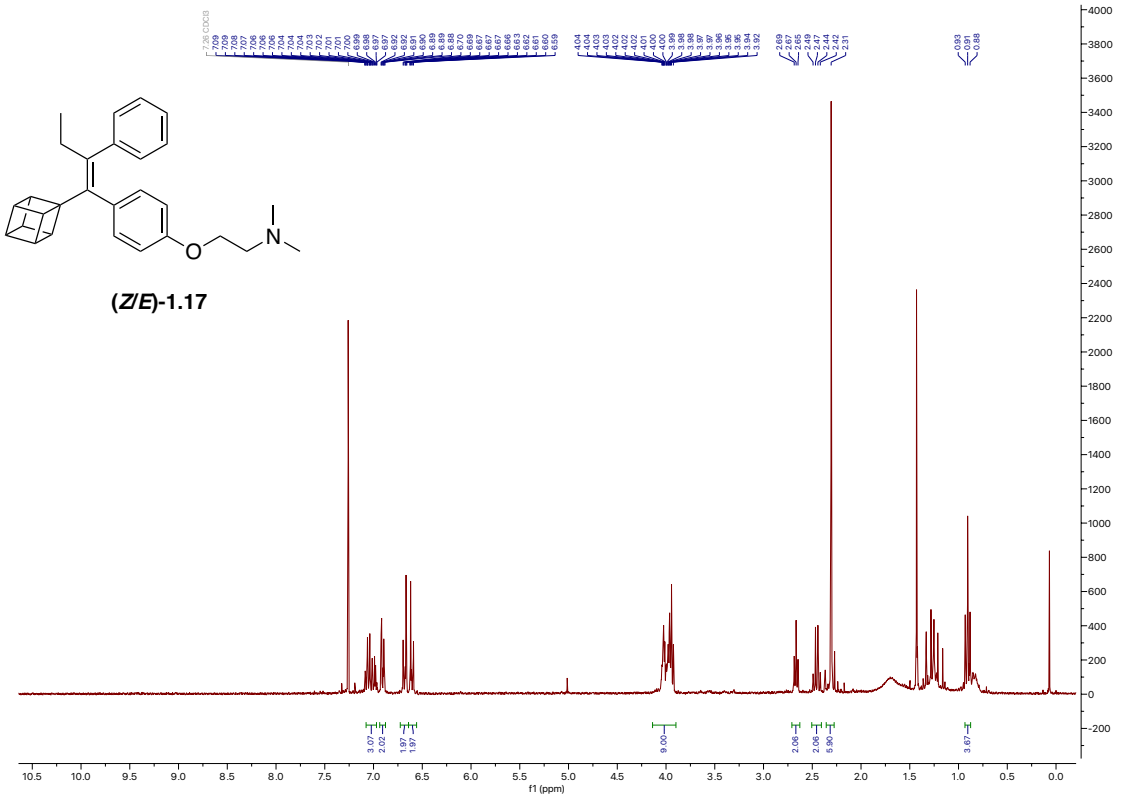

^{13}C NMR (101 MHz, $CDCl_3$) overlay between (*E*)-1.17 and (*Z*/*E*)-1.17 mixture

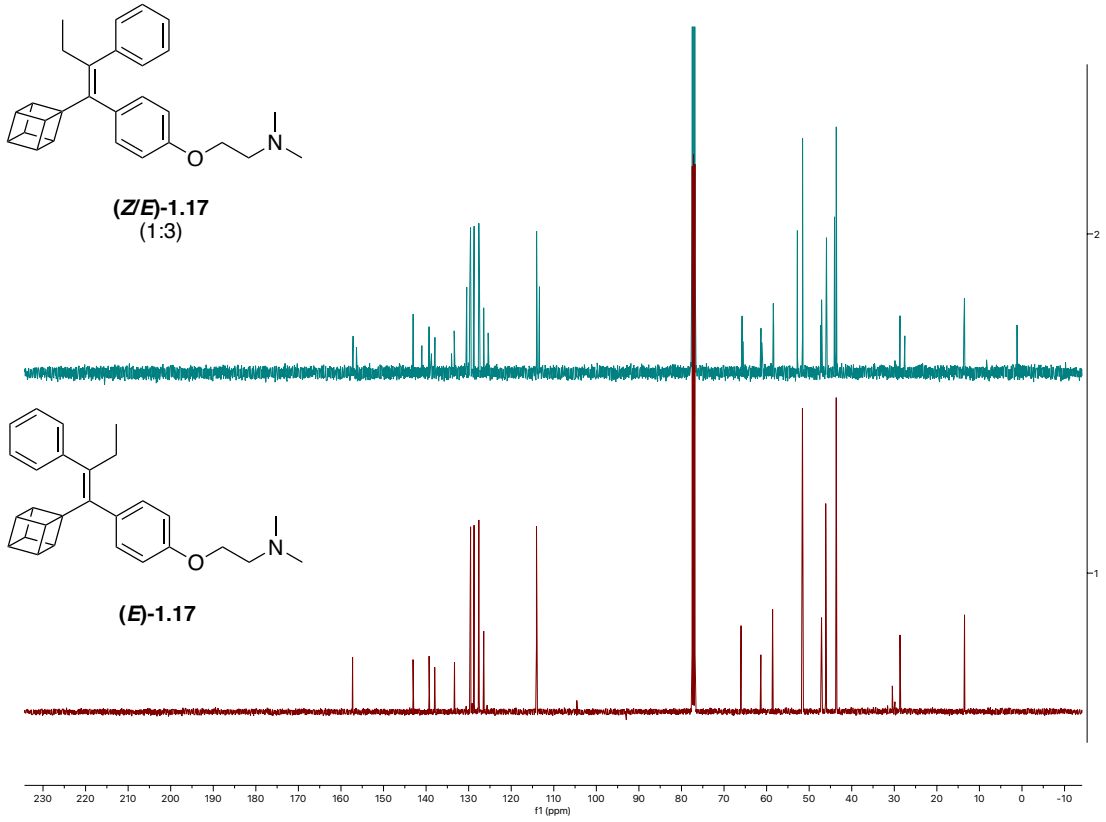

^{1}H NOESY NMR (400 MHz, $CDCl_3$) of (*Z*/*E*)-1.17 mixture – showing *Z*-isomer

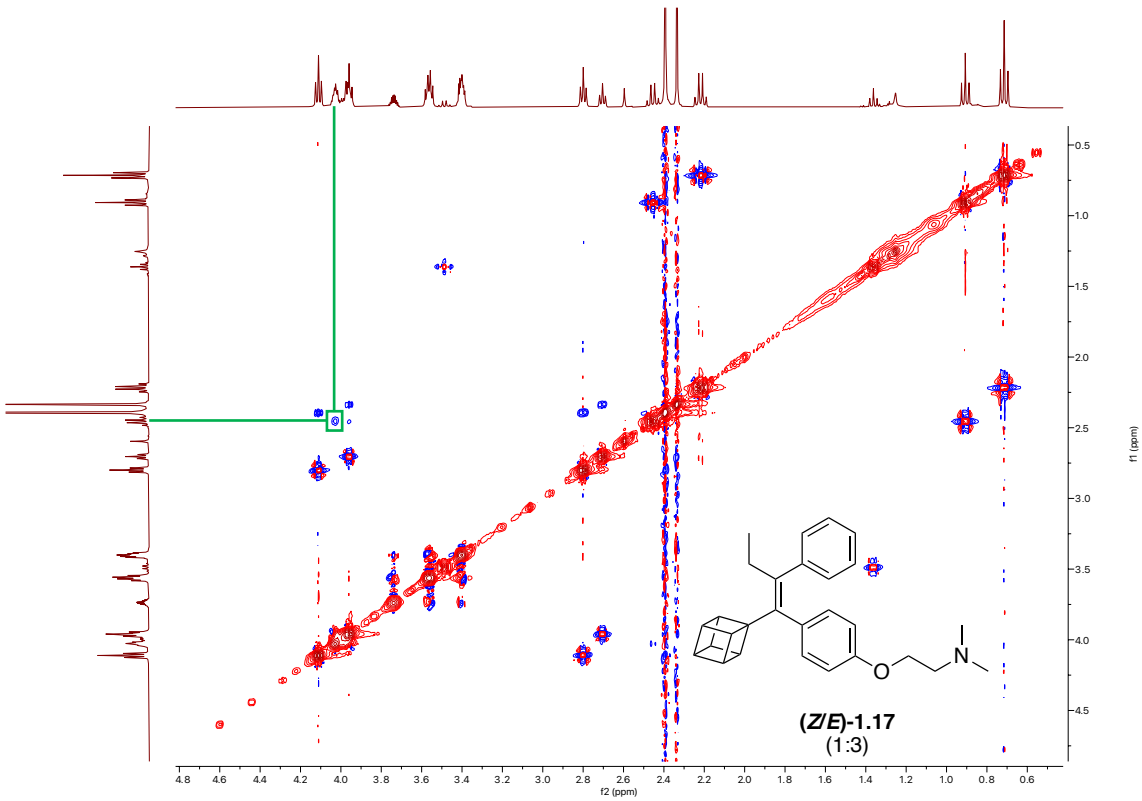

NMR Spectra: ^{1}H NMR (500 MHz, $CDCl_3$) of 3.93

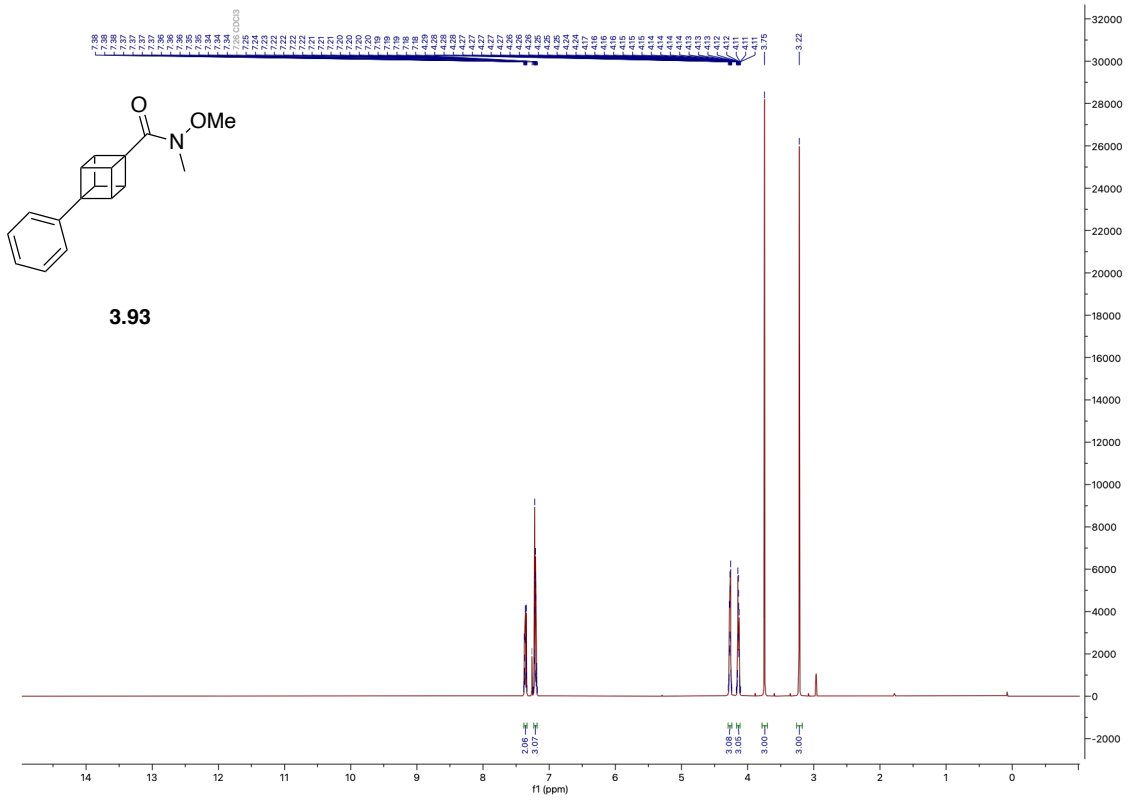

^{13}C NMR (126 MHz, $CDCl_3$) of 3.93

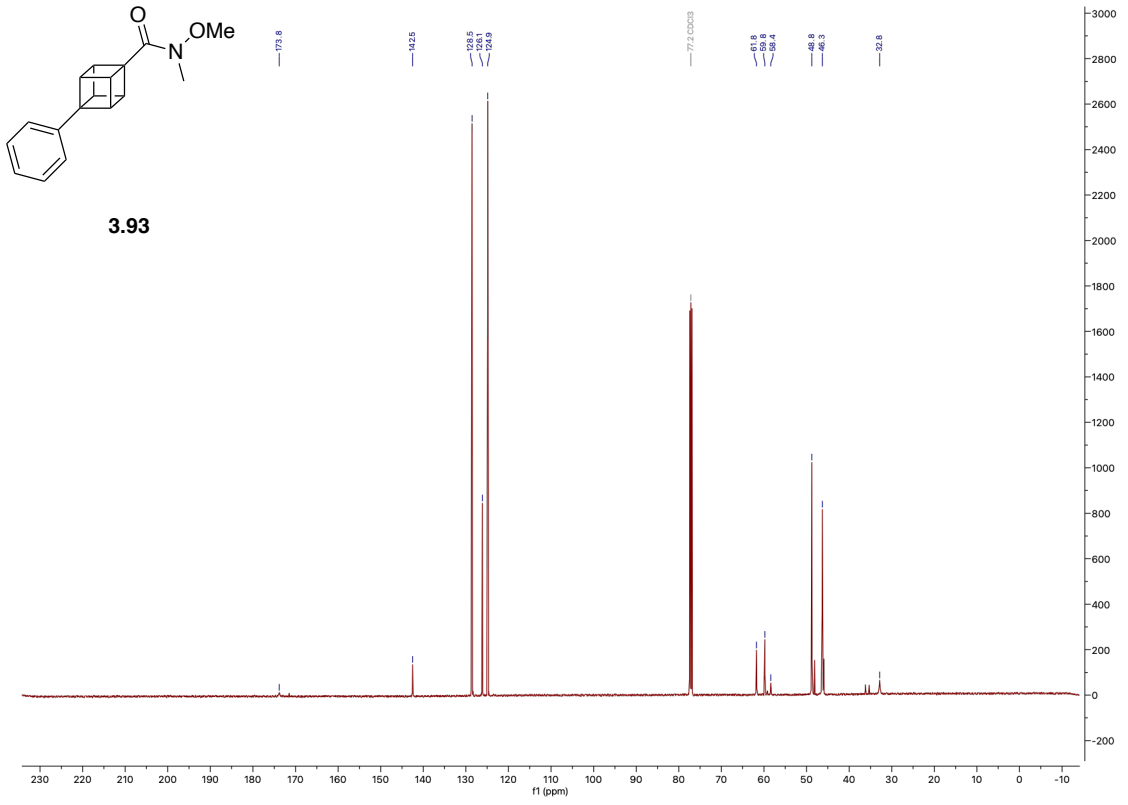

^{1}H NMR (500 MHz, $CDCl_3$) of 3.91a

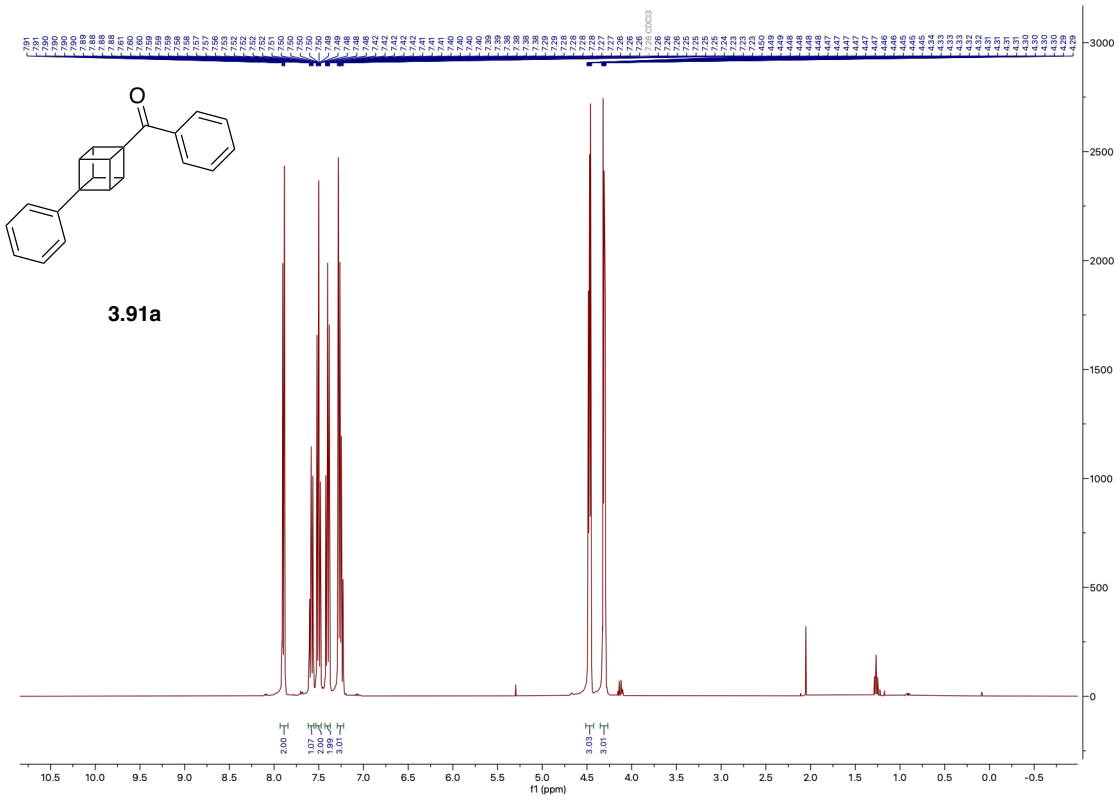

^{13}C NMR (126 MHz, $CDCl_3$) of 3.91a

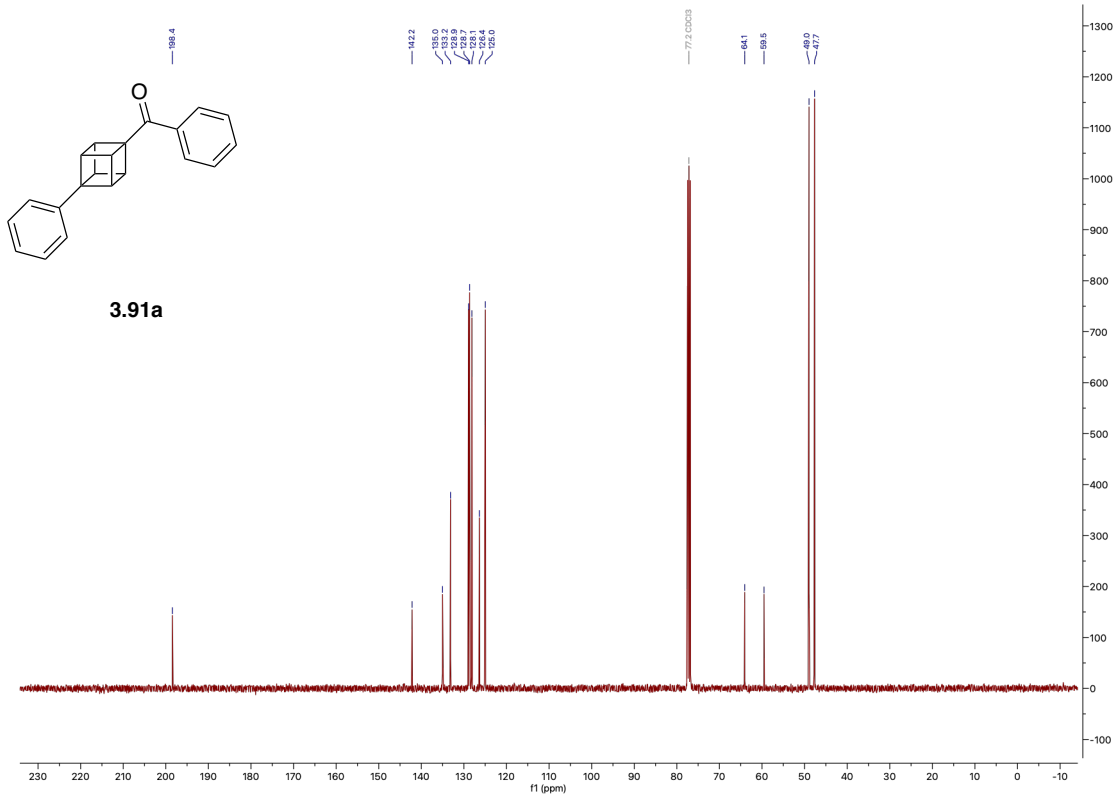

^{1}H NMR (500 MHz, $CDCl_3$) of 3.91b

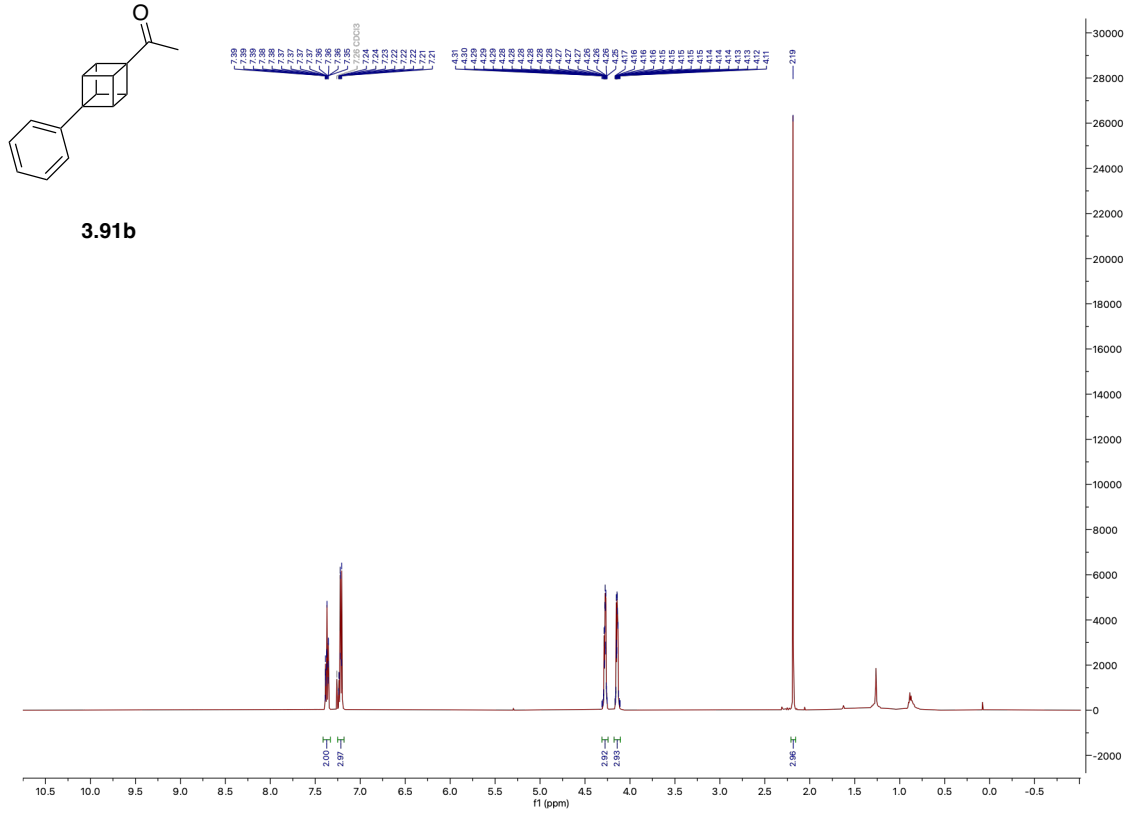

^{13}C NMR (126 MHz, $CDCl_3$) of 3.91b

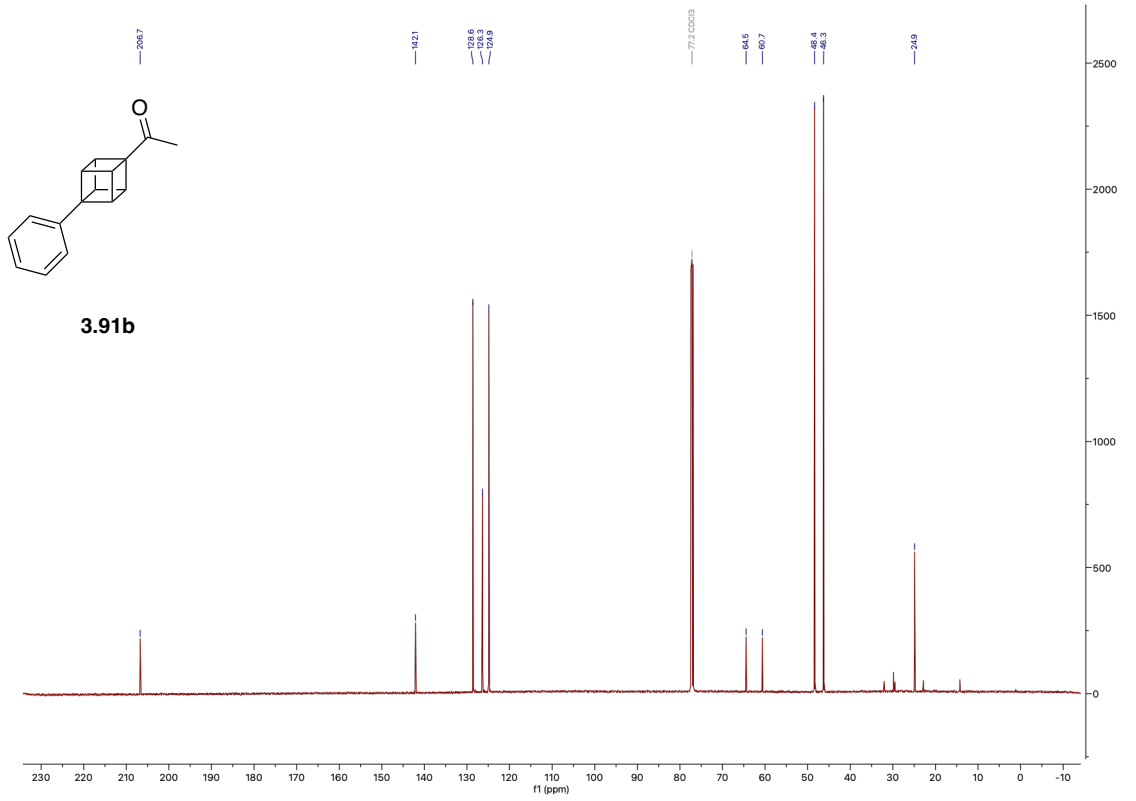

^{1}H NMR (500 MHz, $CDCl_3$) of 3.91c

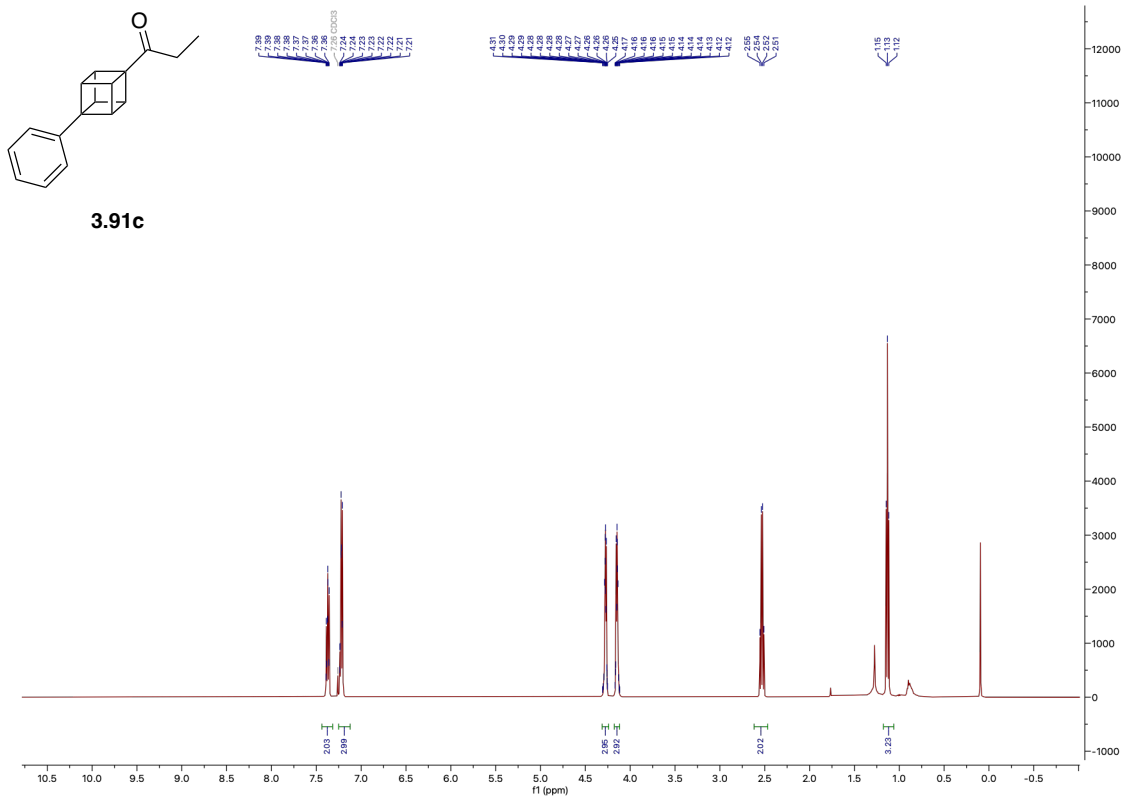

^{13}C NMR (126 MHz, $CDCl_3$) of 3.91c

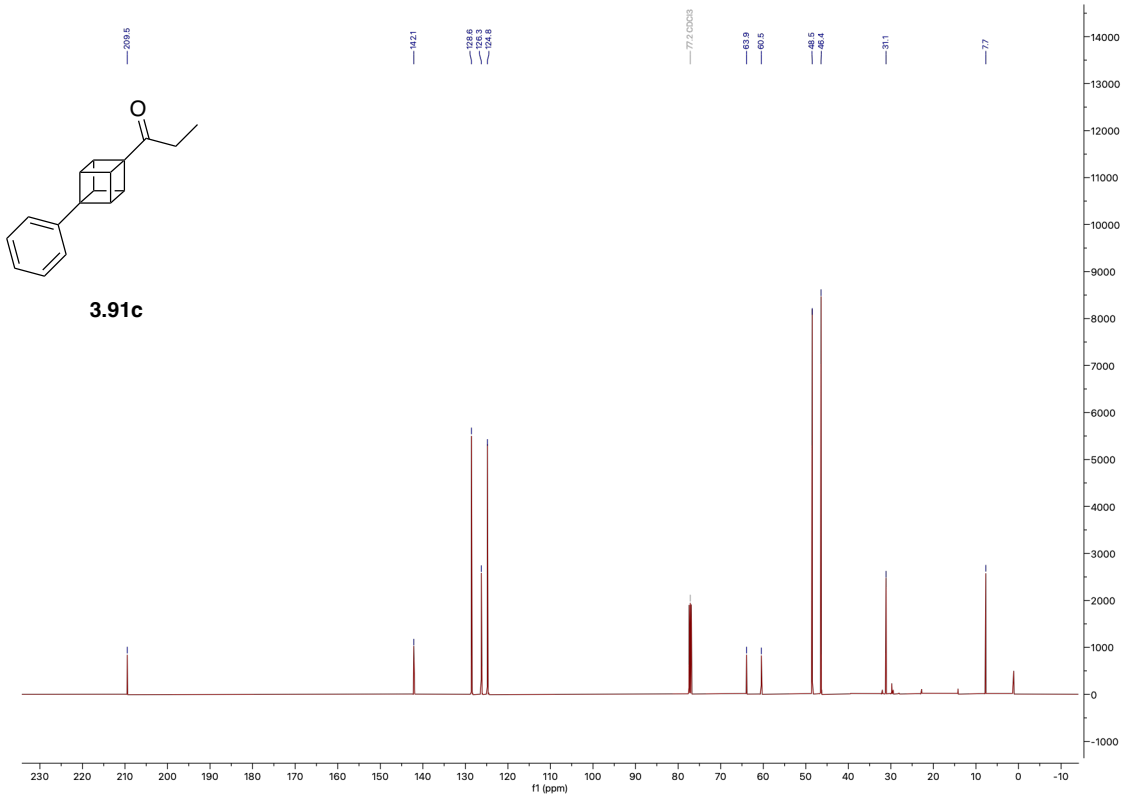

^{1}H NMR (400 MHz, $CDCl_3$) of 3.98

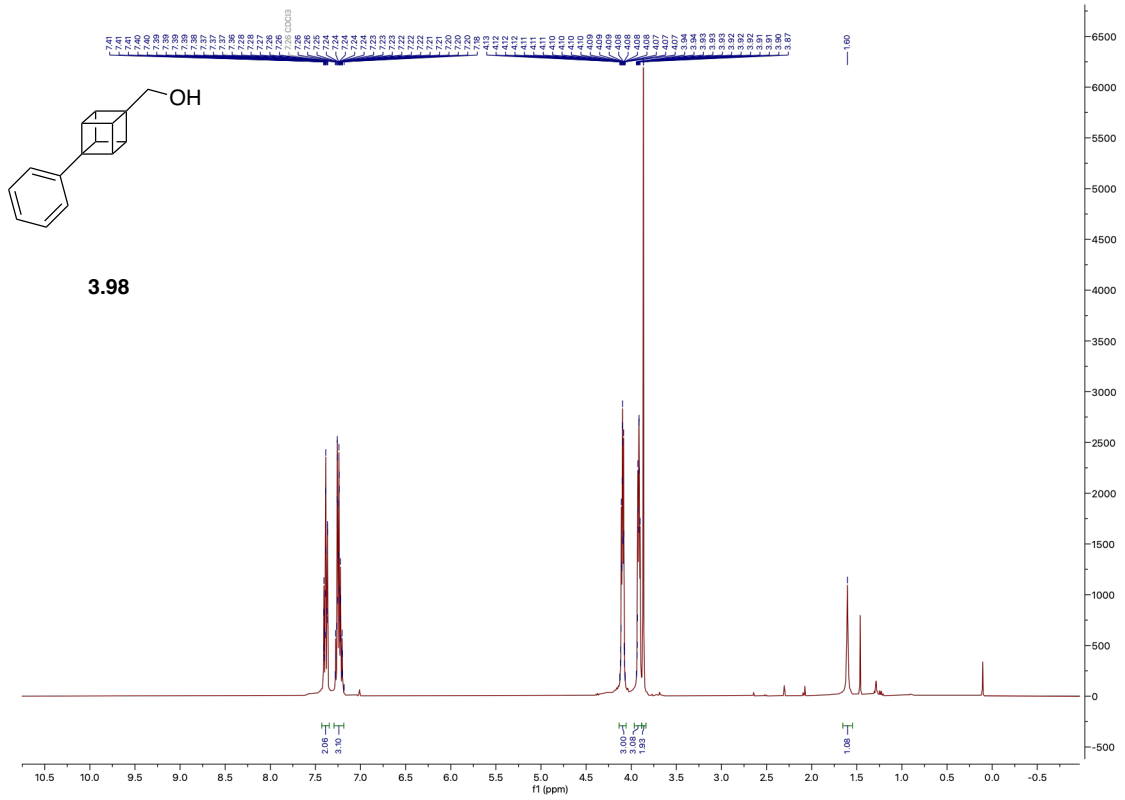

^{13}C NMR (101 MHz, $CDCl_3$) of 3.98

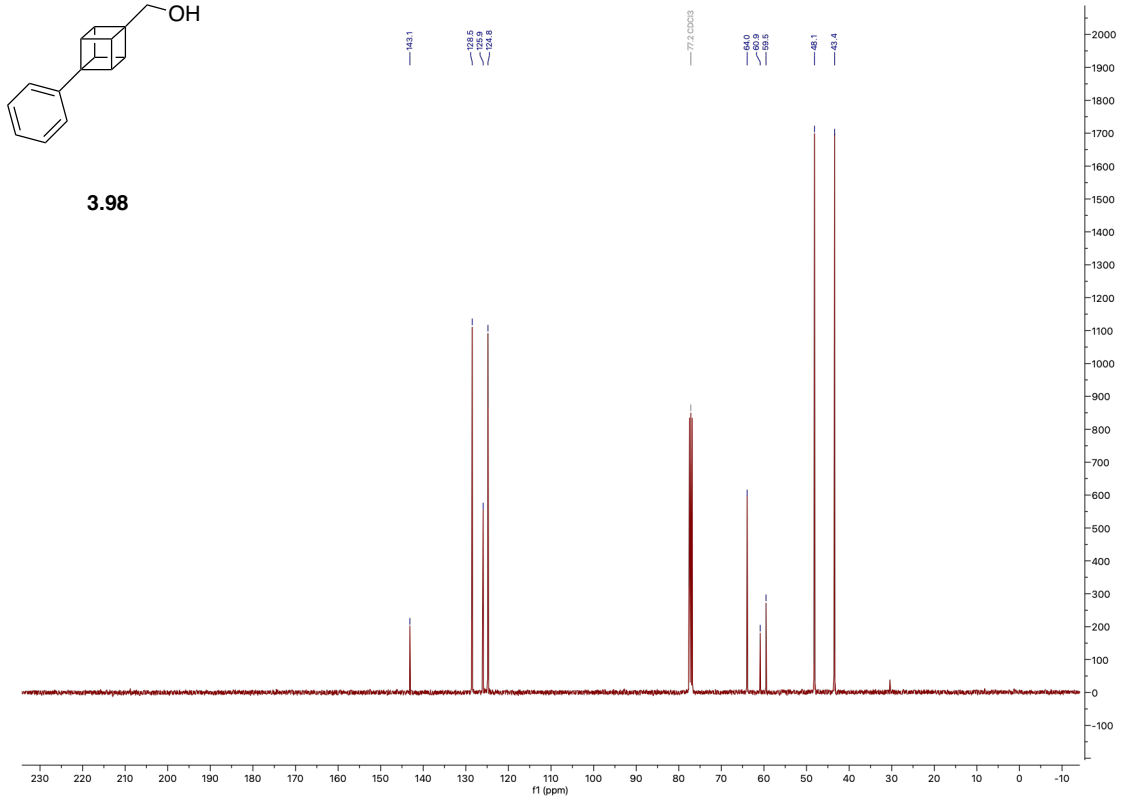

^{1}H NMR (400 MHz, $CDCl_3$) of 3.91d

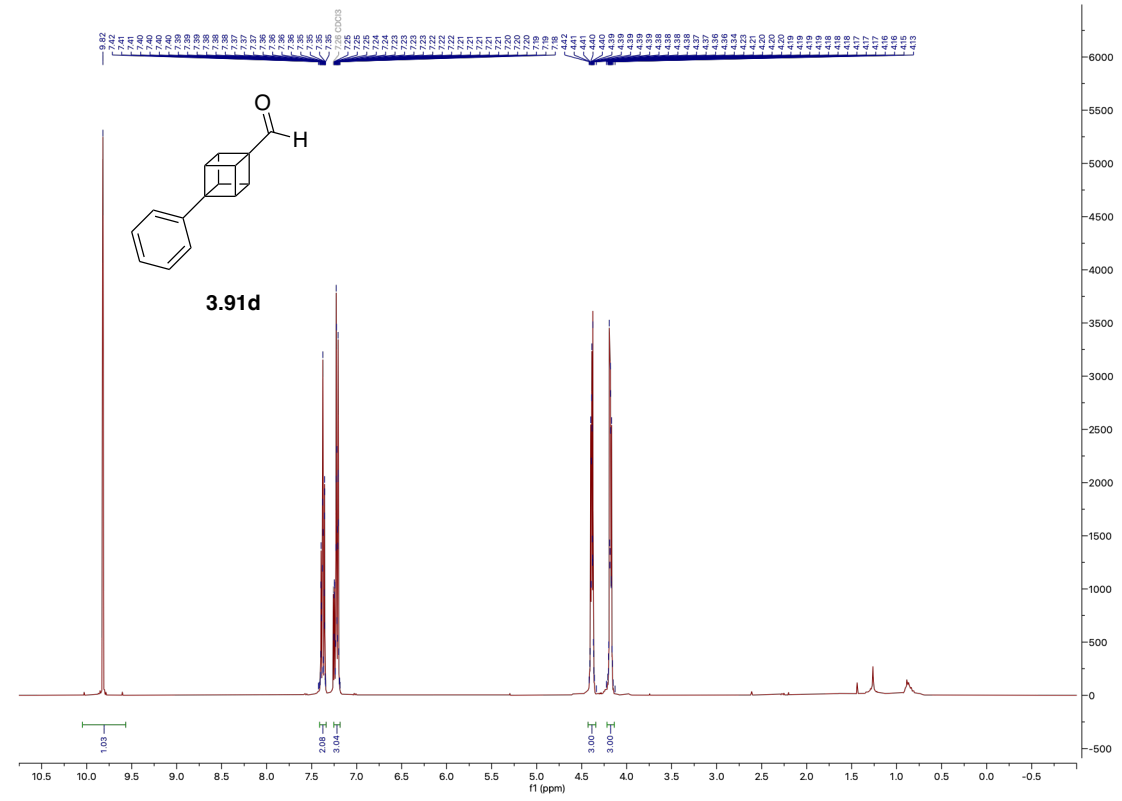

^{13}C NMR (101 MHz, $CDCl_3$) of 3.91d

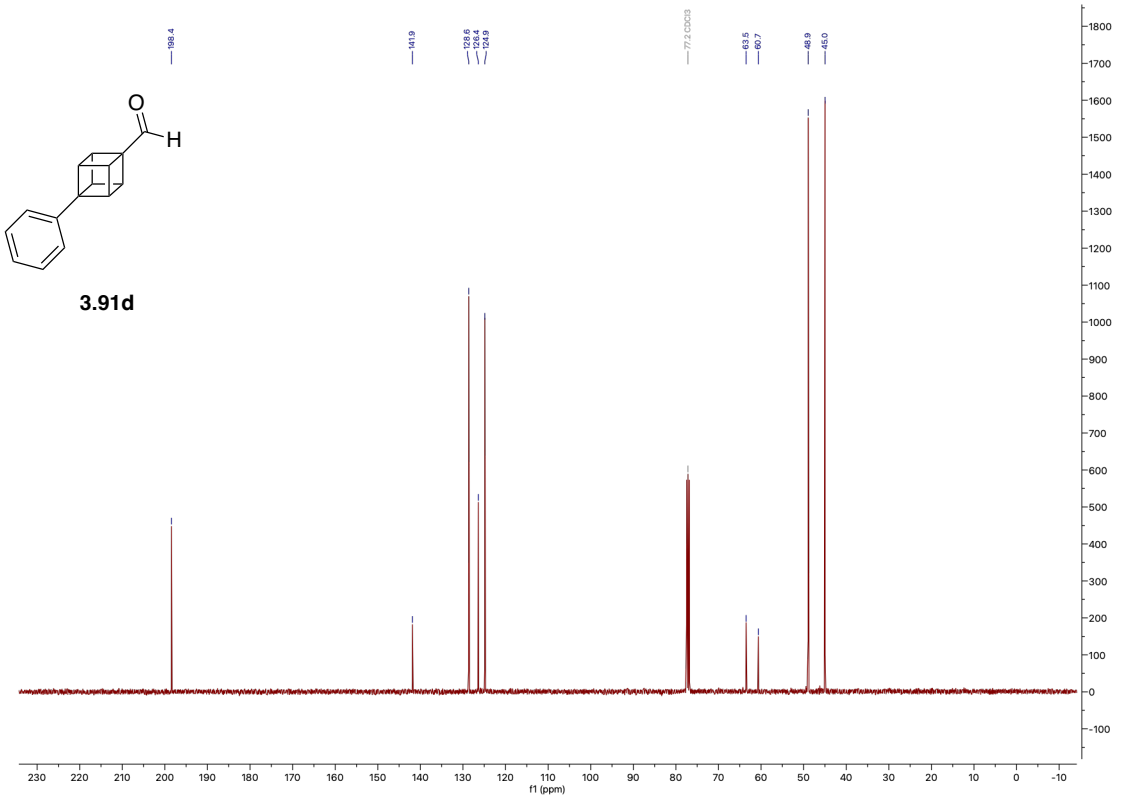

^{1}H NMR (400 MHz, $CDCl_3$) of 3.91e

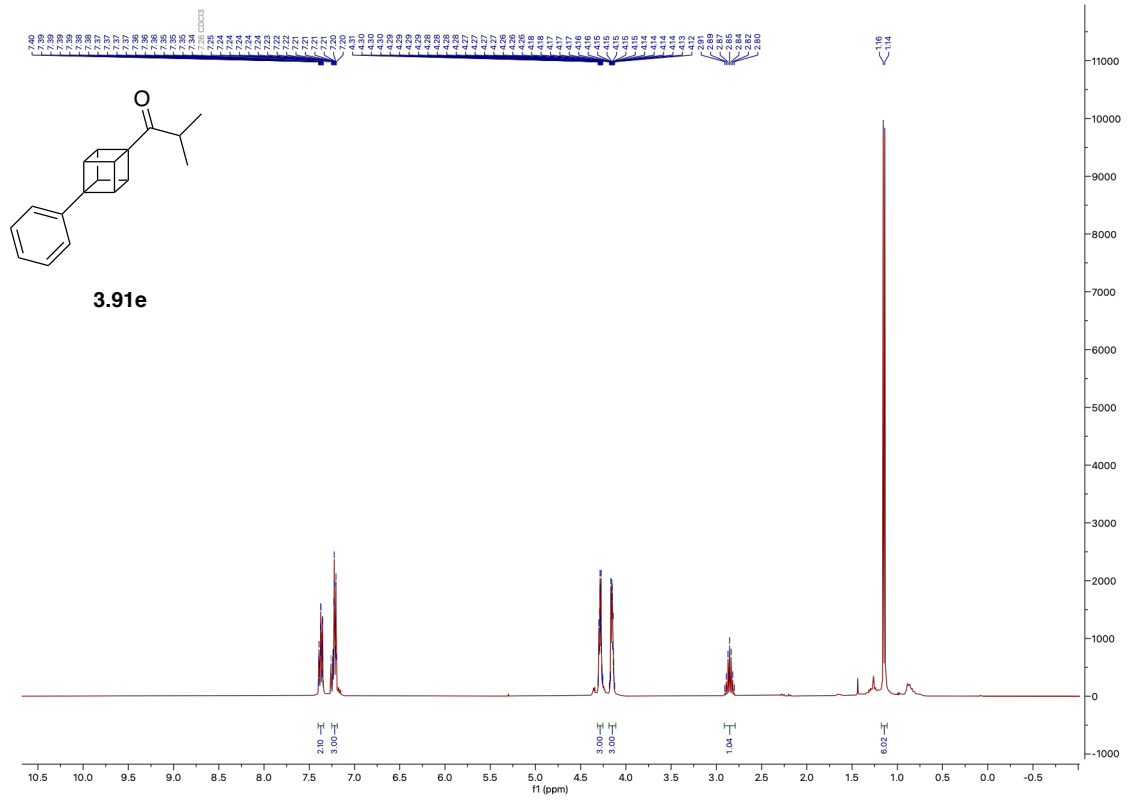

^{13}C NMR (101 MHz, $CDCl_3$) of 3.91e

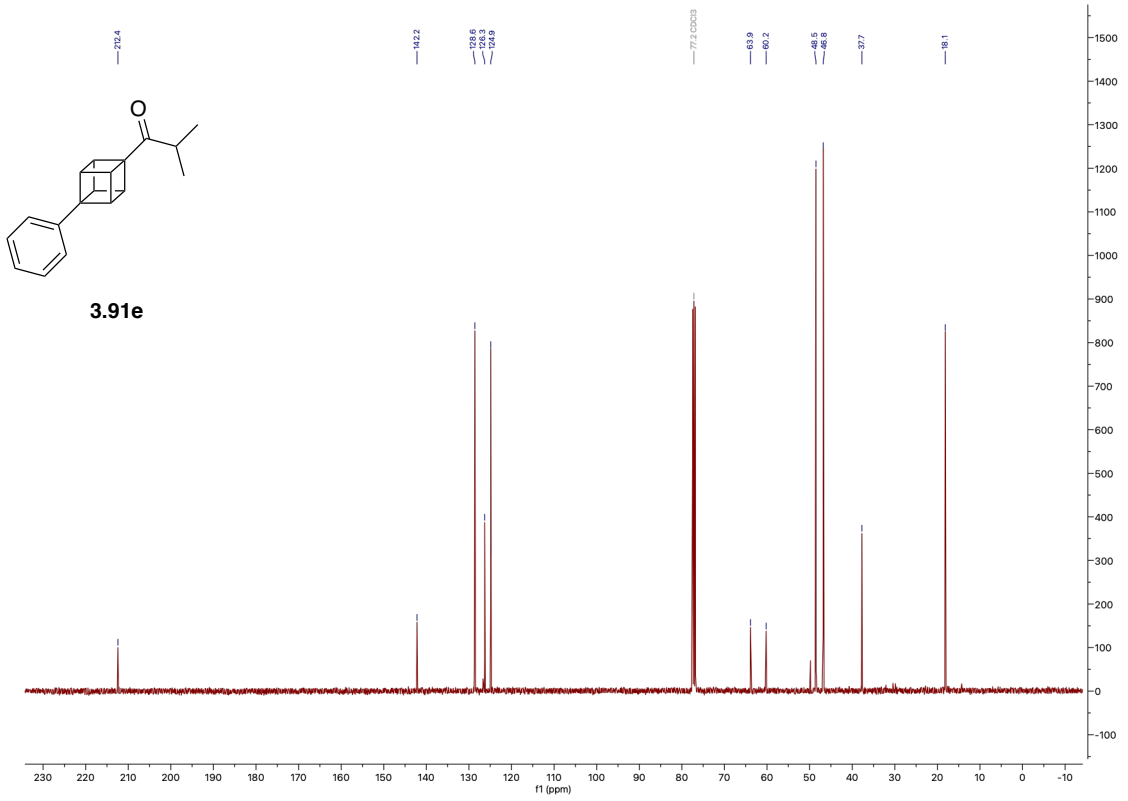

^{1}H NMR (400 MHz, $CDCl_3$) of 3.91f

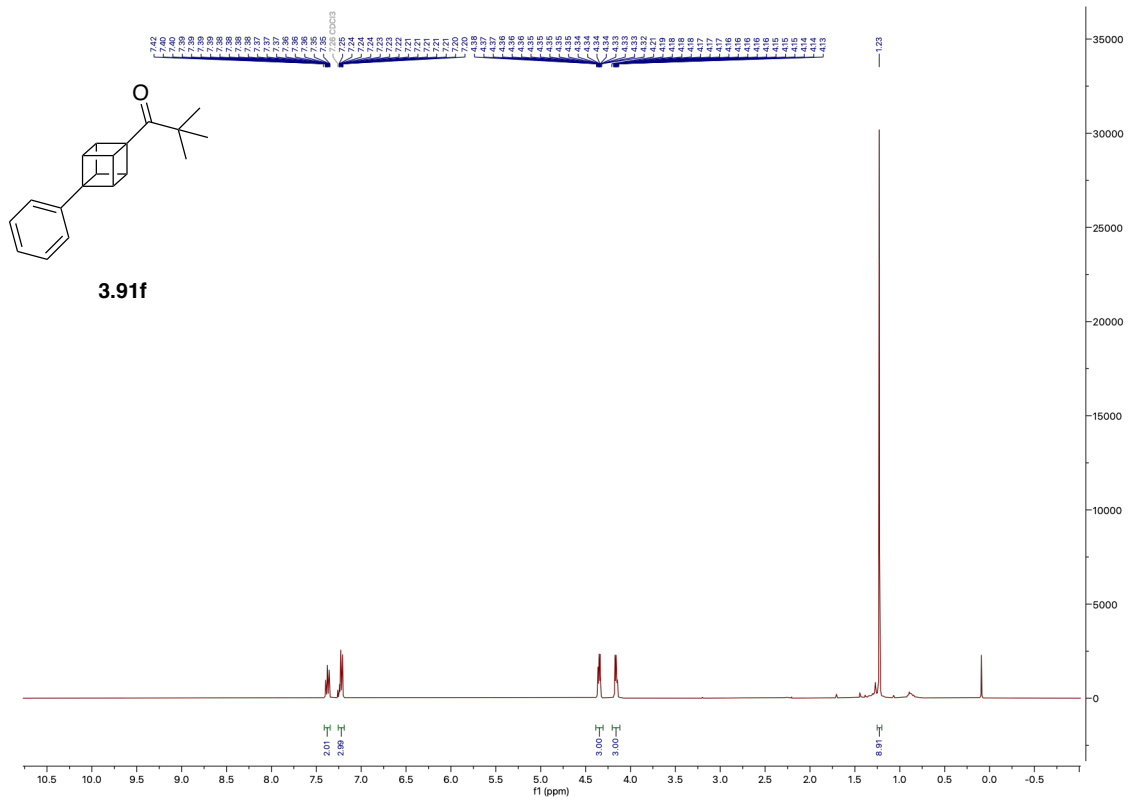

^{13}C NMR (101 MHz, $CDCl_3$) of 3.91f

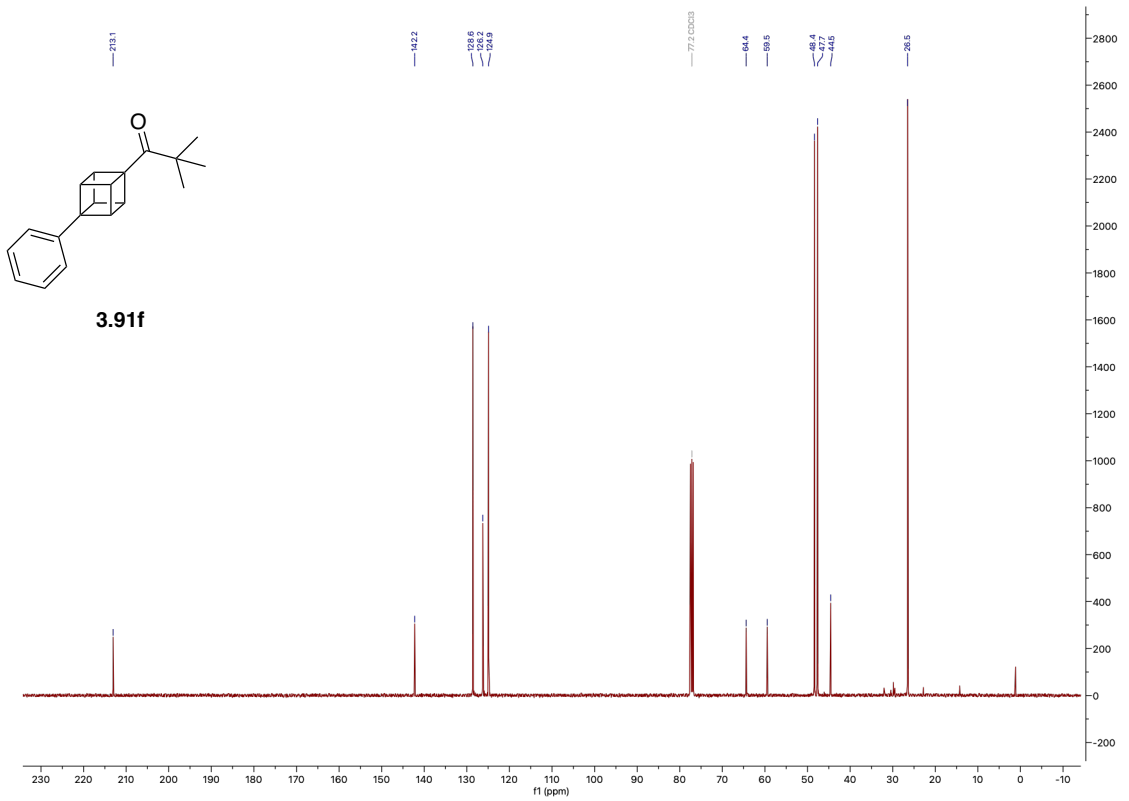

^{1}H NMR (400 MHz, $CDCl_3$) of 3.106

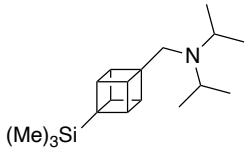

3.106

^{13}C NMR (101 MHz, $CDCl_3$) of 3.106

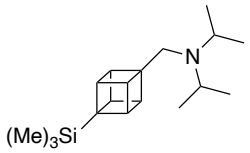

3.106

^{1}H NMR (500 MHz, $CDCl_3$) of 3.107

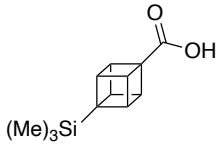

3.107

^{13}C NMR (126 MHz, $CDCl_3$) of 3.107

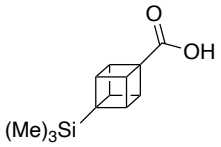

3.107

^{1}H NMR (500 MHz, $CDCl_3$) of 3.108

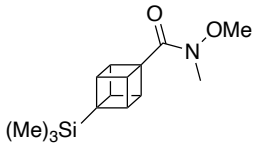

3.108

^{13}C NMR (126 MHz, $CDCl_3$) of 3.108

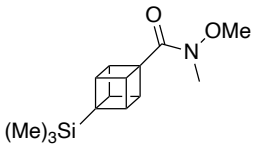

3.108

^{1}H NMR (400 MHz, $CDCl_3$) of 3.91g

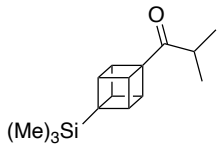

3.91g

^{13}C NMR (101 MHz, $CDCl_3$) of 3.91g

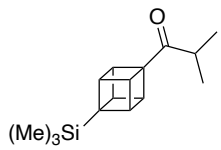

3.91g

^{1}H NMR (400 MHz, $CDCl_3$) of 3.91h

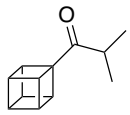

3.91h

^{13}C NMR (101 MHz, $CDCl_3$) of 3.91h

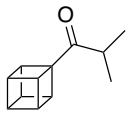

3.91h

^{1}H NMR (400 MHz, $CDCl_3$) of 3.110

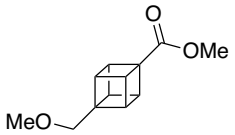

3.110

^{13}C NMR (101 MHz, $CDCl_3$) of 3.110

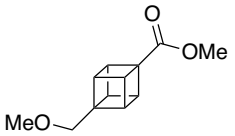

3.110

^{1}H NMR (400 MHz, $CDCl_3$) of 3.111

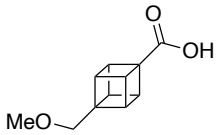

3.111

^{13}C NMR (101 MHz, $CDCl_3$) of 3.111

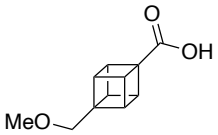

3.111

^{1}H NMR (400 MHz, $CDCl_3$) of 3.112

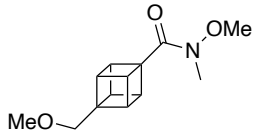

3.112

^{13}C NMR (101 MHz, $CDCl_3$) of 3.112

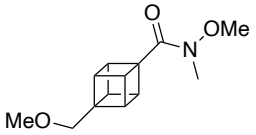

3.112

^{1}H NMR (400 MHz, $CDCl_3$) of 3.91i

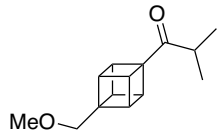

3.91i

^{13}C NMR (101 MHz, $CDCl_3$) of 3.91i

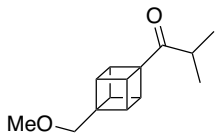

3.91i

^{1}H NMR (500 MHz, $CDCl_3$) of 3.115

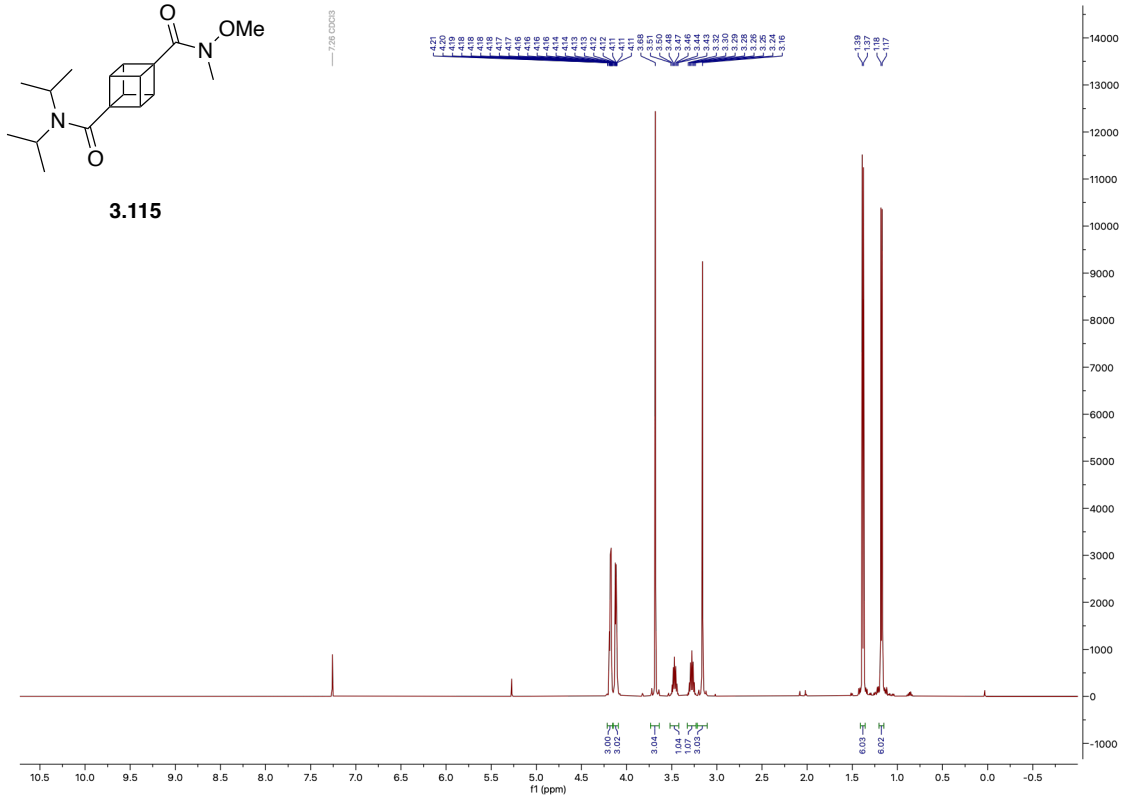

^{13}C NMR (126 MHz, $CDCl_3$) of 3.115

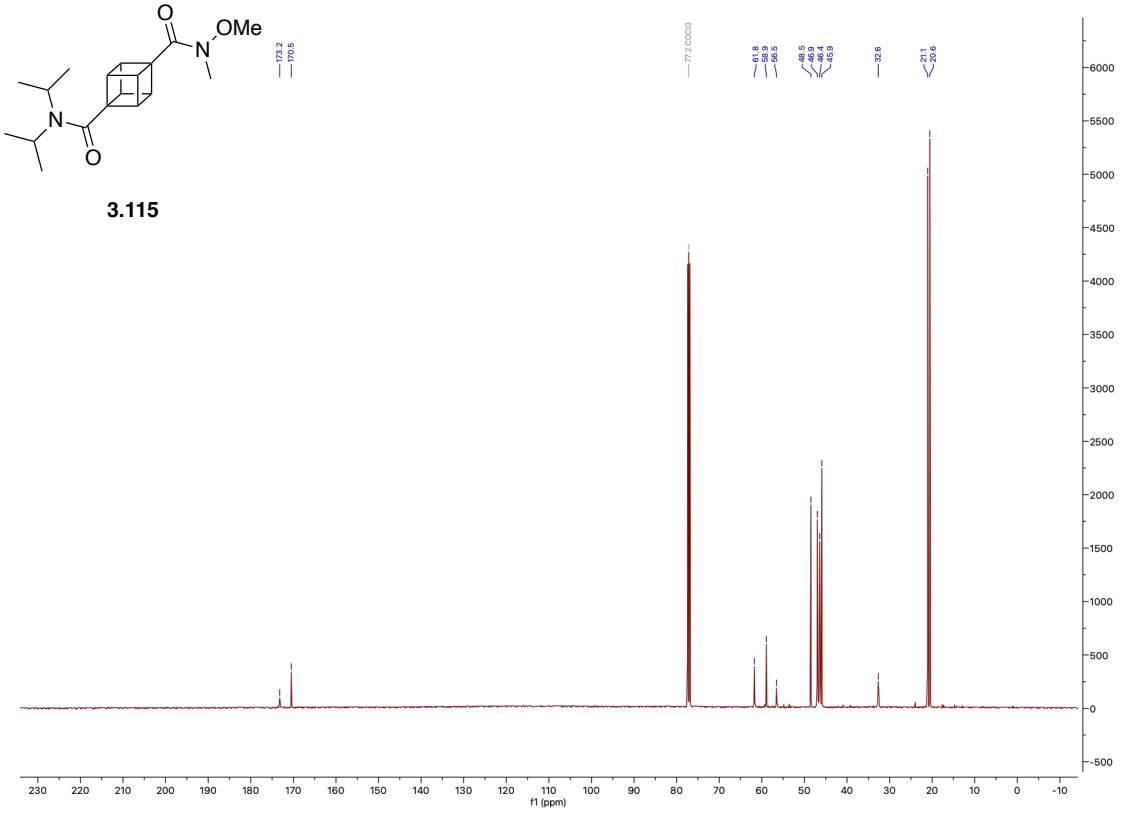

^{1}H NMR (400 MHz, $CDCl_3$) of 3.91j

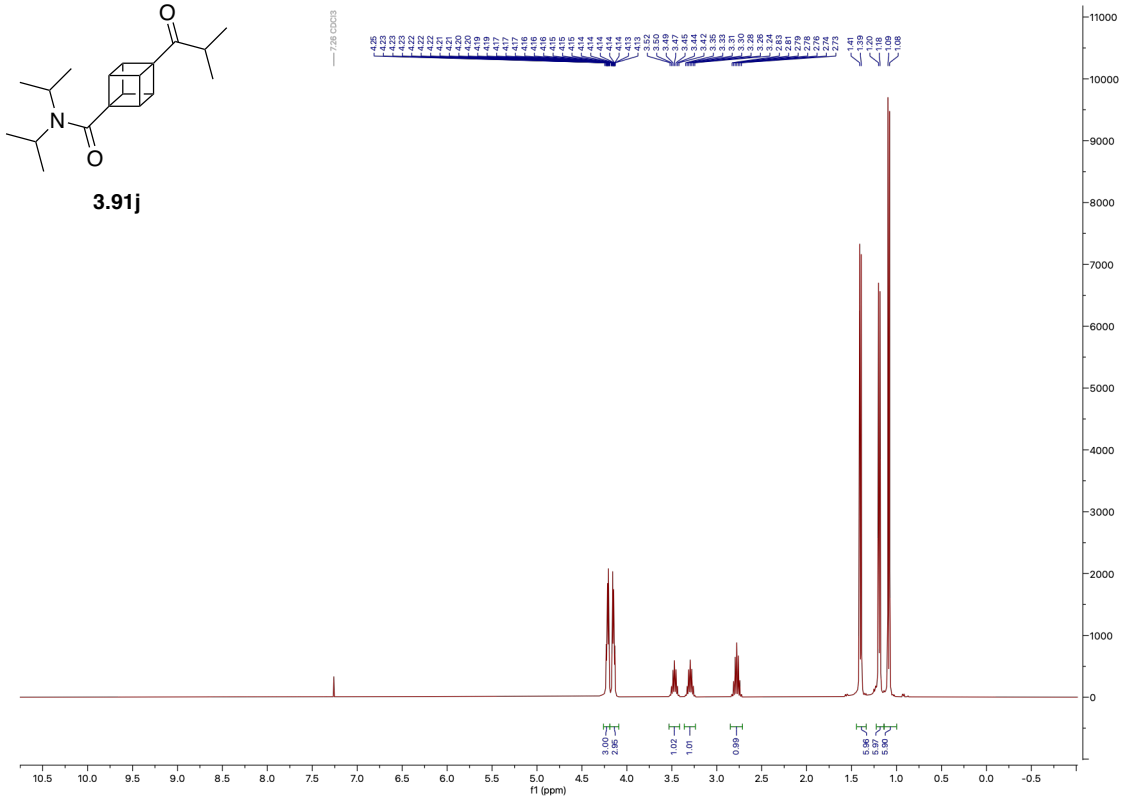

^{13}C NMR (101 MHz, $CDCl_3$) of 3.91j

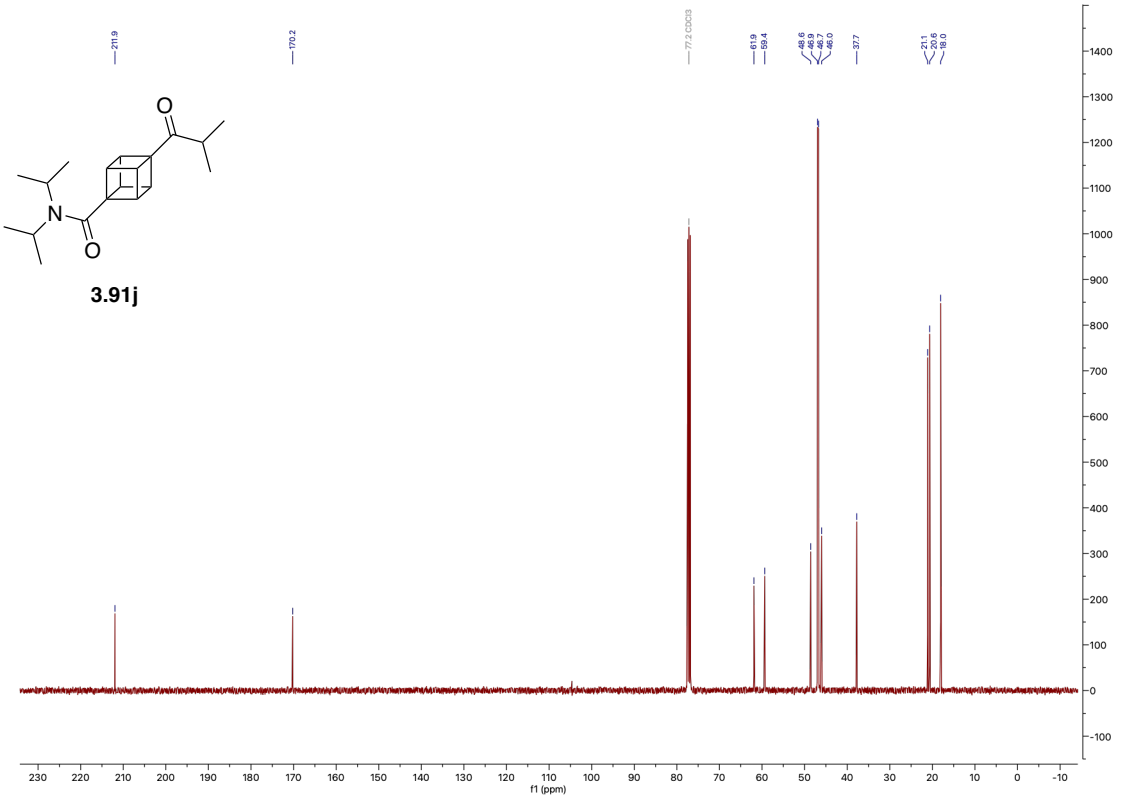

^{1}H NMR (400 MHz, $CDCl_3$) of 3.118

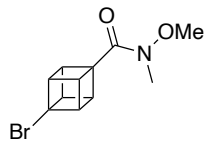

3.118

^{13}C NMR (101 MHz, $CDCl_3$) of 3.118

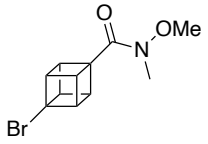

3.118

^{1}H NMR (500 MHz, $CDCl_3$) of 3.91k

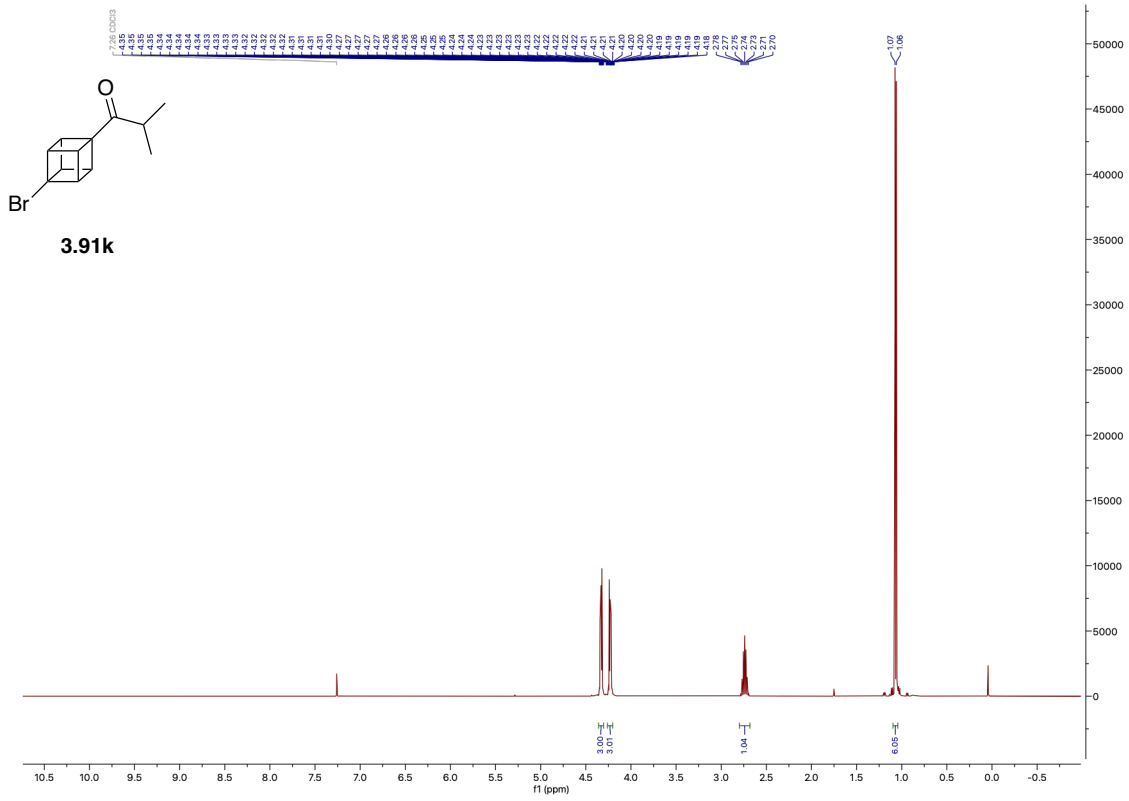

^{13}C NMR (126 MHz, $CDCl_3$) of 3.91k

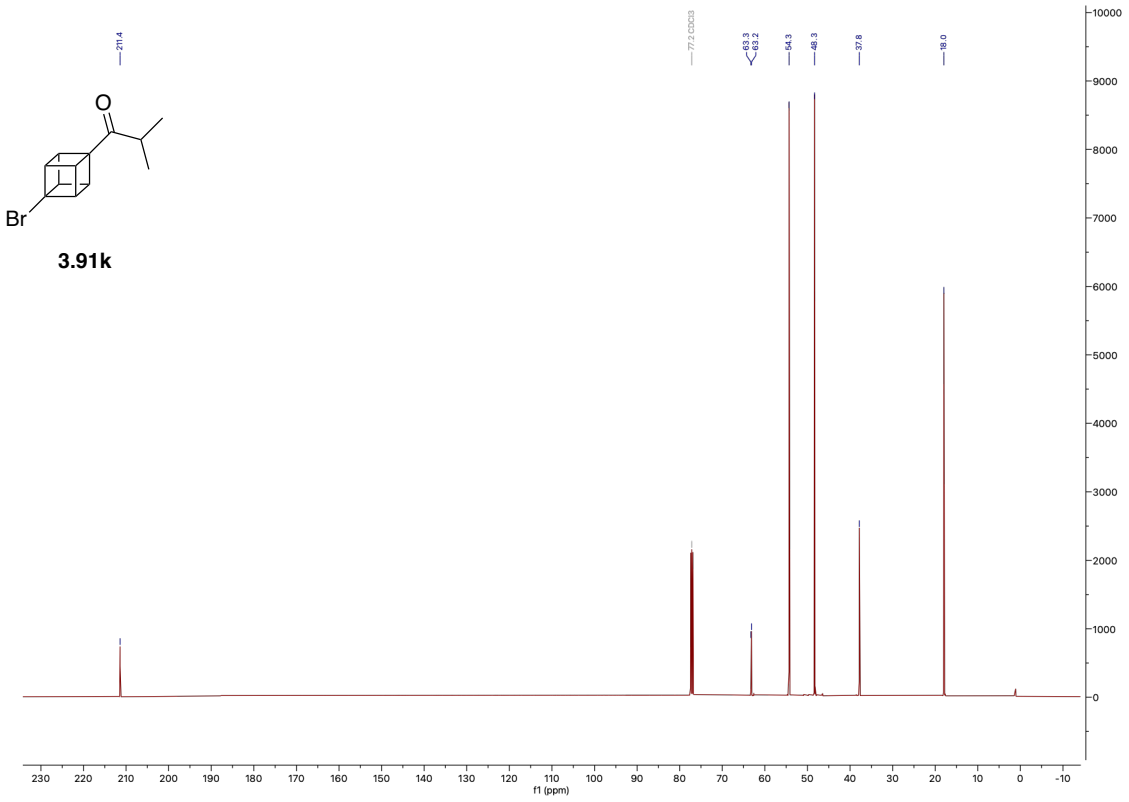

^{1}H NMR (500 MHz, $CDCl_3$) of 3.119

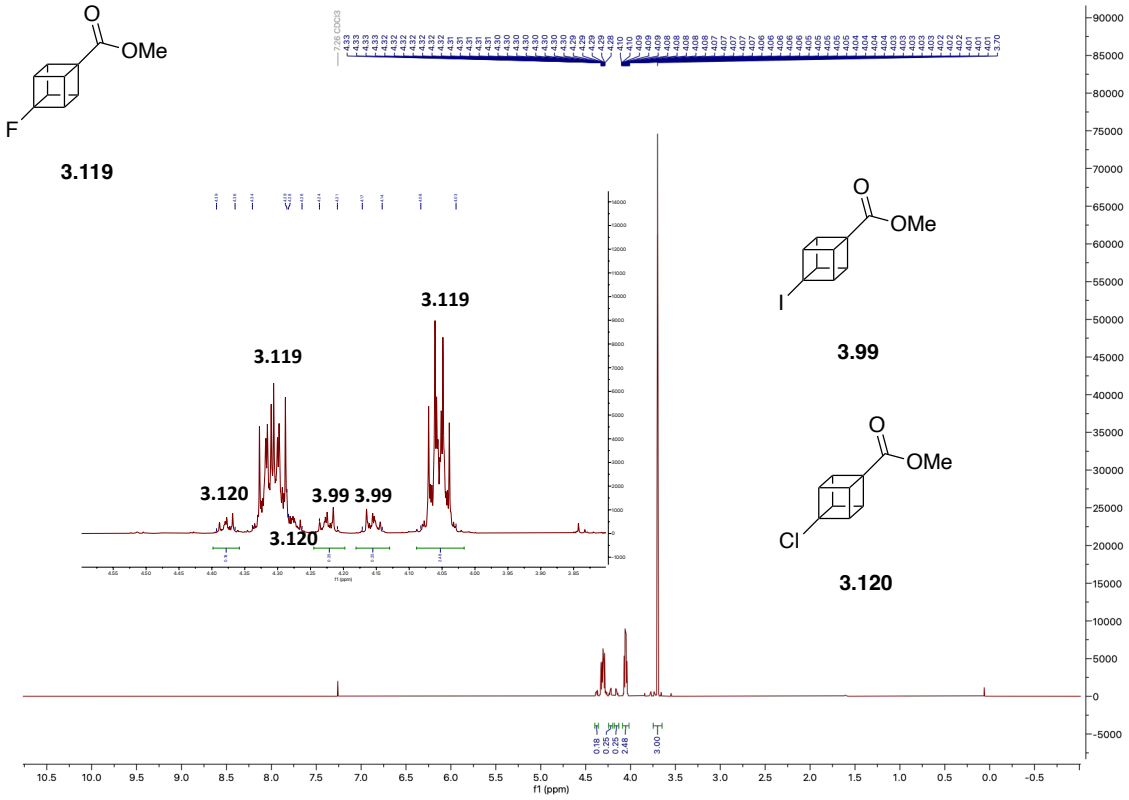

^{13}C NMR (126 MHz, $CDCl_3$) of 3.119

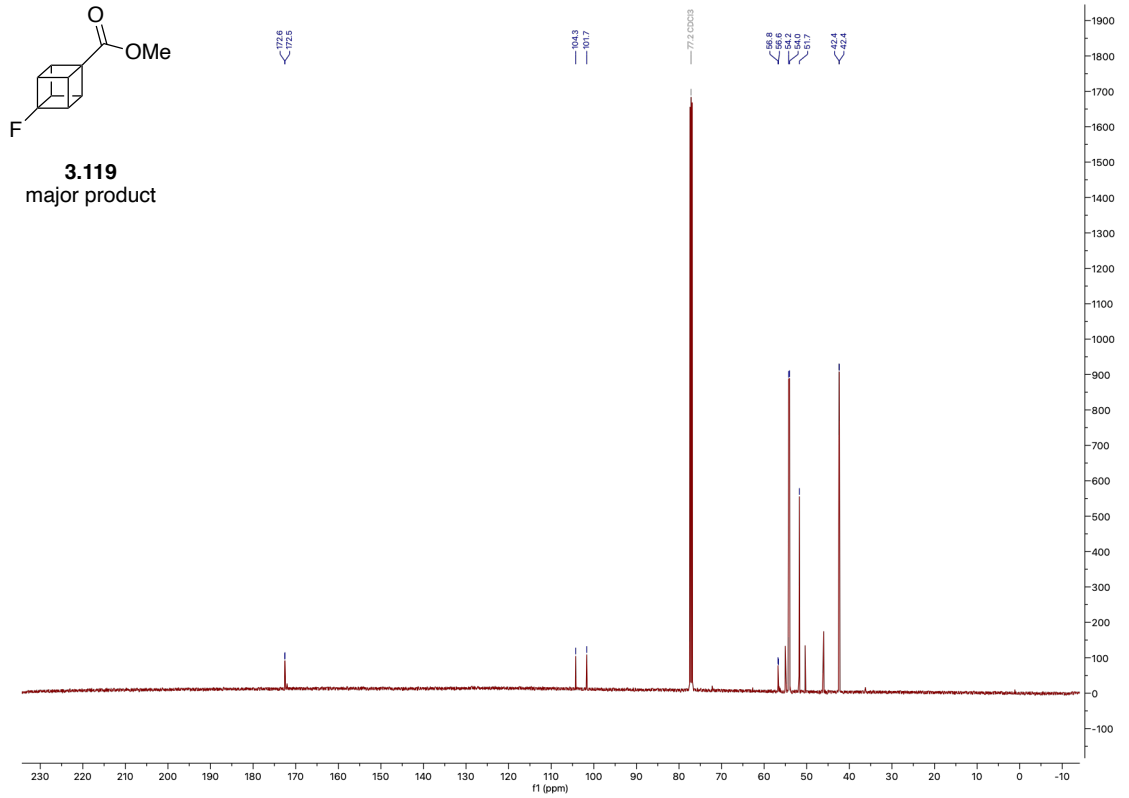

^{13}C NMR (126 MHz, $CDCl_3$) of 3.119 & 3.120 & 3.99

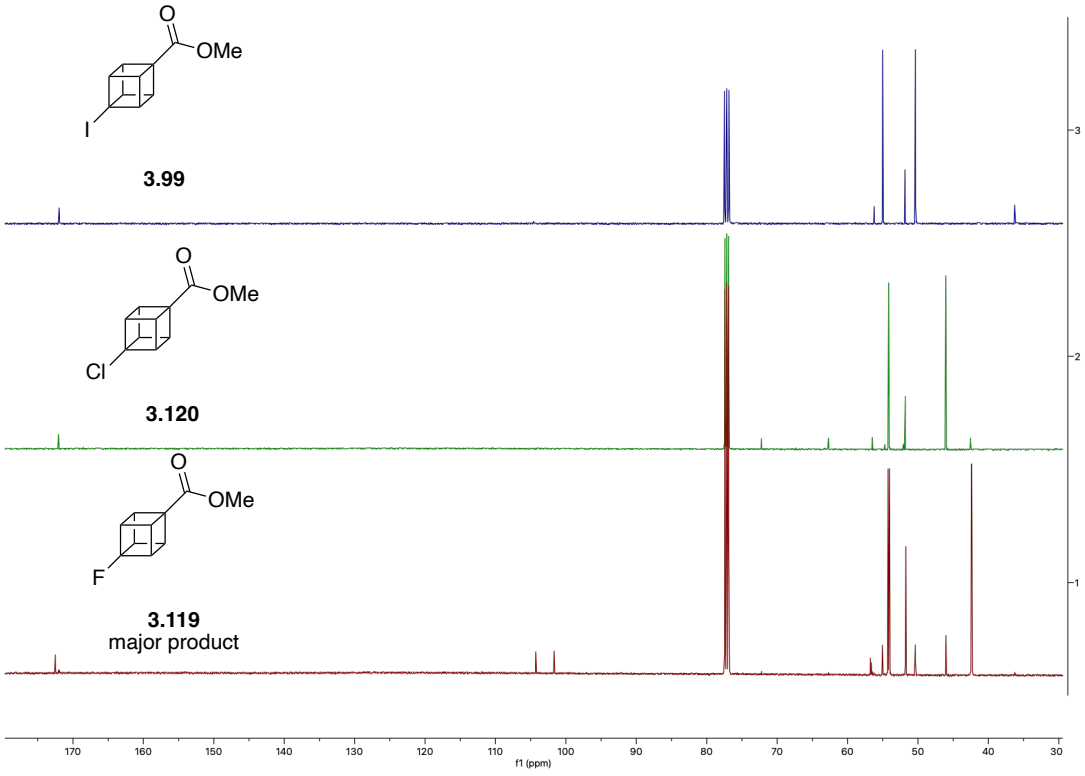

^{13}C NMR (126 MHz, $CDCl_3$) of 3.119 & 3.120 & 3.99 zoom

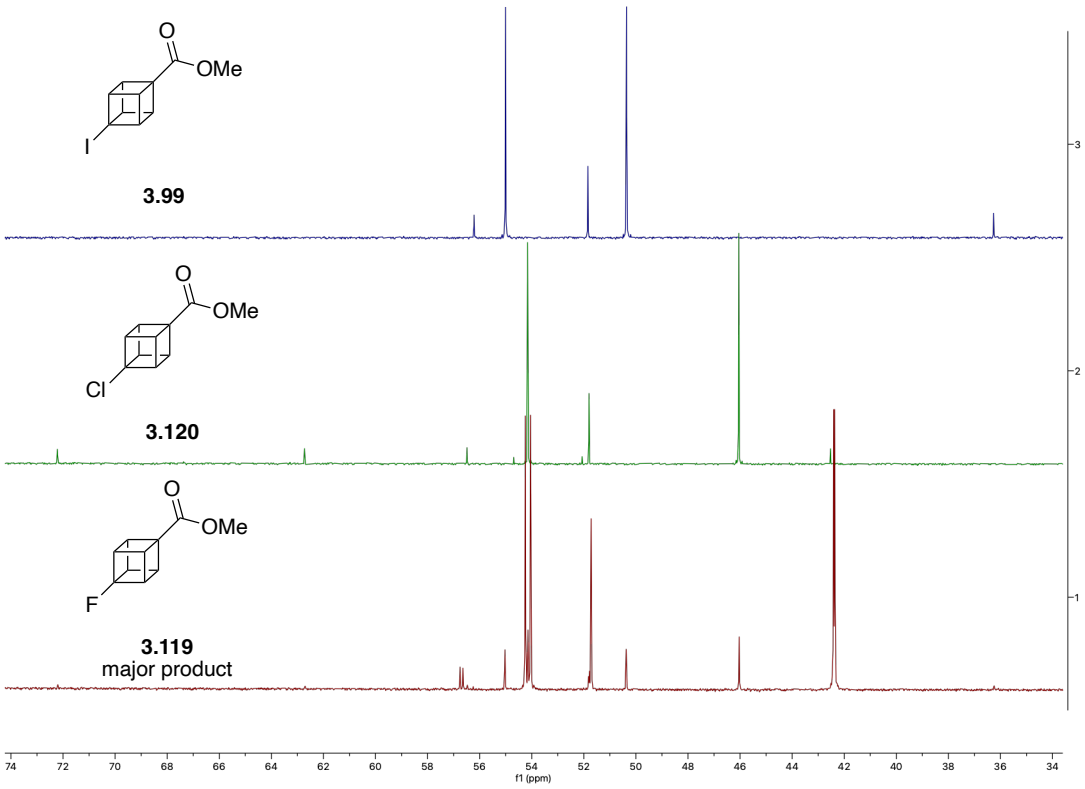

$^{19}F\{1H\}$NMR (471 MHz, $CDCl_3$) of 3.119

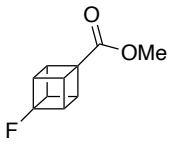

3.119

^{1}H NMR (500 MHz, $CDCl_3$) of 3.120

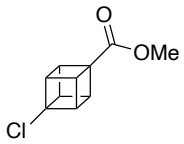

3.120

^{13}C NMR (126 MHz, $CDCl_3$) of 3.120

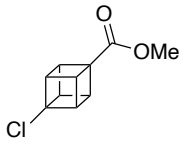

3.120

^{1}H NMR (400 MHz, $CDCl_3$) of 3.121

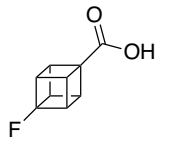

3.121

^{13}C NMR (101 MHz, $CDCl_3$) of 3.121

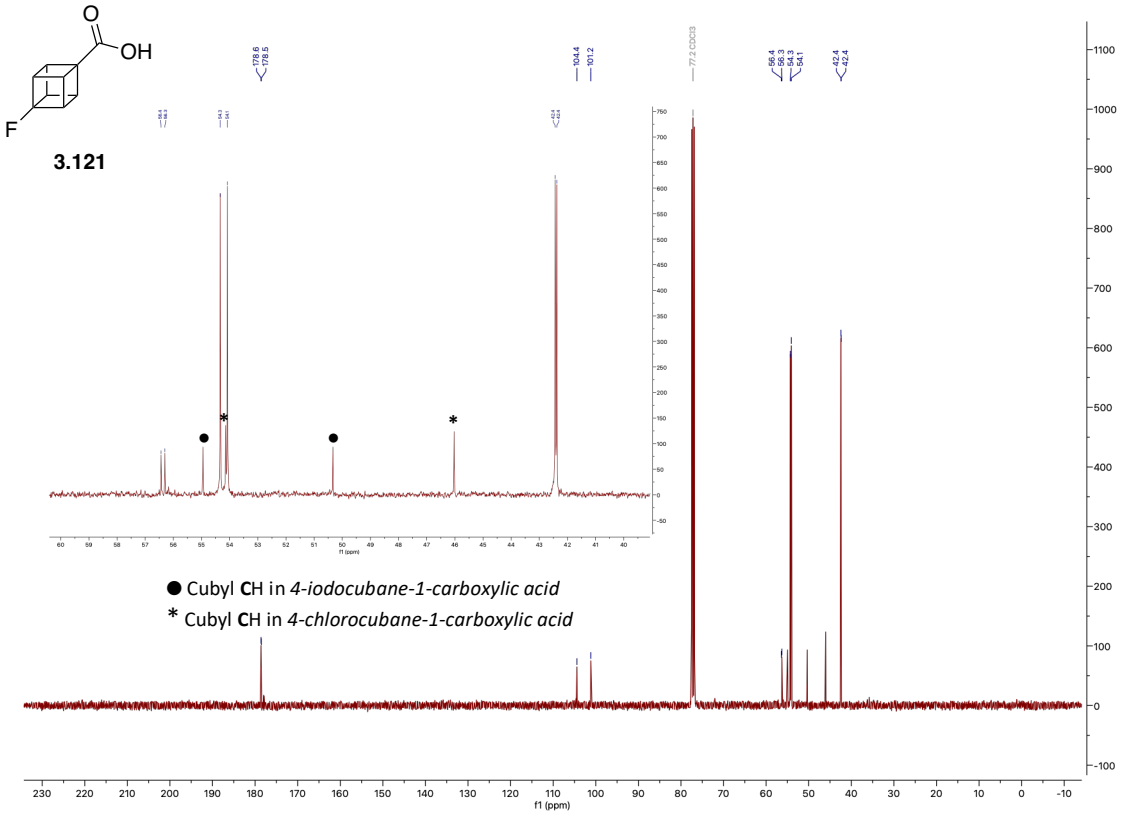

^{19}F{1H}NMR (376 MHz, $CDCl_3$) of 3.121

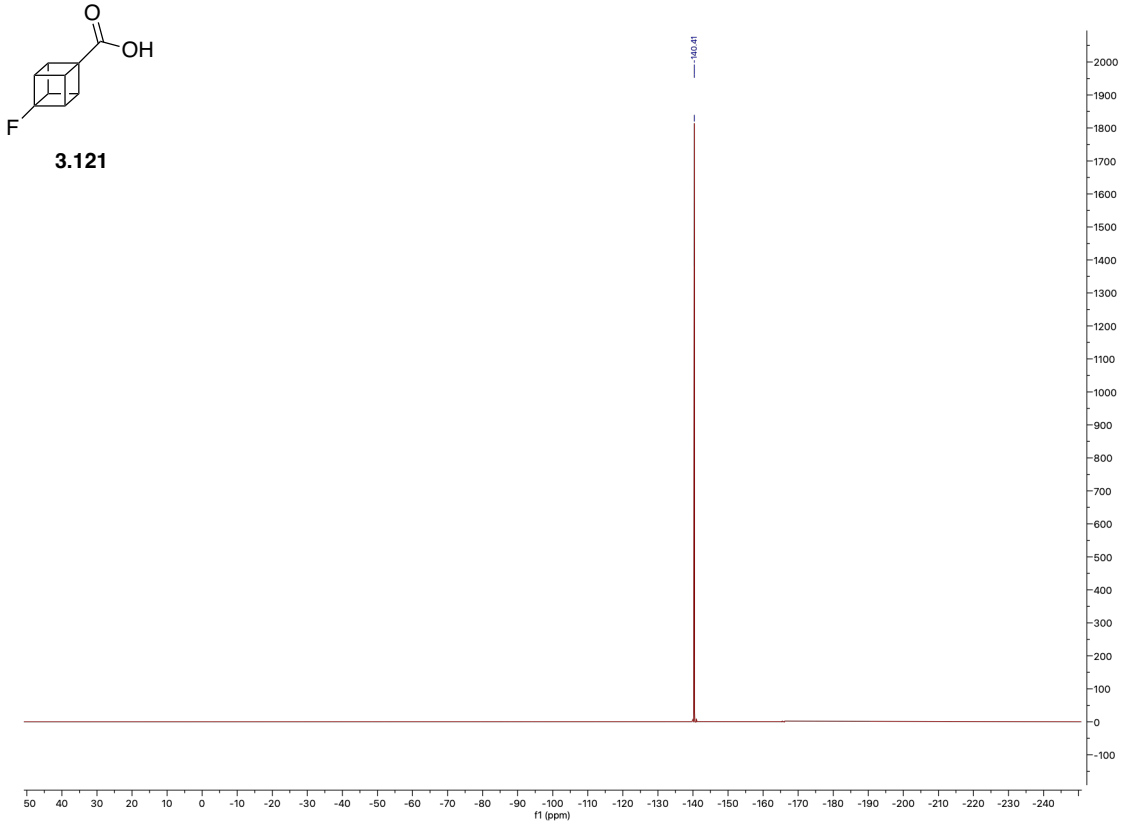

^{1}H NMR (500 MHz, $CDCl_3$) of 3.122

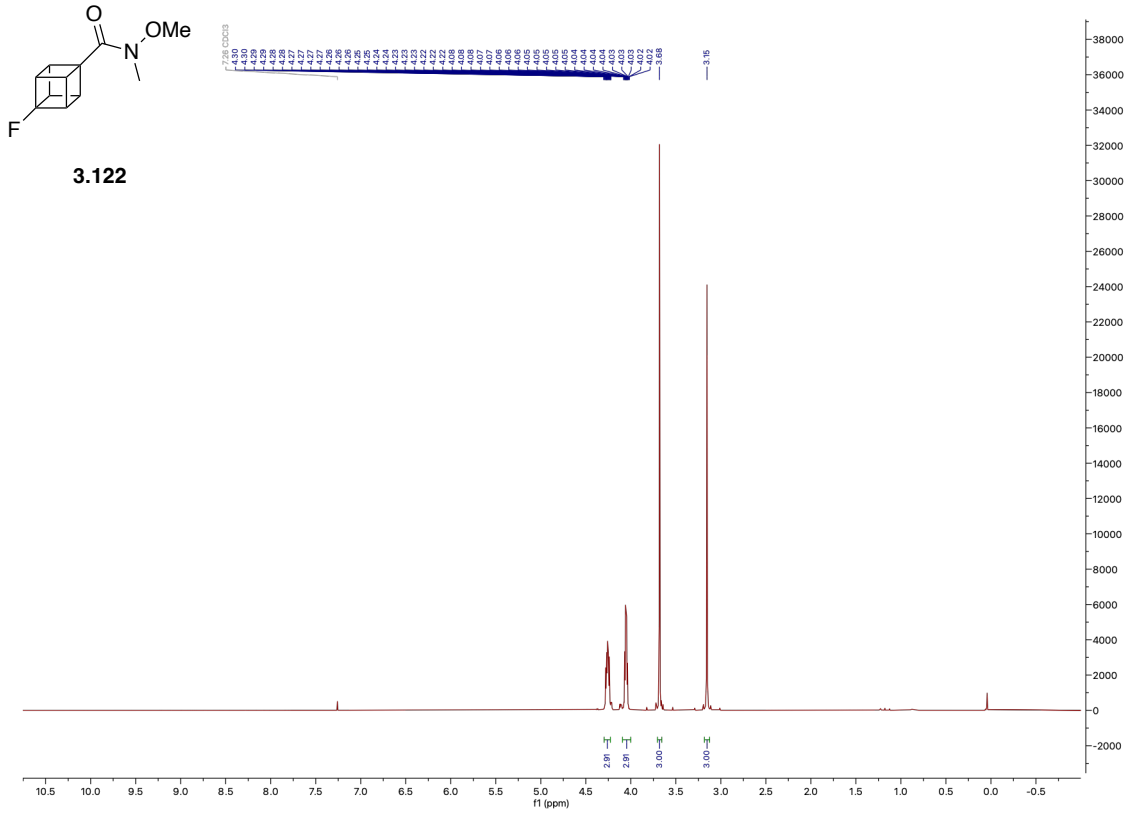

^{13}C NMR (126 MHz, $CDCl_3$) of 3.122

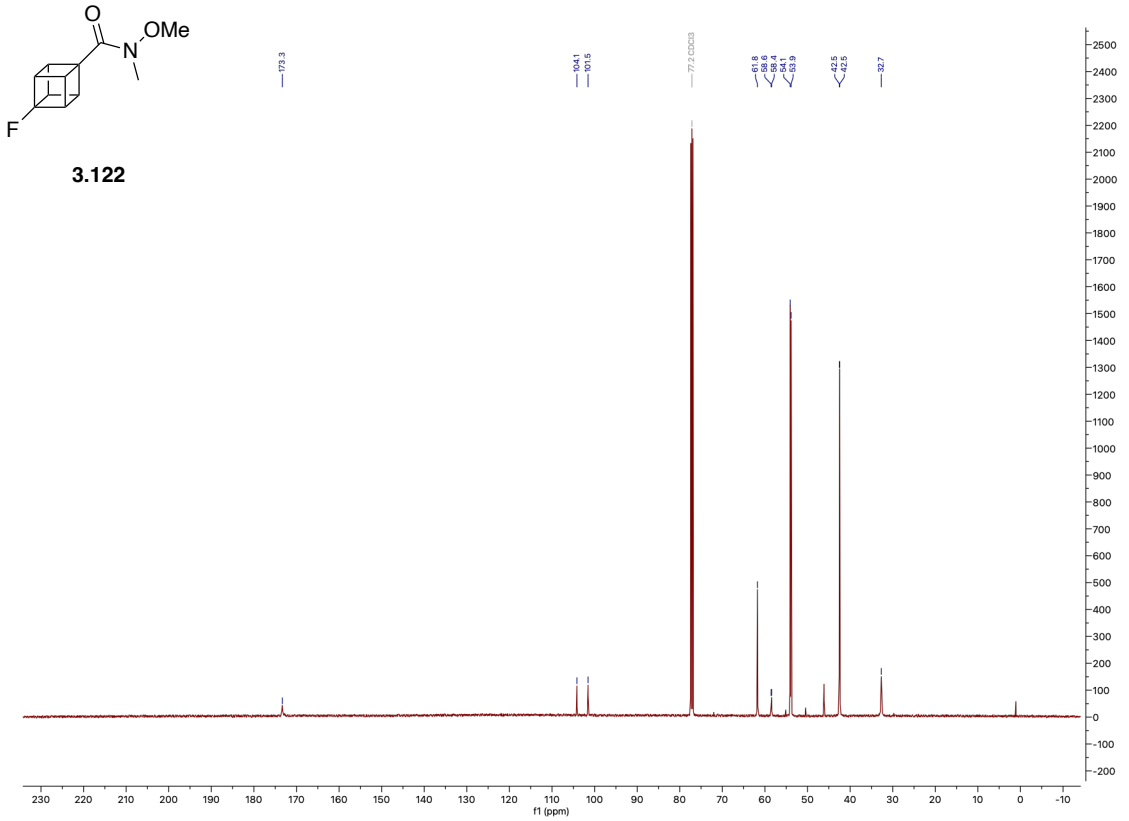

$^{19}F\{1H\}$NMR (471 MHz, $CDCl_3$) of 3.122

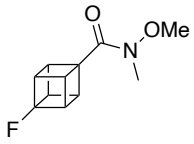

3.122

^{1}H NMR (400 MHz, $CDCl_3$) of 3.91l

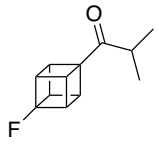

3.91l

^{13}C NMR (101 MHz, $CDCl_3$) of 3.91l

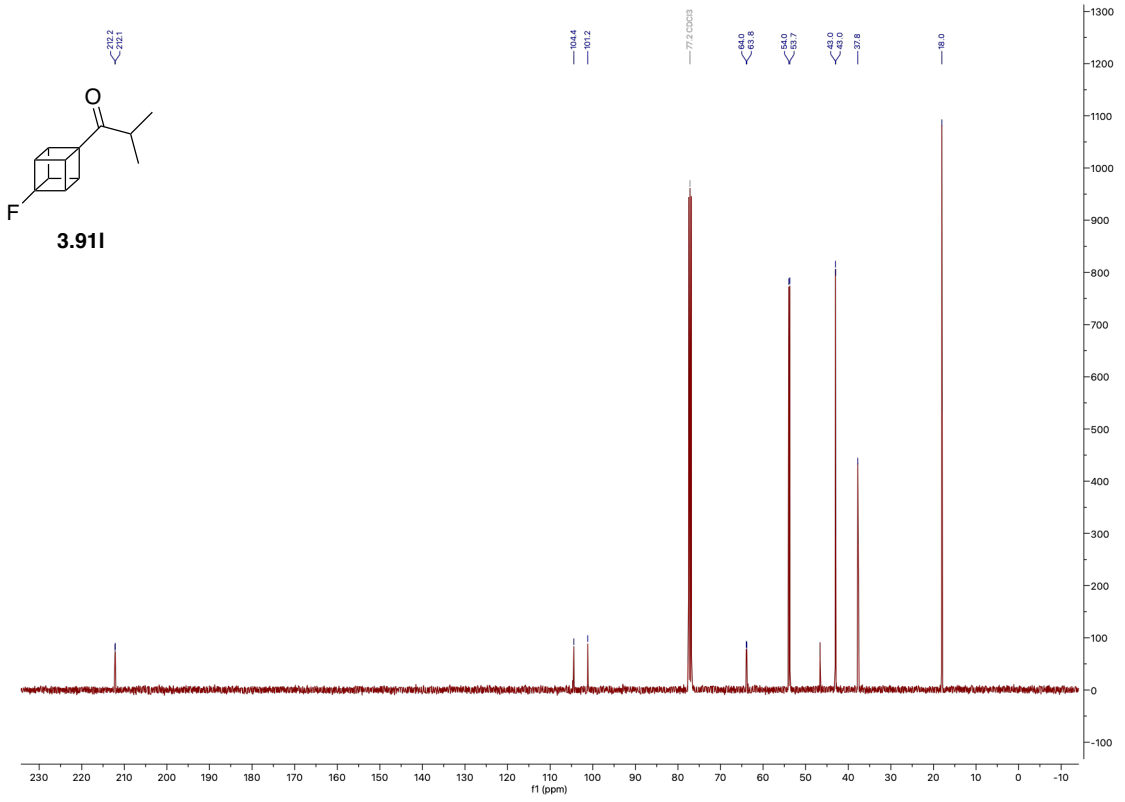

^{19}F{1H}NMR (376 MHz, $CDCl_3$) of 3.91l

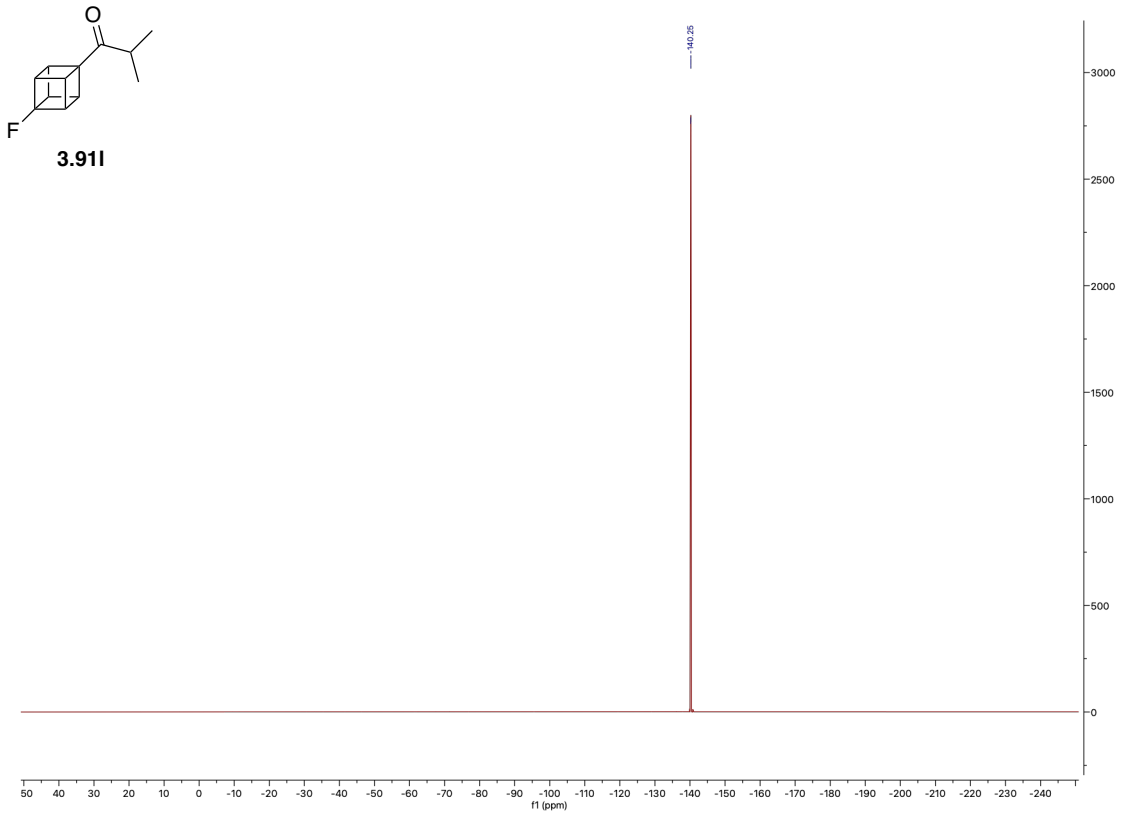

^{1}H NMR (500 MHz, $CDCl_3$) of 3.94a

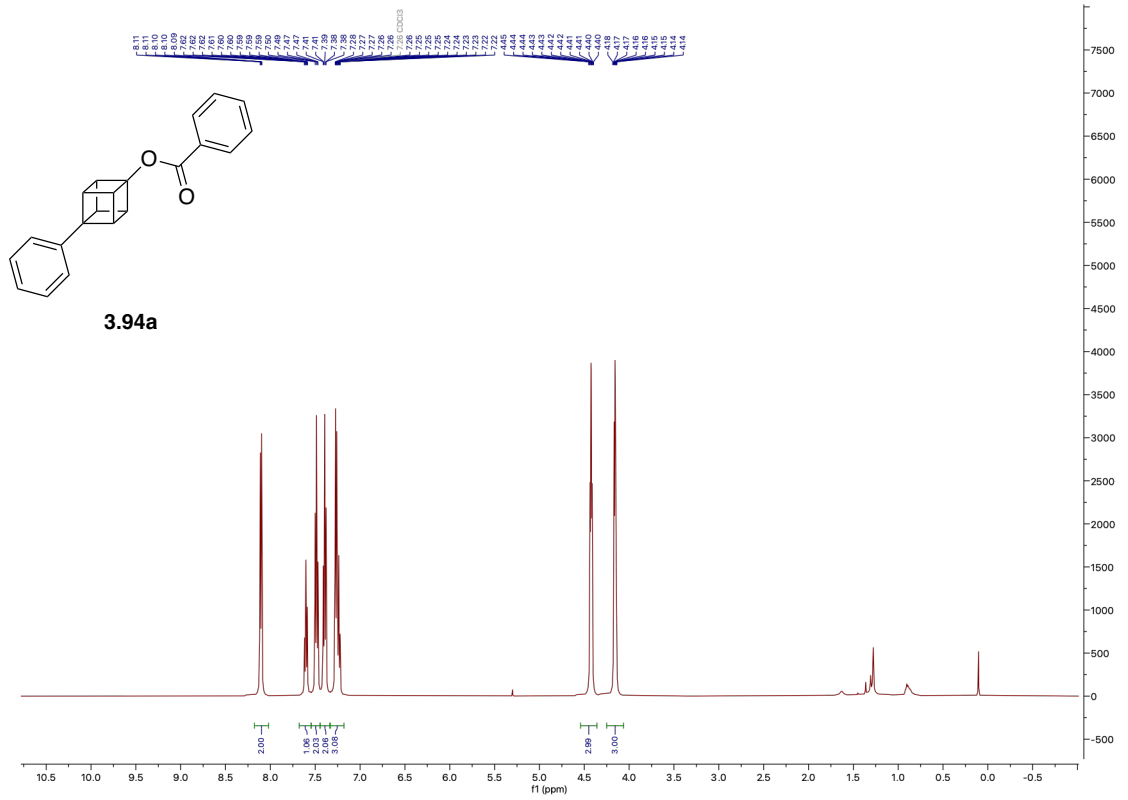

^{13}C NMR (126 MHz, $CDCl_3$) of 3.94a

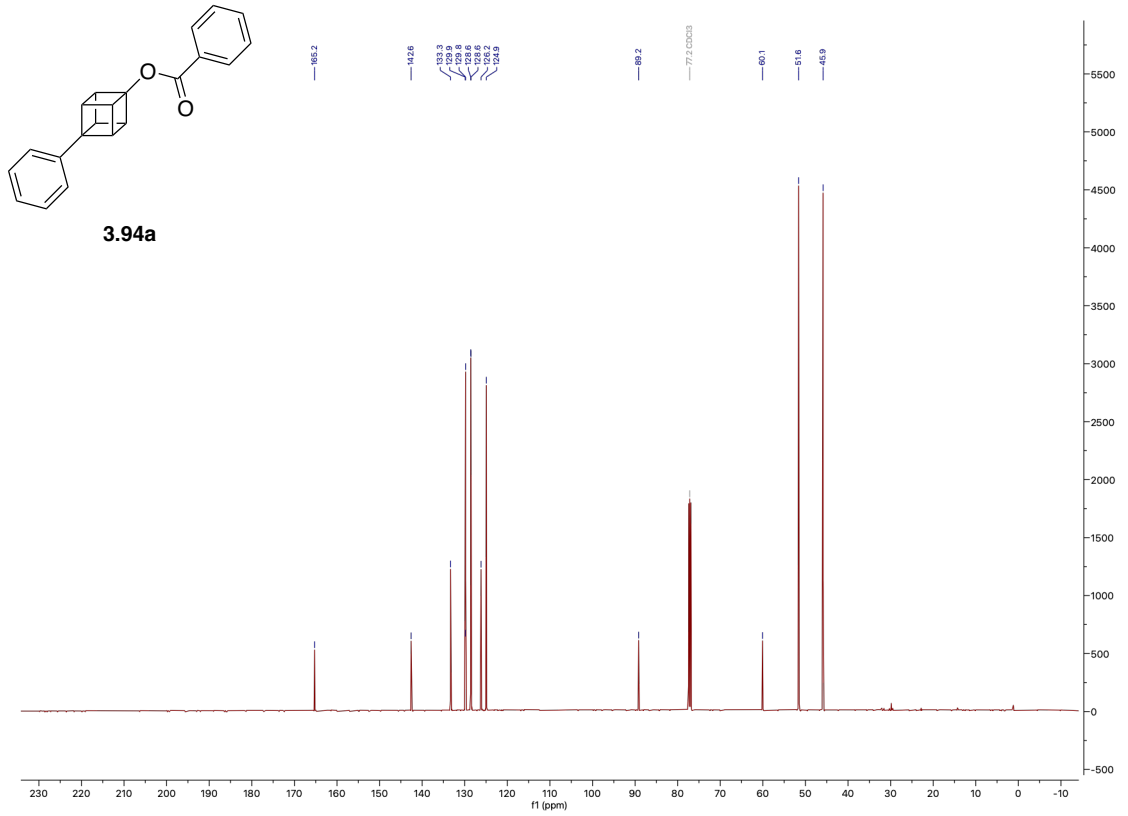

^{1}H NMR (400 MHz, $CDCl_3$) of 3.95a

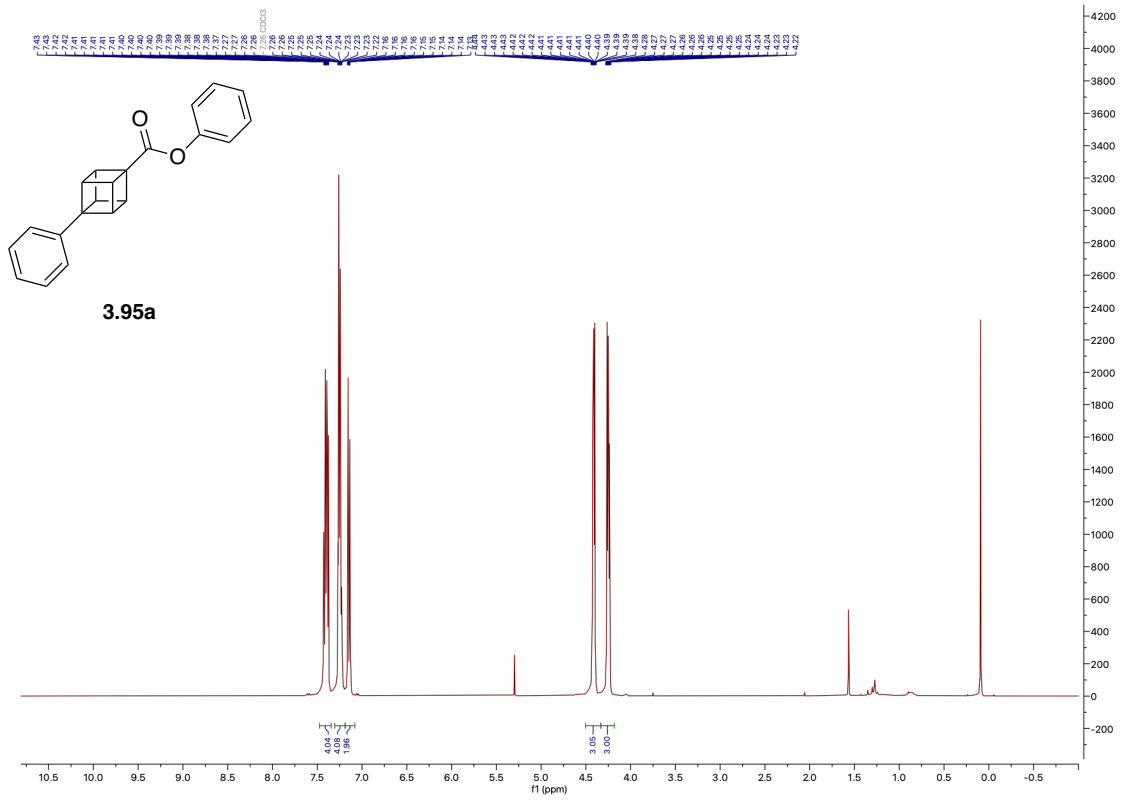

^{13}C NMR (101 MHz, $CDCl_3$) of 3.95a

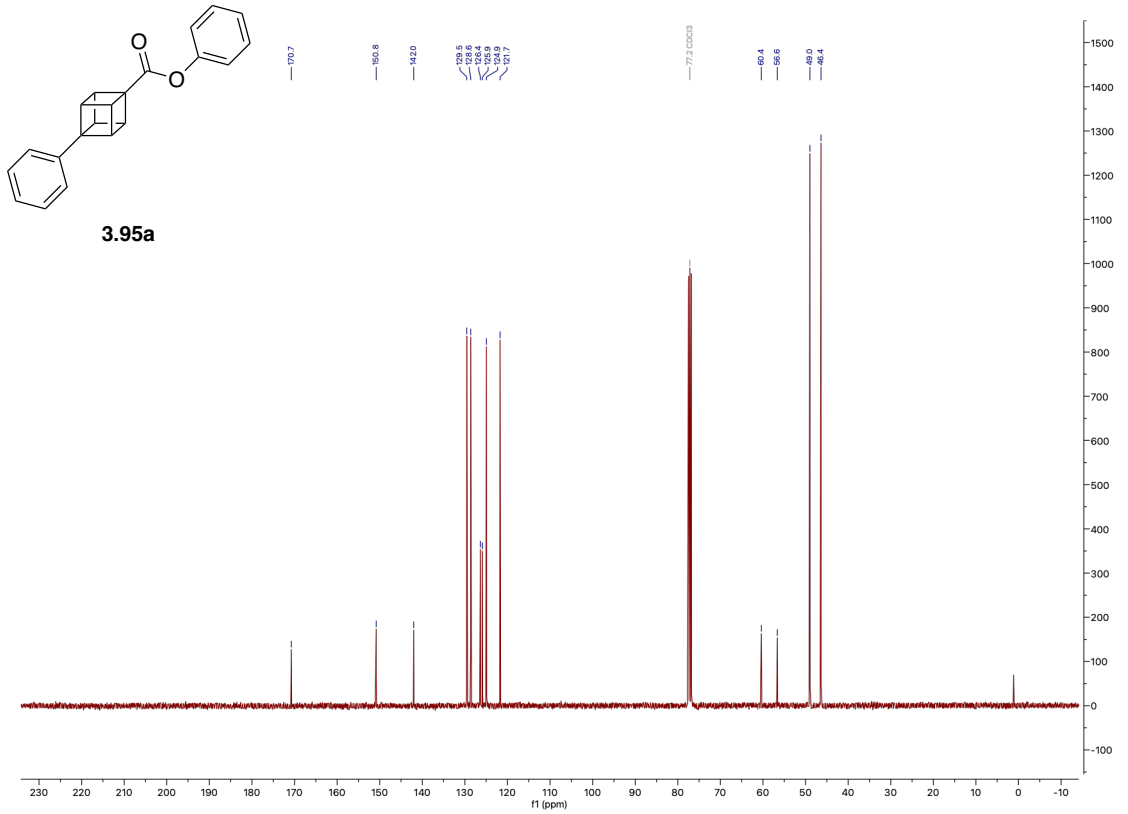

^{1}H NMR (400 MHz, $CDCl_3$) of 3.94b

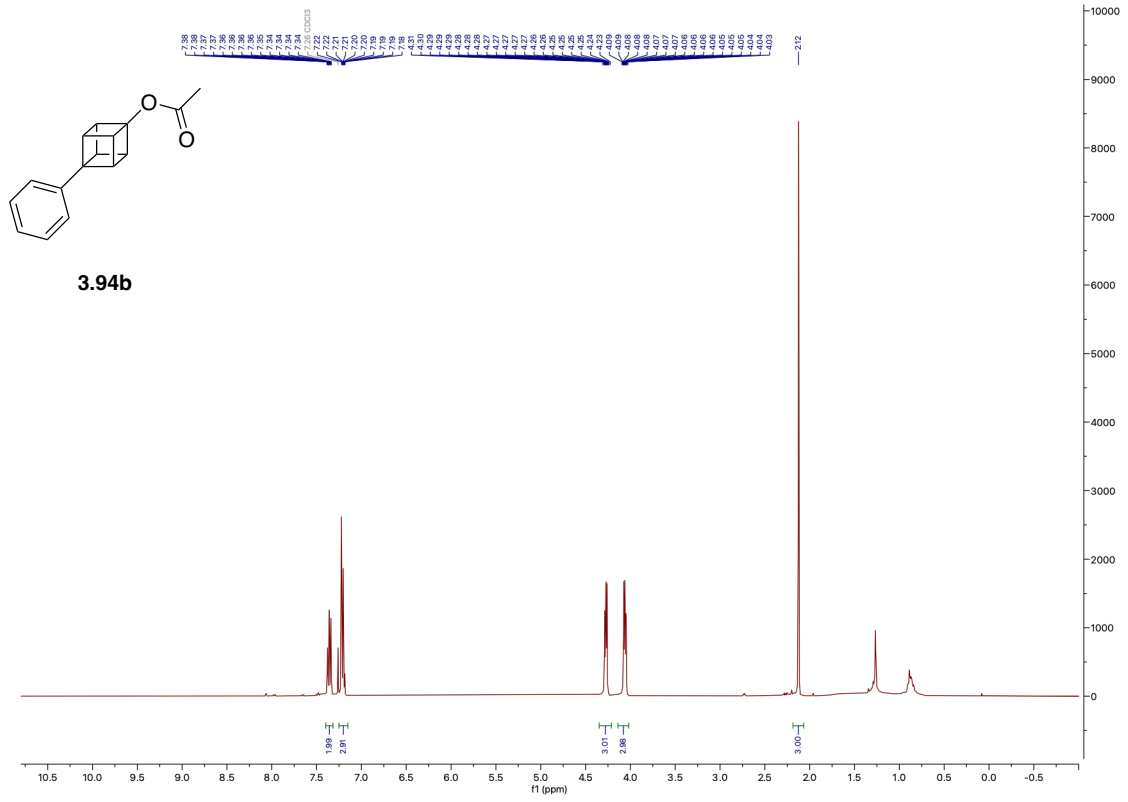

^{13}C NMR (101 MHz, $CDCl_3$) of 3.94b

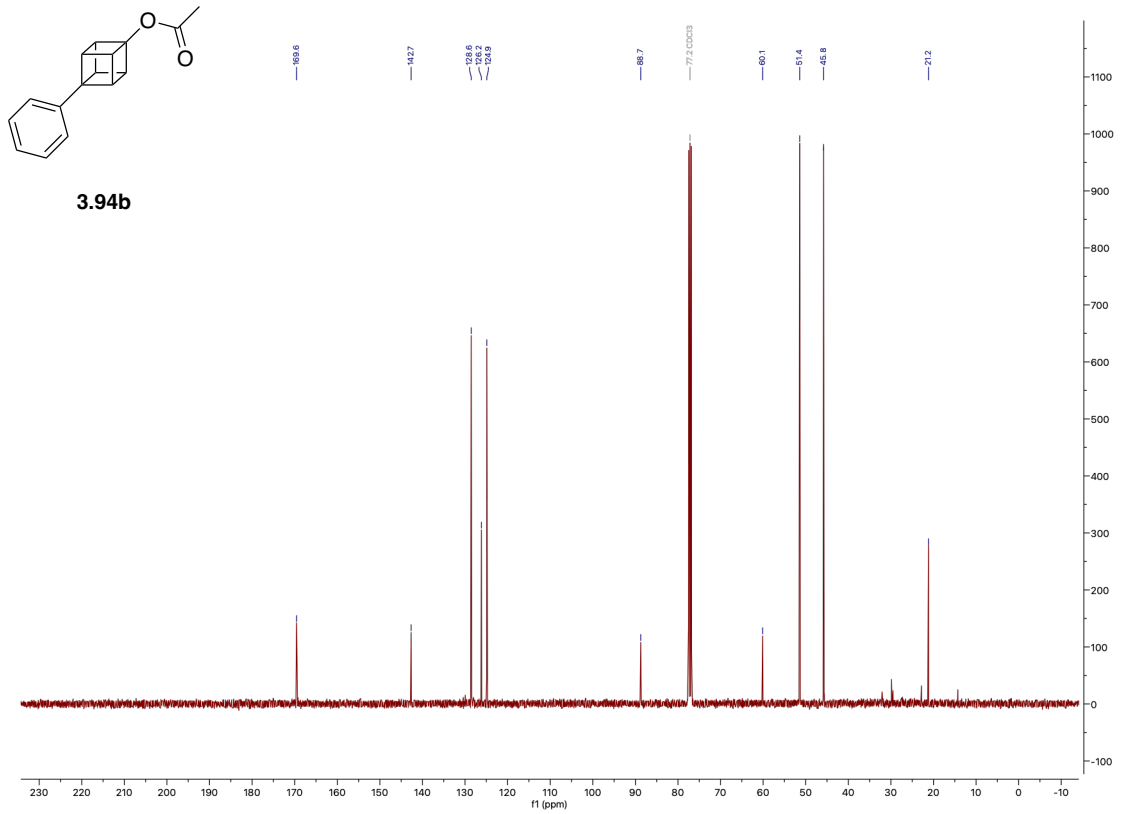

^{1}H NMR (400 MHz, $CDCl_3$) of 3.94c

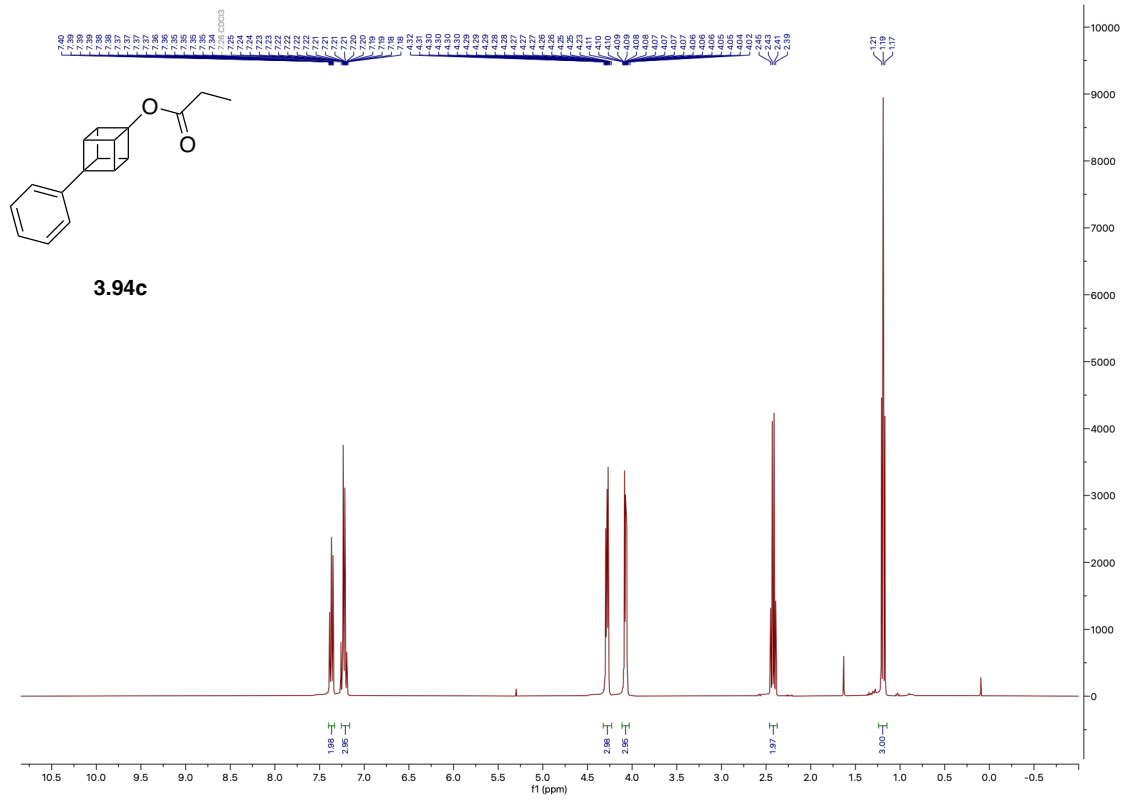

3.94c

^{13}C NMR (101 MHz, $CDCl_3$) of 3.94c

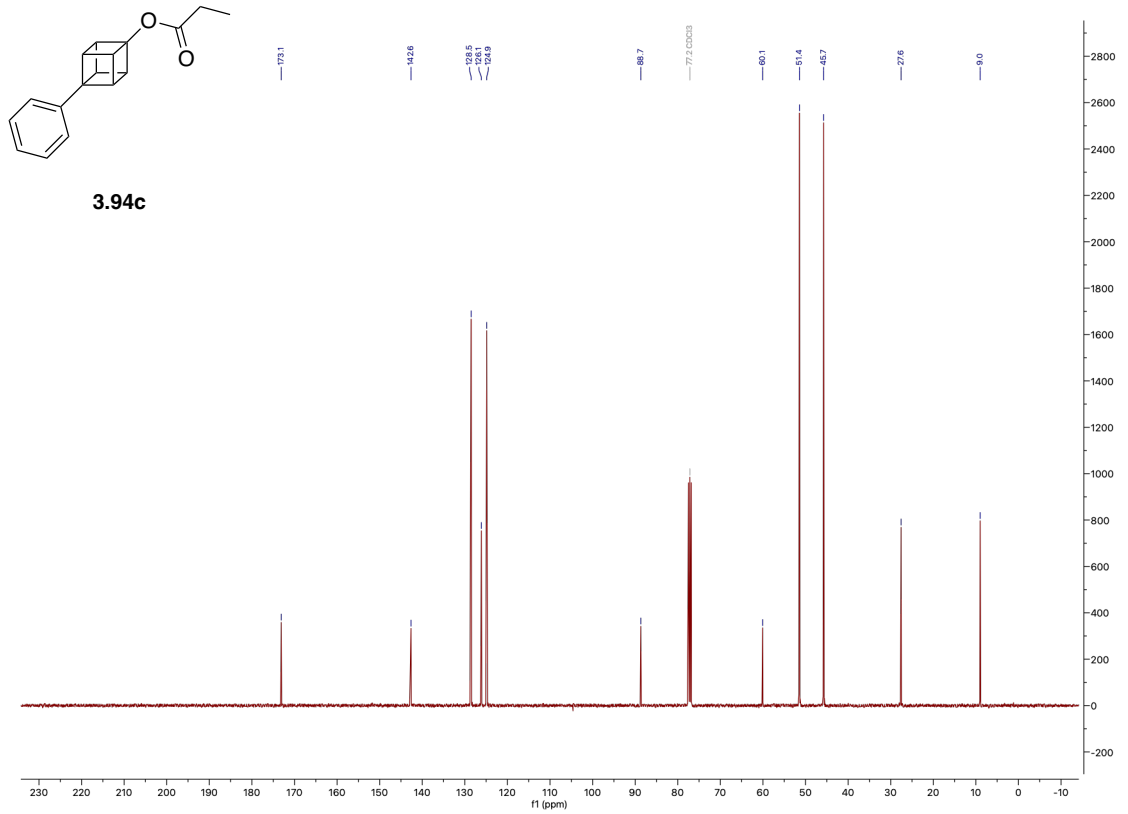

3.94c

^{1}H NMR (400 MHz, $CDCl_3$) of 3.94d

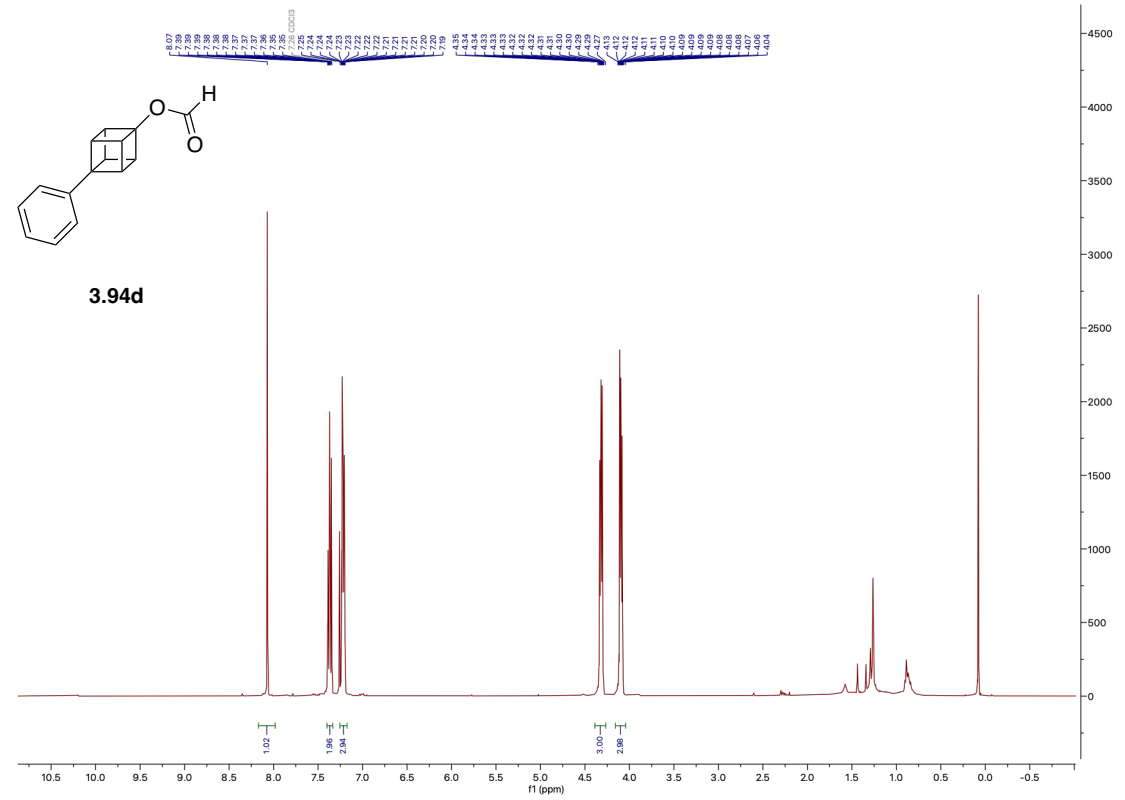

^{13}C NMR (101 MHz, $CDCl_3$) of 3.94d

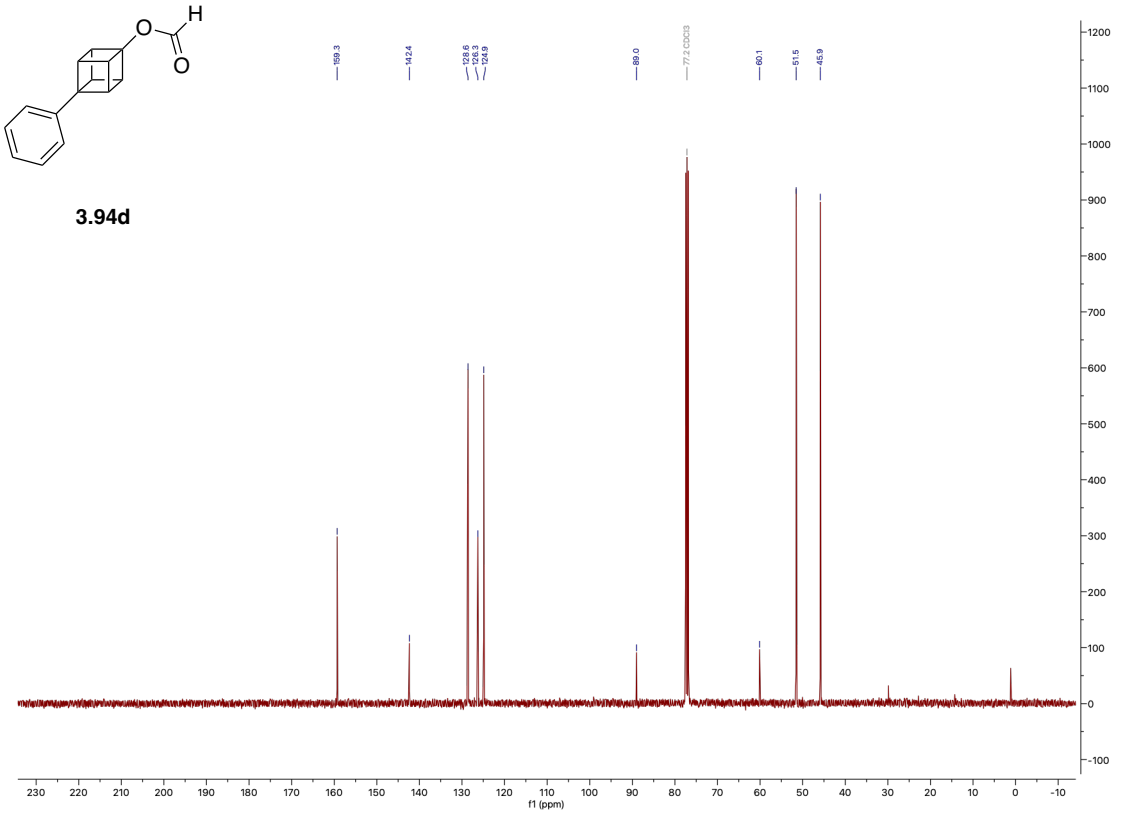

^{1}H NMR (400 MHz, $CDCl_3$) of 3.94e

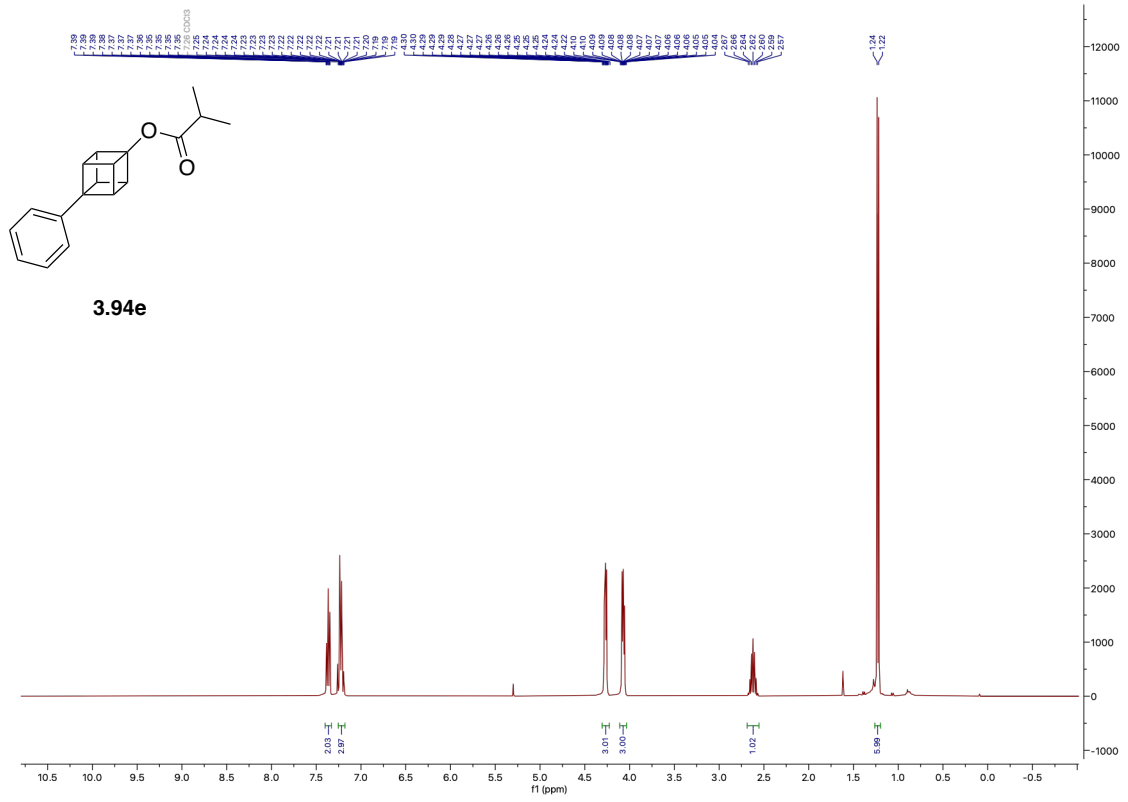

3.94e

^{13}C NMR (101 MHz, $CDCl_3$) of 3.94e

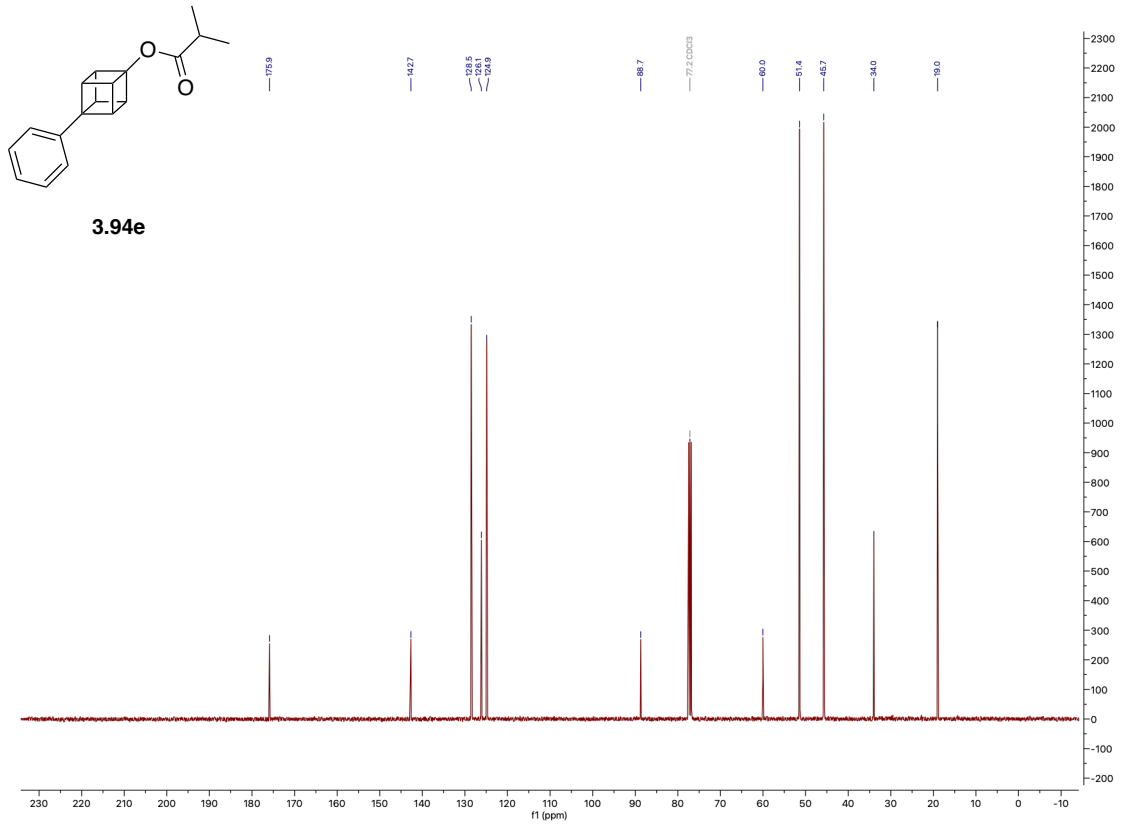

3.94e

^{1}H NMR (400 MHz, $CDCl_3$) of 3.95e

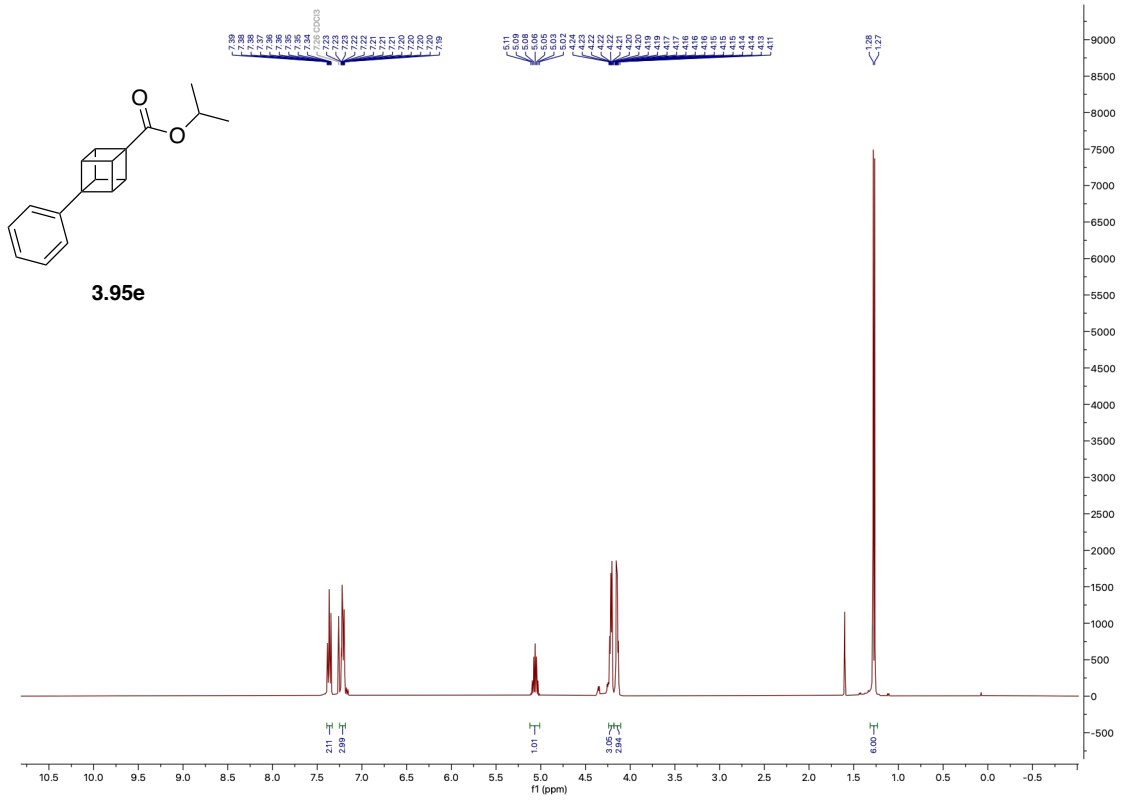

^{13}C NMR (101 MHz, $CDCl_3$) of 3.95e

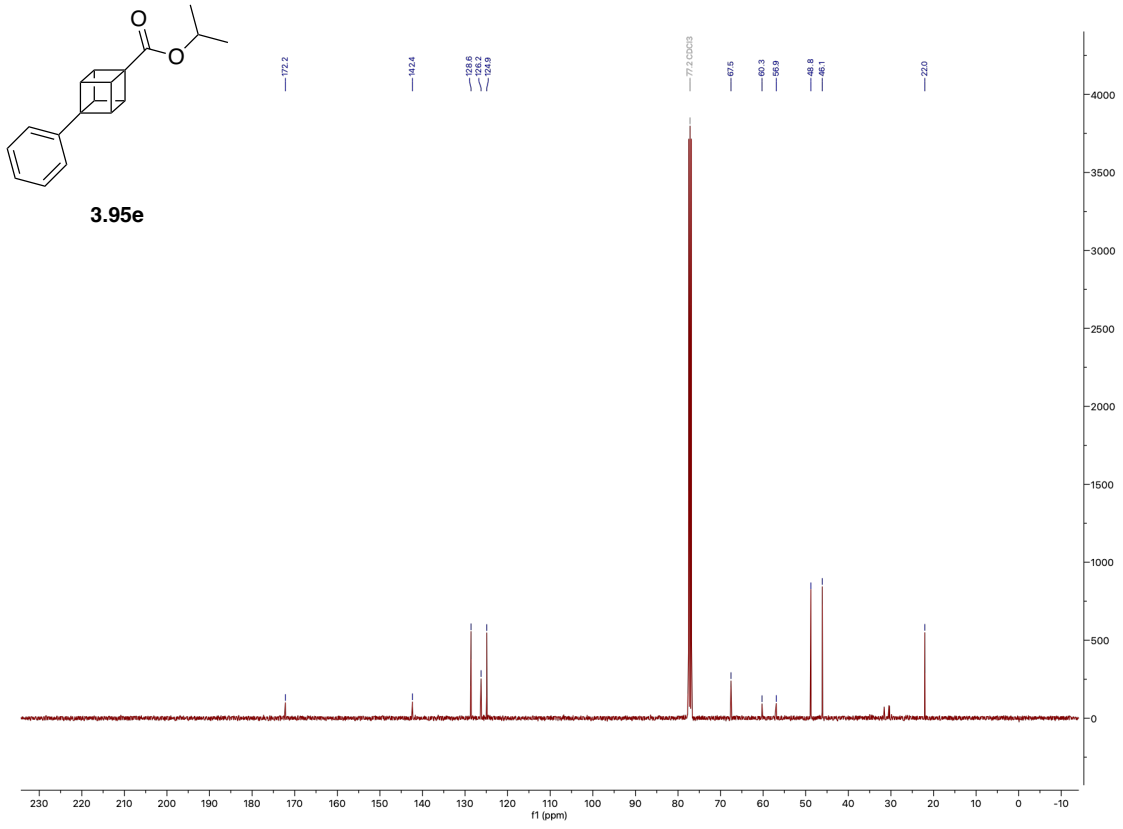

^{1}H NMR (400 MHz, $CDCl_3$) of 3.95f mixed with 3.91f in a ratio of 1:9

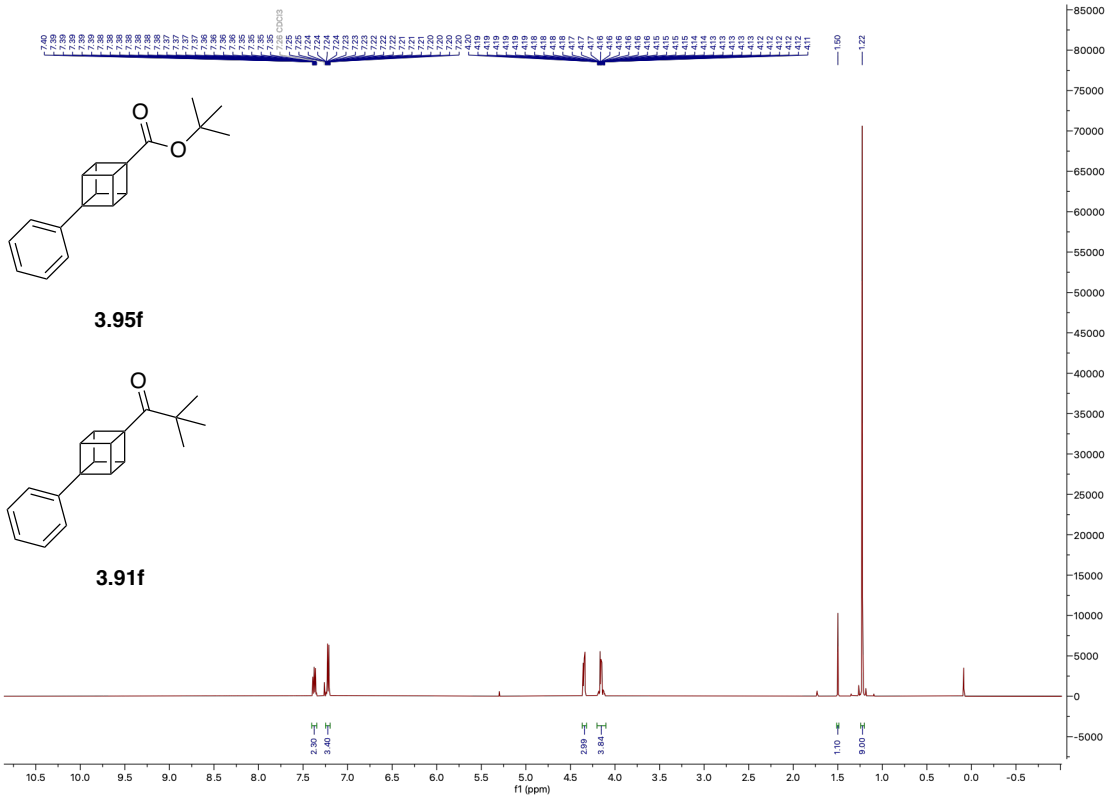

^{13}C NMR (101 MHz, $CDCl_3$) of 3.95f mixed with 3.91f in a ratio of 1:9

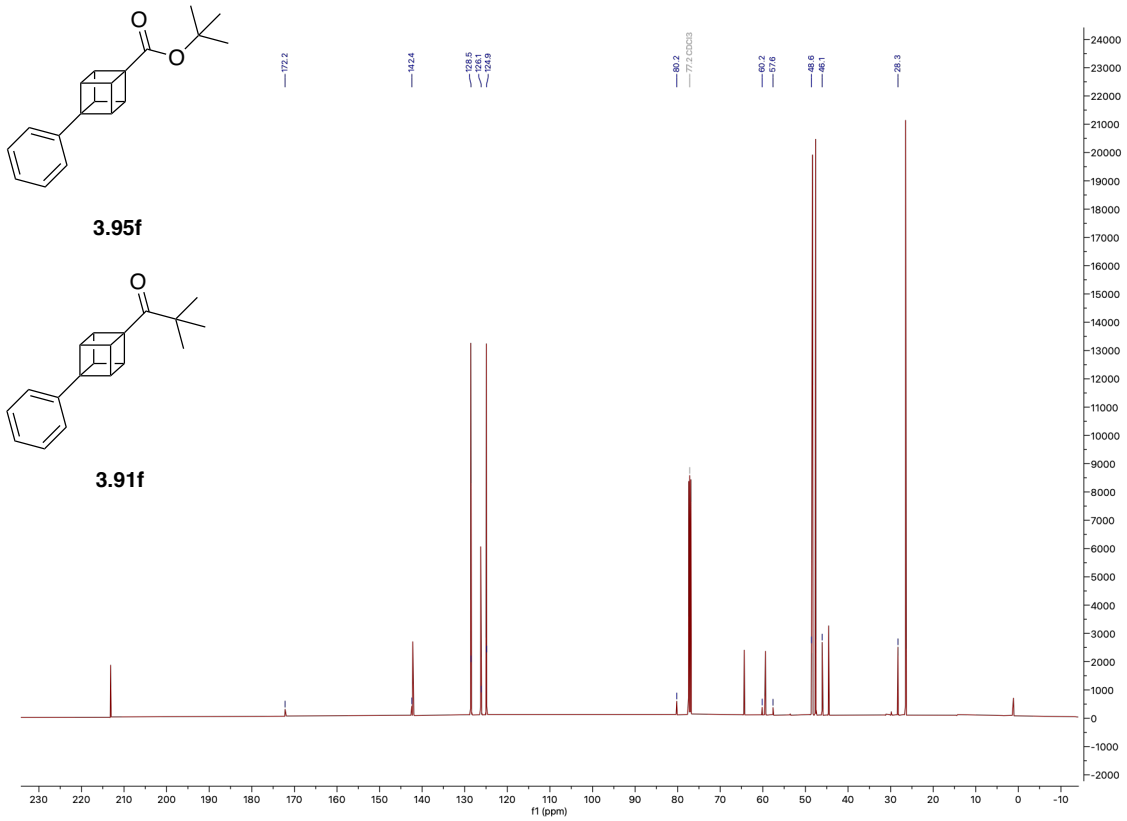

^{1}H NMR (400 MHz, $CDCl_3$) of 3.94g

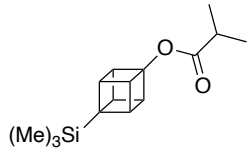

3.94g

^{13}C NMR (101 MHz, $CDCl_3$) of 3.94g

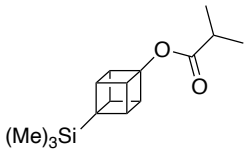

3.94g

^{1}H NMR (400 MHz, $CDCl_3$) of 3.95g

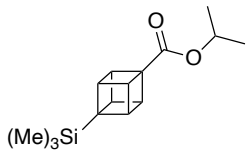

3.95g

^{13}C NMR (126 MHz, $CDCl_3$) of 3.95g

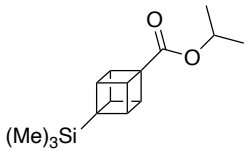

3.95g

^{1}H NMR (400 MHz, $CDCl_3$) of 3.94h

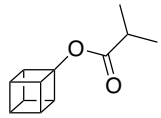

3.94h

^{13}C NMR (101 MHz, $CDCl_3$) of 3.94h

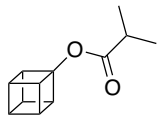

3.94h

^{1}H NMR (500 MHz, $CDCl_3$) of 3.95h

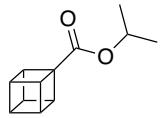

3.95h

^{13}C NMR (126 MHz, $CDCl_3$) of 3.95h

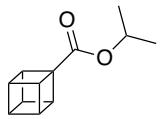

3.95h

^{1}H NMR (500 MHz, $CDCl_3$) of 3.94i

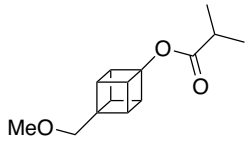

3.94i

^{13}C NMR (126 MHz, $CDCl_3$) of 3.94i

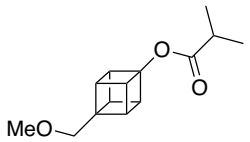

3.94i

^{1}H NMR (500 MHz, $CDCl_3$) of 3.95i

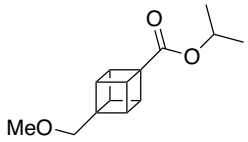

3.95i

^{13}C NMR (126 MHz, $CDCl_3$) of 3.95i

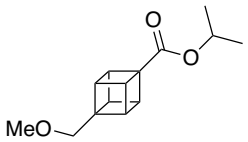

3.95i

^{1}H NMR (500 MHz, $CDCl_3$) of 3.94j

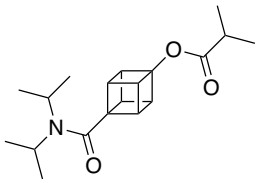

3.94j

^{13}C NMR (126 MHz, $CDCl_3$) of 3.94j

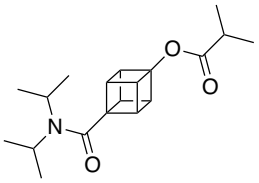

3.94j

^{1}H NMR (500 MHz, $CDCl_3$) of 3.95j

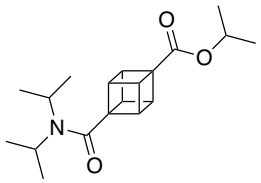

3.95j

^{13}C NMR (126 MHz, $CDCl_3$) of 3.95j

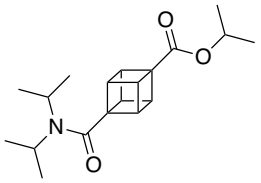

3.95j

^{1}H NMR (500 MHz, $CDCl_3$) of 3.94k

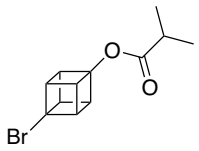

3.94k

^{13}C NMR (126 MHz, $CDCl_3$) of 3.94k

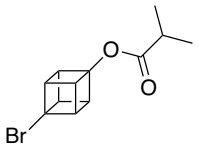

3.94k

^{1}H NMR (400 MHz, $CDCl_3$) of 3.95k

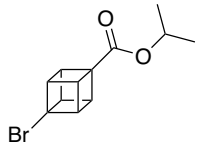

3.95k

^{13}C NMR (101 MHz, $CDCl_3$) of 3.95k

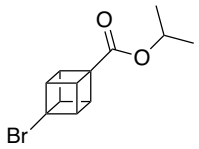

3.95k

^{1}H NMR (500 MHz, $CDCl_3$) of 3.94l

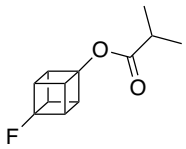

3.94l

^{13}C NMR (126 MHz, $CDCl_3$) of 3.94l

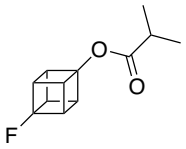

3.94l

$^{19}F\{1H\}$NMR (471 MHz, $CDCl_3$) of 3.94l

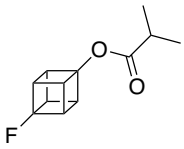

3.94l

^{1}H NMR (400 MHz, $CDCl_3$) of 3.95l

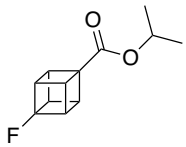

3.95l

^{13}C NMR (101 MHz, $CDCl_3$) of 3.95l

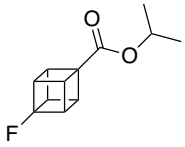

3.95l

^{19}F{1H}NMR (376 MHz, $CDCl_3$) of 3.95l

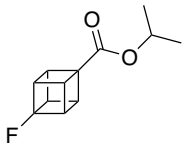

3.95l

^{1}H NMR (300 MHz, $CDCl_3$) of 4.11

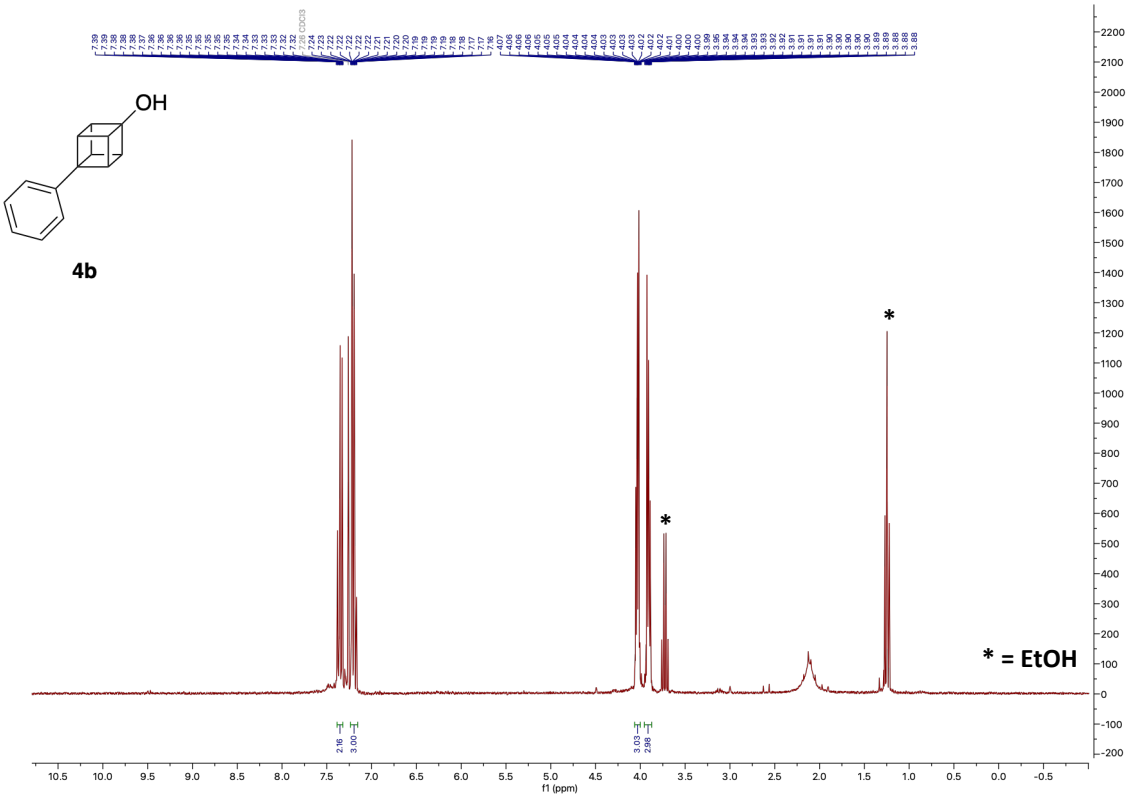

^{1}H NMR (300 MHz, $CDCl_3$) overlay of 4.11 and 3.94b

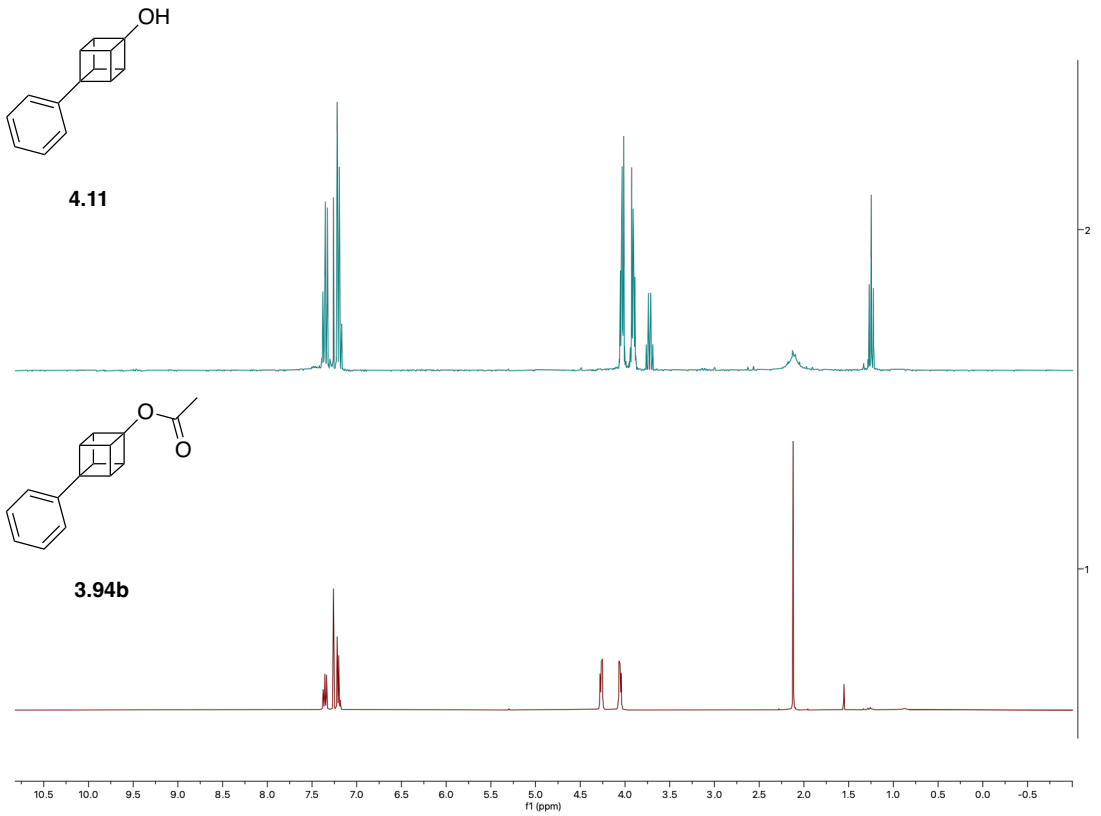

^{1}H NMR (300 MHz, $CDCl_3$) decomposition of 4.11 within 1 h in $CDCl_3$

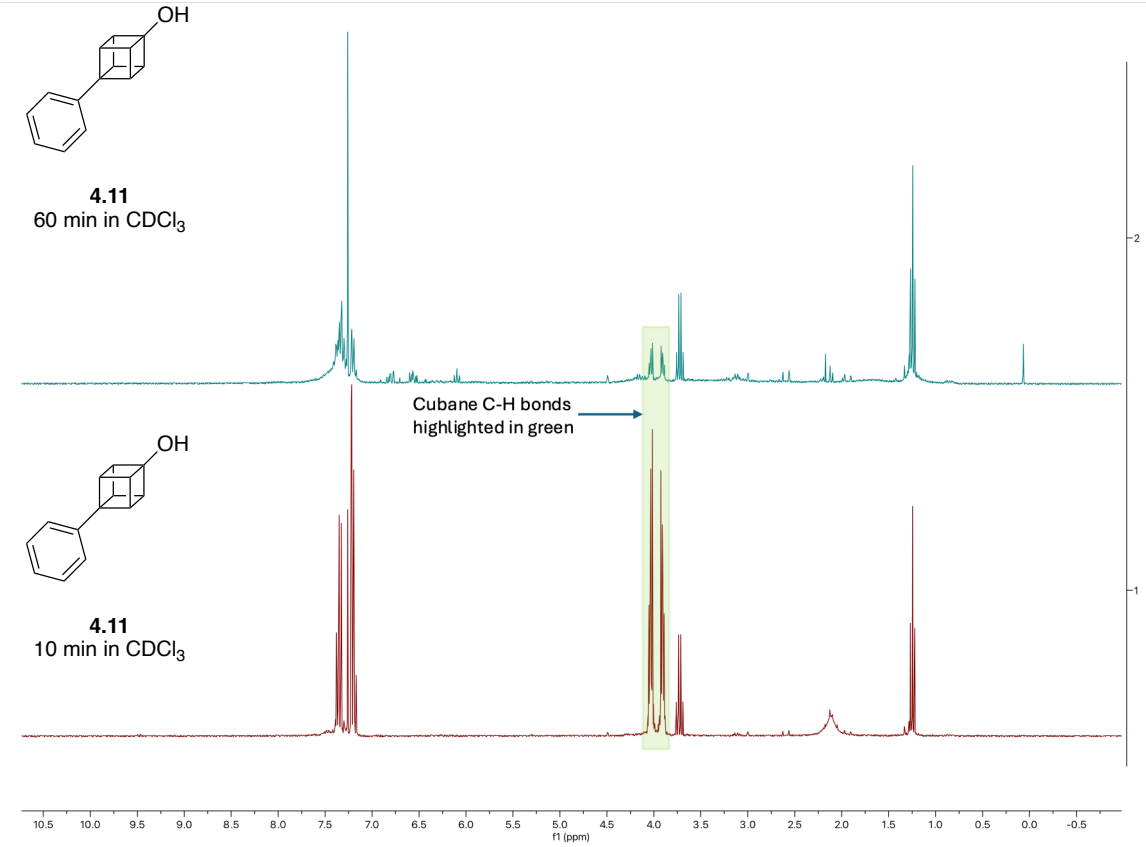

^{1}H NMR (400 MHz, Acetic Acid-d_3) 4.11 in Acetic Acid-d_3 for 24 h

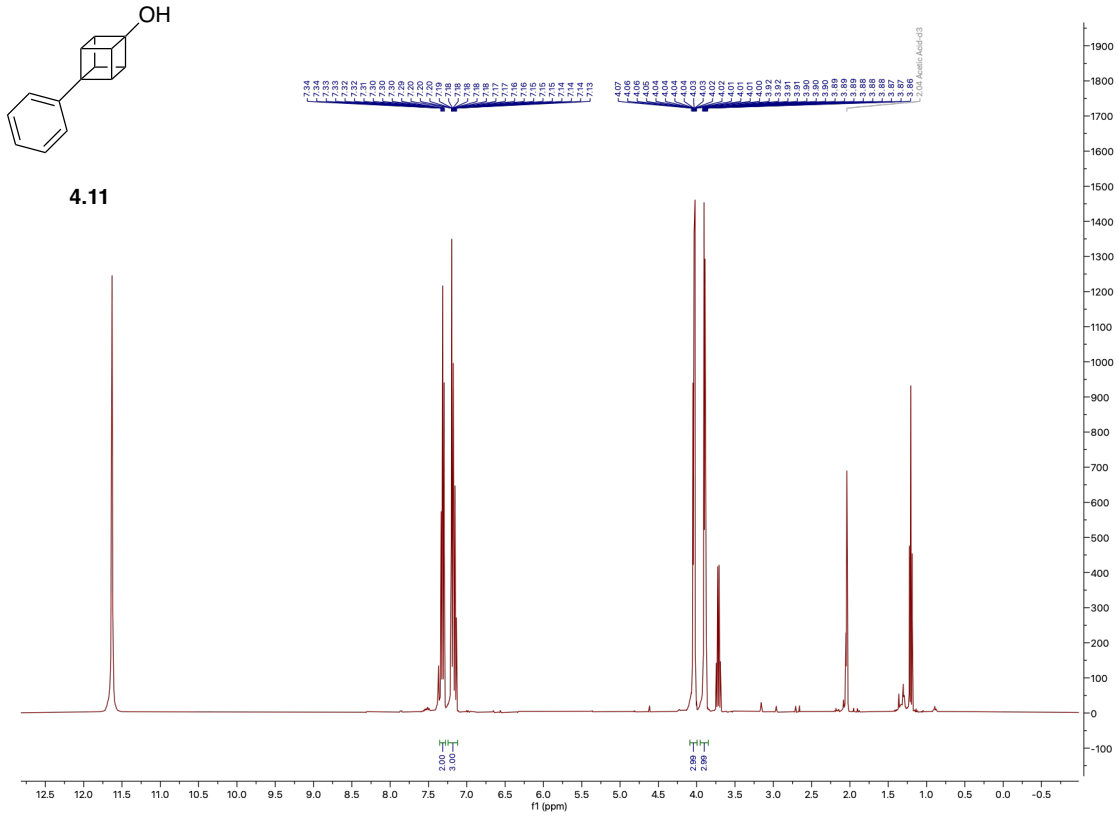

^{1}H NMR (400 MHz, $CDCl_3$) of 4.14

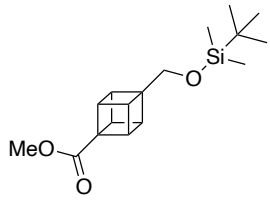

4.14

^{13}C NMR (101 MHz, $CDCl_3$) of 4.14

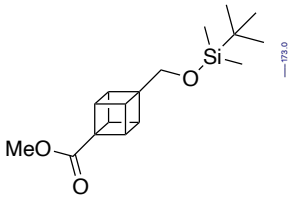

4.14

^{1}H NMR (400 MHz, $CDCl_3$) of 4.15

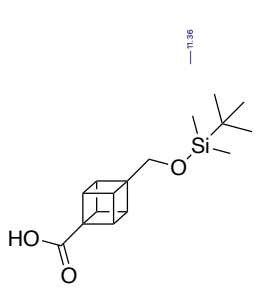

4.15

^{13}C NMR (101 MHz, $CDCl_3$) of 4.15

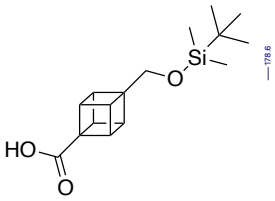

4.15

^{1}H NMR (500 MHz, $CDCl_3$) of 4.16

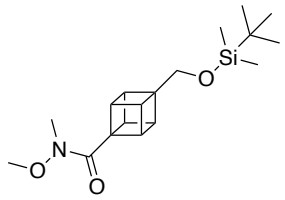

4.16

^{13}C NMR (126 MHz, $CDCl_3$) of 4.16

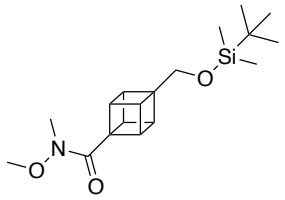

4.16

^{1}H NMR (400 MHz, $CDCl_3$) of 4.17

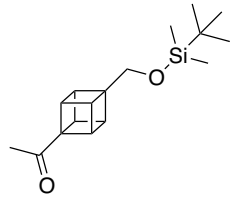

4.17

^{13}C NMR (101 MHz, $CDCl_3$) of 4.17

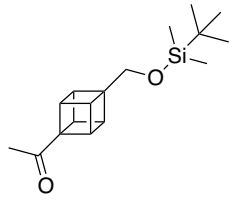

4.17

^{1}H NMR (500 MHz, $CDCl_3$) of 4.18

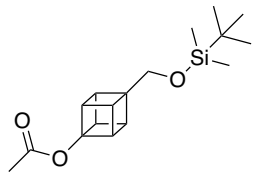

4.18

^{13}C NMR (126 MHz, $CDCl_3$) of 4.18

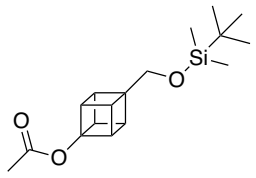

4.18

^{1}H NMR (400 MHz, $CDCl_3$) of 4.19

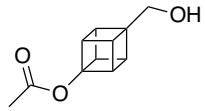

4.19

^{13}C NMR (101 MHz, $CDCl_3$) of 4.19

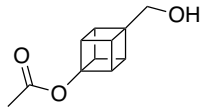

4.19

^{1}H NMR (400 MHz, $CDCl_3$) of 4.20

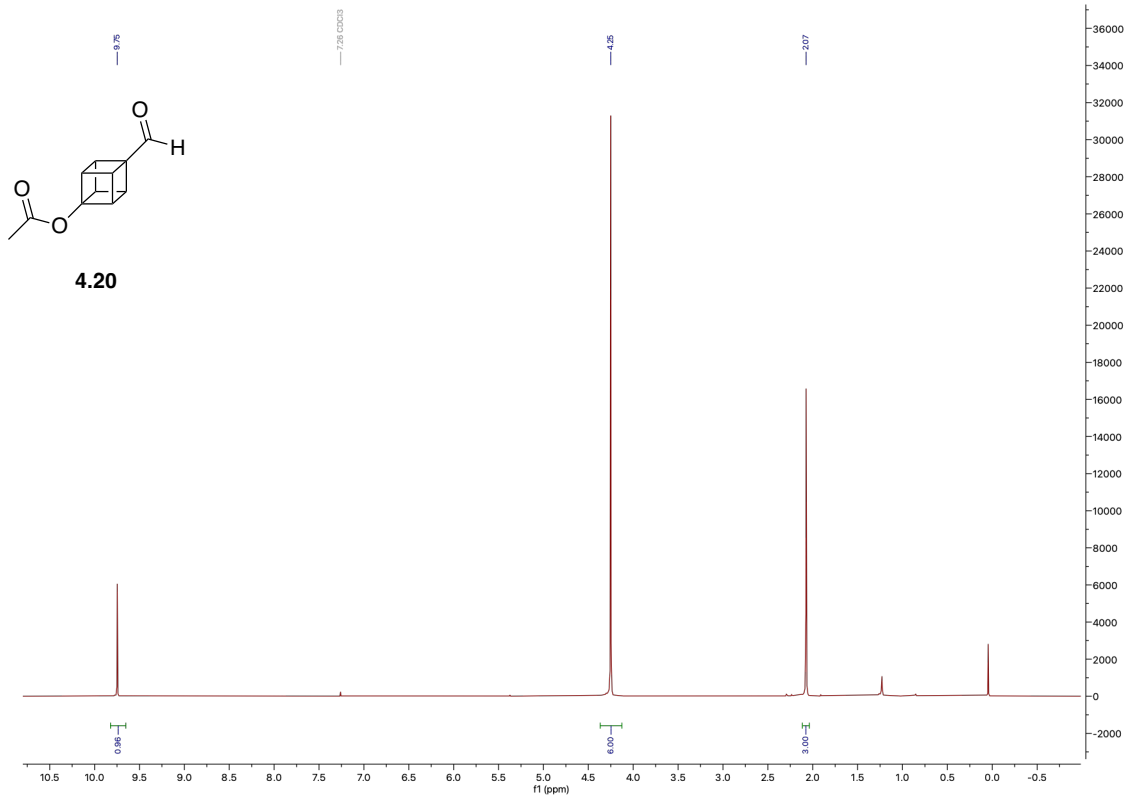

4.20

^{13}C NMR (101 MHz, $CDCl_3$) of 4.20

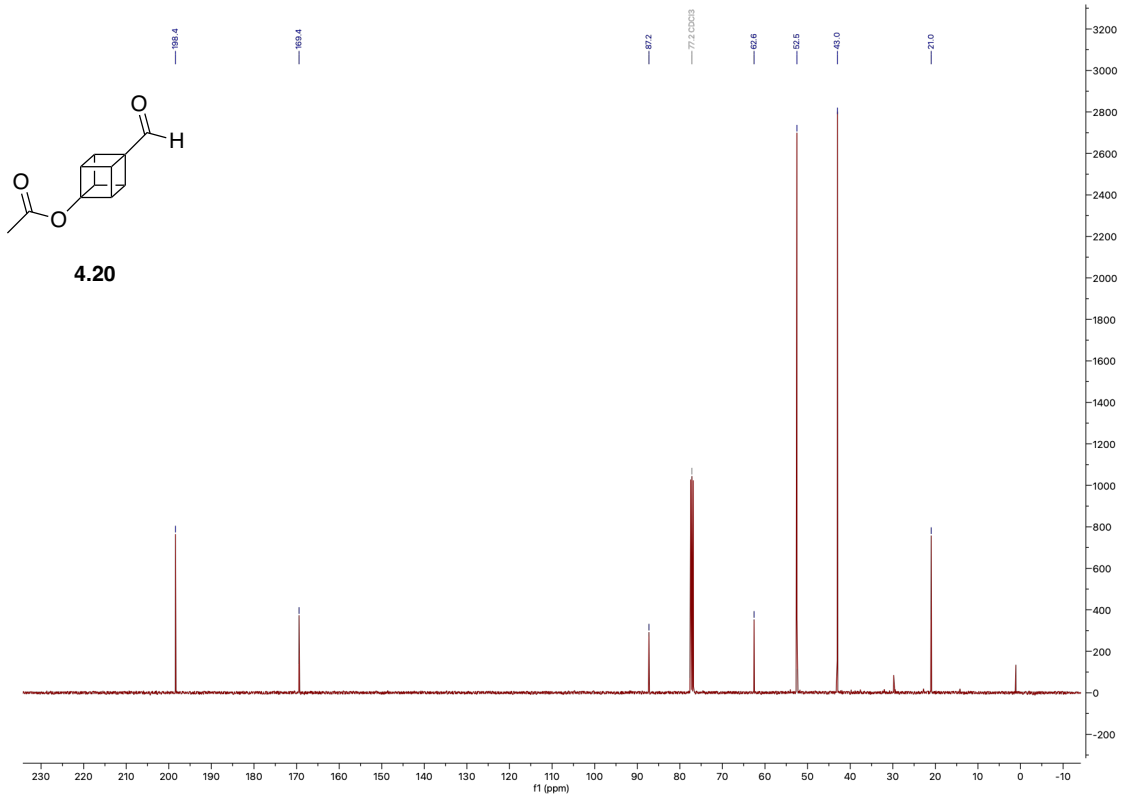

4.20

^{1}H NMR (500 MHz, DMSO-d_6) of 4.23a

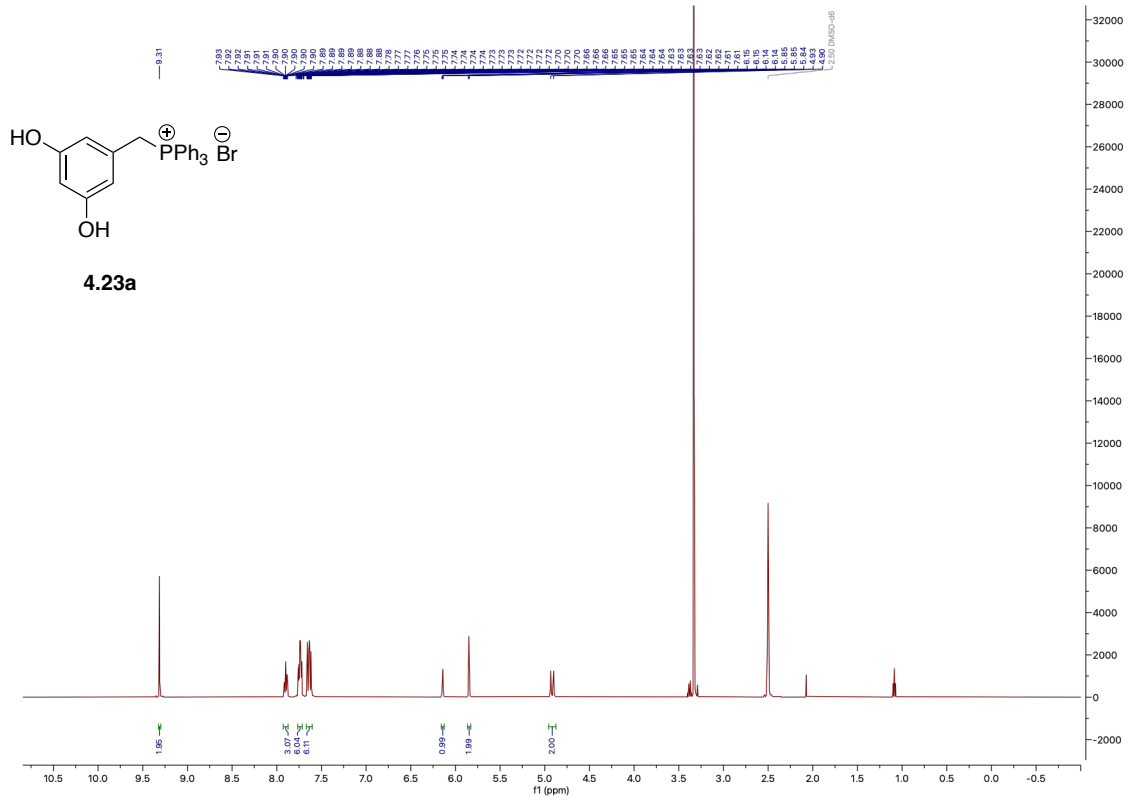

^{13}C NMR (126 MHz, DMSO-d_6) of 4.23a

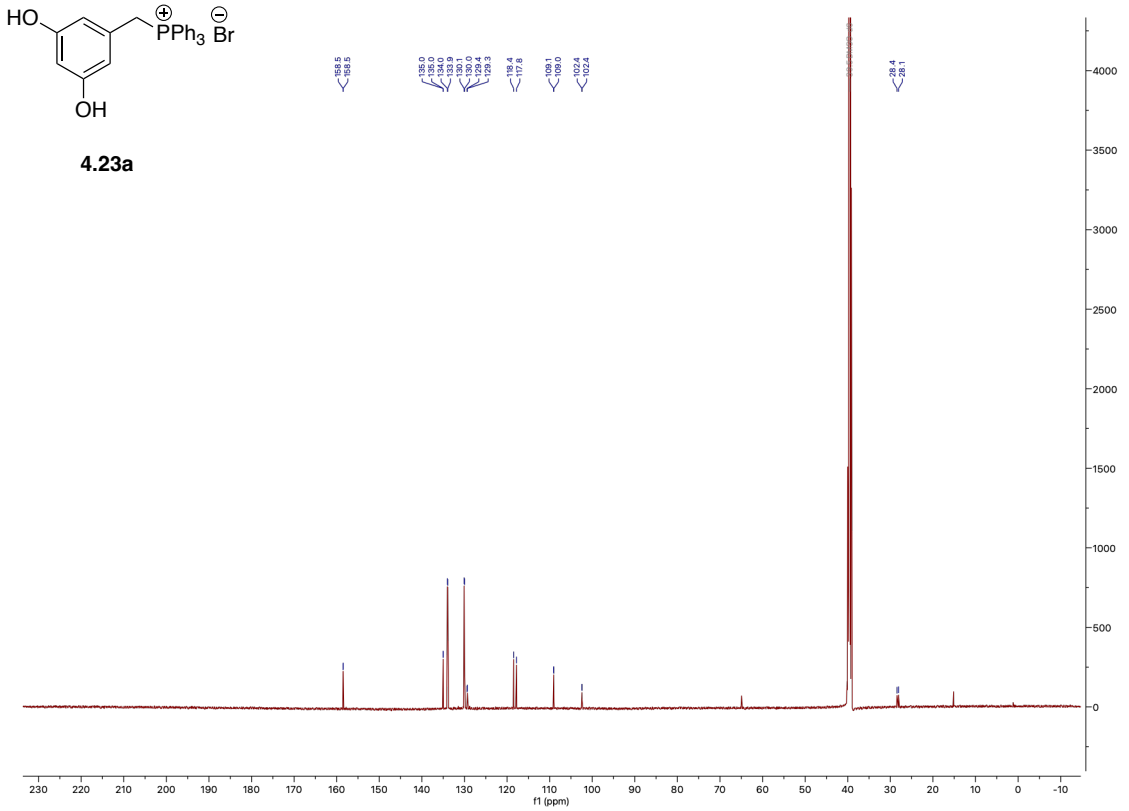

^{31}P NMR (162 MHz, DMSO-d_6) of 4.23a

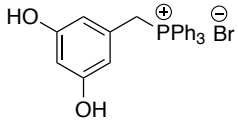

4.23a

^{1}H NMR (400 MHz, $CDCl_3$) of 4.25

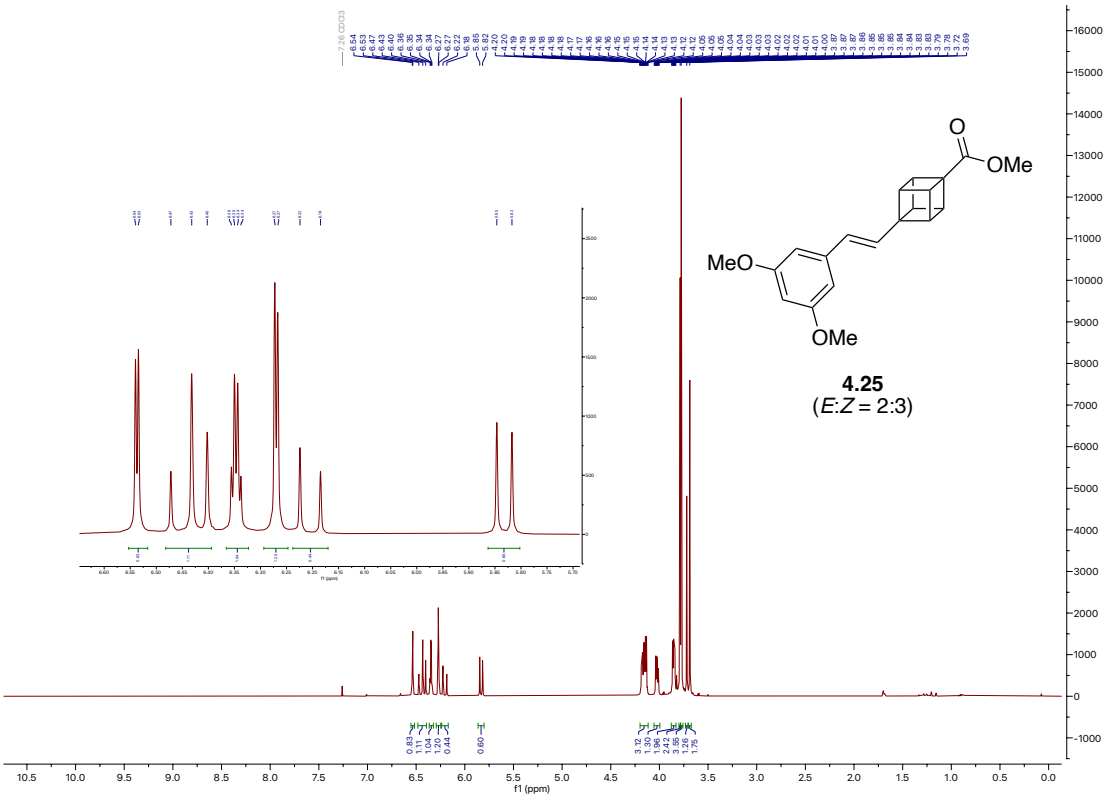

4.25
(*E*:*Z* = 2:3)

^{13}C NMR (101 MHz, $CDCl_3$) of 4.25

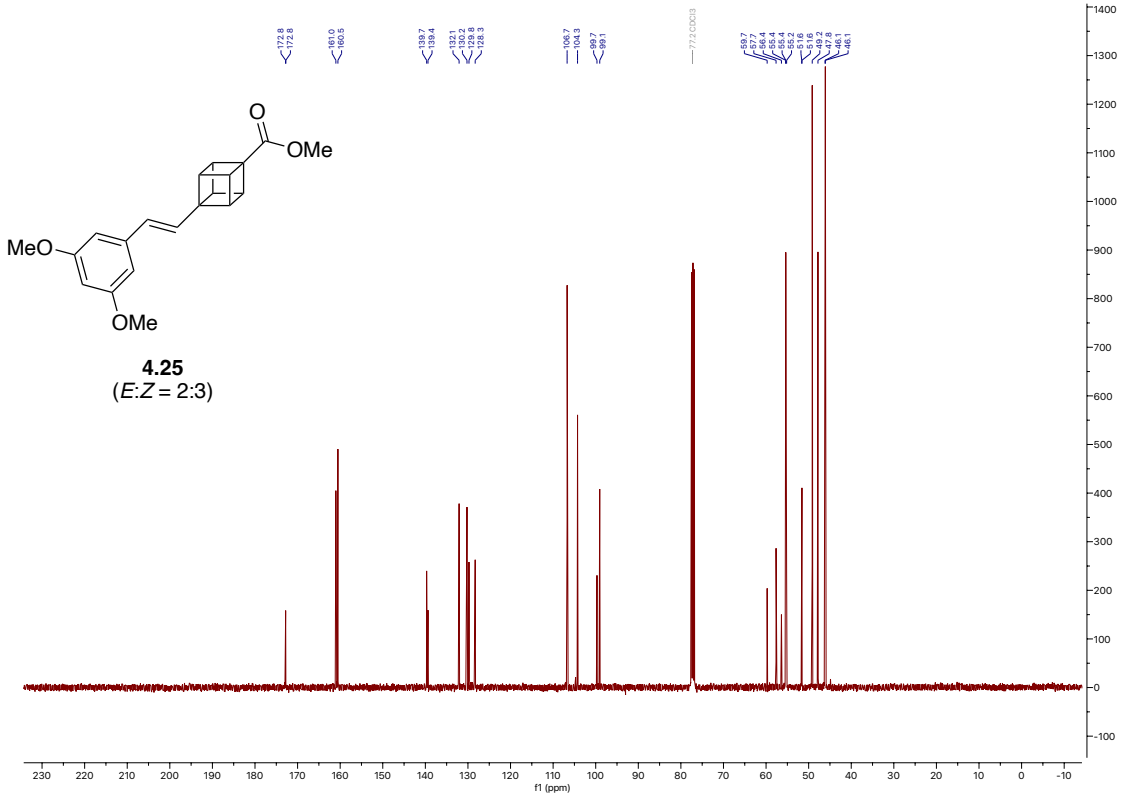

^{1}H NMR (500 MHz, DMSO-d_6) of 4.26a

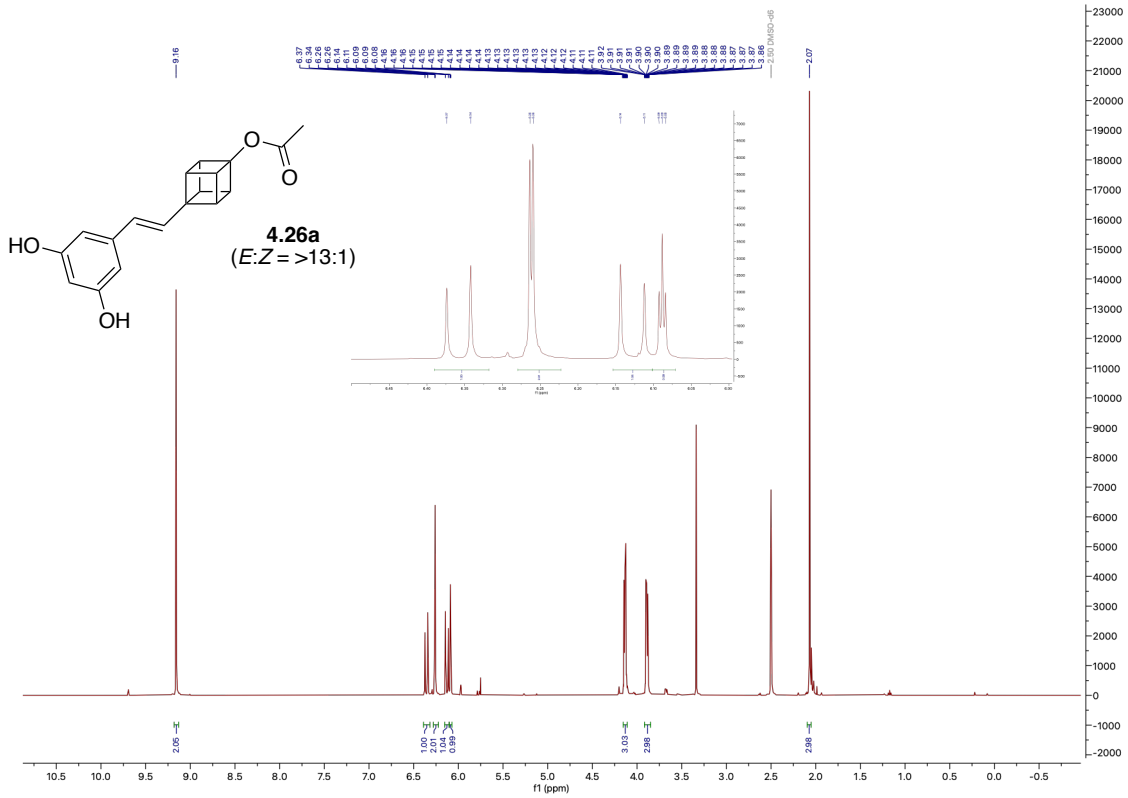

^{13}C NMR (126 MHz, DMSO-d_6) of 4.26a

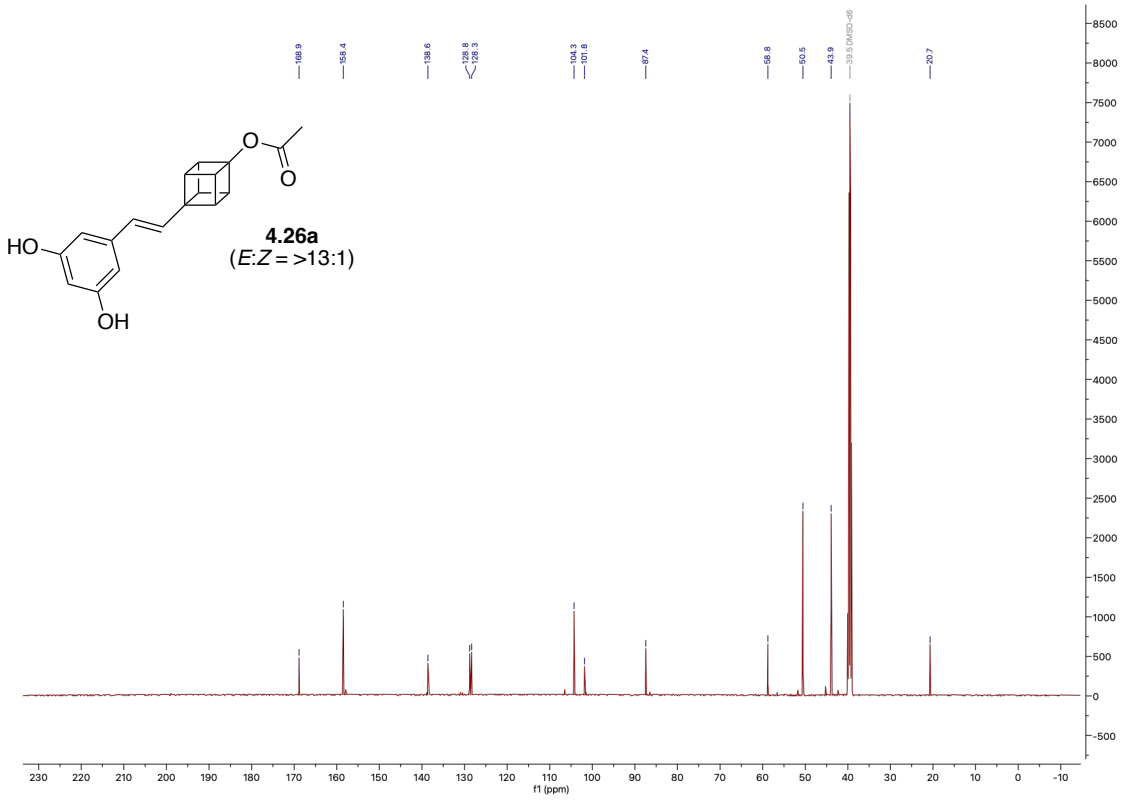

^{1}H NMR (400 MHz, $CDCl_3$) of 4.26b

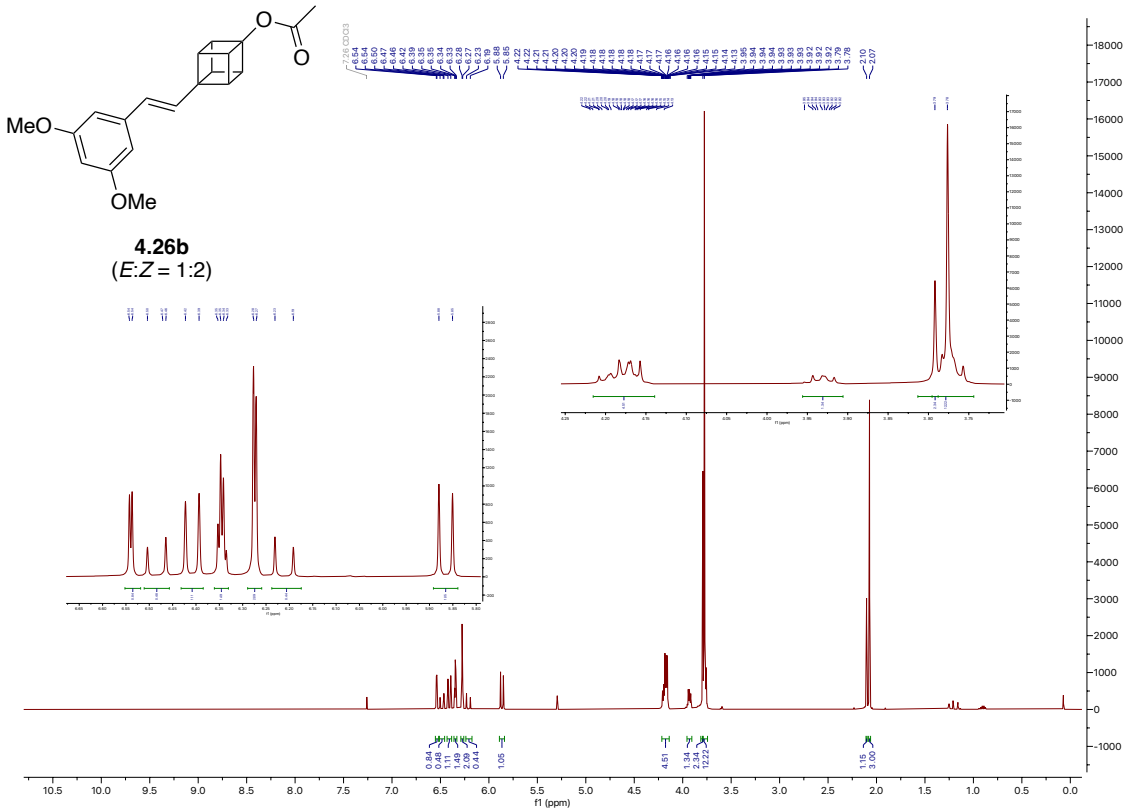

^{13}C NMR (101 MHz, $CDCl_3$) of 4.26b

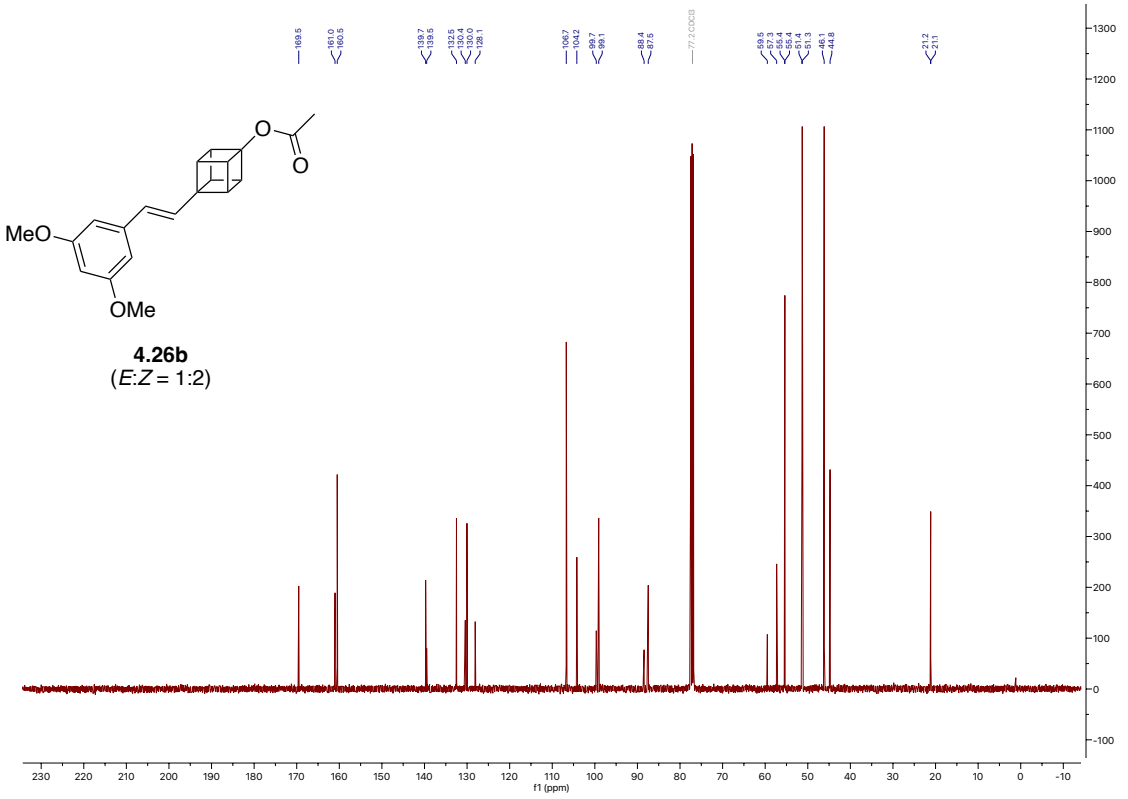

^{1}H NMR (500 MHz, DMSO-d_6) of 4.13a

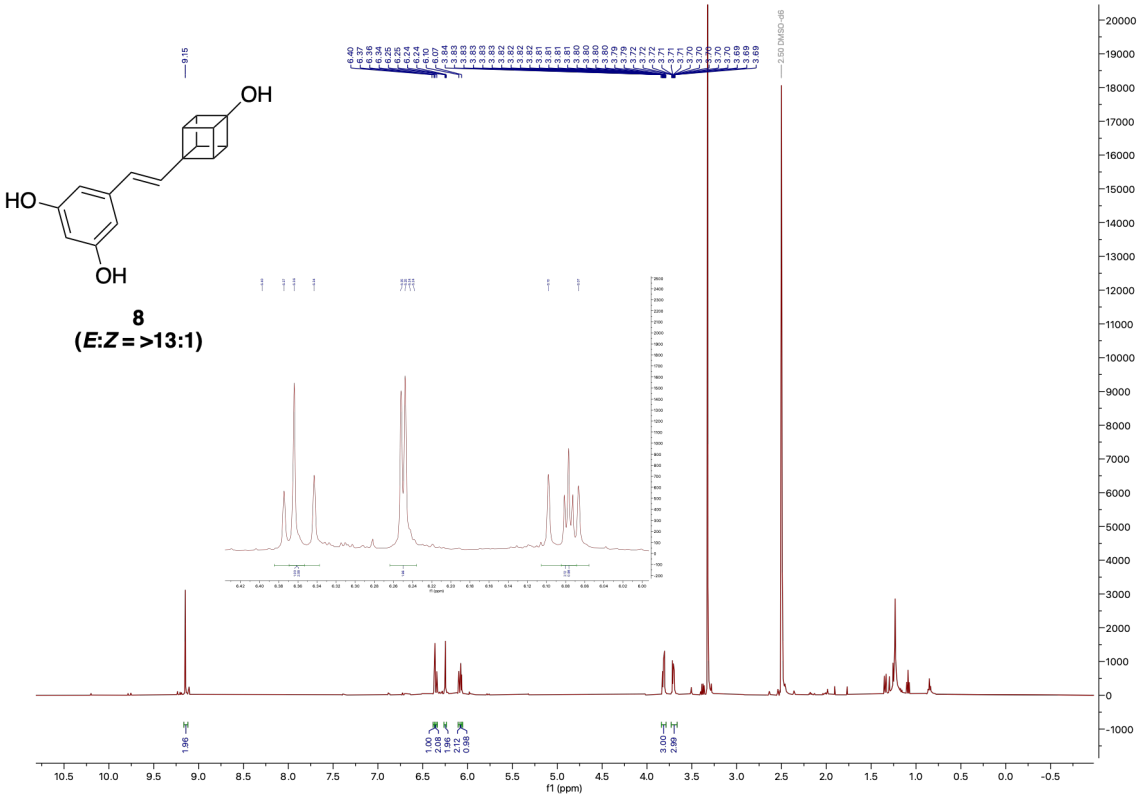

^{13}C NMR (126 MHz, DMSO-d_6) of 4.13a

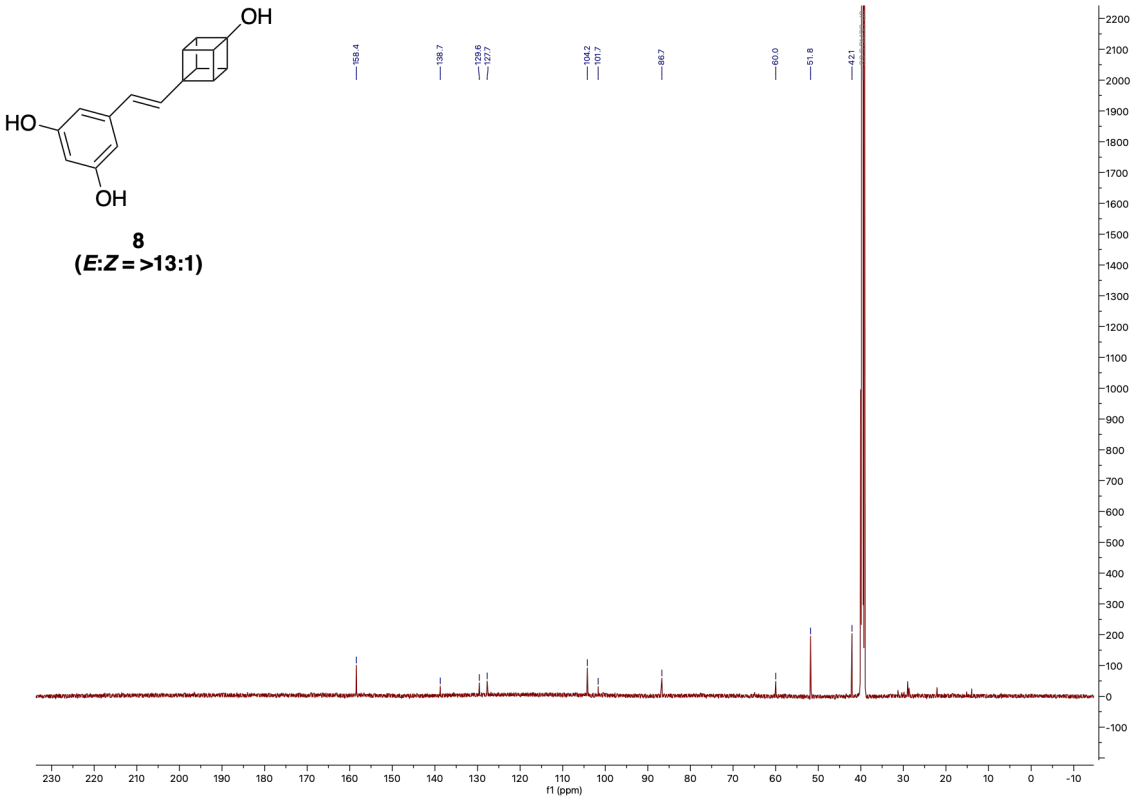

^{1}H NMR (400 MHz, DMSO-d_6) of 4.13b